

**ENHANCED HYDROGEN ECONOMICS VIA CO-
PRODUCTION OF FUELS AND CARBON PRODUCTS**
DE-FC26-06NT42761

FINAL REPORT

Period of Performance 1 Apr 2006-March 31 2011

Original Submission: 15 August 2011

Resubmitted: 11 October 2011

Principal Investigator:

Elliot B. Kennel

Co-Investigators:

**Abhijit Bhagavatula, Dady Dadyburjor, Santhoshi Dixit, Ravinder Garlapalli,
Liviu Magean, Mayuri Mukkha, Olufemi A. Olajide, Alfred H. Stiller,
Christopher L. Yurchick, John W. Zondlo**

**West Virginia University
Department of Chemical Engineering
College of Engineering and Mineral Resources
PO Box 6102
Morgantown WV 26506-6102**

Sponsored by:

**U.S. Department of Energy
National Energy Technology Laboratory
626 Cochran Mills Road
PO Box 10940
Pittsburgh PA 15236-0940**

Project Monitor: John Stipanovich

DISCLAIMER:

This report was prepared as an account of work sponsored by an agency of the United States Government. Neither the United States Government nor any agency thereof, nor any of their employees, makes any warranty, express or implied, or assumes any legal liability or responsibility for the accuracy, completeness, or usefulness of any information, apparatus, product, or process disclosed, or represents that its use would not infringe privately owned rights. Reference herein to any specific commercial product, process, or service by trade name, trademark, manufacturer, or otherwise does not necessarily constitute or imply its endorsement, recommendation, or favoring by the United States Government or any agency thereof. The views and opinions of authors expressed herein do not necessarily state or reflect those of the United States Government or any agency thereof.

ABSTRACT

This Department of Energy National Energy Technology Laboratory sponsored research effort to develop environmentally cleaner projects as a spin-off of the FutureGen project, which seeks to reduce or eliminate emissions from plants that utilize coal for power or hydrogen production. New clean coal conversion processes were designed and tested for coproducing clean pitches and cokes used in the metals industry as well as a heavy crude oil. These new processes were based on direct liquefaction and pyrolysis techniques that liberate volatile liquids from coal without the need for high pressure or on-site gaseous hydrogen.

As a result of the research, a commercial scale plant for the production of synthetic foundry coke has broken ground near Wise, Virginia under the auspices of Carbonite Inc. This plant will produce foundry coke by pyrolyzing a blend of steam coal feedstocks. A second plant is planned by Quantex Energy Inc (in Texas) which will use solvent extraction to coproduce a coke residue as well as crude oil. A third plant is being actively considered for Kingsport, Tennessee, pending a favorable resolution of regulatory issues.

Table of Contents

TABLE OF CONTENTS.....	4
LIST OF FIGURES	6
LIST OF TABLES.....	11
I. EXECUTIVE SUMMARY	15
II. INTRODUCTION.....	16
2.1 Background.....	16
2.1.1. FutureGen Project	17
2.1.2. Research Objectives.....	21
2.1.3 Identification of Hydrogen, Fuels and Carbon Products	22
2.1.4 Mass, Energy, and Cost Balances	23
2.1.5 Delayed Coker Experimental Simulation.	25
2.1.6 Liquid Product Characterization and Optimization	27
2.1.7 Parametric Optimization	28
2.1.8 Anode and Electrode Tests	29
2.1.9 Needle Coke.....	30
2.1.10 Plant Design.....	32
2.1.11 Technology Transfer Plan.....	32
2.2 Direct Liquefaction in China	33
III. EXPERIMENTAL.....	45
3.1 Experimental Procedures	45
3.1.1 Reactor Fill Procedure	45
3.1.2 Hydrogenation Protocol.....	48
3.1.3 Coal Digestion and Solvent Extraction.....	49
3.1.4 Nitrogen Ram.....	50
3.1.5 Hydrogen Tank Replacement	51
3.1.6 Centrifugation	51
3.1.6.1 Lower Kittanning Centrifuge Trials.....	52
3.1.6.2 Powder River Basin Centrifuge Trials.....	57
3.1.6.3 Centrifugation Issues	62
3.1.6.4 Additional Centrifuge Trials.....	70
3.2 Trickle Bed Hydrogenation Reactor.....	76
3.2.1 Introduction to Trickle Bed Hydrogenation.....	76
3.2.2 Catalyst Selection.....	78
3.2.3 Hydrogenation of Naphthalene to Tetralin	79
3.2.4 Thermodynamics of Hydrogenation Reactions	80
3.2.5 Trickle Bed Reactor Kinetics.....	82
3.2.6 Reactor Design.....	87
3.2.7 Reactor Operation	96
3.2.8 Control Experiment without Catalyst	103
3.2.9. Hydrogenation of Naphthalene with Ni-Mo Catalyst.....	105
3.2.10 Determination of Rate Constants.....	121
3.2.11 Hydrogenation with Variable Hydrogen Flow Rate	126
3.2.12 Trickle Bed Hydrogenation of Coal Tar Distillate.....	136
3.2.13 Trickle Bed Concluding Observations	141
3.3 Pyrolysis of Coal--Mild Gasification.....	144

3.3.1	Devolatilization of Low Rank Western Coals	144
3.3.2	Injection Carbon Synthesis	152
3.3.3	Feedstocks for Synthetic Metallurgical Coke	164
3.3.4	Studies with Eastern Bituminous Coals	166
3.3.4	Thermocracking of United Coal Co. Star Bridge Prep Plant Coal Fines.....	174
3.4	Delayed coking	184
3.5	Continuous Coking of Centrifuge Tails	191
3.6	Needle Coke	195
3.7	Fuel Properties of Coal Liquids	201
3.7.1	Recovered Coal Solvent as Gasoline Additive	201
3.8	Testing of Lignite Pitch	203
3.8.1	Evaluation of Lignite	203
3.8.2	Petrography of Texas Lignite (Koppers# 08-2720)	204
3.8.2.1	WVU Sample of Reactor Solids Koppers# 08-2719	205
3.8.2.2	WVU Sample of Lignite After RXN Koppers# 08-2721	206
3.8.2.3	WVU Sample of Coked Lignite 600° –Koppers# 08-2722.....	206
3.8.2.4	Data Summary for Lignite	207
3.8	Trials of Reformulated Lignite Pitch.	241
3.9	CARBON DIOXIDE EMISSIONS	245
3.9.1	Energy Cost of Mining.....	247
3.9.2	Energy Cost of Coal Crushing	248
3.9.3	Energy Cost of Liquefaction	248
3.9.4	Energy Cost of Liquefaction	249
3.9.5	Energy Cost of Distillation	249
3.9.6	Energy Balance for Canadian Oil Sands.....	251
3.9.7	Combustion of burner off-gas in a boiler (coke)	253
3.9.8	Combustion of fuel gas in a Coking Reactor	253
3.9.9	Water Gas Shift Process in an H ₂ Reactor	254
3.9.10	Refining of Synthetic Crude	254
3.9.11	Transportation of Fuel.....	254
3.10	Greenhouse Footprint.....	255
3.10.1	Gross Domestic Product and Its Correlation to Carbon Dioxide.....	260
3.10.2	Carbon Dioxide Intensity	264
3.10.3	Energy Intensity	266
3.10.4	Greenhouse Gas Footprint	271
IV.	SYSTEM DESIGN	274
4.1	Process Description.....	274
4.2	Additional System Analysis.....	285
4.3	Modular Plant Design	291
4.4	Carbonite Plant in Virginia	294
	APPENDIX I. GAS AND LIQUID ANALYSES	302
	APPENDIX II OTHER PROCESSES	351
A2.1	Exxon Donor Solvent Process.....	351
A2.2	H-COAL PROCESS	353
	APPENDIX III. REFERENCES.....	355

List of Figures

Figure 1. Process Diagram for Carbon Products Process for Synthetic Pitch and Coke Precursors.....	19
Figure 2. US production of primary aluminum is in a state of long-term decline, as estimated by the US Geological Survey.	20
Figure 3. Overall Project Flowchart.	22
Figure 4. Simdist boiling point curves for hydrogenated coal liquid, showing favorable yields for liquid fuels. The effect of dissolving coal is to shift the entire curve to the right. Low aliphatic content is the primary reason limiting use of coal liquids for fuel use.	28
Figure 5. Polarized Light Photomicrograph of Needle Coke (picture credit: Ralph Gray & J. C. Crelling, SIU Carbondale).	30
Figure 6. Shenhua Group Direct Liquefaction Concept.	34
Figure 7. Artist's Rendition of Shenhua Direct Liquefaction Facility, scheduled to begin production later this year.	34
Figure 8. Block Diagram of Headwaters/HTI process (courtesy Headwaters).	35
Figure 9. Simplified Mass Balance for Direct Liquefaction.	39
Figure 10. Flowchart for direct liquefaction processes involving needle coke.	44
Figure 11. Overview of the Reactor System.	45
Figure 12. High Pressure Autoclave Reactor, with Pressure Relief Valve and Gauge visible in the background.	46
Figure 13. The blue tank in the rear is a holding tank to allow vented gas to be temporarily stored and slowly vented.	47
Figure 14. Ash Content (percent) as a function of centrifuge time.	53
Figure 15. Approximately 17 pounds of solid material was removed from PRB extract.	58
Figure 16. Ash Level in Centrifuge Tails.	59
Figure 17. Ash Level in PRB Centrate.	60
Figure 18. Viscosity at 50 °C for 25.67 g of Alberta coal dissolved in 70.42 g of CTD and 3.91 g of unhydrogenated oil.	64
Figure 19. Viscosity at 70 °C for 25.67 g of Alberta coal dissolved in 70.42 g of CTD and 3.91 g of unhydrogenated oil.	65
Figure 20. Viscosity at 90 °C for 25.67 g of Alberta coal dissolved in 70.42 g of CTD and 3.91 g of unhydrogenated oil.	66
Figure 21. Viscosity at 50 °C for 25.67 g of Alberta coal dissolved in 70.42 g of CTD and 3.91 g of hydrogenated oil.	67
Figure 22. Viscosity at 70 °C for 25.67 g of Alberta coal dissolved in 70.42 g of CTD and 3.91 g of hydrogenated oil.	68
Figure 23 Viscosity at 90 °C for 25.67 g of Alberta coal dissolved in 70.42 g of CTD and 3.91 g of hydrogenated oil.	69
Figure 24. T. F. Hudgins Spinner-II Model 60SE centrifuge, mounted on a 55 gallon drum containing coal extract.	71
Figure 25. T. F. Hudgins specifications for SAE 30 Oil, using the Model 60SE unit. Extracted coal achieved a much lower turbine speed at 90 psig due to higher viscosity.	71
Figure 26. Schematic of a typical hydroprocessing trickle bed reactor.	79
Figure 27. Hydrogenation of Naphthalene to Tetralin and Decalin,	80
Figure 28. Conversion of naphthalene in a batch reactor at 325 °C and 75 atm using CoO-MoO ₃ /Al ₂ O ₃ catalyst.	84
Figure 29. First-order kinetic plot of the hydrogenation of naphthalene at 200 °C using reduced iron catalyst.	86
Figure 30. First-order kinetic plot of vapor phase reactions on pre-reduced iron catalyst.	87
Figure 31. Trickle Bed Reactor System Schematic.	89
Figure 32. Trickle Bed Reactor System.	92
Figure 33. Hydrogenation Reaction of Naphthalene in the Trickle Bed Reactor.	93
Figure 34. SEM Image of the Ni/Mo/Al ₂ O ₃ Catalyst Showing the Quadrilobal Shape.	93
Figure 35. SEM Image of the Longitudinal View of the Ni/Mo/Al ₂ O ₃ Catalyst Particle.	94
Figure 36. FTIR spectra of varying concentrations of Naphthalene in n-Hexadecane.	101
Figure 37. FTIR Spectra of varying concentrations of Tetralin in n-Hexadecane.	102

Figure 38. Absorbance vs Concentration for varying concentrations of Naphthalene and Tetralin in n-Hexadecane.	102
Figure 39. Plot of Absorbance vs Wavenumber for different samples taken at 425 °C without catalyst.	104
Figure 40. Plot of concentration vs time for the blank test performed at 425 °C.	104
Figure 41. FTIR spectroscopy results at 340 °C and liquid flow rate 90 ml/hr.	106
Figure 42. FTIR spectroscopy results at 340 °C and liquid flow rate 127 ml/hr.	107
Figure 43. FTIR spectroscopy results at 340 °C and liquid flow rate 155 ml/hr.	108
Figure 44. FTIR spectroscopy results at 340 °C and liquid flow rate 267 ml/hr.	109
Figure 45. Integral Method of Analysis of Data at 340 °C.	110
Figure 46. Integral Method of Analysis of Data at Various Temperatures.	121
Figure 47. Plot of $\ln(1/1-X_n)$ vs W/Q to Determine the Rate Constants.	122
Figure 48. Solubility Coefficient of hydrogen in n-hexadecane vs Temperature.	124
Figure 49. Arrhenius Plot to Determine the Apparent Activation Energy.	126
Figure 50. Plot of $\ln(1/1-X_n)$ vs W/Q to determine the rate constants at reduced hydrogen flow rates.	134
Figure 51. Arrhenius Plot to Determine and Compare the Apparent Activation Energy at Higher and Lower Hydrogen Flow Rates.	135
Figure 52. Procedure for Solvent Extraction, Step 1.	137
Figure 53. Procedure for Solvent Extraction, Step 2.	137
Figure 54. Procedure for Solvent Extraction, Step 3.	138
Figure 55. FTIR Analysis of Coal Tar Distillate Samples.	139
Figure 56. Percentage of Carbon in Feed and Product.	140
Figure 57. Percentage of Hydrogen in Feed and Product.	140
Figure 58. Percentage of Nitrogen in Feed and Product.	141
Figure 59. Percentage of Sulfur in Feed and Product.	141
Figure 60. PRB Coal Fines of ¼ inch and below. A nickel and penny are shown for scale.	145
Figure 61. Experimental set-up to conduct the batch pyrolysis experiment.	145
Figure 62. Laboratory Experiment Underway during the three hour process time. Devolatilized vapors are combusted via the flare in the rear of the chamber.	146
Figure 63. Ignition of the Non-condensable gases at about 275 C (original poor quality).	146
Figure 64. SGS Proximate Results, PRB Fines.	150
Figure 65. SGS Proximate Results, PRB Char.	151
Figure 66. General Layout of the Devolatilization Apparatus.	153
Figure 67. Batch Pyrolyzer Ejecting Steam Vapor from PRB coal at ~112 °C.	154
Figure 68. Igniting the flare coal gas starting at about 300 °C with coal liquids being condensed.	154
Figure 69. Pyrolysis of the PRB coal with the collection of gas samples and coal liquids being condensed in the glass flask at about 600 °C.	155
Figure 70. Figure 70PRB Coal Char After Pyrolysis.	155
Figure 71. Batch Pyrolyzer ejecting steam from Pocahontas 3 coal, thus reducing moisture in the condensed coal liquids.	160
Figure 72. Flare gas (mainly light volatiles) ignited at about 300 C.	160
Figure 73. Condensing coal liquids and flaring non-condensable gases.	160
Figure 74. Most of the gases and liquids have been removed from the coal at about 550 C indicating that the pyrolysis conversion was complete and the experiment was terminated.	161
Figure 75. The agglomerated char produced from the pyrolysis process compared to a small sample of the crushed coal feedstock.	161
Figure 76. Conceptual Layout of a Blast Furnace.	166
Figure 77. Collection of all the char and coal liquids produced during the batch pyrolysis test of this high volatile and high caking eastern bituminous coal.	167
Figure 78. Coke Residue from Unsized PRB Coal.	172
Figure 79. Coke Residue from Partial Coking of PRB Ground to -20 Mesh.	172
Figure 80. UCC Star Bridge Coal Prep Plant, near Elkins WV.	174
Figure 81. Mr. Dwayne Ware, Superintendent and Dr. Wolfe collecting coal waste samples.	176
Figure 82. Samples were taken from thickener underflow at the Prep Plant.	177
Figure 83. Samples were taken from the bottoms of the spirals from froth flotation.	177
Figure 84. Samples were also taken from the heavy medium circuit.	178
Figure 85. Batch Pyrolysis Process with coal liquid condenser and coal gas flare.	179

Figure 86. Overview of Modified Coking System.....	185
Figure 87. Paragon Kiln and Controller.....	186
Figure 88. Condenser and holding tank.....	186
Figure 89. Coking Vessel.....	187
Figure 90. Water Cooled Condenser.....	188
Figure 91. Distillation and Delayed Coking System.....	189
Figure 92. Coking Vessel Charged with Lower Kittanning Coal. Red hot filaments are barely visible at left.	190
Figure 93. View of the Coking Vessel from the Top.....	190
Figure 94. Close-up showing active heater coils in the kiln.	191
Figure 95. Overview of modified Lucifer tube furnace outlet, showing fume hood, vapor condenser, vacuum pump and nitrogen gas delivery system.	192
Figure 96. Chrome Plated Steel Boat Containing Coke Precursor.	192
Figure 97. Furnace inlet, showing a loaded boat mounted under the rotating screw drive. The tube underneath the boat is a gas line. The screw itself is not visible in this photograph.....	193
Figure 98. Furnace inlet, showing the screw drive at the tube of the tube.....	193
Figure 99. Delayed Coking System and Trap Arrangement.....	194
Figure 100. Scrubbing System at Coker Outlet.	195
Figure 101. SIMDIST Incremental Yields for CCTD Solvent (no coal dissolved).	197
Figure 102. SIMDIST Incremental Yields for KW/PHO/CTD Centrate.....	198
Figure 103. Simulated Distillation of Solvent (HO/CTD) by Gas Chromatograph.....	198
Figure 104. Simulated Distillation of KW/HO/CTD by Gas Chromatograph (Koppers).....	199
Figure 105. Photomicrographs of Texas Lignite showing: humocollinite, humotelinite with closed cellular structures, humotextinite with open cellular structure, humodensinite (attrital vitrinite), fusinite and shrinkage cracks from desiccation. Reflected light in Air, X250.....	213
Figure 106. Photomicrographs of Texas Lignite showing: humocollinite, humotelinite with open and closed cellular structures, humotextinite with open cellular structure, humodensinite (attrital vitrinite), semifusinite fusinite and shrinkage cracks from desiccation. Reflected light in Air, X250.....	214
Figure 107. Photomicrographs of Texas Lignite showing: humocollinite, humotelinite with cellular structures, humodetrinite (attrital huminite) exinite, semifusinite, fusinite, fine sized inerts and mineral matter. Reflected light in Oil, X600.	215
Figure 108. Photomicrographs of Texas Lignite showing: humocollinite, humotelinite with open and closed cellular structures, humodetrinite (attrital huminite) exinite, semifusinite, fusinite, fine sized inerts and mineral matter. Reflected light in Oil, X600.	216
Figure 109. Photomicrographs of Texas Lignite showing: humodetrinite (attrital huminite) exinite, semifusinite, fusinite, fine sized inerts and mineral matter. Reflected light in Oil, X600.	217
Figure 110. Photomicrographs of Oil Plus Lignite After Reaction (8-15-08) showing: vitropast (altered), fungal spore (inert), humodetrinite (attrital huminite) exinite, semifusinite, fusinite, fine sized inerts and mineral matter. Reflected light in Oil, X600.....	218
Figure 111. Photomicrographs of Oil Plus Lignite After Reaction (8-15-08) showing: vitropast (altered), inert, desiccation cracks in vitropast; mineral matter, pyrite and epoxy mounting media. X250.....	219
Figure 112. Photomicrographs of Oil Plus Lignite After Reaction (8-15-08) showing: vitropast (altered), coarse inert (>50 microns), fine sized inerts (<50 microns), quartz and coarse mineral matter. Reflected light in Oil, X600.....	220
Figure 113. Photomicrographs of Oil Plus Lignite After Reaction (8-15-08) showing: vitropast (altered), coarse inert (semifusinite), fine sized inerts (<50 microns), clay, mineral matter and epoxy mounting material. Reflected Light in Oil, X600.....	221
Figure 114. Photomicrographs of Oil Plus Lignite After Reaction (8-15-08) showing: vitropast (altered), inerts, fine sized inerts (<50 microns), disseminated clay and quartz. Reflected light in Oil, X600.....	222
Figure 115. Photomicrographs of solid from reactor after reaction (extracted) showing: vitropast (altered), pitch like alteration product, inert, sclerotia (inert) and epoxy mounting media. Reflected light in Oil, X135.	223
Figure 116. Photomicrographs of solid from reactor after reaction (extracted) showing: slightly altered lignite (huminite), vitropast (altered), inert, semifusinite, fungal spore and epoxy mounting media. Reflected light in Oil, X600.	224
Figure 117. Photomicrographs of solid from reactor after reaction (extracted) showing: slightly altered lignite (huminite), vitropast (altered), various sized inert, fusinite, and epoxy mounting media. Reflected light in Oil, X600.....	225

Figure 118. Photomicrographs of solid from reactor after reaction (8-15-08) showing: slightly altered lignite (huminite), vitropast (altered), dull particle with high amount of inert, semifusinite, fusinite, pyrite, clay layer, epoxy mounting media. Reflected light in Oil, X600.	226
Figure 119. Photomicrographs of lignite after reaction (8-14-08) showing: slightly altered lignite (huminite), vitropast (altered), various sized inert, fusinite, and epoxy mounting media. Reflected light in Oil, X600.	227
Figure 120. Photomicrographs of lignite after reaction (8-14-08) showing: unaltered lignite (humodetrinite), slightly and highly altered lignite, vitropast (altered-atrital), exinite, semifusinite, fusinite, quartz and epoxy mounting media. Reflected light in Oil, X600.	228
Figure 121. Photomicrographs of Lignite After Reaction (8-14-08) showing: unaltered lignite (humodetrinite), vitropast (collinite and attrital), vitropast from textinite (open structure). sclerotia, clay, mineral matter and epoxy. Reflected light in Oil, X600.	229
Figure 122. Photomicrographs of Lignite After Reaction (8-14-08) showing: unaltered lignite (humodetrinite), vitropast (collinite and attrital), vitropast with desiccation cracks, semifusinite, fungal spore, inert, mineral matter and epoxy. Reflected light in Oil, X600.	230
Figure 123. Photomicrographs of coked lignite at 600 °C (8-14-08) showing: slightly altered lignite (huminite), vitropast with desiccation cracks, semifusinite, loose attrital particle and epoxy media. Reflected light in air, X135.	231
Figure 124. Photomicrographs of coked lignite at 600 °C (8-4-08) showing: slightly altered lignite (attrital), exinite, vitropast from collinite-telinite-textinite, semifusinite, fusinite, mineral matter (clay) and epoxy mounting media. Reflected light in oil, X600.	232
Figure 125. Photomicrographs of coked lignite at 600 °C (8-4-08) showing: slightly altered lignite (huminite), altered attrital huminite, highly altered huminite, coarse inert (fusinite) and epoxy mounting media. Reflected light in oil, X600.	233
Figure 126. Photomicrographs of coked lignite-600 °C (8-4-08) showing: high-intermediate and low degree of carbonization, altered huminite (attrital), fungal spore, shale calcite, clay shale and epoxy mounting media. Reflected light in oil, X600.	234
Figure 127. Photomicrographs of coked lignite at 600 °C (8-4-08) showing: high-intermediate and low degree of carbonization, altered collinite and attrital huminite, fusinite, oxidized inert, dull attrital particle and epoxy mounting media. Reflected light in oil X600.	235
Figure 128. FTIR Liquid in Collection Flask.	236
Figure 129. FTIR Residue H in flask.	236
Figure 130. FTIR Liquid in Flask 1.	237
Figure 131 FTIR Solution in Flask 2.	238
Figure 132, FTIR Solution in Flask 3.	238
Figure 133. Solution in Flask 4.	238
Figure 134. Estimates of “Well-to-Wheels” carbon dioxide footprint estimates (kilograms of carbon dioxide per barrel of product) from the Canadian Association of Petroleum Producers (CAPP). All sources of hydrocarbon products are within 20% of each other (http://www.canadasoilsands.ca/en/img/img_gas_climate_change.gif).	246
Figure 135. Energy Return on Investment for different commodity fuels, estimated by Merrill Lynch.	248
Figure 136. Oil Sands Energy Return on Investment. D represents only the direct energy flows, I represents Indirect energy flows, L represents Labor energy demand, and E represents the Environmental energy demand.	252
Figure 137. Recent Monthly Mean Carbon Dioxide measured at Mauna Loa. CO ₂ concentration is defined as the number of molecules of carbon dioxide divided by the number of all molecules in air, including CO ₂ itself, after water vapor has been removed, expressed as parts per million (ppm). (Illustration credit: NOAA).	257
Figure 138. Carbon balance, from NASA Earth Observatory. The units are GigaTonnes of carbon per year. Illustration credit: NASA Earth Observatory; http://www.nasa.gov/centers/langley/news/researchernews/rn_carboncycle.html on 15 Nov 2010.	258
Figure 139. CRDIAC Estimate of total Carbon Emissions.	259
Figure 140. Global Average Temperature as estimated by the National Climatic Data Center, from January 2002 to Sept 2010. The least squares fit (black line) of the data is generally dismissed in favor of the IPCC estimate (red line).	260
Figure 141. World Gross Domestic Product.	262
Figure 142. Comparative CO ₂ Intensity by Country.	266
Figure 143. Energy Intensity for Top 20 GDP Nations, MJ/\$GDP (Purchase Power Parity).	268

Figure 144. Process Diagram for Carbon Products Process for Synthetic Pitch and Coke Precursors.....	275
Figure 145. Estimated Cash Flow for a 20,000 TPY Carbon Products Plant with FutureGen.	282
Figure 146. Estimated Net Present Value.	283
Figure 147. Estimated Discounted Cash Flow Rate of Return.	283
Figure 148. Estimated Discounted Payback Period.....	283
Figure 149. Cumulative Cash Position.	284
Figure 150. Estimated Rate of Return on Investment.	284
Figure 151. Estimated Payback Period.....	285
Figure 152. Simplified Mass Balance Options for Direct Liquefaction.	287
Figure 153. Component modules for use in a microrefinery for reprocessing used motor oil.....	292
Figure 154. Side view of a typical module.	293
Figure 155. A micro plant used for reprocessing spent motor oil.....	293
Figure 156. Wolfe process for devolatilizing coal to create crude oil and metcoke (www.USPTO.com).....	294
Figure 157. Richard Wolfe (2nd from right) participated in experiments on-site at WVU, along with Liviu Magean, guest researcher Alain Lui, Elliot Kennel and Femi Olajide.....	295
Figure 158. Bench scale coking reactor used to co-produce coked coal (Carbonite™) as well as coal liquids.....	296
Figure 159. Olajide and Wolfe with heavy and light fractions of recovered coal oil from bench scale experiments.	296
Figure 160. Carbonite synthetic coke produced from Powder River Basin and other steam coals.....	297
Figure 161. Coal conveyor at the Carbonite Plant near Norton VA.	297
Figure 162. A tunnel kiln is used to heat treat coke at high temperature, liberating additional volatiles. Similar kilns are in use in the ceramic industry.....	298
Figure 163. Drying kilns at the Norton VA site.....	298
Figure 164. Briquetting machine, used for producing coke briquettes.	299
Figure 165. Synthetic foundry coke from the 1990's predecessor of Carbonite.....	299
Figure 166. Foundries use coke to enhance the properties of metal products such as gray iron.....	300
Figure 167. Carbonite compared with conventional coke. Carbonite coke was broken into pieces in order to more closely resemble the appearance of conventional slot oven metallurgical grade coke.....	300
Figure 168. Process Schematic of a Typical Exxon Donor Solvent Process.	351
Figure 169. Graphical Representation of Product Yield from lignite, Dry-ash-free basis.	352
Figure 170. Process Schematic of a Typical H-Coal Process.	353
Figure 171. Process Schematic of Shenhua Direct Coal Liquefaction Process.	354

List of Tables

Table 1. Estimated Domestic and World Markets for Carbon Products.....	17
Table 2. Mass, Energy, and Cost Balance without FutureGen.	24
Table 3. Mass, Energy and Cost Balance with FutureGen, Liquids = \$60/barrel.....	25
Table 4. Approximate Distillation Cuts by Number of Carbons and Boiling Ranges.	27
Table 5. Estimated Commodity Prices Based on WTI Crude @ \$60/BBL.....	37
Table 6. Estimated Domestic and World Markets for Carbon Products.....	38
Table 7. Elemental Analysis of Bituminous Coal (Lower Kittanning).....	38
Table 8. Input Feedstock Materials Costs, Max Fuels Yield.	40
Table 9. Output Materials Values, Max Fuels Yield.	40
Table 10. Input Feedstock Materials Costs, Binder Pitch Production.	41
Table 11. Output Materials Value, Binder Pitch Production.	41
Table 12. Output Materials Value, Mesophase Pitch Production.	42
Table 13. Output Materials Value, Needle Coke Production.....	42
Table 14. Summary of Parameters Used to Calculate Energy Balance.....	43
Table 15. Proximate Analysis of Lower Kittanning Coal in Centrifuge Tails.....	52
Table 16. Proximate Analysis of Centrate from Lower Kittanning Coal Extract.....	53
Table 17. Lower Kittanning Prepped Coal, Elemental Analysis, Raw Data.....	54
Table 18. Lower Kittanning Elemental Analysis, Average Values.....	54
Table 19. H/C, S/C and N/C for Clean Lower Kittanning Centrate.	54
Table 20. Progression in H/C, S/C and N/C for Lower Kittanning Centrifuge Tails.	54
Table 21. H/C, S/C and N/C for Clean Lower Kittanning Centrate.	54
Table 22. Lower Kittanning (Kingwood) Centrifuge Tails Elemental Analysis, Raw Data, 0917.....	54
Table 23. Lower Kittanning (Kingwood) Centrifuge Tails Elemental Analysis, Avg Values.....	55
Table 24. Lower Kittanning (Kingwood) Centrifuge Tails Elemental Analysis, Raw Data.....	55
Table 25. Lower Kittanning (Kingwood) Centrifuge Tails Elemental Analysis, Avg Values.....	55
Table 26. Lower Kittanning (Kingwood) Centrifuge Tails Elemental Analysis, Raw Data.....	55
Table 27. Lower Kittanning (Kingwood) Centrifuge Tails Elemental Analysis, Avg Values.....	55
Table 28. Lower Kittanning (Kingwood) Centrifuge Tails, Elemental Analysis, Raw Data.....	56
Table 29. Lower Kittanning (Kingwood) Centrifuge Tails, Elemental Analysis, Avg Values.....	56
Table 30. Lower Kittanning (Kingwood) Centrate Elemental Analysis, Raw Data.....	56
Table 31. Lower Kittanning (Kingwood) Centrate Elemental Analysis, Avg Values.....	56
Table 32. Proximate Analysis Results for Centrifuge Tails with PRB Coal.....	58
Table 33. Proximate Analysis Results for Centrate from PRB Coal Extract.....	59
Table 34. Powder River Basin Centrifuge Tails, Raw Data, 1026.	60
Table 35. Powder River Basin Centrifuge Tails, Avg Values, 1026.	60
Table 36. Powder River Basin Centrifuge Tails, Raw Data, 1029.	61
Table 37. Powder River Basin Centrifuge Tails, Avg Values, 1029.	61
Table 38. Powder River Basin Centrifuge Tails, Raw Data.	61
Table 39. Powder River Basin Centrifuge Tails, Avg Values.	61
Table 40. Powder River Basin Centrate, Raw Data.....	61
Table 41. Powder River Basin Centrate, Avg Values.....	62
Table 42. Powder River Basin Centrate, Raw Data.....	62
Table 43. Powder River Basin Centrate, Avg Values.....	62
Table 44. Viscosity data at 50 °C for 25.67 g of Alberta coal dissolved in 70.42 g of CTD and 3.91 g of unhydrogenated oil.....	64
Table 45. Viscosity data at 70 °C for 25.67 g of Alberta Coal dissolved in 70.42 g of CTD and 3.91 g of unhydrogenated oil.....	65
Table 46. Viscosity data at 90 °C for 25.67 g of Alberta Coal dissolved in 70.42 g of CTD and 3.91 g of unhydrogenated oil.....	66
Table 47. Viscosity at 50 °C for 25.67 g of Alberta Coal, 70.42 g of CTD and 3.91 g of hydrogenated oil.....	67

Table 48. Viscosity data at 70 °C for 25.67 g of Alberta Coal dissolved in 70.42 g of CTD and 3.91 g of hydrogenated oil.....	68
Table 49. Viscosity data at 90 °C for 25.67 g of Alberta Coal dissolved in 70.42 g of CTD and 3.91 g of hydrogenated oil.....	69
Table 50. April 22, 2009 Kingwood/CTD/AGOIL	73
Table 51. April 23, 2009 Kingwood/CTD/AGOIL + 35 kg Methyl Naphtalene.....	73
Table 52. Weight of the Tails.....	75
Table 53. Proximate Analysis of Centrate (Kerosene Added).....	75
Table 54. Proximate Analysis of Tails (Kerosene Added).....	75
Table 55. Proximate Analysis of Centrate (Methyl Naphthalene added).....	75
Table 56. Proximate Analysis of Tails (Methyl Naphthalene added).....	75
Table 57. Temperature Program for Activating the Catalyst.....	95
Table 58. Boiling Points of Components and Reactor Feed at Atmospheric Pressure and Operating Pressure	96
Table 59. Operating Conditions for Hydrogenation of Naphthalene in the TB Ratio of Hydrogen Flow rate to Liquid Flow Rate = 750.....	98
Table 60. Operating Conditions for Hydrogenation of Naphthalene in the TBR Ratio of Hydrogen Flow rate to Liquid Flow Rate = 100.....	99
Table 61. Elemental Analysis of Koppers Coal Tar Distillate.....	99
Table 62. Absorbance values for Different Concentrations of Naphthalene in n-Hexadecane.....	101
Table 63. Absorbance values for Different Concentrations of Tetralin in n-Hexadecane.....	101
Table 64. Results for Blank Test Performed at 425 °C and 1200 psig Without Catalyst.....	103
Table 65. Temperature 340 °C, Liquid Flow Rate: 90 ml/hr, H ₂ Flow Rate: 1.125 L/min.....	105
Table 66. Temperature 340 °C, Liquid Flow Rate: 127 ml/hr H ₂ Flow Rate: 1.5625 L/min.....	106
Table 67. Temperature 340 °C, Liquid Flow Rate: 155 ml/hr, H ₂ Flow Rate: 1.9375 L/min.....	107
Table 68. Temperature 340 °C, Liquid Flow Rate: 267 ml/hr, H ₂ Flow Rate: 3.375 L/min.....	108
Table 69. Combined data for all the runs at 340 °C with varying flow rates. Initial concentration of naphthalene in the feed, C _{ao} = 10% by weight.....	109
Table 70. Temperature 360 °C, Liquid Flow Rate: 130 ml/hr, H ₂ Flow Rate: 1.625 L/min.....	111
Table 71. Temperature 360 °C, Liquid Flow Rate: 163 ml/hr, H ₂ Flow Rate: 2.0 L/min.....	111
Table 72. Temperature 360 °C, Liquid Flow Rate: 200 ml/hr, H ₂ Flow Rate: 2.5 L/min.....	112
Table 73. Temperature 360 °C, Liquid Flow Rate: 316 ml/hr, H ₂ Flow Rate: 4.0 L/min.....	112
Table 74. Combined data for all the runs at 360 °C with varying flow rates.....	113
Table 75. Temperature 380 °C, Liquid Flow Rate: 120 ml/hr, H ₂ Flow Rate: 1.5 L/min.....	113
Table 76. Temperature 380 °C, Liquid Flow Rate: 140 ml/hr, H ₂ Flow Rate: 1.75 L/min.....	114
Table 77. Temperature 380 °C, Liquid Flow Rate: 160 ml/hr, H ₂ Flow Rate: 2.0 L/min.....	114
Table 78. Temperature 380 °C, Liquid Flow Rate: 180 ml/hr, H ₂ Flow Rate: 2.25 L/min.....	115
Table 79. Temperature 380 °C, Liquid Flow Rate: 375 ml/hr, H ₂ Flow Rate: 4.6875 L/min.....	115
Table 80. Combined data for all the runs at 380 °C with varying flow rates.....	115
Table 81. Temperature 425 °C, Liquid Flow Rate: 125 ml/hr, H ₂ Flow Rate: 1.5625L/min.....	116
Table 82. Temperature 425 °C, Liquid Flow Rate: 140 ml/hr, H ₂ Flow Rate: 1.75 L/min.....	116
Table 83. Temperature 425 °C, Liquid Flow Rate: 160 ml/hr, H ₂ Flow Rate: 2 L/min.....	117
Table 84. Temperature 425 °C, Liquid Flow Rate: 230 ml/hr, H ₂ Flow Rate: 2.875 L/min.....	117
Table 85. Temperature 425 oC, Liquid Flow Rate: 275 ml/hr, H2 Flow Rate: 3.5 L/min.....	118
Table 86. Combined data for all the runs at 425 °C with varying flow rates.....	118
Table 87. Temperature 450 °C, Liquid Flow Rate: 120 ml/hr, H ₂ Flow Rate: 1.5 L/min.....	118
Table 88. Temperature 450 °C, Liquid Flow Rate: 145 ml/hr, H ₂ Flow Rate: 1.875 L/min.....	119
Table 89. Temperature 450 °C, Liquid Flow Rate: 170 ml/hr, H ₂ Flow Rate: 2.125 L/min.....	119
Table 90. Temperature 450 °C, Liquid Flow Rate: 225 ml/hr, H ₂ Flow Rate: 2.9375 L/min.....	120
Table 91. Combined data for all the runs at 450 °C with varying flow rates.....	120
Table 92. Values of the obtained apparent rate constants at various temperatures.....	123
Table 93. Solubility coefficients for hydrogen at various temperatures using n-hexadecane as the solvent.....	124
Table 94. Temperature 340 °C, Liquid Flow Rate: 150 ml/hr, H ₂ Flow Rate: 0.25 L/min.....	127
Table 95. Temperature 340 °C, Liquid Flow Rate: 165 ml/hr, H ₂ Flow Rate: 0.275 L/min.....	127
Table 96. Temperature 340 °C, Liquid Flow Rate: 200 ml/hr, H ₂ Flow Rate: 0.333 L/min.....	128
Table 97. Temperature 340 °C, Liquid Flow Rate: 245 ml/hr, H ₂ Flow Rate: 0.408 L/min.....	128
Table 98. Combined data for all the runs at 340 °C with reduced H ₂ flow rates.....	129

Table 99. Temperature 380 °C, Liquid Flow Rate: 140 ml/hr, H ₂ Flow Rate: 0.233 L/min.	129
Table 100. Temperature 380 °C, Liquid Flow Rate: 175 ml/hr, H ₂ Flow Rate: 0.3 L/min.	130
Table 101. Temperature 380 °C, Liquid Flow Rate: 200 ml/hr, H ₂ Flow Rate: 0.333 L/min.	130
Table 102. Temperature 380 °C, Liquid Flow Rate: 240 ml/hr, H ₂ Flow Rate: 0.4 L/min.	131
Table 103. Combined data for all the runs at 380 °C with reduced H ₂ flow rates.	131
Table 104. Temperature 425 °C, Liquid Flow Rate: 160 ml/hr, H ₂ Flow Rate: 0.266 L/min.	132
Table 105. Temperature 425 °C, Liquid Flow Rate: 200 ml/hr, H ₂ Flow Rate: 0.333 L/min.	132
Table 106. Temperature 425 °C, Liquid Flow Rate: 240 ml/hr, H ₂ Flow Rate: 0.4 L/min.	133
Table 107. Combined data for all the runs at 425 °C with reduced H ₂ flow rates.	133
Table 108. Values of the apparent rate constants at various temperatures at reduced hydrogen flow rates.	134
Table 109. Elemental Analysis of Trickle Bed Reactor Feed.	139
Table 110. Elemental Analysis of Trickle Bed Reactor Product.	139
Table 111. Comparison of Conversions at Higher and Lower Hydrogen Flow rates for Same Residence Times and Temperatures.	143
Table 112. Elemental Analysis of PRB Coal and Char from Wolfe Mild Gasification Process.	148
Table 113. Proximate Analysis of PRB Coal and Char.	148
Table 114. Proximate Analysis of PRB Coal, PRB Char and Anthracite Used as an Injection Carbon.	156
Table 115. Hargrove Grindability Index (HGI) of PRB Coal and Char.	156
Table 116. PRB Coal and Char as compared to the Anthracite Injection Carbon.	157
Table 117. Analysis of the PRB Coal Gas, Measured by Koppers, Inc.	158
Table 118. Heavy Coal Oil Liquid (Wolfe, 1998).	158
Table 119. Pitch Properties (Wolfe, 1998).	158
Table 120. Gas Analysis (Wolfe, 1998).	159
Table 121. Comparison of Poca 3, PRB and Anthracite.	162
Table 122. Analysis of the Non-Condensable Gases from Pocahontas 3 Coal.	163
Table 123. Properties of Petroleum-Derived Coke from Delayed Cokers.	165
Table 124. Proximate Analysis of Different Coals and Chars.	169
Table 125. Proximate Analysis of WV Hi-Vol Blend.	169
Table 126. Calorimetric Measurements for WV Hi-Vol Blended Coal.	170
Table 127. Calorimetric Measurements for WV Hi-Vol Blended Coal.	171
Table 128. Coal Liquid Analysis for the Light oil.	173
Table 129. Proximate Analysis of the UCC Coal and Coal Waste Samples from Prep Plant.	178
Table 130. Proximate Analysis of the Dried Thickener Underflow Coal Waste and the Char remaining after the volatiles were removed during pyrolysis at 650 C.	180
Table 131. Pyrolysis Coal Gas Analysis Collected From the Coal Waste Test.	181
Table 132. Elemental Analysis for Spiral Waste, Raw Measurements.	181
Table 133. Elemental Analysis for Spiral Waste, Avg Values.	182
Table 134. Elemental Analysis for Thickener Underflow, Raw Measurements.	182
Table 135. Elemental Analysis for Thickener Underflow, Avg Values.	182
Table 136. Elemental Analysis for Belt Fines, Raw Measurements.	182
Table 137. Elemental Analysis for Belt Fines, Raw Measurements.	182
Table 138. Elemental Analysis for Heavy Media Waste, Raw Measurements.	182
Table 139. Elemental Analysis for Heavy Media Waste, Avg Values.	183
Table 140. Coking Trials with Kingwood/Lower Kittanning Centrifuge Tails.	194
Table 141. Proximate Analysis of PHO/CTD/KW Centrate.	196
Table 142. Proximate Analysis of PHO/CTD/KW Tails.	196
Table 143. Gas Chromatograph Results from Kingwood/CCTD.	200
Table 144. Summary of Octane Results.	202
Table 145. ICP Heavy Metal Scan for a Blend of 40% Ethanol, 60% Coal Liquid.	202
Table 146. Sample Description and Koppers Designators.	203
Table 147. Petrographic Maceral Composition of Jewett TX Lignite Sample.	208
Table 148. Vitrinite Reflectance Distribution of Jewett TX Lignite.	209
Table 149. Petrographic Composition of Texas Lignite After Reaction for WVU.	210
Table 150. Vitrinite Reflectance Distribution of Four Residual Products from Texas Lignite.	211
Table 151. Sample Matrix for Koppers using Texas Lignite samples.	212
Table 152. Elemental Analysis Group 1: Oil & Lignite.	239

Table 153. Elemental Analysis Group 2: Lignite+C ₁₀ H ₁₂ after Reaction.	239
Table 154. Elemental Analysis Group 3: Coked Texas Lignite,	239
Table 155. Elemental Analysis Group 4: Solid in Reactor.	239
Table 156. Elemental Analysis Group 5: Texas Lignite.	239
Table 157. Elemental Analysis Group 6: Lignite after Reaction.	240
Table 158. Proximate Analysis for Oil & Lignite.	240
Table 159. Proximate Analysis for Lignite & C ₁₀ H ₁₂ .	240
Table 160. Proximate Analysis for Coked Texas Lignite.	240
Table 161. Proximate Analysis for Lignite.	240
Table 162. Proximate Analysis for Solid.	240
Table 163. Proximate Analysis for Texas Lignite.	241
Table 164. Conversion of WVU extract into pitch.	241
Table 165. Evaluation of Lignite and Binder Pitch Blend.	242
Table 166. Evaluation of Lignite and Binder Pitch Blend.	242
Table 167. Pilot Plant Trials for 2010 and 2007.	242
Table 168. Pilot Plant Forming.	243
Table 169. Green to Bake.	243
Table 170. WG Graphite Properties.	244
Table 171. Composition of Natural gas.	252
Table 172. Composition of Coke.	252
Table 173. Sources of CO ₂ emissions.	253
Table 174. Coke Combustion Parameters.	253
Table 175. Fuel Gas Combustion parameters.	254
Table 176. Top 20 Largest GDP, as Estimated by CIA Factbook, 2009.	261
Table 177. Carbon Dioxide Emissions of the Top 20 GDP Nations.	263
Table 178. Carbon Dioxide Intensity for the Top 20 GDP Nations.	265
Table 179. Energy Intensity for the Top 20 GDP Nations.	267
Table 180. Chemical Enthalpy Divided by CO ₂ Mass for Different Fuels.	268
Table 181. Comparative Efficiency and Yields for Synthetic Fuels.	273
Table 182. Characteristics of Kingwood Lower Kittanning Coal.	278
Table 183. Approximate Mass Balance for Carbon Products Plant with FutureGen.	278
Table 184. Economic Assumptions.	279
Table 185. Utility Price Assumptions.	280
Table 186. Equipment Summary.	281
Table 187. Monte Carlo Analysis Parameters.	282
Table 188. Elemental Analysis of Input Feedstocks and Products.	286
Table 189. Progressive Mass Balance for a Representative Sub-Bituminous Coal Conversion Process.	288
Table 190. Financial Assumptions for Extrapolation of 1999 Estimates to 2008.	289
Table 191. Adjusted Capital Investment from CTL Plants.	291
Table 192. Exxon Conditions for Texas Lignite Conversion.	352

I. EXECUTIVE SUMMARY

This Department of Energy National Energy Technology Laboratory sponsored research effort to develop environmentally cleaner projects as a spin-off of the FutureGen project, which seeks to reduce or eliminate emissions from plants that utilize coal for power or hydrogen production. New clean coal conversion processes were designed and tested for coproducing clean pitches and cokes used in the metals industry as well as a heavy crude oil. These new processes were based on direct liquefaction and pyrolysis techniques that liberate volatile liquids from coal without the need for high pressure or on-site gaseous hydrogen.

The project team successfully aligned itself with a combination of established companies such as Koppers Inc and GrafTech International Ltd, while also establishing relationships with entrepreneurial companies such as Quantex Energy Inc and Carbonite Inc. As a result of the research, a commercial scale plant for the production of synthetic foundry coke has broken ground near Wise, Virginia under the auspices of Carbonite Inc. This plant will produce foundry coke by pyrolyzing a blend of steam coal feedstocks. A second plant is planned by Quantex Energy Inc (in Texas) which will use solvent extraction to coproduce a coke residue as well as crude oil. A third plant is being actively considered for Kingsport, Tennessee, pending a favorable resolution of regulatory issues.

There are two main processes that have proven to be economical for coproducing clean solid products and clean liquids. First, pyrolysis is the boiling of volatile liquids from coal or processed coal materials. By so doing, it is possible to tailor the composition of coal derivatives in such a way that they become suitable for use as cokes, especially metallurgical coke and foundry coke. These cokes are used in the metals industry, especially for making steel. The devolatilized liquids can either be burned to produce thermal energy for the process, or collected and processed in a refinery, much like crude oil.

The second major process is solvent extraction, in which coal is dissolved in a heated heavy oil, then filtered or centrifuged to remove mineral matter, and finally reconstituted as a pure heavy hydrocarbon. Solvent extraction processes can also produce cokes such as anode grade coke, which is used in the aluminum industry. Liquid crude oil also results as a coproduct.

At the start of the project, FutureGen was thought of as a potential source for hydrogen, which could be used to assist the processing of coal, especially for solvent extraction processes. Hydrogenated heavy oils are usually very effective coal solvents. In addition, hydrogen-assisted cracking (sometimes referred to as hydrocracking, not to be confused by processes that use steam instead of gaseous hydrogen) can be used to upgrade pitches and heavy oils to produce lighter fuels and chemicals.

However, FutureGen shifted from coal gasification to oxyfuel combustion in about 2008, which decreases the direct potential synergism between FutureGen and direct liquefaction. Nevertheless, the fundamental processes of pyrolysis and solvent extraction can be used separately, and are currently both on their way to be independently commercialized.

II. INTRODUCTION

2.1 Background

This solvent extraction process is analogous to the direct liquefaction processes, such as the Exxon Donor Solvent process or H-Coal process used for production of synthetic crude oil, with the following distinctions:

a. Typical direct liquefaction processes require the addition of about 7-12% hydrogen by mass, whereas the present process is aimed at 0.0% to 0.5% absorption. This, in turn, permits lower pressures, temperatures, and exposure times compared to typical direct liquefaction. Certain types of carbon products such as coke and pitch actually require lower hydrogen content than the level that exists naturally in many types of coal. Hence there is no reason to have to add hydrogen if pitch and coke are considered to be acceptable products.

b. Many direct liquefaction processes used naphthalene-tetralin conversion as the donor solvent, whereas the present process achieves equivalent performance with coal tar distillates as the solvent. Because naphthalene has a higher price than the intended product (synthetic crude petroleum, for example), it is essential to recover as much solvent as possible. By contrast, the present process is compatible with inexpensive coal tar distillates, with a price *below* the price of the intended products (pitches, cokes, as well as syncrude). Hence solvent recovery and recycling is not necessitated by process economics, and direct production of liquid products can be economically viable.

c. Although conventional direct liquefaction efforts have usually been aimed at producing a synthetic sweet crude petroleum and have sought to avoid producing carbon-rich pitches, the current process actively seeks to produce carbon-rich pitches, because there is an enormous market for them. As shown in Table 1, anode coke alone represents a 3.6 million tons per year domestic market, about half of which is imported and calcined (heat treated) domestically. This is the equivalent in mass of 26 million barrels per year of crude petroleum. Moreover, delayed coker yield is usually only a few percent anode grade coke, hence as much as a billion barrels per year of petroleum-based feedstocks are actually processed in order to obtain coke. Anode coke domestic production is on the decline, so there is a chance that a new process could become the preferred process.

Table 1. Estimated Domestic and World Markets for Carbon Products.¹

Product	Primary Feedstocks	Main Applications	Domestic Annual Sales, Tons	Worldwide Annual Sales, Tons
Binder Pitch ²	Coal Tar Pitch Petroleum pitch	Anodes (Al smelting) Arc furnace electrodes (steelmaking)	800,000	1,500,000
Impregnation Pitch	Petroleum pitch Coal Tar Pitch	Electrodes, Composites	180,000	380,000
Mesophase Pitch	Petroleum Pitch Coal Tar Pitch	High performance composites, fibers	800	3700
Anode Coke ³ Uncalcined Calcined	Petroleum Resid	Anodes (Al smelting)	1,800,000 3,600,000	8,000,000 6,200,000
Needle Coke	Petroleum Pitch (US) PP + CTP (Japan)	Arc furnace electrodes (Steelmaking)	400,000	1,300,000
Carbon Fiber (PAN) ⁴	Petrochemicals	Non-graphitic composites	10,000	24,000
Pitch Fibers ⁵	Coal tar pitch, Petroleum Pitch	Graphitic composites	200	3000
Carbon Black ⁶	Petroleum Pitch, Coal Tar Pitch	Rubber additives, various other	1,800,000	8,000,000
Carbon Foam ⁷	Petrochemicals, Coal, Coal Tar Pitch	Structures, electrochemical systems,	200	200
Carbon Nanofibers ⁸	Natural Gas, Gasified Coal	Polymer additives	50	150
Carbon Nanotubes	Various	TBD	30	100

2.1.1. FutureGen Project

The FutureGen project was originally envisioned as a means to fuel the Hydrogen Economy via coal gasification, while producing no environmental emissions. Yet the use of just a fraction of a percent of the output of FutureGen for production of carbon products and liquid fuels can greatly increase the economic attractiveness of the capability. An enhanced process combining FutureGen with a process for producing carbon products via solvent extraction of coal is described below:

Step 1. Production of a hydrogen-enhanced solvent, obtained by combining less than 1% hydrogen with coal tar distillate oils. This reaction occurs catalytically in a continuously fed

reactor at nominal conditions of 1000 psi and 425 °C. FutureGen can supply both hydrogen as well as process heat for this reaction.

Step 2. Ground coal is combined with the hydrogen enhanced solvent and digested under conditions similar to Step 1. Typically 2-3 parts solvent are used per 1 part coal. Optionally, Steps 1 and 2 can be carried out simultaneously, although pumping requirements are simpler if ground coal is added in a semi-batch mode. Then, the reactor is repressurized to conditions similar to Step 1. Typically 90% of the dry-ash-free coal is digested within 20 minutes.

Step 3. Solids are removed from the digest via centrifugation and/or filtration. Generally two passes are needed in order to lower the ash content from 3% to less than 0.1%. In a commercial operation collocated with FutureGen, the liquid solution could be sent off-site at this point either to a pitch processing (distillation) plant, or directly to a delayed coking facility. The solids can be consumed as fuel for FutureGen.

Step 4. The resultant solid-free solution is distilled. By monitoring the viscosity and softening point, the bottoms can be tailored to create either a pitch (such as binder pitch or impregnation pitch) or a coke precursor. It is possible to recycle a portion of the liquid products and re-hydrogenate it to create additional solvent, or alternatively, to create liquid products directly. The choice will likely be made on the basis of economics.

Step 5. Coke precursor is sent to a delayed coker. The delayed coker heats the coke precursor solution to above its melting point and injects it in very large tanks, whereupon it slowly devolatilizes over a 24-hour period. The volatiles are collected in the form of liquids, and the bottoms become green coke. The bottoms are usually removed by the use of high-pressure water hoses to cut out the green coke from the holding tanks. Thus, both Steps 4 and 5 produce liquid products.

Step 6. The green coke is sent, usually by barge, to a calcining company where it is heat treated to 1350 °C, resulting in cokes including anode and needle grade cokes. In addition, some additional liquid products may be collected; although, calciners usually use the volatiles to fuel the high-temperature furnace.

Figure 1 illustrates this basic process. DOE-funded research at West Virginia University has led to the development of new processes to manufacture synthetic binder pitch, under contract to DOE (DE-FC26-03NT41873).

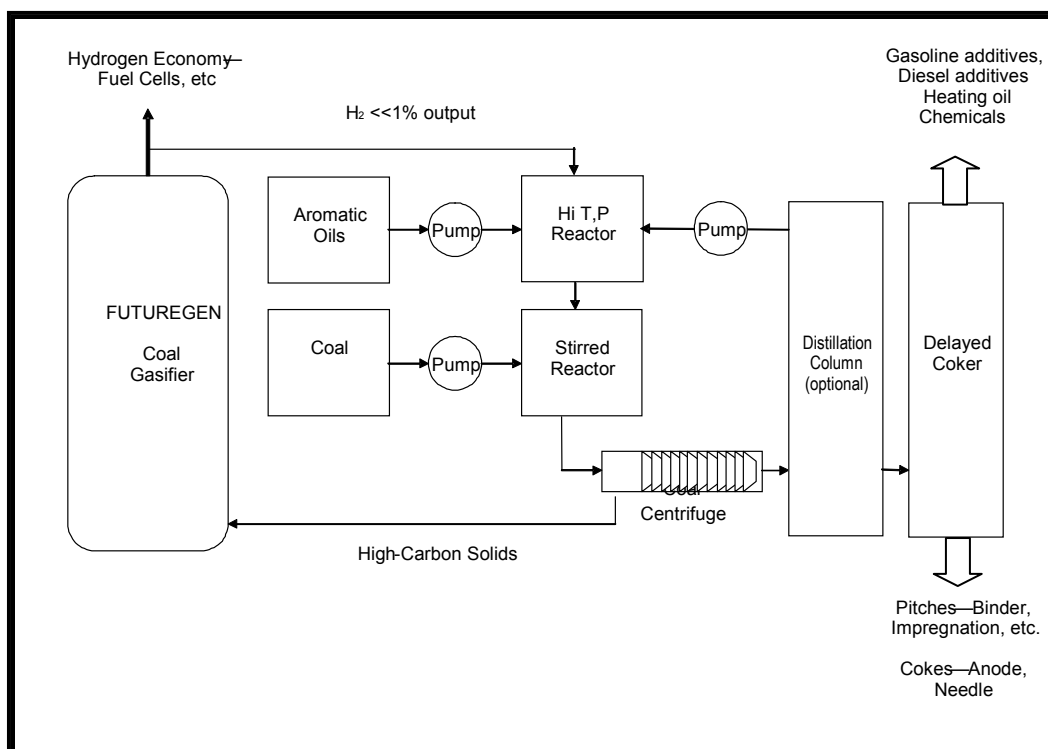


Figure 1. Process Diagram for Carbon Products Process for Synthetic Pitch and Coke Precursors.

The metals smelting industry is suffering from the combined effects of expensive petroleum (~\$90 per barrel at the time of this report), as well as high growth rate of overseas demand, particularly from China and India. The net result has been significant increases in the price of carbon commodities.

The long-term trend is that refineries will seek to maximize production of liquid fuels. A variety of techniques, including catalytic cracking, hydrocracking, and modified distillation processes can be used to increase the yield of liquid products. The result is less petropitch and resid bottoms, and the bottoms that are produced are of significantly lower quality for conversion to anode coke. For that reason, anode coke has suffered from worsening quality over the past two decades, as evidenced by increasing levels of sulfur and heavy metals.^{9,10}

The aluminum industry is critically dependent upon carbon for the aluminum production process. Because aluminum is made via an electrolysis process, it is necessary to consume about 0.4 pounds of carbon for every pound of aluminum produced (the basic reaction being $3C + 2Al_2O_3 \rightarrow 4Al + 3CO_2$). The carbon is supplied in the form of a high-current anode, which in turn is manufactured from anode coke (85%) and binder pitch (15%).

For that reason, the aluminum industry is threatened by the potential decline in coke production. In the US, aluminum production has increased at a rate of about 4% annually during that period, while anode coke supplies have declined. From a peak of 4,121,000 Metric Tonnes in 1991 or about 20.9% of global production, by 2009 the US produced only 1,727,000 Metric Tonnes or 4.6% of global production. Figure 2 shows this disturbing trend. This pathetic performance suggests that the US may soon lose its prominence as a global producer of aluminum unless something can be done to reverse the long term trends.

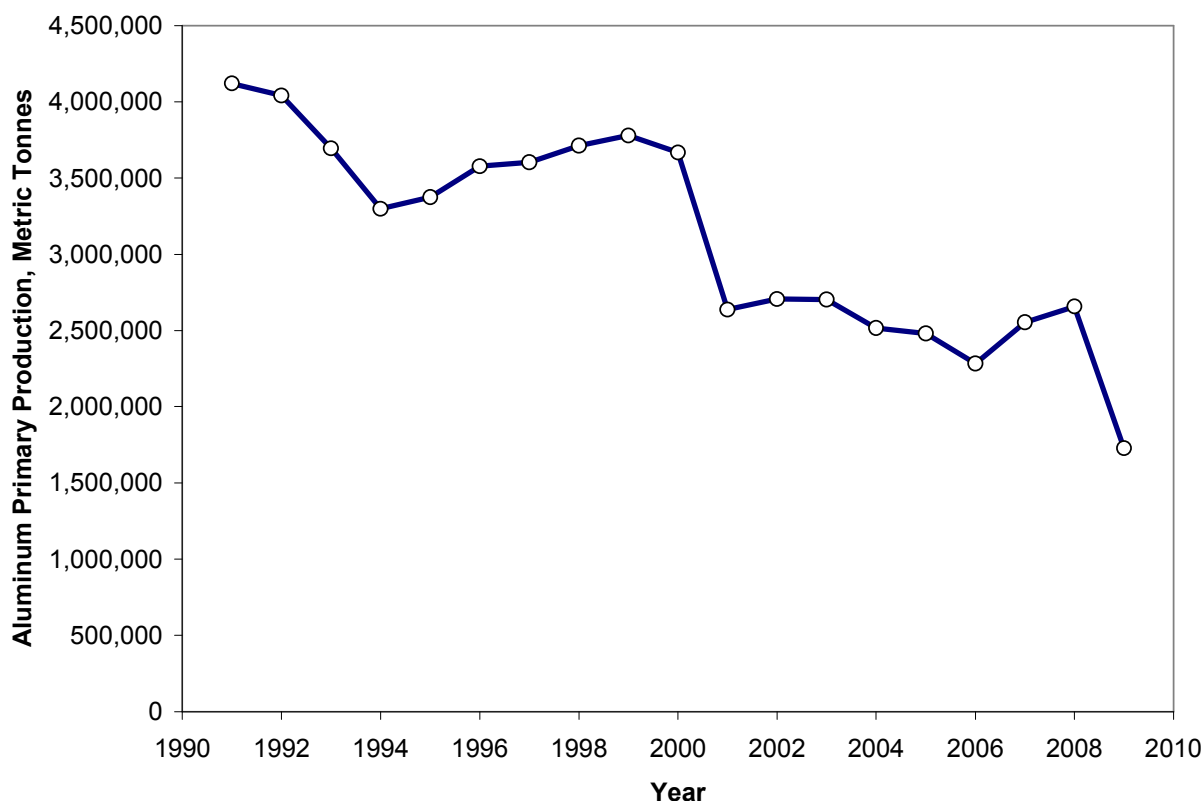


Figure 2. US production of primary aluminum is in a state of long-term decline, as estimated by the US Geological Survey.

For that reason, it is perceived that the metals smelting industry must develop alternate sources of anode coke in the near future.

An overall strategy to co-produce hydrogen as well as liquid fuels and carbon products relies on an evolutionary approach. Initially, demonstration plants will be based upon conventional gas reforming and delayed coking. Ultimately, the future of hydrogen may depend upon a coal gasification approach similar to that of FutureGen. FutureGen initially was based on a concept to build the world's first integrated sequestration and hydrogen production research power plant, although the project later evolved into an oxyfuel concept, to emphasize carbon sequestration first, and hydrogen generation at some point in the future.

At the present time, there is considerable uncertainty about what sort of regulations will be used to reduce CO₂ emissions from the commercial power sector. In addition, the future of hydrogen in automobiles is the subject of a raging debate in the commercial marketplace, as automakers have already begun to achieve efficiency gains via the use of battery-augmented hybrids and electric cars. It is difficult to predict whether America will be better served by augmenting the present supply of hydrocarbon fuels, or by developing hydrogen for new automotive fuel cells. The point is, by combining mild coal liquefaction processes with hydrogen production via coal gasification, the country gains the ability to produce liquid fuels in addition to hydrogen.

The production of carbon in a delayed coker inherently results in liquid-fuel byproducts, as the organic vapors must be distilled away in order to produce green coke. These vapors must be condensed and recovered as useful additives. Delayed coking is the process used to make most anode coke today. Briefly, the delayed coker requires a molten feedstock that can be heated and injected into a drum, where it is allowed to polymerize over approximately a one day period (hence the term “delayed coker” since the material is converted to coke some time after it is heated). The green coke is cut out of the drums using high-pressure water jets. A synthetic pitch could be designed for use in a delayed coker in the same way. The essential synthesis process would be similar to that used for producing binder pitch, except that additional fractional distillation is required in order to modify the fluidity so that the pitch mimics the temperature-dependent flow characteristics of petroleum pitch or petroleum resid. The recovered liquids would be useful as solvent to dissolve additional coal, or could be used as a separate product stream if the price of the chemical product exceeds that of coke precursor. Coke produced from a synthetic pitch precursor would be very low in vanadium and nickel and low in sulfur.

The process of mild liquefaction has been tested at the pilot scale for the production of binder pitch with DOE sponsorship in accordance with specs provided by Koppers Industries (the world’s largest pitch producer), Alcoa (the world’s largest aluminum producer, and thus the world’s largest consumer of carbon anodes), and GrafTech (the world’s largest graphite producer).

2.1.2. Research Objectives

The overall objective of this effort was to develop the means to enhance both environmental characteristics as well as profitability of hydrogen production via coal gasification systems such as FutureGen by using only a small amount of the hydrogen produced to create liquid products as well as carbon products. The process heat and hydrogen are useful to liquefy coal. In addition, the gasification capability is important because it provides a means to use carbon-rich insolubles (also containing ash) from the liquefied coal, in a way that is both profitable and ecologically sound.

The material and energy balances can be weighted according to the commodity prices of the feeds that are utilized as well as the products, thus establishing the limits for processing costs. In addition, the process must be validated technically for the production of key commodities such as anode coke and transportation fuels. At a fundamental level, petroleum has a higher ratio of hydrogen to carbon than coal does. That is why it is easier to refine petroleum to produce transportation fuels. For that reason, coal-based feedstocks should be used to produce carbon-rich products such as pitches and cokes as part of the suite of products. The remainder, being of higher hydrogen content, is more like low-grade petroleum crude that can be refined into commodity liquid products. This establishes the technical and business cases for the development of products, as illustrated in Figure 3 below.

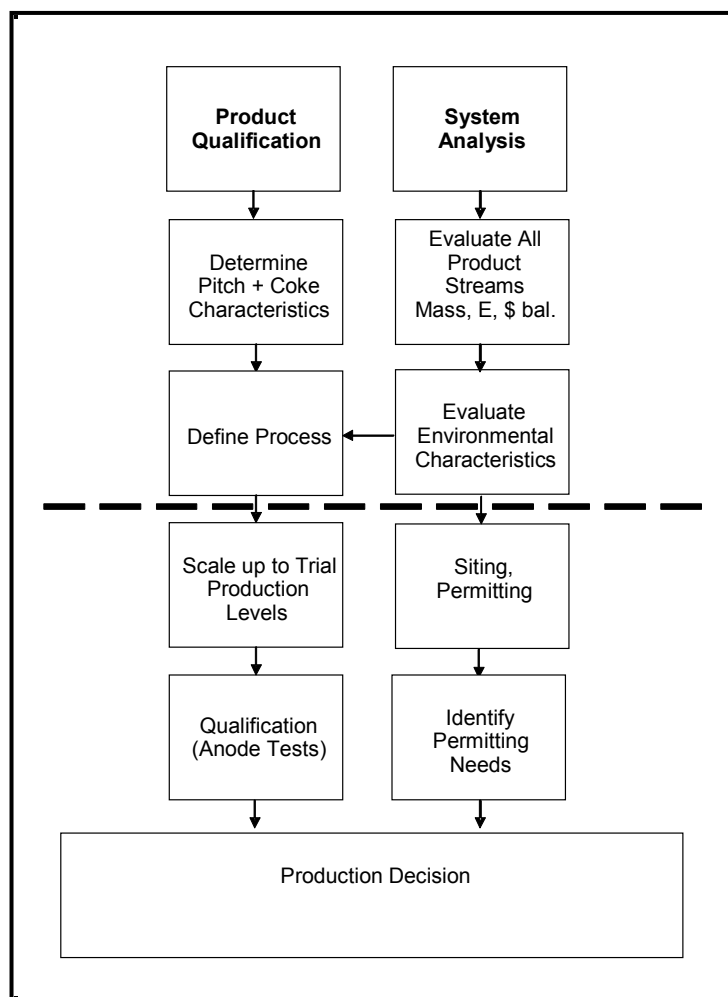


Figure 3. Overall Project Flowchart.

2.1.3 Identification of Hydrogen, Fuels and Carbon Products

A suite of products can be produced by combining a conventional natural gas reforming plant with a solvent extraction capability oriented towards pitches and cokes of interest to metals smelters.

The FutureGen project was intended to form the core of the national capability of producing hydrogen. For that reason, hydrogen was considered as means of enhancing conversion of coal to crude oil. As a baseline, a small amount of hydrogen was used in the proposed process to enhance coal solubility in aromatic oils, thereby creating a solvent. The proportion of hydrogen, solvent, and coal is typically 1:200:80. A hydrogen-to-solvent mass ratio of 1:200 or less is typically used, which is sufficient to liquefy 90% of bituminous coal to produce pitch and coke precursors at WVU's pilot scale plant. The process requires a temperature of 450 °C in order to function. Thus assuming a specific heat of 500 J/kg°C, and permitting thermal losses of 15%, the process requires about 270 MJ per ton. Because the

temperature and energy requirements are well within the operating specifications of FutureGen, this project does not impose special requirements on that operation.

A point design was created for a commercial demonstration unit capable of producing liquid products and carbon products using hydrogen-assisted solvent extraction. Based on the assumption that a pilot scale plant would require a capital investment of at least \$10 million dollars (with that figure being achieved only at sites presently licensed to handle pitch and coal processing), and realizing the margins associated with commodity hydrocarbon products would likely be less than \$100 per ton, a cash-flow-positive operation would likely require a minimum of 20,000 tons per year of products. Using other yardsticks, this corresponds to about one barge per month of product, which is also a reasonable quantity. According to the FutureGen Prospectus as of March 31, 2005, FutureGen will produce about 1 million tons of carbon dioxide to be sequestered. This corresponds to about 270,000 tons of carbon per year. Thus, 20,000 tons of carbon processed annually would be a reasonable baseline, based on the amount produced in a FutureGen plant.

2.1.4 Mass, Energy, and Cost Balances

Detailed mass, energy and cost balances were performed for a suite of products produced from coal via mild hydrogenation and solvent extraction. In 2006, the concept was to leverage the availability of hydrogen from FutureGen, while also taking advantage of the potential utilization of centrifuge tails as a gasification fuel. Table 2 illustrates the case in which FutureGen was assumed to not be available and hydrogen is supplied via tube trailer (Cost estimates are from Simbeck and Chang, NREL/SR-540-32525). The margin is positive but relatively small, about \$34 based on 3 tons of products. Table 3 illustrates the case in which the value of the coker-derived liquid products is at least equal to the value of crude petroleum. Allowance is made for the assumption that additional hydrogen may be needed to raise the quality. These preliminary calculations show that the value added per ton of feedstock can potentially exceed \$200 per ton or roughly \$16 per barrel.

Table 2. Mass, Energy, and Cost Balance without FutureGen.

	Mass	Specific Energy	Specific Energy	Cost per US ton	Extended Cost
Feedstocks	US Tons	kJ/kg	BTU/ton	\$/ton	\$/ton of coal
Solvent (middle distillation cut)	2.5	45000	19149	\$200	\$500
Catalyst	0.0015	0	0	\$2,000	\$3
Raw Coal, -50 mesh,dry	1	29375	12500	\$60	\$60
tube trailer hydrogen	0.0125	142000	60426	\$3,991	\$50
Energy Costs		600			\$61
Total Feed	3.514		17395	\$192	\$673
				PRICE	
Green Stage Products				\$/US ton	
Solid plus residual solvent	0.1	9000	3830	-\$15	-\$2
Unrecovered gas+vapors	0.05	42000	17872	-\$15	-\$1
Fuels + liquid chemicals	2.75	45000	19149	\$260	\$715
Green Coke	0.614	32000	13617	\$130	\$80
Total	3.514			\$226	\$793
Value added per ton of feed				\$34	\$119

Table 3. Mass, Energy and Cost Balance with FutureGen, Liquids = \$60/barrel.

	Mass	Specific Energy	Specific Energy	Cost per US ton	Extended Price
Feedstocks	US Tons	kJ/kg	BTU/ton	\$/ton	\$/ton of coal
Solvent (middle distillation cut)	1.125	45000	19149	\$200	\$225
Catalyst	0.0015	0	0	\$2,000	\$3
Recycle Solvent	1.375	45000	19149	\$200	\$275
Raw Coal, -50 mesh, dry	1	29375	12500	\$60	\$60
tube trailer hydrogen	0	142000	60426	\$3,991	\$0
On-site Hydrogen	0.025	142000	60426	\$907	\$23
Heating Energy Solvent+ H ₂		600			\$4
Heating Energy H-Solvent/Coal Slurry		600			\$4
Separations cost undissolved solids		160			\$5
Distillation Energy		400			\$2
Total Material Feed	3.5015		17673	\$171	\$600
Green Stage Products				Price per US ton	
Solid plus residual solvent	0.1	9000	3830	\$20	\$2
Unrecovered gas+vapors	0.05	42000	17872	-\$15	-\$1
Recycle solvent	1.375	45000	19149	\$200	\$275
Fuels + liquid chemicals	2.75	45000	19149	\$433	\$1,192
Binder Pitch	0	36000	15319	\$300	\$0
Green Coke	-0.7735	32000	13617	\$130	-\$101
Total	3.5015			\$391	\$1,367
Value Added				\$221	\$767

2.1.5 Delayed Coker Experimental Simulation.

In an industrial scale delayed coker, the sheer scale of the unit is sufficient to ensure that the internal temperature will remain high over the 24-hour period required to form cokes. However, for a subscale unit, the possibility of substantial cooling requires that a heater be used in order to moderate the temperature. In addition, the formation of pores in coke is due to the devolatilization and subsequent creation of flow channels from the vapors present in the coke precursor. This, in turn, affects the degree of anisotropy in the coke after calcining. Thus, a heated vertical tank is required to develop appropriate flow fields. With these factors in mind, a heated canister system was designed for delayed coking, based on a simple vertical pipe. The facility is outfitted for handling hydro-treated solvents and coal digests.

A stainless steel pipe was used as the basis for a coker, suitable for a batch size is up to 5 gallons. Anode-grade coke is created by devolatilization of aromatic heavy liquid feedstocks at some 500 °C, in accordance with standard protocols in delayed coker units. In order to verify that the system adequately simulates conditions in a delayed coker. Accordingly, precursor pitch is heated in the reactors and injected into the delayed coker. Condensable vapors are collected in a water cooled condenser.

Properties of interest include:

- a. Proximate Analysis, to determine Volatile Condensable Matter (VCM) Content, weight percent, dry basis. Ash content and moisture content are also determined.
- b. Sulfur, weight percent.
- c. Heavy metals content, especially Nickel and Vanadium content, ppm (related to the oxidation rate in air of the final product).
- d. Real density, g/cm³.
- e. Electrical resistivity, ohm-m.
- f. Flexural strength, ksi.
- g. Avg grain size, microns.
- h. Coefficient of thermal expansion, ppm/°C.
- i. Coke yield, percent, similar to Conradson Carbon measurement.

Hydrogen-assisted solvent extraction is used to produce liquefied coal. Laboratory-scale experiments will establish the amount of distillation required in order to produce a feedstock capable of being heated to 500 °C with a vapor pressure of 60 psig or less, in order to be consistent with typical industrial practices. The light distillates have boiling points and molecular weights consistent with diesel and gasoline, but the aromatic fraction is likely too high. For that reason, the light distillates may be re-hydrotreated and recycled as solvent. The bottoms, representing about half of the total coal solution, can be considered to be the feedstock for the delayed coker.

Laboratory scale cokes are production of anode-grade or superior-quality cokes, larger scale tests is accomplished in the modified facility with several-gallon batches of solvent-assisted, hydrogen-extracted coal.

In industry, coke is assigned to grades ranging from shot coke (unacceptable for use in metals smelting), anode grade, needle grade, intermediate premium needle grade, normal premium needle grade and super premium needle grade. “Needle” refers to the microscopic appearance of the anisotropic grain structure, which results in graphitic structure. The price that anode grade coke commands can vary widely. At the start of the project, anode grade coke price was as low as \$130 per ton, with needle coke prices in the range of \$600 per Metric Tonne. By

2011, prices listed on Alibaba.com were in the range of \$600 to \$800 per Metric Tonne. Needle grade coke was in the range of \$950 to \$1500 per Metric Tonne. To compare this with inflation, a calculation based on the Consumer Price Index (CPI) yields an inflation factor of 12.0 percent between 2006 and the present.

2.1.6 Liquid Product Characterization and Optimization

The protocol for characterizing coal liquids is as follows:

Coal is digested and separated into liquid phases. An anode coke precursor is obtained according to process steps 1-4, listed above. Liquids are obtained at two main points in the system: first, liquids are produced by distilling the coal/solvent solution obtained after removing the insoluble solids in Step 3. As shown in **Figure 4**, these coal-derived liquids have a boiling point range which is reasonably consistent with typical requirements. However, coal-derived liquids tend to be highly aromatic, making them less suitable for use in fuels. If these condensed liquids do not have a high market value, it is possible to re-hydrogenate the condensed liquids and recycle them as a coal solvent.

Conversely, delayed cokers are operated at a high enough temperature to break down heavy molecules, resulting in a higher content of aliphatic compounds, which are much more likely to be suitable for fuels applications.

A list of fuels relevant distillation cuts is shown below.

Table 4. Approximate Distillation Cuts by Number of Carbons and Boiling Ranges.

Product	Number of Carbon Atoms	Boiling Range
LPG	3-4	< -1 °C
Gasoline	5-9	36-150 °C
Kerosene	10-14	174-250 °C
Diesel Fuel	12-18	217-317 °C
Fuel Oil	12-20	217-350 °C
Resid	>20	>350 °C

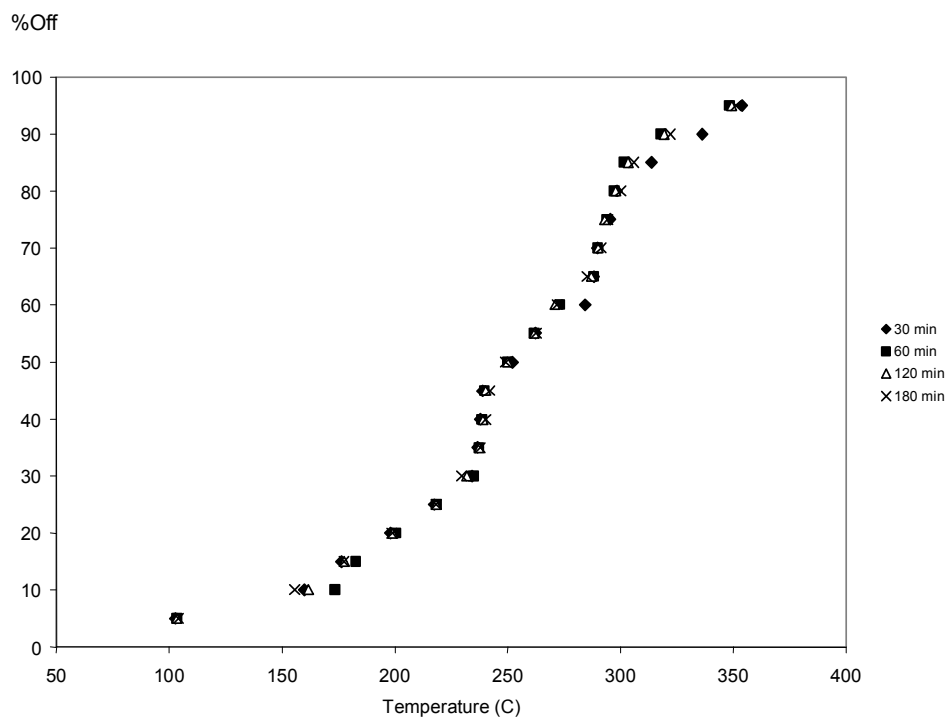


Figure 4. Simdist boiling point curves for hydrogenated coal liquid, showing favorable yields for liquid fuels. The effect of dissolving coal is to shift the entire curve to the right. Low aliphatic content is the primary reason limiting use of coal liquids for fuel use.

Liquid products are then characterized for purity, quality, additives, fuel physical properties, fuel energy value, trace components, trace contaminants, and many other fuel quality, safety and regulatory parameters according to ASTM and other appropriate standards. Nuclear Magnetic Resonance (NMR) spectroscopy is used to determine the ratio of aliphatic and aromatic hydrocarbons. A key objective of this task is to determine how the aliphaticity of liquid products is enhanced through the delayed coking process. Key parameters to be varied include the hydrogen consumption, coal throughput and reactor temperature, pressure and residence time.

2.1.7 Parametric Optimization

A survey of operating delayed cokers identified ranges of material specifications which can be considered. Requirements were developed for viscosity, coke yield, and other requirements imposed by delayed coking facilities.

Parametric studies on the composition of the liquid-phase products is carried out using tools such as elemental analysis, simulated distillation, and thermogravimetric analysis according to ASTM, SAE, and other relevant standards. The yields of categories of products, such as gasoline, diesel fuel, aviation fuel, heating oils, etc., is estimated for distillates of the coal digest as well as condensed liquids from the delayed coker.

This task is carried out analytically using a statistical design of experiments approach, and is supported by experimental analysis, thus determining the most important input and output parameters.

Several different scenarios are of interest. First is the need to develop feedstocks that closely replicate the behavior of current state-of-the-art feeds to existing delayed cokers. This serves to maximize the chance that the new feedstocks produced is acceptable to current delayed coker operators, and minimize the chance of rejection.

Another optimization that is performed is the variation of processing conditions (hydrogen pressure, temperature and residence time) during the hydrogen assisted solvent extraction phase (Steps 1 and 2) that result in maximizing the content of aliphatic gasoline, diesel and other products of interest.

A self-sustaining capability means that more solvent is produced than consumed in the process. This may require additional hydrotreatment in order to increase the fraction of lighter distillates, or alternatively is possible for certain coals with high H/C ratio.

2.1.8 Anode and Electrode Tests

Having demonstrated proof of concept in Phase I, a Phase II effort was initiated to extend the proposed process beyond laboratory-scale efforts in order to better validate the technical and economic merits of the proposed process. Additional investment in the technology, possibly including a new partner from the refining industry, was sought, resulting in a license agreement and substantial investment by Quantex Energy Inc in this technology.

Although anode coke is not the most profitable item in the suite of products that result from a delayed coker, the ability to fabricate viable anode coke from coal is extremely important because it justifies large scale plants. Accordingly, subscale anodes were fabricated using anode coke produced in this task. Tests for air burn, density, resistivity, coefficient of thermal expansion, and other standard industry tests can be performed with laboratory scale samples (a few tens of pounds per batch). Needle-grade cokes have much higher value than anode grade and thus are considered for use in arc furnace electrodes and other large scale applications for graphite.

Large-scale manufacturing of carbon products inherently involves the concomitant production of comparable quantities of liquid products. These liquid products were distilled and segregated into liquid products of potential commercial interest, i.e., diesel fuel. The liquid products were characterized according the same battery of tests identified in Task 3. While successful fabrication of anode coke establishes the feasibility of delayed coking processes incorporating coal-based feedstocks, it remains the case that the majority of revenues will likely come from liquid products. Accordingly, liquid products such as diesel fuel are concomitantly evaluated with the corresponding solid products.

2.1.9 Needle Coke

Needle coke is an attractive commodity for coal-derived carbon product technology because of its high value, relatively large market size and excellent match to the technical characteristics of synthetic coal tar.

Conventional needle coke is typically produced by controlled coking of high purity decant oil. The term “needle” refers to the acicular morphology of the coke which occurs due to the high degree of liquid crystal alignment that occurs as the coke is sheared during formation (see Figure 5). Highly aromatic feedstocks result in enhanced crystalline structure.

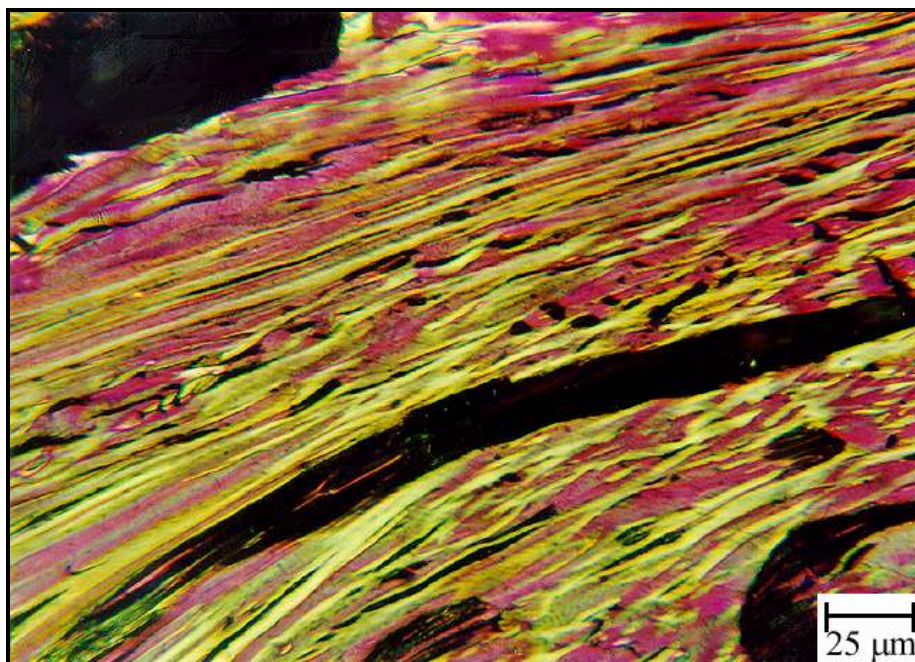


Figure 5. Polarized Light Photomicrograph of Needle Coke (picture credit: Ralph Gray & J. C. Crelling, SIU Carbondale).

Needle coke can not be easily fabricated from coal tar due to the presence of small particulate carbons (referred to in the industry as quinoline insolubles or QI's, although strictly speaking QI denotes a more general class of materials than pyrolytic carbon). QI's result from incomplete pyrolysis of high temperature volatiles from tar. The effect of QI's in a coke precursor is to interrupt the domain growth of the needle-like structure required to produce needle cokes. It is possible to remove QI's through processes such as filtration or centrifugation, but so far it has not been proven economical to do so.

A solvent extracted synthetic feedstock maintains the qualities of low heavy metal contamination, zero QI's and high aromaticity. Hence the propensity to produce needle grade coke is very high.

The chief difficulties in using solvent extracted coal liquids for needle coke feedstocks will include obtaining low impurity levels. Processes such as centrifugation and filtration have tended to be problematic at some level, and so maximum ash levels need to be specified.

Coefficient of thermal expansion is generally used to separate needle grade into sub-grades, including Super Premium, Normal Premium, Intermediate Premium, and Regular sub-grades. The exact values of CTE are available from GrafTech International, Ltd. However, as a goal CTE of less than 0.65 ppm/°C is desired.

Other properties of interest include electrical resistivity, thermal conductivity, index of graphitization, density, reactivity, etc. Ideally these should be measured after full graphitization at 2900 °C, although data taken after heat treatment at lower temperatures can usually be correlated with the equivalent performance at full graphitization.

Accordingly, bench scale needle coking protocols were trialed at GTI as well as WVU, using a protocol for fabricating needle coke from Manganaro, Krupinski and Smith published in 1971.¹¹

a. The pitch precursor is thermally treated batch-wise in a 4-liter electrically heated kettle. 2000 gram charges were used.

b. The pitch is rapidly heated to 390 °C, maintained at this temperature, and then sampled after 7, 31 and 55 hours. The heat treated samples were analyzed for softening point, benzene insolubles (BI) and QI.

c. Optionally, the heat-treated samples can be carbonized by heating at 470 °C, 510 °C and 530 °C for 24 hours.

Maganaro et al. interpret the mechanism of needle coke formation as follows:

a. Beta resins (quinoline soluble, toluene insoluble resins) form from the benzene soluble constituents.

b. At 390 °C, spherules start to develop from beta resins.

c. At higher temperatures (to 470 °C) and time, the spherules grow until they become sufficiently large to distort and coalesce. Continued growth leads to the development of a striated needle-like material. These stages can be observed with polarized light microscopy.

d. In the temperature range of 470 oC to 530 oC, further solidification and development of the coke structure occurs.

Maganaro et al. concluded that the spherules are the precursor to highly oriented needle-like grains. The presence of QI's, in a concentration of higher than about 2.5%, interferes with the development of needle-shaped grain structures by blocking the coalescence of the spherules, and thus prevents their fusion to the needle-like grain state.

Synthetic pitches, having no QI's, are thus expected to be candidates for creating needle grade cokes.

2.1.10 Plant Design

The purpose of this task is to design a plant for hydrogen-assisted solvent extraction of coal, which can be co-located with FutureGen, such that a delayed coker feedstock is produced while meeting technical, economic and environmental requirements. It is based upon the initial point design created in Task 1. The capacity of the plant will probably be in the range of 20,000 tons per year. In 2006, the assumption was that FutureGen would be a coal gasification unit suitable for coproducing electricity and hydrogen. By 2011, however, FutureGen had shifted to an oxyfuel design and at present is no longer intended to produce hydrogen. WVU thus correctly foresaw the difficulties in hydrogen production. In addition, national politics seem to favor domestic production of fossil fuels.

Cost estimation is carried out using industry-standard cost methodologies and data bases. Synergism between FutureGen and the proposed carbon products and liquid fuels capability has been quantified. For example, production of a delayed coker feedstock requires a temperature of at least 450 °C. While this can be accomplished by combustion or electric heating, the preferred solution is to use process heat from the coal gasifier in the form of dry steam, which can be supplied by FutureGen.

Supply options for hydrogen were considered as well. FutureGen or some other syngas based concept might supply hydrogen in pipelines of at least 600 psi and ambient temperature, which is more than sufficient for the requirements of the liquefaction process proposed herein. Similarly, the use of tails from the solids separation process might have a disposal cost associated with them, but a gasifier could utilize carbon-rich solids as a gasification fuel, mixed in with other coal feeds.

The delayed coker feed would be supplied in liquid form to some other site. The delayed coker itself would not be collocated on-site, as the feed could be transported via barge or railcar. Transportation costs and other logistical considerations are specifically developed. Permitting considerations are identified at the federal, state and local levels. Handling and storage of coal, hydrogen as well as coal-derived liquids are special concerns. Because FutureGen is designed for zero or near-zero emissions, then carbon products production should carry the same requirements.

The plant is designed so that it can operate separately from the coal gasification unit. Among other items, this might require a backup steam plant and provisions for accepting hydrogen from tube trailers or LH2 railcars. Backup means for handling solid residue will also be identified. However, the intent would ultimately be to operate the plant in conjunction with the coal gasifier in order to maximize the economic effectiveness.

Similarly, a hydrogen-assisted solvent extraction plant requires minimal design modifications are required from FutureGen or some other gasifier. A modular design, i.e., one in which most of the plant is capable of being broken down into modules and shipped to the point of use by rail or barge, is preferred in order to minimize construction costs at the site.

2.1.11 Technology Transfer Plan

Technology transfer in this case consisted of producing a plant design that was largely implemented by industry, beyond the current project, which will produce commercial cokes and blending agents for transportation fuels. This took the form of a license agreement with Quantex

Energy, with the result being a commercial demonstration plant in Texas. In addition a plant to produce Carbonite, a purified coke to be used as a form of

West Virginia University is ideally suited for this task, due to its strong relationships with the dominant players in this business, including Alcoa, the world's largest producer of aluminum; GrafTech, the world's largest consumer of needle coke for graphite electrodes and specialty graphites; CII Carbon, the number two calciner in the country and Koppers, the world's largest pitch producer. In addition, Dr. Richard Wolfe of Wolfe Engineering headed efforts in artificial metallurgical coke, including the design, manufacture and operation of a pilot scale plant involving mild gasification technology to manufacture formed metallurgical coke.

This objective was accomplished because of license agreements with WVU and Quantex Energy Inc, a Canadian Corporation that seeks to demonstrate commercialize coal conversion. A second plant has broken ground in Virginia on behalf of Carbonite Inc, with the intention of producing clean coke from steam coal blends. These are discussed in greater detail in Chapter 4.

2.2 Direct Liquefaction in China

Direct liquefaction technology has been brought to a high state of the art by the Shenhua Group in China, which is building a direct liquefaction coal-to-liquids plant with a nominal output of 20,000 bpd beginning in 2007. An important distinction, however, is that the WVU system is used to produce a *heavy crude* which is suitable for coproduction of carbon products as well as liquid fuels, whereas the Shenhua plant is being developed to produce a *light crude* which devoted to maximum generation of liquid fuels (see Figure 6 and Figure 7). Economic analysis presented herein argues the case for producing heavy crude as a means for increasing revenue and decreasing cost. The Shenhua technology is believed to be similar to the technology developed by Hydrocarbon Technologies Inc (HTI), a subsidiary of Headwaters Inc, as shown in Figure 8.¹²

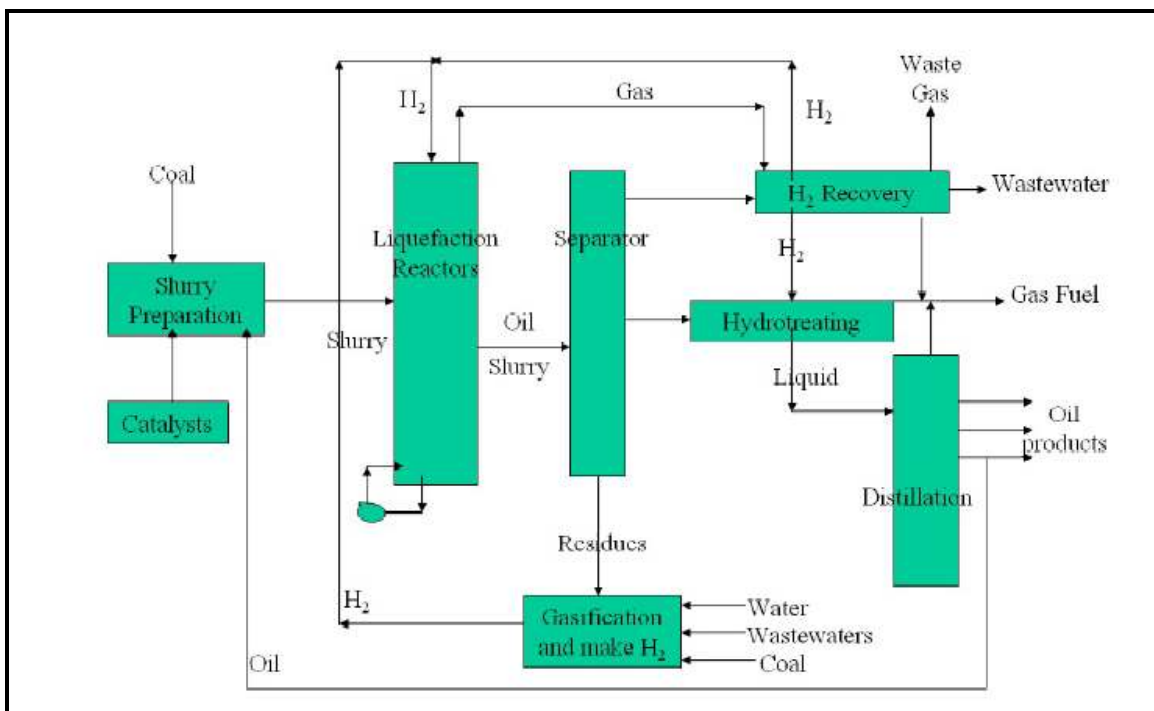


Figure 6. Shenhua Group Direct Liquefaction Concept.¹³



Figure 7. Artist's Rendition of Shenhua Direct Liquefaction Facility, scheduled to begin production later this year.¹⁴

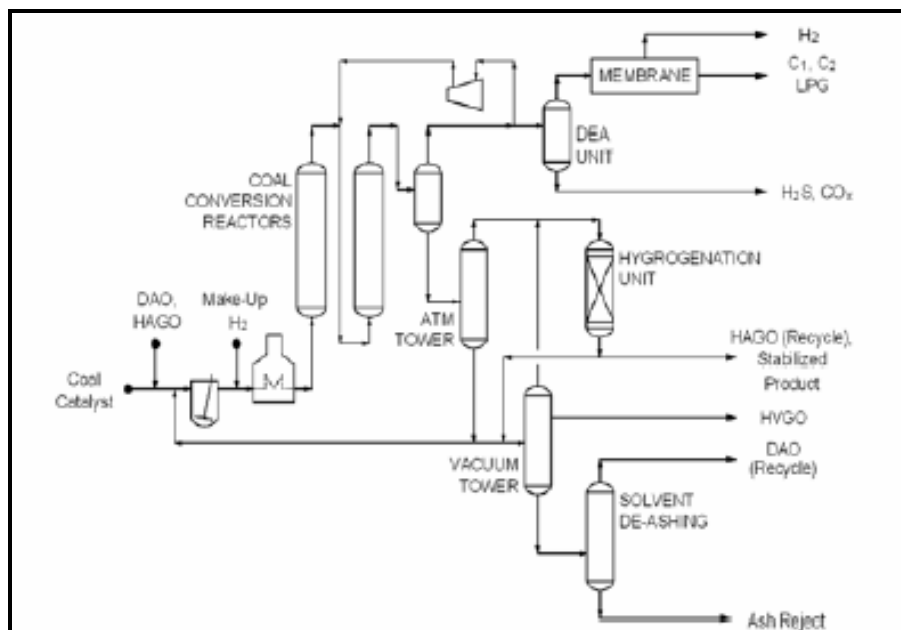


Figure 8. Block Diagram of Headwaters/HTI process (courtesy Headwaters).

In the HTI coal Process, pulverized coal is dissolved in recycled coal-derived heavy process liquid under typical hydrogenation temperature of 435 to 460°C in the presence of elevated hydrogen overpressure (about 170 bars or 2466 psig). These parameters are slightly higher than the parameters used in the WVU system. Hydrogenation occurs at 415 °C with hydrogen overpressure between 1500 psig and 2000 psig. Thus, instead of producing the lightest, most aliphatic hydrocarbon crude possible, a greatly reduced amount of hydrogen is used, thus resulting in a heavy, more aromatic crude.

In the Headwaters/HTI process, most of the coal structure is broken down in the first-stage reactor. Liquefaction is completed in the second-stage reactor. The Headwaters/HTI proprietary GelCat Catalyst is dispersed in the slurry for both stages. The intermediate coal liquids from the mild hydrogenation step must be further upgraded using conventional refining techniques to produce gasoline, jet and diesel fuels. The liquefaction process generally adds an amount of hydrogen equal to about 8-12% of the mass of the coal (dry, ash-free basis).

Heavy aromatic crudes have unique properties that make them especially suitable for value added products such as needle grade coke, anode grade coke, binder pitch and others. Specifically, coal derived synthetic crudes can be low in heavy metal impurities; low in sulfur and high in aromatic content, resulting in superior anisotropy when these materials are converted to carbon materials. Accordingly, coal derived synthetic crudes may produce a proportionately higher percentage of revenues from distillation bottoms, compared to traditional petroleum or oil sands crudes. Conversely, refiners of conventional petroleum or oil sands generally seek to maximize the yield of liquid products, since these usually command the highest price on the open market. Hence, the production of heavy synthetic crudes via direct liquefaction of coal may be more attractive than the production of light synthetic crudes from coal.

For example, in recent history, the price of needle coke (i.e., coke with a highly oriented graphitic atomic structure, commonly used to make synthetic graphite) has remained above \$500 per ton for certain sub-grades. This corresponds to about \$69 per equivalent barrel of petroleum.

Similarly, products such as binder pitch, impregnation pitch and anode grade coke have recently commanded prices in the range of \$200-\$300 per ton (\$27 to \$41 per equivalent barrel).

Coal derived aromatic oils can be candidate precursors for these carbon products. Aromaticity is desirable because such compounds are able, upon thermal conversion to pure carbon, to promote long range graphitic order or anisotropy. In this respect, coal derived precursors may be more suitable than their petroleum based counterparts, which tend to be more aliphatic, which tends to result in the formation of more disordered carbon upon coking.

If acceptable revenues can be obtained from the heavy fractions from coal derived synthetic crudes, this suggests that the aim of direct liquefaction of coal might be to produce a heavy aromatic crude rather than a lighter “sweet crude”. The heavy aromatic coal-derived synthetic crude might be similar to oil sands in that substantial upgrading would be required in order to produce viable fuels. Unlike oil sands, however, coal derived synthetic crude would contain reduced levels of impurities.

Efforts at West Virginia University have typically emphasized the use of solvent extraction. Briefly, a commodity solvent (such as a coal tar distillation product) is hydrogenated to enhance its ability to digest coal. Crushed coal is then digested in the solvent resulting in conversion of up to 90% of the dry, ash-free coal to the liquid state. Industrial processes involving coal-derived solvents as liquefaction solvents generally isolate process-derived recovered solvents, which can be recycled back to the process, thereby minimizing the addition of fresh solvent. The chemical composition of these recycle solvents controls the overall behavior of the coal liquefaction process.

The solids are removed via centrifugation, resulting in a 100% liquid synthetic crude. The solid fuel is intended to be blended in with the feed to a gasification unit such as FUTUREGEN, which is the DOE project to demonstrate zero emissions coproduction of hydrogen and electricity.

The synthetic crude can be refined to produce a combination of gas products, liquid products and carbon products. As is usually the case for hydrocarbon refiners, a variety of options exist for the final products. In particular, three scenarios are considered:

- a. Production of a Syncrude that matches light or intermediate crude, with the intention of maximizing the yield of transportation fuels and in particular gasoline.
- b. Production of an aromatic heavy Syncrude, with co-production of a binder pitch.
- c. Production of an aromatic heavy Syncrude, with co-production of a mesophase pitch.
- d. Production of an aromatic heavy Syncrude with co-production of needle grade coke.

Table 5 compiles commodity prices of products of interest for direct liquefaction of coal. Conversion between mass and volume is based upon an equivalent barrel of West Texas Intermediate (WTI) Crude, having a density of 0.8365 g/cm³.¹⁵ Thus, one barrel of WTI Crude is the equivalent of 0.1458 short tons. Commodity prices are subject to considerable fluctuation even in time scales of a few months. In general, however, the commodity prices tend to move with the price of crude petroleum, such that the ratio of the commodity price to crude oil price may be more stable with time. Hence the commodity prices (including the six-year-old data from the University of Kentucky Study) are normalized to the price of WTI crude in the second

column.¹⁶ The third column estimates the price per barrel (mass-equivalent), based on a WTI Crude price of \$60 per barrel and 0.1458 tons per barrel, and the fourth column is the equivalent price per ton. The date and source of information are listed in the last two columns.

Approximate world market data is contained in Table 6.

Table 5. Estimated Commodity Prices Based on WTI Crude @ \$60/BBL.

Commodity	Lower Heating Value, MJ/kg	Normalized Cost	Price per Equiv BBL	Price per Ton	Source
Gasifier Fuel (e.g., FUTUREGEN)	-	0.0194	\$1	\$8	EK, 2007
Powder River Basin Sub-Bituminous Coal	19	0.0238	\$1	\$10	EIA, 2007
Central Appalachian Bituminous Coal	27	0.1166	\$7	\$48	EIA, 2007
Metallurgical Coke	32	0.4374	\$26	\$180	EK, 2007
Calcined Anode Coke	32	0.4860	\$29	\$200	EK, 2007
Coal Tar Pitch	-	0.6097	\$37	\$251	EK, 2007
Heavy Oil Sands (Lloyd Bend)	43	0.6878	\$41	\$283	EIA, 2007
Natural Gas (Pipeline Receipt)	-	0.7238	\$43	\$298	EIA, 2007
Residual Fuel Oil (RFO)	-	0.7300	\$44	\$302	EIA, 2007
Binder Pitch	42	0.9234	\$55	\$380	EK, 2007
Low Sulfur FCC Decant Oil	-	0.9505	\$57	\$391	UK, 2001
Crude Oil (W.Texas Int.)	42	1.0000	\$60	\$412	EK, 2007
Creosote Oil	-	1.1584	\$70	\$477	UK, 2001
Gasoline	45	1.3955	\$84	\$574	EIA, 2007
Premium Calcined Needle Coke	32	1.4455	\$87	\$595	EK, 2007
Toluene	-	1.4752	\$89	\$607	UK, 2001
Crude Naphthalene	43	1.5049	\$90	\$619	UK, 2001
Xylenes, Mixed	-	1.5446	\$93	\$636	EK, 2007
Benzene	-	1.8911	\$113	\$778	UK, 2001
Mesophase Pitch	-	3.4000	\$204	\$1400	EK, 2007
Hydrogen (refinery)	142	5.3461	\$321	\$1361	EK, 2007
Hydrogen (tube trailer)	142	9.7201	\$583	\$4,000	EK, 2007

EIA = DOE Energy Information Administration, Mar 2007; UK = University of Kentucky, Phase II Quarterly Technical Progress Report, DE-AC22-91PC91040, April 2001; EK = telephone interviews with commodity producers by Elliot Kennel, Mar 2007.

Table 6. Estimated Domestic and World Markets for Carbon Products.¹⁷

Product	Primary Feedstocks	Main Applications	Domestic Annual Sales, Tons	Worldwide Annual Sales, Tons
Binder Pitch ¹⁸	Coal Tar Pitch Petroleum Pitch	Anodes (Al smelting) Arc furnace electrodes (steelmaking)	800,000	1,500,000
Impregnation Pitch	Petroleum Pitch Coal Tar Pitch	Electrodes, Composites	180,000	380,000
Mesophase Pitch	Petroleum Pitch Coal Tar Pitch	High performance composites, fibers	800	3700
Anode Coke	Petroleum Pitch	Anodes (Al smelting)	1,800,000	8,000,000
Needle Coke	Petroleum Pitch (US) PP + CTP (Japan)	Arc furnace electrodes (Steelmaking)	400,000	1,300,000
Carbon Fiber (PAN) ¹⁹	Petrochemicals	Non-graphitic composites	10,000	24,000
Pitch Fibers ²⁰	Coal tar pitch, Petroleum Pitch	Graphitic composites	200	3000
Carbon Black ²¹	Petroleum Pitch, Coal Tar Pitch	Rubber additives, various other	1,800,000	8,000,000
Carbon Foam ²²	Petrochemicals, Coal, Coal Tar Pitch	Structures, electrochemical systems,	200	200
Carbon Nanofibers ²³	Natural Gas, Gasified Coal	Polymer additives	50	150
Other Carbon Nanomaterials	Various	TBD	<1	<1

To determine the materials costs associated with liquefaction, it is necessary to consider the hydrogen content of the feed material as well as the desired product. A representative coal sample was provided by the Kingwood Mine (Alpha Natural Resources) preparation plant. The elemental analysis in Table 7 lists the composition by mass.

Table 7. Elemental Analysis of Bituminous Coal (Lower Kittanning).

Element	Average	% Rel. S. D.
Nitrogen%	1.737767498	2.2299
Carbon%	77.93449148	1.0471
Hydrogen%	5.33333683	1.029
Sulfur%	1.83043015	22.9324

The atomic H/C ratio is described by

$$\left(\frac{H}{C}\right)_{at} = \frac{m_H A_C}{m_C A_H} ,$$

where m_H is the mass of hydrogen, m_C is the mass of Carbon, A_C is the atomic mass of carbon and A_H is the atomic mass of hydrogen. Thus,

$$\left(\frac{H}{C}\right)_{at} \approx 0.82 .$$

A light crude would require $\left(\frac{H}{C}\right)_{at}$ of about 2.00 or higher. Thus the required mass ratio would be

$$\frac{m_H}{m_C} \approx \frac{2.00}{12} = .17$$

A mass balance is set up, according to the basic solvent extraction process in Figure 9.

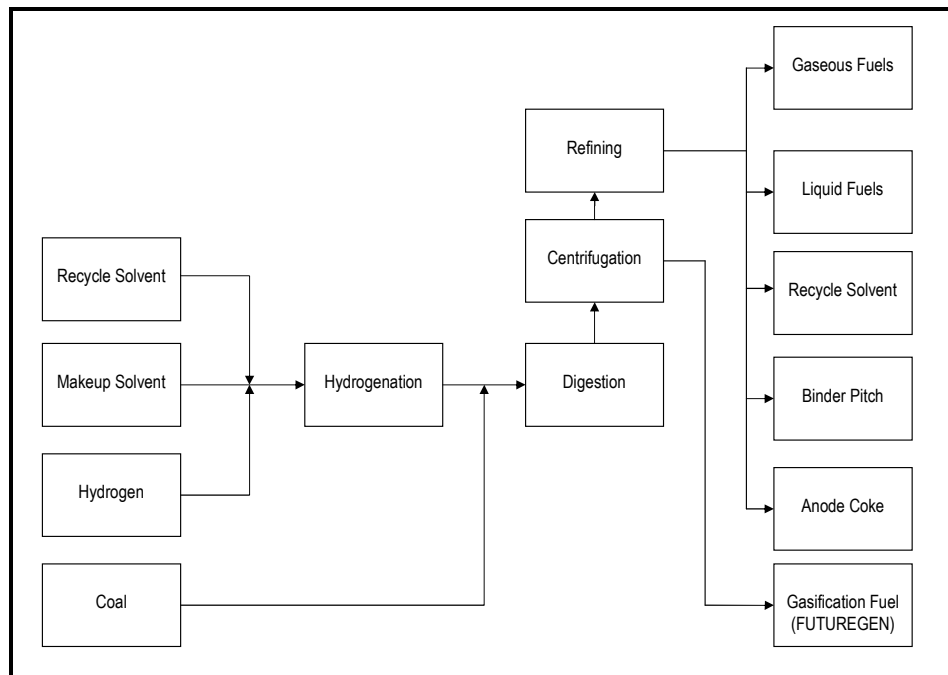


Figure 9. Simplified Mass Balance for Direct Liquefaction.

a. *Maximum transportation fuel yields.* Crude petroleum has an H/C atomic ratio of about 2.0, translating to a mass ratio of about 0.17.²⁴ Thus, the data from Table 7 suggests that it may be necessary to add hydrogen equal to about 12% of the starting mass of coal in order to produce a light crude. An approximate mass balance appears below in Table 8 and Table 9. The input cost and output value considers only the market price of the feedstocks, and does not include processing cost. Higher hydrogenation levels certainly translate to higher upgrading costs. The input makeup solvent is assumed to be pure naphthalene, under the assumption a solvent rich in naphthalene would be required in order to absorb the required amount of hydrogen. As a result, the feedstock cost is approximately \$33 per barrel, approximately 57% of which is due to the cost of hydrogen.

Table 8. Input Feedstock Materials Costs, Max Fuels Yield.

Input Feedstock	Mass Fraction, %	Unit Cost	Extended Cost
Central Appalachian Bituminous Coal	80	\$42	\$34
Hydrogen (refinery)	9.6	\$1,361	\$131
Naphthalene Solvent	10.4	\$619	\$64
Total cost (per ton)			\$229
Total cost (per barrel)			\$33

Table 9. Output Materials Values, Max Fuels Yield.

Output Product	Mass Fraction, %	Unit Value	Extended Value
Synthetic Crude	85	\$412	\$350
FUTUREGEN fuel	15	\$8	\$1
Total Value (per ton)	100		\$351
Total Value (per barrel)			\$51
Net Value Added (per barrel)			\$18

b. *Production of an aromatic heavy Syncrude and binder pitch.* In this scenario, as with the subsequent scenarios, very little hydrogen is consumed, as the intent is to produce a synthetic crude. Accordingly a low-performance hydrogen donor solvent is acceptable, and thus a heavy oil such as petroleum decant oil or coal tar distillate can be substituted for the naphthalene-enriched solvent used to produce a light crude. The production of binder pitch from coal direct liquefaction products has been demonstrated successfully at the bench scale.²⁵ The value of heavy crude is significantly lower than that of light crude (about 70%, based on the values shown in Table 5). High ash residue is assumed to be useful as a feed for a coal gasifier, representing another low value product. However, binder pitch is a relatively high value product, which partially offsets the low value associated with the other two main coproducts. This scenario is described in Table 10 and Table 11.

Table 10. Input Feedstock Materials Costs, Binder Pitch Production.

Input Feedstock	Mass Fraction, %	Unit Cost	Extended Cost
Central Appalachian Bituminous Coal	89	\$42	\$34
Hydrogen (refinery)	0.4	\$1,361	\$5
Coal Tar Solvent	10.6	\$251	\$64
Total cost (per ton)			\$103
Total cost (per barrel)			\$15

Table 11. Output Materials Value, Binder Pitch Production.

Output Product	Mass Fraction, %	Unit Value	Extended Value
Synthetic Crude (heavy)	60	\$283	\$170
FUTUREGEN fuel	15	\$8	\$1
Binder Pitch	25	\$380	\$95
Total Value (per ton)	100		\$266
Total Value (per barrel)			\$39
Net Value Added (per barrel)			\$24

c. *Production of an aromatic heavy Syncrude, with co-production of a mesophase pitch.*

The production of mesophase pitch requires an aromatic pitch with low levels of microscopic particulates (e.g., quinoline insolubles). This pitch is then heated in a quiescent state to promote the formation of liquid crystals, resulting in a mesophase pitch. Mesophase pitches can be used as a binder for graphitic materials with high thermal conductivity. The presence of particulates can interfere with the growth of ordered graphitic domains. Normally coal tars derived from metcoke production have several percent quinoline-insoluble carbon particles, which mainly result from partial pyrolysis of hydrocarbon vapors. Solvent extracted synthetic coal pitch would not have pyrolytic quinoline insolubles present, but might have inorganic mineral matter or fixed carbon present. Thus, an effective mesophase pitch precursor would have to be centrifuged to remove most of the particulates. The required levels have not been determined experimentally, although proof of concept has been accomplished using precursor pitches that are greater than 99.9% liquid phase. Because additional thermal processing is required, it is estimated that the total yield of mesophase pitch would be somewhat lower than the corresponding yield of binder pitch. Yet, as shown in **Table 1**, the ultimate market potential for mesophase is probably only a few thousand barrels per year. Thus mesophase pitch can be considered as a high value niche product, but might not represent a sufficiently large market for large scale production. The output product summary is contained in Table 12.

Table 12. Output Materials Value, Mesophase Pitch Production.

Output Product	Mass Fraction, %	Unit Value	Extended Value
Synthetic Crude (heavy)	65	\$574	\$373
FUTUREGEN fuel	15	\$8	\$1
Mesophase Pitch	20	\$1,400	\$280
Total Value (per ton)	100		\$654
Total Value (per barrel)			\$95
Net Value Added (per barrel)			\$71

d. *Production of an aromatic heavy Syncrude with co-production of needle grade coke.* Needle grade coke is normally produced from the residues created by the delayed coking of high quality decant oil. Alternatively, an aromatic heavy crude might be used as a substitute for decant oil. The input material feedstock list would be similar to that shown in Table 10, with the products described in Table 13. The world market price for needle coke is over a million tons per year, making it a suitable niche product for a small refinery used for coal liquids. The yield of needle grade coke is small, because the coking operation required to produce needle grade coke removes volatile components from this product stream via thermocracking, thereby permitting increased yield of a crude hydrocarbon component.

Table 13. Output Materials Value, Needle Coke Production.

Output Product	Mass Fraction, %	Unit Value	Extended Value
Synthetic Crude (heavy)	75	\$574	\$431
FUTUREGEN fuel	15	\$8	\$1
Needle Grade Coke	10	\$595	\$60
Total Value (per ton)	100		\$491
Total Value (per barrel)			\$72
Net Value Added (per barrel)			\$57

The results suggest that carbon products produced from low hydrogenation levels via a direct liquefaction process result in increased value added compared to the light crudes that could be produced from a more severe hydrogenation. This is primarily due to the fact that hydrogen is relatively expensive compared to the hydrocarbon crudes that are sought. In addition, significantly less processing is involved in producing an aromatic heavy synthetic crude, which likely results in much lower processing cost in order to produce a heavy aromatic synthetic crude versus a light synthetic crude. Accordingly, since it requires less effort, lower energy, less material expense and results in more net revenue, profitability may favor lower hydrogenation levels. Nevertheless, most of the direct liquefaction efforts worldwide appear to be aimed at high hydrogenation levels and maximization of liquid fuels.

The energy balance is problematic because of the large number of chemicals present and the different possible reactions that can occur, as well as the different sources of energy loss (e.g., thermal insulation loss). Thus it is a highly empirical quantity. Malhotra estimated that the overall thermal energy efficiency of direct liquefaction processes to produce a light crude is roughly 65%.²⁶ A process with lower hydrogenation levels would presumably be more efficient due to decreased residence time and lower enthalpy change in the hydrogenation step.

Thermal losses probably account for about half of the thermal energy required for coal liquefaction, as estimated by considering effects such as heating of coal tar distillate, enthalpy of hydrogenation, heating of a coal/solvent slurry, enthalpy of digestion, separations energy, distillation energy, etc. These quantities can be estimated using the parameters listed in Table 14 below, combined with the previously calculated mass balances. Thermophysical property data was estimated from literature values.²⁷ The centrifuge power requirement was extrapolated based on the manufacturer's rating for a Sharples Pennwalt decanter-type centrifuge.

Table 14. Summary of Parameters Used to Calculate Energy Balance.

Parameter	Value
Specific heat of coal tar distillate	2.1 kJ/kg°C
Heat of Vaporization of coal tar distillate	300 kJ/kg
Specific heat of coal	1.2 kJ/kg°C
Centrifuge electric power requirement	90 kJ/kg
Centrifuge Tails Heating Value	15 MJ/kg
Coal Heating Value	30 MJ/kg
Solvent Heating Value	40 MJ/kg
Hydrogen Heating Value	120 MJ/kg

The energy required to hydrotreat may be modeled as a sensible heat rise of coal tar distillate, based on a CTD/coal ratio of 2:1, or

$$\dot{q}_{HT} = m_{CTD} C_{CTD} (T_{CTD2} - T_{CTD1}) \quad ,$$

where m_{CTD} is the mass of coal tar distillate, equal to at least twice the mass coal slurried; C_{CTD} is the specific heat of the coal tar distillate, and T_{CTD2} is the peak hydrogenation temperature, and T_{CTD1} is the initial temperature. To this, an additional penalty for the enthalpy of reaction (that is, hydrogenation) and thermal losses should be added. These terms are probably comparable in magnitude to the sensible heat.

In the pilot scale system, the solvent is permitted to cool down to under 200 °C in order to permit the vapor pressure to decrease to a near-atmospheric level before coal is added. Although it is possible that the coal and solvent could be combined at a higher temperature in a commercial system, it is probably conservative to assume that the solvent would be reheated by about half the original temperature rise. That is,

$$\dot{q}_D = m_{CTD} C_{CTD} (T_{CTD4} - T_{CTD3}) + m_{Coal} C_{Coal} (T_{CTD4} - T_{Coal1})$$

where T_{CTD3} is the temperature to which the hydrotreated coal tar distillate is cooled, T_{CTD4} is the temperature to which the slurry is heated, m_{coal} is the mass of coal slurried with the solvent, C_{coal} is the specific heat of coal, and T_{Coal1} is the starting temperature of the coal.

The separations energy assumes that a single pass is sufficient to remove solids. Distillation energy is calculated as the energy required to raise the temperature of a model compound to the appropriate boiling temperature, plus the enthalpy of vaporization.

The processes are summarized in Figure 10. The estimates are considered preliminary, based on literature values and engineering estimates, and are not backed up by hard experimental data. It might also be noted that if this plant were collocated with a coal gasification plant such as FutureGen, process heat might be available at reduced cost. However, for the purposes of an engineering estimate, this possibility was ignored. Thus, the energy value of the input feedstocks is estimated at 117.25 MWH (100 MWH of which is coal), and the energy value of the output feedstocks is 87.4 MWH, for an overall efficiency of 74.5%.

This is reasonable in light of Malhotra's estimate of 65% for a process involving severe hydrogenation levels (i.e., 10% hydrogen addition versus less than 1%). Lower hydrogenation level implies lower temperature, lower pressure, shorter residence time and reduced enthalpy of reaction, all of which suggest that efficiency should be inversely correlated to hydrogenation level.

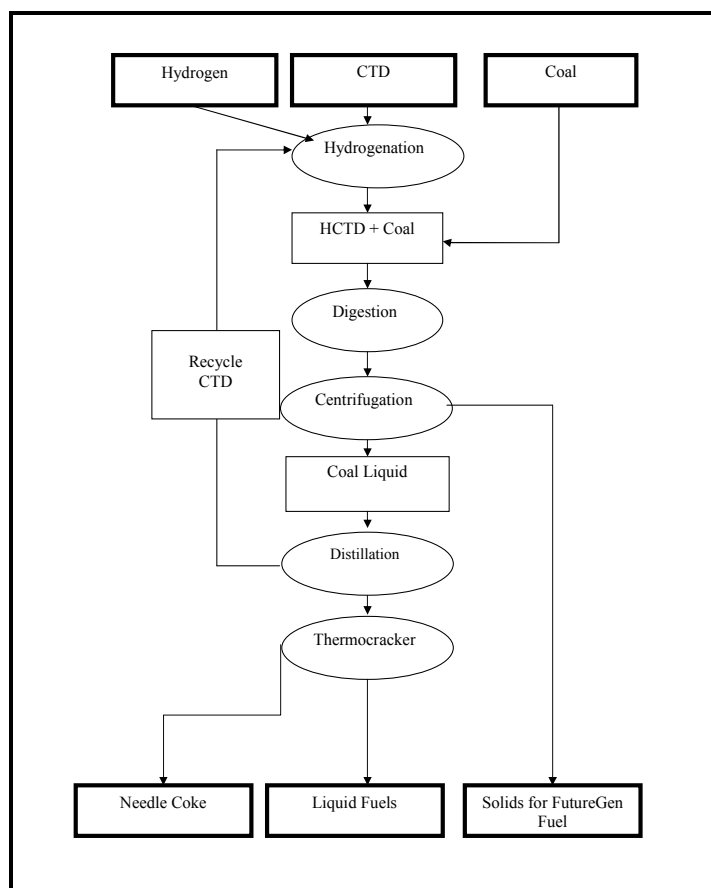


Figure 10. Flowchart for direct liquefaction processes involving needle coke.

III. EXPERIMENTAL

3.1 Experimental Procedures

3.1.1 Reactor Fill Procedure

A high pressure stirred autoclave reactor was used for reactions including digestion, hydrogenation, hydrodesulfurization and other variations. “Hydrogenation” refers to the addition of hydrogen to the working media, in a chemical absorption reaction, typically at pressures of 1000 psig or higher. “Hydrodesulfurization” refers to the use of hydrogen to remove sulfur from the medium by creating hydrogen sulfide. “Hydrotreatment” is sometimes used interchangeably with hydrodesulfurization but other times is used in a more general sense to encompass several or all of the reactions that might occur to alter the properties of the working medium.

These experiments were carried out in two separate locations. A ten gallon reactor was installed in a separate building located opposite the Engineering Science Building. A five gallon reactor was located in Room 317, Engineering Research Laboratory, shown schematically in Figure 11. Specific safety features are described below:

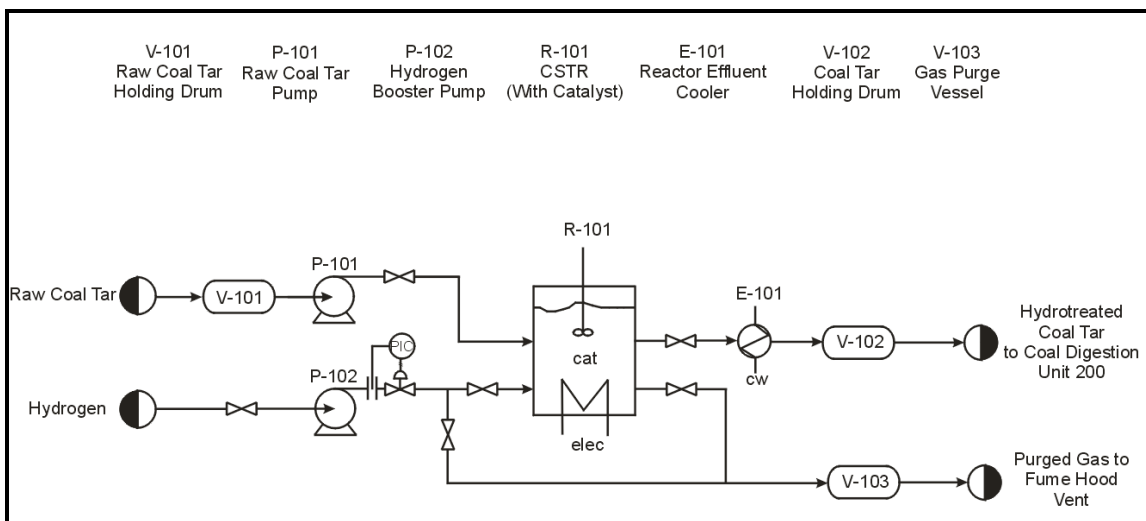


Figure 11. Overview of the Reactor System.

A pressure relief valve (PRV) is mounted on the top (rear) of the hydrogenation reactor, in series with the original equipment manufacturer’s rupture disk (See Figure 12). The rupture disk is designed to yield at 3000 psig. When a flammable mixture is used, however, a rupture disk is not necessarily the best solution, because it results in immediate dispersion of the flammable mixture throughout the fume hood; should that somehow ignite. Accordingly, the PRV permits only the excess gas to be released, and then continues to hold pressure. The PRV vents into the 50 gallon holding tank located in Fume Hood 2, which slowly vents the contents to

the fume hood. The holding tank has a needle valve which is normally open, with a flame arrestor at the end of it, permitting flammable gas to be slowly vented over a period of at least 15 minutes, thus ensuring that the effluent will remain below the lower explosive limit (LEL) at all times. In addition, a pressure gauge is installed between the rupture disk and PRV. Thus, when the rupture disk yields, the pressure gauge reads some finite pressure, providing the operator a sign that the rupture disk has yielded.



Figure 12. High Pressure Autoclave Reactor, with Pressure Relief Valve and Gauge visible in the background.

A holding tank is used to allow the operator to vent gases from the reactor, as shown in Figure 13 below. The volume of the holding tank is 50 gallons and the pressure rating is 200 psig. At ambient temperature, this corresponds to 3200 standard liters. By comparison, during normal operation the reactor should have no more than about 1.5 gallons of head space at 2000 psig or less, corresponding to 232 standard liters. Even if the reactor were to be (accidentally) filled with pure hydrogen at 3000 psig, this is still only 350 standard liters. Therefore, in the unlikely event that the reactor were to suddenly release all of its contents, the contents would not be dispersed into the fume hood, but instead would be contained in the holding tank. It would then slowly vent through a needle valve and flame arrestor at the top of the tank over a period of 15 minutes or longer.



Figure 13. The blue tank in the rear is a holding tank to allow vented gas to be temporarily stored and slowly vented.

The purpose of the flame arrestor is to ensure that, in the unlikely event that air is mixed with the hydrogen and coal tar vapors, and is somehow ignited, the flame will not propagate back through the piping to the holding tank or the reactor.

An electrical grounding cable is used to ground the reactor and the product holding tank (that is, a 55 gallon drum that contains the product). This assures that a potential difference can not be created between the product and the holding tank, minimizing the probability of a static discharge.

A tank of water is used to cool the product as it is released from the reactor. The product leaves the reactor at 400 °C, and is cooled to about 100 °C or below at the exit point. The vessel itself is close to ambient temperature. By reducing the temperature of the product, the vapor pressure is reduced and the chances of reaching an explosive or flammable concentration of vapor are minimized.

An additional step is to continuously bleed a small amount of nitrogen to the product tank, thus inerting the contents and reducing the ability of the atmosphere to feed any fire or explosive situation that might otherwise be created.

The power cable is doubly insulated, using a PVC duct to protect it against chemical spills or “wear and tear.” Thermal insulation is used to ensure that the product line can not accidentally contact the polymer insulation and melt it.

A pneumatically driven pump is used to transfer the neat solvent (Koppers coal tar distillate) and the reactor. This can be operated without opening the reactor, so that the contents are not exposed to air.

3.1.2 Hydrogenation Protocol

PPE Requirement: Flame resistant lab coat, goggles, steel-toed shoes, chemically resistant gloves are mandatory.

1. Coal Tar Distillate (CTD) should be liquid enough to pump. If not, heat to about 70 °C in 55 gallon drum overnight.
2. The reactor must be depressurized. Pressure is released by opening Valve 1 and 2 to release gas to the vent tank. The vent tank valve should be open to allow gas to be bled in the fume hood at a slow rate. Valve 3 should be closed.
3. Weigh the barrel of CTD and record in the lab book. Open valve 4 and turn on the air-actuated pump (prime if necessary). Transfer 27 lbs max of CTD to the reactor.
4. Close valves 1, 2, 3 & 4 are off, and make sure that the fume hoods are on and functioning and that water coolant is flowing to the Magnadrive and water cooling heat exchanger.
5. Purge the reactor by pressurizing to ~100 psig and releasing the gas to the holding tank. Nitrogen is preferred since it is inert, but hydrogen can also be used.
6. If necessary, tighten bolts on reactor to 200 ft-lbs torque using a torque wrench. The sequence of bolt tightening is based on a “star pattern” posted above the reactor. The bolts should be tightened by increments using a torque wrench to 100, 150, 200, 200 and 200 psig, or until the torque wrench no longer rotates the bolts.
7. Turn on heat to the reactor.
8. Monitor the temperature and pressure every five minutes or as directed by the supervisor.
9. ***If the reactor has not been externally pressurized and the pressure goes above 200 psig at less than 400 °C, this means that the reactor may be overfilled, and a potential overpressure situation may be created. Immediately turn off the heater power, turn off the Magnadrive, and then vent the product line, Valve 3. At least 3.0 liters should be released. If this is not effective, immediately initiate the emergency shutdown procedure.
10. The target reactor temperature can be determined by the supervisor, but should be less than 450 °C. If the reactor temperature exceeds 460 °C, immediately initiate the reactor shutdown procedure.
11. As the reactor approaches within 25 °C, of the target, adjust the temperature limit device to ensure temperature overshoot is minimized.
12. Pressurize the reactor by opening the valve at the hydrogen tank. The target pressure can be determined by the supervisor, but should never exceed 2200 psig. If the pressure reaches

this level, vent the reactor gas from Valve 1. If this not effective, immediately initiate the emergency shutdown procedure.

13. Within 5 minutes of pressurizing the reactor, a flammable gas detector should be used to determine if any flammable gas is present near the system.

14. When hydrogenation is complete, record final time, temperature, and pressure.

15. Turn off valve to hydrogen source.

16. Turn off stirrer and heater switch.

17. Using insulated gloves, open the reactor outlet, Valve 3, to the product drum and slowly empty liquid contents of reactor. This process should take 15 minutes or longer. When the pressure drops to 1000 psig, valve off the flow and take a test tube sample for Fourier Transform Infrared (FTIR) or Nuclear Magnetic Resonance (NMR) testing. Then resume draining the reactor. When the reactor seems to be completely drained, turn off Valve 3, and open Valve 1 to refill the reactor.

18. At the end of the day turn off the lever switches to the hydrogenation reactor and Magnadrive, by pulling both levers down. Ensure that the hydrogen gas is valved off at the bottle, at the regulator and also with the black valve after the regulator.

3.1.3 Coal Digestion and Solvent Extraction

PPE Requirement: Flame resistant lab coat, goggles, steel-toed shoes, chemically resistant gloves are mandatory.

The following procedure is used for digestion:

1. A slurry is first made by combining the Hydrogenated Coal Tars with the crushed coal in a small feed vessel. The coal is crushed to a particle size of approximately -50 mesh and dried to eliminate any free moisture. The normal ratio is 2:1 (solvent: coal).

2. Verify that the reactor vents are all open.

3. Turn on the heat to the feed vessel.

4. Stir the feed vessel at 450 rpm for about 30 minutes or until the mixture is fluid enough to be easily transferred into the 10 gallon reaction vessel. The temperature set point is 90 °C.

5. The feed vessel is then hoisted above the reaction vessel and the slurry is drained into the reactor, making sure, firstly, that the reactor vents are all open.

6. Once all of the contents of the feed vessel are in the reaction vessel, the reactor is then sealed and the feed port plug is torqued to 150 ft-pounds to ensure a good seal is made.
7. Close all vents on the reaction vessel. The reactor is now prepped for the reaction.
8. After the reactor is completely sealed, the stirrer is increased to 750 rpm and the reaction heater is turned on and set at 420°C.
9. The process temperature, reactor pressure, and the hour and minute of the day, is then recorded every 15 min. to insure that successive runs are consistent with each other as well as giving early warning signs that could indicate a problem with the reactor at reaction temperatures.
10. Once the process temperature reaches the reaction temperature, typically 350 °C to 420°C, a data point is then taken every 5 min. for one hour to record the relationship between the reaction and the process pressure in the reactor.
11. Once the process temperature has remained at 420°C for one hour, the reaction is assumed to be over, the process heater is turned off and the process is ready to be cooled.

3.1.4 Nitrogen Ram

1. During the heating and reaction process some of the un-dissolved coal may settle in the section of pipe between the valve and the vessel and may form a plug that becomes compacted by the high pressures during the reaction process. This plug is broken free by forcing nitrogen at high pressures through the bottom of the reactor.
2. Upon cooling to 150°C the reactor is still under pressure. The stirrer should be slowed back to 450 rpm before the reactor can be vented.
3. Open reactor vent slightly to allow the pressure to vent slowly. Releasing the pressure too quickly will cause the contents in the reactor to be pushed out of the reactor through the vent line. Once the pressure in the reaction vessel reaches zero psi, close the vents on the reactor to prepare to use the air ram.
4. When the vents are closed and the pressure is at zero in the reaction vessel, the tank that supplies nitrogen to the air ram should be turned on. The regulator should be set between 200 and 400 psi. After pressurizing the air ram, open the valve to the reactor before opening the valve to the air ram, then close the valve to the air ram before closing the valve to the reactor.
5. Repeat Step 4 repeatedly, stepping up the pressure as needed, until the plug breaks loose.
6. After the plug is broken free check the pressure in the reaction vessel. If the pressure is over 70 psi, slowly vent the pressure for the reactor. If not, check to make sure the vent valve is closed and then open the valve to the nitrogen line.

3.1.5 Hydrogen Tank Replacement

PPE Requirement: Flame resistant lab coat, goggles, steel-toed shoes, chemically resistant gloves are mandatory.

1. Valve off the hydrogen tank as well as the valve downstream from the regulator and the black valve downstream from the regulator valve.
2. Remove the empty hydrogen tank. Note that hydrogen regulator threads are left-tighten, right-loosen.
3. Bring in the new hydrogen tank and strap. Attach the regulator.
4. Check for hydrogen leaks using the combustible gas detector and/or Snoop (soap bubbles).

3.1.6 Centrifugation

Centrifugation capability was significantly enhanced by the addition of a larger compressor. As noted previously, the centrifuge is designed to operate with some 100 psig input pressure, but the house air supply was not sufficient to supply the full required pressure.

Accordingly, a Sullair rotary air compressor was purchased and refurbished in order to supply increased air flow. This was complicated by the lack of 3 phase 230 VAC power in the laboratory. Instead, 3-phase 208 VAC was available. It was determined that the compressor was operating in an off-optimum mode due to the lower voltage, so a step-up transformer was used to boost the input voltage to the required level. A second issue was the bearing surfaces between the stationary spindle and the rotor in the centrifuge. Although it was realized previously that all bearing surfaces need to be lubricated for optimum effectiveness, a review of the cleaning protocol revealed that a bearing surface in the lid of the unit was being unintentionally ignored.

After correcting these issues, the centrifuge appeared to be operating at a much higher effectiveness.

However, the centrifuge was not able to achieve low ash levels. For the manufacture of needle coke, GrafTech specifications require an ash level of 0.02% for a 100% synthetic needle coke, or a factor of 25 below the requirement for binder pitch @20/80 ratio.

With Kingwood coal, the centrifuge (prior to increasing the input voltage as mentioned above) was able to achieve an ash level of only about 0.4%.

After making the corrections described above, the collection efficiency was dramatically improved, but the ash level did not drop as much as expected. The reasons for this are discussed below.

3.1.6.1 Lower Kittanning Centrifuge Trials

Approximately 30 gallons of extract was manufactured using recovered solvent and Lower Kittanning sub-bituminous coal. The solvent/coal ratio was 3:1. Ash was removed via centrifugation. The temperature was kept at 50 °C to 70 °C in order to produce a low viscosity fluid. Additional recovered light liquids were added prior to the 10-1 run in order to make up for evaporative losses.

Proximate analysis results revealed a disappointing trend, as shown in Table 15 and Table 16. The ash fraction in the centrifuge tails was initially measured at about 10%, versus an ash fraction in the liquid centrate of about 0.7%, meaning a separation ratio of about 14.

Subsequent trials were less effective, producing yield of only 2-3 pounds after 4 hours of centrifugation, consistent with a centrifuge with less than optimal performance. The low ash yield in the 9-21 data suggests that very little difference was established between the centrate and the tails during that run.

Moreover, the centrate was not cleaned effectively, resulting in an ash content of 0.7%, which is probably too high for anode grade coke as well as the more stringently-specified needle grade coke.

Table 17 and Table 18 summarize the results of Elemental Analysis for Lower Kittanning coal, as received from the Kingwood Mine Prep Plant. The sulfur content is about 1.5%, corresponding to a sulfur to carbon mass ratio of about 1.9% (see Table 19).

Table 20 summarizes the progression of H/C, S/C and N/C in the centrifuge tails after successive runs in a Spinner II centrifuge, with an average residence time of about four hours. Table 21 shows the ratios for the clean centrate. Elemental Analysis runs are shown in Table 22 through Table 31.

Table 15. Proximate Analysis of Lower Kittanning Coal in Centrifuge Tails.

Name	Moisture	Volatile	Ash
9-18-07KWC S 1	3.36	62.68	9.04
9-18-07KWC S 2	2.88	64.46	8.67
9-18-07KWC S 3	3.19	64.53	8.67
9-21-07KWC S 1	3.98	73.84	2.84
9-21-07KWC S 2	4.51	75.5	2.17
9-21-07KWC S 3	4.55	75.95	1.83
9-27-07KWC S 1	2.6	65.51	9.64
9-27-07KWC S 2	2.83	65.32	9.73
9-27-07KWC S 3	2.72	65.31	9.93
10-1-07KWC S 1	1.65	65.22	10.61
10-1-07KWC S 2	2.08	64.71	10.72
10-1-07KWC S 3	2.07	65.26	10.31
10-2-07KWC AF S 1	2.54	69.84	7.33
10-2-07KWC AF S 2	2.97	71.86	5.94
10-2-07KWC AF S 3	2.51	74.71	4.49
10-3-07KWC AF S 1	2.02		8.53
10-3-07KWC AF S 2	2.2		8.53
10-3-07KWC AF S 3	2.52	66.3	8.64

Table 16. Proximate Analysis of Centrate from Lower Kittanning Coal Extract.

Name	Moisture	Volatile	Ash
9-17-07KWC L 1	4.57	80.5	1.08
9-17-07KWC L 2	4.85	80.38	1.11
9-17-07KWC L 3	4.66	80.63	1.05
9-18-07KWC L 1	5.48	77.05	0.98
9-18-07KWC L 2	5.92	76.44	1.01
9-18-07KWC L 3	5.8	76.63	0.98
10-1-07KWC AF L 1	2.62	81.58	0.72
10-1-07KWC AF L 2	3.31	80.9	0.74
10-1-07KWC AF L 3	4.26	80.01	0.74
10-2-07KWC B4 L 1	2.85	81.49	0.74
10-2-07KWC B4 L 2	2.82	81.46	0.69
10-2-07KWC B4 L 3	3.05	81.24	0.66
10-3-07KWC B4 L 1	2.98	81.22	0.72
10-3-07KWC B4 L 2	3.9	80.44	0.71
10-3-07KWC B4 L 3	3.74	80.5	0.69

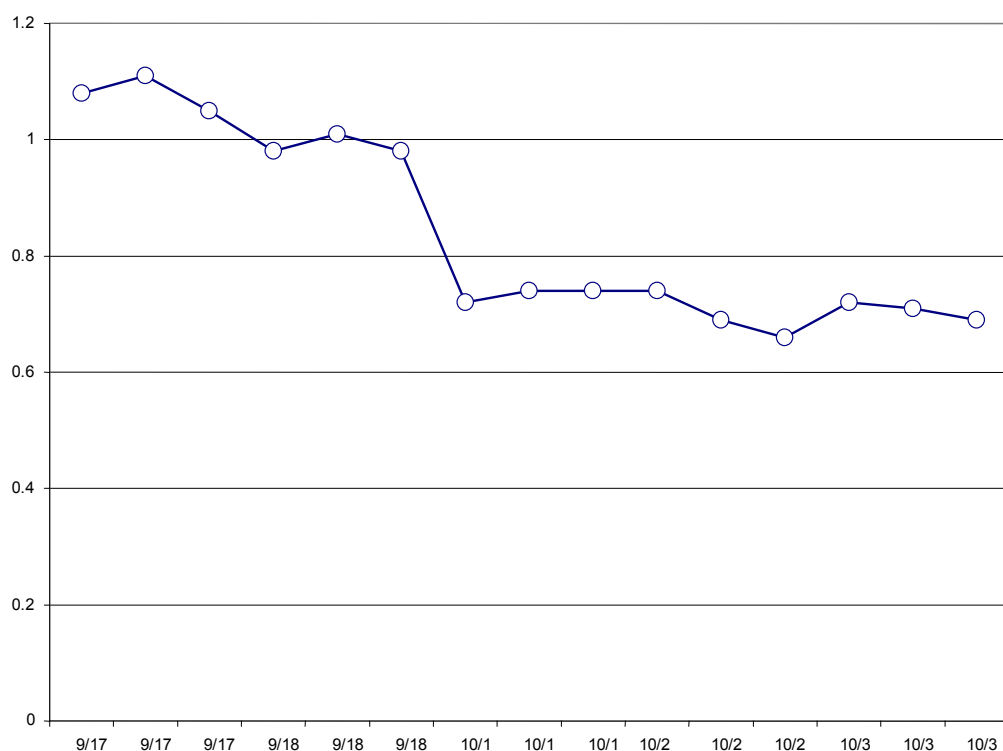


Figure 14. Ash Content (percent) as a function of centrifuge time.

Table 17. Lower Kittanning Prepped Coal, Elemental Analysis, Raw Data.

Group No : 6	Element %			
Sample Name	Nitrogen%	Carbon%	Hydrogen%	Sulfur%
Kwood ROM Coal	1.657230258	77.03638458	5.097712517	1.90096283
Kwood ROM Coal	1.706855059	78.63188934	5.099193573	1.191754818
Kwood ROM Coal	1.644464374	78.05722809	5.089699745	1.408089995

Table 18. Lower Kittanning Elemental Analysis, Average Values.

3 Sample(s) in Group No : 6				
Component Name	Average	Std. Dev.	% Rel. S. D.	Variance
Nitrogen%	1.669516563	0.03296004	1.9742	0.0011
Carbon%	77.90850067	0.8080834	1.0372	0.653
Hydrogen%	5.095535278	0.005107687	0.1002	0
Sulfur%	1.500269214	0.3634787	24.2276	0.1321

Table 19. H/C, S/C and N/C for Clean Lower Kittanning Centrate.

	H/C ratio	S/C ratio	N/C ratio
Lower Kittanning Prepped Coal	0.065404	0.019257	0.021429

Table 20. Progression in H/C, S/C and N/C for Lower Kittanning Centrifuge Tails.

	H/C ratio	S/C ratio	N/C ratio
Lower Kittanning Centrifuge Tails 2007 0917	0.070719	0.000724	0.009598
Lower Kittanning Centrifuge Tails 2007 0918	0.068264	0.006583	0.010892
Lower Kittanning Centrifuge Tails 2007 0921	0.07043	0.000849	0.00833

Table 21. H/C, S/C and N/C for Clean Lower Kittanning Centrate.

	H/C ratio	S/C ratio	N/C ratio
Lower Kittanning Centrate 2007 0918	0.07001	0.00065	0.008465

Table 22. Lower Kittanning (Kingwood) Centrifuge Tails Elemental Analysis, Raw Data, 0917.

Group No : 1	Element %			
Sample Name	Nitrogen%	Carbon%	Hydrogen%	Sulfur%
09-17-07 KWC S	0.90368396	88.18517303	6.134052753	0.031087967
09-17-07 KWC S	0.80128789	89.02332306	6.34750843	0.106475607
09-17-07 KWC S	0.854052723	89.41292572	6.373677731	0.055457313

Table 23. Lower Kittanning (Kingwood) Centrifuge Tails Elemental Analysis, Avg Values.

3 Sample(s) in Group No : 1				
Component Name	Average	Std. Dev.	% Rel. S. D.	Variance
Nitrogen%	0.853008191	0.05120603	6.003	0.0026
Carbon%	88.87380727	0.6273838	0.7059	0.3936
Hydrogen%	6.285079638	0.131446	2.0914	0.0173
Sulfur%	0.064340295	0.03847083	59.7927	0.0015

Table 24. Lower Kittanning (Kingwood) Centrifuge Tails Elemental Analysis, Raw Data.

Group No : 2	Element %			
Sample Name	Nitrogen%	Carbon%	Hydrogen%	Sulfur%
09-18-07 KWC S	0.831915259	81.81243896	5.64530468	0.546172977
09-18-07 KWC S	0.926286519	81.67047119	5.558180332	0.519613743
09-18-07 KWC S	0.912652493	81.73438263	5.536105156	0.548517644

Table 25. Lower Kittanning (Kingwood) Centrifuge Tails Elemental Analysis, Avg Values.

3 Sample(s) in Group No : 2				
Component Name	Average	Std. Dev.	% Rel. S. D.	Variance
Nitrogen%	0.890284757	0.05100706	5.7293	0.0026
Carbon%	81.7390976	0.07110123	0.087	0.0051
Hydrogen%	5.579863389	0.05773864	1.0348	0.0033
Sulfur%	0.538101455	0.01605369	2.9834	0.0003

Table 26. Lower Kittanning (Kingwood) Centrifuge Tails Elemental Analysis, Raw Data.

Group No : 4	Element %			
Sample Name	Nitrogen%	Carbon%	Hydrogen%	Sulfur%
09-21-07 KWC S	0.748035371	88.96126556	6.290157318	0.072676279
09-21-07 KWC S	0.707199633	89.23164368	6.25555706	0.058516491
09-21-07 KWC S	0.769513309	88.88900757	6.264988422	0.09563987

Table 27. Lower Kittanning (Kingwood) Centrifuge Tails Elemental Analysis, Avg Values.

3 Sample(s) in Group No : 4				
Component Name	Average	Std. Dev.	% Rel. S. D.	Variance
Nitrogen%	0.741582771	0.031654	4.2684	0.001
Carbon%	89.0273056	0.1806124	0.2029	0.0326
Hydrogen%	6.270234267	0.01788669	0.2853	0.0003
Sulfur%	0.07561088	0.01873487	24.778	0.0004

Table 28. Lower Kittanning (Kingwood) Centrifuge Tails, Elemental Analysis, Raw Data.

Group No : 6	Element %			
Sample Name	Nitrogen%	Carbon%	Hydrogen%	Sulfur%
10-01-07 KWC OW S	0.780030012	89.17974854	6.414375305	0.070917636
10-01-07 KWC OW S	0.716904461	89.17779541	6.581765175	0.106611803
10-01-07 KWC OW S	0.739629388	88.71237946	6.502914906	0.108406216

Table 29. Lower Kittanning (Kingwood) Centrifuge Tails, Elemental Analysis, Avg Values.

3 Sample(s) in Group No : 6				
Component Name	Average	Std. Dev.	% Rel. S. D.	Variance
Nitrogen%	0.745521287	0.03197256	4.2886	0.001
Carbon%	89.0233078	0.2692736	0.3025	0.0725
Hydrogen%	6.499685129	0.08374166	1.2884	0.007
Sulfur%	0.095311885	0.02114508	22.1852	0.0004

Table 30. Lower Kittanning (Kingwood) Centrate Elemental Analysis, Raw Data.

Group No : 3	Element %			
Sample Name	Nitrogen%	Carbon%	Hydrogen%	Sulfur%
09-18-07 KWC L	0.725556254	88.89108276	6.192035198	0.057650957
09-18-07 KWC L	0.74326992	89.30202484	6.350174904	0.102118224
09-18-07 KWC L	0.801701784	90.0440979	6.237167835	0.014507738

Table 31. Lower Kittanning (Kingwood) Centrate Elemental Analysis, Avg Values.

3 Sample(s) in Group No : 3				
Component Name	Average	Std. Dev.	% Rel. S. D.	Variance
Nitrogen%	0.756842653	0.03984595	5.2648	0.0016
Carbon%	89.41240184	0.5843785	0.6536	0.3415
Hydrogen%	6.259792646	0.08146136	1.3013	0.0066
Sulfur%	0.058092306	0.04380691	75.4091	0.0019

It was clear that the point of diminishing returns had been reached, so efforts to further clean the extract were terminated, and modifications were made to the centrifuge as described previously. In the meantime Powder River Basin extract had been produced, and it was decided to investigate its properties.

3.1.6.2 Powder River Basin Centrifuge Trials

Sub-bituminous Powder River Basin (PRB) sub-bituminous coal is of great interest because of its great abundance, low sulfur and low price. Hence it was decided to carry out trials with this coal. At this time the centrifuge capability had been substantially upgraded.

A 55 gallon drum of extract was prepared using run-of-mine PRB coal. Because of the high moisture content of PRB coal, it is necessary to heat the coal to ~110 °C before permitting it to be loaded in a reactor. Nevertheless, it is supposed that substantial amounts of OH compounds are likely present and which might contribute to a high vapor pressure.

Although the continuously stirred tank reactor is fully capable of handling high pressure, for these experiments 2000 psig was set as the absolute limit. High vapor pressure also brings with it significant reflux cooling within the reactor unit. In this case, the 20-cm thick steel top of the reactor can act as a heat sink and greatly increase the ramp time to temperature and/or limit the maximum attainable temperature in the reactor.

This indeed proved to be problematic, and thus the digestion protocol was modified such that the digestion temperature was limited to 385 °C.

Experience with Lower Kittanning (Kingwood Mine) bituminous coal has indicated that a temperature of 415 °C is sufficient to guarantee substantial conversion of coal to the liquid state. Thus there was some uncertainty as to whether the reduced digestion temperature would be effective, especially in view of the fact that recovered solvent was being used rather than fresh solvent. Nevertheless, because the PRB mineral matter is clay-like rather than rock-like, as is the case for Lower Kittanning, it seems plausible that PRB coal might be easier to digest at somewhat lower temperature. The faster rise in vapor pressure may also imply increasing chemical activity in the reactor. At any rate, the experiments were carried out with a digestion temperature of 385 °C.

The first trial with the Spinner II Model 600 centrifuge appeared to meet expectations. Approximately 17 pounds of material was collected in a four hour trial, with a measure ash content of about 22% according to proximate analysis (see Figure 15). This was accompanied by a reduction of ash content in the product drum to 0.74%.

Three successive runs were also effective in accumulating a full load of material (~15 pounds) in the centrifuge rotor, making a total of 60 pounds removed from the 55 gallon drum. However, although the material in the rotor was definitely a clay-like solid at 50 °C (determined with a thermocouple probe within minutes of opening the unit), proximate analysis indicated that the material contained relatively low ash. By the last run, the solids contained only about 1% ash, versus 0.4% ash in the centrate, yet the tails were clearly solid.

The solution to this enigma is to suppose that there was a higher softening point phase in the solution. In other words, some polymeric material with a slightly higher density may have formed, causing it to be separated by the centrifuge.

In support of this hypothesis, Mettler softening point measurements reveal an apparent softening point of 85 °C in the nominal liquid phase, even though the substance appears to be a thick liquid at ambient temperature. Since centrifugation occurs at no higher than 70 °C, this is consistent with the view that some higher melting point phase is present in the solution along with a lower melting point carrier. Mettler results for the tails show a softening point of 125 °C

for the tails midway through the centrifugation process, and 185 °C for the tails at the completion of the processing.

This trend is borne out by the proximate and elemental analysis described below in Table 32 through Table 43.



Figure 15. Approximately 17 pounds of solid material was removed from PRB extract.

Table 32. Proximate Analysis Results for Centrifuge Tails with PRB Coal.

Name	Moisture	Volatile	Ash
PRB/RSC Solids 10-26-07	5.14	49.46	22.27
PRB/RSC Solids 10-26-07 2	5.08	50.12	22.14
PRB/RSC Solids 10-26-07 3	5.05	50.38	22.47
PRB/RSC Solids 10-29-07 1	4.56	69.45	4.11
PRB/RSC Solids 10-29-07 2	5.19	68.17	4.48
PRB/RSC Solids 10-29-07 3	5.95	65.83	4.99
PRB/RSC Solids 10-30-07 1	7.39	58.28	3.74
PRB/RSC Solids 10-30-07 2	6.88	59.29	3.7
PRB/RSC Solids 10-30-07 3	4.94	61.64	3.55
PRB/RSC Solids 10-31-07 1	5.5	80.86	1.06
PRB/RSC Solids 10-31-07 2	5.93	80.51	1.06
PRB/RSC Solids 10-31-07 3	4.24	81.96	0.96

Figure 16 shows the ash level in the centrifuge tails. An ideal centrifuge would show a nearly constant ash level, rather than the declining level observed. This is consistent with the presence of a phase with a high softening point but containing relatively little ash.

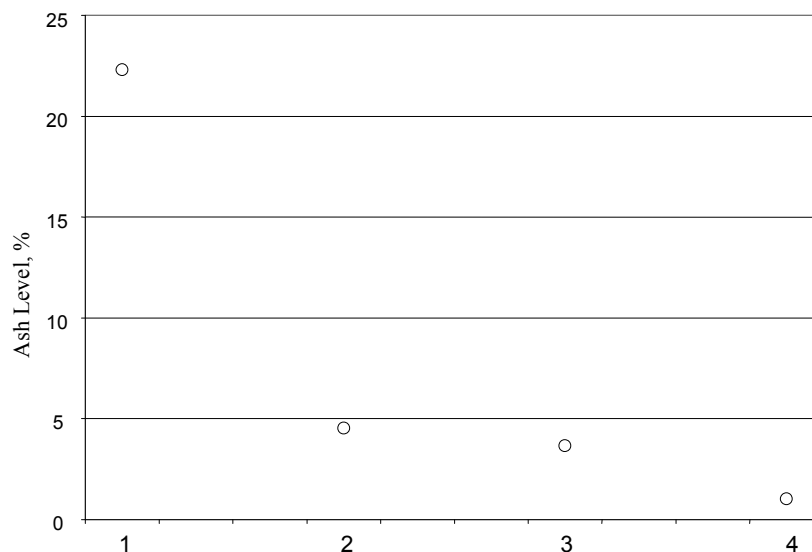


Figure 16. Ash Level in Centrifuge Tails.

Proximate analysis for the centrate shows that an initial cleaning was highly successful. The tails contained 22% x 17 lbs = 3.7 pounds of ash, yet subsequent trials removed much less ash from the centrate, as shown in Figure 17.

Table 33. Proximate Analysis Results for Centrate from PRB Coal Extract.

Name	Moisture	Volatile	Ash
PRB/RSC Liquids 10-26-07 1	3.05	79.96	0.74
PRB/RSC Liquids 10-26-07 2	3.83	79.01	0.76
PRB/RSC Liquids 10-26-07 3	3.85	78.75	0.8
PRB/RSC Liquids 10-30-07 1	7.77	81.6	0.42
PRB/RSC Liquids 10-30-07 2	7.07	81.77	0.48
PRB/RSC Liquids 10-30-07 3	8.41	78.87	0.49
PRB/RSC Liquids 10-31-07 1	7.59	83.46	0.42
PRB/RSC Liquids 10-31-07 2	6.73	83.98	0.43

As shown in Figure 17, the ash level in the centrate was not reduced below about 0.4%. This was sufficient to meet some commercial applications, but insufficient for impregnation pitch or conversion to mesophase pitch. However, since the rotor was filled with apparently solid product, the working fluid must have contained some high softening point phase(s).

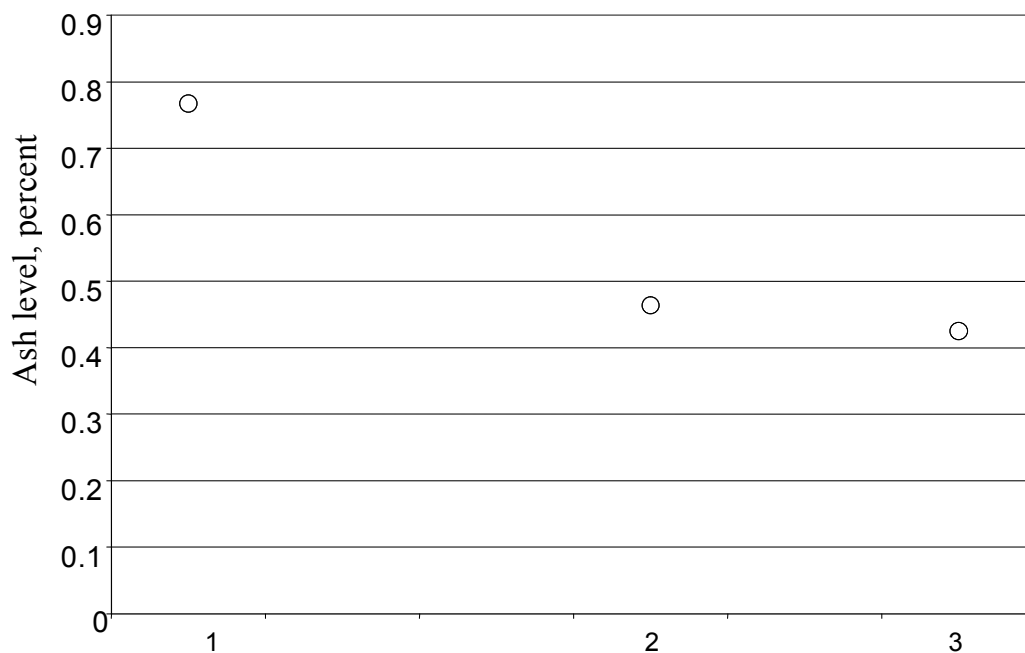


Figure 17. Ash Level in PRB Centrate.

Table 34. Powder River Basin Centrifuge Tails, Raw Data, 1026.

Group No : 1	Element %			
Sample Name	Nitrogen%	Carbon%	Hydrogen%	Sulfur%
PRB/RSC Solids 10-26-07	1.093943119	77.3214798	5.169940472	0.456435919
PRB/RSC Solids 10-26-07	1.024790049	72.57388306	4.817178249	0.65795362
PRB/RSC Solids 10-26-07	1.097207665	77.86791229	5.251233101	0.409735799

Table 35. Powder River Basin Centrifuge Tails, Avg Values, 1026.

3 Sample(s) in Group No : 1				
Component Name	Average	Std. Dev.	% Rel. S. D.	Variance
Nitrogen%	1.071980278	0.04090052	3.8154	0.0017
Carbon%	75.92109172	2.911615	3.8351	8.4775
Hydrogen	5.079450607	0.2307427	4.5427	0.0532
Sulfur%	0.508041779	0.1319106	25.9645	0.0174

Table 36. Powder River Basin Centrifuge Tails, Raw Data, 1029.

Group No : 3	Element %			
Sample Name	Nitrogen%	Carbon%	Hydrogen%	Sulfur%
PRB/RSC Solids 10-29-07	1.046601057	86.3208313	5.81327486	0.015859684
PRB/RSC Solids 10-29-07	1.066816807	85.79718018	5.867721081	0.119129784
PRB/RSC Solids 10-29-07	1.097691655	87.21548462	5.838663101	0.019864652

Table 37. Powder River Basin Centrifuge Tails, Avg Values, 1029.

3 Sample(s) in Group No : 3				
Component Name	Average	Std. Dev.	% Rel. S. D.	Variance
Nitrogen%	1.07036984	0.02572995	2.4038	0.0007
Carbon%	86.4444987	0.7171939	0.8297	0.5144
Hydrogen%	5.839886347	0.02724371	0.4665	0.0007
Sulfur%	0.05161804	0.05850117	113.3347	0.0034

Table 38. Powder River Basin Centrifuge Tails, Raw Data.

Group No : 4	Element %			
Sample Name	Nitrogen%	Carbon%	Hydrogen%	Sulfur%
PRB/RSC Solids 10-30-07	1.231309414	86.09437561	5.371357918	0.011369278
PRB/RSC Solids 10-30-07	1.213133335	85.30443573	5.354231834	0
PRB/RSC Solids 10-30-07	1.123520851	84.43251801	5.501383781	0.040964235

Table 39. Powder River Basin Centrifuge Tails, Avg Values.

3 Sample(s) in Group No : 4				
Component Name	Average	Std. Dev.	% Rel. S. D.	Variance
Nitrogen%	1.1893212	0.05770491	4.8519	0.0033
Carbon%	85.27710978	0.8312657	0.9748	0.691
Hydrogen%	5.408991178	0.08047124	1.4877	0.0065
Sulfur%	0.017444504	0.02114707	121.2248	0.0004

Table 40. Powder River Basin Centrate, Raw Data.

Group No : 2	Element %			
Sample Name	Nitrogen%	Carbon%	Hydrogen%	Sulfur%
PRB/RSC Liquids 10-26-07	0.837416351	90.49252319	6.408792973	0.056268808
PRB/RSC Liquids 10-26-07	0.853012443	89.90281677	6.461357117	0.142173231
PRB/RSC Liquids 10-26-07	0.878010035	90.27101898	6.493767262	0.111598253

Table 41. Powder River Basin Centrate, Avg Values.

3 Sample(s) in Group No : 2				
Component Name	Average	Std. Dev.	% Rel. S. D.	Variance
Nitrogen%	0.856146276	0.02047749	2.3918	0.0004
Carbon%	90.22211965	0.2978788	0.3302	0.0887
Hydrogen%	6.454639117	0.04288363	0.6644	0.0018
Sulfur%	0.103346764	0.0435426	42.1325	0.0019

Table 42. Powder River Basin Centrate, Raw Data.

Group No : 1	Element %			
Sample Name	Nitrogen%	Carbon%	Hydrogen%	Sulfur%
PRB Liquids	0.899367511	91.5116806	6.634878635	0.011611334
PRB Liquids	0.807782233	91.29979706	6.742752552	0.071325041
PRB Liquids	0.778650522	91.59593201	6.716526508	0.051018193

Table 43. Powder River Basin Centrate, Avg Values

3 Sample(s) in Group No : 1				
Component Name	Average	Std. Dev.	% Rel. S. D.	Variance
Nitrogen%	0.828600089	0.06299353	7.6024	0.004
Carbon%	91.46913656	0.1525827	0.1668	0.0233
Hydrogen%	6.698052565	0.05625976	0.8399	0.0032
Sulfur%	0.044651523	0.0303617	67.997	0.0009

3.1.6.3 Centrifugation Issues

Experimental measurements of viscosity of different material combinations suggest that a *rheopectic* (also referred to as *anti-thixotropic*) effect may be the root of centrifugation difficulties.

A Newtonian fluid is one that has a linear relationship between viscosity and shear stress. Conversely, some fluids are non-Newtonian and thus the viscosity can change with shear as well as time. In rheopectic fluids, the longer the fluid undergoes shearing force, the greater the viscosity, a phenomenon known as *shear thickening*.

In the case of centrifugation of coal liquids, when the centrifuge imparts shear to the dissolved coal slurry, the result is an increase in viscosity. When this happens, the fluid resists centrifugation, and it is difficult to obtain low ash levels. This is exactly what has occurred in material systems tested with hydrogenated oil (HO).

To test this hypothesis, viscosities were measured at about 50 °C, 70 °C and 90 °C for different concentrations of coal (identified as Alberta Coal by Quantex Energy Inc) dissolved in

coal tar distillate and agricultural oil. A Brookfield viscometer was used for this experiment. 25.67 g of Alberta Coal was dissolved in 70.42 g of coal tar distillate (from Koppers Inc) and 3.91 g of agricultural oil. Viscosity was measured using the standard viscometer. The experiment was repeated for the same amounts of samples with the hydrogenated oil. The different parameters associated with the viscosity measurement for the hydrogenated oil are given below.

In the case in which non-hydrogenated oil is included in the solvent blend, the viscosity shows only a slight time dependent effect. At 50 °C (see Table 44, Figure 18) the viscosity increases from 280 cP to 310 cP over a 20 minute period. Similar effects are observed at 70 °C and 90 °C, as shown in Table 45 and Table 46 as well as Figure 19 and Figure 20. In addition the equilibrium values of viscosity are seen to decrease with temperature, as expected.

However, for the case in which hydrogenated oil is used in the solvent blend, strongly non-Newtonian, rheopectic behavior is observed. As shown in Figure 21 (see also Table 47), the viscosity increases from 95 cP to 140 cP over a 24 minute period. Moreover, at higher temperatures, higher viscosity is observed instead of lower viscosity as given in Figure 22 and Figure 23 and Table 48 and Table 49. At 90 °C, the viscosity more than doubles over a 30 minute period.

Table 44. Viscosity data at 50 °C for 25.67 g of Alberta coal dissolved in 70.42 g of CTD and 3.91 g of unhydrogenated oil.

Time (min)	Temperature (°C)	RPM	Torque	Viscosity, cP	Shear Stress	Shear Rate
0:00	50.4	100	5.60%	280	78.4	28
2:00	50.3	100	5.80%	295	82.6	28
4:00	50.3	100	6.00%	300	84.0	28
6:00	50.4	100	6.10%	305	84.0	28
8:00	50.3	100	6.10%	305	84.0	28
10:00	50.3	100	6.10%	305	85.4	28
12:00	50.3	100	6.10%	305	85.4	28
14:00	50.3	100	6.10%	305	85.4	28
16:00	50.5	100	6.20%	305	86.8	28
18:00	50.3	100	6.10%	305	85.4	28
20:00	50.4	100	6.20%	310	86.8	28
22:00	50.4	100	6.20%	310	86.8	28
24:00	50.3	100	6.20%	310	86.8	28
26:00	50.3	100	6.20%	310	86.8	28
28:00	50.4	100	6.30%	310	86.8	28
30:00	50.4	100	6.30%	310	86.8	28
32:00	50.4	100	6.30%	310	86.8	28
34:00	50.4	100	6.30%	310	86.8	28

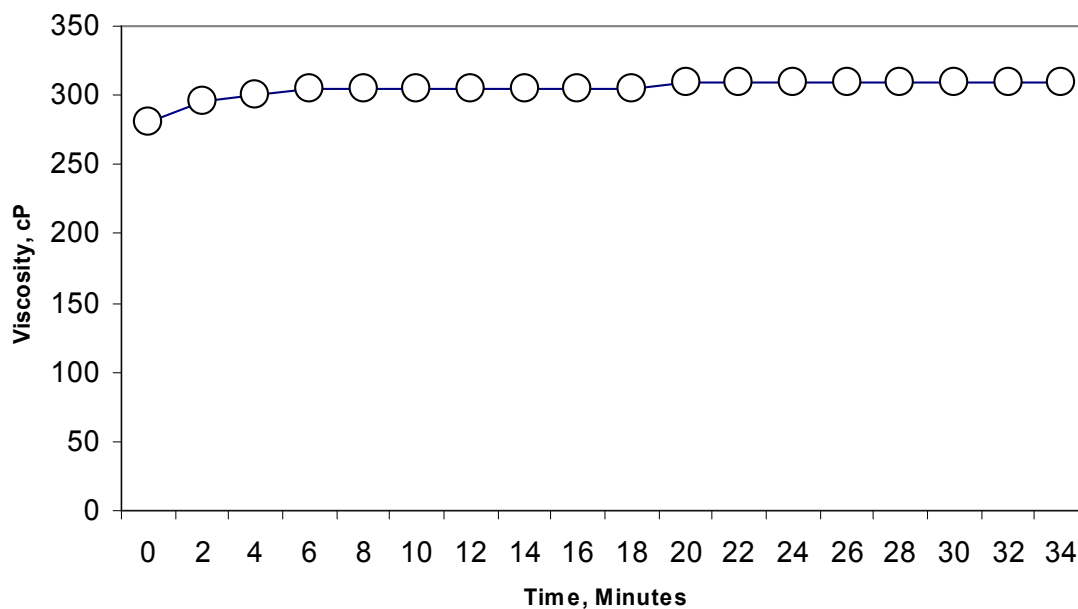


Figure 18. Viscosity at 50 °C for 25.67 g of Alberta coal dissolved in 70.42 g of CTD and 3.91 g of unhydrogenated oil.

Table 45. Viscosity data at 70 °C for 25.67 g of Alberta Coal dissolved in 70.42 g of CTD and 3.91 g of unhydrogenated oil.

Time (min)	Temperature (°C)	RPM	Torque	Viscosity, cP	Shear Stress, dyne/cm ²	Shear Rate sec ⁻¹
0:00	70.5	100	4.30%	210	60.2	28
2:00	70.5	100	4.20%	210	58.8	28
4:00	70.5	100	4.30%	215	60.2	28
6:00	70.3	100	4.40%	220	61.6	28
8:00	70.4	100	4.50%	225	63.0	28
10:00	70.4	100	4.50%	230	64.4	28
12:00	70.3	100	4.70%	230	65.8	28
14:00	70.4	100	4.80%	240	67.2	28
16:00	70.4	100	4.70%	240	65.8	28
18:00	70.3	100	4.80%	240	67.2	28
20:00	70.3	100	4.80%	240	67.2	28
22:00	70.4	100	4.80%	240	67.2	28
24:00	70.4	100	4.80%	240	67.2	28

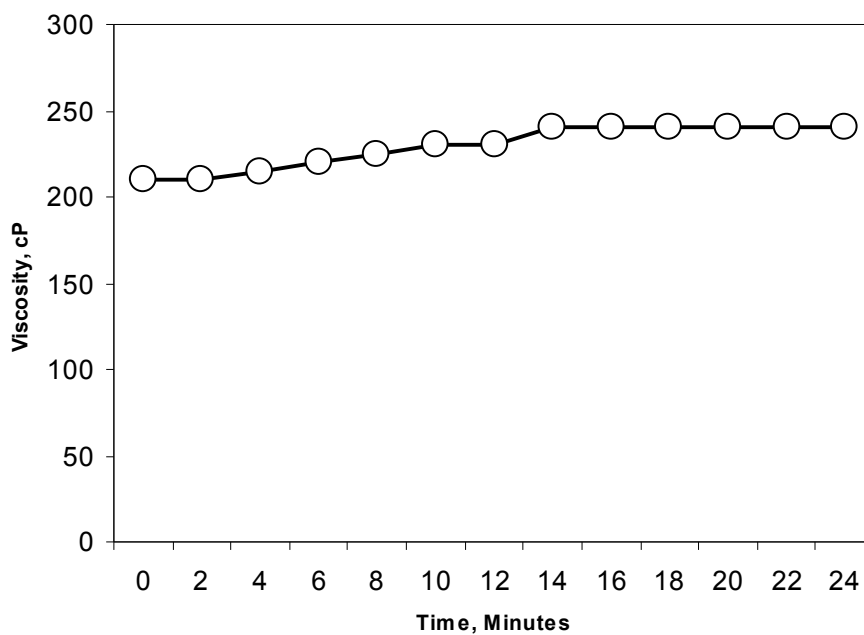


Figure 19. Viscosity at 70 °C for 25.67 g of Alberta coal dissolved in 70.42 g of CTD and 3.91 g of unhydrogenated oil.

Table 46. Viscosity data at 90 °C for 25.67 g of Alberta Coal dissolved in 70.42 g of CTD and 3.91 g of unhydrogenated oil.

Time (min)	Temperature (°C)	RPM	Torque	Viscosity, cP	Shear Stress, dyne/cm ²	Shear Rate sec ⁻¹
0:00	90.2	100	4.60%	230	64.4	28
2:00	90.2	100	4.60%	230	64.4	28
4:00	90.5	100	4.60%	230	64.4	28
6:00	90.4	100	4.60%	225	64.4	28
8:00	90.5	100	4.60%	230	64.4	28
10:00	90.4	100	4.70%	235	64.4	28
12:00	90.4	100	4.60%	230	64.4	28
14:00	90.4	100	4.60%	230	64.4	28
16:00	90.4	100	4.60%	230	64.4	28
18:00	90.5	100	4.60%	230	64.4	28
20:00	90.4	100	4.60%	230	64.4	28
22:00	90.3	100	4.60%	230	64.4	28
24:00	90.4	100	4.60%	230	64.4	28

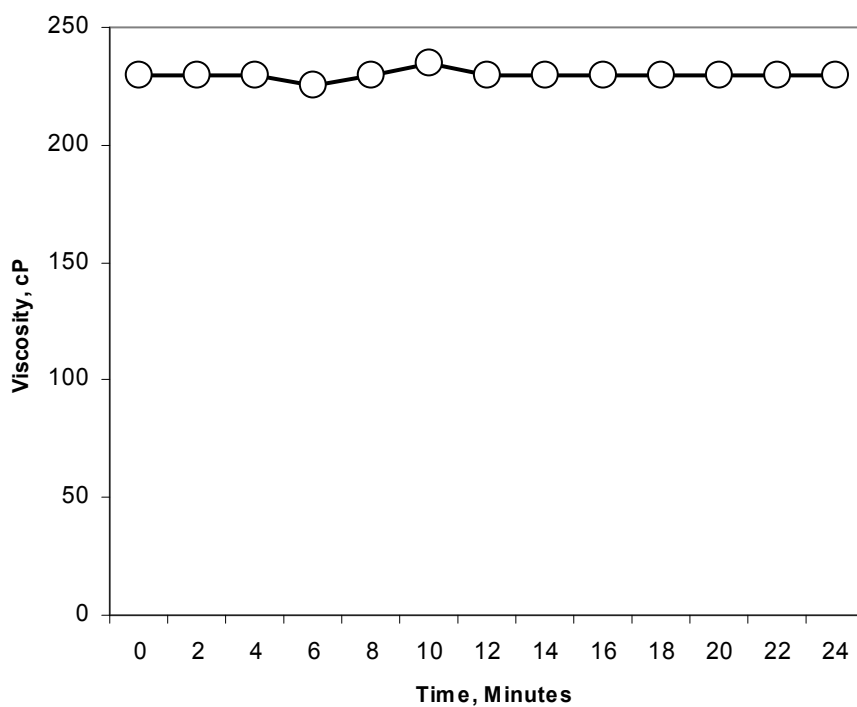


Figure 20. Viscosity at 90 °C for 25.67 g of Alberta coal dissolved in 70.42 g of CTD and 3.91 g of unhydrogenated oil.

Table 47. Viscosity at 50 °C for 25.67 g of Alberta Coal, 70.42 g of CTD and 3.91 g of hydrogenated oil.

Time (min)	Temperature (°C)	RPM	Torque	Viscosity, cP	Shear Stress, dyne/cm²	Shear Rate sec⁻¹
0:00	50.5	100	1.90%	95	26.6	28
2:00	50.5	100	2.10%	105	29.5	28
4:00	50.3	100	2.40%	125	33.6	28
6:00	50.4	100	2.50%	150	39.2	28
8:00	50.4	100	2.30%	120	30.8	28
10:00	50.3	100	2.50%	125	35	28
12:00	50.4	100	2.50%	130	35	28
14:00	50.4	100	2.60%	130	36.4	28
16:00	50.3	100	2.60%	135	36.4	28
18:00	50.3	100	2.80%	140	37.8	28
20:00	50.4	100	2.80%	135	37.8	28
22:00	50.4	100	2.70%	135	36.4	28
24:00	50.3	100	2.70%	140	37.8	28
26:00	50.3	100	2.80%	140	37.8	28
28:00	50.4	100	2.80%	140	37.8	28
30:00	50.3	100	2.80%	140	37.8	28
32:00	50.3	100	2.80%	140	37.8	28

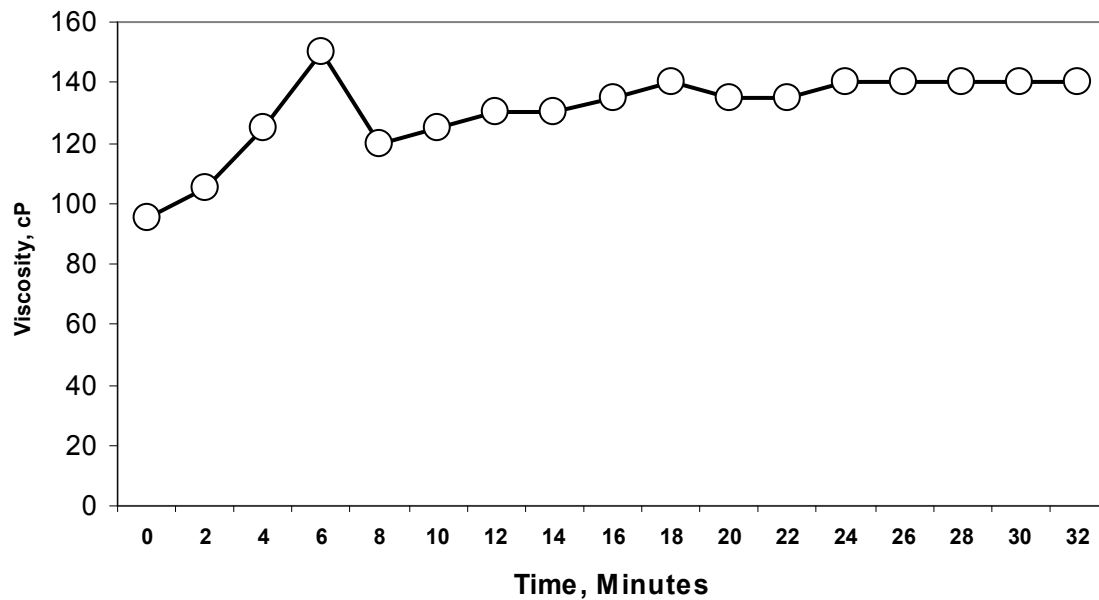


Figure 21. Viscosity at 50 °C for 25.67 g of Alberta coal dissolved in 70.42 g of CTD and 3.91 g of hydrogenated oil.

Table 48. Viscosity data at 70 °C for 25.67 g of Alberta Coal dissolved in 70.42 g of CTD and 3.91 g of hydrogenated oil.

Time (min)	Temperature (°C)	RPM	Torque	Viscosity, cP	Shear Stress, dyne/cm ²	Shear Rate sec ⁻¹
0:00	70.2	100	4.70%	230	64.4	28
2:00	70.5	100	4.30%	215	63.0	28
4:00	70.3	100	4.20%	210	58.8	28
6:00	70.4	100	4.20%	210	58.8	28
8:00	70.4	100	4.30%	215	60.2	28
10:00	70.3	100	4.30%	220	58.8	28
12:00	70.4	100	4.30%	220	60.0	28
14:00	70.4	100	4.30%	215	60.2	28
16:00	70.3	100	4.40%	215	60.2	28
18:00	70.3	100	4.50%	225	63.0	28
20:00	70.4	100	4.50%	225	63.0	28
22:00	70.4	100	4.40%	220	61.6	28
24:00	70.3	100	4.50%	225	63.0	28
26:00	70.3	100	4.60%	235	65.8	28
28:00	70.4	100	4.60%	235	65.8	28
30:00	70.3	100	4.80%	235	68.6	28
32:00	70.3	100	4.80%	235	65.8	28

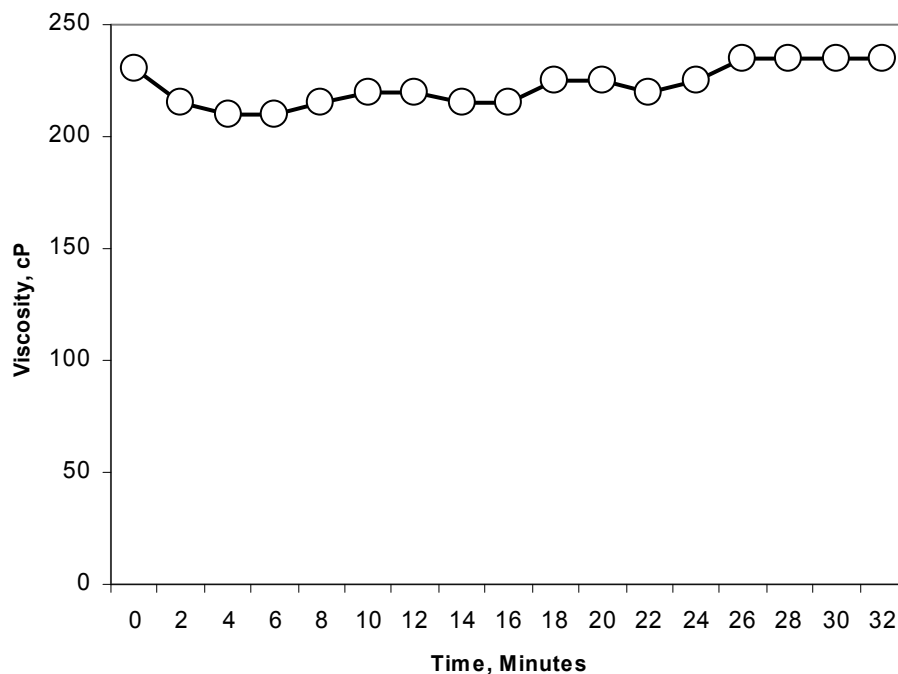


Figure 22. Viscosity at 70 °C for 25.67 g of Alberta coal dissolved in 70.42 g of CTD and 3.91 g of hydrogenated oil.

Table 49. Viscosity data at 90 °C for 25.67 g of Alberta Coal dissolved in 70.42 g of CTD and 3.91 g of hydrogenated oil.

Time (min)	Temperature (°C)	RPM	Torque	Viscosity, cP	Shear Stress, dyne/cm ²	Shear Rate sec ⁻¹
0:00	90.4	100	2.00%	105	29.4	28
2:00	90.3	100	2.50%	125	36.4	28
4:00	90.3	100	2.90%	145	40.6	28
6:00	90.3	100	3.10%	160	44.8	28
8:00	90.4	100	3.30%	170	47.6	28
10:00	90.3	100	3.60%	175	50.4	28
12:00	90.4	100	3.70%	185	51.8	28
14:00	90.5	100	3.80%	190	53.2	28
16:00	90.4	100	4.00%	200	56.0	28
18:00	90.5	100	4.10%	205	57.4	28
20:00	90.2	100	4.30%	215	60.2	28
22:00	90.4	100	4.30%	215	60.2	28
24:00	90.4	100	4.30%	215	61.6	28
26:00	90.6	100	4.40%	220	63.0	28
28:00	90.5	100	4.50%	225	64.4	28
30:00	90.2	100	4.70%	235	65.8	28
32:00	90.3	100	4.60%	235	65.8	28
34:00	90.4	100	4.60%	235	65.8	28
36:00	90.4	100	4.70%	235	65.8	28

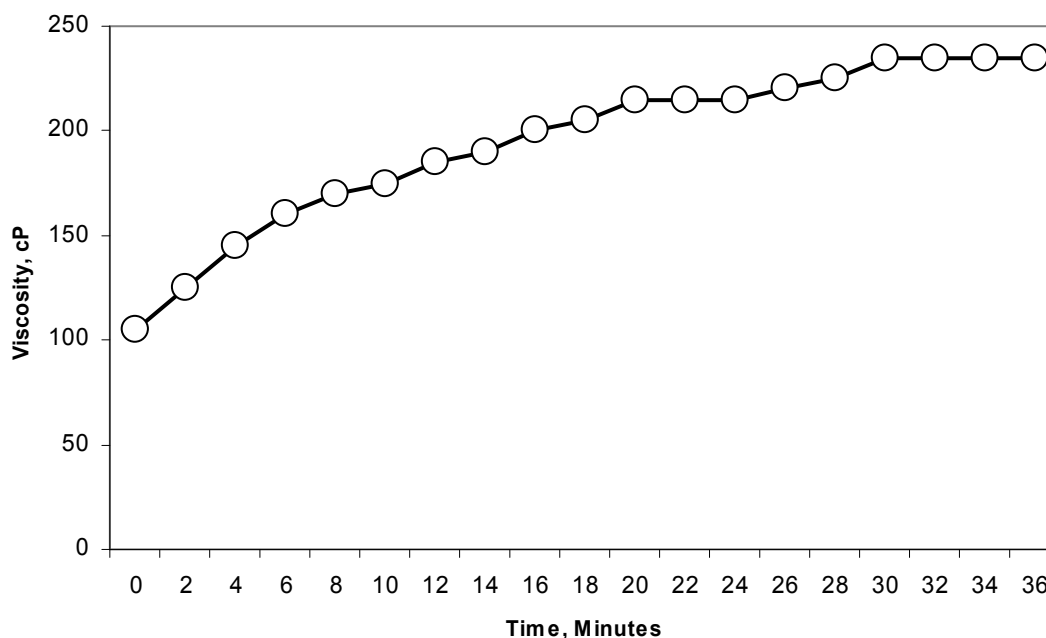


Figure 23 Viscosity at 90 °C for 25.67 g of Alberta coal dissolved in 70.42 g of CTD and 3.91 g of hydrogenated oil.

By extrapolating this data at standard conditions, it may well be that under very high shear conditions (that is, centrifugation), the viscosity increases, possibly by an order of magnitude or more. If so, the fluid would resist centrifugation strongly. This is in fact what is observed empirically.

Hydrogenated oil may be undesirable from the standpoint of centrifuging solid particles. The precise mechanism is not completely understood at this time. However, from an empirical point of view there are other solvents, specifically non-hydrogenated agricultural oil, which do not demonstrate the same behavior.

This suggests that alternative solvent blends may need to be developed, in order to be more compatible with centrifugation.

3.1.6.4 Additional Centrifuge Trials

As indicated in the previous section, the difficulty in producing a low-ash centrate is likely related to the rheopectic nature of the two-phase suspensions produced via the process, with hydrogenated oil playing a key role. Previously, levels of 0.1% ash were obtained using the T. F. Hudgins Inc Spinner II Model 600 centrifuge. After modifying the protocol by using hydrogenated oil as an alternative way to add hydrogen to the system rather than using catalytic hydrogenation using high pressure gaseous hydrogen, it was found that the same centrifuge was unable to reduce the ash content below about 0.5%. This level is marginal for binder pitch and too high for most types of impregnation pitch preferred by GrafTech Inc.

In the previous section, it was argued that this is probably due to the creation of a rheopectic phase. Nevertheless, in parallel with this science-based approach, engineering based approaches were also pursued. Briefly, the conclusion is also that the centrifuge behaves normally but has difficulty in achieving highest performance with the combination of materials currently being used to dissolve coal.

Specifically, it was suspected the Spinner II Model 600 centrifuge might be pneumatically underpowered. The reason is that the jets or nozzles in the centrifuge rotor had been enlarged by the manufacturer in order to accommodate the viscous coal derived oils expected in the current process. The jets produce thrust as liquid is expelled under pressure from the rotor, which acts as a turbine blade. Hence a larger nozzle diameter means that additional mass flow rate must be accommodated, meaning that the amount of pneumatic power might need to be increased by some unspecified amount.

To rule out that possibility, a smaller centrifuge was trialed. A Model 60 unit, with an order of magnitude smaller capacity was substituted, as shown in Figure 24. Approximate performance is shown Figure 25 for motor oil.



Figure 24. T. F. Hudgins Spinner-II Model 60SE centrifuge, mounted on a 55 gallon drum containing coal extract.

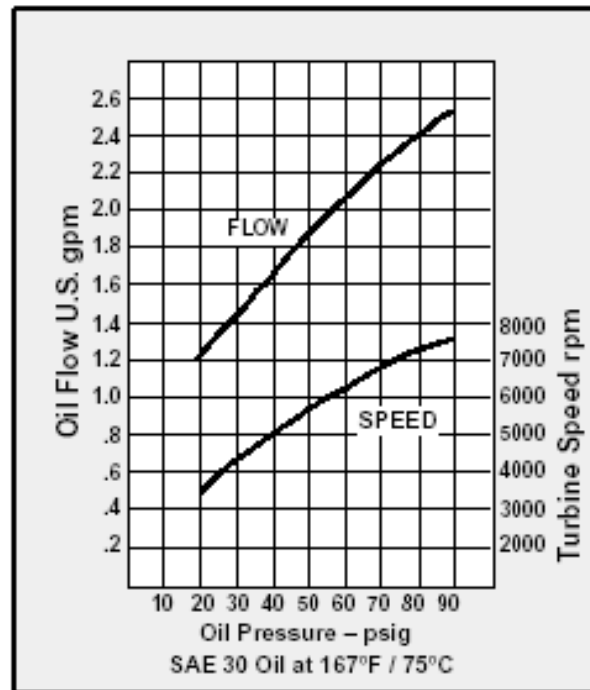


Figure 25. T. F. Hudgins specifications for SAE 30 Oil, using the Model 60SE unit. Extracted coal achieved a much lower turbine speed at 90 psig due to higher viscosity.

Other attempts were made to observe changes in centrifuge performance. To verify that non-Newtonian viscosity changes are the primary reason for lower ash removal, the mass of ash removed was recorded concomitantly with centrifuge RPM. It was found that the centrifuge

RPM was indeed slow for those fluids demonstrating non-Newtonian viscosity changes, as shown by the Table 50 and Table 51. The data recorded includes the time, fluid temperature, cycles per minute in the double diaphragm pump, compressor pressure, tank pressure, inlet pressure and RPM of the centrifuge. The latter is estimated using a vibration gauge.

Table 50. April 22, 2009 Kingwood/CTD/AGOIL

TIME	TEMP	CYC/MIN	P/COMP	P/TANK	P/INLET	RPM
11.30	91	35	75	75	42	700
11.45	88	34	70	75	43	700
12.00	88	35	70	70	44	780
12.15	88	35	70	74	44	750
12.30	88	35	70	75	43	750
12.45	89	36	70	73	43	750
1.05	89	35	70	73	43	760
1.15	89	35	70	74	44	780
1.30	90	35	70	73	44	780
1.45	90	35	70	74	44	780
2.00	90	35	70	74	43	780
2.15	90	35	70	74	44	780
2.30	91	35	70	74	44	780
2.45	91	35	70	74	44	780
3.00	91	35	70	74	44	780
3.15	91	35	70	74	44	780
3.30	91	35	70	74	44	780

The weight of the tails- 4.4

Table 51. April 23, 2009 Kingwood/CTD/AGOIL + 35 kg Methyl Napthalene.

TIME	TEMP	CYC/MIN	P/COMP	P/TANK	P/INLET	RPM
12.10	90	36	75	85	48	1300
12.25	87	36	75	70	43	2050
12.40	87	36	75	70	43	2100
12.55	88	36	75	70	43	2150
1.10	89	36	75	70	43	2100
1.25	89	36	75	70	43	2100
1.40	90	36	75	70	43	2100
1.55	91	36	75	70	43	2100
2.10	91	36	75	70	43	2100

The weight of the tails – 3.8

The addition of methyl naphthalene resulted in immediately increasing the centrifuge speed from about 800 rpm to 2000 (as shown in Table 51). It probably also resulted in the formation of a separate quasi-solid phase, much of which likely appeared in the tails. Hence the ash yield of the tails was only around 6%, according to the data of Table 52, which is about the same as the original coal; hence, it is not an impressive result. This is described in Table 53 and Table 54.

Repeating the experiment with methyl naphthalene also improved the ability of the centrifuge to spin, but did not improve the yield, as shown in Table 55 and Table 56. In that sense, the experiment failed to achieve its desired result. However, if some other solvent were

used to reduce the viscosity without also creating a separate liquid phase, there is reason for optimism to believe that the overall ash removal could be effectively enhanced.

In conclusion, this series of experiments suggests that the centrifuge probably works at close to the manufacturer's specifications. The likely problem is that there is a shear thickening effect, possibly also involving surface tension with the ash particles, which reduces the ability of the centrifuge to remove solids from the current blend of materials.

A chemical solution should be sought by judiciously changing the solvent blend.

Table 52. Weight of the Tails.

Date	14-Apr	15-Apr	17-Apr	22-Apr	23-Apr	28-Apr	Total
Weight(lb)of Tails	3.8	12.2	15.8	4.4	3.8	3.6	43.6
Product weight	215.4						

Table 53. Proximate Analysis of Centrate (Kerosene Added).

Sample	Moisture	Volatiles	Ash	Fixed Carbon
22/04/09KWCTDAGOILKero Cen 1	5.75	75.32	0.54	18.39
22/04/09KWCTDAGOILKero Cen 2	5.08	75.99	0.48	18.45
22/04/09KWCTDAGOILKero Cen 3	5.31	75.65	0.53	18.51
Average	5.38	75.65	0.52	18.45

Table 54. Proximate Analysis of Tails (Kerosene Added).

Sample	Moisture	Volatiles	Ash	Fixed Carbon
22/04/09KWCTDAGOILKeroTail 1	3.06	66.05	6.15	24.74
22/04/09KWCTDAGOILKeroTail 2	2.54	66.92	5.94	24.6
22/04/09KWCTDAGOILKeroTail 3	2.65	66.36	6.22	24.77
Average	2.75	66.44	6.10	24.70

Table 55. Proximate Analysis of Centrate (Methyl Naphthalene added).

Sample	Moisture	Volatiles	Ash	Fixed Carbon
23/04/09KWCTDAGOILMethCen 1	6.12	76.3	0.42	17.16
23/04/09KWCTDAGOILMethCen 2	7.01	75.28	0.47	17.24
23/04/09KWCTDAGOILMethCen 3	7.5	74.94	0.47	17.09
Average	6.876666667	75.51	0.45	17.16

Table 56. Proximate Analysis of Tails (Methyl Naphthalene added).

Sample	Moisture	Volatiles	Ash	Fixed Carbon
23/04/09KWCTDAGOILMethTail 1	3.23	66.77	5.86	24.14
23/04/09KWCTDAGOILMethTail 2	2.52	67.63	5.65	24.2
23/04/09KWCTDAGOILMethTail 3	3.47	66.78	5.72	24.03
Average	3.073333333	67.06	5.74	24.12

3.2 Trickle Bed Hydrogenation Reactor

3.2.1 *Introduction to Trickle Bed Hydrogenation*

In order to achieve improved kinetics of hydrogenation, a trickle bed approach was used. This offers more intimate contact between gaseous hydrogen, catalyst and liquid. The first objective of the research described herein is to study and understand the process of hydrogenation, the design and operation of a trickle bed reactor and the corresponding reaction kinetics involved in the same. The required parts and the materials of construction are to be specified based on the operating conditions. Also, the components are to be set up and the operating conditions and procedures required for the experiments are to be determined. The catalyst which is to be used in the process must also be specified.

It is very important to take all safety aspects into consideration when designing the reactor and performing experiments. Therefore, the system must have numerous safety features. Since, high pressures and high temperatures are involved, the material of construction must be chosen such that it will withstand the operating conditions. The pressure and temperature must be monitored continuously to ensure that the operating conditions are maintained. Pressure relief valves must be installed at various points in the system. Because of the potential hazards of hydrogen gas, the apparatus was installed in a walk-in fume hood.

Once constructed, it is necessary to test the experimental set up to verify that each and every component is working properly. A leak check must also be performed as a precautionary measure. The system must then be checked for isothermal conditions. It must be ensured that the temperature along the reactor is constant in order to obtain more precise results. The trickle bed reactor was used to study the kinetics of a well-known reaction, i.e., hydrogenation of naphthalene to tetralin.

The main objective of the literature review is to study similar work done by other researchers in the area of coal liquefaction and hydrogenation of coal tar distillates and apply that understanding and knowledge of the basic operating conditions in designing the trickle bed reactor. A brief description about the formation of coal is discussed in this section. Also discussed are major processes used in the industry for converting coal into liquid fuels. A basic review of the previous research work done at West Virginia University (WVU) on the hydrotreatment of coal using coal-derived solvents is also presented. Since the present work involves the use of a trickle bed reactor for hydrogenating aromatic hydrocarbons, a major part of the literature review is devoted to the work done on trickle bed reactors in the past by other researchers. The hydrogenation of coal tar distillates and model compounds such as naphthalene in a trickle bed reactor in the presence of a hydrotreating catalyst has been studied in the present work.

The advantages of a Trickle Bed Reactor over a Continuously Stirred Tank Reactor (CSTR) in carrying out multiphase reactions are as follows:

1. In Trickle Bed Reactors, the gas and liquid flow regimes approach plug flow.²⁸ Also, the residence time of the liquid and gaseous reactants is high and hence high conversion may be achieved.
2. The pressure drop is relatively low when compared to CSTR.

3. The liquid-to-catalyst ratio is low thus limiting the side reactions.
4. Problems due to flooding are not encountered.
5. The catalyst load per unit volume of the reactor is high.
6. The liquid hold up is low compared to CSTR.
7. The trickle bed reactor is operated in a continuous manner and not batchwise like the CSTR.
8. The design and construction of a Trickle Bed Reactor is simpler and cheaper than a large CSTR especially for reactions at high pressure and high temperature.

Despite having many advantages, these small-scale trickle bed reactors do have a number of limitations. The commercial reactors are two orders of magnitude longer than the lab scale reactors. The liquid velocities in commercial scale reactors are higher by a factor of about 100 as compared to lab scale reactors. Low liquid velocity in small-scale trickle bed reactors leads to major problems such as poor wetting of the catalyst, wall effects and backmixing. So, the experimental data generated by the lab-scale trickle bed reactors may not always be useful for scale-up purposes.

In trickle bed reactors, part of the catalyst surface is covered by gas and part by liquid. The liquid phase and the gas phase, which consists of vaporized compounds introduced with the feed, are allowed to flow co-currently downwards through the reactor. A co-current operation allows for better distribution of the liquid over the catalyst and also allows for higher liquid flow rates without flooding.²⁹ Hence, it is proposed that the kinetics of the reaction would be much faster since the hydrogen will simultaneously be in the presence of both liquid and the catalyst. Thus, the determination of the minimum practical residence time for the desired catalytic hydrotreatment of coal tar distillates is the ultimate goal of this research.

Trickle bed reactors in the petroleum industry are operated at different conditions depending on the type of feed and the nature of reaction.³⁰ Trickle bed reactors are operated at high pressures in the range of 20-30 MPa in order to reduce the rate of deactivation of the catalyst.³¹ Also, this high pressure operation of the trickle bed reactors increases the solubility of the gaseous reactant thereby attaining higher conversion and better heat transfer. Viscous feeds which have high boiling points are treated at low liquid flow rates. The ratio of flow rates of gas and liquid in the trickle bed reactor is of major concern as it will affect the concentrations of gas and liquid in contact with the catalyst. Another important factor which affects the reactor performance is the wetting efficiency which reflects the fraction of external surface of the catalyst covered by flowing liquid. The flow rates of gas and liquid also affect the wetting efficiency of the catalyst. Huang et al. concluded that neglecting the wetting efficiency of catalyst particles would lead to a misleading conclusion in reaction kinetics. High volatilities of feedstocks, high gas flow rates and low liquid flow rates decrease the wetting efficiency of the catalyst particles.³² The gas flow rates are generally in the range of 250-900 m³ H₂/m³ oil.³³ But, a very high value of the hydrogen-to-oil ratio would result in the increase of the process cost. The optimum value of the ratio of hydrogen to hydrocarbon used in petroleum industries are

2000 to 3000 std.cu.ft./bbl for hydrodesulfurization of heavy gas oil, 3000 to 5000 std.cu.ft./bbl for hydrodesulfurization of heavy residue and 5000 to 10000 std.cu.ft./bbl for a hydrocracking operation ($1 \text{ std.cu.ft./bbl} = 0.18 \text{ m}^3 \text{ H}_2/\text{m}^3 \text{ oil at STP}$).³⁴ Apart from this, the effectiveness of the catalyst also plays a major part in the reaction kinetics and the nature of the products. In order to achieve higher flow rates, catalysts employed in trickle bed reactors are spheres or cylindrical pellets. However, cylindrical catalyst pellets tend to pack together causing liquid to channel through the bed while spherical catalyst particles cause the liquid to channel to the wall. The liquid is mainly held in the catalyst pores which causes liquid hold up and hence different wetting characteristics are obtained in trickle bed reactors. The liquid trickles over the catalyst and the gas flows continuously through the voids at low liquid and high gas flow rates. Conversely, the liquid phase becomes continuous and the gas phase passes through the voids in the form of bubbles for high liquid flow rates and low gas flow rates.

3.2.2 Catalyst Selection

The choice of a hydrotreating catalyst depends upon the type of reaction for which it is intended. The performance of hydroprocessing units is hugely influenced by the catalyst and the type of reactor for a particular feed. Physical properties such as density, porosity, size and shape of a catalyst are crucial parameters in the hydroprocessing of heavy feeds.³⁵ These parameters are feed dependent implying a catalyst giving optimum results for a particular feed may not give the same results for a different feed. The size and shape of catalyst particles ensure efficient catalyst utilization.³⁶ Generally, a catalyst for hydrotreating heavy hydrocarbon oil is a porous carrier composed of one or more inorganic oxides of at least one element selected from among those of Groups II, III and IV of the Periodic Table, and at least one catalytic metal component composited with the carrier. The catalytic metal component is selected from among those of Groups VB, VIB, VIII and IB of the Periodic Table.³⁷ Most common commercial hydrotreating catalysts are Ni-Mo/Al₂O₃, Co-Mo/Al₂O₃, Ni-W/Al₂O₃ and their sulfided forms. Earlier studies reveal that Ni-Mo/Al₂O₃ catalyst shows higher hydrogenation activity as compared to Co-Mo and Ni-W catalysts.³⁸ Also, nickel catalysts, due to their lower temperature requirements and cost effectiveness, are preferred over noble metal catalysts such as platinum, palladium, iridium and rhodium.³⁹ Therefore, as a part of this research, Ni-Mo/Al₂O₃ has been selected as the catalyst for the hydrogenation of naphthalene and coal tar distillates.

Most commercial hydroprocessing reactions are carried out at high pressure ($> 1000 \text{ psig}$) and high temperature ranging between $320 \text{ }^\circ\text{C}$ and $450 \text{ }^\circ\text{C}$ in trickle bed reactors in which the liquid hydrocarbons and gaseous hydrogen flow co-currently downward through a fixed bed of the solid catalyst. Partially reacted fluids are mixed with cold hydrogen gas which is introduced through the top of the reactor. Commercial hydroprocessing reactors contain various zones of catalyst beds separated by quench zones. Catalyst particles are normally cylindrical, spherical, trilobe or quadrilobe extrudates having a particle diameter between 1 and 2 mm. But, a disadvantage for the spherical or cylindrical catalyst particles is that they are not efficient enough for hydrotreating secondary petroleum fractions such as residuum. Therefore, shaped catalyst particles (polylobal extrudates) are used for hydroprocessing heavy feedstocks, in particular for hydrodesulfurization and for processes influenced by diffusion such as trickle bed hydrogenation. Also, polylobal extrudates exhibit lower pressure drops as compared to smaller spherical or cylindrical particles having the same external particle area. A schematic of a typical

hydroprocessing reactor is shown in Figure 26. In commercial trickle bed reactors, complete wetting of the catalyst particles occurs due to the presence of liquid distributors and redistributors. It is to be noted here that the transport of molecules from the gas phase to the active surface of the catalyst faces resistances from bulk gas to gas-liquid interface, from gas-liquid interface to bulk liquid, from bulk liquid to external catalyst surface, and finally diffusional resistances within the pores of the catalyst pellet.

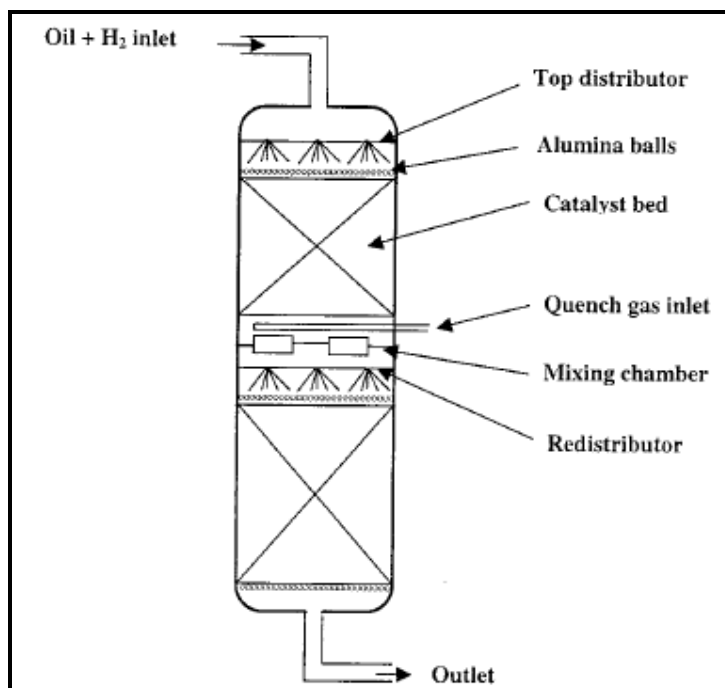


Figure 26. Schematic of a typical hydroprocessing trickle bed reactor.

Small diameter catalyst particles are used in trickle bed reactors and microreactors in order to negate the effects of channeling and backmixing of liquid. Data available in the literature suggest that the maximum catalyst particle diameter in order to avoid channeling and wall effects is approximately 0.4 mm for a reactor with internal diameter of about 8 mm.⁴⁰ Therefore, a commercial Ni-Mo/Al₂O₃ catalyst with a particle diameter of 1.0 mm is used in the present work in which the internal diameter of the reactor is about 20 mm (0.782"). Also, Sie et al. reported that effects of backmixing in a microreactor could be avoided if the catalyst particle diameter is less than 0.2 mm.⁴¹ However, the data obtained by using such small diameter particles may not be very helpful when the bench-scale system is being used to duplicate the results obtained in a commercial process.

3.2.3 Hydrogenation of Naphthalene to Tetralin

As discussed earlier, naphthalene is one of the major aromatic substances present in coal tar distillate. Naphthalene is the simplest model compound resembling the polynuclear aromatics in coal and coal liquids. Much research has been done in the area of reaction kinetics based on the hydrogenation of naphthalene to tetralin in a trickle bed reactor. Naphthalene hydrogenation

can thus represent some reactions occurring during the primary coal liquefaction processes. Naphthalene when hydrogenated at high pressure and high temperature in the presence of a hydrotreating catalyst forms 1,2,3,4 tetrahydronaphthalene (Tetralin) which on further hydrogenation forms cis-decalin and trans-decalin. Most of the research concerning hydrogenation of naphthalene has been done on the sulfided forms of commercial catalysts such as Ni-Mo/Al₂O₃ and Co-Mo/Al₂O₃. The hydrogenation reaction is shown in Figure 27.

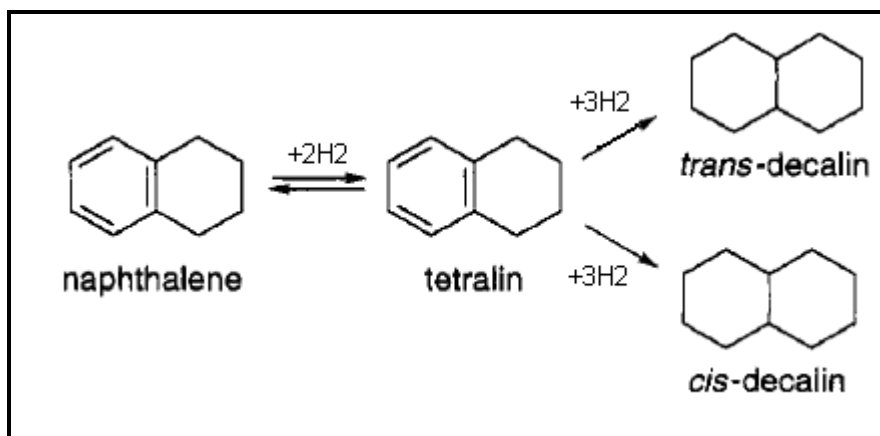


Figure 27. Hydrogenation of Naphthalene to Tetralin and Decalin,

Guin et al. performed the high pressure hydrogenation of naphthalene in a trickle bed reactor using a reduced iron catalyst and compared the results with a commercial Ni-Mo/Al₂O₃ catalyst.⁴² The hydrogenation reaction was performed at a pressure of 6.9 MPa and temperatures ranging between 160°–300°C. It was observed that the secondary hydrogenation reaction to form decalin occurred only in the presence of reduced iron catalyst and not in the presence of commercial Ni-Mo/Al₂O₃ catalyst. The trickle bed experiments by Guin and Zhan showed that the reduced iron catalyst deactivated more rapidly than Ni-Mo/Al₂O₃ and hence could not be used as a catalyst for coal liquefaction.

3.2.4 Thermodynamics of Hydrogenation Reactions

Girgis and Gates reviewed the kinetics and thermodynamics of high pressure catalytic hydroprocessing of aromatic hydrocarbons.⁴³ They concluded that the hydrogenation of aromatic hydrocarbons was a reversible process and that the equilibrium conversion would always be less than 100% under practical processing conditions. Also, the hydrogenation reactions are exothermic reactions in which the extent of reaction at equilibrium decreases with the increase in temperature at lower pressures. Therefore, it is very important to operate at high hydrogen partial pressure in order to hydrogenate the aromatic hydrocarbons to an appreciable extent under typical hydroprocessing conditions. This effect of pressure is in agreement with the Le Chatelier principle. Apart from this, kinetics of reactions conducted in trickle bed reactors require high temperatures, due to which the gaseous reactant expands and does not dissolve sufficiently into the liquid. Therefore, elevated pressures (up to 30 MPa) are necessary to improve the gas solubility and the mass- and heat-transfer rates, to handle large gas volumes at less capital expense, and to slow down the catalyst deactivation.

The thermodynamic data required for calculating the equilibrium constants during liquid phase reactions involving aromatic hydrocarbons are not available readily. Work done by Shaw et al. in this regard proved that gas phase equilibrium constants can be used as a good approximation to estimate the equilibrium constants of the reactions occurring in liquid phase.⁴⁴ This is because the properties which mainly affect equilibrium constants, entropy and enthalpy, do not change significantly from gas phase to liquid phase. More recently, S.A. Ali discussed the thermodynamic aspects of aromatic hydrogenation and reviewed the thermodynamic data available in the literature.⁴⁵ It was found that the heat released during the hydrogenation of aromatic hydrocarbons increased proportionately with the number of moles of hydrogen taking part in the reaction. It was also observed that the heat release per mole of hydrogen consumed did not differ by much during the hydrogenation of different hydrocarbons. This theory was proved earlier by Reid et al. who concluded that the heat released during the hydrogenation of aromatic compounds is between 58 and 70 kJ/mole of hydrogen. A generalized correlation to calculate the equilibrium constant, proposed by Ali, is represented as the following:

$$-\log K = [-1.8399 \log T_K + 13.716] \log C_n + [21 - 321 \log T_K - 139.33] \quad \text{Equation 1}$$

where K is the equilibrium constant, T_K is the temperature in degrees Kelvin and C_N is the carbon number which can be varied between 6 and 12. This correlation is valid for a temperature range of 200 °C to 400 °C with an error of about 3-5 %.

Recent studies by Rautanen et al. reported that the dehydrogenation of tetralin to form naphthalene was highly dependent on the concentration of tetralin and the rate of hydrogenation of naphthalene but independent of pressure and temperature.⁴⁶ A low hydrogenation rate accompanied by a high concentration of tetralin favored the formation of naphthalene in the experiments performed by Rautanen et al. over a temperature range of 85-160 °C and a pressure range of 20-40 bar using a Ni/Al₂O₃ catalyst. In addition, it was also observed that the dehydrogenation reaction of tetralin to form naphthalene was a minor reaction and that only a miniscule amount of naphthalene was formed under the above mentioned conditions. Frye and Weitkamp measured the equilibrium hydrogenation of several multi-ring aromatic hydrocarbons such as naphthalene, phenanthrene, acenaphthene and biphenyl in the vapor phase at different temperatures ranging between 300 °C and 450 °C and pressures ranging between 5 atm and 60 atm.⁴⁷ Their results indicate that the equilibrium constants for the hydrogenation of multi-ring aromatic hydrocarbons are less than unity at typical hydroprocessing temperatures (temperatures greater than 340 °C). Further studies by Weitkamp suggested that the rate of hydrogenation for the first ring of naphthalene is about 20 to 40 times greater than that of the last ring. The work done by Sapre and Gates further substantiated this result.⁴⁸ Furthermore, Sapre and Gates generalized that naphthalene and substituted naphthalenes are an order of magnitude more reactive than benzene and substituted benzenes. Also the hydrogenation of naphthalene is sequential with the rate of primary reaction. This indicates that the hydrogenation of naphthalene to tetralin is an order of magnitude faster than that of the secondary reaction, i.e., from tetralin to decalin. Guin and Zhan also investigated the extent of hydrogenation on Ni-Mo/Al₂O₃ and pre-reduced iron catalysts at different temperatures ranging from 160 °C to 300 °C at 1000 psi pressure in a trickle bed reactor. The extent of hydrogenation was represented as:

$$A_H = (2M_{TET} + 5M_{DEC}) / (5(M_{NAPH} + M_{TET} + M_{DEC})) \quad \text{Equation 2}$$

where A_H = Extent of hydrogenation of naphthalene
 M_i = Moles of compound i in the reaction products.

The extent of hydrogenation of naphthalene varies between 0 and 1 as the products vary from totally aromatic to completely saturated. If no decalin is present in the product, the extent of hydrogenation of naphthalene cannot exceed 0.4 corresponding to 100% tetralin according to the reaction stoichiometry.⁴⁹

3.2.5 Trickle Bed Reactor Kinetics

Earlier studies by Satterfield revealed that in a trickle bed reactor, the kinetics of any reaction can be represented as first-order model though the actual kinetics may be different.⁵⁰ In order to assume first-order kinetics in a trickle bed reactor the following assumptions have to be made:

1. There should not be any dispersion of the reactant in the axial or radial direction, i.e. plug flow of the liquid must be considered.
2. It has to be assumed that the liquid is saturated with gas at all times and that there are no mass or heat transfer limitations between the gas and liquid, between liquid and solid catalyst and inside the catalyst particles.
3. The gaseous reactant must be in great excess when compared to the liquid reactant and isothermal conditions must be maintained during the process.
4. The reaction occurs only at the liquid-catalyst interface and that no vaporization or condensation occurs.

Consider the irreversible unimolecular reaction of the form:



The rate equation for the irreversible unimolecular reaction shown above can be represented as:

$$-r_A = -dC_A/dt = kC_A \quad \text{Equation 4}$$

Equation (2.4) can be integrated to:

$$-\ln (C_A/C_{A0}) = kt \quad \text{Equation 5}$$

Equation (2.5) can further be represented as:

$$-\ln (1-X_A) = kt \quad \text{Equation 6}$$

where C_{A0} = Initial concentration of reactant A, mol/liter
 C_A = Concentration of reactant A at any time, t , mol/liter
 X_A = Conversion of reactant A, $(C_{A0} - C_A)/C_{A0}$

k = Reaction Rate constant, Sec^{-1}
 t = Time, sec

A plot of $\ln(1-X_A)$ or $\ln(C_A/C_{A0})$ vs t gives a straight line passing through origin for the form of the rate equation as shown in Equation (2.4).

In a similar manner as described above, consider the irreversible bimolecular reaction of the form:



The corresponding rate equation for the irreversible bimolecular reaction represented in (2.7) is:

$$-r_A = -dC_A/dt = -dC_B/dt = kC_AC_B \quad \text{Equation 8}$$

where C_B = Concentration of the reactant B at any time, t , mol/liter.

If the initial concentration of reactant B is much larger than that of A, then C_B remains approximately constant at all times, and Equation (2.8) approaches Equation (2.4) for the first-order reaction. Thus, the second-order reaction becomes a pseudo first-order reaction.

In order to utilize an ideal plug flow reactor model for determining the kinetics in a trickle bed reactor, the following criterion suggested by Mears and reviewed by Satterfield must hold true:

$$L/d_p > \left[20 \frac{n * D_{al}}{V_L * d_p} \right] \ln \left(\frac{C_{in}}{C_{out}} \right) \quad \text{Equation 9}$$

where L = Length of the reaction zone, cm

d_p = Diameter of the catalyst particle, cm

D_{al} = Axial dispersion coefficient of the liquid, cm^2/sec

V_L = Superficial velocity of the liquid, cm/sec

n = Order of the reaction

C_{in} = Inlet concentration of the reactant, mol/liter

C_{out} = Outlet concentration of the reactant, mol/liter

The axial dispersion coefficient, D_{al} , used in Equation (2.9) can be estimated using Equation (2.10) for small deviations from plug flow.

$$1 - X_A = \exp \left[-k\tau + (k\tau)^2 \frac{D_{al}}{V_L * L} \right] \quad \text{Equation 10}$$

where X_A = Conversion of the reactant at steady state

k = Rate constant of the reaction, sec^{-1}

τ = Residence time of the reaction, sec

D_{al} = Axial dispersion coefficient of the liquid, cm^2/sec

V_L = Superficial velocity of the liquid, cm/sec

L = Length of the reaction zone, cm

The studies done by Sapre and Gates and Zhan and Guin further confirm that the hydrogenation of naphthalene to tetralin follows first-order kinetics in the presence of excess hydrogen. Sapre and Gates performed the high pressure hydrogenation of aromatic hydrocarbons, namely, benzene, biphenyl, naphthalene and 2-phenylnaphthalene in a batch reactor at 75 atm and 325 °C in the presence of sulfided $\text{CoO-MoO}_3/\text{Al}_2\text{O}_3$ catalyst. They concluded that each reaction network consisted of the reversible hydrogenation of the aromatic hydrocarbon to give a hydroaromatic hydrocarbon which further experienced slow hydrogenation. For instance, when the reactants were naphthalene and hydrogen, tetralin was obtained as the primary product while tetralin was further hydrogenated slowly to give trans-decalin. The reaction network was represented as a pseudo first-order in the hydrocarbon reactants. Figure 28 shows the conversion of naphthalene in the experiments performed by Sapre and Gates.

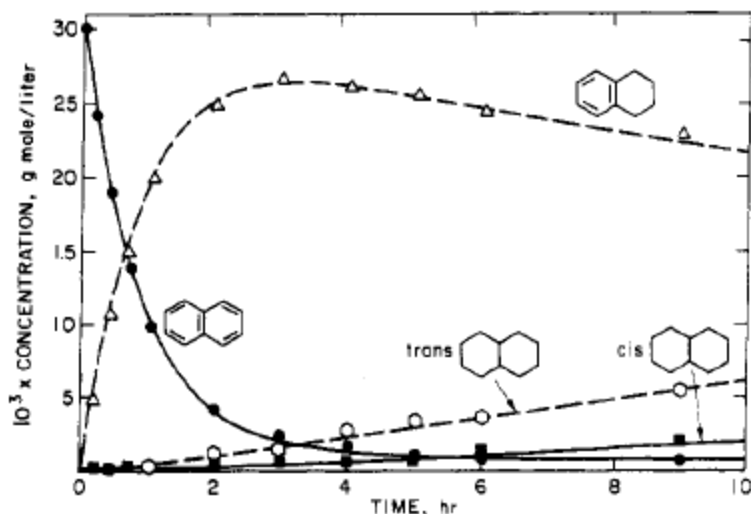


Figure 28. Conversion of naphthalene in a batch reactor at 325 °C and 75 atm using $\text{CoO-MoO}_3/\text{Al}_2\text{O}_3$ catalyst.⁵¹

It can be seen that, for these reaction conditions, the concentration of tetralin passes through a maxima at about 3 hr and that the conversion of naphthalene within this period is almost 90%. The pseudo first-order rate constant for the overall disappearance of each component was determined using the conversion data. The rate constant for the hydrogenation of naphthalene was determined to be $(58.9 \pm 3.6) \times 10^{-6} \text{ m}^3/\text{kg}\cdot\text{sec}$. Since the primary hydrogenation reactions are reversible, Sapre and Gates observed a deviation from the pseudo first-order behavior as equilibrium was approached. Therefore, for the determination of the rate constant to provide the best representation of the reaction network over the whole range of conversion data, all the data were used, and it was assumed that each reaction in each network was pseudo first-order in the organic reactant.

Zhan and Guin performed the high pressure hydrogenation of naphthalene in a trickle bed reactor using reduced iron catalyst. The liquid phase hydrogenation of naphthalene was carried out in a trickle bed reactor at a pressure of 6.9 MPa and a temperature of 200 °C with varying flow rates of both liquid and gaseous reactants. They proposed a first-order, plug flow model to study the reactor performance, whose expression is similar to Equation (2.6) described earlier in

this section. The expression for the plug flow model proposed by Zhan and Guin is shown in Equation 11.

$$\ln(1/(1-X_n)) = k_L \cdot W/Q_L \quad \text{Equation 11}$$

where X_n = Conversion of naphthalene, $(C_{N0}-C_N)/C_{N0}$
 C_{N0} = Initial concentration of naphthalene in the feed, mol/cm³
 C_N = Final concentration of naphthalene at steady state, mol/cm³
 W = Weight of the catalyst, g
 Q_L = Volumetric flow rate of the liquid feed, ml/min
 k_L = Rate constant of the liquid phase hydrogenation reaction, ml/g-min

A plot of $\ln(1/(1-X_n))$ vs W/Q_L (which is directly proportional to time) gave a straight line passing through origin as shown in Figure 29, indicating that the hydrogenation reaction was a first-order reaction.

Zhan and Guin also studied the reaction kinetics of the hydrogenation of naphthalene in the vapor phase. Cyclohexane was used as the feed solvent and the hydrogenation reaction was carried out in vapor phase in the temperature range of 160 °C to 300 °C. They proposed an empirical power-law rate model similar to Equation 8 to represent the kinetics of the vapor phase reaction. Equation 12 was used to represent the vapor phase reaction kinetics.

$$r_N = k_{app} C_N^a C_H^b \quad \text{Equation 12}$$

where r_N = Reaction rate of naphthalene, mol/g-min
 k_{app} = Apparent rate constant of vapor phase reaction, mol/g-min/(mol/cm³)²
 C_N = Concentration of naphthalene at time t, mol/cm³
 C_H = Concentration of hydrogen in the gaseous mixture under reaction conditions, mol/cm³
a, b = Reaction orders of naphthalene and hydrogen respectively.

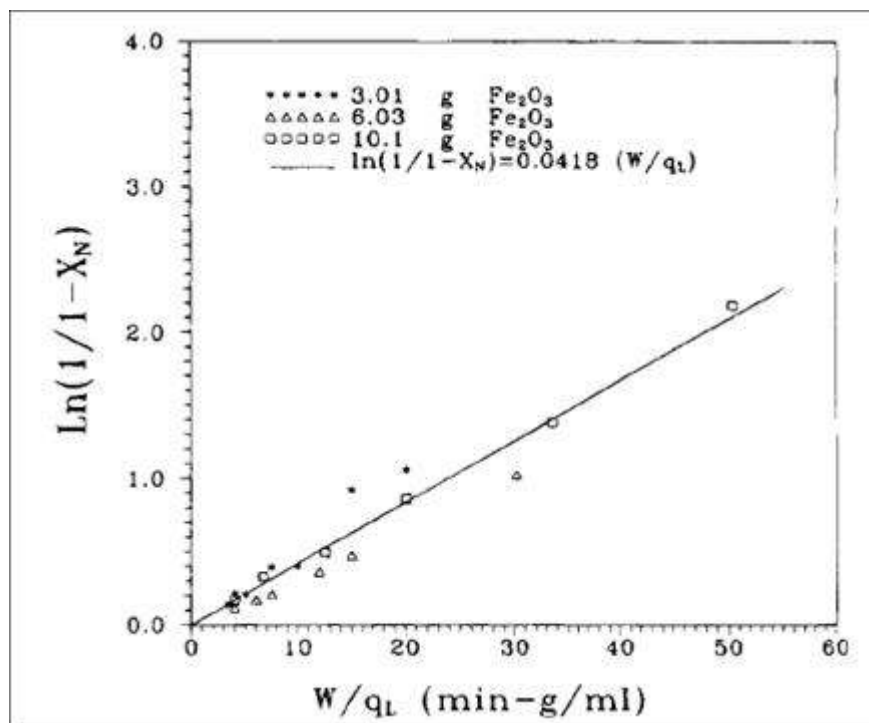


Figure 29. First-order kinetic plot of the hydrogenation of naphthalene at 200 °C using reduced iron catalyst.⁵²

The concentration of hydrogen was considered to be a constant since the flow rate of hydrogen was large compared to that of naphthalene and thus less than 1% of the hydrogen entering the system reacted. Equation 13 represents the modified expression for the plug flow reactor model for the hydrogenation of naphthalene in vapor phase.

$$\ln (1/(1-X_n)) = k_{app}C_{H_0}^b \cdot W/Q \quad \text{Equation 13}$$

where C_{H_0} = Initial feed concentration of hydrogen, mol/cm³
 Q = Volumetric flow rate of feed, ml/min

A plot of $\ln(1/(1-X_n))$ vs W/Q gave a straight line passing through origin as shown in Figure 30, indicating that the hydrogenation reaction was a first-order reaction even in the vapor phase. Also, the calculated value of the apparent activation energy for the hydrogenation of naphthalene was about 44 KJ/mol.

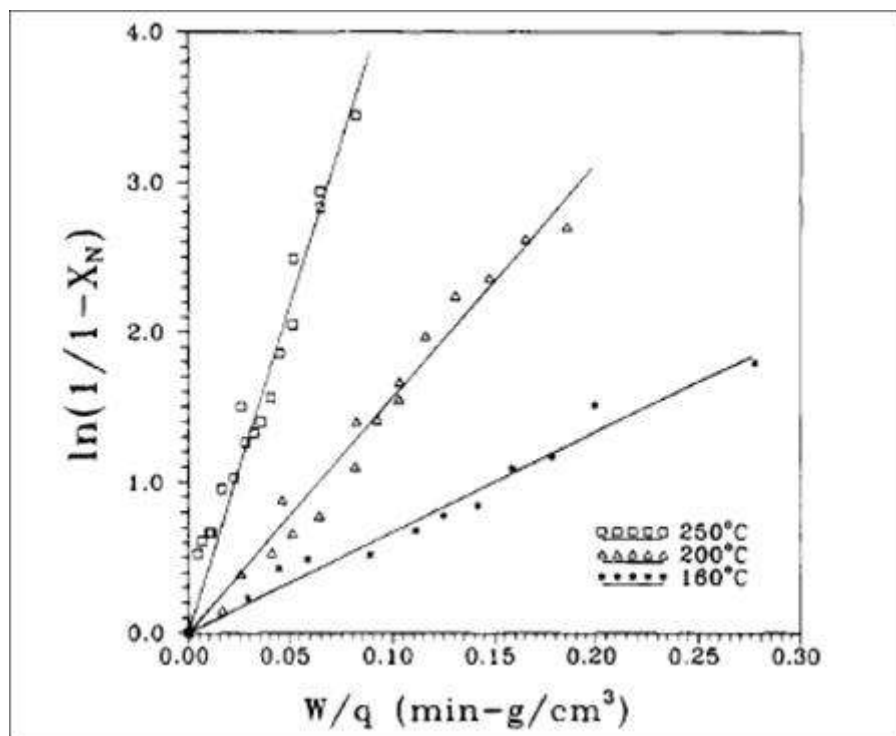


Figure 30. First-order kinetic plot of vapor phase reactions on pre-reduced iron catalyst.⁵³

3.2.6 Reactor Design

The hydrogenation of the coal tar distillates is to be studied in a trickle bed reactor at a temperature of 340-425 °C and a pressure of up to 1200 psig. Figure 31 is the schematic diagram of the newly designed trickle bed reactor system used for this study. Both hydrogen as well as the liquid feed were allowed to flow downward co-currently in the trickle bed reactor. The liquid feed was pumped using a high pressure diaphragm pump supplied by Milton Roy metering pumps (Model # MBH 0718 HPFCBM4SES T11NN22). The rated capacity of the pump is 3.1 GPH and the rated pressure is 3130 psi. Check valves (CV) are fitted on the feed line in order to maintain the flow in one direction. A mass flow controller (FC) (Brooks Instrument Model # SLA 5850S 1BAB4B1A1) in the H₂ feed line was adjusted in order to maintain the flow rate of gas. The flow controller regulates hydrogen flow up to 10 SLPM. A heating tape (H-1) was wound around the feed line in order to preheat the feed entering the reactor to a temperature of around 250 °C. The reactor (RU) is a one-inch outer diameter stainless steel TP-316 L pipe with a wall thickness of 0.109 inches. The length of the reactor is 20 inches and its internal diameter is 0.782 inches. Since the internal diameter of the reactor is relatively small compared to its length, the temperature variation in the radial direction of the catalyst bed can be considered negligible. The reactor was heated to the required operating temperature using a heating tape wrapped around the outside of the reactor. The reactor temperature was controlled using a PID temperature controller (Omega Engineering, Inc. Model 4002KC). Copper rods running axially were installed on the external surface of the reactor for better heat distribution along the reactor since the thermal conductivity of copper is very high, ~ 360 W/m-K at 400 °C. The copper rods were wrapped with the heating tape (H-2) and the entire assembly was insulated with a thick

“fiberfrax” wool blanket. The main purpose of having the copper rods and insulation was to maintain nearly isothermal conditions along the length of the reactor. Temperatures were monitored at various points along the reactor using K-type thermocouples (TC). Four thermocouples were mounted at various points on the outside of the reactor for continuous monitoring of the axial temperature profile and one thermocouple (TC1) was placed directly inside the catalyst bed. These temperatures were monitored using a 10 point temperature scanner provided by Omega Engineering, Inc (Model # DP 1001).

Based on the criteria for selection of catalyst for a hydrotreatment process as described earlier, the catalyst used in this process is a Nickel-Molybdenum (Ni/Mo/Al₂O₃- KF-843-1.3Q) catalyst which was supplied by Albemarle Catalysts located in Pasadena, Texas. The catalyst was placed in the middle of the reactor and was retained in a basket. The length of the reaction zone is five inches (which can be varied) and the remaining space in the reactor was filled with glass beads which were used as packing material. These glass beads have the same diameter as that of the catalyst in order to promote an evenly distributed flow in the entrance and exit ends of the catalyst. The reactor effluent was collected in a separating vessel (TA1) where the liquid and vapor were disengaged. A back pressure regulator (BPR) is also provided in order to maintain the desired system operating pressure.

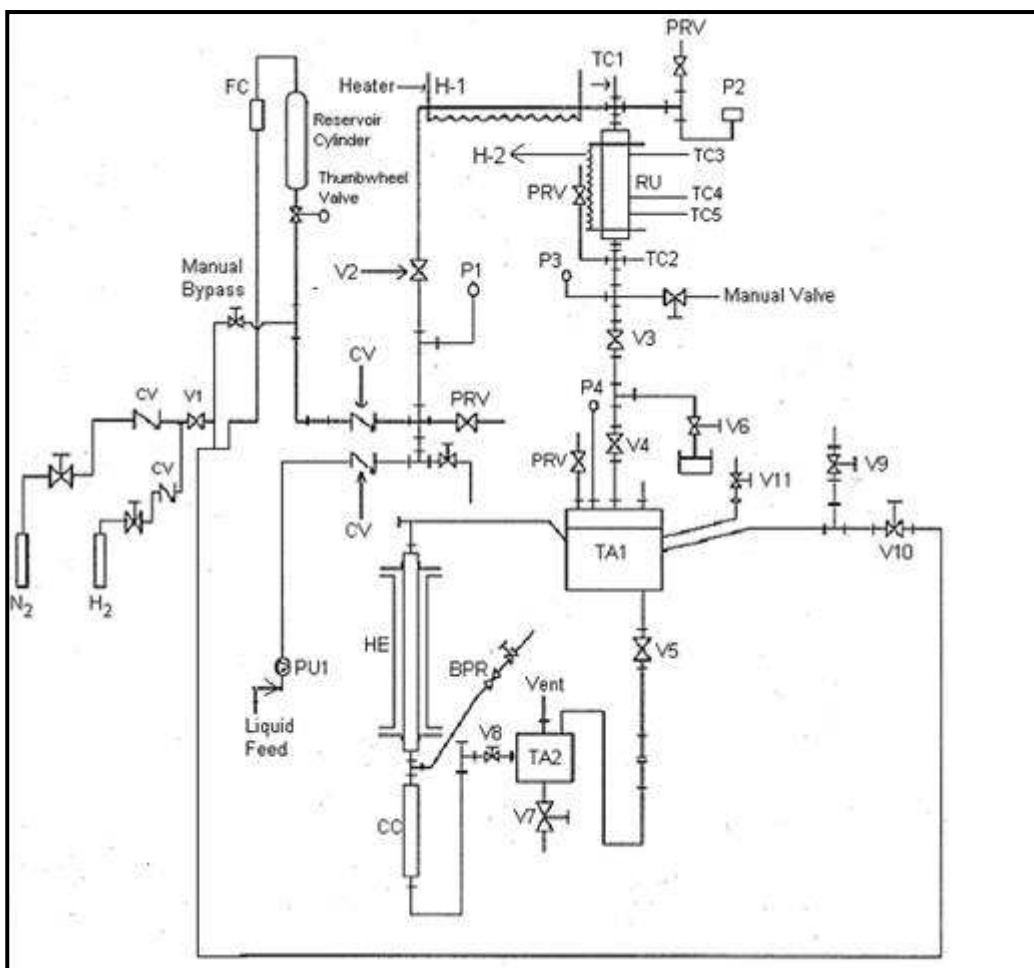


Figure 31. Trickle Bed Reactor System Schematic.

CV- Check Valve	PU1- High Pressure Pump	TCx- Thermocouples
TA1- Holding Tank	RU- Reactor Unit	Px- Pressure Gauges
PRV- Pressure Relief Valve	FC- H ₂ Mass Flow Controller	
BPR- Back Pressure Regulator		

Once disengaged from the liquid, the vapor then flows to a heat exchanger (HE) to knock out any remaining liquids before the hydrogen is vented through the back-pressure regulator. Pressure gauges are mounted at various points of the system. A pressure transducer (P2) is also provided at the top of the reactor to monitor the pressure of the incoming feed.

The hydrogen is fed into the system via a CV and a mass flow controller (FC). The gas feeding system also includes a nitrogen cylinder. Nitrogen gas is used for purging the trickle bed reactor system before activating the catalyst. The hydrogen and the nitrogen cylinders are equipped with separate CVs so that both the gases do not mix with each other while flowing into the reactor system. The gas outlet line is equipped with a Back Pressure Regulator (BPR- Model # KPB 1S0A422P2- 0000) that maintains the overall gas pressure in the system constant. With the aid of the FC and the BPR the hydrogen flow and pressure can be controlled in a precise manner. The hydrogen supply is a 2,000 psig high-pressure hydrogen cylinder. The remotely controlled valve V1 is the main hydrogen shut-off valve. Valves V2, V3, V4 and V5 supplied by Swagelok (Model # MS-131-DA) are also remotely controlled valves. The liquid is fed into the system with a Milton Roy high-pressure diaphragm metering pump (PU1) as noted above.

The system also includes a sample port from which the samples are taken without depressurizing the reactor. The manual sampler valve, V6, is located between the remotely controlled valves V3 and V4. When a sample is taken, V3 and V4 are closed. The product enclosed in the volume between V3 and V4 can be drained off the system via V6. When valves V1, V2, V3, and V4 are opened, the system is in “run mode”. The product from the RU will trickle down to the high-pressure holding tank, TA1. The TA1 is a 1-gallon autoclave that is under the same pressure as the RU. TA1 is held approximately at room temperature. TA1 is drained through the V5. V5 will not open unless V3 and V4 (marked V34 on the control panel) are closed. V3 and V4 are controlled in unison with one switch.

After passing through V5, the product is collected in a standard low-pressure 8-gallon steel tank (TA2) that is under atmospheric pressure with an open vent pipe. The 8-gallon tank is drained via a manual valve (V7) at its base.

The gas from the RU and the autoclave is mainly hydrogen. However, there will also be small amounts of hydrocarbon gases from the CTD. The hydrogen and other gases exit the autoclave at reactor pressure and pass a double-pipe heat exchanger (HE) where the CTD fractions condense. The condensate is collected in a one-foot long condensate collector (CC). It is made of the same material as the RU. The remaining hydrogen exits the system via the BPR and is vented into the fume hood. The condensate collector can be emptied into the 8-gallon tank via valve V8. Emptying the TA1 into TA2 should be done at a relatively low pressure. The valve V9 is used for depressurizing TA1. This is done in order to drop the process pressure. When TA1 is emptied into TA2, TA1 can be re-pressurized with the valve V10. If TA1 is not re-pressurized, there might be a fast gas/liquid rush through the catalyst when V34 is opened again. This might damage the catalyst bed and possibly other components.

The RU is attached to the system with unions. The RU with its heater can easily be removed from the system without elaborate disassembly of the rest of the system. This makes it relatively easy to perform experiments with different types or amounts of catalysts. The system is designed for use at temperatures up to 500 °C and pressure of 3000 psig, although typical operating conditions are temperatures up to 450 °C and 1200 psig pressure.

The design allows monitoring of the temperature difference between the RU wall and the catalyst. The relatively low thermal mass of the RU makes it possible to change the RU

temperature relatively fast in order to study reactions at various temperatures. The system also allows a wide range of hydrogen and liquid flow rates. The system is mainly remotely controlled with the exception of a few valves which are operated manually. A data logger is connected to the system in order to monitor continuously the temperatures of the RU wall, the RU exit port, and the catalyst. The RU temperature is controlled with the aid of the PID controller. The valves V1 through V5 are activated by compressed air. The air is controlled with the aid of electric solenoid valves. The pressure in the system is monitored from the control panel. The pressure transducer (P2) is placed relatively close to the RU input port. The system is equipped with a number of redundant pressure gauges and pressure relief valves (PRVs) for safety purposes. The 1-gallon autoclave has a rupture disk assembly as an additional safety feature. The rupture disk assembly (RD) is routed into a collection tank. V11 is used to reduce the exhaust flow rate from TA1 if RD ruptures. The other PRVs are also routed into the collection tank. Since the remotely controlled valves are indirectly relay controlled it is possible to add logical safety features integrated with the relay wiring. There are a few Boolean conditions that protect the system and the operator from the most dangerous operational procedures. For example, it is impossible to start the pump PU1 unless all the valves from the input line down to TA1 are open. It is also impossible to drain TA1 through V5 if V3 and V4 between the RU and TA1 are open. This would cause a flow rush through the system that could harm the catalyst or other components. To be able to drain the entire system from top to bottom, there is a manual switch to override the valve V5 opening restrictions. A photograph of the entire Trickle Bed Reactor system is shown in Figure 32. The reactor is in the upper right, the feed system is in the center and the effluent collection system is at the lower right.

As mentioned earlier, the hydrogenation of naphthalene was carried out initially in the trickle bed reactor as a “model” reaction which simulates the hydrogenation of the multi-component coal-derived liquids. Since the reactor system is a small lab-scale unit intended for experiments to optimize process parameters, the feed used here is a mixture of 10% by weight of naphthalene and 90% by weight of n-hexadecane.



Figure 32. Trickle Bed Reactor System

In order to assess the reactor performance the model compound naphthalene (Sigma-Aldrich, purity >99%) dissolved in n-hexadecane (Acros Organic, 99% purity) was used as the reactant. The solution is a mixture of 10% by weight of naphthalene dissolved in 90% by weight of n-hexadecane which was then hydrogenated at high temperature and high pressure over a Ni/Mo support catalyst. The desired chemical reaction occurring in this process is the hydrogenation reaction depicted in Figure 33. It has to be noted here that the solvent n-hexadecane was acting as an inert material and did not take part in the overall reaction in the trickle bed reactor.

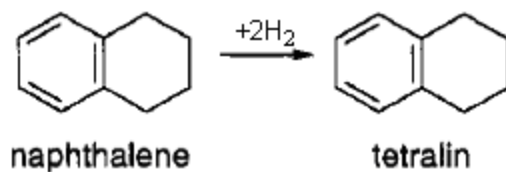


Figure 33. Hydrogenation Reaction of Naphthalene in the Trickle Bed Reactor.

Nickel/Molybdenum on an Aluminum Oxide support (Ni/Mo/Al₂O₃) was used as the catalyst for this process. The catalyst is a commercial hydrotreating catalyst as described previously. This catalyst in its sulfided form is a very effective catalyst for hydrogenation of polynuclear aromatic hydrocarbons such as naphthalene as described by Mann et al.⁵⁴ Based on the criteria for selection of the hydrotreating catalyst and data available in the literature, Ni-Mo/Al₂O₃ was chosen as the catalyst for this process. The catalyst particles, supplied by Albemarle Catalysts, are quadrilobe extrudates having an overall diameter of 1.0 mm. Figure 34 and Figure 35 are SEM images showing the shape of the catalyst particle being used in this work.

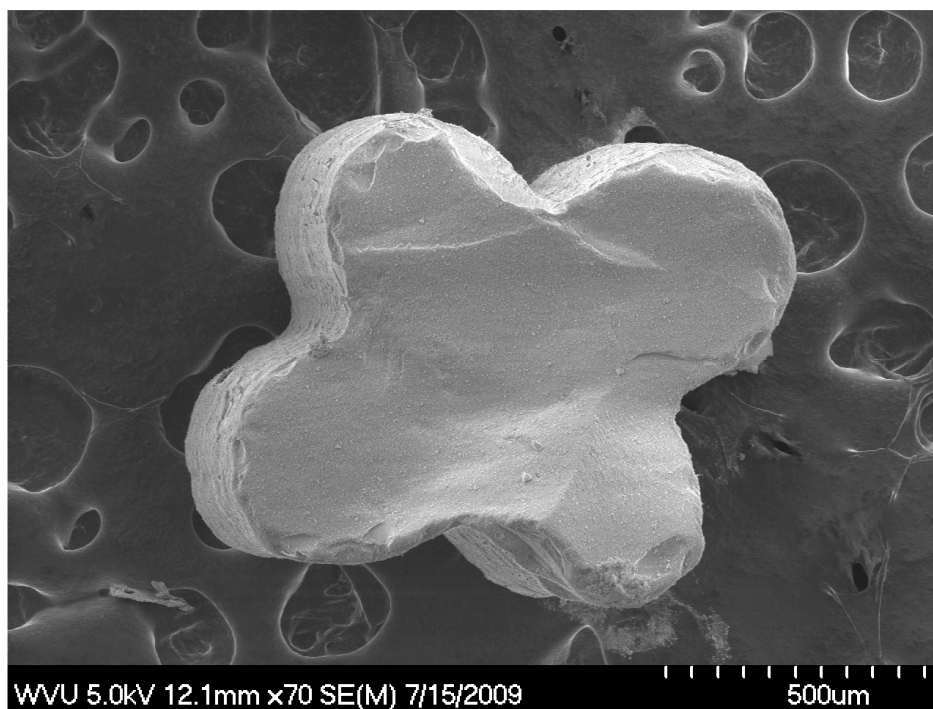


Figure 34. SEM Image of the Ni/Mo/Al₂O₃ Catalyst Showing the Quadrilobal Shape.

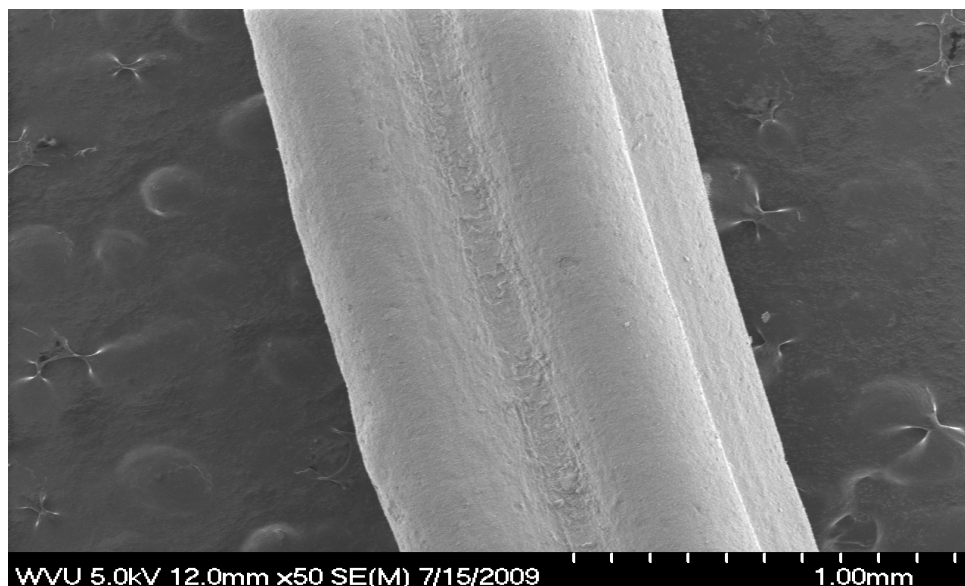


Figure 35. SEM Image of the Longitudinal View of the Ni/Mo/Al₂O₃ Catalyst Particle.

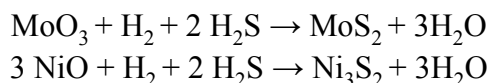
The catalyst was loaded in the middle of the reactor with the catalyst bed height being five inches. The catalyst obtained from the manufacturer (Albemarle Catalysts) is the form of its oxide. The oxides of molybdenum and nickel must be converted into their sulfides for the catalyst to be in the active state for hydrotreating.

Proper presulfiding results in the highest catalyst activity and would ensure a longer catalyst life with less frequent regenerations. The presulfiding reactions are exothermic and release water. Presulfiding is done by addition of the required amount of sulfur in a short period of time and at a low temperature. Above 200 °C there should always be a sulfur compound present. The catalyst was activated in-situ using presulfiding sulfur compounds that are added to the catalyst after it has been loaded into the reactor. As per the manufacturer's direction, the in-situ presulfiding procedure consists of four steps:

1. Catalyst drying: Fresh catalyst is a very hygroscopic material. It contains up to 10% water when loaded in moist weather. The presence of water affects the particle strength and deactivates the catalyst easily. Therefore, the catalyst must be completely dry before loading into the reactor and the loading must take place in completely dry weather. The catalyst bed is heated slowly with dry gas flowing up to 175 °C. Air, nitrogen or hydrogen can be used as the drying gas. Nitrogen is used as the drying gas in the present procedure.

2. Soaking in oil: Since the sulfiding reactions are exothermic, the liquid presulfiding sulfur compound should be present as a heat sink during sulfidation of the catalyst. Liquid feed should be introduced only after the catalyst has been completely dried. Cracked feedstocks should never be used during this process, because they significantly decrease the catalyst activity. 99% pure liquid wax paraffin oil spiked with 2.5 wt% carbon disulfide is used as the liquid phase for activating the catalyst in the present work.

3. Conversion of the oxides to sulfides: Proper presulfiding of the catalyst is obtained by supplying the stoichiometric amount of sulfur in a short period at a low temperature. The stoichiometric amount of sulfur can be calculated from the metals content of the catalyst according to the following reactions:



For the catalyst being used in the present work (Ni-Mo/Al₂O₃- KF-843-1.3Q), the stoichiometric amount of sulfur level on the catalyst is 12 wt%. These data are provided by the catalyst manufacturer, Albemarle Catalysts. The conversion of oxides to sulfides is kinetically controlled; therefore H₂S is released at a predetermined rate. This is usually observed when 40-60 % of the required stoichiometric amount of sulfur has been added. Premature H₂S breakthrough may be an indication of channeling or maldistribution in the reactor.

4. Saturation with sulfur: Once the H₂S is released, the remaining amount of sulfur must be added at elevated temperatures. The maximum activity of the catalyst is achieved once the catalyst is fully sulfided with the required stoichiometric amount of sulfur.

The catalyst was activated using the presulfiding liquid phase, a mixture of 99% pure liquid wax paraffin oil spiked with 2.5 wt% carbon-di-sulfide (CS₂). For activating the catalyst, the system was first purged with nitrogen for 30 min at 100°C. Hydrogen was then flushed through the system for 30 minutes at 290 psig. After purging, the presulfiding liquid phase, cut in at a liquid hourly space velocity (LHSV) of 5.33 hr⁻¹, was pumped into the reactor at a pressure of 435 psig with no hydrogen flow. After 3 hours of soaking at this condition, the hydrogen flow was set at 0.107 L/min and oil flow at a LHSV of 1.33 hr⁻¹. The temperature of the system was then increased to 250 °C and maintained constant for 5 hrs. This process was continued until the temperature of the system was raised to 320 °C. The temperature was held constant for 6 hrs at this temperature. Once this was achieved, the presulfiding liquid phase is changed to the actual hydrocarbon test feed. The temperature program for activating the catalyst is shown in Table 57.

Table 57. Temperature Program for Activating the Catalyst.

Temperature (°C) from	Increase to (°C)	Held for (hours)
100	250	5
250	300	5
300	320	6

3.2.7 Reactor Operation

The operating conditions employed for the baseline model compound hydrogenation studies were temperatures of 340-450 °C and a pressure of 1200 psig. A constant pressure of 1200 psig was chosen in the present study in order to maintain the feed mixture of naphthalene and n-hexadecane in the liquid phase. The effects of maintaining a high hydrogen partial pressure in a trickle bed reactor have been discussed earlier. The boiling point of the liquid mixture comprising naphthalene and n-hexadecane is calculated using the additivity rule, according to which the boiling point of a mixture is a function of the boiling points of the pure components and their respective mole fractions.

$$T_{mixture} = \sum_{i=1}^n T_i \cdot X_i \quad \text{Equation 14}$$

where $T_{mixture}$ = Boiling point of the liquid mixture, K
 T_i = Boiling point of the i^{th} component, K
 X_i = Mole fraction of the i^{th} component in the mixture

Since the boiling points and the mole fractions of the pure components in the liquid feed are known, it is easy to calculate the normal boiling point of the mixture using Equation (3.1). But this estimation is valid only at atmospheric pressure. It is a known fact that boiling points of substances vary with pressure. The boiling point of the liquid feed at elevated pressures was calculated by using an application devised by Goodman et al.⁵⁵ The boiling points of the pure components and the liquid mixture being used in this study are given in Table 58 at both atmospheric pressure as well as operating pressure.

Table 58. Boiling Points of Components and Reactor Feed at Atmospheric Pressure and Operating Pressure

Component	Mole Fraction in reactor feed, X_i	Boiling Point at atmospheric pressure, °C	Boiling Point at 1200 psig, °C
Naphthalene	0.164	218.0	544.4
n-Hexadecane	0.836	287.0	654.4
Reactor Feed	1.000	275.7	636.5

As seen from the preceding table, the calculation indicates that the hydrocarbon feed remains in the liquid phase under the reactor operating conditions used in this study.

Both hydrogen as well as the liquid feed were allowed to flow downward co-currently in the trickle bed reactor. Generally, low liquid flow rates and high gas flow rates are employed for the hydrotreating process in a Trickle Bed Reactor. For this hydrogenation study, the volumetric flow rate of the liquid was varied between 100 ml/hr and 300 ml/hr and the hydrogen flow rate was varied between 1 L/min and 4 L/min. The ratio of hydrogen flow rate to that of the liquid flow rate was maintained constant at $750 \text{ m}^3 \text{ H}_2 / \text{m}^3 \text{ oil}$. The ratio of flow rates of gas and liquid was constant at all times as it affects the concentration of gas and liquid in contact with the catalyst. The flow rates of gas and liquid also affect the wetting efficiency of the catalyst which is defined as the fraction of external surface of the catalyst covered by flowing liquid. The effects of incomplete wetting of the catalyst particles have been discussed earlier.

Once the entire study of the hydrogenation of naphthalene under the above mentioned conditions was completed, the ratio of hydrogen flow rate to that of the liquid flow rate was reduced to $100 \text{ m}^3 \text{ H}_2 / \text{m}^3 \text{ oil}$ and the reaction was again performed between temperatures of 340-450 °C and 1200 psig pressure. This was done to check if there was any change in the rate of reaction, order of reaction and activation energy at lower gas flow rates. The limitation of the Brooks Mass Flow Controller is that it does not allow the gas flow rate to be lower than 200 cc/min. Hence, the lowest possible ratio of hydrogen flow rate to liquid flow rate which could be obtained was 100. Table 59 and Table 60 provide the list of reaction conditions at which the hydrogenation of naphthalene to tetralin was performed in the trickle bed reactor. Prior to operating the trickle bed reactor at the aforementioned operating conditions, a blank test run without the catalyst was conducted at 425 °C and 1200 psig pressure. The catalyst particles were replaced by glass beads of the same size as that of the catalyst. This test was done to compare the conversion of naphthalene to tetralin with and without the catalyst. Ideally, in the absence of catalyst particles, the conversion of naphthalene to tetralin should be minimal. In order to ensure accurate values for the liquid flow rate, the weight of the feed entering the reactor was measured gravimetrically every two minutes. A plot of mass of feed vs time gave a straight line indicating that the mass flow rate of feed was constant. The slope of the plot gives the mass flow rate of the liquid feed entering the reactor. The rate constant and the order of the reaction were then found using integral method of analysis of data.

Table 59. Operating Conditions for Hydrogenation of Naphthalene in the TB Ratio of Hydrogen Flow rate to Liquid Flow Rate = 750.

Temperature (°C)	Liquid Flow Rate (ml/hr)	Hydrogen Flow Rate (L/min)
340	90	1.1250
	125	1.5625
	155	1.9375
	270	3.3750
360	130	1.6250
	160	2.0000
	200	2.5000
	320	4.0000
380	120	1.5000
	140	1.7500
	160	2.0000
	180	2.2500
	375	4.6875
425	125	1.5625
	140	1.7500
	160	2.0000
	230	2.8750
	275	3.5000
450	120	1.5000
	145	1.8750
	170	2.1250
	225	2.9375

Table 60. Operating Conditions for Hydrogenation of Naphthalene in the TBR Ratio of Hydrogen Flow rate to Liquid Flow Rate = 100.

Temperature (°C)	Liquid Flow rate (ml/hr)	Hydrogen Flow Rate (L/min)
340	150	0.250
	165	0.275
	200	0.333
	245	0.408
380	140	0.233
	175	0.300
	200	0.333
	240	0.400
425	160	0.266
	200	0.333
	240	0.400

Once the hydrogenation of naphthalene was completed in the trickle bed reactor at various operating conditions, the naphthalene feed was replaced by Koppers Coal Tar Distillate. In order to prove that the trickle bed reactor could be used for the hydrogenation of coal derived solvents, a preliminary run was performed at an operating temperature of 425 °C and a pressure of 1200 psig. An elemental analysis of the Koppers Coal Tar Distillate is given in Table 61.

Table 61. Elemental Analysis of Koppers Coal Tar Distillate.

Sample	Element	Percentage
Koppers Coal tar Distillate	Carbon	89.80
	Hydrogen	7.62
	Nitrogen	1.16
	Sulfur	0.37

As the reaction proceeded, the samples were collected every 60 minutes and analyzed using Fourier Transform Infrared Spectroscopy (FTIR). In order to obtain a baseline for this analysis, different concentrations of naphthalene and tetralin dissolved in n-hexadecane were first prepared and analyzed to obtain the wavenumber at which their respective peaks were occurring. A plot of absorbance vs. concentration gives the calibration curve for obtaining the concentration of the hydrogenated samples. For the case of analyzing hydrogenated coal tar distillate samples, Fourier Transform Infrared Spectroscopy could not be used. This is due to the fact that literally hundreds of compounds are present in the coal tar distillate sample, and hence, no specific IR band could be selected. Instead, an elemental analysis was done on both feed and product samples. Elemental analysis gives the exact percentage of carbon, hydrogen, nitrogen and sulfur in the feed as well as the product. Since it was only desired to verify the change in percentage of hydrogen from feed to product, elemental analysis was preferred over FTIR analysis.

The results of the hydrogenation of naphthalene to tetralin as well as the hydrogenation of coal tar distillates in the trickle bed reactor are discussed in this chapter. To start with, the results of the Fourier Transform Infra Red calibration of different concentrations of naphthalene and tetralin dissolved in n-hexadecane are provided. Secondly, the results of the blank test run performed in the absence of catalyst at 425 °C are discussed. Thirdly, the analysis of various samples collected during the runs at different temperatures (340 °C to 450 °C) is presented. Fourthly, the results for various samples analyzed during the runs performed under reduced flow rate of hydrogen are presented. Finally, the result of the elemental analysis of hydrogenation of coal tar distillates in the trickle bed reactor is provided.

Fourier Transform Infra Red (FTIR) analysis was used to characterize different samples of naphthalene and tetralin with varying concentrations using n-hexadecane as the solvent. The spectrum for naphthalene dissolved in n-hexadecane is shown in Figure 36. A unique peak corresponding to naphthalene alone occurs at a wavenumber of 781 cm^{-1} . It was also observed that the absorbance of naphthalene increases up to a certain value, i.e., 10% and then decreases. This is due to the fact that naphthalene does not completely dissolve in n-hexadecane for concentrations higher than 10% by weight. Therefore, a mixture of 10% by weight of naphthalene dissolved in 90% by weight of n-hexadecane was chosen as the feed. The values of absorbance for different concentrations of naphthalene in n-hexadecane are given in Table 62. The FTIR spectrum for tetralin dissolved in n-hexadecane is shown in Figure 37. The absorbance values for different concentrations of tetralin in n-hexadecane are given in Table 63. The FTIR results indicate that a unique peak corresponding to tetralin alone occurs at a wavenumber of 741 cm^{-1} .

Table 62. Absorbance values for Different Concentrations of Naphthalene in n-Hexadecane.

Absorbance	Concentration % of Naphthalene
0	0
0.201587	5
0.372501	10
0.268161	15

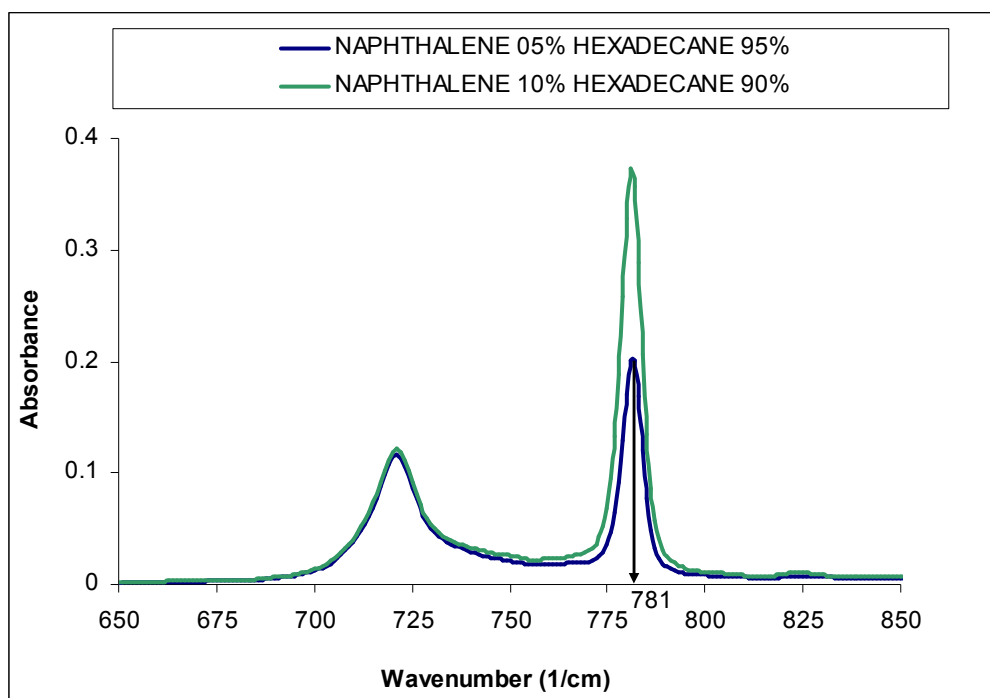


Figure 36. FTIR spectra of varying concentrations of Naphthalene in n-Hexadecane.

Table 63. Absorbance values for Different Concentrations of Tetralin in n-Hexadecane

Absorbance	Concentration % of Tetralin
0	0
0.105962	5
0.187101	10
0.265565	15

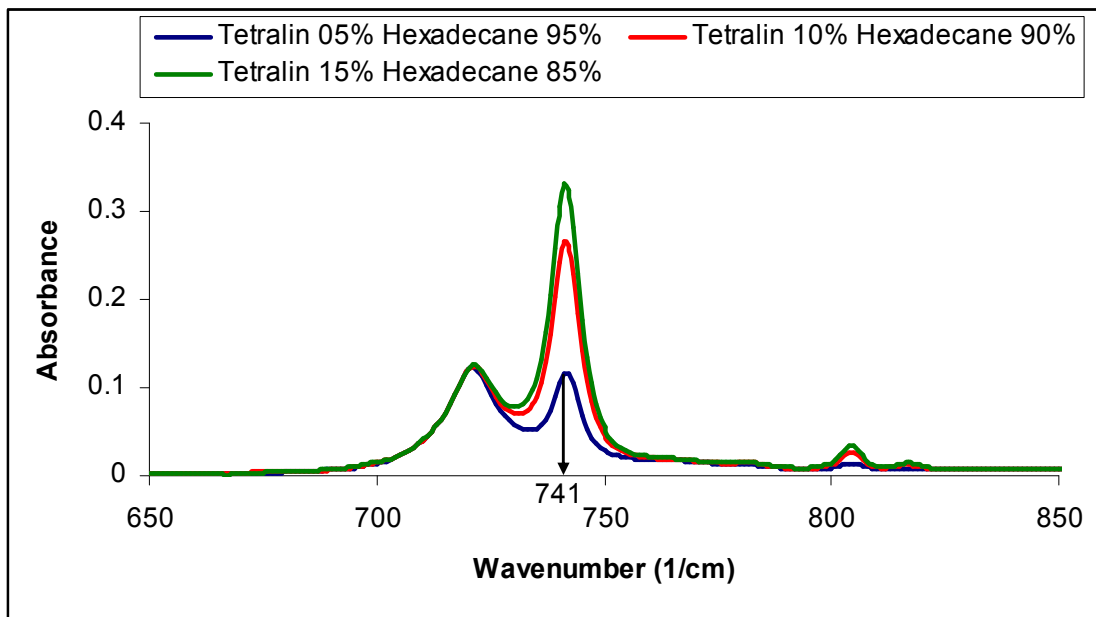


Figure 37. FTIR Spectra of varying concentrations of Tetralin in n-Hexadecane.

The Absorbance vs Concentration calibration plot for both naphthalene and tetralin is shown in Figure 38. This plot was then subsequently used for obtaining the concentrations of the hydrogenated samples from the trickle bed reactor.

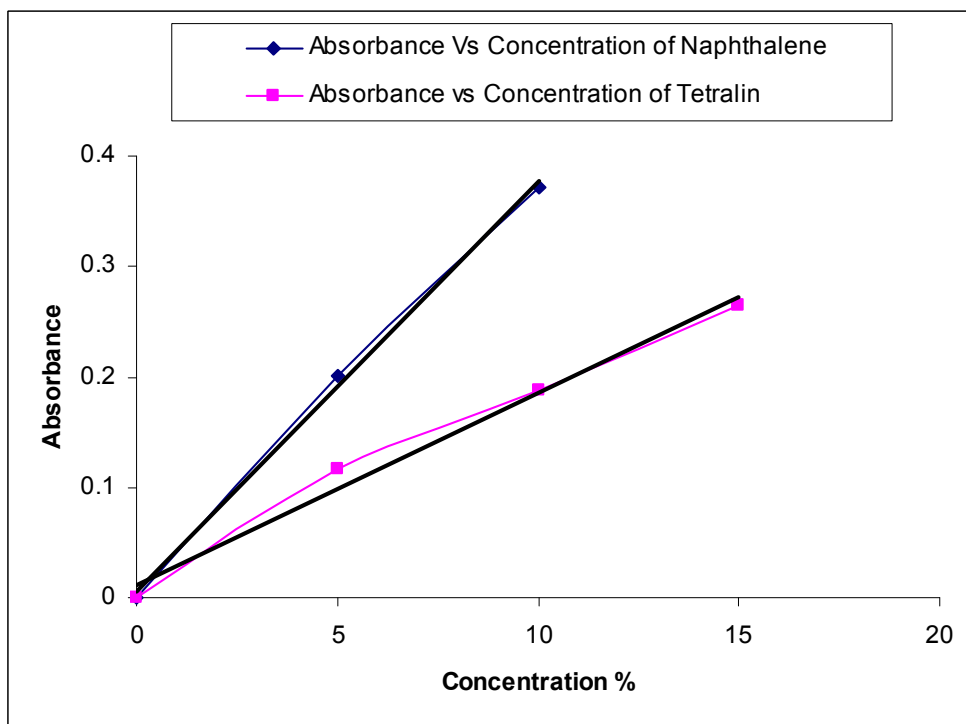


Figure 38. Absorbance vs Concentration for varying concentrations of Naphthalene and Tetralin in n-Hexadecane.

3.2.8 Control Experiment without Catalyst

Once the baseline calibration analysis was performed and the results analyzed, a blank test was performed for the hydrogenation of naphthalene in the trickle bed reactor at the operating temperature of 425 °C and 1200 psig pressure. The liquid feed flow rate for this test was 135 ml/hr and the hydrogen gas flow rate was maintained at 1.6875 L/min. This test was carried out in the absence of catalyst particles which were replaced by glass beads of the same size as that of the catalyst particles. The blank test was performed to show that the hydrogenation reaction would not occur even at the maximum operating conditions and that naphthalene would not be hydrogenated to tetralin in the absence of a catalyst. As the reaction proceeded, hydrogenated samples were collected every 60 min and analyzed using FTIR spectroscopy. The results for the blank test are shown in Table 64.

Table 64. Results for Blank Test Performed at 425 °C and 1200 psig Without Catalyst.

Time (min)	Absorbance (at 781 cm ⁻¹)	Absorbance (at 741 cm ⁻¹)	% Concentration (naphthalene)	% Concentration (tetralin)	Conversion, X _n (C _{ao} -C _a)/C _{ao}
0	0.367212	0	10	0	-
60	0.353684	0.031212	9.2	0.8	0.08
120	0.352304	0.031138	9.2	0.8	0.08
180	0.33415	0.035858	8.8	1.2	0.12
240	0.327669	0.03628	8.8	1.2	0.12
300	0.329986	0.037498	8.8	1.2	0.12

C_{ao} = Initial concentration of naphthalene in the feed, 10 % by weight.

C_a = Final concentration of naphthalene in the hydrogenated sample.

The results of the FTIR spectroscopy for all the samples taken for the blank test are shown in Figure 39. From the plot of Absorbance vs Wavenumber, it can be clearly stated that the hydrogenation reaction of naphthalene is not proceeding at more than 12% conversion. The conversion of naphthalene to tetralin is only 12 % which is very little when compared to the conversion in the presence of a catalyst indicating that the hydrogenation reaction occurring is due to catalytic activity. It can be seen from Table 65 that the absorbance of naphthalene at 781 cm⁻¹ is not changing appreciably and also the peaks of tetralin at 741 cm⁻¹ are not increasing with

time which is the expected result. A plot of concentration vs residence time shown in Figure 40 confirms the result. It should also be pointed out that, from the results presented in Table 65, the sum of the concentrations of naphthalene and tetralin add to 10% for all the samples. This indicates a good mass balance and the lack of any further conversion of tetralin to decalin. Thus, the FTIR method of analysis appears to be well suited for this study.

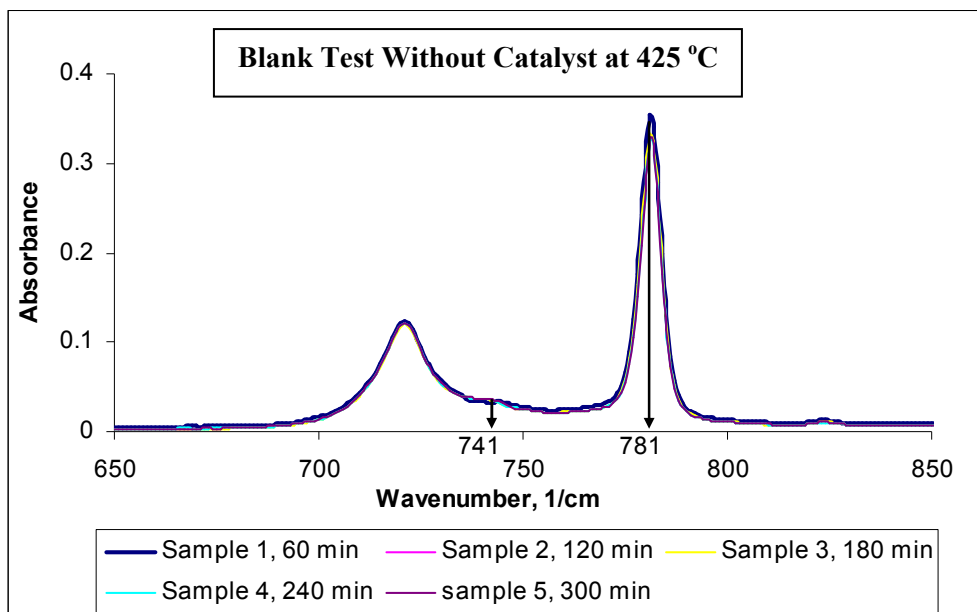


Figure 39. Plot of Absorbance vs Wavenumber for different samples taken at 425 °C without catalyst

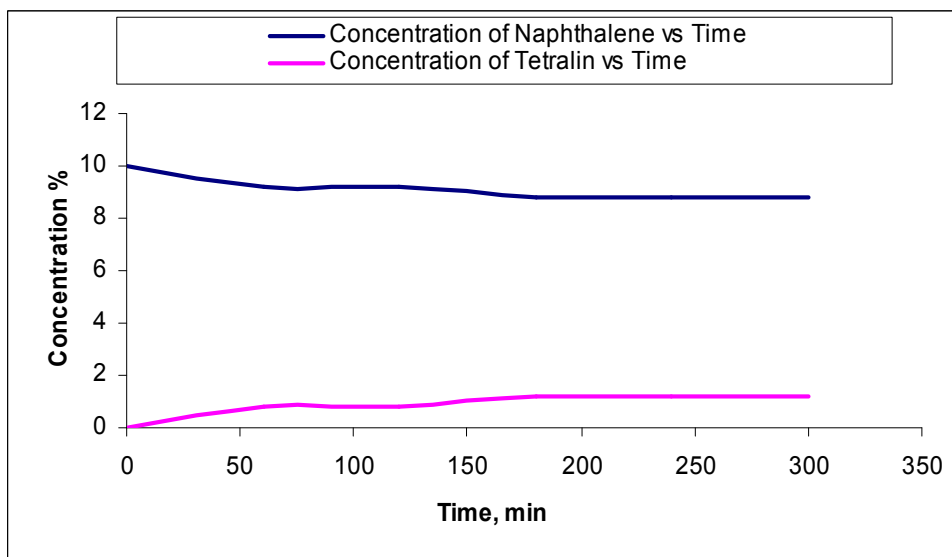


Figure 40. Plot of concentration vs time for the blank test performed at 425 °C.

3.2.9. Hydrogenation of Naphthalene with Ni-Mo Catalyst

Following the blank test, the hydrogenation of naphthalene in the trickle bed reactor in the presence of the sulfided Ni-Mo/Al₂O₃ catalyst was studied at different temperatures ranging from 340 °C to 450 °C. The results for all the runs at 5 different temperatures, 340 °C, 360 °C, 380 °C, 425 °C and 450 °C are presented as described earlier. The extent of reaction for the hydrogenated samples was tested using a FTIR analysis at a wavenumber of 781 cm⁻¹ and 741 cm⁻¹ for naphthalene and tetralin respectively. The experimental results indicate that naphthalene has been converted to tetralin. It should be noted here that no other peaks other than those for naphthalene and tetralin have been observed at any time during the reaction. This is a clear indication that further hydrogenation of tetralin to form cis-decalin and trans-decalin is not occurring in the trickle bed reactor.

The hydrogenation reaction was performed at different flow rates of the liquid ranging from 90 ml/hr to 300 ml/hr. The hydrogen gas flow rate was varied accordingly so as to keep the ratio of flow rate of gas to liquid constant throughout at 750. Also, the pressure was kept constant at 1200 psig for all runs. Table 65 through Table 68 provide the results for the hydrogenation of naphthalene with varying liquid and gas flow rates at 340 °C in the presence of a catalyst. It can be observed from these results that as the flow rate of liquid increases, the conversion levels of naphthalene decrease due to decreased residence time in the catalyst bed. FTIR spectroscopy results for all the runs done at 340 °C with varying flow rates of gas and liquid are shown in Figure 41 through Figure 44.

Table 65. Temperature 340 °C, Liquid Flow Rate: 90 ml/hr, H₂ Flow Rate: 1.125 L/min.

Time (min)	Absorbance (at 781 cm ⁻¹)	Absorbance (at 741 cm ⁻¹)	% Concentration (naphthalene)	% Concentration (tetralin)	Conversion X _n (C _{ao} -C _a)/C _{ao}
0	0.367821	0	10	0	
60	0.29324	0.056596	7.6	2.4	0.24
120	0.253296	0.064206	6.6	3.2	0.34
180	0.219384	0.075903	5.8	3.6	0.42
270	0.135581	0.108063	3.4	5.6	0.66
330	0.138739	0.112702	3.4	5.6	0.66

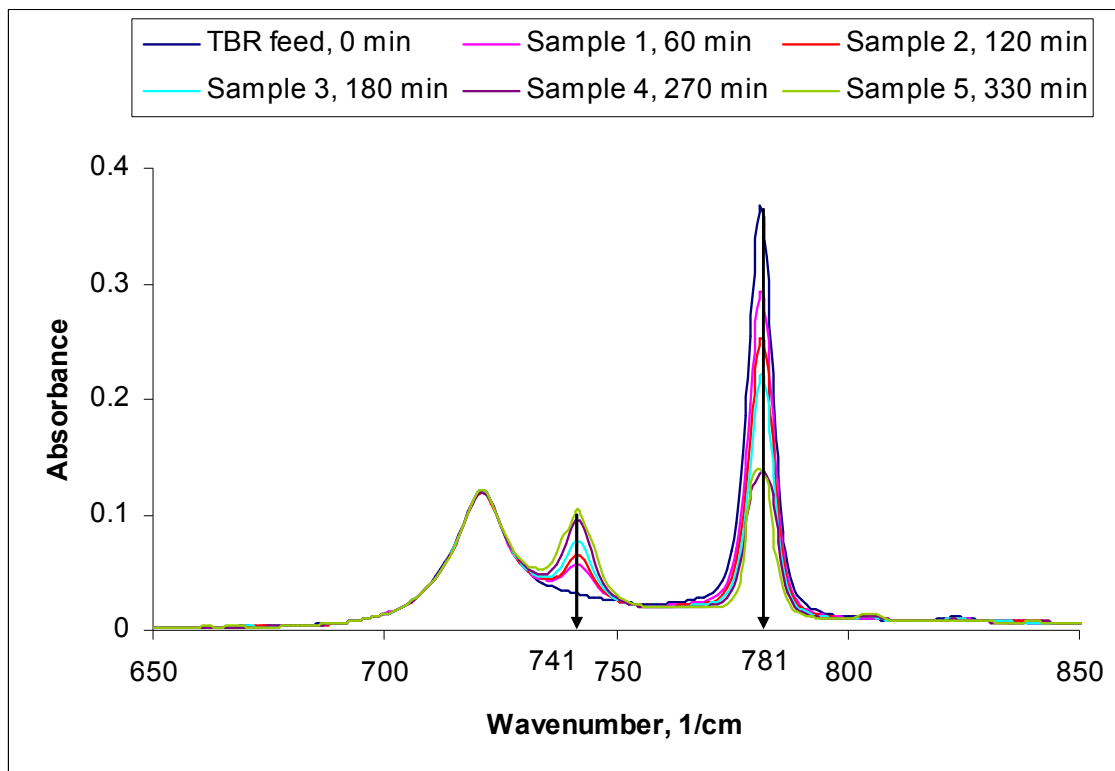


Figure 41. FTIR spectroscopy results at 340 °C and liquid flow rate 90 ml/hr.

Table 66. Temperature 340 °C, Liquid Flow Rate: 127 ml/hr H₂ Flow Rate: 1.5625 L/min.

Time (min)	Absorbance (at 781 cm ⁻¹)	Absorbance (at 741 cm ⁻¹)	% Concentration (naphthalene)	% Concentration (tetralin)	Conversion X _n
0	0.362415	0	10	0	
60	0.248117	0.069652	6.6	3.2	0.34
120	0.190439	0.093370	5.0	4.8	0.50
180	0.191821	0.101677	5.0	4.8	0.50
240	0.191814	0.098259	5.0	4.8	0.50

Table 67. Temperature 340 °C, Liquid Flow Rate: 155 ml/hr, H₂ Flow Rate: 1.9375 L/min.

Time (min)	Absorbance (at 781 cm ⁻¹)	Absorbance (at 741 cm ⁻¹)	% Concentration (naphthalene)	% Concentration (tetralin)	Conversion X _n
0	0.367775	0	10	0	
60	0.253187	0.066575	6.6	3.2	0.34
120	0.228919	0.086481	6.0	4.0	0.40
180	0.208854	0.091669	5.4	4.4	0.44
240	0.207735	0.089981	5.4	4.4	0.46
300	0.208722	0.092007	5.4	4.4	0.46

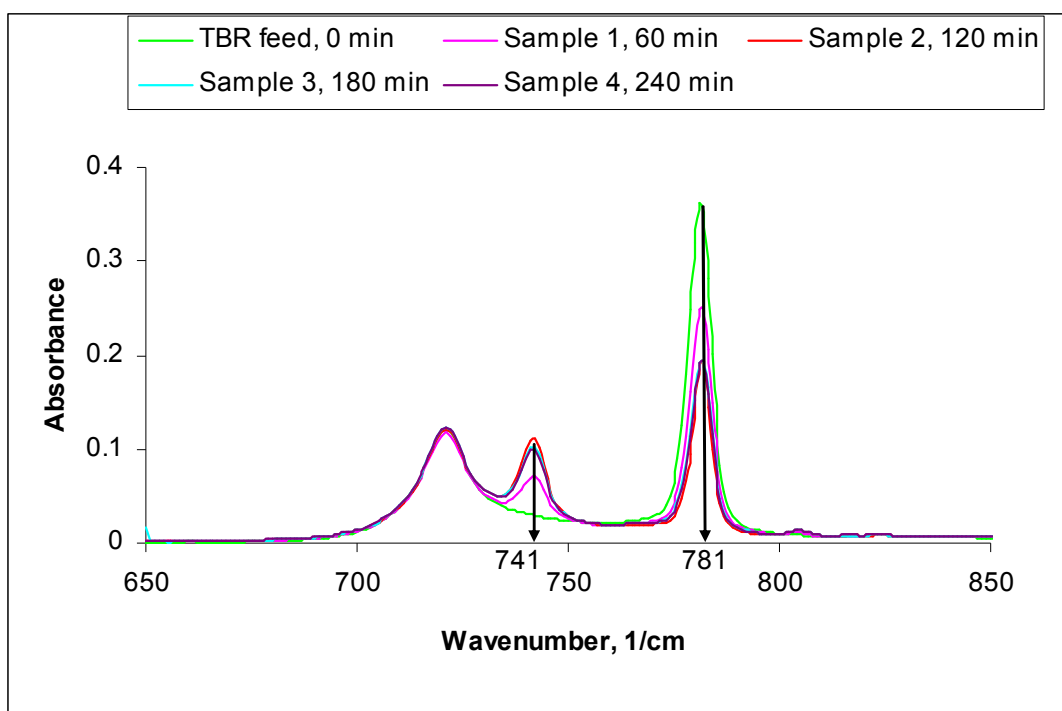


Figure 42. FTIR spectroscopy results at 340 °C and liquid flow rate 127 ml/hr.

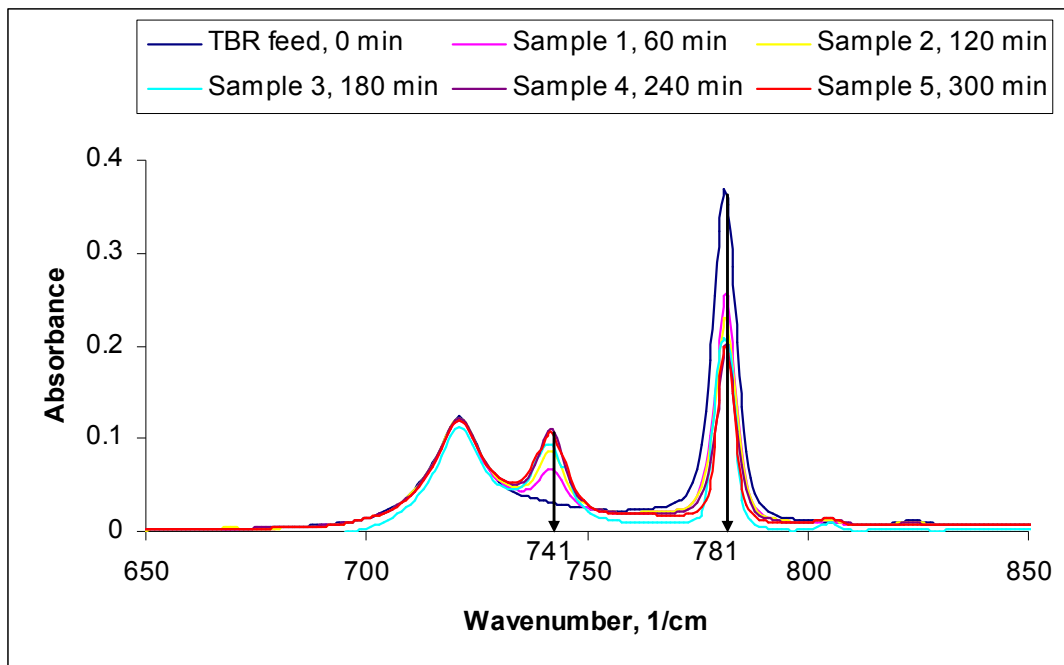


Figure 43. FTIR spectroscopy results at 340 °C and liquid flow rate 155 ml/hr.

Table 68. Temperature 340 °C, Liquid Flow Rate: 267 ml/hr, H₂ Flow Rate: 3.375 L/min.

Time (min)	Absorbance (at 781 cm ⁻¹)	Absorbance (at 741 cm ⁻¹)	% Concentration (naphthalene)	% Concentration (tetralin)	Conversion X _n
0	0.373039	0	10	0	
60	0.287753	0.046417	7.6	2.0	0.24
120	0.266692	0.062836	7.0	2.8	0.30
180	0.241438	0.074863	6.4	3.2	0.36
240	0.246662	0.072567	6.4	3.2	0.36
300	0.24195	0.072951	6.4	3.2	0.36

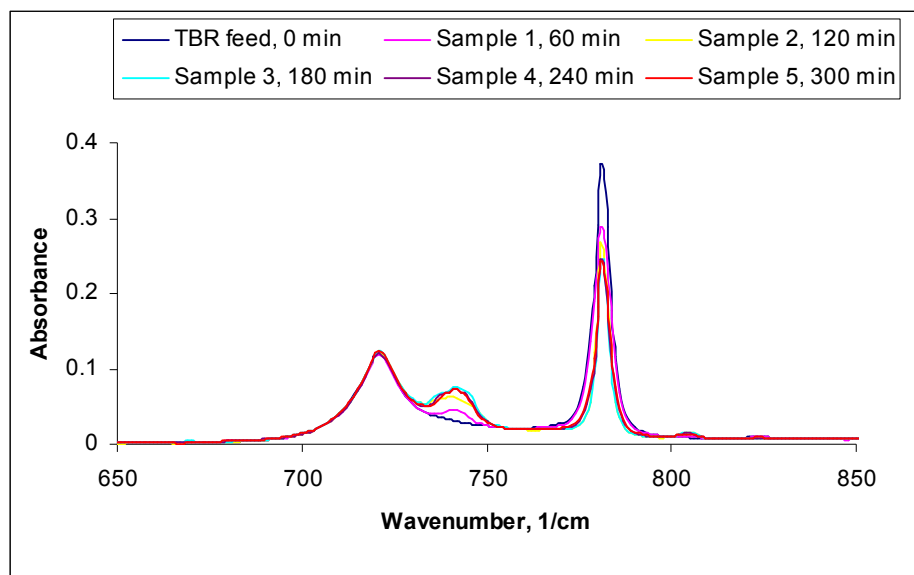


Figure 44. FTIR spectroscopy results at 340 °C and liquid flow rate 267 ml/hr.

The FTIR spectroscopy results indicate that as time proceeds, the absorbance of naphthalene in the hydrogenated samples decreases indicating that the concentration of naphthalene in the hydrogenated samples is decreasing while that of tetralin is increasing, thereby proving that the hydrogenation reaction is indeed occurring in the trickle bed reactor. In most cases it takes about 180 min for the reaction to reach steady state. It should be noted that in all but a few cases, the sum of the wt% of naphthalene and tetralin is approximately equal to 10%, indicating a reasonable mass balance for the system.

An integral method of analysis of the above data models the hydrogenation reaction as a first-order reaction. This result is in accordance with the results available in literature. Table 69 provides the combined data of all the runs done at 340 °C with varying flow rates.

Table 69. Combined data for all the runs at 340 °C with varying flow rates. Initial concentration of naphthalene in the feed, $C_{a0} = 10\%$ by weight.

Residence Time, min (V/V_0)	Final concentration of naphthalene, C_a %	Conversion, X_n %
26.667	3.4	66
18.898	5.0	50
15.484	5.4	46
8.988	6.4	36

V = Volume of the reaction zone, taken as the volume of the catalyst bed = 40 cc.

V_0 = Volumetric flow rate of the feed, ml/hr.

A plot of $-\ln (C_a/C_{a0})$ vs Residence time gives a straight line passing through origin indicating that the reaction is a first-order reaction as shown in Figure 45. Residence time is defined as the time required to treat one reactor volume of feed or the time taken by the reactant to pass through the volume of catalyst bed. Each of the data points associated with a specified residence time is taken as the final steady state value from Table 70 Table 66 through Table 68. The slope of the plot gives the rate constant of the hydrogenation reaction at 340 °C. The good straight-line fit of the data confirms that the hydrogenation reaction is indeed following first-order kinetics. To obtain the rate of reaction and activation energy for the hydrogenation reaction, the hydrogenation reaction has to be run at different temperatures and different flow rates. Thus, the reaction was run at different temperatures ranging from 340 °C to 450 °C. Table 70 through Table 91 describes the results obtained for all the runs at temperatures of 360 °C to 450 °C in the presence of a catalyst.

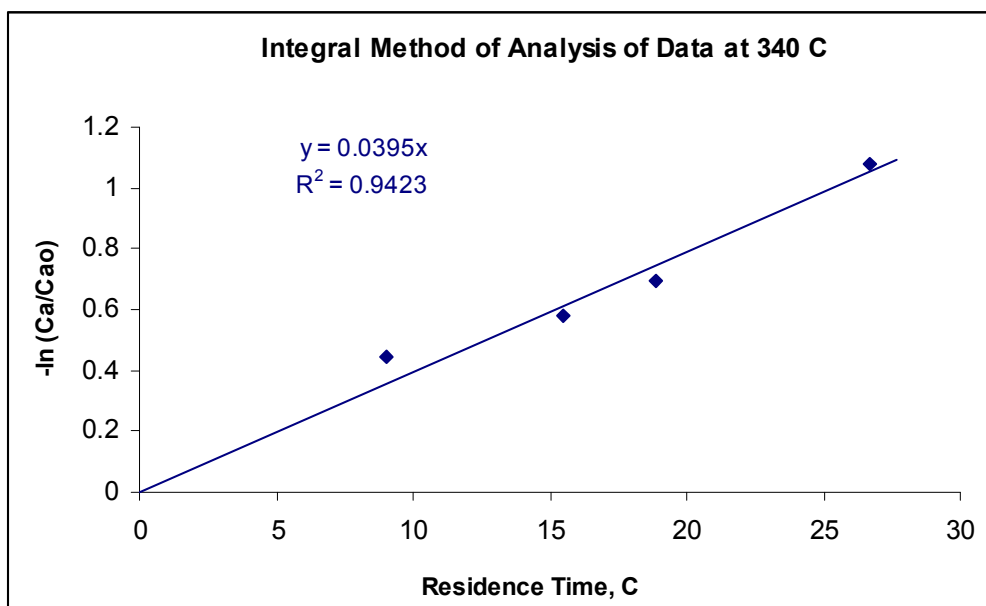


Figure 45. Integral Method of Analysis of Data at 340 °C.

Table 70. Temperature 360 °C, Liquid Flow Rate: 130 ml/hr, H₂ Flow Rate: 1.625 L/min.

Time (min)	Absorbance (at 781 cm ⁻¹)	Absorbance (at 741 cm ⁻¹)	% Concentration (naphthalene)	% Concentration (tetralin)	Conversion Xn
0	0.364127	0	10	0	
60	0.295789	0.047385	8	2	0.2
120	0.165312	0.102286	4.4	5.2	0.56
180	0.164145	0.104543	4.4	5.2	0.56
240	0.166755	0.101053	4.4	5.2	0.56

Table 71. Temperature 360 °C, Liquid Flow Rate: 163 ml/hr, H₂ Flow Rate: 2.0 L/min.

Time (min)	Absorbance (at 781 cm ⁻¹)	Absorbance (at 741 cm ⁻¹)	% Concentration (naphthalene)	% Concentration (tetralin)	Conversion Xn
0	0.352092	0	10	0	
60	0.255487	0.069856	6.8	3.2	0.32
120	0.191068	0.091126	5	4.6	0.5
180	0.175657	0.098397	4.6	5.2	0.54
240	0.134634	0.11278	3.2	5.6	0.68
300	0.136839	0.115327	3.2	5.6	0.68

Table 72. Temperature 360 °C, Liquid Flow Rate: 200 ml/hr, H₂ Flow Rate: 2.5 L/min.

Time (min)	Absorbance (at 781 cm ⁻¹)	Absorbance (at 741 cm ⁻¹)	% Concentration (naphthalene)	% Concentration (tetralin)	Conversion Xn
0	0.359659	0	10	0	
60	0.264782	0.043762	7.2	2.2	0.28
120	0.18851	0.084047	5.0	4.4	0.52
180	0.185173	0.094392	4.6	4.8	0.52
240	0.183346	0.090583	4.6	4.8	0.52

Table 73. Temperature 360 °C, Liquid Flow Rate: 316 ml/hr, H₂ Flow Rate: 4.0 L/min.

Time (min)	Absorbance (at 781 cm ⁻¹)	Absorbance (at 741 cm ⁻¹)	% Concentration (naphthalene)	% Concentration (tetralin)	Conversion Xn
0	0.365962	0	10	0	
60	0.271163	0.059013	7.2	2.8	0.28
120	0.233378	0.070742	6.4	3.2	0.36
180	0.227505	0.071671	6	3.6	0.4
240	0.225589	0.073901	6	3.6	0.4

The results at 360 °C follow a similar pattern as that of the results obtained at 340 °C (see Table 70 through Table 73). However, the conversion of naphthalene is higher at 360 °C indicating that the conversion and the rate of reaction increase with increasing temperature. Table 74 provides the combined data of all the runs done at 360 °C with varying flow rates.

Table 74. Combined data for all the runs at 360 °C with varying flow rates.

Residence Time, min (V/V ₀)	Final concentration of naphthalene, Ca	Conversion, Xn %
18.461	3.4	66
14.724	4.4	56
12	4.6	54
7.595	6	40

Similar to the data obtained at 340 °C, it can be observed from these results that as the flow rate of liquid increases, the conversion of naphthalene decreases due to decreased residence time in the catalyst bed. The concentration of naphthalene and tetralin in the hydrogenated samples is calculated using Figure 38 (Absorbance vs Concentration for varying concentrations of naphthalene and tetralin in n-hexadecane).

Table 75. Temperature 380 °C, Liquid Flow Rate: 120 ml/hr, H₂ Flow Rate: 1.5 L/min

Time (min)	Absorbance (at 781 cm ⁻¹)	Absorbance (at 741 cm ⁻¹)	% Concentration (naphthalene)	% Concentration (tetralin)	Conversion Xn
0	0.378675	0	10	0	
60	0.326741	0.048056	8.0	2.0	0.20
150	0.076200	0.123518	2.0	6.8	0.80
180	0.073638	0.131480	1.8	6.8	0.82
240	0.069580	0.134602	1.8	7.2	0.82

Table 76. Temperature 380 °C, Liquid Flow Rate: 140 ml/hr, H₂ Flow Rate: 1.75 L/min

Time (min)	Absorbance (at 781 cm ⁻¹)	Absorbance (at 741 cm ⁻¹)	% Concentration (naphthalene)	% Concentration (tetralin)	Conversion X _n
0	0.365163	0	10	0	
60	0.127969	0.113552	3.6	6.0	0.64
120	0.133269	0.116943	3.6	6.2	0.64
180	0.135585	0.116755	3.6	6.2	0.64
240	0.088432	0.123012	2.4	6.4	0.76
300	0.090759	0.122732	2.4	6.4	0.76

Table 77. Temperature 380 °C, Liquid Flow Rate: 160 ml/hr, H₂ Flow Rate: 2.0 L/min.

Time (min)	Absorbance (at 781 cm ⁻¹)	Absorbance (at 741 cm ⁻¹)	% Concentration (naphthalene)	% Concentration (tetralin)	Conversion X _n
0	0.364163	0	10	0	
60	0.232962	0.046719	6.2	2.2	0.38
120	0.181965	0.097251	4.8	5.2	0.52
180	0.139181	0.104464	3.6	5.6	0.64
240	0.094783	0.117830	2.6	6.4	0.74
300	0.097449	0.122354	2.6	6.4	0.74

Table 78. Temperature 380 °C, Liquid Flow Rate: 180 ml/hr, H₂ Flow Rate: 2.25 L/min.

Time (min)	Absorbance (at 781 cm ⁻¹)	Absorbance (at 741 cm ⁻¹)	% Concentration (naphthalene)	% Concentration (tetralin)	Conversion X _n
0	0.356907	0	10	0	
60	0.274165	0.050987	7.6	2.2	0.24
120	0.211892	0.074674	5.8	3.8	0.42
180	0.152713	0.092938	4.2	5.2	0.58
240	0.107983	0.107939	2.8	6.0	0.72
300	0.100702	0.111322	2.8	6.0	0.72
330	0.103864	0.122598	2.8	6.4	0.72

Table 79. Temperature 380 °C, Liquid Flow Rate: 375 ml/hr, H₂ Flow Rate: 4.6875 L/min.

Time (min)	Absorbance (at 781 cm ⁻¹)	Absorbance (at 741 cm ⁻¹)	% Concentration (naphthalene)	% Concentration (tetralin)	Conversion X _n
0	0.363409	0	10	0	
60	0.264349	0.054547	7.2	2.8	0.28
120	0.224311	0.079615	5.8	3.8	0.42
180	0.226347	0.085546	5.8	4.2	0.42
240	0.216995	0.088103	5.8	4.2	0.42

Table 80. Combined data for all the runs at 380 °C with varying flow rates.

Residence Time, min (V/V ₀)	Final concentration of naphthalene, Ca	Conversion, X _n %
6.40	5.8	42
13.54	2.8	72
15.48	2.6	74
17.14	2.4	76
20.44	1.8	82

Table 81. Temperature 425 °C, Liquid Flow Rate: 125 ml/hr, H₂ Flow Rate: 1.5625L/min.

Time (min)	Absorbance (at 781 cm ⁻¹)	Absorbance (at 741 cm ⁻¹)	% Concentration (naphthalene)	% Concentration (tetralin)	Conversion Xn
0	0.366152	0	10	0	
60	0.289194	0.052512	7.6	2.4	0.24
120	0.106563	0.115734	2.8	6.0	0.72
180	0.101346	0.122681	2.4	6.4	0.76
240	0.068048	0.136542	1.6	7.6	0.82
300	0.067198	0.134559	1.6	7.6	0.82

Table 82. Temperature 425 °C, Liquid Flow Rate: 140 ml/hr, H₂ Flow Rate: 1.75 L/min

Time (min)	Absorbance (at 781 cm ⁻¹)	Absorbance (at 741 cm ⁻¹)	% Concentration (naphthalene)	% Concentration (tetralin)	Conversion Xn
0	0.368959	0	10	0	
60	0.222854	0.074493	6.0	4.0	0.4
120	0.181572	0.075486	4.8	4.0	0.52
180	0.135524	0.104455	3.6	5.6	0.64
240	0.083762	0.109639	2.0	6.0	0.80
300	0.081570	0.127540	2.0	6.8	0.80

Table 83. Temperature 425 °C, Liquid Flow Rate: 160 ml/hr, H₂ Flow Rate: 2 L/min

Time (min)	Absorbance (at 781 cm ⁻¹)	Absorbance (at 741 cm ⁻¹)	% Concentration (naphthalene)	% Concentration (tetralin)	Conversion Xn
0	0.370084	0	10	0	
30	0.219326	0.069332	6.0	3.6	0.40
60	0.169540	0.095983	4.4	5.2	0.56
120	0.139389	0.106864	3.6	5.8	0.64
180	0.093285	0.123274	2.2	6.8	0.78
240	0.087775	0.130843	2.2	6.8	0.78
300	0.086783	0.131479	2.2	6.8	0.78

Table 84. Temperature 425 °C, Liquid Flow Rate: 230 ml/hr, H₂ Flow Rate: 2.875 L/min.

Time (min)	Absorbance (at 781 cm ⁻¹)	Absorbance (at 741 cm ⁻¹)	% Concentration (naphthalene)	% Concentration (tetralin)	Conversion Xn
0	0.368323	0	10	0	
60	0.274125	0.047343	7.2	2.4	0.28
120	0.160610	0.103196	4.2	5.2	0.58
180	0.141910	0.10683	3.6	5.8	0.64
240	0.110631	0.119796	3.2	6.4	0.68
300	0.117459	0.124441	3.2	6.4	0.68
330	0.116874	0.127459	3.2	6.8	0.68

Table 85. Temperature 425 oC, Liquid Flow Rate: 275 ml/hr, H2 Flow Rate: 3.5 L/min

Time (min)	Absorbance (at 781 cm ⁻¹)	Absorbance (at 741 cm ⁻¹)	% Concentration (naphthalene)	% Concentration (tetralin)	Conversion Xn
0	0.371452	0	10	0	
60	0.276021	0.041337	7.4	1.8	0.26
120	0.142487	0.122166	3.8	6.2	0.72
180	0.143571	0.126032	3.8	6.2	0.72
240	0.137019	0.123345	3.8	6.2	0.72

Table 86. Combined data for all the runs at 425 °C with varying flow rates.

Residence Time, min (V/V ₀)	Final concentration of naphthalene, Ca	Conversion, Xn %
8.72	3.8	62
10.43	3.2	68
15.18	2.2	78
17.14	2.0	80
19.20	1.6	84

Table 87. Temperature 450 °C, Liquid Flow Rate: 120 ml/hr, H₂ Flow Rate: 1.5 L/min.

Time (min)	Absorbance (at 781 cm ⁻¹)	Absorbance (at 741 cm ⁻¹)	% Concentration (naphthalene)	% Concentration (tetralin)	Conversion Xn
0	0.360390	0	10	0	
60	0.297821	0.047279	7.8	2.0	0.22
120	0.147563	0.111734	3.8	5.6	0.62
180	0.102282	0.117992	2.4	6.4	0.76
240	0.055048	0.145542	1.4	8.0	0.86
300	0.054483	0.144927	1.4	8.0	0.86

Table 88. Temperature 450 °C, Liquid Flow Rate: 145 ml/hr, H₂ Flow Rate: 1.875 L/min.

Time (min)	Absorbance (at 781 cm ⁻¹)	Absorbance (at 741 cm ⁻¹)	% Concentration (naphthalene)	% Concentration (tetralin)	Conversion X _n
0	0.367082	0	10	0	
60	0.271596	0.049953	7.2	2.2	0.28
120	0.160137	0.095088	4.2	4.8	0.58
180	0.075701	0.123801	1.8	6.4	0.82
240	0.072883	0.129723	1.8	6.8	0.82
300	0.071437	0.130172	1.8	6.8	0.82

Table 89. Temperature 450 °C, Liquid Flow Rate: 170 ml/hr, H₂ Flow Rate: 2.125 L/min.

Time (min)	Absorbance (at 781 cm ⁻¹)	Absorbance (at 741 cm ⁻¹)	% Concentration (naphthalene)	% Concentration (tetralin)	Conversion X _n
0	0.370005	0	10	0	
60	0.281137	0.053709	7.4	2.4	0.26
120	0.249658	0.061681	6.4	2.8	0.36
180	0.157151	0.078235	4.2	4.0	0.58
240	0.103582	0.123846	2.4	6.4	0.76
300	0.102687	0.124278	2.4	6.4	0.76

Table 90. Temperature 450 °C, Liquid Flow Rate: 225 ml/hr, H₂ Flow Rate: 2.9375 L/min.

Time (min)	Absorbance (at 781 cm ⁻¹)	Absorbance (at 741 cm ⁻¹)	% Concentration (naphthalene)	% Concentration (tetralin)	Conversion X _n
0	0.370005	0	10	0	
60	0.278600	0.056747	7.4	2.4	0.26
120	0.177651	0.096338	4.6	4.8	0.54
180	0.126854	0.111715	3.2	5.6	0.68
240	0.120159	0.119602	3.2	6.0	0.68
300	0.121683	0.118439	3.2	6.0	0.68

Table 91. Combined data for all the runs at 450 °C with varying flow rates.

Residence Time, min (V/V ₀)	Final concentration of naphthalene, C _a	Conversion, X _n %
10.66	3.2	68
14.03	2.4	76
16.55	1.8	82
19.51	1.4	86

An integral method of analysis of the experimental data obtained at various temperatures confirms that the hydrogenation reaction follows apparent first-order kinetics. A plot of $-\ln(C_a/C_{a0})$ vs Residence time gives straight lines passing through the origin for all the temperatures as shown in Figure 46.

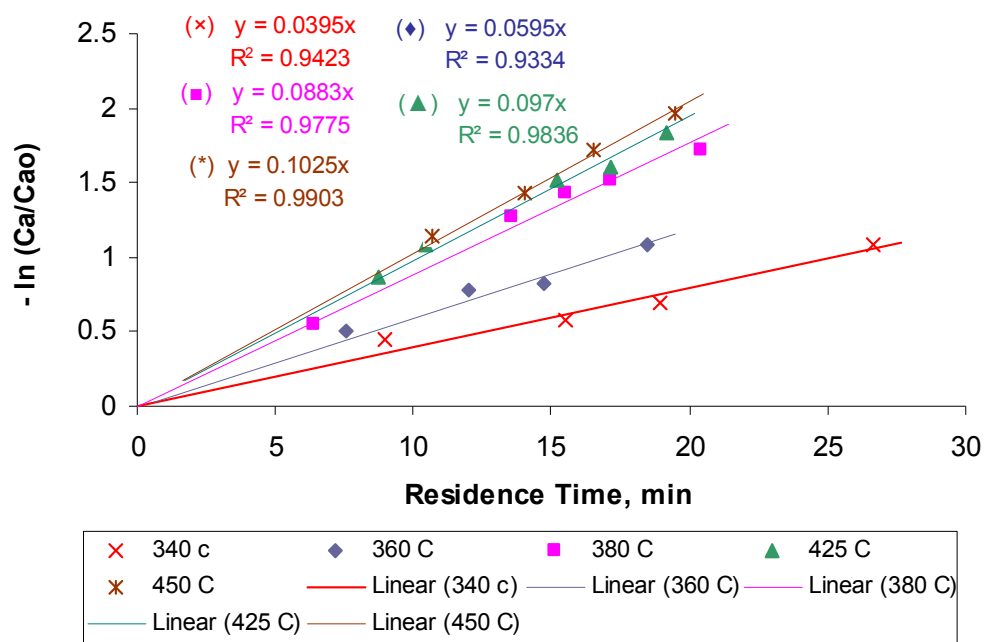


Figure 46. Integral Method of Analysis of Data at Various Temperatures.

3.2.10 Determination of Rate Constants

The integral method described above gives the indication that the reaction occurring in the trickle bed reactor is a first-order reaction. But this method does not take into consideration the concentration of hydrogen saturated in the liquid at reaction conditions. Since, hydrogen is in large excess compared to the liquid feed, the hydrogen concentration can be assumed to be constant and hence the reaction is a pseudo first-order reaction in naphthalene. Based on the reaction scheme for the hydrogenation of naphthalene and the criterion suggested by Mears, an ideal plug flow reactor model was used to fit the experimental data. Taking into consideration the saturated hydrogen concentration at various temperatures, the reaction rate constants for the hydrogenation reaction can be determined. The performance of the reactor can be described by

$$\ln\left(\frac{1}{1-X_n}\right) = K_L * \frac{W}{Q} \quad \text{Equation 15}$$

where X_n = Steady state conversion of naphthalene for a given residence time

K_L = Rate constant of the trickle bed reaction, ml/g-min

W = Weight of the catalyst, g

Q = Volumetric flow rate of the liquid feed, ml/min

In effect, the quantity W/Q is analogous to the residence time of the reaction described earlier. The pseudo first-order rate constant K_L can further be defined as the product of the apparent rate constant K_{app} and the saturated hydrogen concentration in the liquid, C_{H0} as shown in Equation 16 assuming no external mass transfer occurs and that the reaction rate is first-order with respect to hydrogen.

$$\ln\left(\frac{1}{1-X_n}\right) = K_{app} C_{H0} * \frac{W}{Q} \quad \text{Equation 16}$$

where K_{app} = Apparent rate constant for the hydrogenation reaction,
(ml/g-min)/(mol/cm³)

C_{H0} = Saturated hydrogen concentration in the liquid, mol/cm³

The slope of the linear plot of $\ln\left(\frac{1}{1-X_n}\right)$ vs W/Q thus gives the rate constant of the liquid phase

hydrogenation of naphthalene as shown in Figure 47. If this pseudo first-order rate constant is divided by the saturated hydrogen concentration, the apparent rate constant, K_{app} , can be determined. The apparent rate constants thus obtained were used in the calculation of the apparent activation energy of the hydrogenation reaction. The saturated concentration of hydrogen in the liquid has been estimated using Shaw's correlation. It can be clearly seen that the plug flow reactor model gives a reasonably good fit using the linear least squares regression method. The values of the obtained apparent rate constants at various temperatures are given in Table 92.

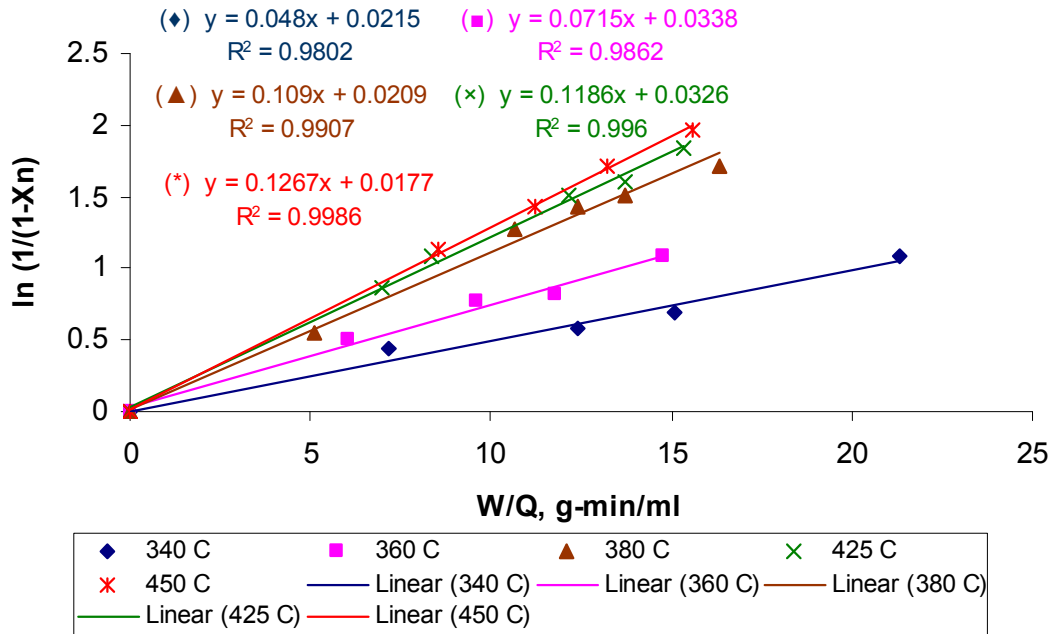


Figure 47. Plot of $\ln(1/(1-X_n))$ vs W/Q to Determine the Rate Constants.

Table 92. Values of the obtained apparent rate constants at various temperatures.

Temperature, °C	Pseudo First-Order Rate Constant, K_L ml/g-min	Saturated Concentration of Hydrogen, mol/cm³	Apparent rate Constant, K_{app} (ml/g-min)/ (mol/cm³)
340	0.0480	0.000805	59.627
360	0.0715	0.000869	82.278
380	0.1059	0.000937	112.779
425	0.1186	0.001112	106.655
450	0.1267	0.001223	103.598

As the temperature increases the pseudo first-order rate constants (K_L) also increase indicating an increase in the rate of hydrogenation but the apparent rate constants decrease slightly at higher temperatures. According to previous studies by other researchers, the apparent rate constant is a function of the intrinsic reaction rate constant and the adsorption equilibrium constants of naphthalene and hydrogen. At high temperatures, the adsorption equilibrium constants decrease due to the more negative values of the adsorption heats of naphthalene and hydrogen. This can be shown by Van't Hoff equation,

$$\ln K = \frac{-\Delta H}{RT^2} \quad \text{Equation 17}$$

At higher temperatures (above 400 °C) the increase in the rate of hydrogenation is not as pronounced as the ones at lower temperatures. This can be attributed to the fact that at higher temperatures, the equilibrium conversion for the hydrogenation of naphthalene to tetralin approaches 100%. Therefore, further increasing the temperature would only lead to the dehydrogenation of tetralin.

J.M. Shaw proposed a correlation to determine the concentration of hydrogen when it is saturated in a liquid phase.⁵⁶ This correlation was proposed to determine the solubility of hydrogen in aromatic, alicyclic and heterocyclic solvents. This correlation is valid over the temperature range of $0.45 \leq T_{r,solvent} \leq 0.97$ and a pressure range of 0.1-30 MPa where $T_{r,solvent}$ is the reduced temperature of the solvent. Shaw assumes that the hydrogen solubility is a function of the reduced temperature of the solvent. According to this correlation, one can express the solubility coefficient of hydrogen as a function of the fugacity coefficient and partial pressure. The solubility per unit volume is then defined as:

$$S^* = S [f/P] \rho_{solvent}^2 \quad \text{Equation 18}$$

Where S^* = Normalized solubility (moles H_2 . L⁻²_{solvent} . MPa⁻¹. kg_{solvent})
 S = Solubility coefficient (moles H_2 . kg⁻¹_{solvent}. MPa⁻¹)
 f = Fugacity Coefficient, MPa

P = Hydrogen partial pressure (MPa)
 ρ_{solvent} = Density of the solvent at STP (kg/L)

This correlation proposed by Shaw was further improved upon and verified experimentally by Cai et al. who calculated the solubility of hydrogen in n-hexadecane for a broad range of temperatures (80-380 °C) and pressures (0.5-12 MPa). The solubility coefficients for hydrogen at various temperatures using n-hexadecane as the solvent are given in Table 93.

Table 93. Solubility coefficients for hydrogen at various temperatures using n-hexadecane as the solvent.⁵⁷

Temperature, °C	Solubility Coefficient, moles H ₂ /(kg solvent·MPa)
80	0.046
130	0.058
183	0.070
250	0.090
330	0.120
380	0.150

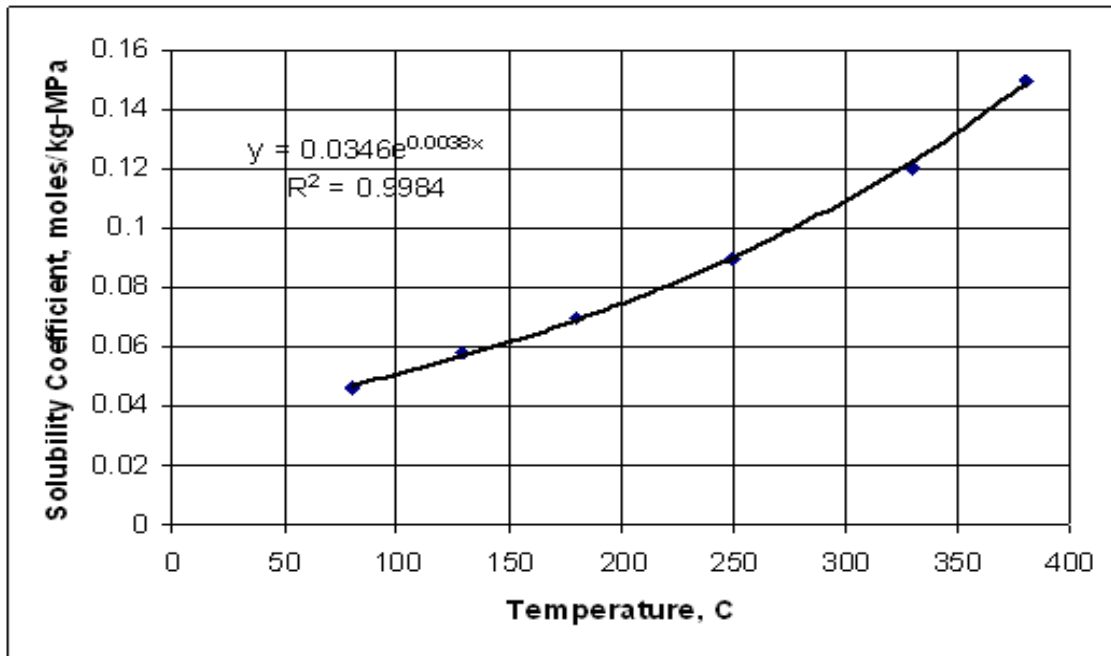


Figure 48. Solubility Coefficient of hydrogen in n-hexadecane vs Temperature.

A plot of Solubility Coefficient vs Temperature for hydrogen saturated in n-hexadecane is shown in Figure 48. The solubility of hydrogen is then be obtained as a product of the solubility coefficient, weight of the solvent and pressure. Figure 48 indicates that the solubility of hydrogen in the solvent increases exponentially as the temperature increases. This plot can

thus be used to extrapolate the data and obtain the solubility coefficient of hydrogen at higher temperatures which are being used in the present study (425 °C and 450 °C).

The rate constants, obtained using the plug flow reactor model, were used to determine the activation energy of the hydrogenation reaction as shown in Figure 49. Equation 19 shows the Arrhenius Law used for calculating the activation energy of a reaction.

$$K_{app} = K_0 \exp\left(\frac{-E_{app}}{RT}\right) \quad \text{Equation 19}$$

where K_{app} = Apparent rate constant of the hydrogenation reaction, ml/g-min/mol/cm³

K_0 = Frequency factor, ml/g-min/mol/cm³

E_{app} = Apparent activation energy of the hydrogenation reaction, KJ/mol

R = Universal gas constant, 8.314 J/mol-k

T = Temperature, K

Also, the apparent activation energy can be expressed as:

$$E_{app} = E + \Delta H \quad \text{Equation 20}$$

where E = Intrinsic activation energy, defined as the activation energy for a reaction in the exothermic direction, KJ/mol, and ΔH = Standard heat of hydrogenation, KJ/mol.

The slope of the plot of $\ln(K_{app})$ and $1/T$ gives the apparent activation energy of the hydrogenation reaction studied in this work. The value of $\ln K_{app}$ decreases slightly at higher temperatures and thus the apparent activation energy also appears to decrease at higher temperatures. This may imply that the hydrogenation reaction is diffusion-controlled at temperatures greater than 380 °C. Also, the saturated hydrogen concentration in the liquid at temperatures greater than 380 °C was obtained by extrapolating the values of the solubility coefficients of hydrogen in n-hexadecane. These extrapolated values of the hydrogen concentration may not actually be true at higher temperatures (425 °C and 450 °C) used in the present study. Therefore, the apparent activation energy was determined only between the temperature range of 340 °C to 380 °C. The calculated value of the apparent activation energy is approximately equal to 53 KJ/mol.

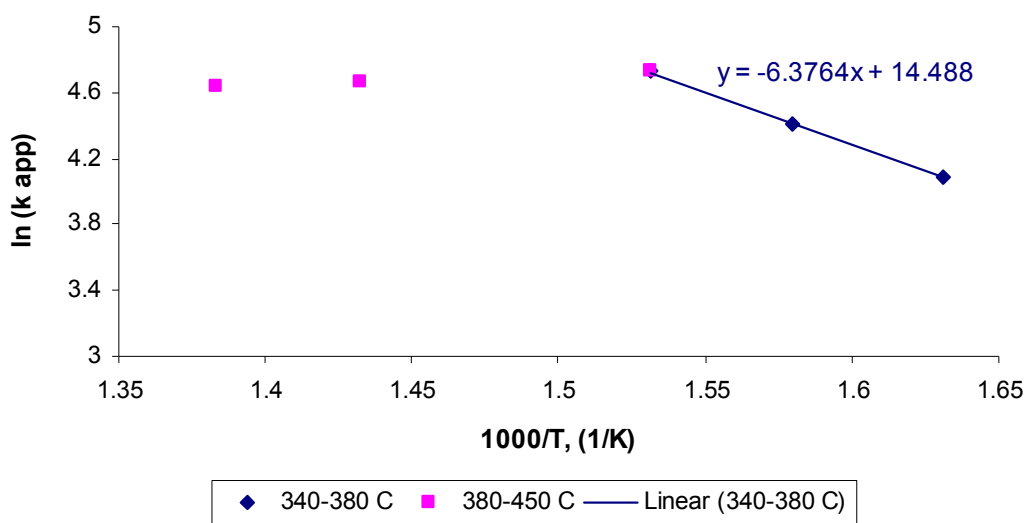


Figure 49. Arrhenius Plot to Determine the Apparent Activation Energy.

3.2.11 Hydrogenation with Variable Hydrogen Flow Rate

The hydrogenation of naphthalene in the trickle bed reactor was also studied by reducing the hydrogen flow rate and thereby reducing the ratio of hydrogen to liquid flow rate in the reactor. The basic operating conditions were the same, i.e., the reactor was operated between temperatures 340 °C and 450 °C and the pressure was maintained constant at 1200 psig while the ratio of hydrogen flow rate to liquid flow rate was reduced to 100 from 750 used earlier. This test was performed to check if there was any influence of the hydrogen flow rate on the rate of hydrogenation since, for a practical system, the hydrogen flow rate would be kept to a minimum. The liquid feed to the trickle bed reactor was also the same, 10% by weight of naphthalene dissolved in 90% by weight of n-hexadecane. This experiment was performed at three different temperatures, 340 °C, 380 °C and 425 °C. The hydrogenated samples were analyzed in the same manner as before by using FTIR spectroscopy. The results of this experiment at all the above mentioned temperatures are given in Table 94 through Table 107.

Table 94. Temperature 340 °C, Liquid Flow Rate: 150 ml/hr, H₂ Flow Rate: 0.25 L/min.

Time (min)	Absorbance (at 781 cm ⁻¹)	Absorbance (at 741 cm ⁻¹)	% Concentration (naphthalene)	% Concentration (tetralin)	Conversion X _n
0	0.372373	0	10	0	
60	0.324521	0.043883	8.4	1.6	0.16
120	0.255972	0.071385	6.8	3.2	0.32
180	0.254589	0.071430	6.8	3.2	0.32
240	0.245907	0.077884	6.4	3.6	0.36
300	0.242916	0.074647	6.4	3.6	0.36

Table 95. Temperature 340 °C, Liquid Flow Rate: 165 ml/hr, H₂ Flow Rate: 0.275 L/min.

Time (min)	Absorbance (at 781 cm ⁻¹)	Absorbance (at 741 cm ⁻¹)	% Concentration (naphthalene)	% Concentration (tetralin)	Conversion X _n
0	0.368276	0	10	0	
60	0.303418	0.051324	8.0	2.0	0.20
120	0.272052	0.058999	7.2	2.8	0.28
180	0.232839	0.083262	6.2	3.8	0.38
240	0.231151	0.081730	6.2	3.8	0.38
300	0.231701	0.080941	6.2	3.8	0.38

Table 96. Temperature 340 °C, Liquid Flow Rate: 200 ml/hr, H₂ Flow Rate: 0.333 L/min.

Time (min)	Absorbance (at 781 cm ⁻¹)	Absorbance (at 741 cm ⁻¹)	% Concentration (naphthalene)	% Concentration (tetralin)	Conversion X _n
0	0.367349	0	10	0	
60	0.332033	0.033416	8.8	1.2	0.12
120	0.308086	0.050365	8.0	2.0	0.20
180	0.287554	0.055907	7.4	2.4	0.26
240	0.273011	0.061402	7.2	2.8	0.28
300	0.272265	0.062408	7.2	2.8	0.28

Table 97. Temperature 340 °C, Liquid Flow Rate: 245 ml/hr, H₂ Flow Rate: 0.408 L/min.

Time (min)	Absorbance (at 781 cm ⁻¹)	Absorbance (at 741 cm ⁻¹)	% Concentration (naphthalene)	% Concentration (tetralin)	Conversion X _n
0	0.371567	0	10	0	
60	0.321033	0.039218	8.4	1.6	0.16
120	0.301909	0.052491	8.0	2.0	0.20
180	0.280528	0.055555	7.6	2.4	0.24
240	0.281370	0.059884	7.6	2.4	0.24
300	0.281439	0.061247	7.6	2.4	0.24

Table 98. Combined data for all the runs at 340 °C with reduced H₂ flow rates.

Residence Time, min (V/V ₀)	Final concentration of naphthalene, Ca	Conversion, Xn %
9.79	7.6	24
12.00	7.2	28
14.54	6.4	36
16.00	6.2	38

Table 99. Temperature 380 °C, Liquid Flow Rate: 140 ml/hr, H₂ Flow Rate: 0.233 L/min.

Time (min)	Absorbance (at 781 cm ⁻¹)	Absorbance (at 741 cm ⁻¹)	% Concentration (naphthalene)	% Concentration (tetralin)	Conversion Xn
0	0.367691	0	10	0	
60	0.303424	0.051106	8.0	2.0	0.20
120	0.264801	0.068300	6.8	3.2	0.32
180	0.18293	0.097213	4.8	5.2	0.52
240	0.140629	0.109911	3.6	5.6	0.64
300	0.141753	0.115439	3.6	6.2	0.64

Table 100. Temperature 380 °C, Liquid Flow Rate: 175 ml/hr, H₂ Flow Rate: 0.3 L/min.

Time (min)	Absorbance (at 781 cm ⁻¹)	Absorbance (at 741 cm ⁻¹)	% Concentration (naphthalene)	% Concentration (tetralin)	Conversion X _n
0	0.376956	0	10	0	
60	0.313928	0.042541	8.2	1.6	0.18
120	0.253335	0.074006	6.4	3.6	0.36
180	0.208921	0.090449	5.6	4.4	0.44
240	0.163075	0.095325	4.2	5.2	0.58
300	0.160784	0.098106	4.2	5.2	0.58

Table 101. Temperature 380 °C, Liquid Flow Rate: 200 ml/hr, H₂ Flow Rate: 0.333 L/min.

Time (min)	Absorbance (at 781 cm ⁻¹)	Absorbance (at 741 cm ⁻¹)	% Concentration (naphthalene)	% Concentration (tetralin)	Conversion X _n
0	0.371695	0	10	0	
60	0.305658	0.050755	8.0	2.0	0.20
120	0.257286	0.068995	6.8	3.2	0.32
180	0.226203	0.080598	6.0	4.0	0.40
240	0.187349	0.090707	5.0	4.8	0.50
300	0.193336	0.092876	5.0	4.8	0.50

Table 102. Temperature 380 °C, Liquid Flow Rate: 240 ml/hr, H₂ Flow Rate: 0.4 L/min.

Time (min)	Absorbance (at 781 cm ⁻¹)	Absorbance (at 741 cm ⁻¹)	% Concentration (naphthalene)	% Concentration (tetralin)	Conversion Xn
0	0.376991	0	10	0	
60	0.313737	0.04498	8.2	1.8	0.18
120	0.240634	0.073831	6.2	3.6	0.38
180	0.22108	0.085766	5.8	4.2	0.42
240	0.214112	0.087494	5.4	4.4	0.46
300	0.213764	0.088369	5.4	4.4	0.46

Table 103. Combined data for all the runs at 380 °C with reduced H₂ flow rates.

Residence Time, min (V/V ₀)	Final concentration of naphthalene, Ca	Conversion, Xn %
10.00	5.4	46
12.00	5.0	50
13.71	4.2	58
17.14	3.6	64

Table 104. Temperature 425 °C, Liquid Flow Rate: 160 ml/hr, H₂ Flow Rate: 0.266 L/min.

Time (min)	Absorbance (at 781 cm ⁻¹)	Absorbance (at 741 cm ⁻¹)	% Concentration (naphthalene)	% Concentration (tetralin)	Conversion Xn
0	0.363744	0	10	0	
60	0.323308	0.046566	8.4	1.6	0.16
120	0.193712	0.101543	5.0	5.0	0.50
180	0.173888	0.112383	4.4	5.6	0.56
240	0.153326	0.118513	3.8	6.0	0.62
300	0.151239	0.118418	3.8	6.0	0.62

Table 105 Temperature 425 °C, Liquid Flow Rate: 200 ml/hr, H₂ Flow Rate: 0.333 L/min.

Time (min)	Absorbance (at 781 cm ⁻¹)	Absorbance (at 741 cm ⁻¹)	% Concentration (naphthalene)	% Concentration (tetralin)	Conversion Xn
0	0.367428	0	10	0	
60	0.250195	0.075043	6.4	3.6	0.36
120	0.232255	0.080640	6.0	4.0	0.40
180	0.167438	0.105354	4.4	5.6	0.56
240	0.172479	0.110258	4.4	5.6	0.56

Table 106. Temperature 425 °C, Liquid Flow Rate: 240 ml/hr, H₂ Flow Rate: 0.4 L/min.

Time (min)	Absorbance (at 781 cm ⁻¹)	Absorbance (at 741 cm ⁻¹)	% Concentration (naphthalene)	% Concentration (tetralin)	Conversion X _n
0	0.371459	0	10	0	
60	0.295164	0.055285	7.6	2.4	0.24
120	0.245230	0.075344	6.4	3.6	0.36
180	0.215485	0.089859	5.6	4.4	0.44
240	0.190958	0.102865	5.0	5.0	0.50
300	0.191487	0.103602	5.0	5.0	0.50

Table 107. Combined data for all the runs at 425 °C with reduced H₂ flow rates.

Residence Time, min (V/V ₀)	Final concentration of naphthalene, C _a	Conversion, X _n %
10	5	50
12	4.4	56
15	3.8	62

It can be observed from these results that for the hydrogenation reaction occurring in the trickle bed reactor at lower hydrogen flow rates, the conversion of naphthalene to tetralin is considerably lower for the same residence times when the ratio of hydrogen to liquid feed entering the reactor is decreased.

The plug flow reactor model was used again to determine the pseudo first-order rate constants and the rate of reaction of the hydrogenation of naphthalene at reduced hydrogen flow rates. Figure 50 shows the plot of $\ln(1/(1-X_n))$ vs W/Q which is used to determine the apparent rate constants of the hydrogenation reaction. The values of the apparent constants at various temperatures are given in Table 108. The values in parentheses are the values of the rate constants at higher hydrogen flow rates.

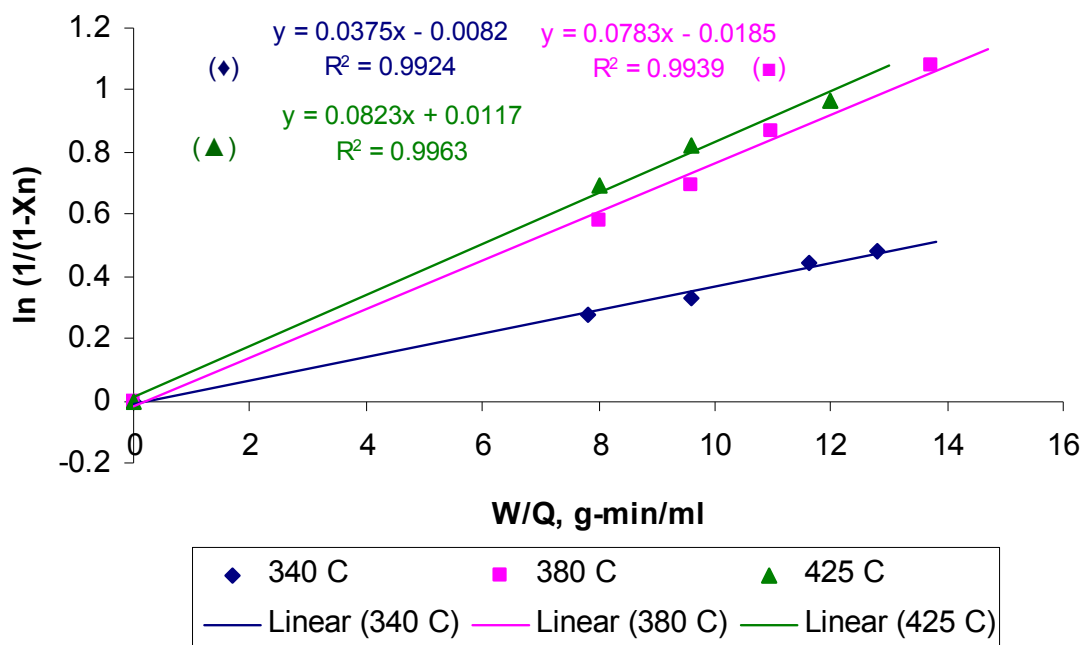


Figure 50. Plot of $\ln(1/(1-X_n))$ vs W/Q to determine the rate constants at reduced hydrogen flow rates.

Table 108. Values of the apparent rate constants at various temperatures at reduced hydrogen flow rates.

Temperature, °C	Pseudo First-Order Rate Constant, K_L ml/g-min	Saturated Concentration of Hydrogen, mol/cm ³	Apparent Rate Constant, K_{app} (ml/g-min)/(mol/cm ³)
340	0.0375 (0.048)	0.000805	46.58 (59.627)
380	0.0783 (0.1059)	0.000937	83.56 (112.779)
425	0.0823 (0.1186)	0.001112	74.01 (106.655)

From Table 108, it is clear that the rate constants and the rate of hydrogenation decreases when the ratio of hydrogen to liquid flow rate entering the reactor is reduced. A possible reason for this is due to the very low flow rate of liquid feed. Since the flow rate of liquid is very low, complete wetting of the catalyst particles may not occur. Hence, the gaseous reactant tends to enter the pores of the catalyst through the region that is not wetted by the liquid. Another reason for this might be the fact that the reaction is diffusion limited or mass transfer controlled. As reviewed by Satterfield, if a reaction is diffusion limited, then at very low liquid flow rates, the

catalyst pores tend to be filled by the gaseous reactant instead of the liquid. This can cause a change in the reaction rate accompanied by a change in diffusivity. As the flow rate of hydrogen in this case is reduced considerably, the amount of hydrogen that enters the catalyst pores is also reduced thereby reducing the rate of hydrogenation.

Even though the rate of hydrogenation decreases, the reduced flow rate of hydrogen should not have any effect on the activation energy, as activation energy is independent of the reactant concentration. A plot of $\ln(K_{app})$ vs $1/T$ is plotted, as shown in Figure 51, to compare the activation energies in both cases, i.e., at the higher and lower hydrogen flow rates. It can be seen that there is not much of a difference in slopes in both the cases. Also, the apparent rate constants at temperatures above 380 °C follow a similar trend as observed previously.

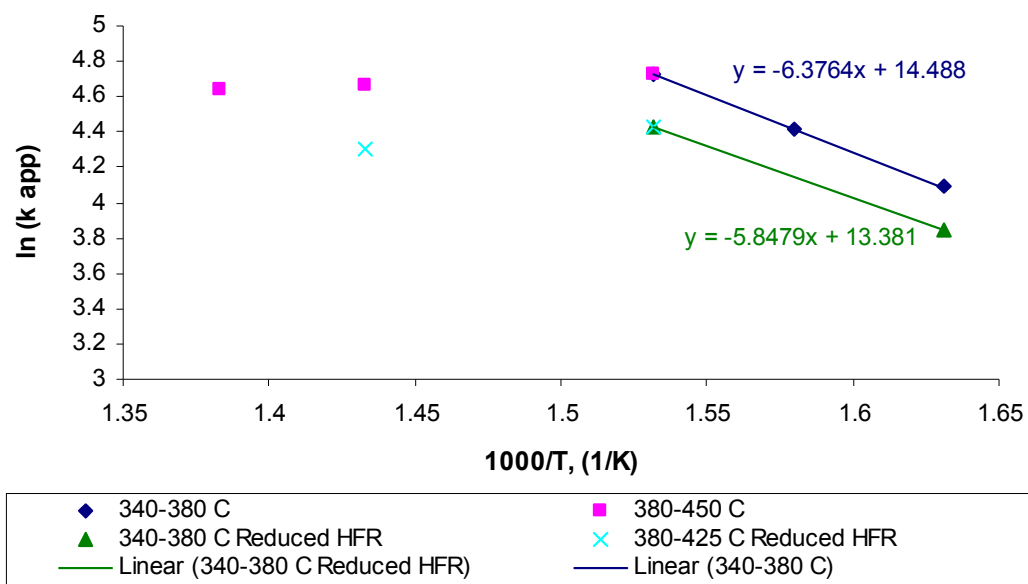


Figure 51. Arrhenius Plot to Determine and Compare the Apparent Activation Energy at Higher and Lower Hydrogen Flow Rates.

From Figure 51, the obtained value of the apparent activation energy for the hydrogenation reaction with reduced hydrogen flow rate is approximately equal to 49 KJ/mol. The activation energy obtained for the previous case at higher hydrogen flow rate was about 53 KJ/mol showing that the difference is less than 10%. These values are also comparable to the literature values. This proves the fact that the plug flow reactor model which was used to assess the performance of the reactor is valid and can be used to predict the values of the rate constants and the activation energy for the liquid phase hydrogenation of naphthalene in the trickle bed reactor. The observed difference may be because of the fact that only two data points were used in the second study for the Arrhenius plot as compared to the three points for the study at higher flow rates.

3.2.12 Trickle Bed Hydrogenation of Coal Tar Distillate

As discussed earlier, naphthalene is the simplest polyaromatic hydrocarbon which can replicate the hydrogenation of coal-derived solvents. Therefore, once the hydrogenation of naphthalene was completed in the trickle bed reactor at various operating conditions, the naphthalene feed was replaced by Koppers Coal Tar Distillate. This was done to verify if the trickle bed reactor could be used for the hydrogenation of coal-derived solvents.

A preliminary run was performed at an operating temperature of 425 °C and a pressure of 1200 psig. Since coal tar distillate is a very viscous compound, it cannot be pumped directly into the trickle bed reactor as it may clog the entire reactor system which might cause undesirable safety concerns. Hence, coal tar distillate was dissolved in a solvent, n-hexadecane, in the same manner as naphthalene, before being fed into the trickle bed reactor. The feed to the trickle bed reactor is a mixture of 30 % by weight of coal tar distillate dissolved in 70 % by weight of n-hexadecane. The percentage of coal tar distillate was increased in the feed to the trickle bed reactor in this case as it was difficult to analyze the feed and product samples with a large percentage of n-hexadecane. The ratio of hydrogen flow rate to that of the liquid flow rate was maintained constant at $750 \text{ m}^3 \text{ H}_2/\text{m}^3 \text{ oil}$. The reactor was operated continuously for 300 min and the product for analysis was collected at the bottom collecting tank of the trickle bed reactor system. An elemental analysis was then done on both the feed as well as the product. Elemental analysis gives the exact percentage of carbon, hydrogen, nitrogen and sulfur in the feed as well as the product. Since the solvent, n-hexadecane is in large excess, it has to first be removed completely before analyzing the samples of feed and product. By extracting out the solvent, only the coal tar distillate was analyzed before and after hydrogenation. It has to be remembered that the solvent was used only as a medium for transporting the coal tar distillate through the trickle bed reactor. It is assumed that the solvent does not participate in the reaction.

The procedure for extracting the solvent, n-hexadecane, from the feed and product solutions in order to perform the elemental analysis appears below, along with illustrations as shown in Figure 52 through Figure 54.

1. Step 1. 30 % by weight of coal tar distillate (CTD) was dissolved in 70 % by weight of n-Hexadecane. Consider 30 g of CTD mixed with 70 g of n-hexadecane. During this process, some amount of CTD stuck to the walls of the container and 1.7 g of CTD was lost as a result of this. Hence, only 28.3 g of CTD dissolved in n-hexadecane. Therefore, the actual percentage of CTD by weight in the mixture was 28.8%.

2. Step 2. To the mixture of CTD and n-Hexadecane, approximately 140 ml of N-methyl-2 pyrrolidone (NMP) was added. NMP is a good solvent for coal tar distillate but a poor solvent for n-hexadecane. Hence, NMP was added to the mixture in order to separate n-hexadecane. Hexadecane, being lighter, separated from the top layer. The resultant bottom layer consisted of a mixture of CTD and NMP. Now, 28.3 g of CTD was present in 140 ml of NMP for a total weight percent of approximately 16.4 % of CTD.

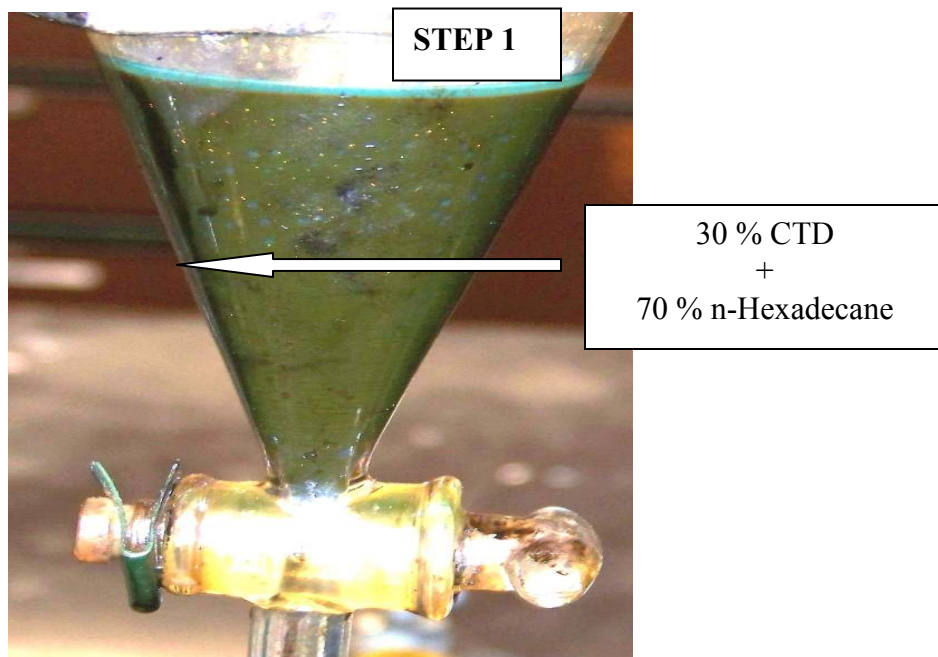


Figure 52. Procedure for Solvent Extraction, Step 1.

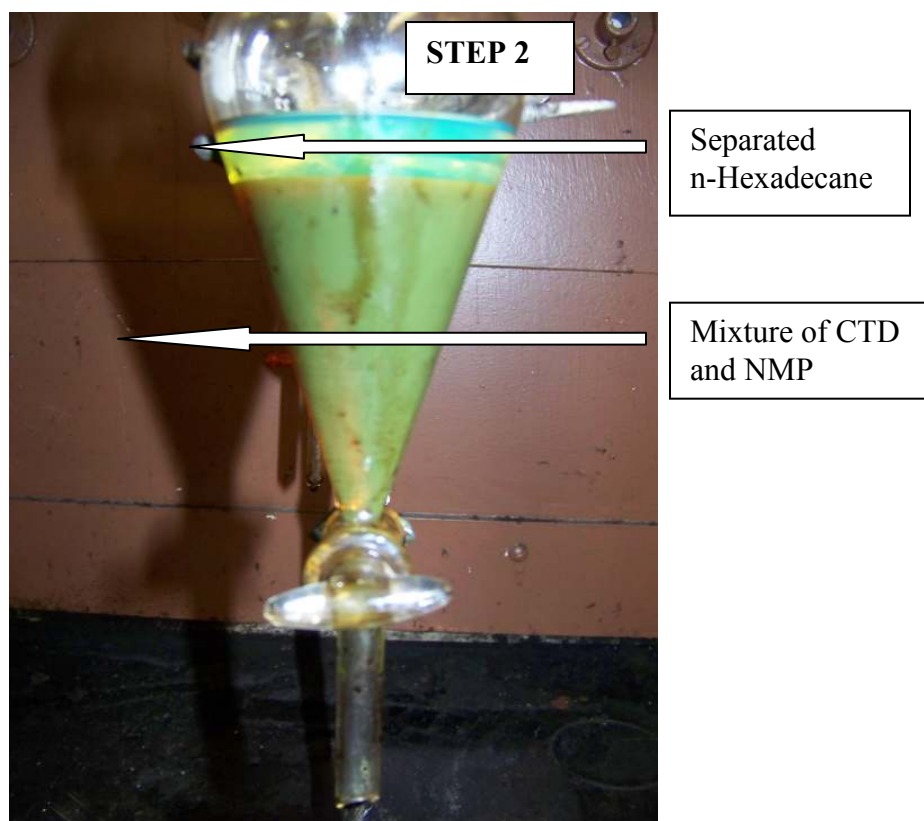


Figure 53. Procedure for Solvent Extraction, Step 2.

Once hexadecane was completely separated, the mixture of CTD and NMP was added to a separatory funnel. In order to calculate the extraction efficiency of CTD for this procedure, 5 ml of the mixture was taken in the separatory funnel. The density of this mixture of CTD and NMP is equal to 0.9 g/cc and hence, the total weight of the mixture was 4.5 g. Hence, the amount of CTD present in 5 ml of the mixture should be 0.738 g. (16.4 % of 4.5 g is the amount of CTD in the mixture).

Step 3: Approximately 75 ml of water was then added to the mixture of 5 ml of CTD and NMP in the separatory funnel to selectively separate NMP from the mixture since NMP is completely miscible with water, while CTD is not. In this manner, the original CTD separated out in the bottom layer of the funnel. About 0.67 g of CTD separated from the bottom layer instead of the theoretical amount of 0.738 g. Therefore, percentage extraction of CTD was about 91 %.

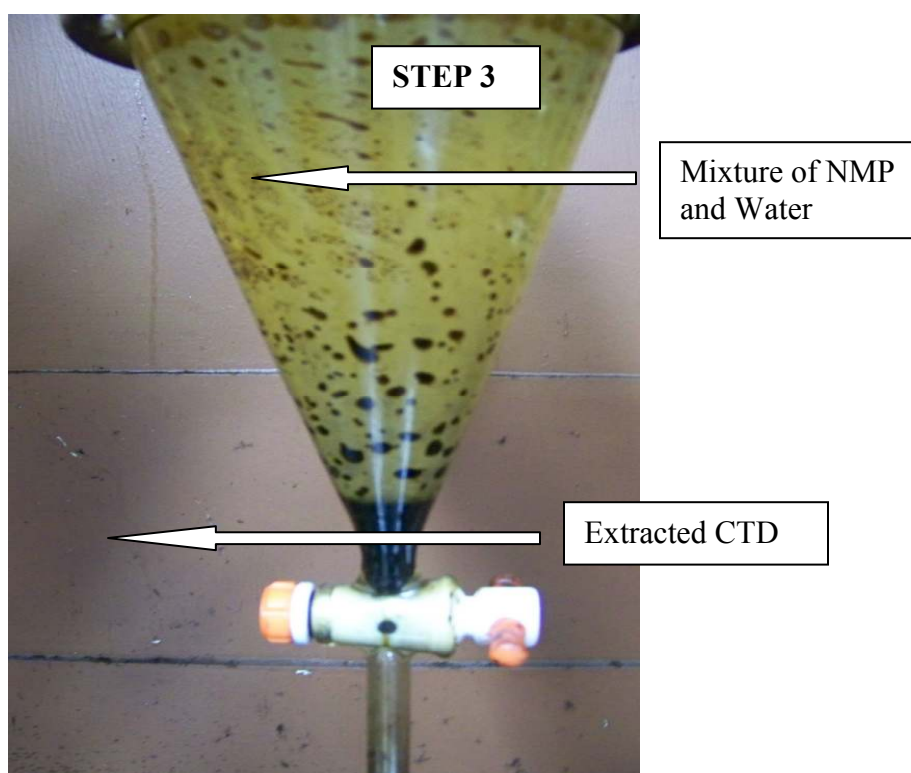


Figure 54. Procedure for Solvent Extraction, Step 3.

An FTIR analysis was done on the coal tar distillate as received from Koppers Inc. and the sample of coal tar distillate extracted using the solvent extraction procedure. Figure 55 shows the result for the FTIR analysis done on both samples. From the plot of Absorbance vs Wavenumber, it can be seen that there is very little difference in the peaks of both samples. In fact, both the spectra nearly overlap each other with the exception of two peaks. This proves that the solvent extraction method described above can be used effectively to extract out the solvent, n-hexadecane. The obtained coal tar distillate can then be analyzed for percentage increase in hydrogen content using an elemental analysis. The same procedure was followed for extracting the solvent from the hydrogenated product also.

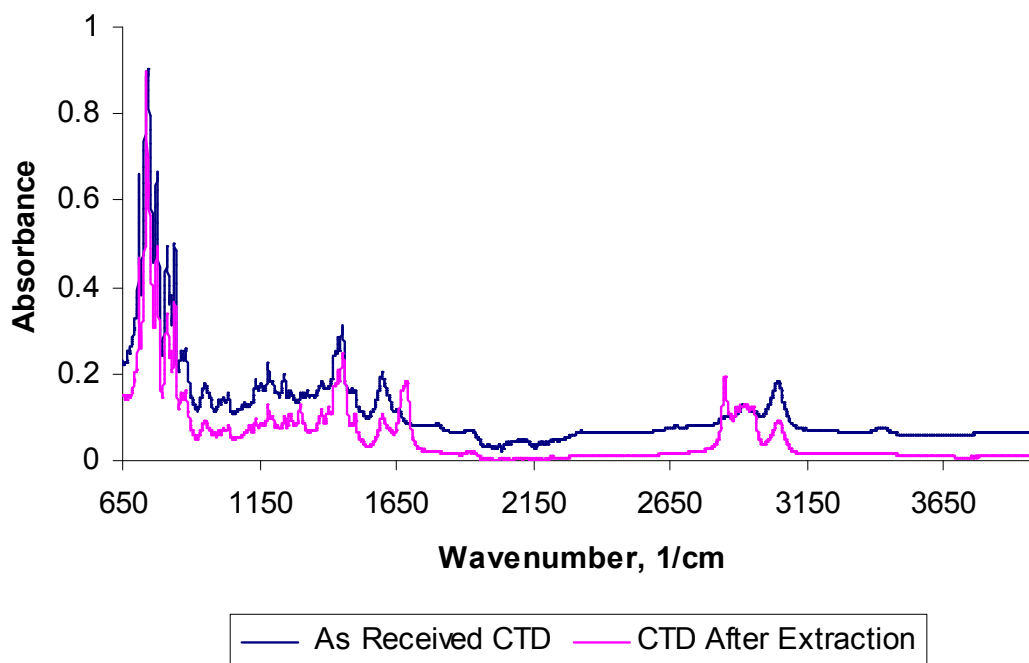


Figure 55. FTIR Analysis of Coal Tar Distillate Samples.

Once the hydrogenated coal tar distillate product was collected and extracted, an elemental analysis was carried out on both the feed and the product. The results of the elemental analysis are given in Table 109 through Table 112.

Table 109. Elemental Analysis of Trickle Bed Reactor Feed.

Sample	Element	Percentage
Trickle Bed Reactor Feed, (Coal Tar Distillate)	Carbon	89.58
	Hydrogen	8.03
	Nitrogen	1.36
	Sulfur	0.34

Table 110. Elemental Analysis of Trickle Bed Reactor Product

Sample	Element	Percentage
Trickle Bed Reactor Product, (Hydrogenated Coal Tar Distillate)	Carbon	89.97
	Hydrogen	10.09
	Nitrogen	0.80
	Sulfur	0.05

From the results of the elemental analysis, it can be clearly seen that there is a definite increase in the percentage of hydrogen from the feed to the product indicating that the trickle bed reactor can indeed be used for hydrogenating coal derived solvents. The percentage increase in hydrogen was observed to be about 25 %. Also, there is almost no change in the percentage of carbon. It can also be observed from Table 109 and Table 110 that there is a drastic change in the percentages of nitrogen and sulfur from feed to the product. The nitrogen percentage decreases by about 41 % while the sulfur percentage decreases by about 85 % from feed to product. This most likely indicates some reaction of hydrogen with the nitrogen and sulfur present in CTD to form ammonia (NH_3) and hydrogen sulfide (H_2S) respectively. Bar graphs showing the percentage changes in elemental composition are shown in Figure 56 through Figure 60.

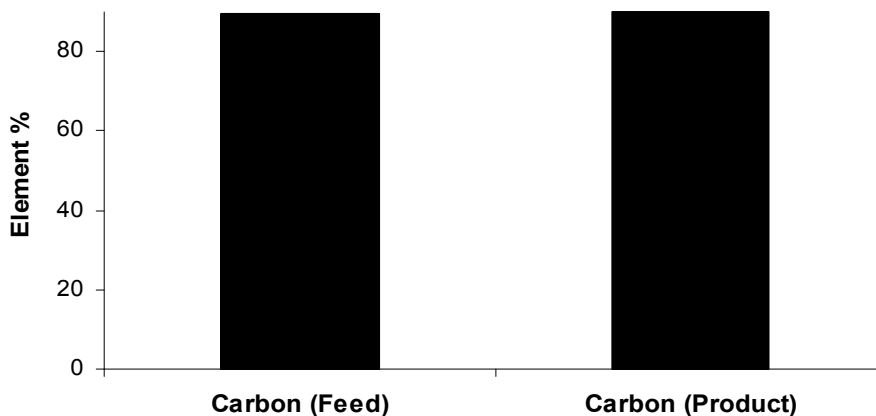


Figure 56. Percentage of Carbon in Feed and Product.

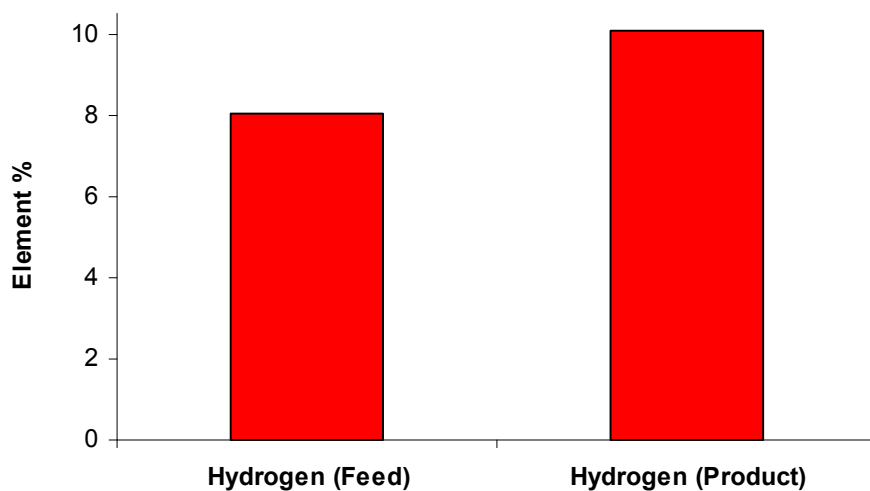


Figure 57. Percentage of Hydrogen in Feed and Product.

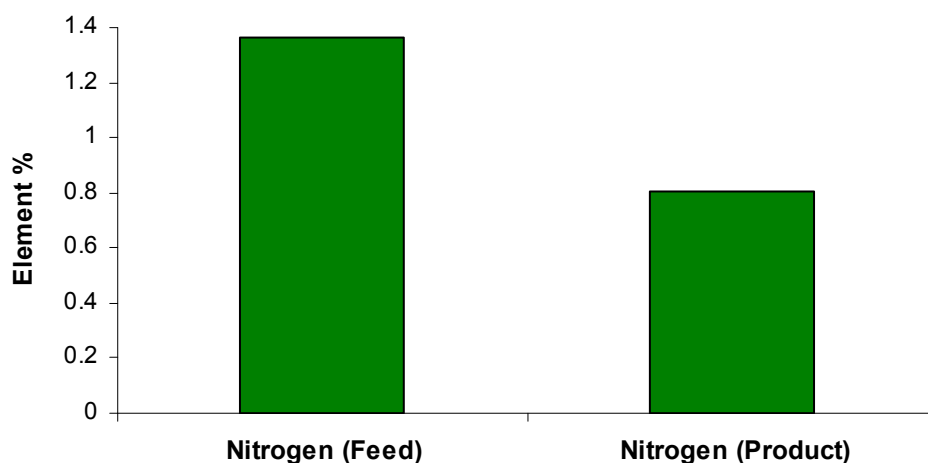


Figure 58. Percentage of Nitrogen in Feed and Product.

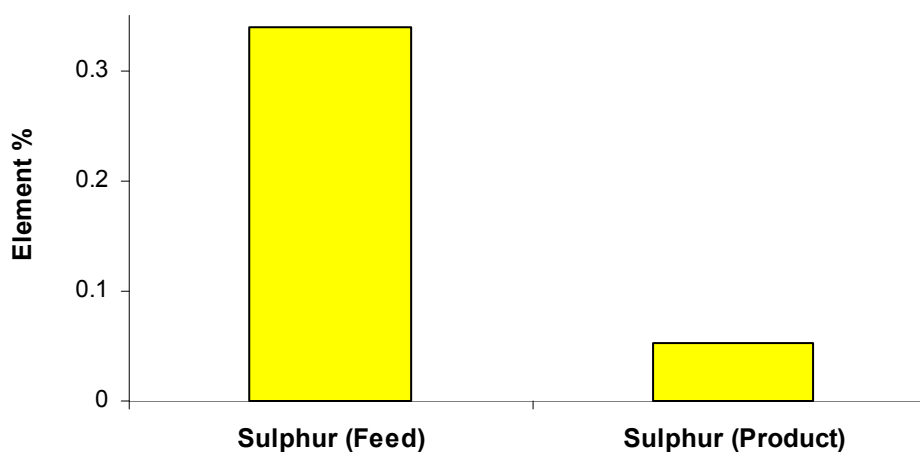


Figure 59. Percentage of Sulfur in Feed and Product.

This is an indication that, while the hydrogenation reactions with the coal tar distillate are occurring in the trickle bed reactor, some denitrification and desulfurization reactions are also occurring.

3.2.13 Trickle Bed Concluding Observations

Based on the results available from the various runs performed on the trickle bed reactor, the following conclusions can be drawn.

1. A trickle bed reactor has been designed, constructed and operated successfully for hydrogenating naphthalene and Koppers coal tar distillate.

2. A Fourier Transform Infra Red spectroscopic analysis of varying concentrations of naphthalene and tetralin dissolved in n-hexadecane indicates that a unique peak of naphthalene occurs at 781 cm^{-1} while that of tetralin occurs at 741 cm^{-1} .
3. Hydrogenation of naphthalene was carried out in the trickle bed reactor at five different temperatures with varying flow rates of liquid and gas. The results from the hydrogenation reaction of naphthalene indicate that the reaction taking place inside the trickle bed reactor is a pseudo-first order reaction since hydrogen is in large excess compared to the liquid feed.
4. The FTIR spectroscopic results indicate that as time proceeds, the absorbance of tetralin in the hydrogenated samples increases indicating that the concentration of tetralin in the hydrogenated samples increases while that of naphthalene decreases, thereby proving that the hydrogenation reaction is indeed occurring in the trickle bed reactor.
5. It can be observed from the results that as the reaction temperature increases, the conversion of naphthalene and the rate of hydrogenation increases. Also, at a particular temperature and pressure, as the flow rate of liquid increases, the conversion levels of naphthalene decrease due to decreased residence time in the catalyst bed.
6. The rate constants and the order of the reaction were found by fitting the experimental data to an ideal plug flow reactor model, taking into consideration the saturated hydrogen concentration in the liquid phase at various temperatures. The plug flow reactor model gave a reasonably good fit using linear least squares regression method.
7. As the temperature increases the rate constants also increase indicating an increase in the rate of hydrogenation but the apparent rate constants decrease slightly at higher temperatures ($425\text{ }^{\circ}\text{C}$ and $450\text{ }^{\circ}\text{C}$). This is because at high temperatures, the adsorption equilibrium constants decrease due to the more negative values of the adsorption heats of naphthalene and hydrogen. Another reason for this could be the fact that the solubility of hydrogen in the solvent increases at a much faster rate at higher temperatures and the hydrogenation reaction is diffusion-controlled. Also, the hydrogen concentration at the higher temperatures was obtained by extrapolating the data of solubility coefficients of hydrogen in n-hexadecane. This method may not be true for temperatures greater than $380\text{ }^{\circ}\text{C}$ used in the present study.
8. The apparent activation energy for the hydrogenation of naphthalene was calculated in the temperature range of $340\text{ }^{\circ}\text{C}$ to $380\text{ }^{\circ}\text{C}$ using the Arrhenius law and it was found to be approximately equal to 53 KJ/mol comparable to the values available in literature.
9. The hydrogenation of naphthalene was also studied by reducing the flow rate of hydrogen to the trickle bed reactor to verify if the hydrogen flow rate had any effect on the rate of hydrogenation. It was observed that the hydrogenation reaction occurs even with lower flow rates of hydrogen but the conversion of naphthalene was considerably lower for the same residence times and temperatures as shown in Table 111. This may be due to mass transfer effects occurring to a greater extent at lower hydrogen flow rates.

10. The apparent activation energy for the hydrogenation of naphthalene at lower hydrogen flow rates was found to be approximately equal to 49 KJ/mol. This value is similar to the value obtained for the higher hydrogen flow rate with the difference being less than 10 %. This verifies that the plug flow reactor model used in this work to assess the performance of the reactor is valid.

Table 111. Comparison of Conversions at Higher and Lower Hydrogen Flow rates for Same Residence Times and Temperatures.

Temperature, °C	Residence Time, min	Conversion % at Higher H₂ Flow Rate	Conversion % at Lower H₂ Flow Rate
340	16	46	38
380	13	72	58
	17	76	64
425	10	68	50
	15	78	62

11. From the results obtained for the hydrogenation of naphthalene in the trickle bed reactor, the optimum operating temperature for the hydrogenation reaction is 380 °C as the rate of hydrogenation at higher temperatures is not as pronounced as it is at 380 °C.

12. Koppers Coal Tar distillate was successfully hydrogenated in the trickle bed reactor. A method to extract the solvent, n-hexadecane, from the feed and product was devised so as to perform elemental analysis on the samples. Thus, the percentage of hydrogen in feed and product was verified.

13. An elemental analysis performed on both feed as well as product indicates that the hydrogen percentage increases by about 25% from feed to product. Thus, it is verified that using the trickle bed reactor can be an effective method for hydrotreating coal tar distillates. Also, a decrease in percentage of other elements like nitrogen and sulfur was observed. The nitrogen and sulfur percentages decreased by about 41% and 85 % respectively indicating that while the hydrogenation reaction with the coal tar distillate is occurring, some denitrification and desulfurization reactions are also occurring in the trickle bed reactor.

3.3 Pyrolysis of Coal--Mild Gasification

3.3.1 Devolatilization of Low Rank Western Coals

As noted above, the tails from the centrifuge, containing undigested fixed carbon as well as mineral matter (ash), represent a significant portion of the output stream from the process. The preferred disposition of these materials is to subject these materials to a partial coking process at a temperature of 450 °C to 650 °C in order to drive off gaseous fuels (primarily methane) as well as condensable vapors that can be utilized for liquid fuels. This process was pioneered in the 1980s and 1990s by Richard A. Wolfe, mainly as a process for producing metallurgical grade “formed coke” using lower cost coals. However, in this case the Wolfe process is seen as the most economical and environmentally conscientious method to utilize the centrifuge tails from the direct liquefaction processes described above.

The solid material, basically a green coke with high ash content would be nominated as a fuel for FutureGen or other gasification system. Alternatively, this material could be blended in with the coal fuel for a conventional combustion system, or possibly incorporated in asphalt or possibly even used to make a low-grade activated carbon.

The centrifuge tails could also be used for the above purposes with little or no treatment, in which case additional value would not be obtained from the hydrocarbons that are present in the system. Thus, this option could be considered as a backup case.

In order to address these issues, experimental tests were initiated based on the Wolfe process, in which coal is partially coked to produce combustible gas and condensable volatiles. The partially coked coal is then suitable for use in a coal gasification system such as FutureGen or other system. The primary purpose of this test was to determine the approximate quality and quantity of the by-products produced from Powder River Basin (PRB) sub-bituminous coal, and to determine whether the acquisition procedures for the gas, liquid and solid products were acceptable. The use of PRB coal was selected as the initial coal because of its non-caking properties and high moisture content. Additional coals have been selected to establish this comparative base line of information on pyrolysis products that can be produced including the amount of hydrogen and methane gas from each coal.

For the initial tests, WVU via its subcontractor Carbonite Inc (Richard A. Wolfe) obtained a representative sample of 25 pounds of PRB coal fines from the a plant in Gillette, WY operated by KFX Corporation (see Figure 60). Ultimate and proximate analysis of the PRB coal were obtained from an outside contractor and compared to in-house measurements using a LECO analyzer and WVU.

A 2000 gram, electrically heated, batch pyrolysis system at WVU including both condenser and gas collectors was designed based on a kettle heater obtained from Ken Krupinski of Koppers, as shown in Figure 61.

The coal was heated to about 600 C within 60 minutes. This temperature was maintained for 30 minutes, following which the unit was allowed to cool down for 90 minutes. The system is shown operating in Figure 62 and Figure 63. Initially, moisture from the coal was boiled off, resulting in a visible emission of steam. At higher temperatures, volatile vapors were produced, which were then be combusted using a pilot light.

Samples were collected for analysis, including the char, coal liquids, and non-condensable gases. Coal liquids and non-condensable gases were sent to Koppers for analysis.

The starting material and the char were analyzed in-house as well as by a third party analytic laboratory.



Figure 60. PRB Coal Fines of $\frac{1}{4}$ inch and below. A nickel and penny are shown for scale.



Figure 61. Experimental set-up to conduct the batch pyrolysis experiment.



Figure 62. Laboratory Experiment Underway during the three hour process time. Devolatilized vapors are combusted via the flare in the rear of the chamber.



Figure 63. Ignition of the Non-condensable gases at about 275 C (original poor quality).

The technical data obtained for the proximate analysis of the coal and by-products is shown in Table 112. Three samples were run in order to ensure that the tests were statistically repeatable. Proximate analysis is shown in Table 113. Additional confirming proximate analyses were carried out by SGS Beckley Laboratory. Data from only one sample was reported. SGS reports 9.95% ash versus an average of 4.89 for the samples measured by WVU in the coal. Measurements for the char showed 12.5% ash for samples measured at WVU (a high of 14.4% and a low of 11.3%) versus 15.0% for samples measured by SGS. These results are reported in Figures 64 and 65.

Based on the relatively high sample-to-sample variation as measured by WVU, the values reported by SGS are consistent with the WVU measurements. It is concluded that the differences are due to sample-to-sample variation and likely not due to differences in technique.

Table 112. Elemental Analysis of PRB Coal and Char from Wolfe Mild Gasification Process.

Summarize Results				
Date :	10/12/2006	13:47:27		
Method Name :	NCHS			
Method Filename :	101206.mth			
Group No : 1	Element %			
Sample Name	Nitrogen%	Carbon%	Hydrogen%	Sulfur%
PRB COAL	0.676678181	56.91474152	6.056604862	0.276702642
PRB COAL	0.602487207	56.64510345	6.262539387	0.110314086
PRB COAL	0.597990155	56.33021927	5.909677029	0.204147592
3 Sample(s) in Group No : 1				
Component Name	Average	Std. Dev.	% Rel. S. D.	Variance
Nitrogen%	0.625718514	0.04418961	7.0622	0.002
Carbon%	56.63002141	0.2925528	0.5166	0.0856
Hydrogen%	6.076273759	0.1772515	2.9171	0.0314
Sulfur%	0.197054774	0.08342073	42.3338	0.007
Group No : 2	Element %			
Sample Name	Nitrogen%	Carbon%	Hydrogen%	Sulfur%
PRB CHAR	1.247597456	74.76076508	1.949725628	0.093554311
PRB CHAR	1.199389696	75.12137604	2.138507366	0.22133483
PRB CHAR	1.302074075	74.04397583	1.592323542	0.112925842
3 Sample(s) in Group No : 2				
Component Name	Average	Std. Dev.	% Rel. S. D.	Variance
Nitrogen%	1.249687076	0.05137407	4.111	0.0026
Carbon%	74.64203898	0.5484248	0.7347	0.3008
Hydrogen%	1.893518845	0.2773961	14.6498	0.0769
Sulfur%	0.142604994	0.06886657	48.2918	0.0047

Table 113. Proximate Analysis of PRB Coal and Char.

Name	Crucible Mass	Initial Mass	Moisture Mass	Volatile Mass	Ash Mass	Moisture	Volatile	Ash	Fixed Carbon
PRB Coal 1	14.063	1.0361	0.7399	0.4089	0.0463	28.58	31.95	4.47	31.63
PRB Coal 2	13.501	1.1435	0.8121	0.4417	0.0526	28.98	32.39	4.6	30.62
PRB Coal 3	13.873	1.2176	0.8731	0.4826	0.0681	28.3	32.07	5.6	30.26
PRB Char 1	14.443	0.9212	0.9081	0.8077	0.1325	1.42	10.91	14.39	63.79
PRB Char 2	15.461	0.949	0.9397	0.8342	0.1114	0.98	11.12	11.73	66.03
PRB Char 3	13.764	0.948	0.9378	0.8292	0.107	1.07	11.46	11.29	65.79

The gas samples were sent to Koppers Inc (Monessen facility). Koppers was able to perform only a qualitative analysis. As expected, the gas was composed of H₂, CO₂, ethylene, ethane, O₂, high levels of N₂, methane and CO.

The results showed that during rapid pyrolysis the PRB coal fines rapidly devolatilize, producing both condensable liquid vapor as well as non-condensable combustible gases. The bench scale system performed very well, but sample collection procedures must be improved for liquid and gas phase samples.



October 13, 2006

Wolfe Engineering & Consulting
P.O. Box 1274
Banner Elk NC 28604
Attn: Dr. Richard Wolfe

Sample identification by
Wolfe Engineering

PRB Fines

Kind of sample Coal
reported to us
Sample taken at -----
Sample taken by Wolfe Engineering
Date sampled -----
Date received September 30, 2006

Analysis report no. 64-64625218

Page 1 of 1

PROXIMATE ANALYSIS

	<u>As Received</u>	<u>Dry Basis</u>	
* % Moisture	26.52	XXXXXX	
% Ash	7.31	9.95	
% Volatile	25.82	35.14	
% Fix Carbon	40.35	54.91	
	100.00	100.00	
% Sulfur	0.45	0.61	
BTU/lb	8378	11402	MAF 12662
So ₂ Lb/Million BTU @ 100%	1.07		

* 60 Mesh Moisture

METHODS

Moisture: ASTM D 2961; Ash: ASTM D 3174; Volatile: ASTM D 3175;
Fixed Carbon: ASTM D 3172 (Calculated Value); Sulfur: ASTM D 4239 (Method B);
Btu/lb: ASTM D 5865; Oxidation: ASTM D 5263; FSI: ASTM D 720

Respectfully submitted,
SGS NORTH AMERICA INC.

Beckley Laboratory

SGS North America Inc. Minerals Services Division
P.O. Box 850, Sophia, WV 25921 t (304) 255-0422 f (304) 255-0417 www.us.sgs.com/minerals

Member of the SGS Group

P-465

GENERAL CONDITIONS OF SERVICE ON REVERSE

Figure 64. SGS Proximate Results, PRB Fines.



October 13, 2006

Wolfe Engineering & Consulting
P.O. Box 1274
Banner Elk NC 28604
Attn: Dr. Richard Wolfe

Sample identification by
Wolfe Engineering

PRB Char

Kind of sample Coal
reported to us

Sample taken at -----

Sample taken by Wolfe Engineering

Date sampled -----

Date received September 30, 2006

Analysis report no. 64-64625219

Page 1 of 1

PROXIMATE ANALYSIS

	<u>As Received</u>	<u>Dry Basis</u>	
* % Moisture	0.10	XXXXXX	
% Ash	14.93	14.94	
% Volatile	7.70	7.71	
% Fix Carbon	77.27	77.35	
	100.00	100.00	
% Sulfur	0.57	0.57	
BTU/lb	12495	12508	MAF 14705
So ₂ Lb/Million BTU @ 100%	0.91		

* 60 Mesh Moisture

METHODS

Moisture: ASTM D 2961; Ash: ASTM D 3174; Volatile: ASTM D 3175;
Fixed Carbon: ASTM D 3172 (Calculated Value); Sulfur: ASTM D 4239 (Method B);
Btu/lb: ASTM D 5865; Oxidation: ASTM D 5263; FSI: ASTM D 720

Respectfully submitted,
SGS NORTH AMERICA INC.

Beckley Laboratory

SGS North America Inc. Minerals Services Division
P.O. Box 650, Sophia, WV 25921 t (304) 255-0422 f (304) 255-0417 www.us.sgs.com/minerals

P-465

GENERAL CONDITIONS OF SERVICE ON REVERSE

Member of the SGS Group

Figure 65. SGS Proximate Results, PRB Char.

3.3.2 Injection Carbon Synthesis

Injection carbon is used in steel blast furnaces to control the chemistry of iron produced. In this sense, it performs a similar function to metallurgical coke; however, injection carbon does not have the same requirement to exhibit structural strength. Powdered anthracite is often used as injection carbon. The ability to inexpensively produce injection carbon would be highly significant if it could be accomplished. Coals that produce a clean char (i.e., powdered carbon as opposed to coke) could potentially be used as sources for injection carbon. Ordinarily, steam coals could not be considered to be effective candidates for injection carbon because they have too much volatility. Hence devolatilized steam coal could potentially fit the requirements for injection carbon.

The protocol for delayed coking tests was modified by the addition of a simpler water cooled condenser and gas collector process, as shown in Figure 66. Larger diameter tubing was used in order to avoid susceptibility to clogging. The system consists of a heated kettle capable of temperatures of approximately 1000 °C, well in excess of the 600 °C required. Originally a “smart” temperature controller was used; however, because of the small size of the unit, the controller was unable to regulate the heater during initial heating. First order overshoot was about 100 °C, which is thought to be excessive. Therefore the controller was replaced by a simple manually controlled Variac. The lines to the condenser are heated in order to avoid condensation at undesired points in the system. A glass condenser is used to condense devolatilized liquids, which are then collected in a flask. A separate line is used to vent steam during initial heating.

The preferred practice would be to have the condenser be vertical, rather than inclined at ~30 degrees. A larger fume hood would have been required, however.

The protocol is approximately as follows:

1. Approximately 1.0 kg of centrifuge tails (or, alternatively, raw coal) is placed in the kettle heater and heated at approximately constant heater power. The power is manually adjusted to permit the temperature come up to 500 °C with minimal overshoot. A temperature of 600 °C can be used to acquire samples more quickly; however, many commercial delayed cokers operate at the 500 °C level, which is the reason for selecting that temperature.
2. The coal samples heated up to about 100 °C to remove the moisture from the PRB coal to reduce the amount of water in the condensed coal liquids (Figure 67).
3. Coal gas can be ignited when the temperature of the sample reaches about 300 °C (see Figure 68). The pyrolysis of the PRB coal with condensing of coal liquids and flaring coal gas are shown in Figure 69.
4. Gas samples are collected from the outlet line. Different sampling devices have been trialed including metal canisters, Mylar bags and plastic bottles. Koppers recommended using a plastic bottles.
5. Liquid samples are collected from the condenser and analyzed at Koppers.

6. The remaining solid char is collected and analyzed at WVU as well as by SGS Minerals Laboratory.

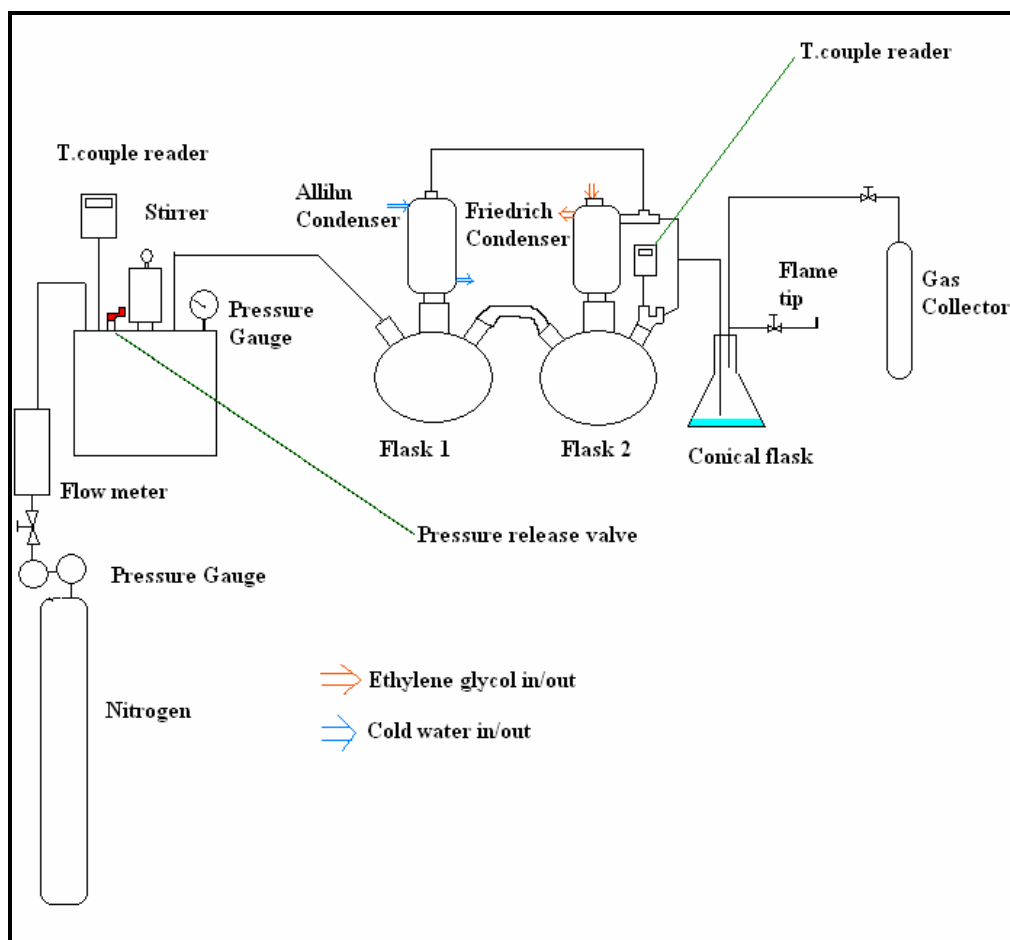


Figure 66. General Layout of the Devolatilization Apparatus.

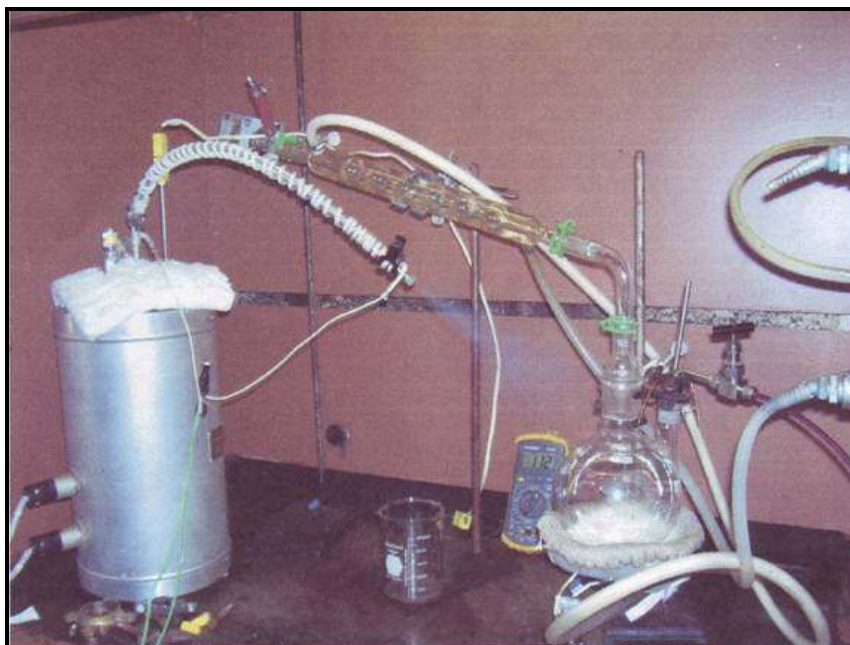


Figure 67. Batch Pyrolyzer Ejecting Steam Vapor from PRB coal at ~112 °C.

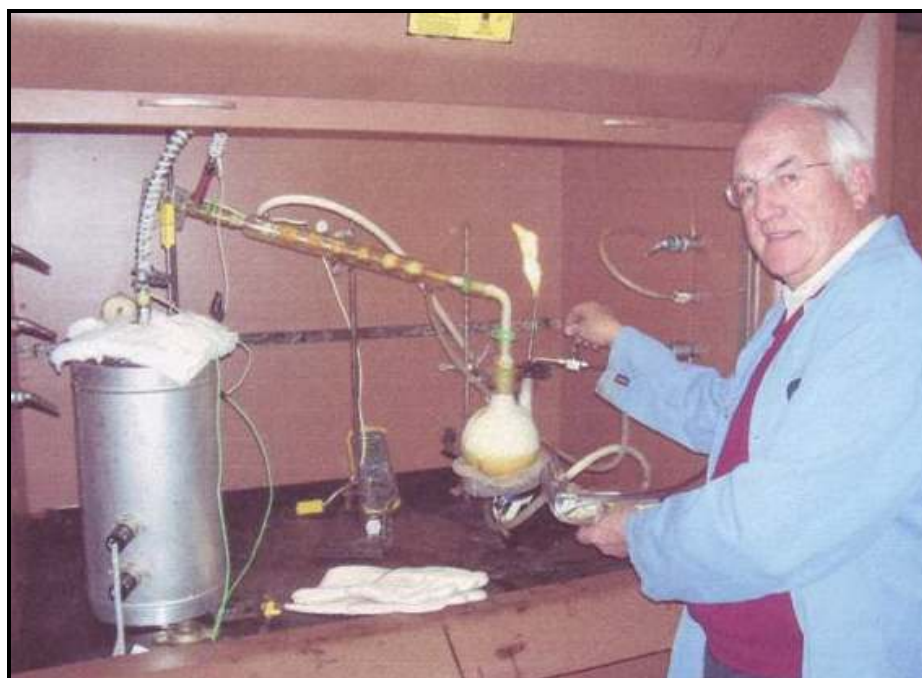


Figure 68. Igniting the flare coal gas starting at about 300 °C with coal liquids being condensed.



Figure 69. Pyrolysis of the PRB coal with the collection of gas samples and coal liquids being condensed in the glass flask at about 600 °C.

Figure 70 shows the general appearance of the coal char resulting from PRB coal. The proximate analysis of the PRB coal char produced after pyrolysis is contained in Table 114. These data are compared to the properties of anthracite. The results are consistent with the view that the PRB coal char could be useful as an injection source.

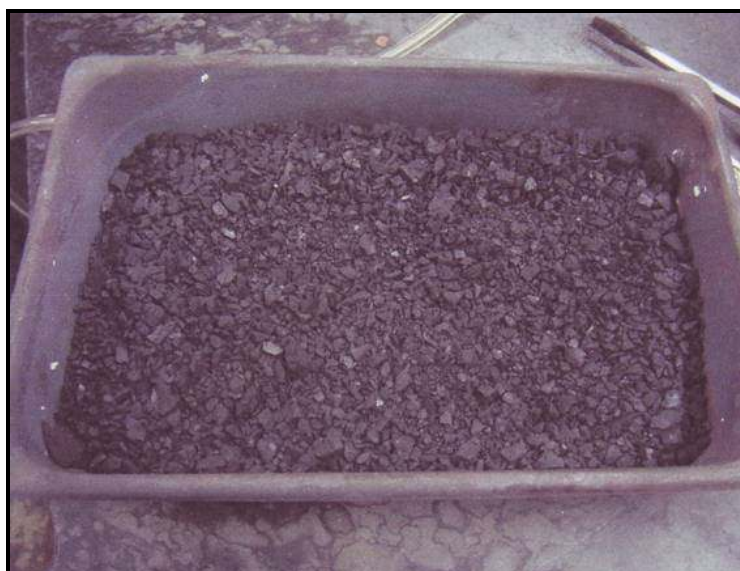


Figure 70. Figure 70PRB Coal Char After Pyrolysis.

Table 114. Proximate Analysis of PRB Coal, PRB Char and Anthracite Used as an Injection Carbon.

	Moisture, %	Ash, %	Volatiles, %	Fixed Carbon. %	Heat Value, Btu/lb	Sulfur, %
PRB Coal (control)	27.11	6.92	33.38	32.59	8,345	0.35
PRB Char 1	0.1	14.93	7.7	77.27	12,495	0.57
PRB Char 2	0.25	13.56	11.43	74.76	12,744	0.49
Anthracite	5.32	14.11	6.55	74.02	11,653	0.65

The second PRB char has higher volatile content and higher moisture than the first PRB char sample. Likely this is due to a shorter time at temperature.

The results in **Table 114** were produced via a rapid pyrolysis, conducted at about 600 °C. The PRB coal fines rapidly de-volatilized. The de-volatilized gases were condensed and then the non-condensable gases such as hydrogen and methane were combusted.

Table 115 shows another important physical characteristic of the char produced from PRB coal and that is the Hargrove Grindability Index which is a measure of the hardness of the coal. These data show that the char produced after pyrolysis is harder than the original coal which was also reported by Wolfe in previous testing with eastern bituminous coal. This means that the char produced should be acceptable from a handling standpoint and strong enough for injection into steel furnaces.

Table 115. Hargrove Grindability Index (HGI) of PRB Coal and Char.

Sample Type	HGI
PRB Coal, as received	57
PRB Coal, dried.	68
PRB Char	45

Another important characteristic that was measured was the screen or sieve analysis which is a measure of the particle sizes of the coal and char as compared to the particle sizes now used with anthracite coal an injection carbon source. These comparison data are shown in **Table 116**. These results show that the PRB char produced from the batch pyrolysis is comparable to the existing injection carbon used in the steel industry.

Table 116. PRB Coal and Char as compared to the Anthracite Injection Carbon.

Passing	Retained Upon	Anthracite Coal Weight%	PRB Coal%	PRB Char%
-----	+1/4 screen	2.47	0.00	0.00
+1/4	6 mesh screen	14.48	42.23	40.50
6 Mesh	16 mesh screen	67.49	40.24	54.20
16 Mesh	0	15.56	17.53	5.30

The coal gas samples were analyzed by Koppers, Inc of Pittsburgh, Pa for the purpose of determining the chemical characteristics of the gas and the heat value of these non-condensable gases. The results shown in Table 117 show that about 45% of the gas was hydrogen (28%) and methane gas (17%).

Also, the gas analysis shows a high percentage of CO₂ which is not expected since air was not intentionally allowed in the delayed coking vessel. Oxygen might have been present if the sample had been substantially oxidized. Alternatively, the possibility of leakage or other experimental error has not been ruled out. Additional trials may resolve this issue.

Table 117. Analysis of the PRB Coal Gas, Measured by Koppers, Inc.

Hydrogen	28.21 %
Methane	17.35 %
Ethylene	0.94 %
Ethane	2.97 %
Acetylene	0.02 %
O ₂	1.74 %
N ₂	9.32 %
CO	6.23 %
CO ₂	33.22 % *

Heat Value of the gas (calculated) was 354 BTU/ft³.

The coal liquids were collected and also analyzed in a Mass Spectrometer by Koppers. Koppers reported that the results are questionable in that there were no low boiling compounds and in fact, the liquids were mainly paraffinic high molecular weight liquids. If this is in fact the preferred reaction pathway, it suggests that additional cracking would be necessary to produce fuels.

For comparison purposes, Table 118 through Table 122 contain data taken from experiments carried out by Dr. Wolfe with Allied Signal in 1998. In that case, the hydrogen and methane made up about 58 % of the gas with less than 1 % carbon dioxide, as one might expect, since during pyrolysis, no combustion occurs.

Table 118. Heavy Coal Oil Liquid (Wolfe, 1998).

Specific Gravity @60 F		1.108
Water, vol. %		9.0 %
Quinoline Insolubles, wt %	Wt. %	4.4 %
Ash, wt %	Wt. %	0.089 %
Ammonium Chlorides	Lbs/1000 gal	300

Table 119. Pitch Properties (Wolfe, 1998).

Softening Point	C	54.40
Toluene Insolubles	Wt. %	16.40
Quinoline Insolubles	Wt. %	10.10
Coking Value	Wt. %	28.60
Ash	Wt. %	0.36
Sulfur	Wt. %	0.45
Distillation to 360 °C	Wt. %	10.50

Table 120. Gas Analysis (Wolfe, 1998).

Gas	Volume %	Wt. Lbs/cub ft.	Btu/cub ft.	Air Required
CH ₄	38.16	0.0171	366.3	3.66
C ₂ H ₆	1.46	0.0012	24.8	0.24
C _x H _{2x} +2	2.25	0.0038	38.3	0.09
H ₂	30.66	0.0017	89.5	0.89
O ₂	4.95	0.0044	--	--
N ₂	19.13	0.0150	--	--
CO	2.76	0.0022	22	0.07
CO ₂	0.65	0.0008	--	--
H ₂ S, COS, SO ₂	0.0037	0.2 X 10 ⁻⁶	1.1	0.01
Totals	100.0237	0.0462 Lbs/SCF	542 Btu/SCF	4.96 SCF/SCF
		(11,700 Btu/#)		

Pyrolysis is a potentially viable means of using coal to produce a viable feed for FutureGen while also producing liquid fuels. Three coals currently considered for use in FutureGen include Powder River Basin sub-bituminous, as well as Pittsburgh #8 and Illinois #6. All of these coals are longtime industry standards.

After devolatilization, Powder River Basin coal seems to be superficially similar to anthracite, suggesting that it may meet specifications as an injection carbon source for steel smelting, as well as being applicable to FutureGen.

About 50 per cent of the PRB coal can be converted into a carbon source with a fixed carbon content of about 77 per cent. The rest is converted to liquids or gas. The surprisingly high carbon dioxide concentration in the gas suggests that more samples should be evaluated, however.

The hardness of the PRB coal char is harder than the original PRB coal which should cause no difficulty in injecting this carbon source.

Both sub-bituminous Powder River Basin (PRB) coal and bituminous Pocahontas No. 3 (Beckley WV) coals were tested, as shown in the sequence of photos starting with Figure 71 through Figure 75 below.



Figure 71. Batch Pyrolyzer ejecting steam from Pocahontas 3 coal, thus reducing moisture in the condensed coal liquids.



Figure 72. Flare gas (mainly light volatiles) ignited at about 300 C.

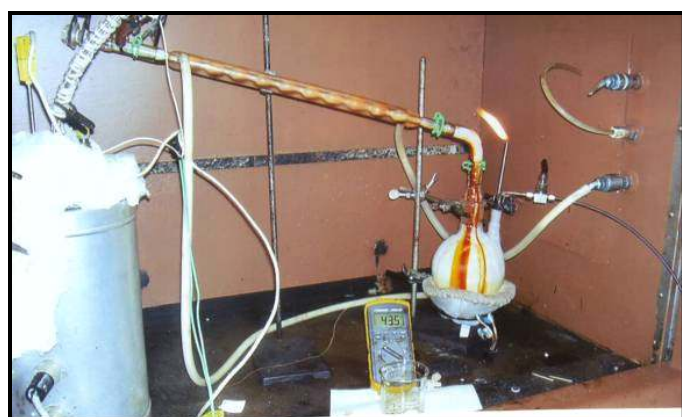


Figure 73. Condensing coal liquids and flaring non-condensable gases

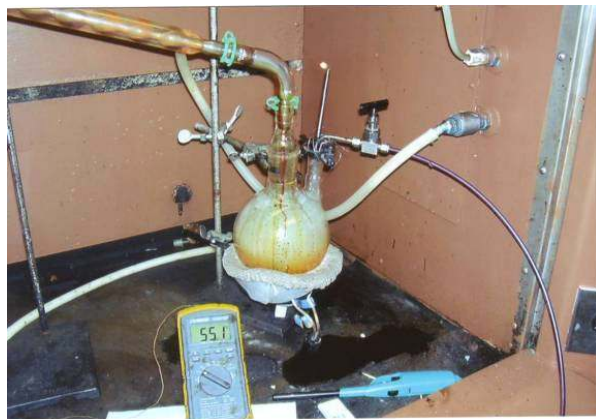


Figure 74. Most of the gases and liquids have been removed from the coal at about 550 C indicating that the pyrolysis conversion was complete and the experiment was terminated.



Figure 75. The agglomerated char produced from the pyrolysis process compared to a small sample of the crushed coal feedstock.

The technical data shown in Table 121 include the proximate analyses of the Pocahontas 3 Beckley seam coal and the char pyrolysis. These data also compares the char properties to anthracite coal properties that are now used as an injection carbon source. Also shown in this table are the results for PRB coal and char as a comparison.

Table 121. Comparison of Poca 3, PRB and Anthracite.

Parameter	Poca 3		PRB		Anthracite
	Raw Coal	Char	Raw Coal	Char	Raw
Moisture, %	6.40	0.27	27.11	0.10	5.32
Volatiles, % dry basis	16.28	5.34	33.38	7.70	6.55
Fixed Carbon, % DB	70.12	85.88	32.59	77.27	74.02
Ash, % DB	7.20	8.51	6.92	14.93	14.11
Sulfur, % DB	0.69	0.66	0.35	0.57	0.65
Lower Heating Value, BTU/lb	13,527	13,930	8,345	12,495	11,653
Free Swelling Index	7	0	0	0	0
Grindability Index	85	49	57	45	45

Thus the carbon char produced from the low volatile Pocahontas 3 type coal is similar in many respects to anthracite coal now used in many applications in the steel industry.

The low volatile coal produced an ~80% yield of carbon char. The PRB coal yielded about 50% char, with a corresponding larger yield of coal liquids.

An important distinction between PRB and Pocahontas 3 is that the carbon char produced from Pocahontas 3 coal becomes highly plasticized at temperatures less than 550 °C, whereas the PRB coal has no such caking property. Therefore the size of the PRB char is directly related to the size of the initial coal being fed to the pyrolyzer.

It is suggested that the caking property will enable the char to be crushed and screened to the appropriate size for an end user, possibly enabling it to be used as an injection carbon source for blast furnaces in place of the more expensive anthracite coal. If so, this could be an important co-product enabled by FutureGen technology.

The collected coal liquids were analyzed by Koppers in Pittsburgh, Pa. and the Environmental Laboratory Services (ELS) in New Castle, Pa. These results are shown in **Table 122** and actual data from the gas analyzer is shown in the appendix. These results show that the coal liquids contain appreciable concentrations (~5%) of benzene, toluene, and xylene (BTX) which is classified as a light oil and is used in the refinery industry for use as a gasoline additive for high octane rating.

As expected, the analysis of the coal liquids showed very little amount of coal tar was produced from this Pocahontas 3 low volatile coal and this observation can be further defined as larger quantities of this coal are processed in the future.

Gas measurements were more problematic. High concentrations of nitrogen and oxygen were observed, suggesting that extensive mixing with air may have occurred, either during the collection step, or, alternatively, during subsequent leakage during the storage step. Because the gas is collected at moderately high temperature, upon cooling it is possible that the container can be at a partial vacuum, raising the possibility that air might leak in the container. Hence, the collection technique and storage need to be refined.

Table 122. Analysis of the Non-Condensable Gases from Pocahontas 3 Coal.

Gas	Mass Percentage		
	365 oC	450 oC	550 oC
CH ₄	15.18	21.11	23.53
C ₂ H ₂	0.02	0.02	0.02
C ₂ H ₄	0.59	0.59	0.37
C ₂ H ₆	5.02	5.02	1.96
H ₂	1.87	8.93	17.35
O ₂	10.94	9.22	8.11
N ₂	64.75	53.58	46.47
CO	0.71	1.16	1.82
CO ₂	0.92	0.37	0.37
TOTAL	100.00	100.00	100.00

Additional data is contained in Appendix I.

The primary purpose of this test was to determine the quantity and quality of the coal by-products (char, coal liquids, and gas) that can be achieved from a high volatile eastern caking coal as compared to a low volatile eastern caking coal and a high volatile PRB basin non-caking western coal located in Wyoming.

The results of this particular test with the high volatile coal confirmed that as much as 70 percent of the coal can be converted into a high value carbon char product of acceptable quality as a carbon injection source and the remaining 30 percent of the gases removed during the pyrolysis process contained about 23 percent condensed coal liquids, about 6 percent non-condensable gases containing mostly methane and hydrogen gases, and about one percent water. These results showed that the yield of char produced from this coal was about 13 percent less in quantity than the char produced from the low volatile coal in Test No. 3 and produced about 20 percent more quantity of char than from the PRB coal. This test also showed that this high volatile eastern coal would produce a larger quantity of coal liquids than the previous two coals tested.

The results of these tests were consistent with results from previous tests. The high volatile PRB coal will not cake nor agglomerate during pyrolysis, so the size of the char produced is directly related to the size of coal being processed. The char yields for PRB coal were about 50 percent and liquid and gas yields about 25 percent and with about 25 % moisture removed. On the other hand, the low volatile caking coal fines, produced a yield of about 83 percent char with about 12 percent volatiles and 5 % moisture removed.

The liquid analyses showed that a high percentage of the liquids recovered during the pyrolysis process were defined as light coal oil with as much as 5 percent Benzene, Toluene, and Xylene (BTX) compounds which make these liquids highly desirable by the oil refinery industry for further processing into transportation fuel additives.

The gas analyses showed that the non-condensable gases contained mostly hydrogen and methane gas with only small amounts of longer chain carbon products.

The primary purpose of this test series is to establish a base line for the hydrogen and carbon products produced from different coals during pyrolysis and how these products can be further processed to support any future generation process. The first tests conducted were with Powder River Basin (PRB) coals from Wyoming because of their low cost, low caking properties and high volatility content. The second series of test were conducted with the low volatile, high caking characteristics of the West Virginia Pocahontas No. 3 Beckley seam of coal. The latest test results as described in this report were for the processing of a typical high volatile, high caking, southern West Virginia Coal blend obtained from a supplier near Beckley WV. This coal blend is expected have similar characteristics to the West Virginia Kingwood coal located in the northern part of West Virginia.

3.3.3 Feedstocks for Synthetic Metallurgical Coke

Metallurgical coke is of interest for large scale coal liquefaction if for no other reason than the finite market for anode grade coke. Motaghi et al. indicate that the long term market for anode grade coke may be as high as 17-20 million tons per year. Assuming that one barrel of crude oil is equal to 320 pounds, then 20 million tons per year corresponds to some 300,000 barrels per day. Of course this is bit of an apples-to-oranges comparison because crude oil is used to produce a variety of products, and not just anode grade coke. Nevertheless, the point is that the size of the world market for anode coke is comparable to a single large Texas refinery.⁵⁸ Fuel grade coke is also produced via delayed coking, but at a greatly reduced price. Table 123 compares the properties of fuel grade coke as well as anode grade coke and needle grade coke.

Because of the limited demand for anode grade coke, in the long run, larger carbon product markets need to be considered. Although estimates of the total global market size vary greatly, metallurgical grade coke represents a significantly larger market than anode grade coke.

According to a study by IntertechPria, the global metallurgical coke market is forecast to reach 460 million metric Tonnes by 2015, or some twenty times higher than the market for anode grade cokes.⁵⁹ Yet a estimate of 750 million metric Tonnes was published in Steel Times International, suggesting that the market may be very volatile.⁶⁰ In recent years, the market demand for metallurgical grade coke has been created by increasing global demand for steel, notably from India and China.

In 2009 the global downturn caused demand for metallurgical coke to plummet. Chinese exports were priced out of the market partly as a result of its 40% export tax. In 2010 iron and steel production recovered somewhat, restoring demand.⁶¹

Coke prices have been volatile, and of course no one knows the future for or any other major commodity, but as of early 2011, at least one estimate for the world market price for metallurgical pegged it at about \$350 per metric Tonne.⁶²

If these trends are long term, and if global demand for liquid products continues to hold as well, then a sound business plan can likely be created on the basis of producing metallurgical grade coke and synthetic crude oil as coal liquefaction derivatives.

Table 123. Properties of Petroleum-Derived Coke from Delayed Cokers.⁶³

Property	Fuel Grade Coke	Calcined Anode Grade Coke	Calcined Needle Grade Coke
Density, kg/m ³	880	7k20-800	670-720
Sulfur, weight percent	3.5-7.5	1.0-3.5	0.2-0.5
Nitrogen, ppm mass	6000		
Nickel, ppm mass	489	200	5-7
Vanadium, ppm mass	141	350	
Volatiles, weight %	12	0.5	0.5
Ash content, wt%	0.35	0.40	0.10
Moisture content, wt%	8-12	0.3	0.1
Hardgrove Grindability	35-70	60-100	
Coefficient of Thermal Expansion x 10 ⁻⁷			1-5

Metallurgical grade coke differs from anode grade coke in several aspects. Since metallurgical grade coke is usually used in blast furnaces, it needs to have physical integrity and resist pulverization as it is dumped into the top of the blast furnace, as conceptually illustrated in Figure 76 below. As the layers of coke, limestone and iron ore sinks under the weight of additional layers from above, the metallurgical grade coke needs to have compression strength. For these reasons, a battery of ASTM tests must be used which differ from the tests used to characterize anode grade coke.

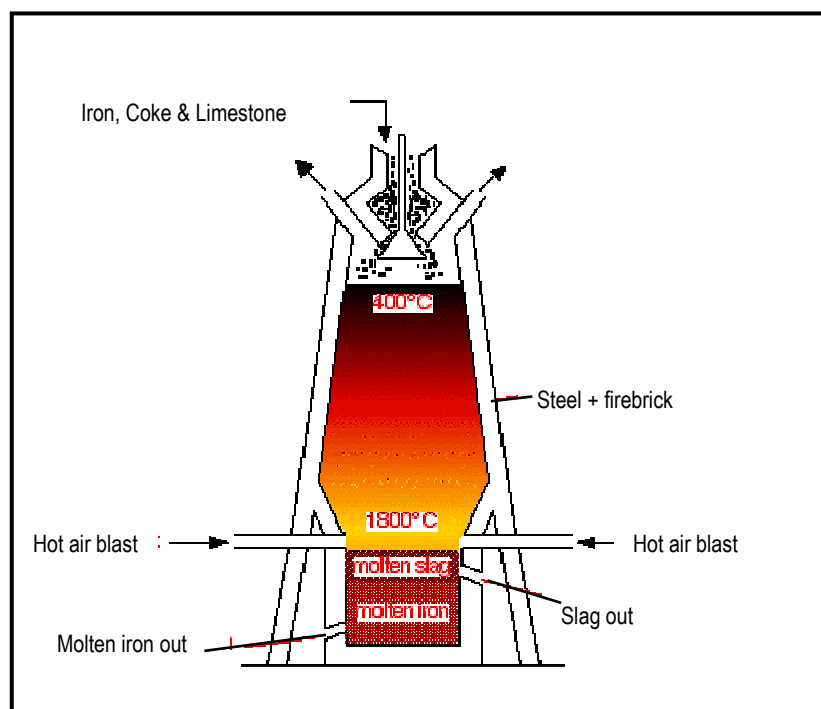


Figure 76. Conceptual Layout of a Blast Furnace.

The Hardgrove Grindability Index measures the extent to which coal can be reduced to smaller particle size. A high index means that the coal is easier to grind, and a low index suggests a coal which is harder to grind.

The Free Swelling Index measurement determines whether a coal will actually swell and form a coke. Coals with a low FSI form a powdery char, and do not create a solid coke at all.

The Coke Reactivity Index (CRI) and Coke Strength after Reaction (CSR) are usually measured together. The CRI/CSR test measures coke reactivity in carbon dioxide at elevated temperatures and its strength after reaction by tumbling. The CRI is based on weight loss, while the CSR is related to the mass fraction of particles above a certain size. Typically, blast furnaces seek coke with a CRI less than 25, and a CSR greater than 60.

The ASTM Stability and Hardness Tumbler Testing is also related to the performance of coke in the harsh blast furnace environment. This test measures the resistance of coke to impact and abrasion, based on the mass fraction of coke having a size of 1" or greater after tumbling in a specified drum. Hardness is characterized by the mass fraction which is 1/4" or greater. Typically blast furnace operators may seek coke with a stability rating of +60.

3.3.4 Studies with Eastern Bituminous Coals

The technical procedure used in conducting this pyrolysis test was similar to previous tests conducted in December, 2006 and March, 2007.

1. Approximately 1.75 kg of blended high volatile eastern coal were prepared in a batch electrically heated coking reactor with a thermocouple placed directly in the coal to measure the temperature of the coal during pyrolysis.
2. The coal sample was heated in the batch process to about 100 C to remove most of the moisture from the coal as a method to reduce the moisture content in the coal liquids..
3. The non-condensable coal gas was ignited at about 250 C which indicated that the initial low volatile gases such as hydrogen and methane were beginning to be removed during the initial stages of the pyrolysis process.
4. Several gas samples were collected during the pyrolysis process.
5. The batch pyrolysis process was maintained at 600 C for about one hour until all the volatiles were removed where the evolving gas was unable to maintain a flare ignition, thus indicated that the pyrolysis of the coal at this temperature was complete. The system was cooled down by removing the insulation and the containment kettle from the electrical heater.
6. After cooling to ambient room temperature, the char and coal liquids were collected (Figure 77). The agglomerated char and coal liquids samples as removed from the batch pyrolysis system.



Figure 77. Collection of all the char and coal liquids produced during the batch pyrolysis test of this high volatile and high caking eastern bituminous coal.

Table 124 contains the proximate analyses of the high volatile coal tested in this experiment, compared with the two previous tests as well as to the anthracite coal properties now used as a carbon injection source in the steel industry. These results suggest that the carbon char produced from the different coals tested compares favorably with the quality of the anthracite coal now used in the steel industry; e.g., as an injection source. The low volatile Pocahontas 3 coal yields a larger quantity of char with less liquids and gas. In contrast, the PRB coal yields less char but a larger quantity of coal liquids and gas. The high volatile eastern coal shows yields of both char and coal liquids in between the other two coals. Also, an interesting and expected observation is that the sulfur remaining in the char after pyrolysis is less than the initial sulfur in the coal. This is as expected since during the pyrolysis process, most of the organic sulfur is removed in the vapor stage and the elemental sulfur is what remains in the char. Therefore, the char has less sulfur than the original coal when the difference in weight percent is considered as in the case for the PRB coal when so much moisture was removed initially for the coal.

Table 124. Proximate Analysis of Different Coals and Chars.

Coal Properties	WV Hi-Vol		Pocahontas 3		Powder River Basin		Anthracite
	Coal	Char	Coal	Char	Coal	Char	
Moisture	1.99	0.43	6.40	0.27	27.11	0.10	5.32
Volatile	35.53	6.70	16.68	5.34	33.38	7.70	6.55
Fixed Carbon	54.88	81.94	70.12	85.88	32.59	77.27	74.02
Ash	7.60	10.93	7.20	8.51	6.92	14.93	14.11
Sulfur	1.13	0.85	0.69	0.66	0.35	0.57	0.65
Heat Value, BTU/lb	13,795	13,377	13,527	13,930	8,345	12,495	11,653
Free Swelling Index	8.5	0	7.0	0	0	0	0

Confirming measurements were made at WVU, and the results are shown in **Table 125** for the WV Hi-Vol blend. The values agree within several percent, the majority of the difference likely due to inhomogeneity and nonuniformity of the samples.

Table 125. Proximate Analysis of WV Hi-Vol Blend.

Test Identifier	Moisture	Volatile	Ash
Coal WV Hi-Vol Blend Wolfe 3/13/07 1	1.44	33.05	5.36
Coal WV Hi-Vol Blend Wolfe 3/13/07 2	1.39	32.69	6.47
Char WV Hi-Vol Blend Wolfe 3/13/07 1	0.8	7.04	9.61
Char WV Hi-Vol Blend Wolfe 3/13/07 2	0.85	7.82	13.46

Table 126 and Table 127 provide confirming calorimetric measurements made at WVU.

Table 126. Calorimetric Measurements for WV Hi-Vol Blended Coal.

Sample ID:	COALWOLFE31307-4		Mode:	Determination
Type:	Final		Date/Time:	03/19/07 00:35:30
Sample Weight:	0.6400		Method:	Dynamic
Spike Weight:	0.0000		Bomb ID:	1
Fuse:	15.0000		EE Value:	2261.6821
Acid:	10.0000		Sulfur:	0.0000
Jacket Temperature:	30.0449		Initial Temp.:	22.7412
Temperature Rise:	2.1292			
			Gross Heat:	13473.5146
				Btu/lb
Sample ID:	COALWOLFE31307-6		Mode:	Determination
Type:	Final		Date/Time:	03/19/07 01:25:29
Sample Weight:	0.6567		Method:	Dynamic
Spike Weight:	0.0000		Bomb ID:	1
Fuse:	15.0000		EE Value:	2261.6821
Acid:	10.0000		Sulfur:	0.0000
Jacket Temperature:	30.0109		Initial Temp.:	21.9097
Temperature Rise:	2.2158			
			Gross Heat:	13667.4688
				Btu/lb

Table 127. Calorimetric Measurements for WV Hi-Vol Blended Coal.

Sample ID:	CHARWOLFE31307-2	Mode:	Determination
Type:	Final	Date/Time:	01/09/00 04:17:38
Sample Weight:	0.6353	Method:	Dynamic
Spike Weight:	0.0000	Bomb ID:	1
Fuse:	15.0000	EE Value:	2397.9153
Acid:	10.0000	Sulfur:	0.0000
Jacket Temperature:	29.9705	Initial Temp.:	23.1758
Temperature Rise:	1.9238		
		Gross Heat:	12999.7490
			Btu/lb
Sample ID:	CHARWOLFE31307-3	Mode:	Determination
Type:	Final	Date/Time:	01/09/00 04:37:06
Sample Weight:	0.8907	Method:	Dynamic
Spike Weight:	0.0000	Bomb ID:	1
Fuse:	15.0000	EE Value:	2397.9153
Acid:	10.0000	Sulfur:	0.0000
Jacket Temperature:	30.0392	Initial Temp.:	22.8734
Temperature Rise:	2.7035		
		Gross Heat:	13050.6104
			Btu/lb

Figure 78 shows the coke residue from unsized PRB coal, and Figure 79 shows coke residue from the same coal ground to -20 mesh. This sample could properly be considered to be low-grade carbon foam. It was noted that grinding to -20 mesh resulted in a uniform, lower density coke.

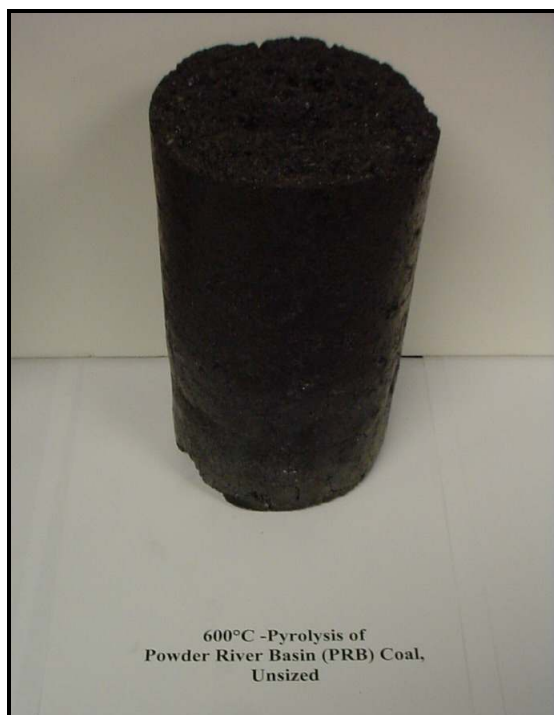


Figure 78. Coke Residue from Unsized PRB Coal.

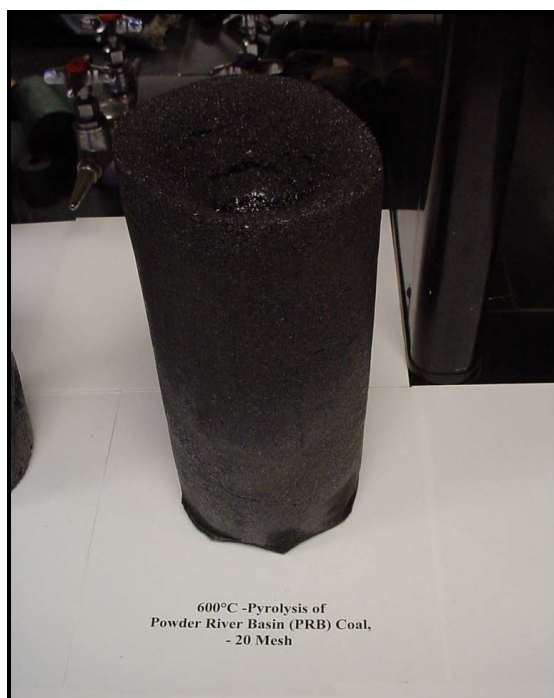


Figure 79. Coke Residue from Partial Coking of PRB Ground to -20 Mesh.

The coal liquids were analyzed by Environmental Laboratory Services (ELS) in New Castle, Pa. These results for the light fractions are shown in **Table 128**, with the data for heavy products included in Appendix I. The results show that the high volatile coal blend produces

about 3.45 percent light coal oil containing mostly benzene, toluene, and xylene (BTX). These coal liquids and those coal liquids from the previous testing of the other coals meet the specifications for selling this by-product to oil refinery industry. For example, the existing coke oven industry produced light coal oil normally contains less than 1.5 % BTX. Coal liquids produced from the pyrolysis process at 600 C contain a higher percentage of light coal oil than the coke ovens which typically operate at about 1100 °C.

Table 128. Coal Liquid Analysis for the Light oil.

REPORT DATE: 03/28/07

Sample Name: Wolfe/WVU WV Hi Vol Blend Coal Liquids
 Sample Date: 03/13/07
 Lab Sample #: HW63469

LABORATORY RESULTS		
<u>Parameter</u>	<u>Result</u>	<u>Method</u>
*Benzene,	0.74 %	EPA 8260B
*Toluene,	1.31 %	EPA 8260B
*Ethyl Benzene,	0.18 %	EPA 8260B
*Xylenes, Total	1.22 %	EPA 8260B

Total Light Oil Compounds	3.45 %	
Flash Point	72 °F	EPA 1010A

Based upon the results obtained in this pyrolysis experiment using a high volatile, high caking, southern West Virginia bituminous coal blend, the following observations can be made:

- a. The high volatile caking type coal produces a high quality carbon char product that appears to meet the specifications for injection carbon and semi-coke applications with in the steel industry.
- b. A carbon yield of a least 70 percent can be achieved during the pyrolysis of a high volatile West Virginia coal of the quality tested in this experiment.
- c. The amount of coal liquids and gas are on the order of about 25 percent when using this type of West Virginia coal.
- d. The quality of the coal liquids are sufficient for selling to the oil refinery industry very similar to the coke oven light oils now sold but of better quality.

e. The quality and heat value of the gas is sufficiently clean to use as a fuel source in the pyrolysis process.

f. In order to provide sufficient heat to operate the pyrolysis system from the recycled gas, it may prove that a high volatile coal, either the eastern coal or the PRB coal, is needed, even though the yield of char would be less.

g. The energy and material balance are one of the important parameters in establishing the economics of this pyrolysis technology in converting coal continuously into liquids, gases, and char and coke products.

3.3.4 Thermocracking of United Coal Co. Star Bridge Prep Plant Coal Fines

Experimental delayed coking trials were carried out using coal wastes obtained from the United Coal Company Star Bridge Coal Preparation Plant near Elkins, WV, shown below (Figure 80). This helps to develop the premise that coal waste could be utilized as a clean fuel in FutureGen or other gasification related projects, while at the same time helping to reduce the amount of mining waste which continues to accumulate as coal is mined. The amount of coal waste may amount to as much as a fourth of the coal that is actually mined.



Figure 80. UCC Star Bridge Coal Prep Plant, near Elkins WV.

United Coal Company of Bristol, Virginia allowed Dr. Wolfe to collect several coal waste samples from their Star Bridge Preparation Plant located near Elkins, West Virginia.

These samples were analyzed for the coal characteristics and then processed through a batch pyrolysis system at West Virginia University.

The purpose of collecting these samples was to conduct a partial coking tests to determine whether the coal residue can be used in FutureGen or other coal gasification applications. In addition, the quality and quantity of coal liquids that might be recovered are also of interest.

This particular coal is a low volatile coal with a volatile content of about 20 % which represents a reasonable “worst case” in terms of coal liquids recovery. It is obvious that coals with higher volatile content would provide the opportunity for the recovery of larger quantities of coal liquids.

Because the price of coal liquids is comparable to the price of crude oil, and because of the additional attention commanded by environmentalism, it is appropriate to reconsider the utility of waste coal and coal fines.

Even with the best physical coal cleaning steps available there still is an enormous amount of coal, particularly the fine size coal from froth floatation cells and spirals, lost in the discarded coal waste. This is a concern to any true Clean Coal fuel cycle operation, including FutureGen and others.

The UCC coal waste samples were collected and the laboratory analysis showed that this coal was a low to mid-volatile coal of about 19-24 % which means that this coal is the worst case for collecting coal liquids from the volatiles. This condition was the primary reason for selecting this particular coal seam for if a measurable quantity of coal liquids could be recovered from this type coal, then the higher volatile coals would be even more economical. The laboratory analysis showed that the thickener underflow stream of fine coal waste contained as much as 48 % coal on a dry basis with a heat value of 6699 BTU/lb and a particle size of 16 mesh by zero. The spiral waste stream showed 33% coal on a dry basis with a heat value of 3138 BTU/lb. The heavy medium coal waste showed, with a secondary heavy medium cleaning step, as much as 54 % coal with a heat value of 7542 BTU/lb which showed a lot coal partings in this coal.

A special batch coal pyrolysis test experiment was undertaken at West Virginia University using the dry thickener underflow waste stream as the source of material. The pyrolysis test was operated at 650 C and the coal liquids and methane gas samples were collected and analyzed. The results showed that the recovered coal liquids were of high quality and of sufficient commercial value and were similar to the light coke oven oils currently purchased by oil refineries at the price of crude oil. Laboratory analyses of these liquids is now underway by Koppers, Inc., but typically these type liquids show the Benzene, Toluene, and Xylene (BTX) averaging around 5% which is higher than the normal 3% from light coke oven coal oils. The volatile levels of the coal waste sample were 16.71% and the char sample after processing at 650 C was 1.58% which accounts for about a 90% volatile removal rate. The material balance during this batch test showed that about 60% of these volatiles were light coal liquids, and the remaining 40% volatiles were incondensable methane gas with a heat value near natural gas levels.

Based upon testing an initial quantity of 2000 grams of coal waste, the amount of coal liquids recovered was about 180 grams. Relating these values to a one ton quantity of this thickener underflow coal waste of the same quality in this study, about 180 pounds of coal liquids (and at 7 pounds per gallon) could be recovered. This equates to about 26 gallons or 0.6 barrel of coal liquids that could be recovered from each ton of the low volatile coal waste processed. At the current price of light coal oil being the same price as crude oil at today's price

of \$80 per barrel, these coal oil liquids have a value of about \$48/ton of coal waste processed. At these prices, the recovery of the coal liquids from selected coal waste would make economic sense. This low volatile coal waste is the worst case and would be further improved when higher volatile coal waste was thermally reprocessed by this technology.

Mr. Dwayne Ware, superintendent of the coal preparation plant and Dr. Wolfe collected the samples as shown in Figure 81 through Figure 84.



Figure 81. Mr. Dwayne Ware, Superintendent and Dr. Wolfe collecting coal waste samples.



Figure 82. Samples were taken from thickener underflow at the Prep Plant.



Figure 83. Samples were taken from the bottoms of the spirals from froth flotation.



Figure 84. Samples were also taken from the heavy medium circuit.

Each of the coal waste samples and the clean coal sample were analyzed at the SGS mineral laboratory in Beckley, West Virginia. The results of these analysis are shown in **Table 129**. The results show that this is mid to low volatile coal with excellent coking properties.

**Table 129. Proximate Analysis of the UCC Coal and Coal Waste Samples from Prep Plant.
(AS RECEIVED BASIS)**

Characteristics	Clean Filter Cake Coal	Thickener Waste	Spiral Waste	Heavy Med.
% moisture	30.42	28.63	5.56	3.42
% ash	5.71	37.39	64.15	43.32
% Volatile	18.74	16.71	14.45	20.2
% Fix Carbon	45.13	17.27	15.84	33.1
	100	100	100	100
% sulfur	0.38	0.21	0.26	0.39
BTU/#	9766	4736	3138	7542
FSI	8	--	--	--
Fluidity ddpn	754	--	---	--
Softening Temp C	405			
Max Fluidity Temp C	449			
Resolidification Temp C	477			
Fluid Range C	72			

Wolfe designed and installed an efficient batch pyrolysis system at WVU with condenser and gas collection capability for converting coal and coal waste into char, coal liquids and gases. Based on recent discussions with Ken Krupinski (Koppers consultant), a second dry-ice-cooled condenser needs to be installed. In Figure 85, it can be seen that volatile vapors are present in the vapor collection flask, and some portion may be vented with the gas. This might affect the mass balance, so that the liquid mass might be understated and the gas mass might be overstated.



Figure 85. Batch Pyrolysis Process with coal liquid condenser and coal gas flare

Proximate results are shown in Table 130. These results show that the dried coal waste has an ash content of about 51% and a volatile content of 17%. The coal char remaining after the pyrolysis experiment at 650 C showed that the ash was about 60% and the volatiles were about 1.59% which indicates that about 90% of the volatiles were removed and converted into gas and coal liquids.

Table 130. Proximate Analysis of the Dried Thickener Underflow Coal Waste and the Char remaining after the volatiles were removed during pyrolysis at 650 C.

Characteristics	Thickener Underflow Coal Waste	Resulting Char
% moisture	1.76	0.56
% ash	50.30	59.58
% Volatile	16.71	1.58
% Fixed Carbon	<u>31.23</u>	<u>38.28</u>
	100	100
% Sulfur	0.29	0.29
BTU/#	6699	5916

From a material balance of the coal liquids produced and the gases produced, the results showed that about 60% of the volatiles were converted into coal liquids and the remaining 40% was incondensable gases such as methane gas. The methane gas analysis is shown in **Table 131**. These results show that the majority of the gas is methane gas with a total heat value similar to natural gas at 1000 Btu/scf. This gas could be recycled to provide the heat source for the process without the need for any additional heat source. Alternatively, such gas could be reformed in a FutureGen system to produce additional hydrogen if desired.

Elemental analysis of the different forms of waste coals is shown in **Table 132** through **Table 139**.



P.O. Box 1028
Bridgeport, WV 26330-0461
Phone: (304) 623-0020
FAX: (304) 624-8065

Analysis#:	51626
Run Date:	10/25/2007
Run Time:	13:58
Cylinder#:	

Customer:	Wolfe Engineering & Consulting	Sample Date:	10/24/2007
Field:	Component Analysis	Sample Time:	0:00
Station:	Waste 1	Collected By:	Richard Wol
Meter:		Effective Date:	10/24/2007
		Sample Pressure:	0.00 PSIG

Component	MOL%	GPM
Methane	74.8086	
Ethane	7.3919	1.97
Propane	1.8355	0.50
I-Butane	0.1330	0.04
N-Butane	0.4028	0.13
I-Pentane	0.5477	0.20
N-Pentane	0.2467	0.09
Nitrogen	1.2883	
CO2	12.0613	
Oxygen	0.4144	
Hexanes+	0.8698	0.38
Total:	100.0000	3.31

Analytical Results at Base Conditions	
BTU/SCF (Dry):	1032.0096
BTU/SCF (Saturated):	1014.9855
PSIA:	14.7300
Temperature (°F):	60.00
Z Factor (Dry):	0.99688
Z Factor (Saturated):	0.99683

Analytical Results at Contract Conditions	
BTU/SCF (Dry):	1032.0096
BTU/SCF (Saturated):	1014.9855
PSIA:	14.7300
Temperature (°F):	60.00
Z Factor (Dry):	0.99688
Z Factor (Saturated):	0.99682

Calculated Specific Gravities	
Ideal Gravity:	0.7778
Real Gravity:	0.7790

Gross Heating Values are Based
on GPA 2145-91, 2172, 2251
Compressibility is Calculated using AGA-8

- Table 132. Elemental Analysis for Spiral Waste, Raw Measurements.**

181

Table 133. Elemental Analysis for Spiral Waste, Avg Values.

3 Sample(s) in Group No : 2				
Component Name	Average	Std. Dev.	% Rel. S.D.	Variance
Nitrogen%	0.801262895	0.07529882	9.3975	0.0057
Carbon%	30.96622403	1.4891	4.8088	2.2174
Hydrogen%	2.457643429	0.07452782	3.0325	0.0056
Sulfur%	0	0	0	0

Table 134. Elemental Analysis for Thickener Underflow, Raw Measurements.

Group No : 3	Element %			
Sample Name	Nitrogen%	Carbon%	Hydrogen%	Sulfur%
Thickener Underflow	0.931117892	44.17263031	2.855177641	0
Thickener Underflow	0.981972158	46.07748032	2.968631268	0
Thickener Underflow	1.023709893	47.10408783	3.05917263	0

Table 135. Elemental Analysis for Thickener Underflow, Avg Values.

3 Sample(s) in Group No : 3				
Component Name	Average	Std. Dev.	% Rel. S.D.	Variance
Nitrogen%	0.978933315	0.04637074	4.7369	0.0022
Carbon%	45.78473282	1.487493	3.2489	2.2126
Hydrogen%	2.960993846	0.1022117	3.4519	0.0104
Sulfur%	0	0	0	0

Table 136. Elemental Analysis for Belt Fines, Raw Measurements.

Group No : 4	Element %			
Sample Name	Nitrogen%	Carbon%	Hydrogen%	Sulfur%
Clean Fines from Belt	1.23564899	78.55104065	4.903787136	0.141470283
Clean Fines from Belt	1.421684742	82.78783417	5.115591049	0.228846774
Clean Fines from Belt	1.388062119	80.09781647	4.964108944	0.150972411

Table 137. Elemental Analysis for Belt Fines, Raw Measurements.

3 Sample(s) in Group No : 4				
Component Name	Average	Std. Dev.	% Rel. S. D.	Variance
Nitrogen%	1.348465284	0.09913757	7.3519	0.0098
Carbon%	80.47889709	2.14395	2.664	4.5965
Hydrogen%	4.99449571	0.1091226	2.1849	0.0119
Sulfur%	0.173763156	0.04793982	27.5892	0.0023

Table 138. Elemental Analysis for Heavy Media Waste, Raw Measurements.

Group No : 5	Element %			
Sample Name	Nitrogen%	Carbon%	Hydrogen%	Sulfur%
Heavy Media Waste	1.019470453	48.34233475	3.488897562	0
Heavy Media Waste	0.984535933	46.38832092	3.400177717	0.05040412
Heavy Media Waste	0.964423597	46.22026825	3.488134146	0.079863451

Table 139. Elemental Analysis for Heavy Media Waste, Avg Values.

3 Sample(s) in Group No : 5				
Component Name	Average	Std. Dev.	% Rel. S. D.	Variance
Nitrogen%	0.989476661	0.02785403	2.815	0.0008
Carbon%	46.98364131	1.179659	2.5108	1.3916
Hydrogen%	3.459069808	0.05100347	1.4745	0.0026
Sulfur%	0.043422524	0.04038687	93.009	0.0016

Based upon the laboratory results obtained in this coal waste partial coking experiment, the following conclusions can be made:

a. Production of FutureGen gasification fuel appears to be a realistic possibility using coal wastes of the types considered. In the past, this may have been considered to be uneconomical, but in today's environment, the high price of liquid fuels and chemicals dictates that coal-wastes be re-evaluated as potential material resources. Although bituminous coal currently sells for three times the price of western US coals, the same is not true for waste coals, including prep plant waste and gob, which are very low price commodities. If fuels and liquids can indeed be extracted while coproducing an inexpensive gasification fuel, it may be worthwhile to consider FutureGen systems for use in the Eastern US.

b. Of the various coal waste streams sampled from the UCC Star Bridge coal preparation plant, the waste stream with the largest amount of coal was from the thickener underflow stream. This coal waste comes from the fine coal circuit and the refuse belt filters. In most preparation plants, the coal recovery rate is not much better than shown in this plant, so the fine coal circuit is typically where most of the coal is lost to waste. The percentage of fine coal in this waste stream was about 49 percent.

c. The coal sampling of the heavy medium waste stream showed a lot coal partings exist in this waste; a secondary heavy medium system could be installed and then the recovery of this coal waste with partings could be used as feed to a pyrolysis process to recovery the coal liquids.

d. The pyrolysis of the thickener underflow waste product in the batch system showed that about 90 percent of the remaining volatiles in the coal waste could be recovered and converted into coal liquids and methane gas. The material balance showed that about 60 percent of the volatiles were converted into a high quality coal liquid, and the remaining 40 percent were methane type gas with a heat value of about 1000 BTU per standard cubic feet.

e. The amount of coal liquids that could be recovered from the coal waste at this preparation plant (which processes typically a mid to low volatile coal) is about 26 gallons per ton of coal waste processed. The price of light coal liquids can be comparable to a barrel of crude oil. At a price of \$80 per barrel, the value of these coal liquids would be about \$48 per ton of coal waste.

3.4 Delayed coking

Originally, it was thought that an effective simulation should use liquid injection into a hot (500 °C) coking vessel. However, discussions with Intertek PARC (Harmarville PA) suggested that this is probably not necessary. Intertek PARC uses canisters that are lowered into a heater. There are limitations to this approach, but the main one is probably the shear size of the unit. An industrial scale delayed coker has significant vertical (buoyant) pressure gradients resulting from the shear size of the unit. Hence the coke produced often has highly elongated vertical pores. Such effects are difficult to reproduce for small scale units, irrespective of the method of introducing the materials to be coked.

Direct coal liquefaction processes also result in synthetic heavy aromatic crudes or tars.

Powder River Basin coal was used as a control test because it is being considered as a fuel for FutureGen. Other coals selected by FutureGen include Illinois #6 and Pittsburgh #8. In addition, PRB is low cost and often quoted as a baseline for determining coal prices. Further, the liquid products resulting from cracking sub-bituminous coal are likely to be more aliphatic than liquids from bituminous coal. Hence PRB liquids may have higher yield of fuels-relevant liquids compared to liquids from bituminous coals.

The delayed coking system was modified to permit injection of hot liquid directly into the coking chamber in order to better simulate the physical processes that occur in an actual delayed coker. Previously, the coking chamber could be lowered in the kiln using a small crane. This was judged to be satisfactory for many experiments, although the wall/fluid interaction is different in the two variants. In the case of hot liquid injection, the wall is pre-heated and thus remains more or less at a constant temperature when the liquid is injected. By contrast, in the canister system, the walls of the canister were cold when the unit was lowered into the kiln. This may result in some difference in the development of bubbles in the working media.

The system also contains a water cooled condenser and storage tank to recapture liquid volatiles. The output in turn is scrubbed using a caustic soda scrubber, and further adsorbed on activated carbon in order to minimize environmental interactions.

However, the main reason to modify the system is actually based on human factors, as it is desirable to avoid lifting and lowering of a heavy object into a hot kiln inside a cramped walk-in fume hood. A diagram of the modified system is shown in Figure 86, with photographs in Figure 87 through Figure 90.

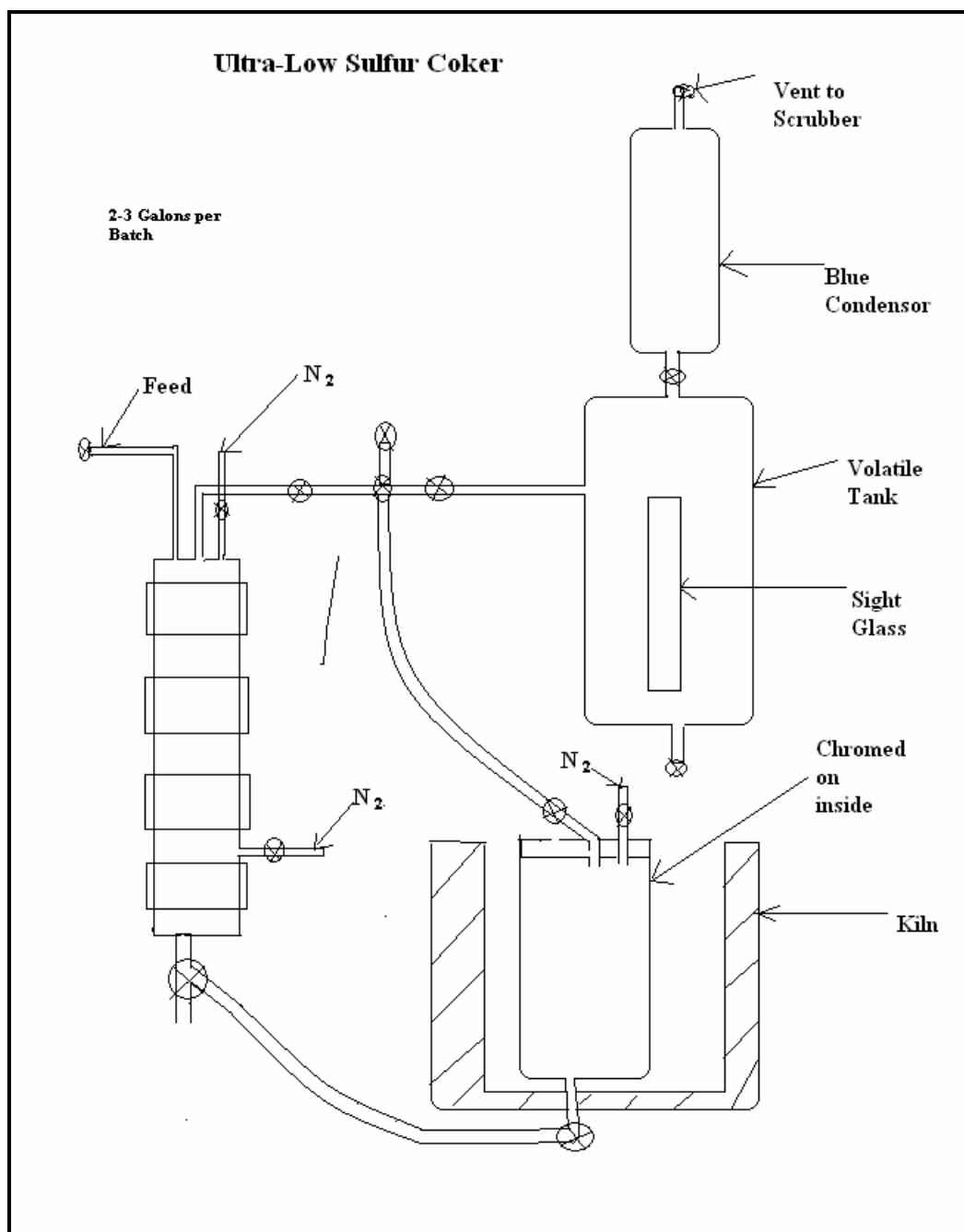


Figure 86. Overview of Modified Coking System.



Figure 87. Paragon Kiln and Controller.



Figure 88. Condenser and holding tank.



Figure 89. Coking Vessel.



Figure 90. Water Cooled Condenser.

A viable coking capability may provide a method to deal with high ash coals. As previously pointed out, if the tails are composed of 80% viable liquefied product and 20% solids, this would be economically attractive only for coals with ash concentration of several percent or less. Otherwise, it is necessary to have some means of recovering liquids from the ash-containing solid fraction.

One of the main potential reasons for not using delayed coking machines to process centrifuge tails is that current cokers—used by the petroleum industry—are presently engaged in upgrading petroleum stocks. Hence, the incorporation of ash in the coker is likely to be a sticking point (literally in figuratively) in persuading the owner of such a facility to use coal feedstocks in a facility that currently produces revenue streams. Thus, the development of a coke product containing ash might have to be undertaken in a completely separate facility.

The process begins with coal tar distillate (CTD) being pumped from a storage drum into the twelve gallon distillation unit using a diaphragm pump. This setup is shown in Figure 91. The drum sits on a scale so that mass of material entering the system can be recorded. Once the CTD is inside of the distillation unit, nitrogen is bubbled through the CTD through a coil at the bottom of the vessel. Then the distillation vessel is heated using five heating bands and the temperature is measured using a thermocouple. The rate of heating the material, the maximum temperature of the vessel, and the amount of time that the process is held at that temperature are all variables that are examined in the testing process.

As the CTD is heated, lighter molecules escape into the vapor phase and are carried out of the distillation unit by N_2 . The vapors, along with nitrogen, enter the side of a collection

vessel. They proceed out of the top of the collection vessel and into the tube side of a shell and tube heat exchanger that is set in the vertical position. Cooling water is run through the shell side of the heat exchanger in order to condense the vapors. The vapors condense and fall back down into the collection vessel. There is also a T-valve installed at the collection vessel vapor input so that samples of condensed vapors can be obtained at any time during the distillation process. The nitrogen and any vapors that did not condense leave the top of the condenser and enter a large expansion tank where the vapor should condense.

Samples of the pitch, or reacted CTD, can be taken directly from the distillation vessel using a sample port that is designed to obtain a well-representative sample across the diameter of the vessel. The pitch and condensed vapor samples are analyzed with the main objective being to make the best possible precursor to further the process into high valued needle coke.

When the distillation process is completed the pitch is still a liquid with low viscosity inside of the heated vessel. It can then be pumped into a coking unit for further processing into needle coke. The coking unit, or coker, is set inside of a kiln in order to obtain the desired temperature of the coking process. The piping is wrapped in heating tape so the pitch does not solidify in the lines while it is being transferred. In addition, the pump is also equipped with a heating element for the same reason.



Figure 91. Distillation and Delayed Coking System.

The pitch is transferred at a very low rate using a Balder sludge pump. The low transfer rate is to avoid any temperature gradients in the coker, which is at a higher temperature than the incoming pitch. The idea is to have the pitch enter the coker slow enough so that the temperature remains constant. The inside of the coker is coated so that the coke can be removed from the

walls of the vessel much more easily. Inside of the coker, heat drives more material into the vapor phase. The vapors and nitrogen, which are added into the top of the coker, also go to the collection vessel and into the condenser.

The delayed coker is shown during operation in Figure 92 through Figure 94.



Figure 92. Coking Vessel Charged with Lower Kittanning Coal. Red hot filaments are barely visible at left.



Figure 93. View of the Coking Vessel from the Top.



Figure 94. Close-up showing active heater coils in the kiln.

3.5 Continuous Coking of Centrifuge Tails

A Lucifer Tube Furnace was modified to permit continuous feeding of coal derivative centrifuge tails in order to produce coke. The centrifuge tails were produced by dissolving Kingwood Mine Lower Kittanning bituminous coal in hydrogenated (0.5% additional hydrogen) Koppers coal tar distillate, in a ratio of 1 part coal to 3 parts coal tar distillate.

The Lucifer Tube Furnace was converted to a continuous belt feed using an auger drive which slowly turns in order to pull chrome-plated boats containing coal derivatives at a constant rate. Because some of the components of the belt drive contain carbon steel, the temperature capability of the furnace in belt mode is reduced to about 600 °C, versus the normal furnace capability of 1350 °C. Figure 95 shows the general layout of the furnace. A forced air fume hood is placed above the furnace outlet to remove any vapors or gases that may be generated from the experiment. Prior to exhausting, the air is further scrubbed using a chilled condenser as well as activated carbon filter (not shown) to ensure that vapors and sulfur effluents are minimized.



Figure 95. Overview of modified Lucifer tube furnace outlet, showing fume hood, vapor condenser, vacuum pump and nitrogen gas delivery system.

Figure 96 shows a boat loaded with coke precursor. The boats are made from aluminum in order to reduce the tendency of coke to adhere to its surface. Chrome-plated steel is another alternative if high temperature is required. The boats have simple hooks so that they can be suspended from the rotating screw.



Figure 96. Chrome Plated Steel Boat Containing Coke Precursor.

Figure 97 shows the boat suspended from the rotating screw at the inlet of the reactor. The drive motor slowly rotates the screw, which causes the boat to move into the tube. Figure 98 shows a slightly different perspective, such that the screw is visible at the top of the inside of the loading section.



Figure 97. Furnace inlet, showing a loaded boat mounted under the rotating screw drive. The tube underneath the boat is a gas line. The screw itself is not visible in this photograph.

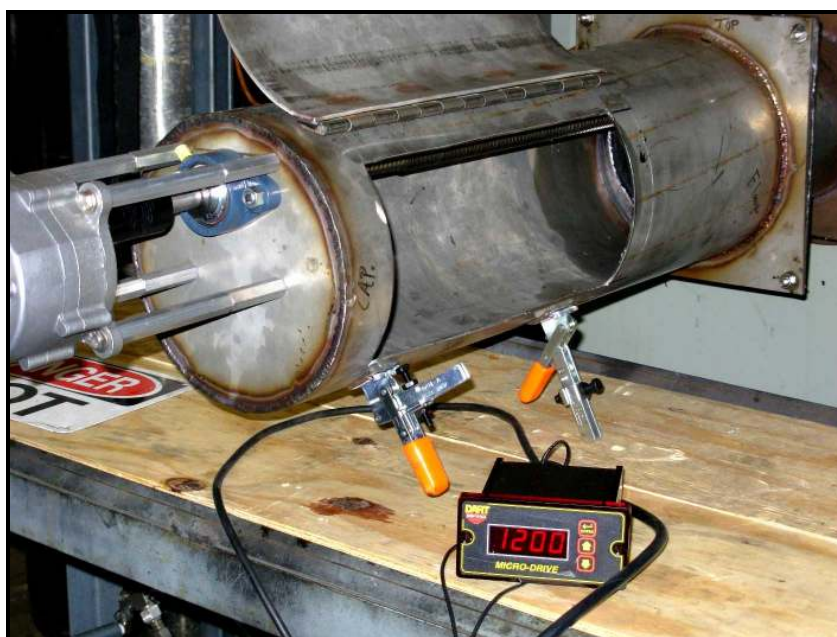


Figure 98. Furnace inlet, showing the screw drive at the tube of the tube.

Volatile vapors are trapped from the furnace effluent using a refrigerated loop with activated carbon, so that minimal quantities of organic vapors are released to the environment.

To process centrifuge tails, the furnace temperature was set at 450 °C. The central zone temperature of the furnace temperature varied during the run from 463C to 446C. The inert atmosphere was nitrogen, with a total flow set at 30 CFH. The drive speed was set at 40 inches per hour. The approximate size of the hot zone is 20 inches, so that the processing time was about 30 minutes.

The exhaust fan was used throughout the run to ensure that gases were continuously exhasuted.

Approximately 291 grams of the centrifuge tails were placed in an aluminum boat. Upon completion of the run, 119 grams of solid remained, indicating that (i.e. approx. 60% weight reduction). Proximate analysis is shown in Table 140.

The intent was to produce a volatile content of some 15%. Thus the results were very close to the goal despite this being a first attempt.

Subsequent tests verified that the ash composition met the requirements of the Dakota Gasification Company. At the time, FutureGen was intended to include gasification as part of the project, although later the power plant design was changed to an oxyfuel combustion system. Nevertheless, a successful result for the Dakota Gasification Company would suggest that requirements for other gasification projects would also be achievable.

Table 140. Coking Trials with Kingwood/Lower Kittanning Centrifuge Tails.

Sample	Moisture	Volatiles	Ash
Cent Tails neat	5.53	61.84	6.14
Cent Tails after coking	0.42	12.76	18.40

A scrubbing system was developed using two 55 gallon drums of activated carbon as well as a cold-trapping system (see Figure 99 and Figure 100). This system is estimated to be effective at containing at least 99% of the volatiles that are evolved.

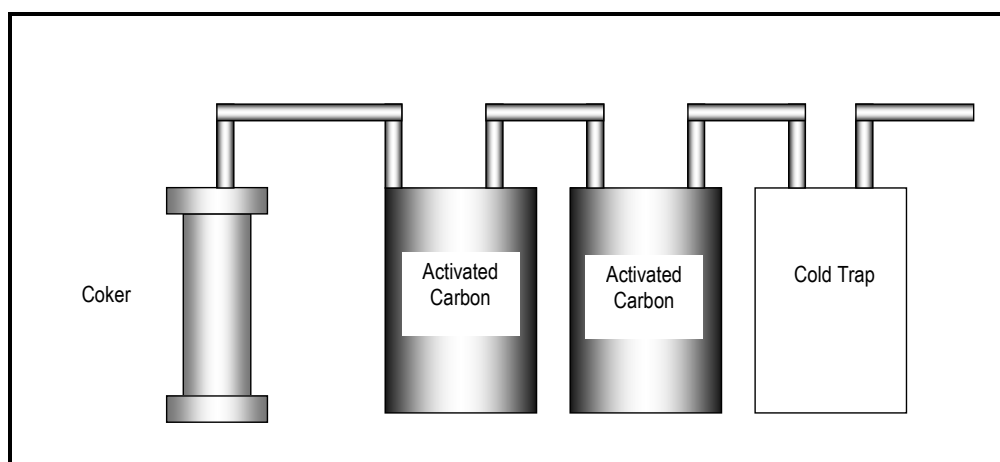


Figure 99. Delayed Coking System and Trap Arrangement.



Figure 100. Scrubbing System at Coker Outlet.

3.6 Needle Coke

In order to produce needle coke, batches of coal extract were produced from both Lower Kittanning (Kingwood Coal) as well as Powder River Basin sub-bituminous coals. Recovered distillate was used as a solvent. It was determined that the resultant solutions had a high softening temperature, making them difficult to process in a centrifuge.

As an alternate formulation, coal was extracted in a combination of coal tar distillate (CTD) with partially hydrogenated oil blends. Two blends were created. The first blend was composed of Lower Kittanning bituminous coal from the Kingwood Mine (KW), which was then dissolved in a blend of partially hydrogenated oil and Koppers CTD. The ratio was 1:1.5:1.5.

The second blend was composed of Lower Kittanning coal in a solution of hydrogenated oil (HO) and Koppers CTD. The ratio was 1 : 0.71 : 2.1.

The slurry was centrifuged in a Thermoelectron 7100 bucket-type centrifuge, resulting in 85% recovery of centrate in both cases.

Preliminary results show that the centrate behaved in SIMDIST as if it was nearly 100% volatile (See Figure 101 through Figure 104). This suggests that the coal was broken down much more effectively than in experiments that did not use hydrogenated oil. This is an extremely favorable result from the standpoint of creating liquid products such as fuels, but a very poor result from the standpoint of creating pitches and cokes. Paradoxically, however, proximate analysis shows that the volatile content is around 75%. Proximate analysis (Table 141 and Table 142) first considers the mass fraction that boils at 105 °C or below. This is referred to as “moisture” although in reality it could also consist of low boiling point hydrocarbons or oxygenates.

In theory, coke yield should be approximately equal to

$$m_c = 100\% * (m_v - m_a),$$

where m_c is the mass fraction of fixed (nonreactive) carbon, m_v is the mass fraction of volatiles,

and m_a is the mass fraction of ash. The mass fraction of ash is the value obtained after complete oxidation.

Thus, the proximate analysis in Table 141 suggests that a residue should be obtained after distillation, although this was not the case during SIMDIST, which showed that almost all of the material was distilled away with minimal residue.

Nevertheless, accepting this surprising result at face value, it implies that the concentration of partially hydrogenated oil needs to be reduced in order to increase the pitch yield.

This is consistent with results obtained via gas chromatography and SIMDIST (Table 143). It appears that the addition of coal results in shifting the curve to the right, as expected. However, there is very little yield of the very heavy molecules with boiling temperature greater than $\sim 450^\circ\text{C}$. Hence the pitch and coke yield appear to be small.

On the other hand, the shifting of the SIMDIST profile to the right is evidence that in fact coal digestion has occurred. Thus, to sum up it appears that hydrogenated oil reduced the pitch yield, and may have affected the sulfur level as well. More testing is needed to verify this, however.

Table 141. Proximate Analysis of PHO/CTD/KW Centrate.

Name	Moisture	Volatile	Ash	Fixed Carbon
PHO/CTD/KW centrate 1	15.85	73.93	0	26.07
PHO/CTD/KW centrate 2	14.31	75.23	0.01	24.76
PHO/CTD/KW centrate 3	12.49	76.98	0.03	22.99

Table 142. Proximate Analysis of PHO/CTD/KW Tails .

	Moisture	Volatile	Ash	Fixed Carbon
PHO/CTD/KW tails 1	12.54	59.78	2.32	37.9
PHO/CTD/KW tails 2	11.39	58.57	3.19	38.24
PHO/CTD/KW tails 3	10.9	61.54	2.26	36.2

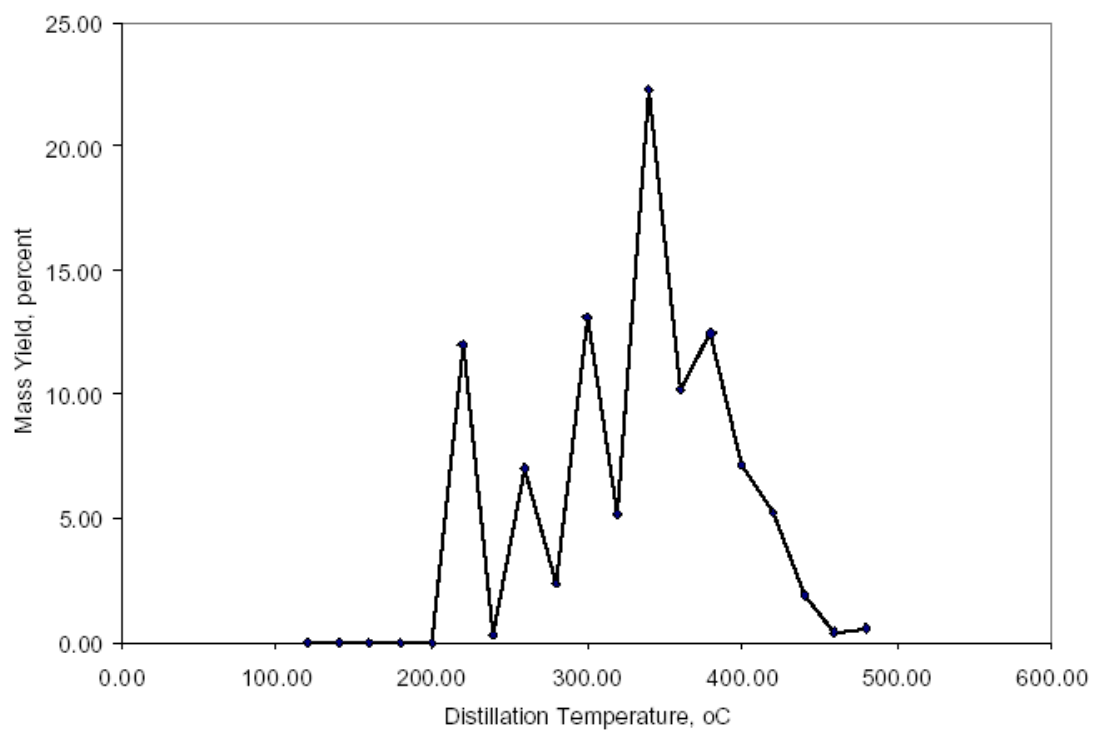


Figure 101. SIMDIST Incremental Yields for CCTD Solvent (no coal dissolved).

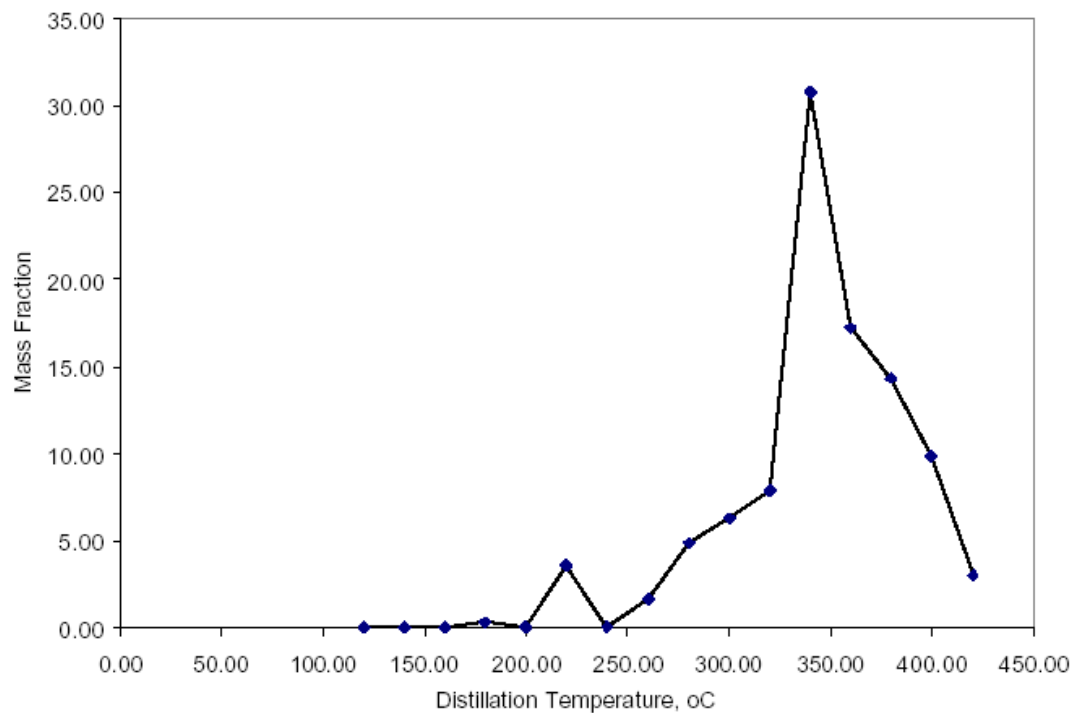


Figure 102. SIMDIST Incremental Yields for KW/PHO/CTD Centrate.

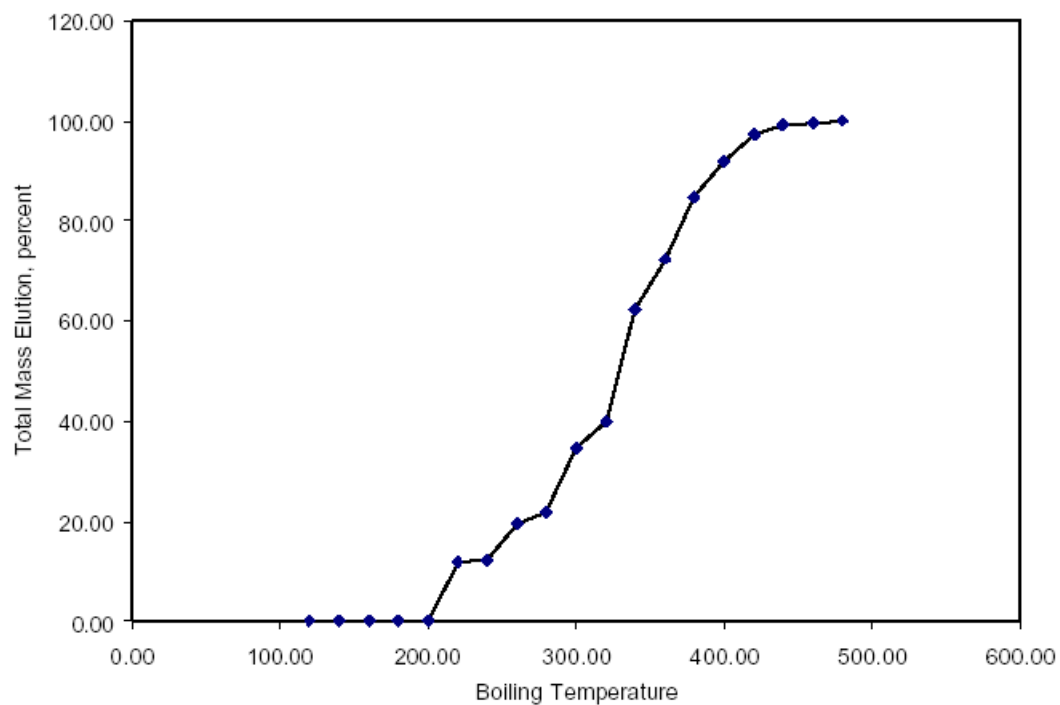


Figure 103. Simulated Distillation of Solvent (HO/CTD) by Gas Chromatograph (Koppers).

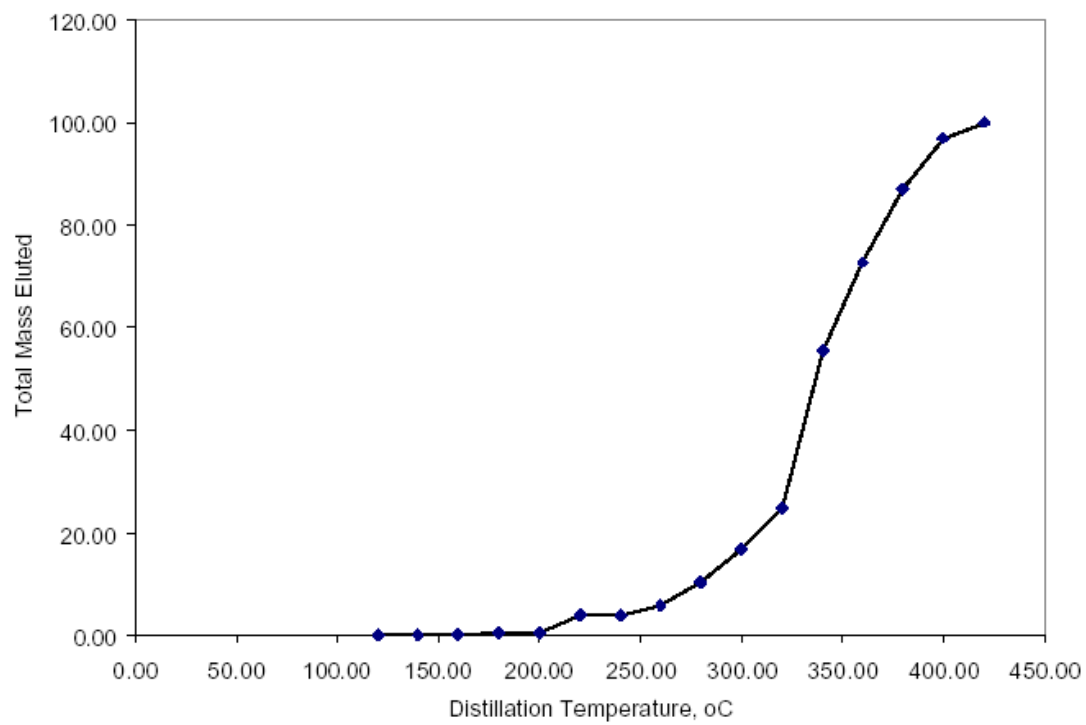


Figure 104. Simulated Distillation of KW/HO/CTD by Gas Chromatograph (Koppers).

Table 143. Gas Chromatograph Results from Kingwood/CCTD.

Boiling Pt		CCTD w/o Coal Wt. %	CCTDKW Centrate Wt. %
	Benzene	0	0
110.6	toluene	0.17	0.05
120	unided	0.63	0
136	ethylbenzene	0.27	0
139	m+p xylene	0	0
145	styrene	0	0
145	o xylene	0.65	0.1
161	3+4 ethyl toluene	0.5	0
165	1,3,5 trimethyl benzene	0	0
	benzonitrile	0	0
	phenol	0	0
168	1,2,4 trimethyl benzene	0	0
	2,3 benzofuran	0	0
	1,2,3 trimethyl benzene	0	0
	indan	0.39	0.115
177	indene	0.16	0.195
180		0	0
190	o cresol	0.18	0
201	m+ p cresol	0.47	0
	non-id	0	0
212	2,4 dimethyl phenol	0.19	0
218	Naphthalene	12.26	3.82
221	benzothiophene	0.33	0
	quinoline	0	0
242	isoquinoline	0	0
	methyl benzothiophene	0.37	0
	2methyl naphthalene	1.62	0.66
	methyl benzothiophene	0.37	0
	1methyl naphthalene	0.88	0.39
		0.46	0.175
256	Biphenyl	0.46	0.255
		1.09	0.415
270	Acenaphthylene	4.01	4.24
	Acenaphthene	2.28	0.525
		0.36	0.11
287	Dibenzofuran	2.2	2.04
		0	0.375
295	Fluorene	3.13	3.35
		1.92	7.575
332	dibenzothiophene	0.44	2.44
		5.5	2.08
	Phenanthrene	17.95	23.805
340	Anthracene	1.87	1.935
		0.45	1.42
	carbazole	0.92	1.17
		13.56	15.04
375	Fluoranthene	9.78	13.495
		0.88	0.745
404	Pvrene	7.36	9.865
		0	1.735
398	benzo(a)fluorene	1.27	0.74
399	benzo(b)fluorene	1.15	0.895
		2.23	0.135
425	Benz(a)anthracene	0.24	0.11
431	Chrysene	1.05	0
	triphenylene	0	0
480	Benzo(b)fluoranthene	0	0
	Benzo(i)fluoranthene	0	0
	Benzo(k)fluoranthene	0	0
> 480 °C		0	0
		100	100

3.7 Fuel Properties of Coal Liquids

3.7.1 Recovered Coal Solvent as Gasoline Additive

Recovered distillates from coal liquefaction were able to achieve high octane performance in synthetic gasoline blends with other fuels.

The distillates were obtained after a mild direct liquefaction process using Kingwood Coal in hydrogenated coal tar. The liquefied coal was distilled to create a binder pitch, resulting in recovered aromatic solvent from the distillation process.

These results are summarized in **Table 144** below. The octane measurements were made by Intertek-PARC, Harmarville PA.

Table 144. Summary of Octane Results.

Blend Composition	Research Octane Number	Motor Octane Number	(R+M)/2
95% Gasoline @ 87.3 Octane 5% coal liquids	93.9	100.6	97.2
90% ethanol 10% coal liquids	137	132.6	134.8

Table 145 (see below) shows the heavy metals present in a blend of 40% ethanol, 60% coal liquids, using Inductively Coupled Plasma (ICP) Spectroscopy performed at the National Research Center for Coal and Energy (NRCCE), Morgantown WV. The results show low levels of contaminants. For example, sulfur is only 1.8 ppm.

Table 145. ICP Heavy Metal Scan for a Blend of 40% Ethanol, 60% Coal Liquid.

Ag	Al	As	Au	B	Bi	Ca	Cd	Ce	Co
	mg/L	mg/L	uS/cm	mg/L	mg/L	mg/L	mg/L	mg/L	mg/L
07/05/06	07/05/06	07/05/06	07/05/06	07/05/06	07/05/06	07/05/06	07/05/06	07/05/06	07/05/06
ND	0.355	0.217	ND	0.005	ND	ND	ND	0.296	ND
Cr	Cu	Er	Fe	Gd	Ho	K	La	Li	Mg
	mg/L	mg/L	uS/cm	mg/L	mg/L	mg/L	mg/L	mg/L	mg/L
07/05/06	07/05/06	07/05/06	07/05/06	07/05/06	07/05/06	07/05/06	07/05/06	07/05/06	07/05/06
0.002	0.001	0.001	0.199	ND	0.001	0.153	ND	ND	ND
Mn	Mo	Na	Nd	Ni	P	Pb	Pd	Pr	Pt
	mg/L	mg/L	uS/cm	mg/L	mg/L	mg/L	mg/L	mg/L	mg/L
07/05/06	07/05/06	07/05/06	07/05/06	07/05/06	07/05/06	07/05/06	07/05/06	07/05/06	07/05/06
0.0.15	0.008	0.270	ND	0.001	ND	ND	0.014	0.574	ND
Rb	S	Sb	Sc	Se	Si	Sm	Sn	Sr	Ti
	mg/L	mg/L	uS/cm	mg/L	mg/L	mg/L	mg/L	mg/L	mg/L
07/05/06	07/05/06	07/05/06	07/05/06	07/05/06	07/05/06	07/05/06	07/05/06	07/05/06	07/05/06
2.037	1.84	0.005	ND	0.504	ND	0.035	0.285	ND	ND
Tl	Tm	V	W	Y	Yb	Zn	Zr		
	mg/L	mg/L	uS/cm	mg/L	mg/L	mg/L	mg/L		
07/05/06	07/05/06	07/05/06	07/05/06	07/05/06	07/05/06	07/05/06	07/05/06		
ND	ND	0.001	ND	ND	ND	0.086	ND		

Blending with ethanol is perceived to be potentially advantageous because the coal liquids are highly aromatic compared to conventional petroleum-derived gasoline. The aromatic liquids are likely to be more soluble in ethanol than in straight-chained aliphatic liquids such as gasoline. Moreover, ethanol has more rapid kinetics than the heavier coal liquids. Hence, coal

liquids blended with ethanol can potentially come closer to duplicating the properties of petroleum-derived gasoline.

Other key tests that need to be performed include tailpipe emissions, seal compatibility, cold flow characteristics, and others.

3.8 Testing of Lignite Pitch

Lignite samples were obtained from the Jewett mine, Texas with the assistance of the University of Texas at Arlington. The analysis of the samples was carried out in the present effort so that the two universities could leverage each others respective efforts. A petrographic examination was initiated by Koppers Inc to evaluate the suitability of this particular lignite as a source of pitch. The protocol for lignite conversion involved first liquefying the coal, followed by distillation at atmospheric pressure and inert (nitrogen) atmosphere in order to obtain a pitch residue.

3.8.1 Evaluation of Lignite

Five samples of Texas lignite and residual products were submitted for petrographic analysis. This is of interest because lignite was previously used for severe hydrogenation experiments as part of the Exxon Donor Solvent (EDS) process, and thus might naturally be considered to be part of a similar liquefaction effort emphasizing heavier products. Jewett TX had been a candidate FutureGen site until being downselected. Table 146 summarizes the samples that were created.

Table 146. Sample Description and Koppers Designators.

Koppers No.	Description
08-2718	Oil + Lignite After RXN 8-15-08
08-2719	Solids from RXN in Reactor
08-2720	Texas Lignite
08-2721	Lignite After RXN 8-14-08
08-2722	Coked Texas Lignite 600 C 8-4-08

The control sample is 08-2720, which is the lignite as received. Digestion was attempted using tetralin at about 400 psig and 400 °C. Following the digestion reaction, the liquids were decanted or distilled off.

The coal and residual samples were prepared for petrographic analysis and photographed at 135X and/or 250X in air and at 600X in reflected light in oil. The coal petrographic analysis for the lignite coal consists of maceral composition and vitrinite (huminites) reflectance. A total of 1000 points were counted for maceral composition and 100 particles of vitrinite (huminites) were measured for reflectance analysis. The petrographic analysis of the four reacted samples covers the composition of residue materials which consist of the altered materials which relate to the reactive macerals and the inert constituents. A total of 1000 points were counted for composition and each sample was photographed at 135X and/or 250X in air to show the particle

microstructure and at 600X in oil to illustrate specific macerals. In addition, 100 particles of Vitrinite like material were measured to determine the degree of thermal alteration or carbonization.

3.8.2 Petrography of Texas Lignite (Koppers# 08-2720)

The Texas coal is a lignite, based on moisture and rank (“huminite” reflectance), which on a dry basis is high in ash at 21.14% and has a moisture 28.77%. The petrographic composition of the Texas lignite coal sample is listed in **Error! Reference source not found.** and the vitrinite (huminite) reflectance distribution is listed in Table 148 and shown in Figure 105 through Figure 109. The precursor of vitrinite in lignite or brown coal stages are combined together petrographically in the ‘Huminite’ group since these macerals bear few resemblances to their later coalification products in bituminous coal. The huminite is divided into 3 maceral subgroups. The maceral names for coarse woody material (+50 μm) with closed cellular structure is called telinite while the woody material with open cellular structure is called textinite. The maceral subgroup name for telinite and textinite is humotelinite. The humic material identified as humocollinite appears as smooth structureless vitrinite like material which has become homogenized by geochemical gelification. The finer sized humic material that is most altered is called attrinite and the less altered humic fines are densinite. The maceral subgroup for densinite and attrinite is called humodetrinite which includes the attrital huminite that is mixed with liptinite and/or inertinite. The liptinite or higher hydrogen materials are subdivided into resinite, sporinite or reproductive spores and pollen and cutinite or leaf coating materials. The inertinite in coal is highest in fixed carbon and is commonly like charcoal in appearance when it is coarse (semifusinite and fusinite) but it is called micrinite, macrinite and inertodetrinite if it is fine (<50 microns) sized. The minerals or ash forming materials are generally clay, bone coal, shale, carbonates and pyrite. The huminite macerals are precursors to the vitrinite maceral group in bituminous coal. The humocollinite is the humic precursor to collinite, the humotelinite and humotextinite are the precursor to telinite or pseudovitrinite and the attrinite and densinite are the precursor to vitrodetrinite. In addition, some of the humotextinite may degrade into semifusinite.

The results show that the Texas lignite has a moderate amount of total reactives at 65.5% and is moderate to high in total inerts at 34.5%. Huminite is the most abundant reactive maceral at 57.2% and consists of 20.4% humocollinite, with 15.6% of humotelinite, 20.0% of densinite and only 1.2% of attrinite. The huminite (vitrinite) exhibits a small range of vitrinite types (V2 through V4). The mean-maximum huminite (vitrinite) reflectance in oil is 0.35% and the V-type distribution is listed in Table 148. There are two processes which occur in the transformation of the original plant material to vitrinite in the coalification process. They are referred to as humicification and gelification. Since the initial differences between plant remains are gradually reduced with increasing coalification, there are more huminite macerals in this lignite coal than vitrinite macerals. The combined exinite and resinite macerals are moderate in amount at 7.0%. The low reflecting huminite produces char with isotropic microtexture.

The percent conversion of dry, ash free coal to liquefaction products in hydrogenation depends largely on the type and rank of the coal concerned. It is generally believed that coals with the highest conversion yields contain the following properties; (A) vitrinite with reflectance less than 0.8%, (B) vitrinite plus exinite content greater than 60%, (C) volatile matter greater than 35% and (D) hydrogen to carbon atomic ratio (dry, ash free) greater than 0.75. In regard to

solvent extraction processes the reactive macerals (huminite and liptinite) should dissolve in coal tar oil at temperatures above 400°C while the mineral matter and organic inerts are reported as part of the residue.

The lignite plus oil sample has moderate amount of ash at 8.78% and has a moisture content of only 1.57%. The petrographic examination of residual solids from coal processing can greatly contribute to our understanding of the behavior of coal macerals in liquefaction or solvent processing. It is important to identify unaltered and altered coal and the degree to which the macerals are changed. In this discussion the reactive macerals (huminite and liptinite) that have low, intermediate and high degrees of alteration are identified as vitroplast.

The composition of the lignite plus oil sample is listed in Table 149 and the reactives (vitroplast) reflectance distribution is listed in Table 150 and shown in Figure 110 through Figure 114. The lignite plus oil sample has 73.4% by volume, of altered reactives or vitroplast which consists of 66.6% with an intermediate degree of altered vitroplast and 6.8% of highly altered vitroplast. The vitroplast occurs as a result of the reactive macerals huminite and liptinite softening and dissolving then solidifying into a gel like material that appears like vitrinite in bituminous coals. The vitroplast in the lignite plus oil sample after RXN has a mean maximum reflectance of 1.77% and the v-types range 0.90 to 2.49. In this study the vitroplast with reflectance over 2.00% should be considered highly altered and the oil plus lignite sample contains vitroplast with the highest degree of alteration in the current group of samples. There is 26.6 % of total inerts which consist of 2.0% coarse organic inerts (semifusinite and fusinite), with 7.8% of fine organic inerts (micrinite, macrinite and inertodetrinite) and 16.8% of inorganic inerts. The coarse organic inerts are particles over 50 microns in size while the fine organic inerts are less than 50 microns. There is a significant difference between the amount of inorganic inerts reported in the petrographic analysis (16.8% - by volume) and the amount reported in the proximate analysis (8.78% - by weight). In general, the amount by volume is usually about half the amount reported by weight.

3.8.2.1 WVU Sample of Reactor Solids Koppers# 08-2719

The composition of the extracted reactor solids from the RXN sample is listed in Table 149 and the reactives (huminite and vitroplast) reflectance distribution is listed in Table 150, with the corresponding photomicrographs shown in Figure 115 through **Error! Reference source not found.** The sample of extracted reactor solids from the RXN has moderate to low amount of ash at 5.60% and has a moisture content of only 1.10%. There is 65.6% of total reactives which consist of 14.0% of unaltered lignite and 51.6% of altered vitroplast. The unaltered lignite consists mostly of humodetrinite at 12.2%, with 1.6% of humocollinite and only 0.2% of exinite. The vitroplast consists of 21.0% slightly altered coal and 30.6% with an intermediate degree of alteration. The huminite and vitroplast in the sample of extracted reactor solids has a mean maximum reflectance of 0.50% and the v-types range 0.20 to 1.19%. This sample contains reactive macerals with the lowest degree of alteration in the current group of residual samples. However, many of the particles appear to be slightly altered even though the reflectance of the reactive materials stay the same or increase only slightly from the parent lignite. There is 34.4 % of total inerts which consist of 8.8% coarse organic inerts (semifusinite and fusinite), with 17.6% of fine organic inerts (micrinite, macrinite and inertodetrinite) and 8.0% of inorganic inerts. The coarse organic inerts are particles over 50 microns in size while

the fine organic inerts are less than 50 microns. As noted in the previous sample, there is a significant difference between the amount of inorganic inerts reported in the petrographic analysis (8.0% - by volume) and the amount reported in the proximate analysis 5.60% - by weight). In general, the amount by volume is usually about half the amount reported by weight.

3.8.2.2 WVU Sample of Lignite After RXN Koppers# 08-2721

The sample of lignite after RXN has a high amount of ash at 35.79% and has a moisture content of only 1.49%. The composition of the lignite after RXN is listed in Table 149 and the reactivities (vitroplast) reflectance distribution is listed in Table 150 and shown in Figure 119 through 122. The lignite after RXN sample has 59.4% by volume of altered reactivities or vitroplast which consists of 49.6% with an intermediate degree of altered coal or vitroplast, 5.0% of slightly altered coal and 2.8% of highly altered coal. It is difficult to determine if the altered coal is a result of the reactive macerals huminite and liptinite softening and dissolving then solidifying or if they occur due carbonization. The altered coal in the lignite after RXN has a mean maximum reflectance of 1.58% and the v-types range 0.60 to 2.29. In this study the altered coal with reflectance over 2.00% should be considered highly altered and the lignite after RXN has the second highest degree of alteration in the current group of samples. There is 40.6 % of total inerts which consist of 4.6% coarse organic inerts (semifusinite and fusinite), with 6.6% of fine organic inerts (micrinite, macrinite and inertodetrinite) and 29.4% of inorganic inerts. The coarse organic inerts are particles over 50 microns in size while the fine organic inerts are less than 50 microns.

3.8.2.3 WVU Sample of Coked Lignite 600° –Koppers# 08-2722

The sample of coked lignite has a high amount of ash at 33.83% and has a moisture content of 2.41%. The composition of the coked lignite is listed in Table 149 and shown in Figure 119 through Figure 122. The reactivities (huminite) reflectance distribution is listed in Table 150 and shown in Figure 123 through Figure 127. In general, coked material is used in reference to coking bituminous coals in which the vitrinite goes through a plastic transformation and re-solidifies to form anisotropic crystalline domains during carbonization while lignite and most sub bituminous coals do not have swelling or agglomerating properties and are referred to as char. In addition, the carbonization temperature for metallurgical coke is around 900 to 1000°C while the temperature for char is significantly less since the charring process is meant to drive off excess moisture and volatiles. The coked lignite has 59.2% by volume of altered reactivities or vitroplast which consists of 54.0% with an intermediate degree of altered coal or vitroplast, with 2.2% of slightly altered coal, 1.6% of highly altered coal and 0.2% of unaltered humodetrinite. It is difficult to determine if the altered coal is a result of the reactive macerals huminite and liptinite softening and dissolving then solidifying or if they occur due carbonization (thermal alteration). The altered coal in the coke lignite has a mean maximum reflectance of 1.40% and the v-types range 0.60 to 1.89. The reflectance measurements indicate a wide difference in the degree of carbonization which range from unaltered coal to highly altered char, as shown in Figures 20 through 23. There is 40.8 % of total inerts which consist of 6.0% coarse

organic inerts (semifusinite and fusinite), with 10.6% of fine organic inerts (micrinite, macrinite and inertodetrinite) and 24.2% of inorganic inerts.

3.8.2.4 Data Summary for Lignite

Data for Jewett Texas lignite are shown in **Error! Reference source not found.** Based on known solubilities, a total of 65 weight percent is believed to be reactive and soluble. Fusinite, semi fusinite and micrinites are charcoal-like materials that are normally insoluble, although in principle these might reactively bond with hydrocarbons and thus become soluble. Moreover, these materials contain chemical enthalpy and could be useful if incorporated in a final product, especially a coke precursor. These materials were estimated at 15.5%. Other mineral matter is estimated at 34.5%. Total solids, then, are estimated at about 50.0%.

Using centrifugation, a liquid phase cannot be realized due to entrainment limitations with the solids. In the case of bituminous coal the amount of mineral matter in retentate (tails) is about 20%, using the Spinner-II type centrifuge. More powerful units might result in doubling that amount, which might yield a liquid fraction of a few weight percent.

Thus, with the current laboratory state of the art, a liquid phase is not expected. Cleaning of the lignite could be accomplished with state of the art wash plants. Hence it is recommended that lignite be supplied to a cleaning facility in order to remove ash to less than 10% of the total dry mass. Unfortunately, the wash plant facility can not clean just a small amount of coal, but must use 2-3 tons of material in order to produce a clean batch.

As an alternative route, thermocracking (i.e. pyrolyzing the material, often under conditions that mimic those found in a typical delayed coker) can be used to devolatilize the dissolved coal and to recover the solvent. The product yield is likely to be a function of processing conditions and thermocracking temperature and time. However, from a mass standpoint, it is not clear whether more product is liberated if the lignite is solubilized before thermal cracking. That is, the expectation is that liquid yield is not higher than about 65% by mass, assuming that dealkylation is avoided. This is true whether or not the material is reacted with a solvent prior to the thermocracking procedure.

The sample matrix is summarized in Table 151. Supporting Elemental Analysis and Proximate Analysis is contained in Table 152 through Table 163. Fourier Transform InfraRed (FTIR) data is shown in Figure 128 through Figure 133.

Table 147. Petrographic Maceral Composition of Jewett TX Lignite Sample.

Koppers No.	08-2720
Date	10-31-2008
Description	<u>Texas Lignite</u>
<u>Reactives</u>	
Huminite (vitrinite) Macerals:	
Humocollinite	20.4
Humotelinite	15.6
<u>Humodetrinite:</u>	
Densinite	20.0
Attrinite	1.2
Exinite - sporinite = 5.4 - cutinite = 0.6	6.0
Resinite – normal = 0.2 terpene = 0.8	1.0
Semifusinite	<u>1.3</u>
Total Reactives	65.5
<u>Inerts</u>	
Semifusinite	2.5
Micrinite - micrinite = 2.4 - macrinite = 0.6 - inertinite = 5.4	8.4
Fusinite	4.6
Mineral Matter:	
- clay 6.2	
- shale 3.2	
- carb. shale 3.6	
- quartz 1.4	
- carbonate 0.8	
- pyrite 0.4	
- bone coal 2.8	<u>19.0</u>
Total Inerts	34.5
Mean-Max. Ro in Oil, %	0.35

Table 148. Vitrinite Reflectance Distribution of Jewett TX Lignite.

Koppers No.	08-2720
Date	10-31-2008
Description	Texas Lignite
Vitrinite Reflectance	
0.20	---
0.21	---
0.22	2.0
0.23	---
0.24	---
0.25	2.0
0.26	---
0.27	---
0.28	4.0
0.9	4.0
Total V-type 2	12.0
0.30	2.0
0.31	---
0.32	4.0
0.33	14.0
0.34	14.0
0.35	8.0
0.36	18.0
0.37	4.0
0.38	10.0
0.39	6.0
Total V-type 3	80.0
0.40	---
0.41	4.0
0.42	2.0
0.43	---
0.44	2.0
0.45	---
0.46	---
0.47	---
0.48	---
0.49	---
Total V-type 4	8.0
Mean-Max. Ro in Oil, %	0.35

Table 149. Petrographic Composition of Texas Lignite After Reaction for WVU.

Koppers No. Date of Analysis	08-2718 10-31-2008	08-2719 10-31-2008	08-2721 10-31-2008	08-2722 10-31-2008
Description	After RXN 8-15-08	From RXN (extracted solids) Reactor Solids	After RXN 8-14-08	600°C 8-4-08
	Oil Lignite		Lignite	Coked Lignite
Reactives				
Unaltered Huminite (vitrinite)				
Humocollinite	---	1.6	---	---
Humotelinite	---	---	---	---
Humodetrinite:	---	12.2	1.6	0.2
Vitroplast :				
Slight degree of Alteration	---	21.0	5.0	2.2
Altered	66.6	30.6	49.6	54.0
High degree of Alteration	6.8	---	2.8	1.6
Exinite	---	0.2	0.4	0.6
Resinite	---	---	---	0.6
Total Vitroplast & Reactives	73.4	65.6	59.4	59.2
Inerts				
Semifusinite	1.4	5.0	3.2	5.0
Micrinite - micrinite	(0.6)	(2.2)	(0.2)	(0.6)
- macrinite	(1.2)	(1.0)	(1.0)	(1.0)
- inertinite	(6.0) 7.8	(14.4) 17.6	(5.4) 6.6	(9.0) 10.6
Fusinite	0.6	3.8	1.4	1.0
Mineral Matter:				
Clay	9.0	1.2	7.4	9.8
Shale	---	1.2	4.6	4.6
Carb. Shale	---	2.8	7.0	5.4
Quartz	3.8	2.8	5.2	1.2
Carbonate	---	---	---	0.2
Pyrite	0.2	---	0.4	1.0
Bone Coal	3.8	---	4.8	2.0
Total Inerts	26.6	34.4	40.6	40.8
Mean-Max. Ro in Oil, %	1.77	0.50	1.58	1.40

Table 150. Vitrinite Reflectance Distribution of Four Residual Products from Texas Lignite.

<i>Koppers No.</i>	08-2718	08-2719	08-2721	08-2722
<i>Date Description</i>	10-31-2008 After RXN 8-15-08 Oil Lignite	10-31-2008 From RXN (extracted solids) Reactor Solids	10-31-2008 After RXN 8-14-08 Lignite	10-31-2008 600°C 8-4-08 Coked Lignite
<i>Vitrinite (V-Type) Reflectance</i>				
0.10 to 0.19	---	---	---	---
0.20 to 0.29	---	12.0	---	---
0.30 to 0.39	---	30.0	---	---
0.40 to 0.49	---	22.0	---	---
0.50 to 0.59	---	12.0	---	---
0.60 to 0.69	---	8.0	2.0	2.0
0.70 to 0.79	---	4.0	---	2.0
0.80 to 0.89	---	4.0	2.0	---
0.90 to 0.99	2.0	4.0	---	2.0
1.00 to 1.09	---	2.0	6.0	8.0
1.10 to 1.19	2.0	2.0	4.0	8.0
1.20 to 1.29	---	---	6.0	6.0
1.30 to 1.39	2.0	---	6.0	14.0
1.40 to 1.49	10.0	---	12.0	16.0
1.50 to 1.59	16.0	---	16.0	20.0
1.60 to 1.69	6.0	---	14.0	12.0
1.70 to 1.79	12.0	---	10.0	8.0
1.80 to 1.89	14.0	---	2.0	2.0
1.90 to 1.99	20.0	---	6.0	---
2.00 to 2.09	8.0	---	4.0	---
2.10 to 2.19	2.0	---	8.0	---
2.20 to 2.29	2.0	---	2.0	---
2.30 to 2.39	2.0	---	---	---
2.40 to 2.49	2.0	---	---	---
2.50 to 2.59	---	---	---	---
2.60 to 2.69	---	---	---	---
2.70 to 2.79	---	---	---	---
2.80 to 2.89	---	---	---	---
2.90 to 2.99	---	---	---	---
Mean-Max. Ro in Oil, %	1.77	0.50	1.58	1.40

Table 151. Sample Matrix for Koppers using Texas Lignite samples.

Texas Lignite Sample ID	Petrographic examination	SIMDIST	GC-MS	
Oil + Lignite after reaction (Aug 06 2008)	TBD			
Lignite + C10H12 after reaction (Aug 28 2008)	X			
Coked Texas Lignite	X			
Solution in Flask #4 500-600 C (aug 15 2008)		X	X	
Solution from Flask #1 + 2 (Aug 28 2008)		X	X	
Lignite after reaction (Aug 14, 2008)	X			
Condensed Vapor in Small tube (aug 14, 2008)		X	X	
Liquid in Flask (aug 01 2008)		X	X	
Solution in Flask #3 (Aug 28. 2008)		X	X	
Liquid from Flask #1 (Aug 08 2008)		X	X	
Solid from Reaction in Reactor, (Aug 08, 2008)	TBD			
Texas Lignite (Aug 04, 2008)	X			
Oil from flask #2 (Aug 08, 2008)		X	X	
Resi H in Flask #1 (aug 06, 2008)		X	X	

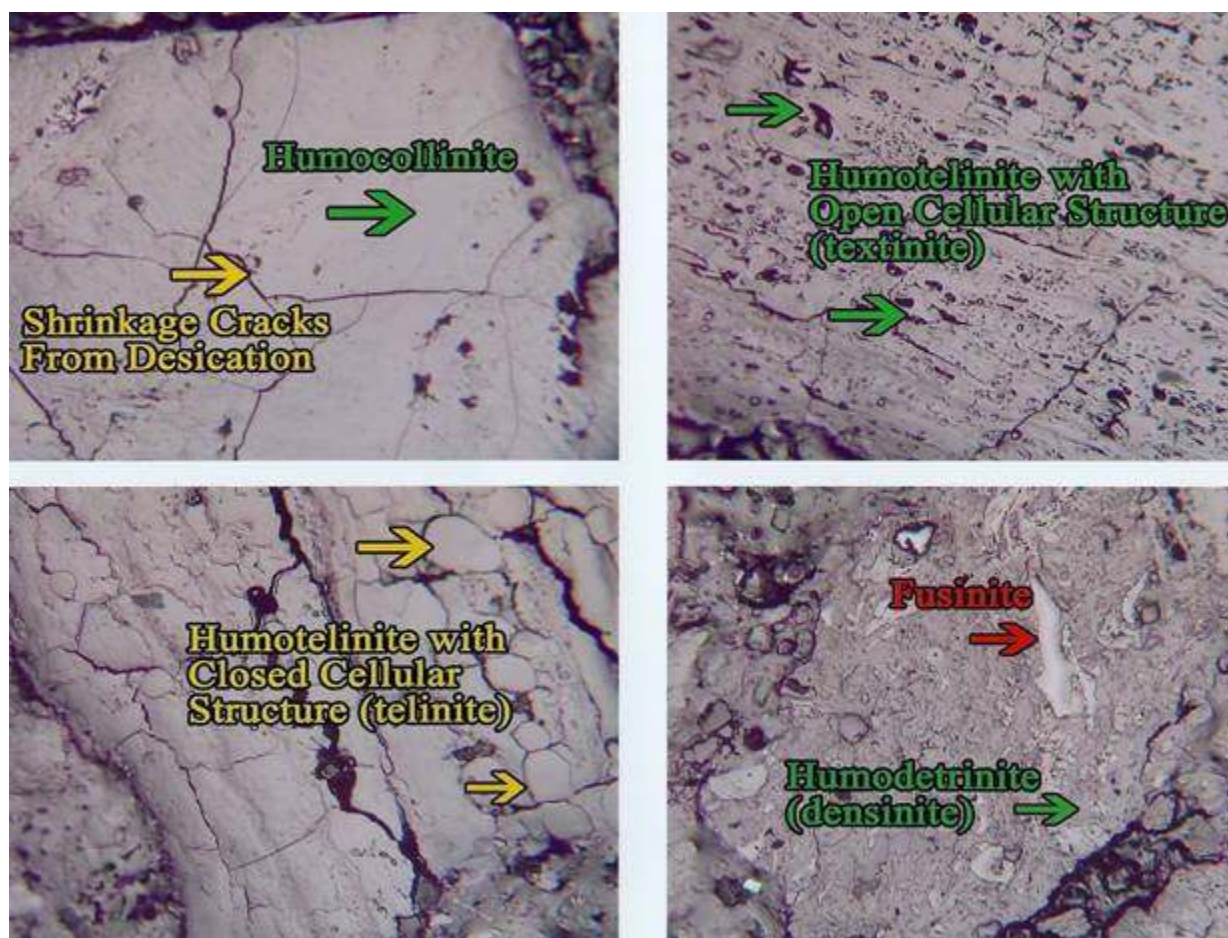


Figure 105. Photomicrographs of Texas Lignite showing: humocollinite, humotelinite with closed cellular structures, humotextinite with open cellular structure, humodensinite (attrial vitrinite), fusinite and shrinkage cracks from desiccation. Reflected light in Air, X250.

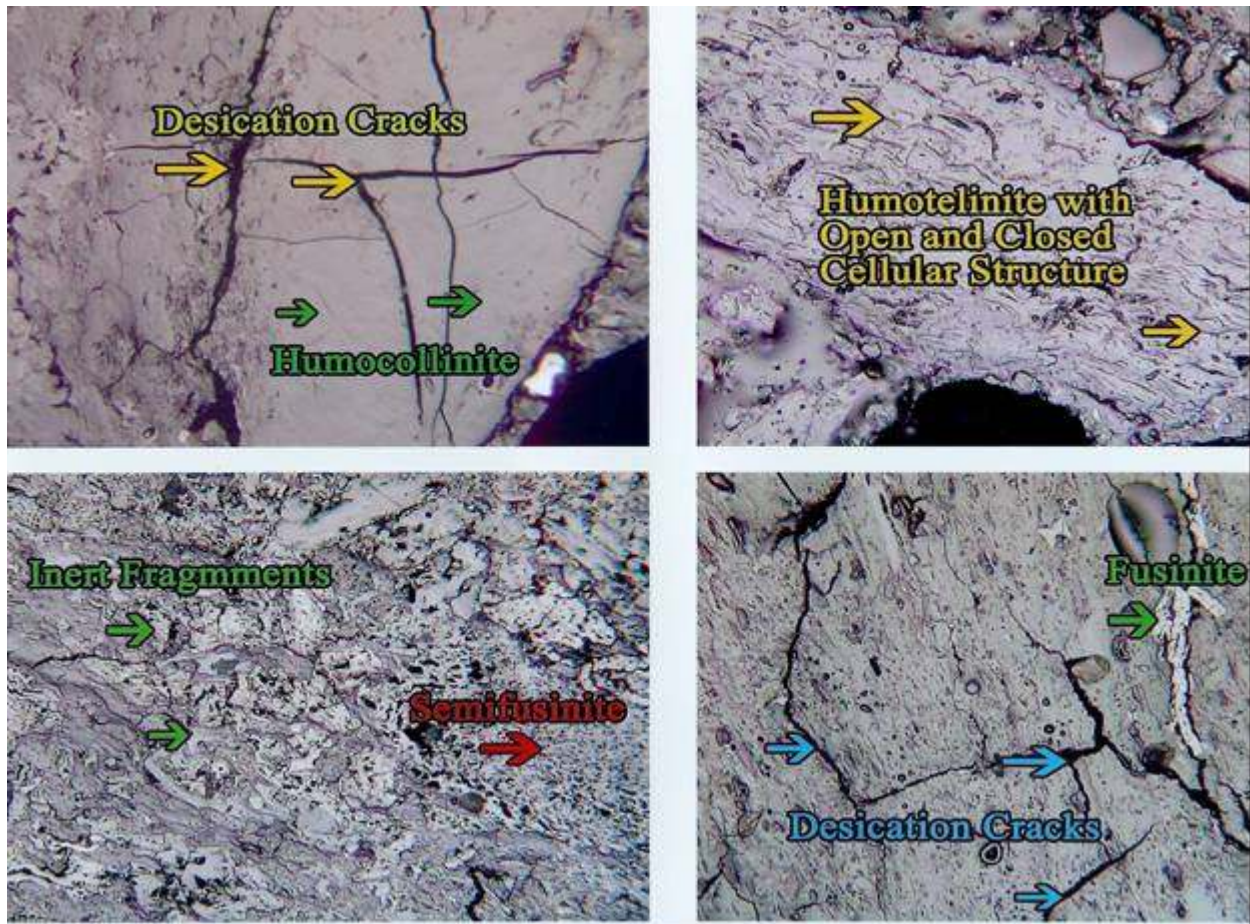


Figure 106. Photomicrographs of Texas Lignite showing: humocollinite, humotelinite with open and closed cellular structures, humotextinite with open cellular structure, humodensinite (attrital vitrinite), semifusinite fusinite and shrinkage cracks from desiccation. Reflected light in Air, X250.

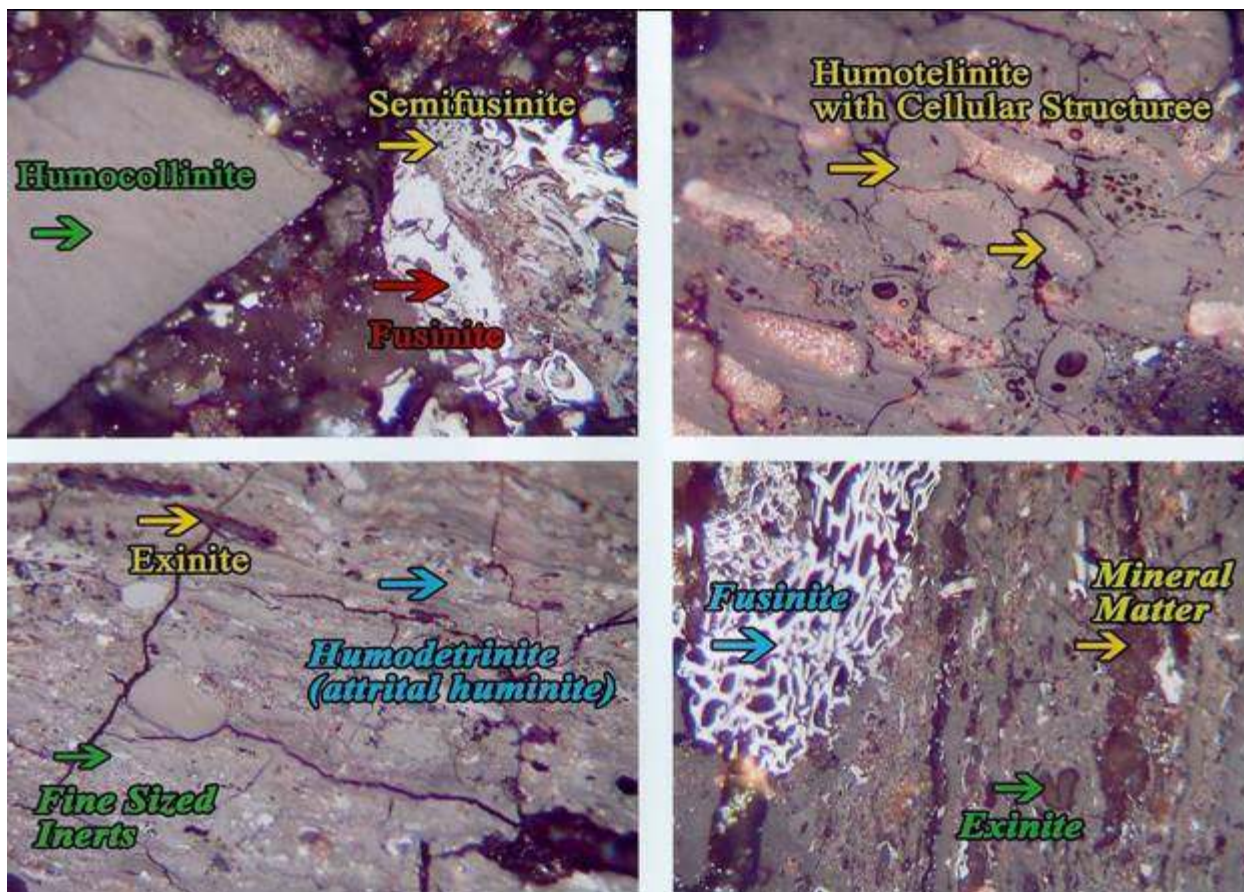


Figure 107. Photomicrographs of Texas Lignite showing: humocollinite, humotelinite with cellular structures, humodetrinite (attrital huminite) exinite, semifusinite, fusinite, fine sized inerts and mineral matter. Reflected light in Oil, X600.

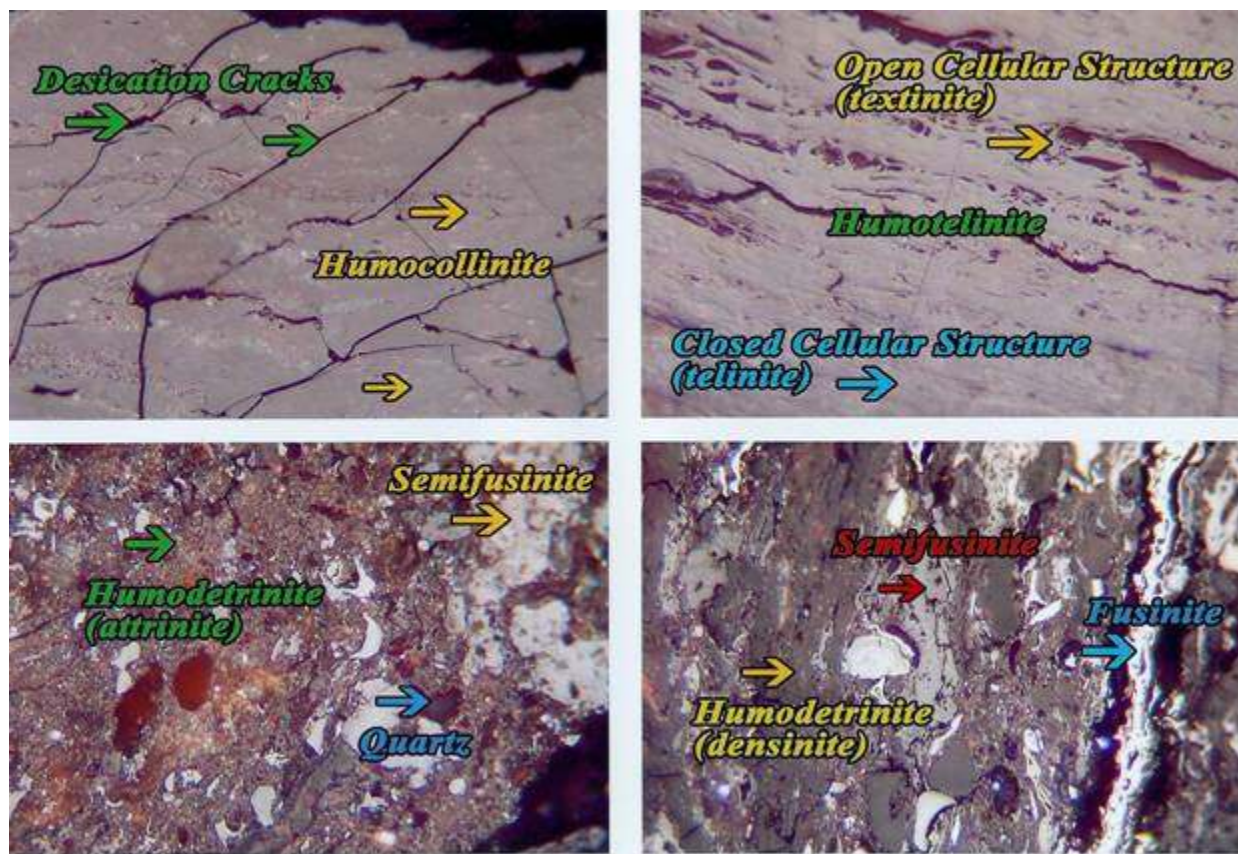


Figure 108. Photomicrographs of Texas Lignite showing: humocollinite, humotelinite with open and closed cellular structures, humodetrinite (attrital huminite) exinite, semifusinite, fusinite, fine sized inerts and mineral matter. Reflected light in Oil, X600.

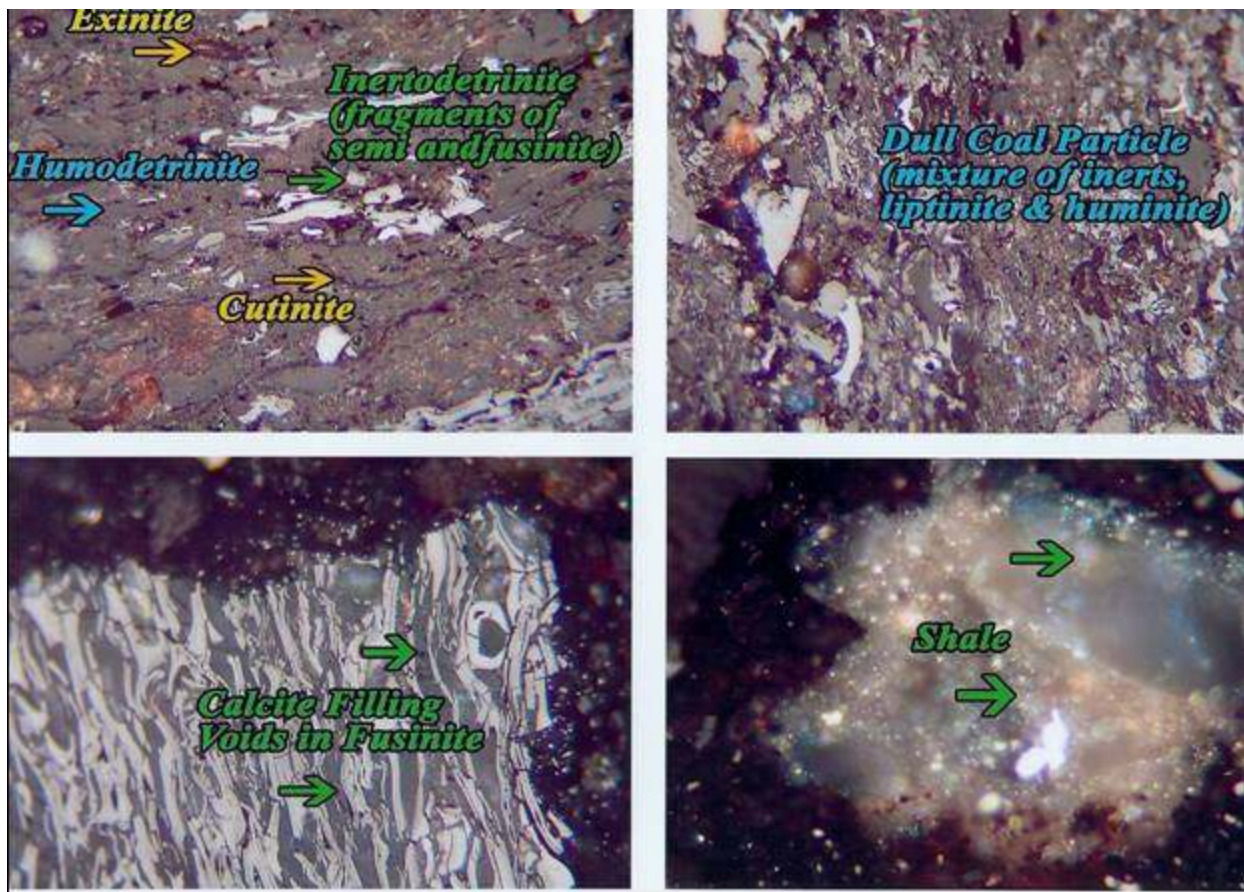


Figure 109. Photomicrographs of Texas Lignite showing: humodetrinite (attrital huminite) exinite, semifusinite, fusinite, fine sized inerts and mineral matter. Reflected light in Oil, X600.

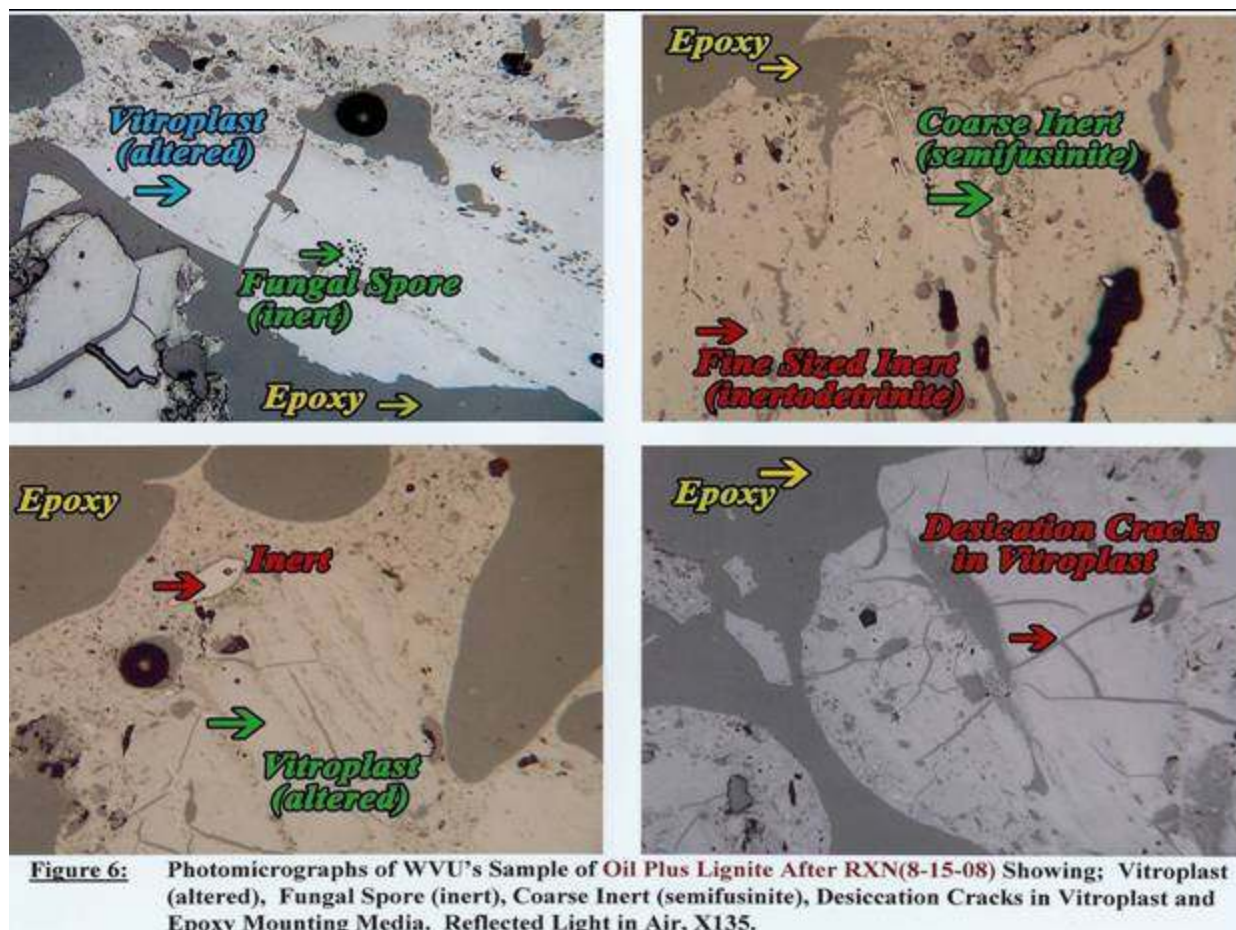


Figure 110. Photomicrographs of Oil Plus Lignite After Reaction (8-15-08) showing: vitroplast (altered), fungal spore (inert), humodetrinite (attrital huminite) exinite, semifusinite, fusinite, fine sized inerts and mineral matter. Reflected light in Oil, X600.

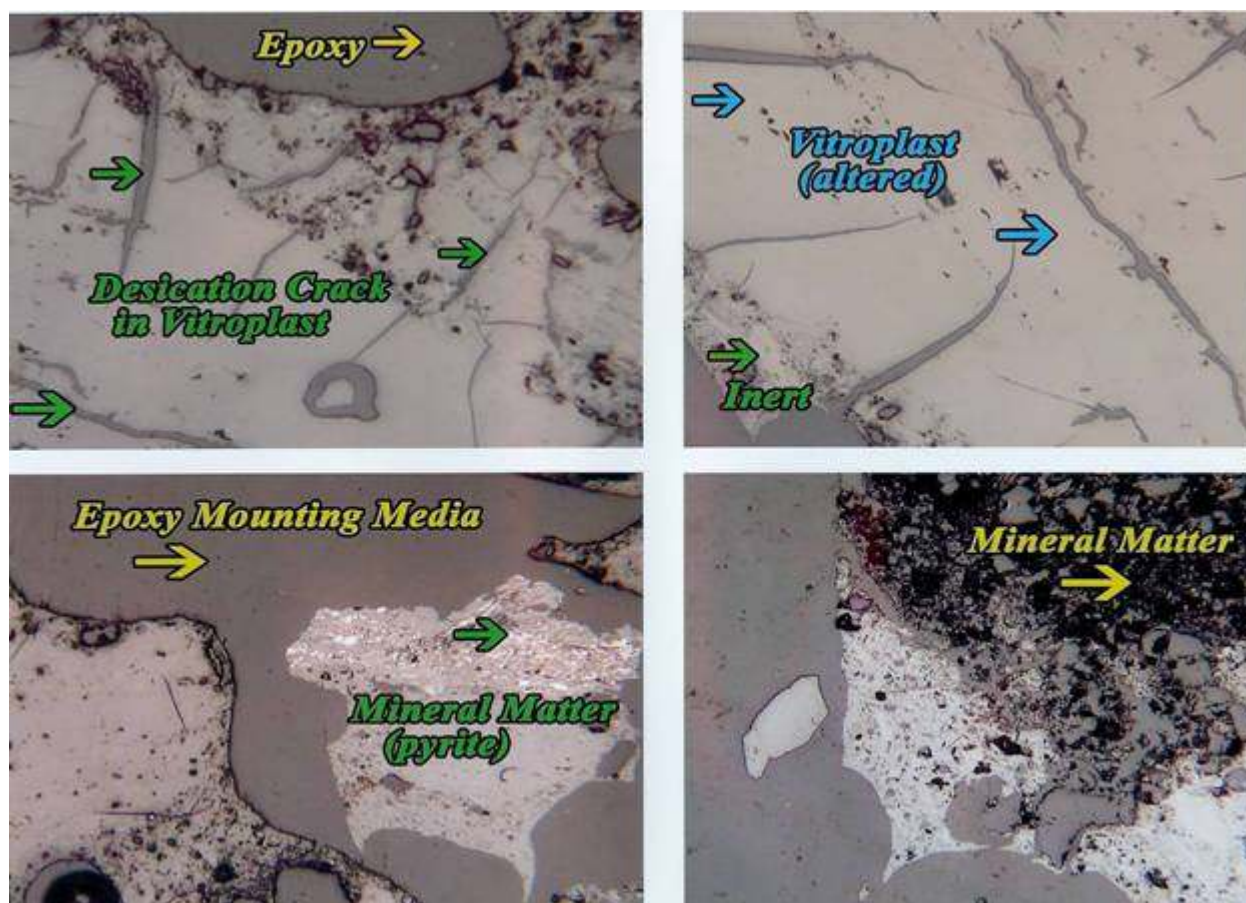


Figure 111. Photomicrographs of Oil Plus Lignite After Reaction (8-15-08) showing: vitroplast (altered), inert, desiccation cracks in vitroplast; mineral matter, pyrite and epoxy mounting media. X250.

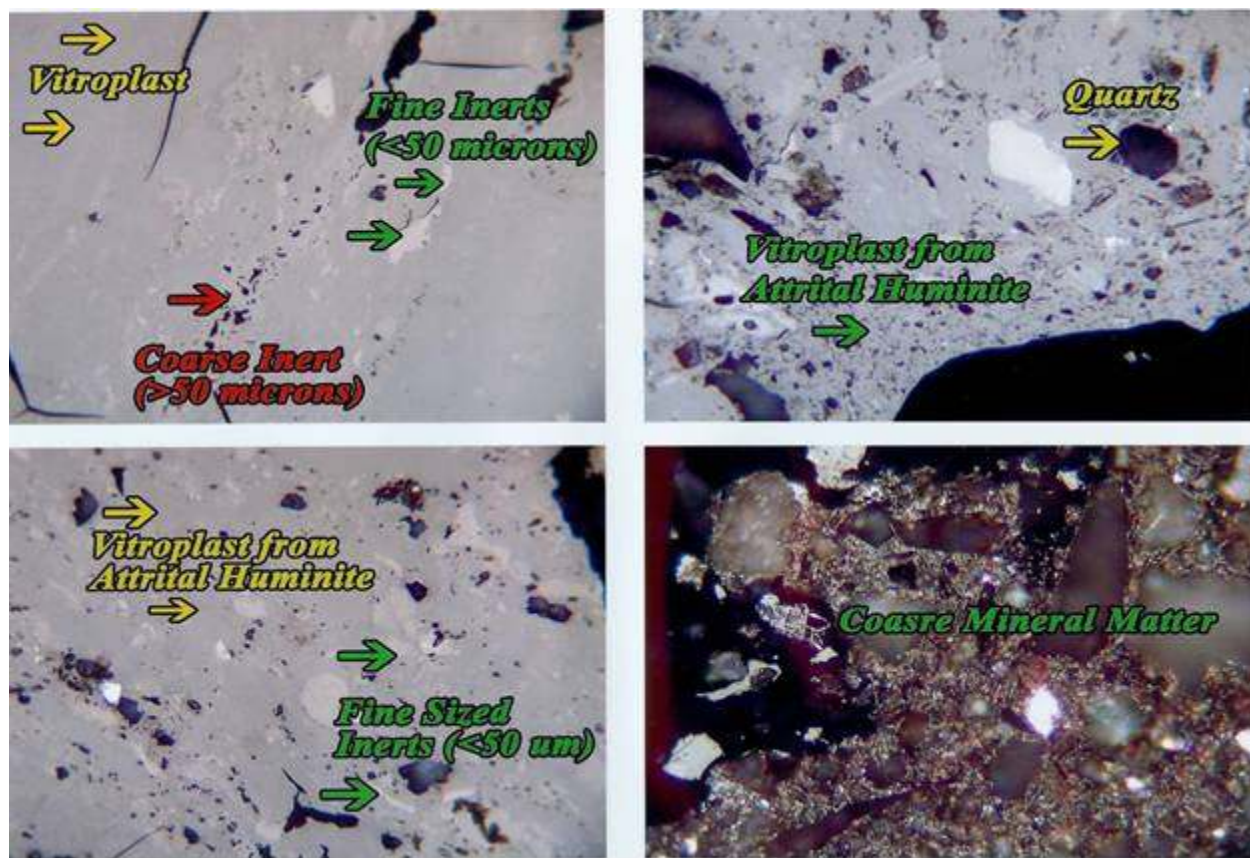


Figure 112. Photomicrographs of Oil Plus Lignite After Reaction (8-15-08) showing: vitroplast (altered), coarse inert (>50 microns), fine sized inerts (<50 microns), quartz and coarse mineral matter. Reflected light in Oil, X600.

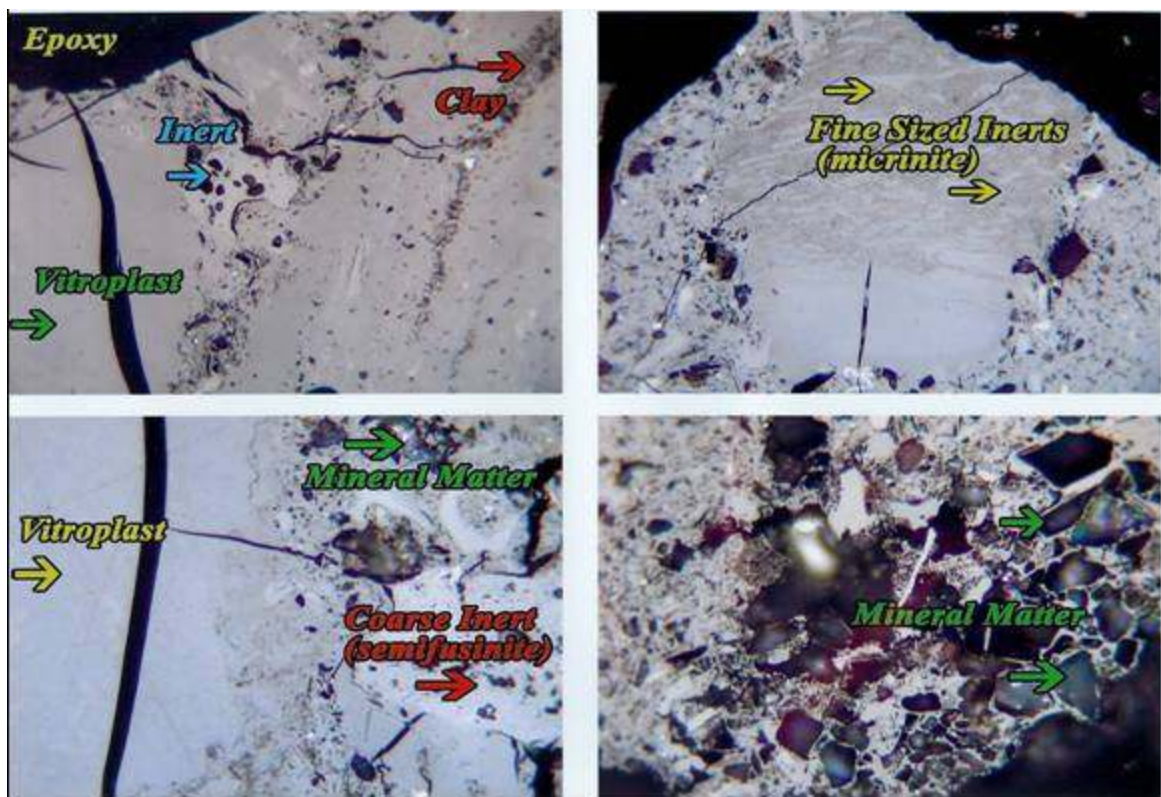


Figure 113. Photomicrographs of Oil Plus Lignite After Reaction (8-15-08) showing: vitroplast (altered), coarse inert (semifusinite), fine sized inerts (<50 microns), clay, mineral matter and epoxy mounting material. Reflected Light in Oil, X600.

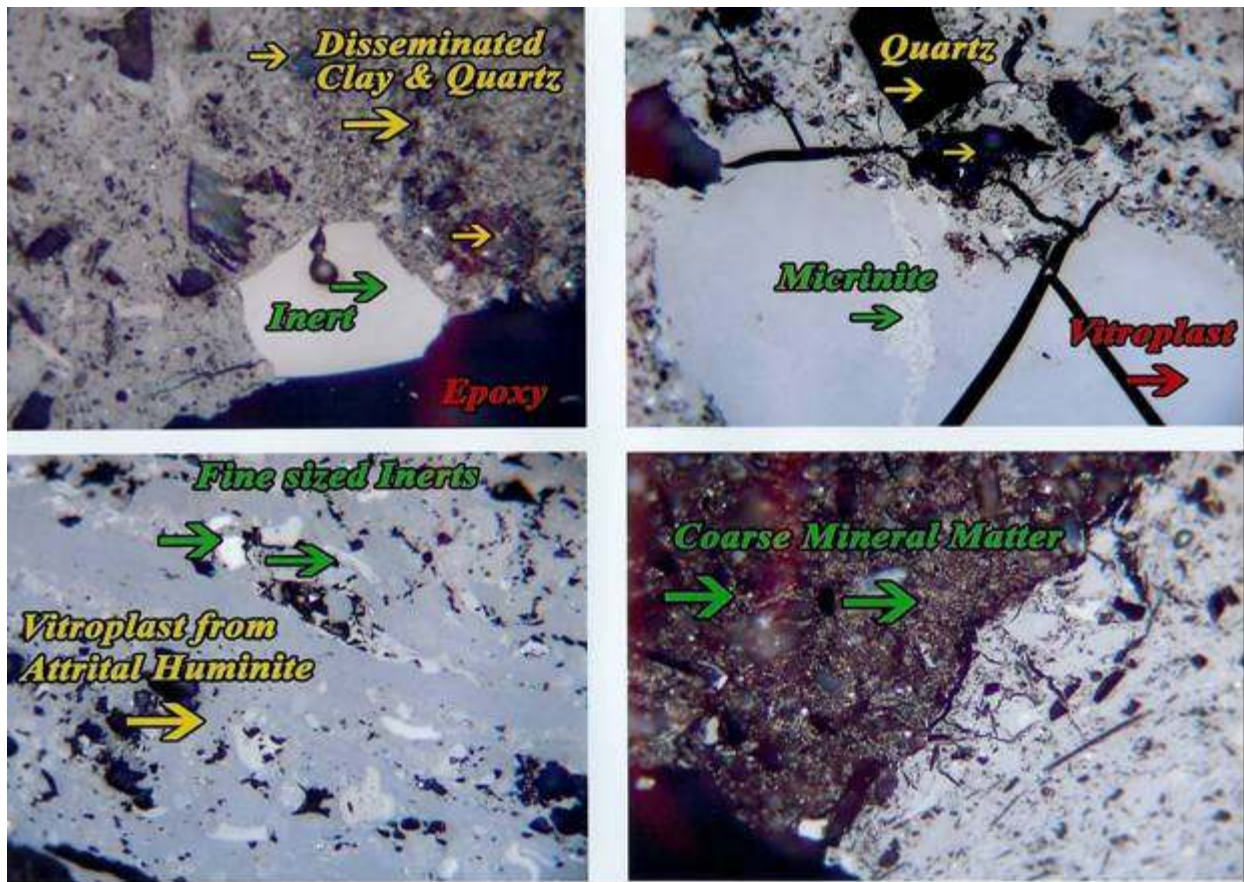


Figure 114. Photomicrographs of Oil Plus Lignite After Reaction (8-15-08) showing: vitroplast (altered), inerts, fine sized inerts (<50 microns), disseminated clay and quartz. Reflected light in Oil, X600.

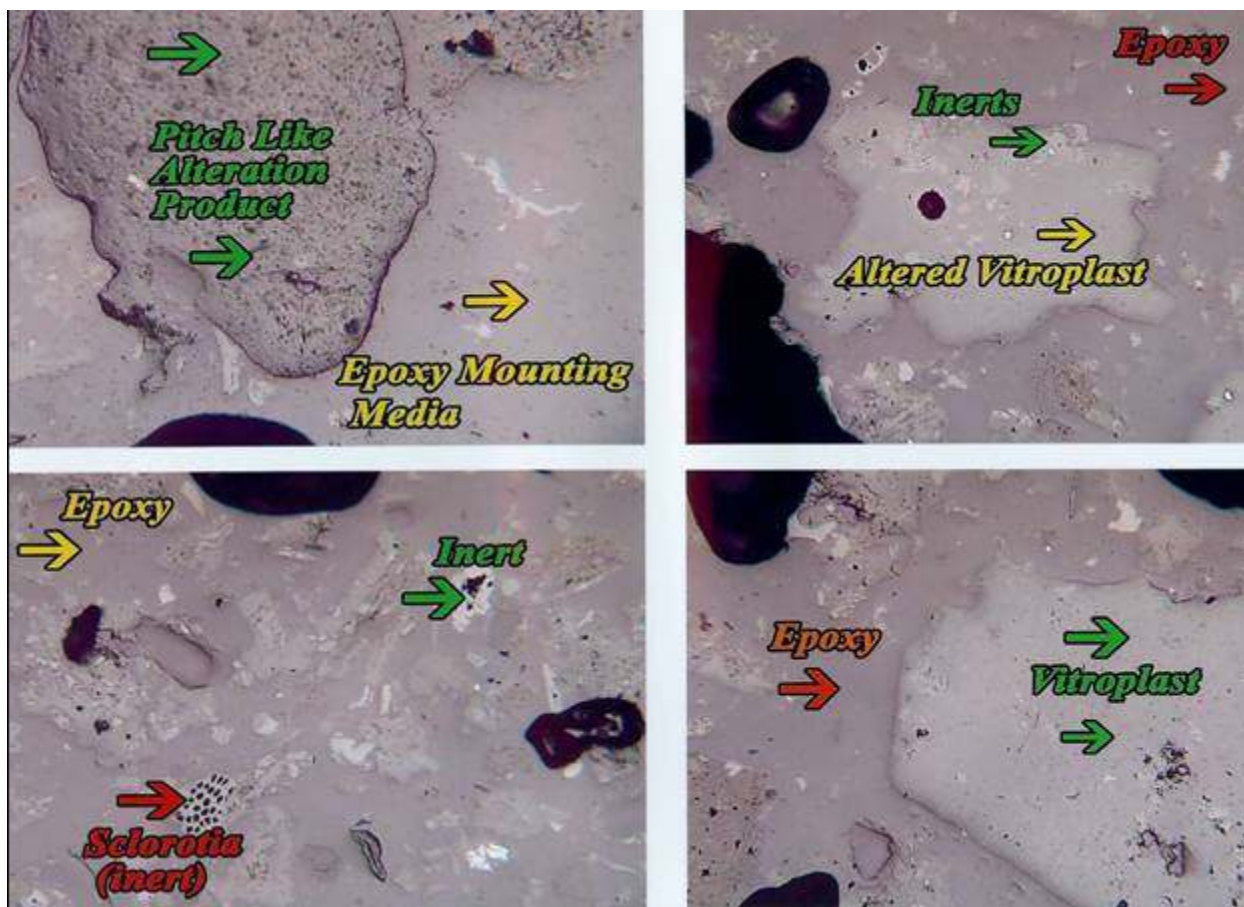


Figure 115. Photomicrographs of solid from reactor after reaction (extracted) showing: vitropplast (altered), pitch like alteration product, inert, sclerotia (inert) and epoxy mounting media. Reflected light in Oil, X135.

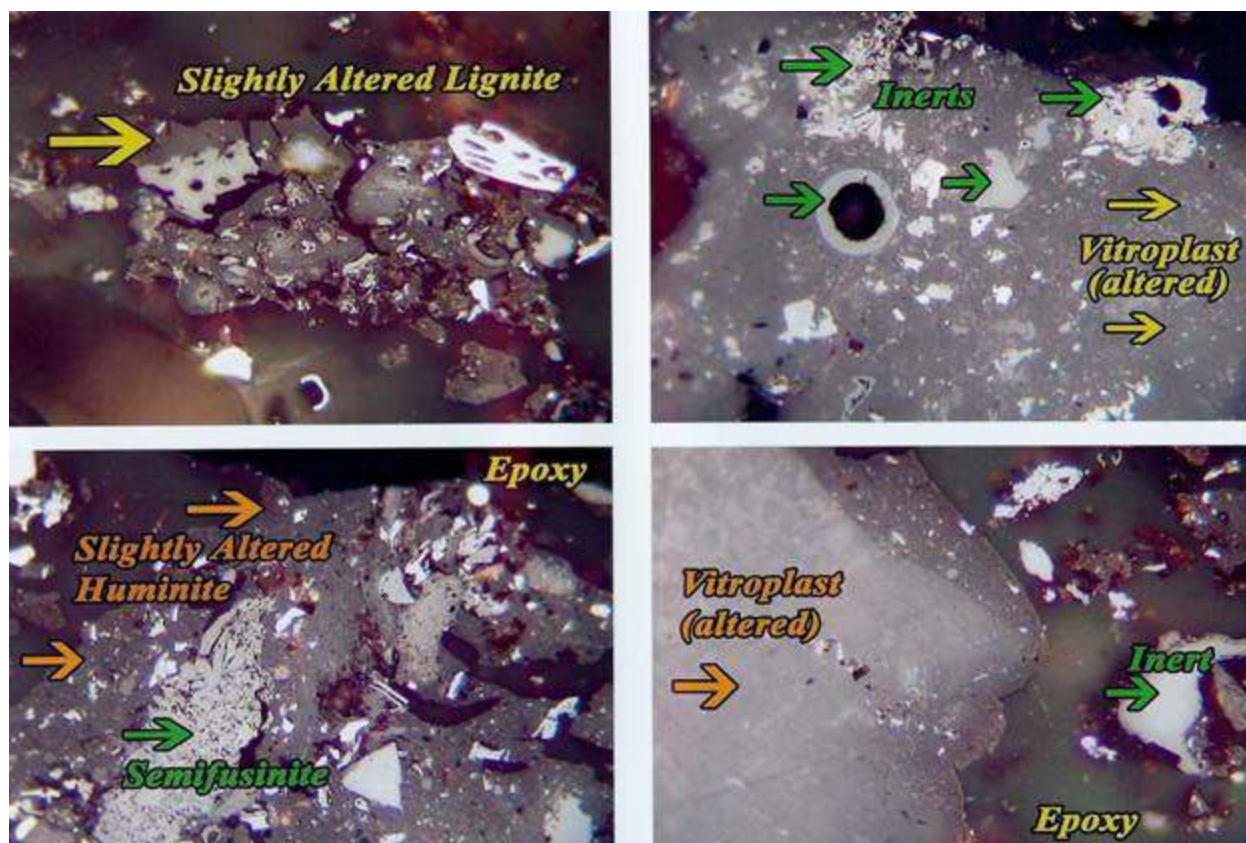


Figure 116. Photomicrographs of solid from reactor after reaction (extracted) showing: slightly altered lignite (huminite), vitroplast (altered), inert, semifusinite, fungal spore and epoxy mounting media. Reflected light in Oil, X600.

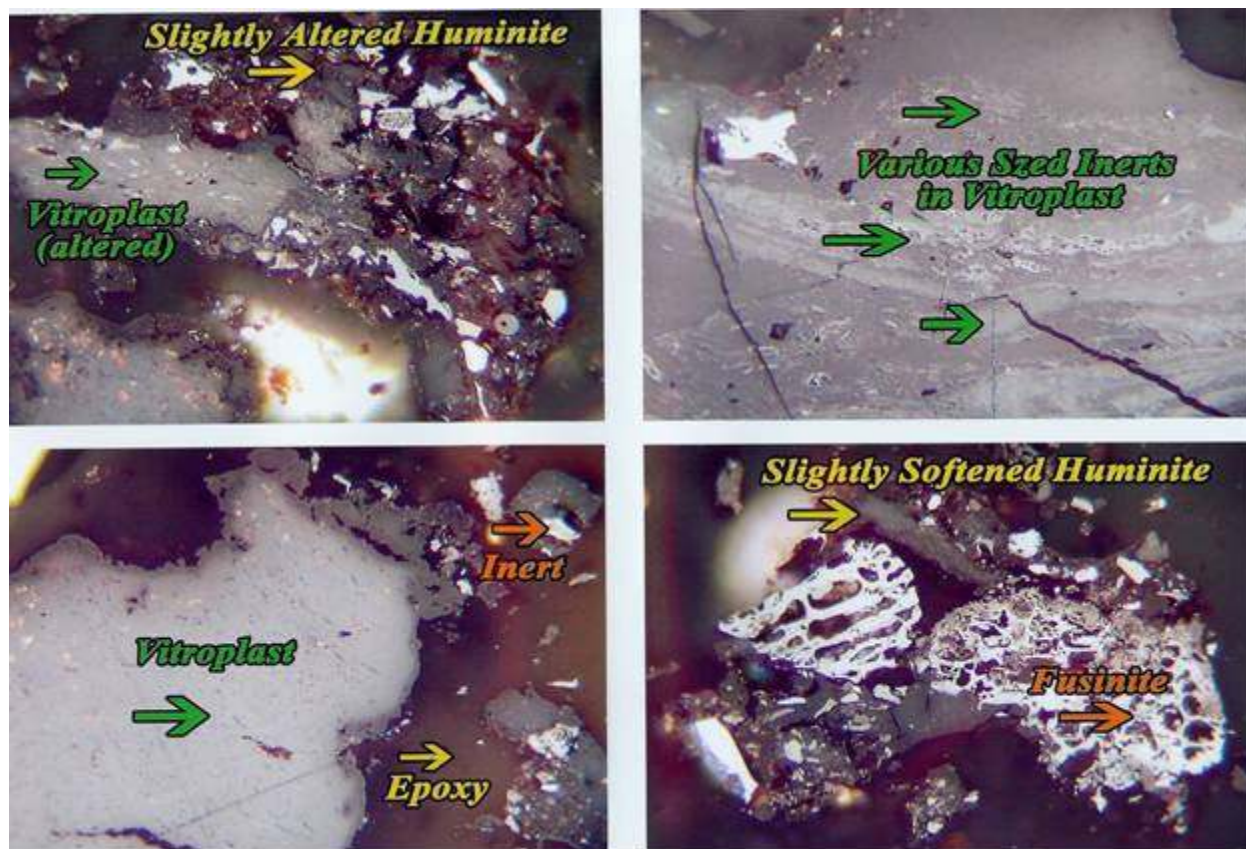


Figure 117. Photomicrographs of solid from reactor after reaction (extracted) showing: slightly altered lignite (huminite), vitroplast (altered), various sized inert, fusinite, and epoxy mounting media. Reflected light in Oil, X600.

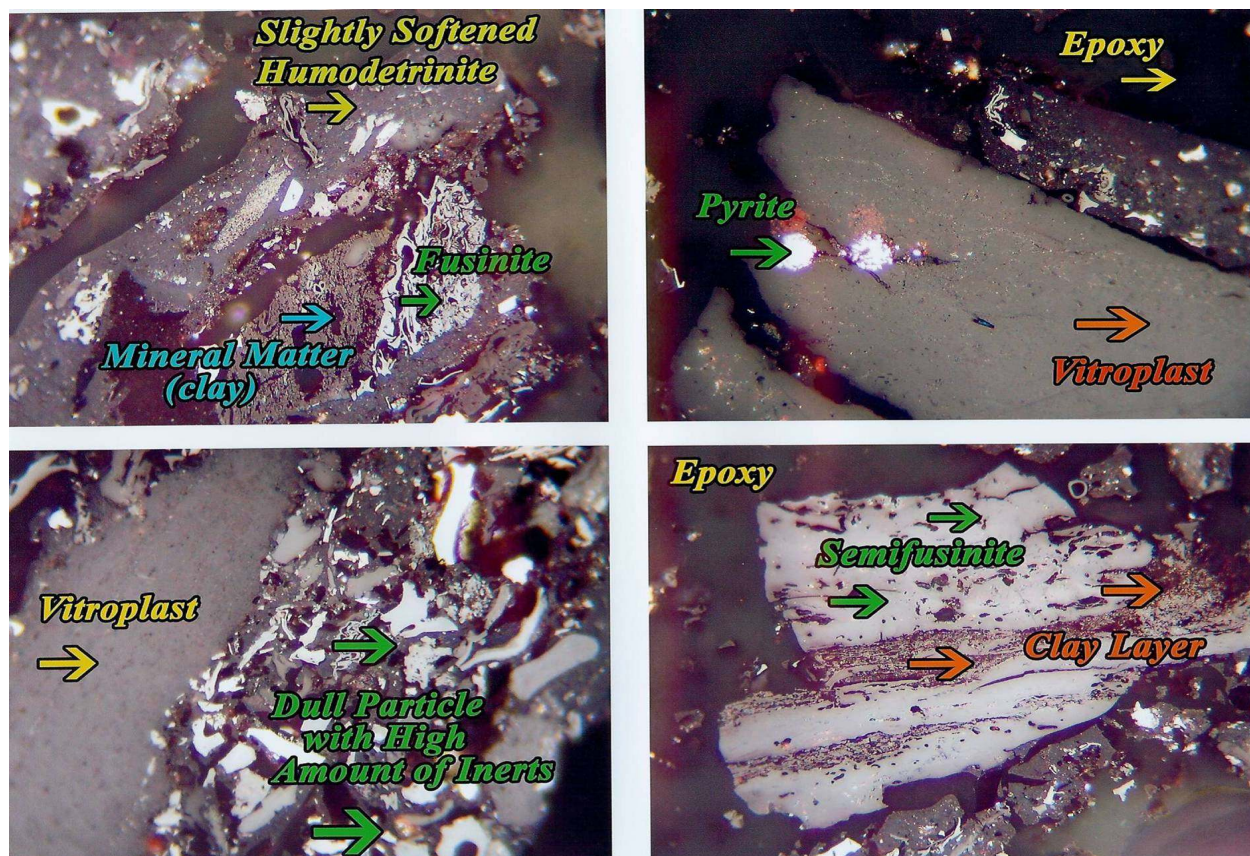


Figure 118. Photomicrographs of solid from reactor after reaction (8-15-08) showing: slightly altered lignite (huminite), vitroplast (altered), dull particle with high amount of inert, semifusinite, fusinite, pyrite, clay layer, epoxy mounting media. Reflected light in Oil, X600.

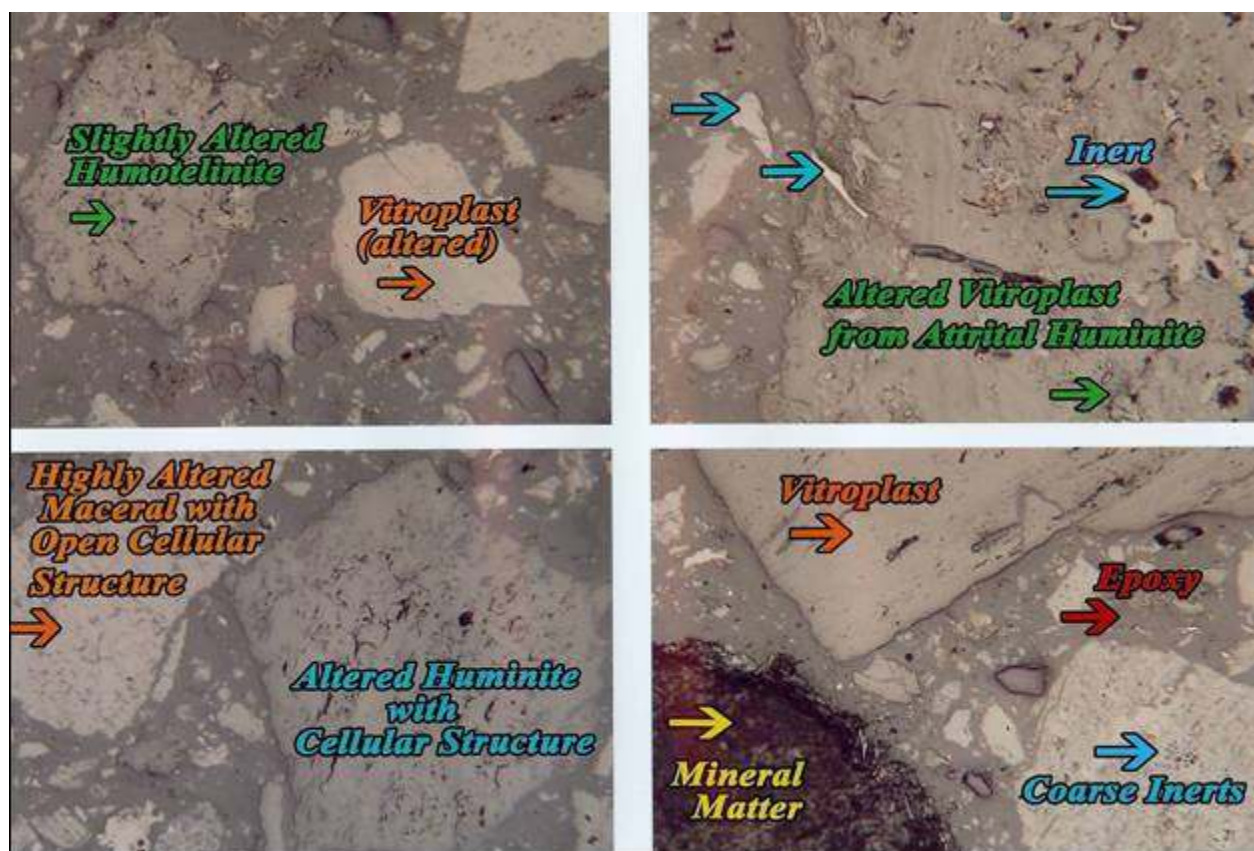


Figure 119. Photomicrographs of lignite after reaction (8-14-08) showing: slightly altered lignite (huminite), vitroplast (altered), various sized inert, fusinite, and epoxy mounting media. Reflected light in Oil, X600.

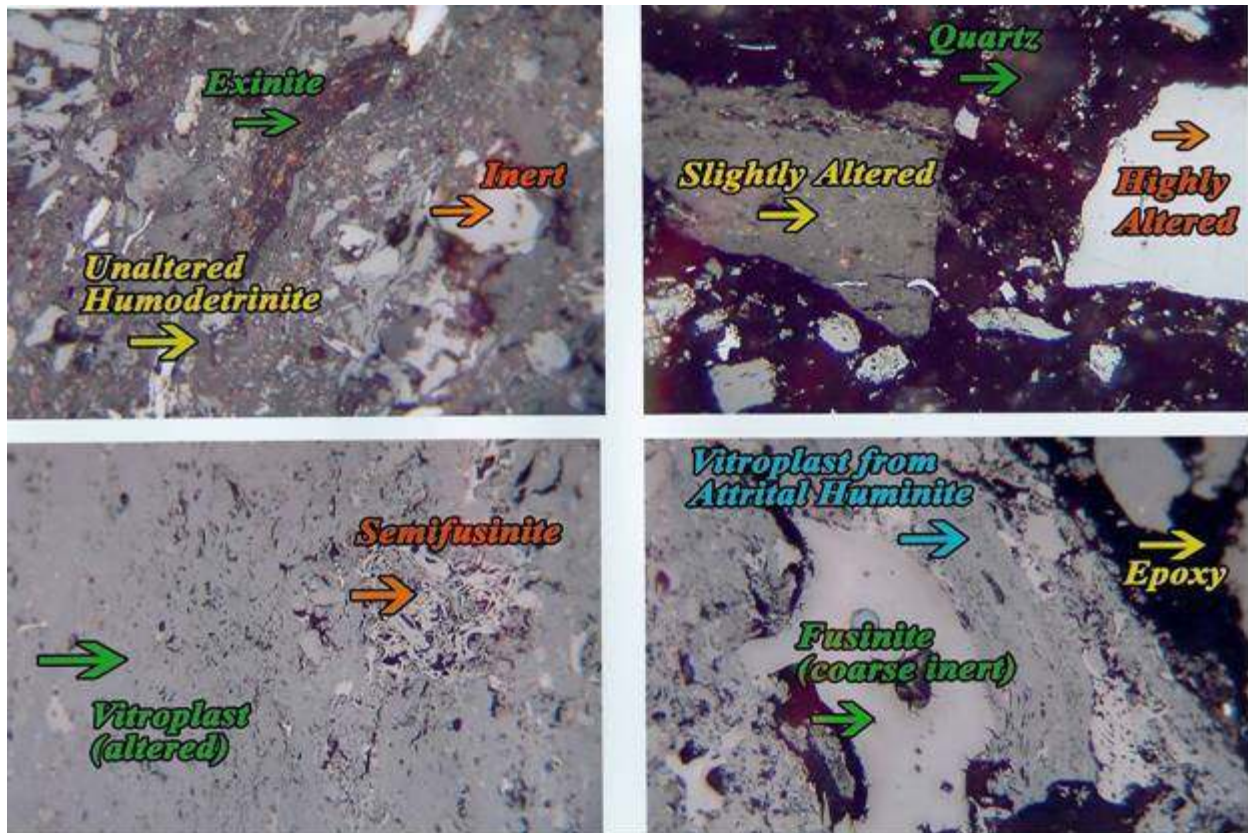


Figure 120. Photomicrographs of lignite after reaction (8-14-08) showing: unaltered lignite (humodetrinite), slightly and highly altered lignite, vitroplast (altered-attrital), exinite, semifusinite, fusinite, quartz and epoxy mounting media. Reflected light in Oil, X600.

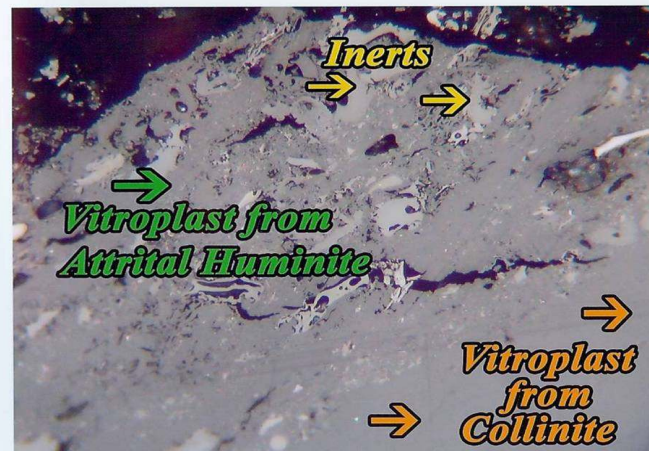
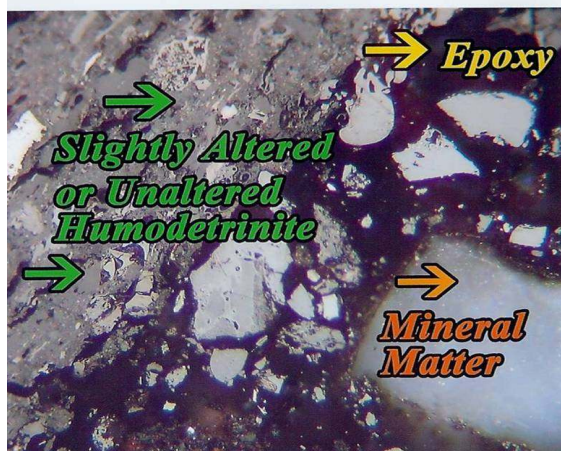
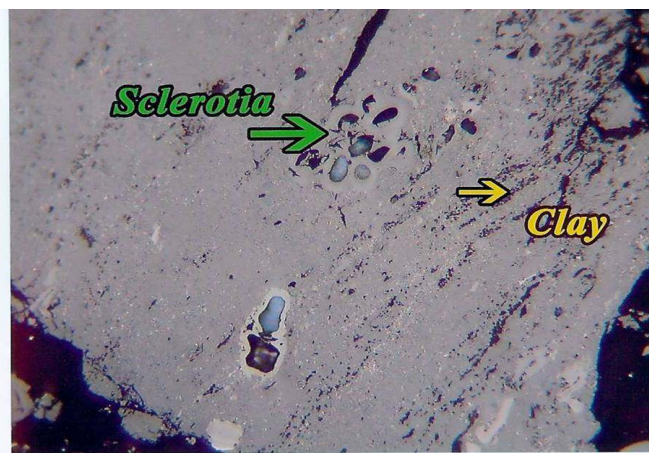


Figure 121. Photomicrographs of Lignite After Reaction (8-14-08) showing: unaltered lignite (humodetrinite), vitroplast (collinite and attrital), vitroplast from textinite (open structure), sclerotia, clay, mineral matter and epoxy. Reflected light in Oil, X600.

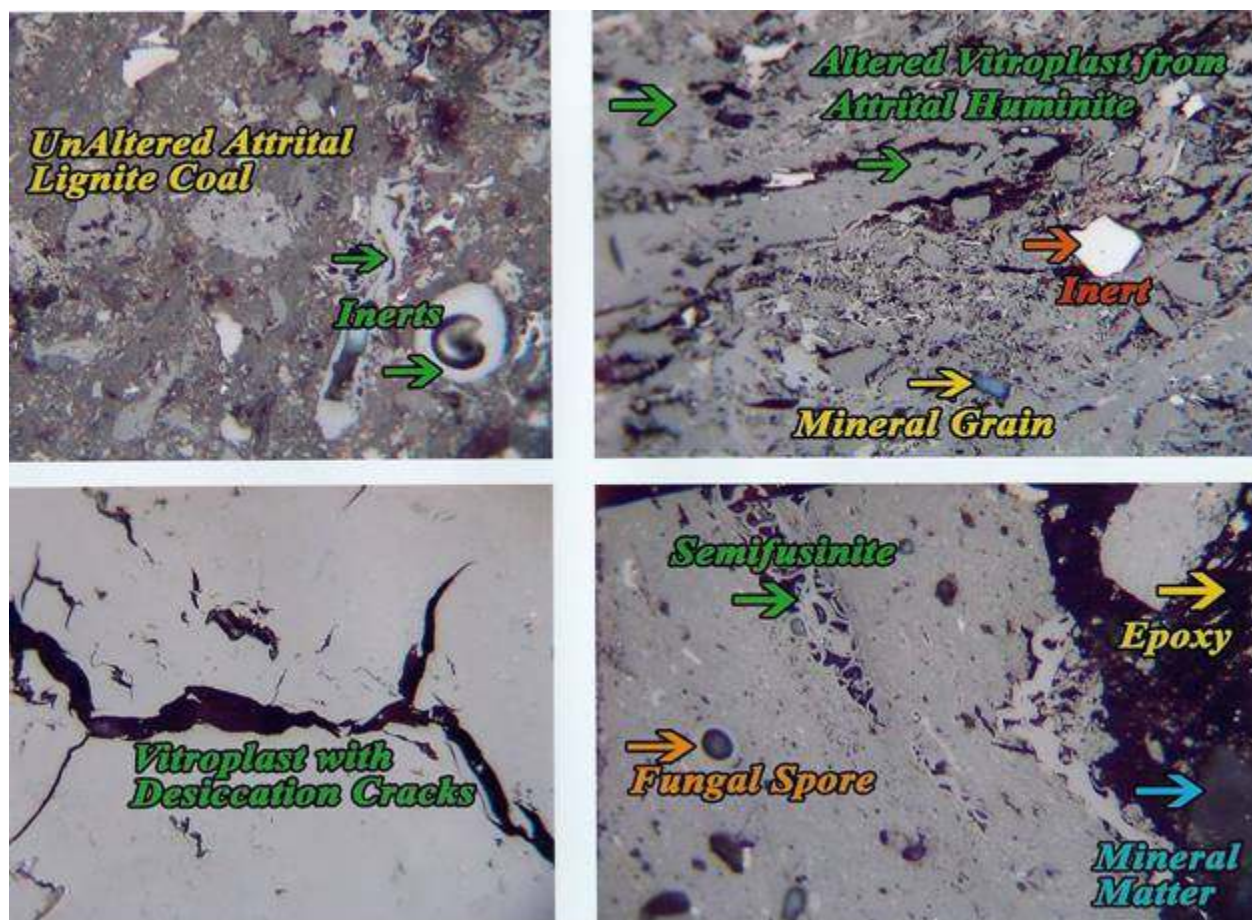


Figure 122. Photomicrographs of Lignite After Reaction (8-14-08) showing: unaltered lignite (humodetrinite), vitroplast (collinite and attrital), vitroplast with desiccation cracks, semifusinite, fungal spore, inert, mineral matter and epoxy. Reflected light in Oil, X600.

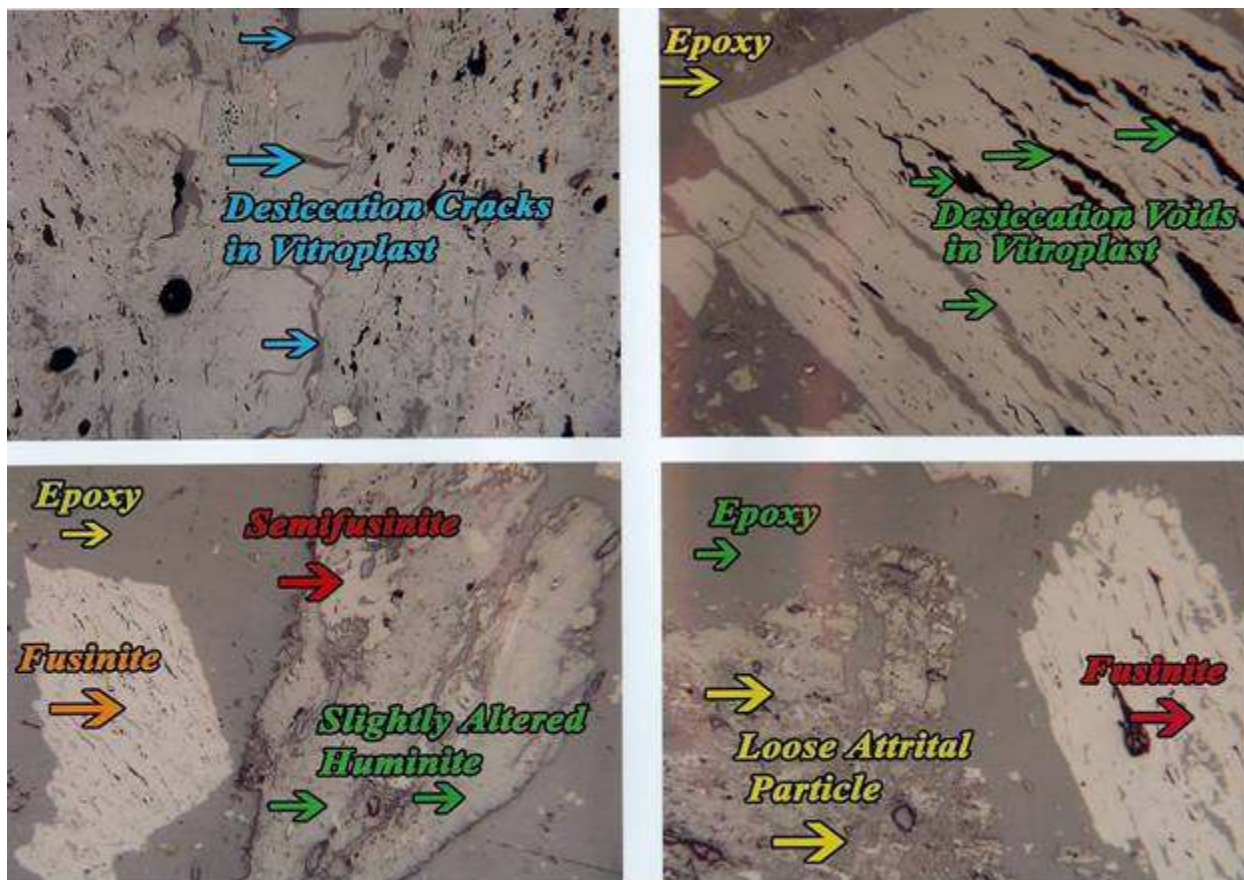


Figure 123. Photomicrographs of coked lignite at 600 °C (8-14-08) showing: slightly altered lignite (huminite), vitroplast with desiccation cracks, semifusinite, loose attrital particle and epoxy media. Reflected light in air, X135.

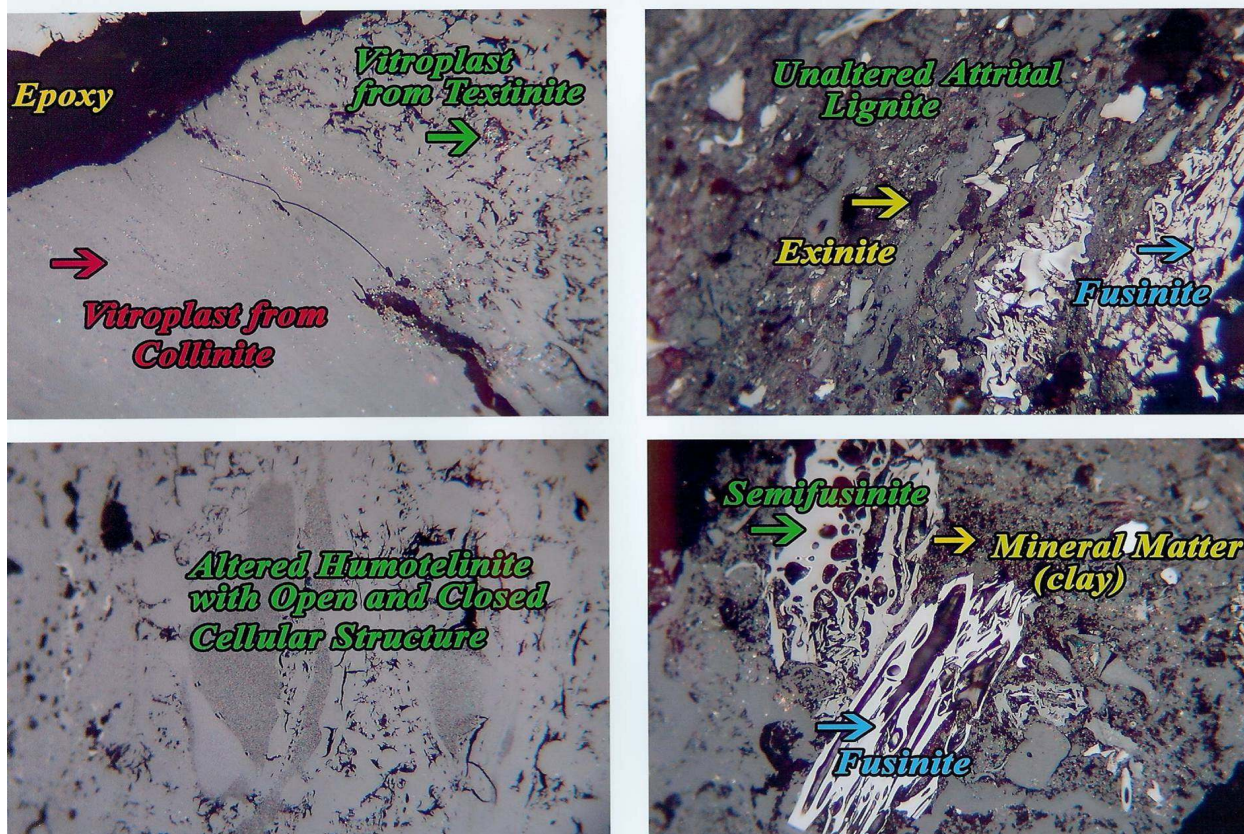


Figure 124. Photomicrographs of coked lignite at 600 °C (8-4-08) showing: slightly altered lignite (attrital), exinite, vitroplast from collinite-telinite-textinite, semifusinite, fusinite, mineral matter (clay) and epoxy mounting media. Reflected light in oil, X600.

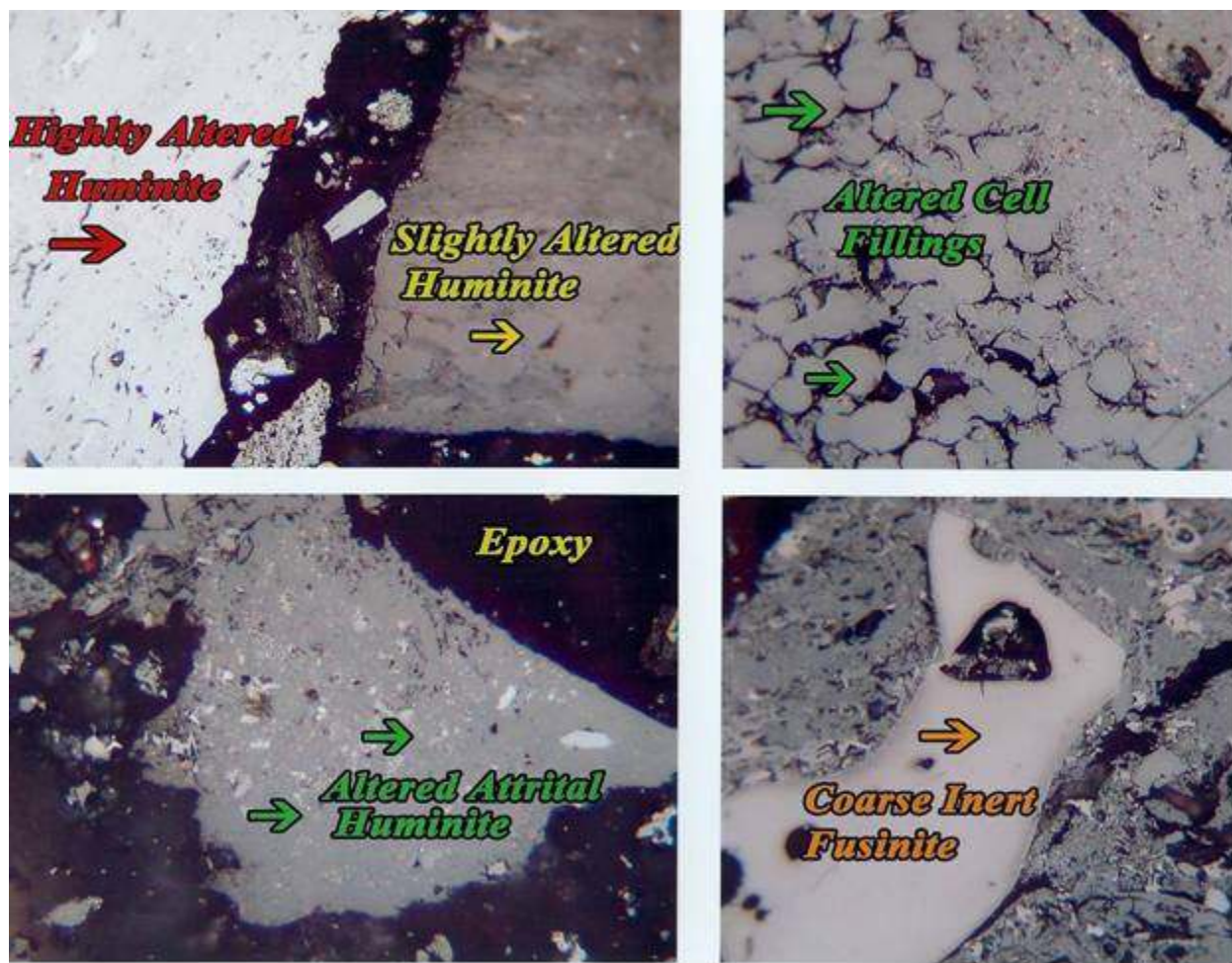


Figure 125. Photomicrographs of coked lignite at 600 °C (8-4-08) showing: slightly altered lignite (huminite), altered attrital huminite, highly altered huminite, coarse inert (fusinite) and epoxy mounting media. Reflected light in oil, X600.

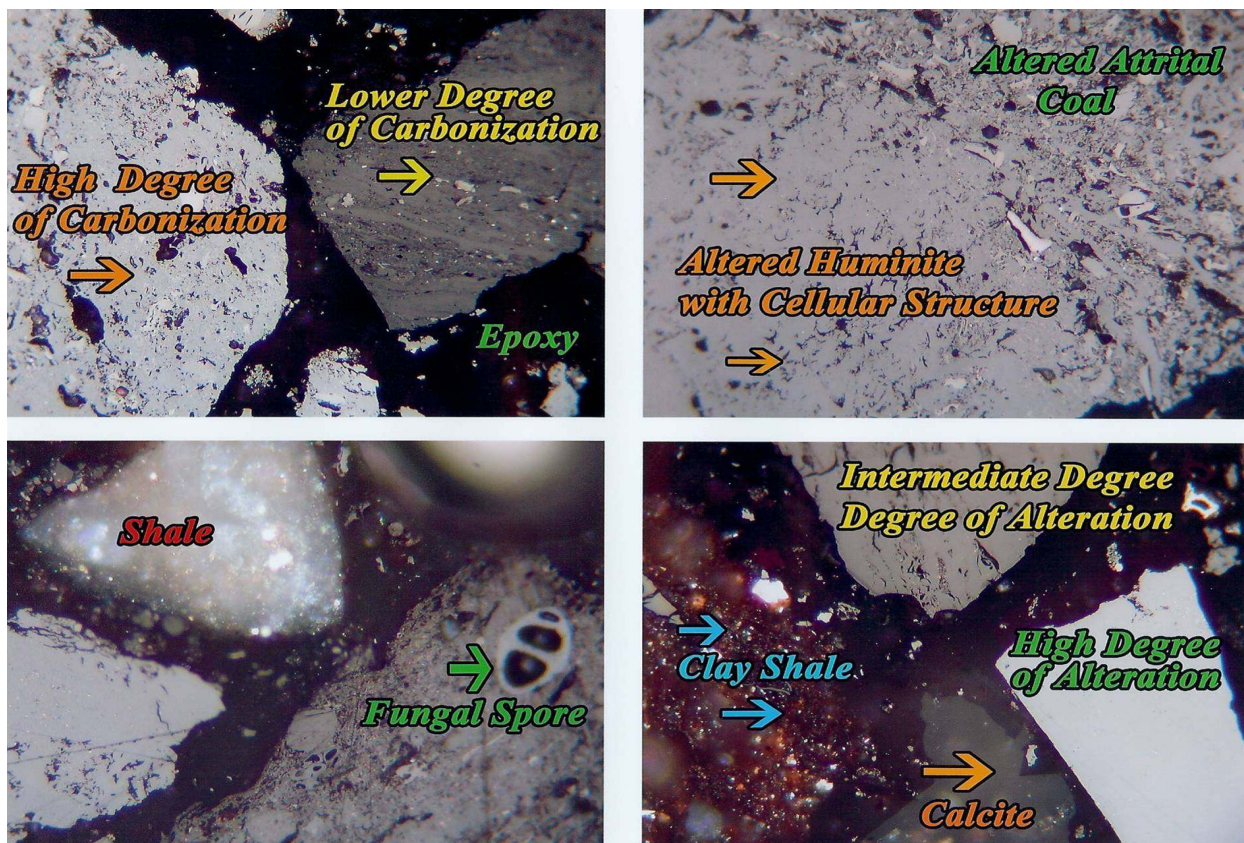


Figure 126. Photomicrographs of coked lignite-600 °C (8-4-08) showing: high-intermediate and low degree of carbonization, altered huminite (attrital), fungal spore, shale calcite, clay shale and epoxy mounting media. Reflected light in oil, X600.

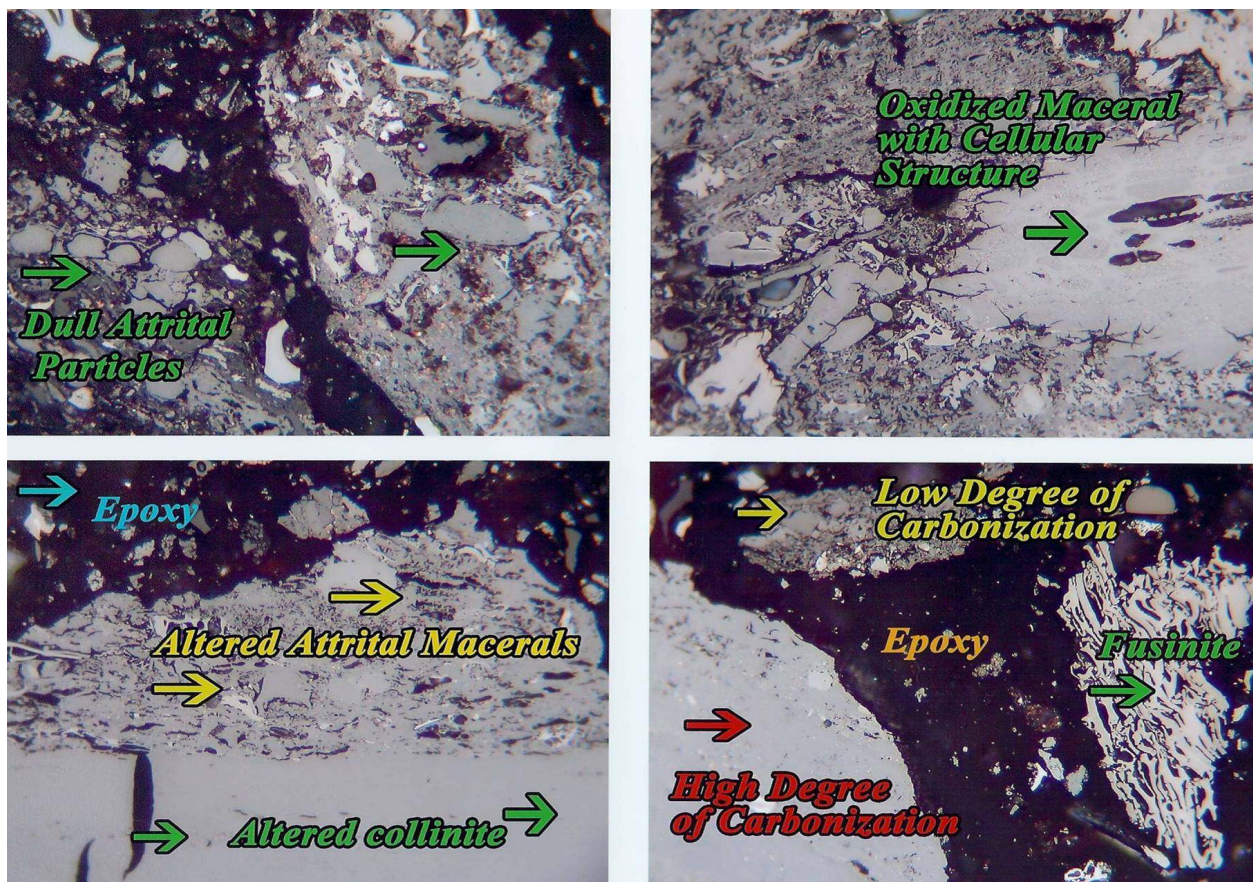


Figure 127. Photomicrographs of coked lignite at 600 °C (8-4-08) showing: high-intermediate and low degree of carbonization, altered collinite and attrital huminite, fusinite, oxidized inert, dull attrital particle and epoxy mounting media. Reflected light in oil X600.

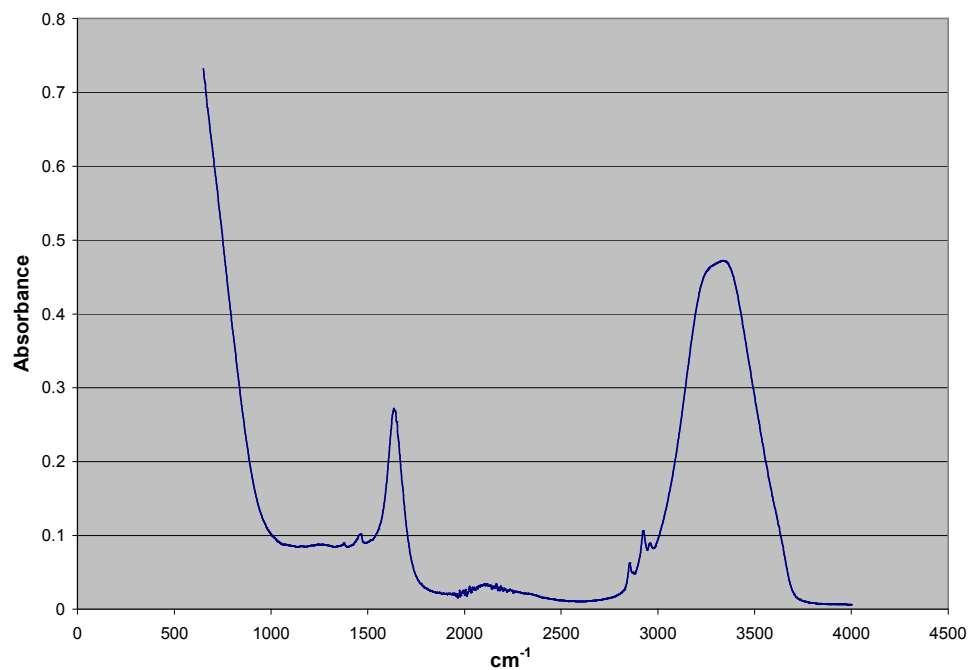


Figure 128. FTIR Liquid in Collection Flask.

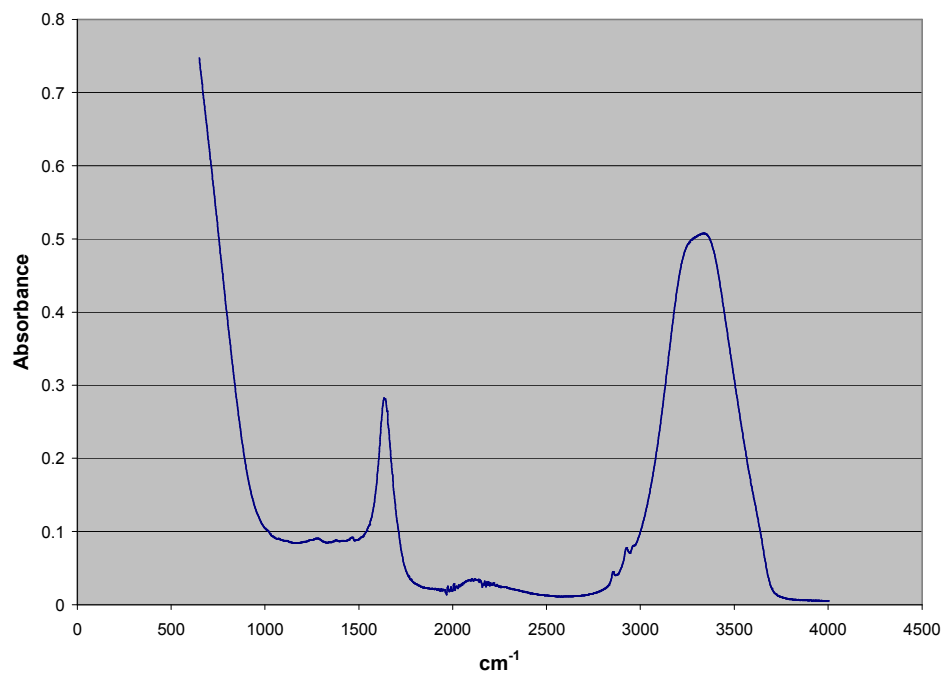


Figure 129. FTIR Residue H in flask.

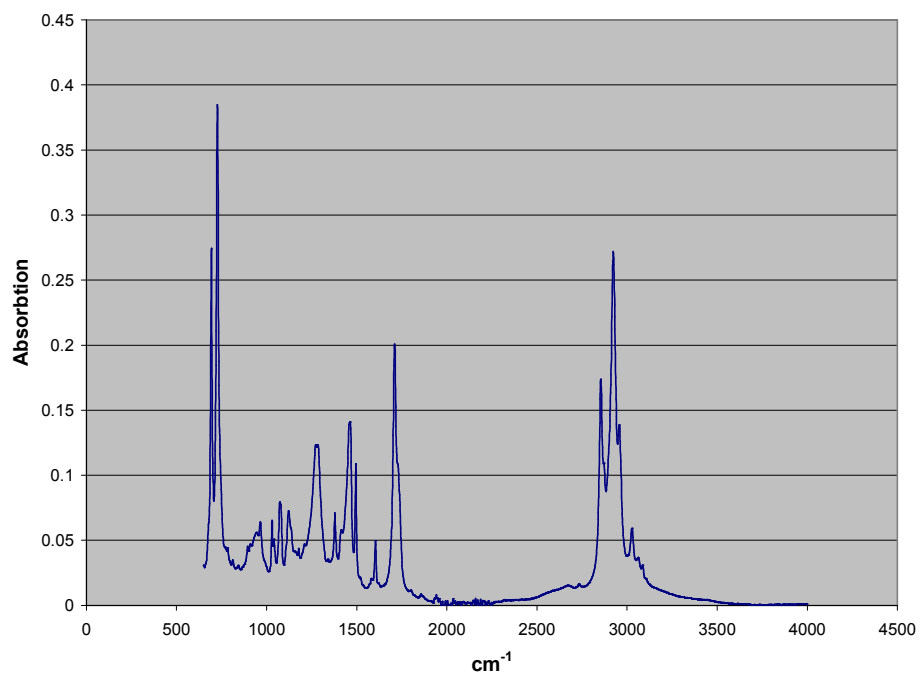


Figure 130. FTIR Liquid in Flask 1.

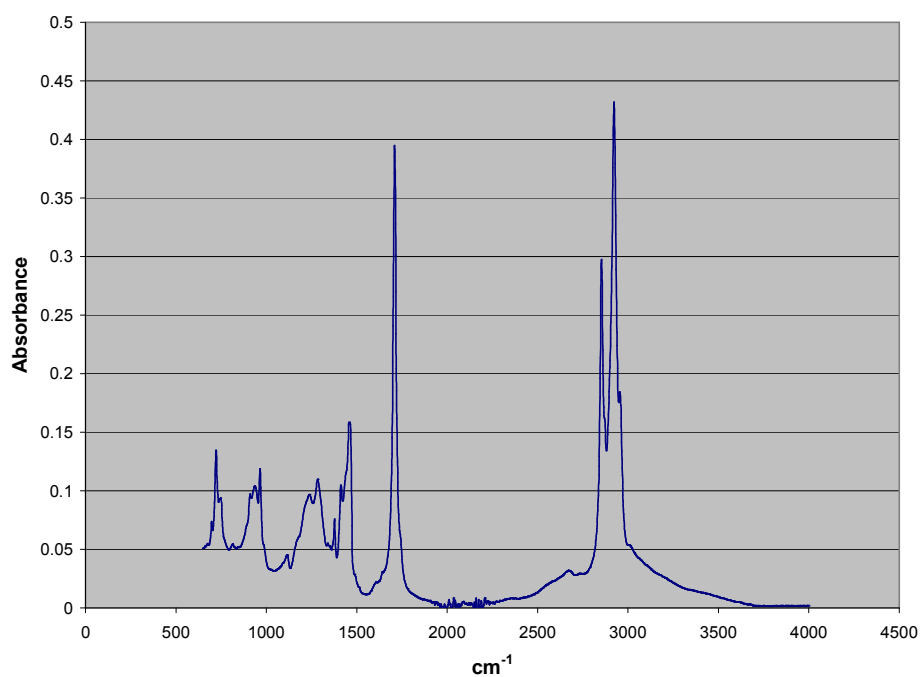


Figure 131 FTIR Solution in Flask 2.

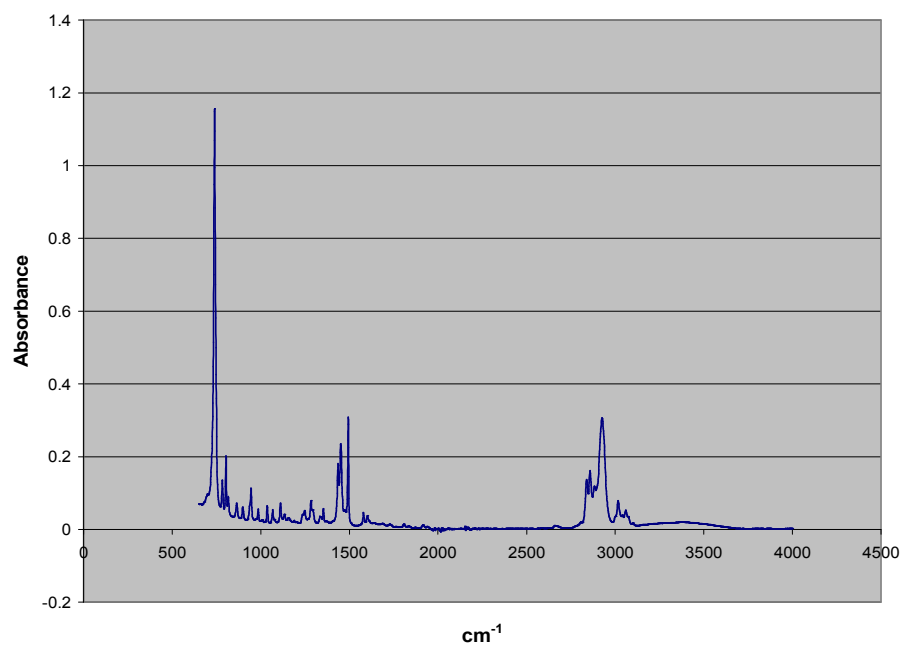


Figure 132, FTIR Solution in Flask 3.

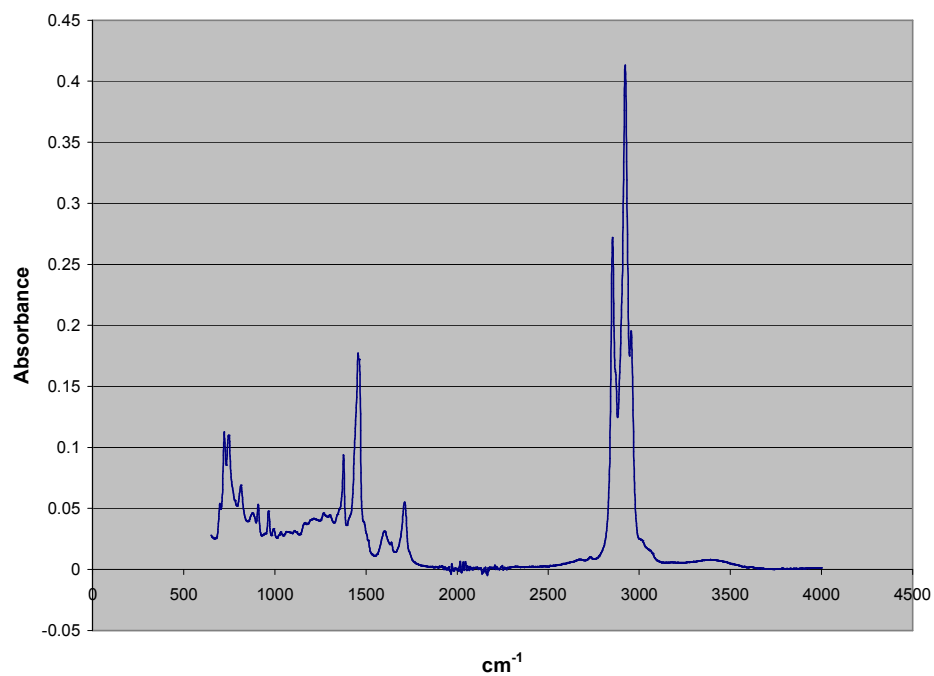


Figure 133. Solution in Flask 4.

Table 152. Elemental Analysis Group 1: Oil & Lignite.

Component Name	Average	Std Deviation	Pct Std Dev
Nitrogen%	0.632106841	0.07257914	11.4821
Carbon%	78.21912638	0.6387663	0.8166
Hydrogen%	10.2014637	0.1520341	1.4903
Sulphur%	0	0	0
H/C Ratio	0.130421601		

Table 153. Elemental Analysis Group 2: Lignite+C₁₀H₁₂ after Reaction.

Component Name	Average	Std Deviation	Pct Std Dev
Nitrogen%	1.308192194	0.01208797	0.924
Carbon%	44.60134315	2.895088	6.491
Hydrogen%	1.670570374	0.1321491	7.9104
Sulphur%	0.265684962	0.04004355	15.0718
H/C Ratio	0.037455607		

Table 154. Elemental Analysis Group 3: Coked Texas Lignite,

Component Name	Average	Std Deviation	Pct Std Dev
Nitrogen%	1.468110323	0.0897733	6.1149
Carbon%	50.02894402	5.719777	11.4329
Hydrogen%	2.672159076	0.335629	12.5602
Sulphur%	0.386608601	0.06317361	16.3405
H/C Ratio	0.053412262		

Table 155. Elemental Analysis Group 4: Solid in Reactor.

Component Name	Average	Std Deviation	Pct Std Dev
Nitrogen%	0.638795396	0.04850077	7.5925
Carbon%	66.76225535	9.139135	13.6891
Hydrogen%	7.921565533	1.488226	18.787
Sulphur%	0.665137385	0.964717	145.0403
H/C Ratio	0.118653354		

Table 156. Elemental Analysis Group 5: Texas Lignite.

Component Name	Average	Std Deviation	Pct Std Dev
Nitrogen%	0.944510837	0.009173099	0.9712
Carbon%	33.61059825	0.5498106	1.6358
Hydrogen%	4.11746645	0.6886094	16.7241
Sulphur%	0.300249656	0.1704539	56.7707
H/C Ratio	0.122505003		

Table 157. Elemental Analysis Group 6: Lignite after Reaction.

Component Name	Average	Std Deviation	Pct Std Dev
Nitrogen%	1.400005619	0.1832718	13.0908
Carbon%	49.84944534	7.757624	15.5621
Hydrogen%	1.899187764	0.3254492	17.1362
Sulphur%	0.291790937	0.05553367	19.032
H/C Ratio	0.038098473		

Table 158. Proximate Analysis for Oil & Lignite.

Sample	Moisture	Volatile	Ash	Fixed Carbon
Oil+Lignite Reaction 1	1.57	69.57	8.78	20.08
Oil+Lignite Reaction 2	1.2	70.74	6.33	21.72
Oil+Lignite Reaction 3	1.16	70.28	7.18	21.37
Oil+Lignite Average	1.31	70.20	7.43	21.06

Table 159. Proximate Analysis for Lignite & C₁₀H₁₂.

Sample	Moisture	Volatile	Ash	Fixed Carbon
Lignite+C ₁₀ H ₁₂ after Reaction 1	2.25	15.71	40.9	41.14
Lignite+ C ₁₀ H ₁₂ after Reaction 2	2.31	16.06	42.04	39.59
Lignite+ C ₁₀ H ₁₂ after Reaction 3	1.95	14.12	43.35	40.58
Lignite+ C ₁₀ H ₁₂ Average	2.17	15.30	42.10	40.44

Table 160. Proximate Analysis for Coked Texas Lignite.

Sample	Moisture	Volatile	Ash	Fixed Carbon
Coked Texas Lignite 2	2.41	21.51	33.83	42.25
Coked Texas Lignite 3	2.4	21.35	33.42	42.84
Coked Texas Lignite	2.41	21.43	33.63	42.55

Table 161. Proximate Analysis for Lignite.

Sample	Moisture	Volatile	Ash	Fixed Carbon
Lignite after reaction 1	1.49	17.08	35.79	45.64
Lignite after reaction 2	1.39	15.76	42.58	40.27
Lignite Average	1.44	16.42	39.19	42.96

Table 162. Proximate Analysis for Solid,

Sample	Moisture	Volatile	Ash	Fixed Carbon
Solid in reactor 2	1.25	73.55	5.3	19.89
Solid in reactor 3	1.1	77.16	5.6	16.15
Solid Average	1.18	75.36	5.45	18.02

Table 163. Proximate Analysis for Texas Lignite.

Sample	Moisture	Volatile	Ash	Fixed Carbon
Texas Lignite 1	29.56	27.61	19.03	23.8
Texas Lignite 2	28.77	26.46	21.14	23.63
Texas Lignite 3	28.75	26.23	22.22	22.81
Texas Lignite Avg	29.03	26.77	20.80	23.41

3.8 Trials of Reformulated Lignite Pitch.

GrafTech International carried out studies of WVU extract made from lignite obtained from Quantex Energy Inc. These extracts were converted to pitches via distillation. The results show that a pitch was formed with properties that are potentially relevant for use as a binder pitch, impregnation pitch or coke precursor.

This pitch, when blended with conventional Koppers binder pitch as a control, made an acceptable pitch. Because low rank coals contain more aliphatic chemicals than conventional bituminous coal derived pitches, pitches from sub-bituminous coals, lignite (or even biomass blends) are less desirable for anode and electrode applications. Nevertheless, their use on industrial scale may be possible, as suggested by data in Table 164 through Table 170.

Table 164. Conversion of WVU extract into pitch.

	Binder Pitch	Impregnation Pitch
Pitch Yield, wt%	52.6	59.8
Softening Point, °C	111.6	92.8
MCC, wt%	38.0	33.2
Ash, wt%	1.29	1.16
QI, wt%	1.9	2.1
TI, wt%	30.0	26.3
Flash Point, °C	276	258
Nitrogen, wt%	1.25	--
Mesophase	none	none

Table 165. Evaluation of Lignite and Binder Pitch Blend.

Pitch	Lignite Blend	Control
Softening Point, °C	112.7	111.4
Ash, wt%	0.94	1.17
C, wt%	89.99	92.49
H , wt%	4.93	3.99
N , wt%	1.32	1.02
S , wt%	0.66	0.57
C/H	1.74	1.93
COC, °C	258	266
Coking Value, wt%	37.5	59.2

Table 166. Evaluation of Lignite and Binder Pitch Blend.

Pitch	Lignite Blend	Control
CTE, ppm	0.114	0.140
SR. $\mu\Omega$ -m	15.10	10.04

Table 167. Pilot Plant Trials for 2010 and 2007.

Pitch	Softening Point °C	QI wt%	TI wt%	Coking Value wt%	Ash Wt%
Pilot Trial 2010					
Koppers A	113.7	10.7	26.5	57.8	ND
80:20 CTP:Syn	108.7	12	ND	53.2	0.56
Pilot Trial 2007					
P-18	111.8	13.4	30.4	59.8	0.11
80:20 CTP:Syn	109.7	14.4	31.9	58.5	0.46
75:25 CTP:M50	110.7	13	28.6	55.7	0.16

Table 168. Pilot Plant Forming.

Pitch	Binder Level pph	Green Density g/cm3
Pilot Trials 2010		
Koppers A	26	1.766
80:20 CTP:Syn (93065)	26	1.766
80:20 CTP:Syn (93066)	26	1.774
Pilot Trials 2007		
P-18	29	1.744
P-18	30	1.731
80:20 CTP:Syn	29	1.738
80:20 CTP:Syn	30	1.750
75:25 CTP:M50	27	1.756

Table 169. Green to Bake.

Pitch	Binder Level pph	QI wt%	CV wt%	Green BD g/cm3	Baked BD g/cm3	Density Change
Pilot Trials 2010						
Koppers A	26	10.7	57.8	1.766	1.660	-0.116
80:20 CTP:Syn (93065)	26	12.2	53.2	1.766	1.641	-0.136
80:20 CTP:Syn (93066)	26	12.2	53.2	1.774	1.650	-0.124
Pilot Trials 2007						
P-18	29	13.4	59.8	1.744	1.645	-0.098
P-18	30	13.4	59.8	1.731	1.645	-0.086
80:20 CTP:Syn	29	14.9	58.5	1.738	1.629	-0.109
80:20 CTP:Syn	30	14.9	58.5	1.750	1.622	-0.128
75:25 CTP:M50	27	13	56.0	1.755	1.648	-0.106

Table 170. WG Graphite Properties.

Pitch	BD g/cm3	Flexural psi	YM GPa	SR $\mu\Omega$-m	CTE ppm
Pilot Trials 2010					
Koppers A	1.695	1423	1.40	5.72	0.23
80:20 CTP:Syn (93065)	1.678	1207	1.27	6.14	0.21
80:20 CTP:Syn (93066)	1.685	1252	1.29	6.04	0.22
Pilot Trials 2007					
P-18	1.685	1334	1.40	5.40	0.11
P-18	1.709	1451	1.45	5.17	0.12
80:20 CTP:Syn	1.692	1348	1.37	5.41	0.13
80:20 CTP:Syn	1.681	1319	1.41	5.43	0.12
75:25 CTP:M50	1.680	1159	ND	5.16	0.16

3.9 CARBON DIOXIDE EMISSIONS

Currently there is no approved methodology for evaluating the carbon dioxide footprint for energy production. Hence the science of estimating the carbon dioxide footprint remains in its infancy and is the subject of quite some controversy. To cite an obvious example, early on it was assumed that biofuels would definitely have a much smaller greenhouse gas footprint than fossil fuels. The rationale is based on the fact that biomass is seemingly created largely from atmospheric carbon dioxide, with the process of photosynthesis generating cellulose. Hence the reverse reaction of combustion would seem not to result in net carbon dioxide. This naïve point of view is summarized and critiqued by Johnson.⁶⁴

Johnson as well as many others have pointed out that carbon dioxide may be generated via the use of chemical fertilizers, or via the energies required to plant, cultivate, harvest, process (e.g., fermentation and distillation, for many biofuels) and distribute. These energies could in principle greatly exceed the enthalpy value of the biofuel itself.⁶⁵ Pimentel and Patzek have published articles that suggest that in certain circumstances at least, the amount of energy input for corn ethanol production exceeds the enthalpy that can be generated from the fuel.⁶⁶ If this is correct, it implies that the carbon dioxide signature from biomass must also be larger than that obtained from simply burning fossil fuel inputs.

Without seeking to resolve the issue of the exact value of energy ratio, the point is that simply switching from burning coal to burning biomass may not actually reduce the total carbon dioxide ratio by more than several percent. If this point of view is borne out by improved modeling in the future, the substitution of ethanol for fossil fuel may result in only incremental improvements, and may not bring about order-of-magnitude reductions sought by environmental advocates.

To cite another case, nuclear power is thought to be a real-world alternative to fossil energy, at least for central station power generation. In France, for example, nuclear power already supplies some 79% of the total electrical power produced in that country.⁶⁷ No carbon dioxide is produced during the generation of thermal energy from fission. However, nuclear power is extremely capital intensive. Hence there is at least the suspicion that carbon might be produced during the fabrication of the components. Certainly steel requires the use of metallurgical grade coke to produce in a blast furnace, with additional energy being added in order to process the steel. Even concrete requires energy for its production. The centrifuges used to enrich uranium are likewise highly energy intensive. Labor expenses result in enabling people to consume goods, services and energy from other sources.

While intuitively it seems reasonable to believe that the CO₂ footprint from nuclear power is likely to be less than the same footprint from coal power, upon further reflection the answer is not a simple one. Thus the actual footprint for alternative technologies is difficult to estimate.

Greenhouse gas, or more specifically carbon dioxide, is potentially produced at all phases from “Well to Wheels.” Anytime heat is used, in today’s economy it is likely that that heat derives from hydrocarbon combustion processes in some way, and thus results in carbon dioxide emission.

Some processes, such as those involving gasification and liquefaction, inherently produce carbon dioxide as part of reactions such as methane reforming and water gas shift. These reactions are part of the Fischer Tropsch processing of natural gas, biomass or coal. This

however is not the only or the main reason for the net emission of carbon dioxide. Figure 134 shows estimates of “Well to Wheels” carbon dioxide footprints, as estimated by the Canadian Association of Petroleum Producers.”

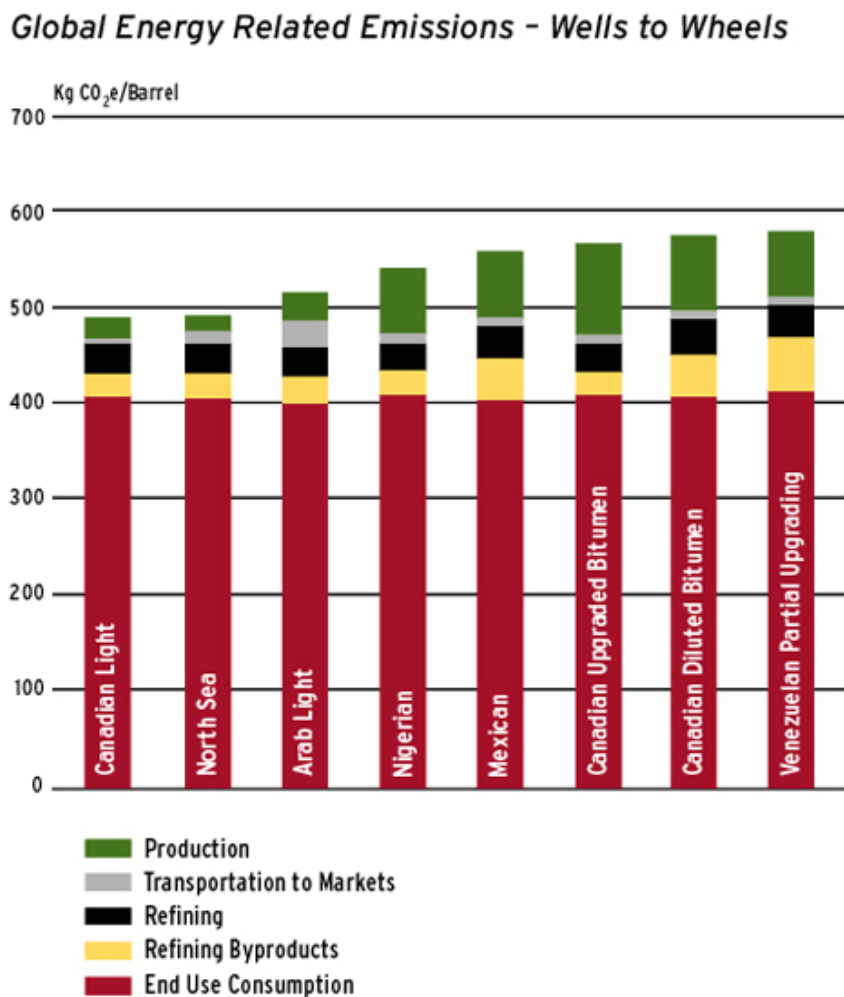


Figure 134. Estimates of “Well-to-Wheels” carbon dioxide footprint estimates (kilograms of carbon dioxide per barrel of product) from the Canadian Association of Petroleum Producers (CAPP). All sources of hydrocarbon products are within 20% of each other (http://www.canadasoilsands.ca/en/img/img_gas_climate_change.gif).⁶⁸

The liquefied coal process involves the production of digested extract from coal followed by separation of the soluble and non-soluble solids from the extract. The next stage of the process is the pitch and condensate production via distillation. These processes are easily quantified via thermodynamic analysis. Carbon dioxide does not result from the process itself. However, thermal energy used in the process might result from the combustion of char or natural gas, and thus could result in the production of CO₂.

The green portion of the bar represents the amount of greenhouse gas produced in the production phase. This is the phase that Quantex seeks to occupy in commercializing its process for converting coal to crude oil. Using a barrel of crude (159 liters) with density 0.92 kg/liter the mass of a barrel is 159 kg. The CO₂ emissions associated with production of Oil Sands about 100 kg per barrel of product judging from Figure 134 or 0.6 kg of CO₂ per kg of product.

Note that if one were conscientious about reducing CO₂ signature, it might be possible to use sources of thermal energy such as solar heat, geothermal energy, or waste heat from some other process, rather than burning char or natural gas. In the present analysis, however, it is (pessimistically) assumed that thermal energy is supplied by burning natural gas or char. When electrical energy is used, it is assumed that the electrical energy is associated with thermal energy produced by burning char at 32 MJ/kg, and the source of thermal energy is three times the amount of the electrical energy consumed. These processes would result in additional expense, and may not be practical, and thus are not further considered.

3.9.1 Energy Cost of Mining

There is a real energy cost associated with mining coal and transporting it. This amount of energy is often compared to the energy value of the fuel by a quantity known as EROI (Energy Return on Investment) or EROEI (Energy Return on Energy Invested) or EROIE (Energy Return on Invested Energy). These terms are all equivalent. This is the energy value of the resource divided by the energy expended in acquiring the resource, or

$$EROI = \frac{Q_{fuel}}{Q_{cost}}$$

The energy efficiency is

$$\eta = 1 - \frac{Q_{cost}}{Q_{fuel}} .$$

There is no standardized method to calculate these quantities and there are a number of agendas that might result in differences in these estimates. Different assumptions may result in different estimates. For example, Figure 135 shows the EROI for several commodity energy products, as estimated by Merrill Lynch.⁶⁹ The EROI of Coal is 80, meaning that there is very little energy expended in acquiring “Coal.” However, the value might differ for Western US coal versus Eastern US coal, mine mouth coal versus prepped coal, etc.

Based on 25 MJ/kg combustion enthalpy for bituminous coal (as an example), the energy cost of producing 1 kg of coal is $1/80 * 25$ MJ or 312 kJ. Assuming this energy is supplied from combustion of char (32 MJ/kg specific energy), 0.00975 kg of carbon is combusted, or .036 kg of CO₂ emitted per kg of product.

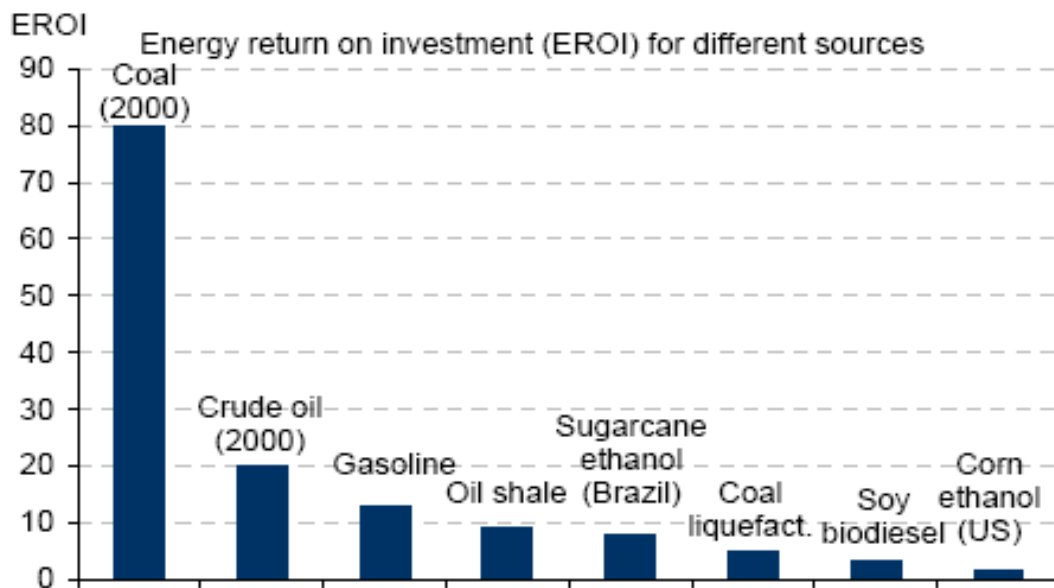


Figure 135. Energy Return on Investment for different commodity fuels, estimated by Merrill Lynch.

These parameters can be estimated for Liquefied Coal as well as Oil Sands, and shown in the analysis below.

3.9.2 Energy Cost of Coal Crushing

Crushing coal to -20 mesh, which is accomplished routinely for many power plants, must add some energy cost. A NIOSH report shows that laboratory coal crushers handle 15 kg samples, with ~5 kJ expended in crushing the samples, or 300 J/kg.⁷⁰ The thermal energy required to produce this amount of electrical work would be some 900 J/kg, translating to 0.0001 kg of CO₂ results from grinding 1 kg of coal. This is negligible compared to the mining (production) cost.

3.9.3 Energy Cost of Liquefaction

In the first stage, coal is reacted with coal tar distillate (solvent) at 400 °C for an hour in a reactor to solubilize coal so that the non-soluble matter can be separated from the solution with ease. Feed ratio of 3 parts of solvent to 1 part of coal by weight is used. During this stage the volatiles are condensed, collected and mixed with the extract from the reactor for further processing. Assuming naphthalene to be the model compound representing solvent, and

Weight of coal into the reactor = 1 kg

Weight of solvent = 3 kg

Initial Temperature, T₁ = 20 °C

Final Temperature, T₂ = 400 °C ,

then the amount of heat energy required to raise the temperature from T_1 to T_2 is given by

$$Q_1 = \sum m_i c_{p_i} (T_2 - T_1) \quad ,$$

where the mass fractions are $m_i = 0.75$ solvent and 0.25 coal.

Using the following parameters:

Specific heat capacity of coal = 1.38 kJ/kg K

Specific heat capacity of naphthalene = 1.72 kJ/kg K

Average specific heat of the feed = 1.635 kJ/kg K

Amount of heat energy required, $Q_1 = 2.49 \text{ MJ}$

Assuming 15% of heat losses, then

$$Q_1 \text{ reactor} = 2.86 \text{ MJ (per kg of input coal).}$$

3.9.4 Energy Cost of Centrifugation

The extract from the reactor is then centrifuged to separate the non-soluble solids from the centrate followed by distillation. A decanter centrifuge is rated at 5 kW for a maximum flow rate of 5 gallons per minute (0.315 liters/sec). This corresponds to an energy cost of 16 kJ/kg .

The distillation process the apparatus is heated under vacuum until a desired temperature is reached (400°C) to produce pitch and volatiles. The volatiles produced during this stage of the process are condensed which is tested for fuel potential. We assume pessimistically that very little of the energy is recuperated. Hence the distillation inlet temperature is only 90°C .

3.9.5 Energy Cost of Distillation

The energy cost of distillation of the liquefied coal can be estimated with the following assumptions:

Weight of liquefied coal = 0.85 kg

Weight of Solvent = 3.00 kg

Initial temperature, $T_3 = 90^\circ\text{C}$

Final temperature, $T_4 = 400^\circ\text{C}$

Amount of heat energy, $Q_2 = 1.95 \text{ MJ}$

Heat Losses (15%), Actual heat, $Q_2 = 2.24 \text{ MJ}$

Heat of vaporization of naphthalene, $\Delta H_v = 43.3 \text{ kJ/mol}$

Moles of Naphthalene = 23.4

Amount of boiling heat, $Q_3 = 1013 \text{ kJ}$

Total heat = $Q_1 + Q_2 + Q_3 = 6.11 \text{ MJ}$

Assuming that the main product is pitch, and assuming also that the yield is about equal to the remaining mass of coal in solution, that is, 0.85 kg, then the product-normalized heat consumption is

$$\frac{Q_{tot}}{m} = \frac{6.11}{0.85} = 7.2 \frac{MJ}{kg} \text{ of pitch product.}$$

It is assumed that the energy needed for processing is obtained by burning char or natural gas.

Enthalpy of char = 32 MJ/kg; natural gas LHV is 45 MJ/kg.

Total amount of char burned = 0.23 kg of char.

CO₂ produced = 0.85 kg of CO₂ per kg of pitch product, or 0.62 kg of CO₂ if natural gas is used to produce thermal energy for the process.

Based on pitch product energy value of 37 MJ/kg, the Energy Efficiency of the process is approximately given by

$$\eta \approx 1 - \frac{7.2}{37} \approx 80\%$$

This covers coal as it enters the reactor to the production of product as it leaves the plant. The use of recuperation would result in a higher energy efficiency. This is comparable to the efficiency of oil refineries, although those refineries dealing mainly with straight-run crude may have efficiencies in the 90% range.

If the pitch is converted to coke plus crude, there should be an additional thermodynamic penalty associated with the devolatilization and cracking process. However, this is smaller than might be imagined, because in the case of delayed coking, the distillation residue (already preheated to 500 °C) is pumped directly to the delayed coker with little or no addition of thermal energy. In this case, the coke and the distilled liquids should both be considered products for the Quantex product, as the coke will surely be used for metallurgical coke or else for anode grade coke. This is not true for Oil Sands, which makes fuel coke that is so high in heavy metal concentration that it is often landfilled.

3.9.6 Energy Balance for Canadian Oil Sands

The acquisition of oil sands is inherently inefficient. Oil Sands can be extracted in two ways: open-pit mining for oil sands at the surface, and *in situ* recovery for underground oil sands. After the excavation or drilling, bitumen is extracted from the remaining mixture of sand and water. A ton of tar sands results in the production of only one-half net barrel of oil. The next phase is either to use hydrogen to upgrade the bitumen to 30° API syncrude, which has a quality comparable to conventional crude oil, or to blend it with higher quality diluents such as conventional oil. Both these products can be refined at existing refineries. An important issue is the degree to which natural gas is required either for process heat or for upgrading the quality and reducing the viscosity of the bitumen. This situation is shown graphically in Figure 136, originally published in the *Oil Drum*. Direct energy flows refer to energy consumed in the acquisition and processing of oil sands. Indirect energy flows would include the energy used to fabricate equipment used in the processing. Labor energy demand contains the energy that is associated with personnel involved in the processing. Finally, the environmental energy demand accounts for additional energy that might be consumed in future processing; e.g., to reduce the signature of CO₂ associated with the process. An EROI of 5.2 is a reasonable estimate, based on Herweyer and Gupta (Figure 136). As previously discussed,

$$EROI = \frac{Q_{fuel}}{Q_{cost}}$$

The energy efficiency is

$$\eta = 1 - \frac{Q_{cost}}{Q_{fuel}}$$

Thus, the efficiency is about 80%, which is very similar to the coal liquefaction case.

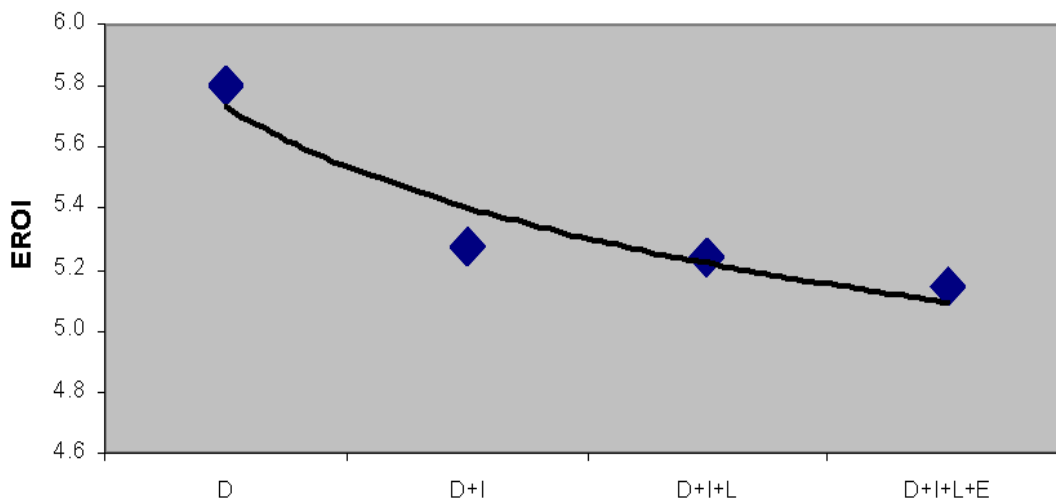


Figure 136. Oil Sands Energy Return on Investment. D represents only the direct energy flows, I represents Indirect energy flows, L represents Labor energy demand, and E represents the Environmental energy demand.⁷¹

There are three main sources of CO₂ emissions associated with bitumen upgrading:

- Combustion of burner off-gas in a boiler (Combustion of Coke).
- Combustion of fuel gas in a coking reactor.
- Water gas shift process in a H₂ plant.

Relevant parameters are contained in Table 171 through Table 174 below.

Table 171. Composition of Natural gas.

Component	Volume (%)
Hydrogen	2.1
Methane	96.8
C-2	0.7
C-3	0.4

Table 172. Composition of Coke

Component	Fluid Coking (Wt %)	Delayed Coking (Wt %)
Carbon	83.7	73.5
Hydrogen	1.8	3
Nitrogen	2	1.8
Sulfur	6.5	6.2
Ash	0.3	3.4
Moisture	4.8	12.1

Table 173. Sources of CO₂ emissions.

	Fluid coking	Delayed coking
Feed Rate (bbl/day)	200000	85000
Syncrude (bbl/day)	170000	65000
Coke combusted	1200	3000
Fuel gas combusted	2500	1500

3.9.7 Combustion of burner off-gas in a boiler (coke)

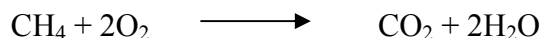
For every Metric Tonne of carbon combusted, 3.67 Metric Tonnes of CO₂ is released. Assumptions are summarized in Table 174. Since Pyrolysis gases are also combusted in the burner, CO₂ emissions are estimated using a carbon content of 70 %. The total amount of CO₂ released from the burner = 3080 Metric Tonnes/day. The total emissions for a 500000 bbl/day production of synthetic crude = 9240 t/day

Table 174. Coke Combustion Parameters.

	estimate
Coke Combusted	1200 t/day
Actual carbon content of coke	83.70%
Carbon content used for CO ₂ emissions calculation	70%

3.9.8 Combustion of fuel gas in a Coking Reactor

The fuels gas in the coking reactor is mainly methane (density = 0.717 kg/m³). Hence the complete combustion of Fuel gas in the reactor is approximated by



Therefore, 1 mole of CH₄ on complete combustion releases 1 mole of CO₂ with density 1.95 kg/m³ at STP.

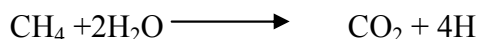
Table 175. Fuel Gas Combustion parameters.

Fuel gas combusted	2500 t/day
Volume of Fuel gas	3486750 m ³ /day
Total amount of CO ₂ released by combustion of fuel gas	6800 t/day
Total emissions for 500,000 bbl/day production of Syncrude	20400 t/day

3.9.9 Water Gas Shift Process in an H₂ Reactor

The amount of hydrogen required for upgrading bitumen to produce 170000 bbl/day of synthetic crude is about 7000000 m³/day. Hydrogen for this process can most economically be produced via the steam reforming of methane or natural gas

Consider the steam reforming of methane in the reactor.



Therefore, for every 4 moles of H₂ formed, 1 mole of CO₂ is released.

Therefore, amount of CO₂ produced = 1.75×10^6 m³/day

Now, 1 mole of CO₂ occupies 22.4 liters at STP.

Therefore, 44 g of CO₂ occupies 22.4 liters at STP.

Therefore, total CO₂ emissions are approximately 3500 t/day.

Total emissions for a 500000 bbl/day production of synthetic crude = 10500 t/day

3.9.10 Refining of Synthetic Crude

During refining of synthetic crude, the CO₂ emissions are thought to mainly result from the production of hydrogen by steam reforming, which is approximately 10,500 t/day.

3.9.11 Transportation of Fuel

Consider the carbon content of the refined fuel be 85 %

Density of fuel = 920 kg/m³,

Total CO₂ emissions are 456.19 kg/bbl

For, 500000 bbl/day, Total CO₂ emissions = 2.2×10^8 kg/day,
which is approximately = 220,000 T/day (metric)

Total amount of CO₂ produced for the whole process = 250,640 T/day.

3.10 Greenhouse Footprint

The production, quantification, regulation of atmospheric carbon dioxide is probably the central issue in determining the future of energy. However, in some ways, the understanding of carbon dioxide is in some ways the same state as the understanding of economics at the time of Adam Smith's *Wealth of Nations*.

At present, it is not even clear whether certain fuels emit net carbon or not. For example, consider the life cycle carbon footprint associated with ethanol (C_2H_5OH). A barrel of ethanol contains 125 kg, of which about 52%, or 65 kg is carbon. Hence, when ethanol is burned about 239 kg of carbon dioxide are produced. This then might have been considered to be the carbon "footprint" associated with carbon dioxide.

Advocates of biomass derived-ethanol, however, were quick to point out that biomass originates as atmospheric carbon dioxide, and is converted to organic matter via the process of photosynthesis. Thus it seemed plausible that the true carbon footprint, or at least the net footprint, might be zero.

Digging deeper, however, other analysts pointed out that the photosynthesis process is enhanced by the use of chemical fertilizers derived from fossil fuels. Similarly, the production of bio ethanol requires that energy be used to plant, harvest, collect and process biomass. Hence, some analysts questioned whether ethanol truly has a lower carbon footprint than oil or coal.

Another example could be wind power. It is commonly assumed that windpower has no greenhouse footprint at all. However, carbon is consumed in the manufacture of the windmill components. In particular steel and aluminum can not be produced without the consumption of coke and/or electrical energy. In addition, labor is required to produce and maintain wind power systems. The people paid to produce wind energy systems are participants in the economy, owning cars and houses and the like. Should this carbon be attached to carbon balance sheet for wind power and other energy systems?

The CO_2 data from Mauna Loa can be used to estimate the mass of carbon dioxide in the earth's atmosphere. This can be done by estimating the total surface area of the earth, and assuming that the earth's atmosphere is mainly close to the earth's surface so that the earth's gravitational constant is approximately the same as a function of altitude. Thus,

$$A_{earth} = 4\pi R_{earth}^2 \quad .$$

The earth's radius is 6.371 km, so that the effective surface area of the earth may be estimated at $5.167 \times 10^{19} \text{ m}^2$. The mass of the atmosphere to first order is obtained by multiplying times the pressure and dividing by the earth's effective gravitational constant.

$$m_{atm} = \frac{A_{earth} p_{atm}}{9.81 \frac{kg}{m^2}} \quad ,$$

With atmospheric pressure equal to 1.013×10^5 Pa, the mass of the earth's atmosphere is thus approximately 5.267×10^{18} kg. The mass of carbon in the atmosphere is then calculated using the mol ratios obtained from the Mauna Loa data, as shown in Figure 137.

$$m_{atm,C} = m_{atm} C_{carbon} \frac{w_C}{w_{air}} ,$$

where the dry mol ratio of carbon in the atmosphere is taken to be 390 parts per million, the molecular weight of carbon w_C is 12.0, and the effective molecular weight of air w_{air} is 28.96 g/mol. Hence, using these assumptions, the total mass of atmospheric carbon is estimated at 8.73×10^{14} kg of carbon, or 873 GTonne of carbon.

Carbon Dioxide emissions are obtained by multiplying by the ratio of atomic masses, or

$$\dot{M}_{CO_2} = \left(\frac{12 + 16 * 2}{12} \right) \dot{M}_C ,$$

or,

$$\dot{M}_{CO_2} = 3.67 \dot{M}_C ,$$

or alternatively, the mass of atmospheric carbon dioxide can be estimated at 3200 GigaTonnes of CO_2 . This corresponds reasonably well with published estimates of 800 GigaTonnes of carbon.⁷²

The carbon content is known to be increasing at an approximately linear rate; i.e., the first time derivative of carbon content is approximately 1.8 ppm carbon dioxide per year, or 0.47% each year, corresponding to approximately 15 GigaTonnes of carbon dioxide per year observed in the atmosphere, as shown in Figure 137 and Figure 138.

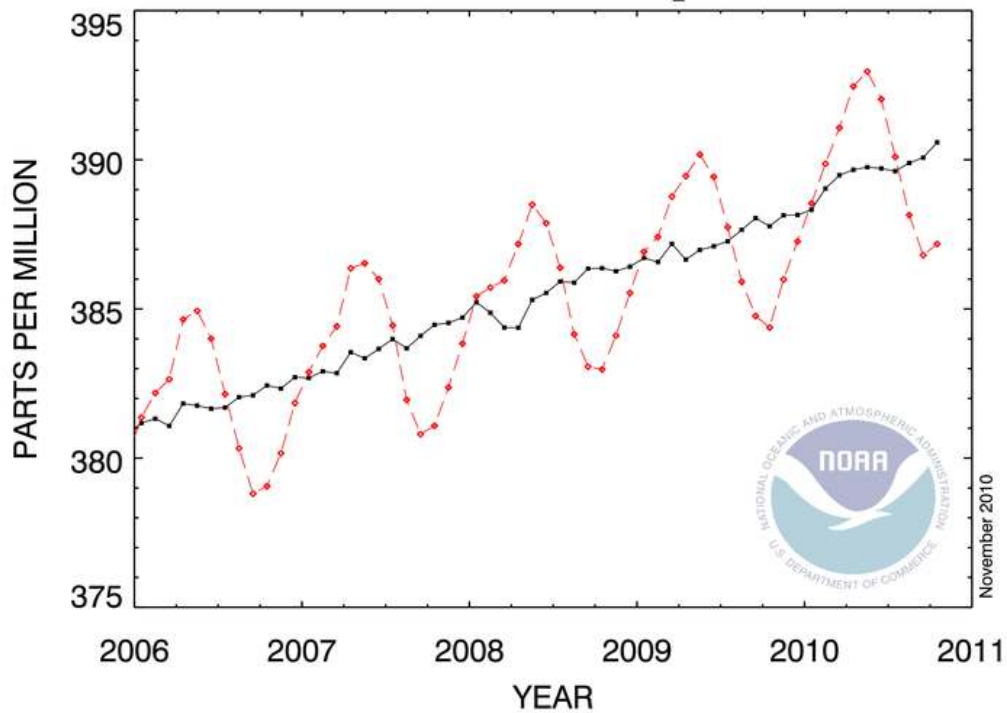


Figure 137. Recent Monthly Mean Carbon Dioxide measured at Mauna Loa. CO_2 concentration is defined as the number of molecules of carbon dioxide divided by the number of all molecules in air, including CO_2 itself, after water vapor has been removed, expressed as parts per million (ppm). (Illustration credit: NOAA).

If, as a thought experiment, anthropogenic emission rate of carbon were somehow kept constant for many years, the atmospheric inventory of carbon dioxide would reach a constant equilibrium, as the leakage rate would eventually balance the anthropogenic emissions rate. Further changes in carbon dioxide inventory would then depend upon the second time derivative of anthropogenic carbon mass. Currently, however, the atmosphere is presumed to be far from saturated, meaning that CO_2 concentration in the atmosphere will continue to rise linearly for many years.

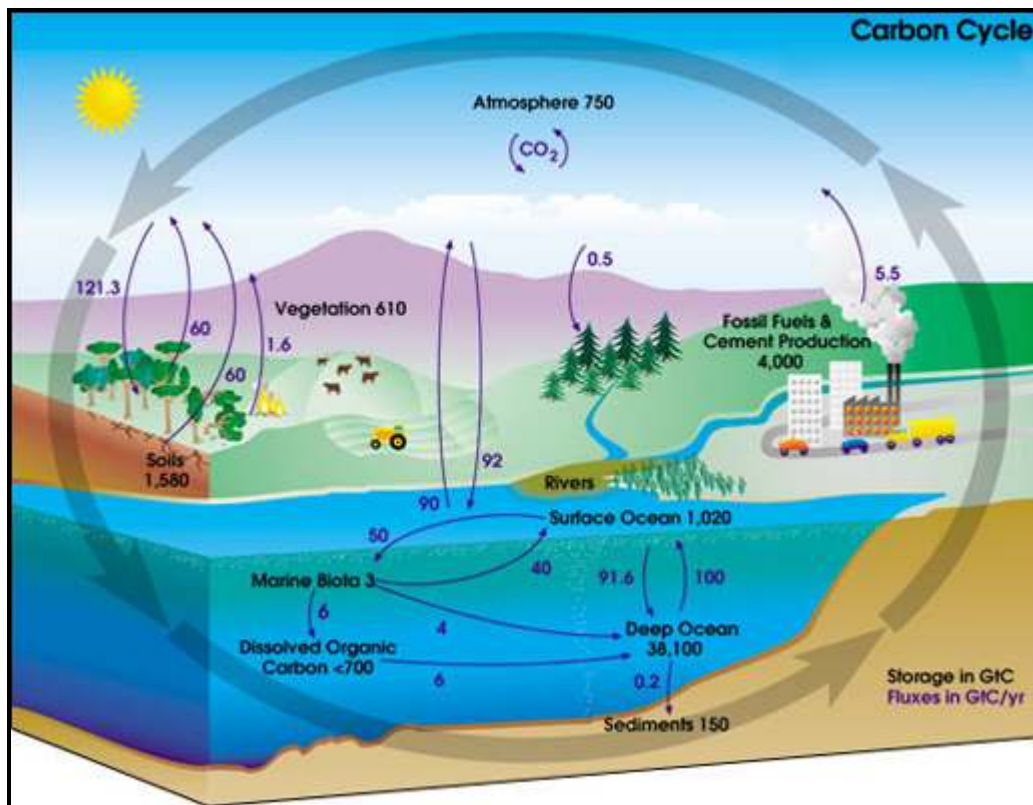


Figure 138. Carbon balance, from NASA Earth Observatory. The units are GigaTonnes of carbon per year. Illustration credit: NASA Earth Observatory; http://www.nasa.gov/centers/langley/news/researchernews/rn_carboncycle.html on 15 Nov 2010.

This net rate of increase of the carbon inventory is substantially lower than the amount of carbon dioxide thought to be emitted into the atmosphere.

The gross emissions of carbon dioxide (i.e., at the point of production) are also increasing, as shown below in the CRDIAC graph in Figure 139. To obtain carbon dioxide emissions, rather than carbon emissions, it is necessary to multiply the ordinate by 3.67.

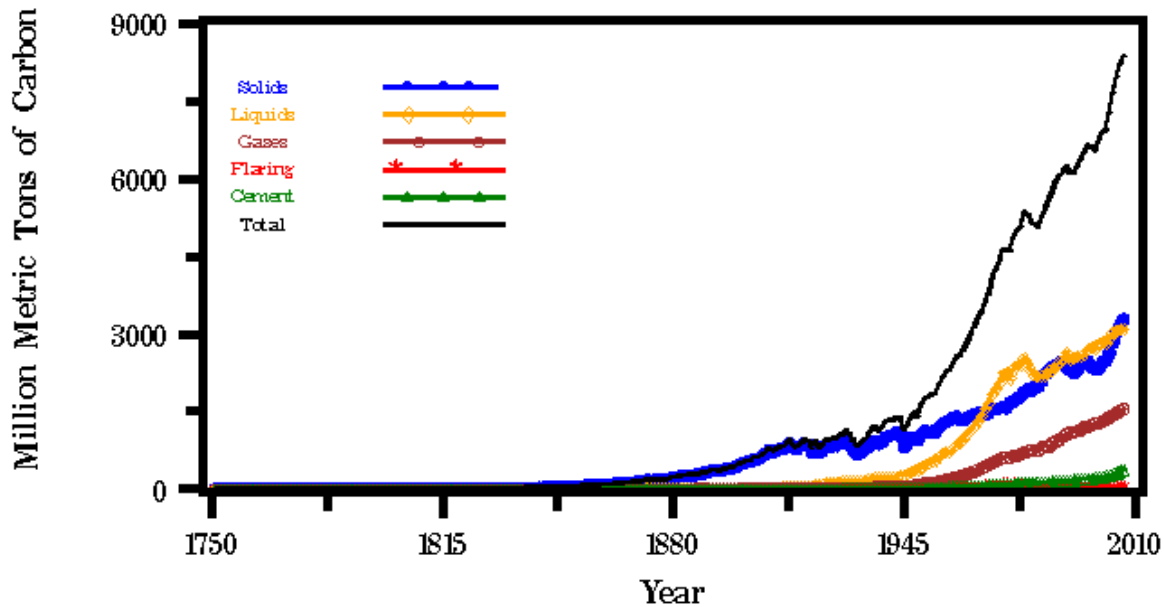


Figure 139. CRDIAC Estimate of total Carbon Emissions.

The emissions rate is of course related to the amount of carbon mass measured in the atmosphere, but not identical. Significant amounts of carbon evidently transferred to other reservoirs other than the atmosphere.

According to the Department of Energy's Carbon Dioxide Information Analysis Center (CDIAC), as of 2008 31.9 GigaTonnes of carbon dioxide were emitted to the atmosphere from anthropogenic sources, and growing by 1.7 percent per year; that is, the second derivative of carbon dioxide mass is some 550 MTonnes per year per year.⁷³

Comparing these values with the measured carbon dioxide, the atmospheric inventory of carbon dioxide is increasing at the rate of only 15 GigaTonnes per year of carbon dioxide rather than 31.9 GigaTonnes emitted. Hence,

$$\Delta M_{CO_2 atm} = 0.47 \Delta M_{CO_2 emitted}$$

This could be true if the lifetime of anthropogenic carbon dioxide in the atmosphere were less than a year; however the environmental community believes that all carbon dioxide persists for much longer times.

This increase in atmospheric carbon dioxide is thought to have a causal relationship with an increase in global average temperature. CO₂ is known to have a high absorption cross section in the infrared spectrum, meaning that some level of warming must certainly be present. The total effect depends upon empirical feedback coefficients. For calculational purposes the Intergovernmental Panel on Climate Change 1999 estimate of 0.02 degrees per year is considered to be the most authoritative estimate of global average temperature change, despite the fact that a linear least squares fit of the actual data shows a pause in the increase of global average temperature over the past nine years, as shown in Figure 140. Global average

temperature did rise significantly from 1976 to 2002, however. Whether or not future global temperature trends will resume the positive ramp of that time period is a matter of some debate.

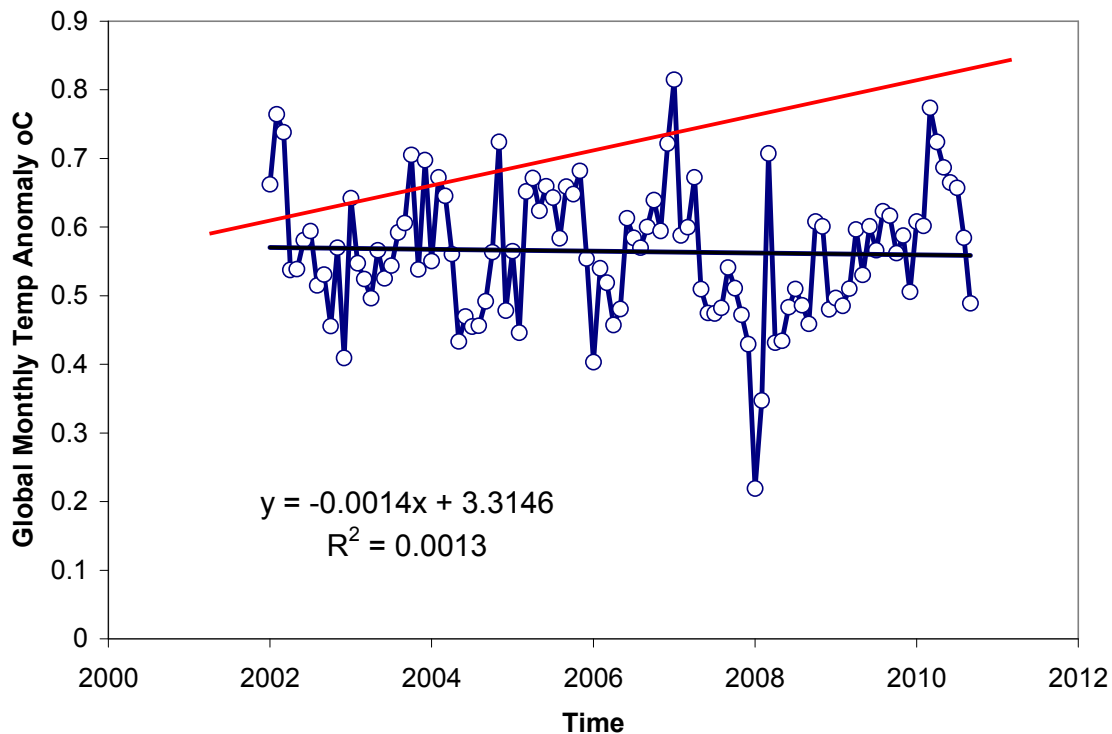


Figure 140. Global Average Temperature as estimated by the National Climatic Data Center, from January 2002 to Sept 2010. The least squares fit (black line) of the data is generally disregarded in favor of the IPCC estimate (red line). Hence it is expected that at some point in time the data will conform more closely to the model.

3.10.1 Gross Domestic Product and Its Correlation to Carbon Dioxide

The emission of carbon dioxide, in turn, is thought to be directly due to the consumption of carbon materials, mainly fuels, in the process of producing economic benefits. Hence it does not come as a surprise that the rise in carbon dioxide coincides with an increase in the global Gross Domestic Product.

In other words, economic activity is strongly correlated with the generation of carbon dioxide. This can be shown by first considering the top 20 largest nations in terms of Gross Domestic Product, as shown in Figure 141 and Table 176. These estimates are made based on Purchasing Power Parity (PPP) which means that they are corrected for differences in cost of living and inflation in different countries.

Table 176. Top 20 Largest GDP, as Estimated by CIA Factbook, 2009.

Rank	Country	GDP (PPP) Billions of USD	GDP(PPP) Percent of World
1	United States	14260	20.38%
2	People's Republic of China	8789	12.56%
3	Japan	4137	5.91%
4	India	3560	5.09%
5	Germany	2811	4.02%
6	United Kingdom	2149	3.07%
7	Russia	2116	3.02%
8	France	2110	3.02%
9	Brazil	2025	2.89%
10	Italy	1760	2.52%
11	Mexico	1482	2.12%
12	Spain	1368	1.95%
13	South Korea	1356	1.94%
14	Canada	1285	1.84%
15	Indonesia	969.2	1.38%
16	Iran	876	1.25%
17	Turkey	863.3	1.23%
18	Australia	824.3	1.18%
19	Republic of China (Taiwan)	717.7	1.03%
20	Poland	690.1	0.99%
	Top 20 GDP	54148.6	77.38%
	World	69980	100.00%

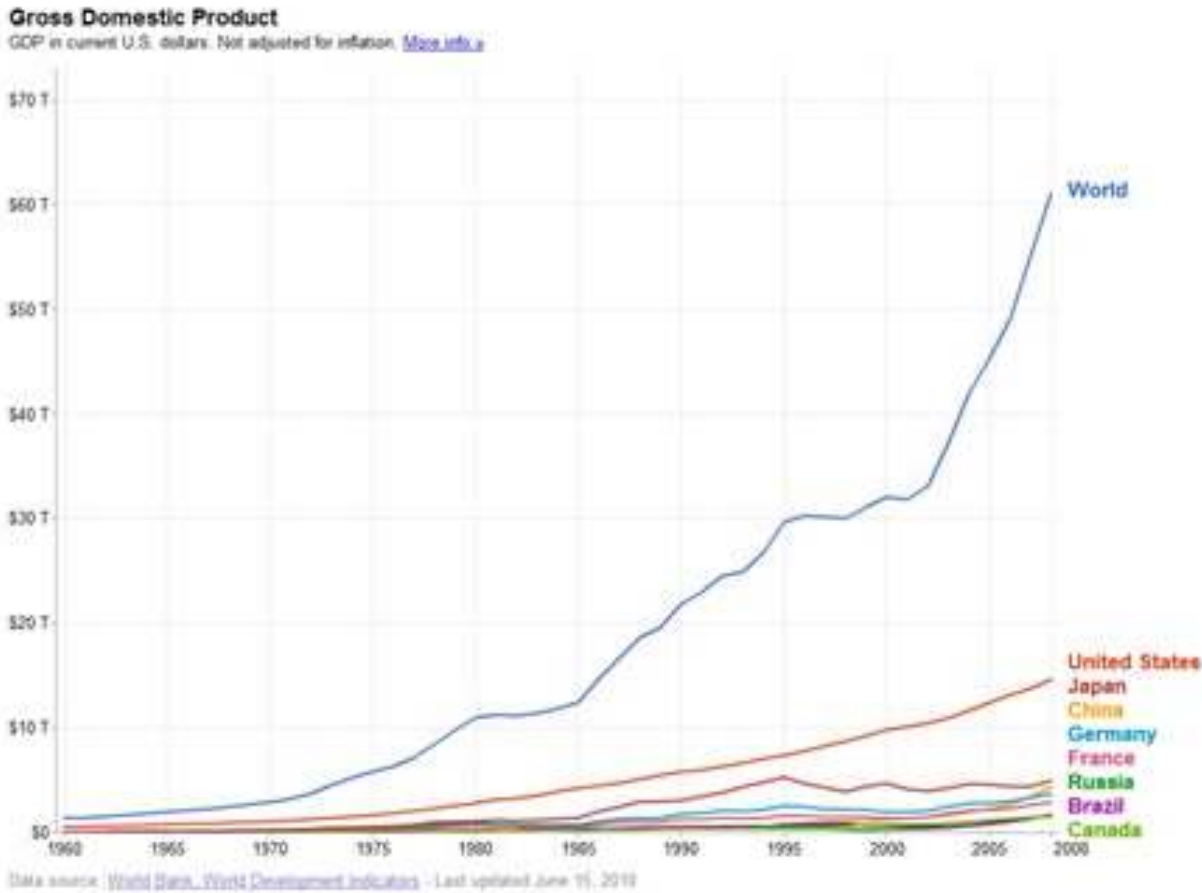


Figure 141. World Gross Domestic Product.⁷⁴

The global GDP growth function can be coarsely approximated as a linear function over the period 1985 to 2010, from GDP growing at = ~12 Trillion dollars to the present GDP = \$69 Trillion dollars. Hence the first time derivative of GDP is about

$$\frac{dGDP}{dt} \approx \frac{6.9 \times 10^{13} - 1.2 \times 10^{13} \text{ USD}}{25 \text{ years}}$$

$$\frac{dGDP}{dt} \approx 2.3 \times 10^{12} \frac{\text{USD}}{\text{year}}$$

Carbon emissions are estimated by country by the International Energy Agency (IEA) in Table 177.⁷⁵ For countries not separately listed by the IEA, 2007 data were used from the Intersociety Panel on Climate Change.⁷⁶ Interestingly, the United States is no longer the number one emitter of carbon dioxide in the world. Rather, that dubious honor now goes to the People's Republic of China. This is due to several factors including extensive utilization of coal for electric power, as well as production of heavy industry commodities such as steel, aluminum and concrete.

Table 177. Carbon Dioxide Emissions of the Top 20 GDP Nations.

Rank	Country	CO2 Emissions, Million Tonnes	CO2 Emissions Percent of World
2	United States	5596	20.38%
1	People's Republic of China	6551	12.56%
5	Japan	1151	5.91%
3	India	1612	5.09%
6	Germany	804	4.02%
9	United Kingdom	510	3.07%
4	Russia	1594	3.02%
16	France	368	3.02%
17	Brazil	368	2.89%
13	Italy	430	2.52%
12	Mexico	471	2.12%
18	Spain	318	1.95%
10	South Korea	503	1.94%
8	Canada	557	1.84%
15	Indonesia	397	1.38%
11	Iran	496	1.25%
20	Turkey	264	1.23%
14	Australia	398	1.18%
7	Republic of China (Taiwan)	750	1.03%
19	Poland	318	0.99%
	Top 20 GDP	23456	79.83%
	World	29381	100.00%

3.10.2 Carbon Dioxide Intensity

The quantity Carbon Dioxide Intensity is defined as

$$I_{CO_2} = \frac{M_{CO_2}}{GDP} \quad ,$$

where GDP is the Gross Domestic Product of some nation, measured in dollars; and M_{CO_2} is one year's worth of total carbon dioxide emissions to the environment from that nation. That the literature often uses "carbon" and "carbon dioxide" interchangeably, introducing needless confusion into the discussion. Of course CO_2 has a mol weight of 44 compared to 12 for carbon only.

The mass of carbon dioxide emissions may seem straightforward enough to measure, but it may be more controversial when it is necessary to assign attribution (i.e., for tax purposes). For example, if one nation burns fossil fuel in a power plant to produce electricity, and that electricity is sent via transmission lines to another country, which country is charged? Or, if a nation imports steel from another nation, which nation should be charged for the carbon emissions that result from manufacturing and transporting the steel?

In addition to the obvious case of carbon dioxide production for energy, carbon dioxide is also produced in the manufacture of cement, metals and other consumer goods which are not necessarily consumed in the nation that produces them.

Note also that the carbon dioxide emitted per year represents a *gross* amount, whereas the *net* amount must be used to calculate the actual inventory of carbon dioxide in the atmosphere.

With these potential misgivings in mind, Table 178 lists the Carbon Dioxide Intensity for the Top 20 GDP Nations in the same order used previously (see also Figure 142). China has a high carbon dioxide intensity because much of that nation's electric power is derived from coal. In addition, it has a great deal of heavy industry and manufacturing which in turn generates a significant amount of carbon emissions.

Table 178. Carbon Dioxide Intensity for the Top 20 GDP Nations.

GDP Rank	Country	Carbon Dioxide Intensity (kg CO2/\$ GDP)	Carbon Dioxide Intensity (Tonne CO2/\$ GDP)
1	United States	0.392	3.92e-4
2	People's Republic of China	0.745	7.45e-4
3	Japan	0.278	2.78e-4
4	India	0.453	4.53e-4
5	Germany	0.286	2.86e-4
6	United Kingdom	0.237	2.37e-4
7	Russia	0.753	7.53e-4
8	France	0.174	1.74e-4
9	Brazil	0.182	1.82e-4
10	Italy	0.244	2.44e-4
11	Mexico	0.318	3.18e-4
12	Spain	0.232	2.32e-4
13	South Korea	0.371	3.71e-4
14	Canada	0.433	4.33e-4
15	Indonesia	0.410	4.10e-4
16	Iran	0.566	5.66e-4
17	Turkey	0.306	3.06e-4
18	Australia	0.483	4.83e-4
19	Republic of China (Taiwan)	1.045	1.045e-3
20	Poland	0.461	4.61e-4
	World	0.420	4.20e-4

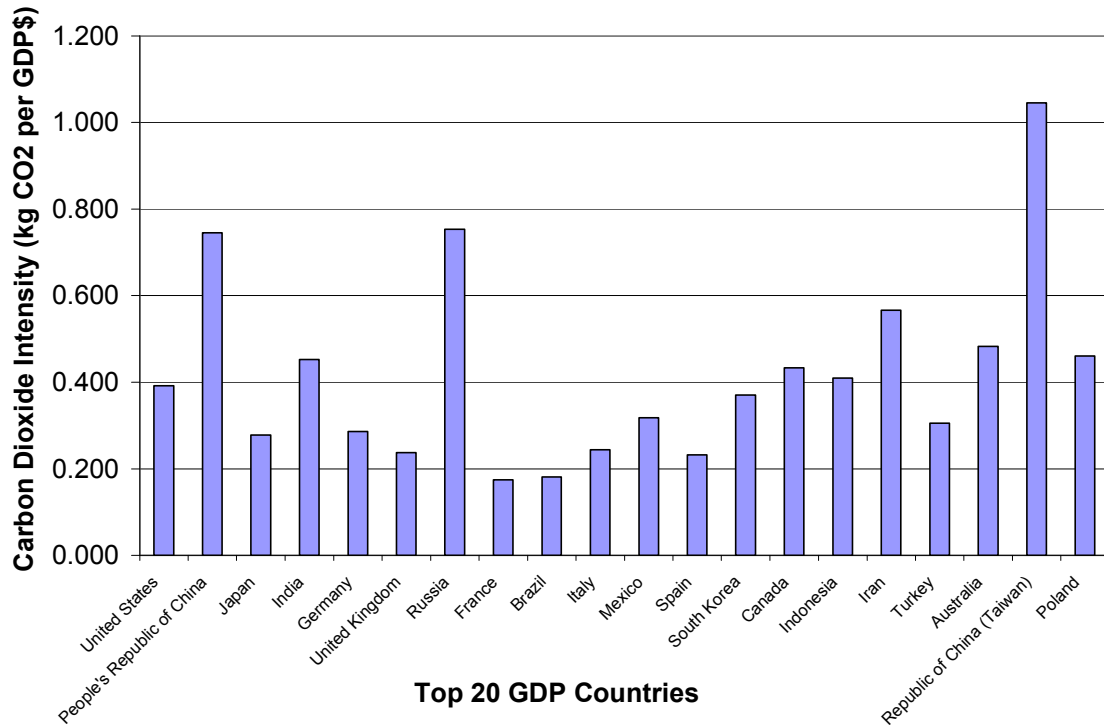


Figure 142. Comparative CO₂ Intensity by Country.

3.10.3 Energy Intensity

Yet another parameter of importance is energy intensity, defined as the total energy consumed by a country or region in a year divided by the annual gross domestic product, or

$$I_E = \frac{E_{consumed}}{GDP}$$

Notionally, energy intensity measures the extent to which a country consumes energy as it produces wealth for its citizens. Thus a low energy intensity could be interpreted as indicative of an energy efficient economy.

However, energy intensity is probably flawed for countries with very low GDP. For example, according to estimates from the Energy Information Administration International Energy Annual 2006, Afghanistan has an energy intensity about a factor of ten lower than the United States. It can hardly be the case that the Afghanistan economy is more energy efficient than that of the United States. However, putting aside those misgivings for the moment, in comparing the top 20 GDP nations, the use of energy intensity seems more reasonable, as countries in which energy prices are high tend to score lower (i.e., better) than the United States, whereas countries which are less advanced in terms of their energy consumption capability tend to score higher (worse). This is shown in Table 179 and Figure 143.

Table 179. Energy Intensity for the Top 20 GDP Nations.⁷⁷

GDP Rank	Country	Energy Intensity (Joules /\$GDP)
1	United States	9.32e6
2	People's Republic of China	1.45e7
3	Japan	6.84e6
4	India	7.88e6
5	Germany	6.77e6
6	United Kingdom	5.52e6
7	Russia	1.98e7
8	France	6.95e6
9	Brazil	7.21e6
10	Italy	5.94e6
11	Mexico	6.45e6
12	Spain	6.57e6
13	South Korea	1.21e7
14	Canada	1.38e7
15	Indonesia	6.64e6
16	Iran	1.48e7
17	Turkey	6.04e6
18	Australia	9.45e6
19	Republic of China (Taiwan)	8.74e6
20	Poland	8.35e6
	World	9.353e6

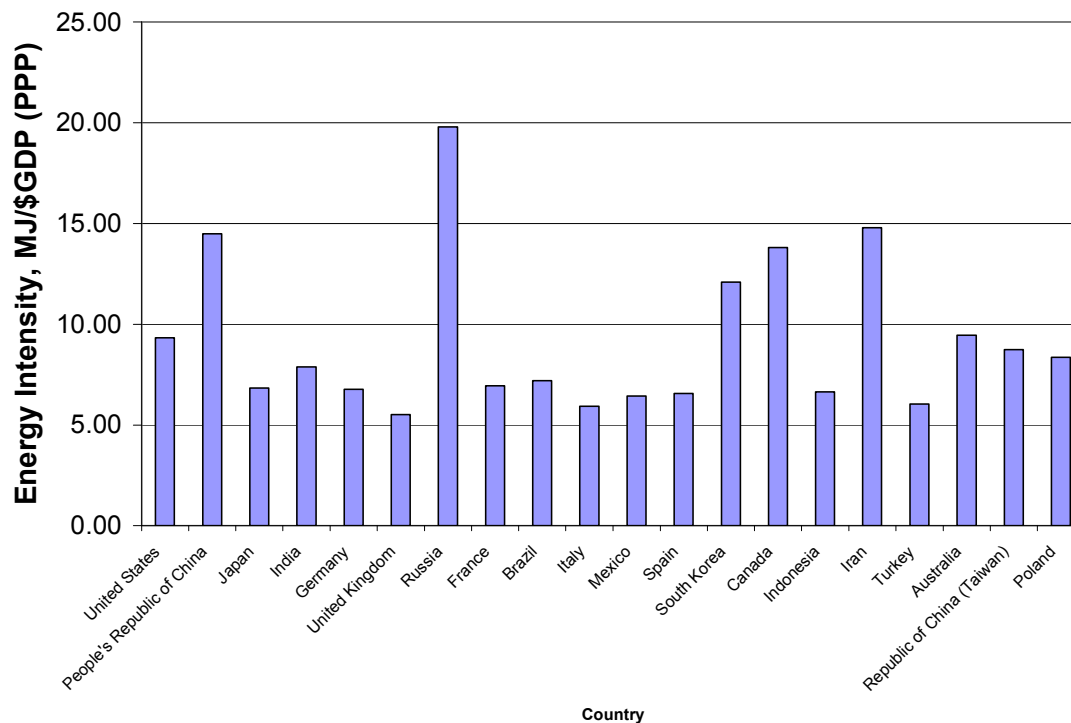


Figure 143. Energy Intensity for Top 20 GDP Nations, MJ/\$GDP (Purchase Power Parity).

Another deficiency of the concept of Energy Intensity is that it does not distinguish between different types of energy. Certainly a kilowatt-hour of electricity is valued differently than a kilowatt hour of thermal energy.

The choice of energy source is vitally important to determining the carbon dioxide footprint. Obviously, the amount of carbon dioxide emitted per unit energy consumed varies according to different fuels, obviously, with natural gas having the highest ratio of enthalpy divided by carbon dioxide emissions.

Table 180 lists chemical enthalpy divided by the mass of carbon dioxide emissions for several fuels. This does not include any penalty for extraction. Hydrogen fuel is not separately included, since despite fantasies of a few years ago, hydrogen is not freely obtainable. Rather, the horrible truth is that it is still most economically generated from natural gas with the addition of thermal energy.

Table 180. Chemical Enthalpy Divided by CO₂ Mass for Different Fuels.

Fuel	Specific Enthalpy, J/kg	CO ₂ Emissions per kg of fuel	Enthalpy/CO ₂ Emissions
		kg	J/kg
Petcoke	3.2E+07	3.67	8.73E+06
Bituminous Coal (Dry, ash-free)	3.5E+07	3.43	1.02E+07
Petroleum Crude	4.5E+07	3.33	1.35E+07
Methane/natural gas	5.6E+07	2.75	2.04E+07

The values in do not include penalties for extraction or for processing. It may sometimes be the case that additional carbon must be burned in order to provide the energy needed to obtain, refine and transport fuels. In some cases, the additional consumption might be as much as two or three times the amount of chemical enthalpy available in the products. For example, in the production of oil sands crude, it is generally conceded that the energy required to produce a barrel of crude is comparable to the chemical enthalpy of that product. Similarly, in the debate concerning corn ethanol, some analysts have suggested that the amount of enthalpy required to produce a kilogram of corn ethanol is higher than the ethanol contained in the product.

The atmospheric carbon dioxide inventory, global average temperature and global GDP can be all be approximated as linear functions of time, at least over the past few decades. Moreover, from a phenomenological point of view, these are not arbitrary correlations, but in fact environmental scientists suggest that modern economic activity causes carbon to be oxidized which in turn causes the change in global average temperature.

Thus,

$$\Delta C_{CO_2} = \frac{\partial C_{CO_2}}{\partial t} \Delta t$$

$$\Delta T = \frac{\partial T}{\partial t} \Delta t$$

$$\Delta GDP = \frac{\partial GDP}{\partial t} \Delta t$$

and the values of the constants are,

$$\frac{\partial GDP}{\partial t} = 1.2 \times 10^{12} \frac{\$}{year}$$

$$\frac{\partial C_{CO_2}}{\partial t} = 1.8 \frac{ppm}{year} = 31.9 \frac{GT (emitted)}{year}$$

$$\frac{\partial T}{\partial t} = .02 \frac{^{\circ}C}{year}$$

The correlation for CO₂ change rate is based on the observed rate of concentration change (i.e., 1.8 ppm/year), whereas the 31.9 GT/year refers to the actual emissions rate.

It is also possible to correlate temperature rise that is believed to result from changes in carbon emission. That is,

$$\Delta T = \frac{.02 \frac{^{\circ}\text{C}}{\text{year}}}{31.9 \times 10^9 \frac{\text{Tonnes}}{\text{year}}} \Delta M_{\text{CO}_2 \text{ emitted}}$$

or,

$$\Delta T = 6.3 \times 10^{-13} \frac{^{\circ}\text{C}}{\text{Tonne}} \Delta M_{\text{CO}_2} \quad .$$

It is also possible to produce a correlation between GDP and global warming, for example:

$$\Delta T = \frac{.02 \frac{^{\circ}\text{C}}{\text{year}}}{1.2 \times 10^{12} \frac{\$}{\text{year}}} \Delta \text{GDP} \quad ,$$

or,

$$\Delta T = 1.7 \times 10^{-14} \frac{^{\circ}\text{C}}{\$} \Delta \text{GDP} \quad .$$

The existence of a correlation does not prove which is the cause and which is the effect, but does suggest a relationship.

Adding to the global Gross Domestic Product results in a discrete change in global average temperature. With advances in low-carbon technologies, it may be eventually possible to reduce the coefficient and thus lessen the impact on global temperature.

A word of caution may be applied here concerning the causal relationship between these parameters. These quantities are correlated, meaning that they all tended increase over the past several years. But this does not necessarily prove that there is a cause and effect relationships. It is possible to dispute the precise relationship between carbon dioxide and GDP, for example, in that there may be other variables that are quite independent of the carbon cycle. Nevertheless, there is adequate reason for believing that a functional relationship does exist, and future modeling efforts may result in much more accurate models than the simplistic first order analysis suggested here.

3.10.4 Greenhouse Gas Footprint

A total model for estimating greenhouse footprint, even in a preliminary way, still needs to be created. Such a model should account for not only the carbon that is produced directly, but also indirect carbon that is produced via emissions from heat sources or reforming processes to generate hydrogen, to cite two common ways by which carbon dioxide might be indirectly produced in a chemical process. Thermal energy might commonly involve combustion of natural gas, and the production of hydrogen via methane reforming and water gas shift necessarily co-produces carbon dioxide along with hydrogen.

A third source of carbon dioxide might be the carbon associated with the capital cost and operational cost which arise from the development of a given enterprise. For example, if steel and concrete are used to create a solar power plant, there are carbon emissions that result from the production of steel and concrete as well as transportation costs. Labor costs will certainly result in people using their paychecks to buy cars, houses and the like which results in additional consumption of fuels. These costs must be included and appropriately averaged over the lifetime of the plant.

Hence, in order to determine the greenhouse footprint for coal liquefaction processes as well as others, a top-down methodology is selected, in which global quantities such as carbon dioxide emission, energy production and gross domestic product are parameterized and compared. Once global relationships are discerned, they are applied to determine the carbon dioxide footprint and the economic footprint of individual plants.

a. First the direct carbon dioxide production is calculated based on the amount of carbon dioxide produced in the process. For example, if syngas is produced in some process, it usually results in the coproduction of carbon dioxide in the same reaction.

b. Secondary sources of carbon dioxide are calculated. For a process which has some efficiency η , defined as the normalized chemical enthalpy of the products minus energy expended in processing, then the thermal energy requirement for the process is proportional to $(1 - \eta)$. If possible, the carbon dioxide emission should be calculated based on the actual technology used in the process. If specific information is not available, however, then the mass of carbon dioxide produced per unit energy can be estimated according to the country-specific parameters Energy Intensity and Carbon Dioxide Intensity, or

$$M_{CO_2} = \frac{I_{CO_2}}{E_{Consumed}}$$

Secondary sources of carbon dioxide need to be considered. For example if a hypothetical plant requires N kilowatt-hours per year, the actual emissions at the are minimized by stipulating that this energy be supplied only as electricity. In reality, however, if that electricity is produced by burning fossil fuels, then it seems sensible to count the carbon burned to provide that electricity. By similar reasoning, the carbon dioxide footprint accounting system needs to determine how much of that carbon dioxide burden should be assigned to the power plant, and how much needs to be assigned to the chemical plant operator that opted to not buy N kilowatt-hours worth of thermal energy on site, and instead caused $3N$ kWh(T) to be produced at the power plant.

c. Carbon dioxide resulting from capital cost must also be estimated. Ideally this would be estimated based on knowledge of the specific design of the process. However, if information is unavailable, this can still be crudely estimated by applying the country-specific carbon dioxide intensity to the value of the capital investment. This is probably best expressed as a “levelized” amount, which is to say an average over the projected lifetime of the system.

d. Carbon dioxide resulting from the general economy surrounding the plant can be estimated using the country-specific Energy Intensity to determine the amount of GDP associated with that quantity of energy, i.e.,

$$\Delta GDP = \frac{E_{consumed}}{I_E} \quad .$$

Then the corresponding Carbon Dioxide Intensity can be used to determine that amount of carbon dioxide associated with that portion of the economy,

$$M_{CO_2} = \Delta GDP * I_{CO_2} \quad ,$$

or,

$$M_{CO_2} = E_{consumed} \frac{I_{CO_2}}{I_E} \quad .$$

The above outlined approach is compiled in a spreadsheet model which might be used to compare different energy production enterprises. As examples, Table 181 lists some processes with different yields and thermal efficiencies. The efficiency of the CTL/Quantex efficiency was previously estimated at 80% based upon thermal modeling. Thermal energy is needed to heat coal and solvent to allow melting and dissolution; with electrical energy used for distillation; with thermal energy also required in the final distillation process. These simple processes do not require large quantities of energy and so for that reason the efficiency can certainly be higher than other direct liquefaction protocols, much of which also include energy intensive steps such as hydro-upgrading in the same process.

The efficiency of Fischer Tropsch systems utilizing coal are about 27%, according to estimates shown in Table 181 below. Efficiency is defined as the chemical enthalpy of the products divided by the total amount of energy expended in the processing of those products. Hence this is not quite an “apples to apples” comparison since the products differ according to the process. In particular, Fischer Tropsch processes result in diesel fuel which is close to being a finished product, whereas heavy crude produced in the Quantex process would require additional processing in order to result in a comparable product stream. The WVU/Quantex process does not hydrogenate as other Direct Liquefaction processes do; hence efficiency can be significantly higher than the Gulf Direct Liquefaction process. The yield of products from the Quantex process is essentially 100% since generally there are no waste products from coal processing. However, the processing energy is assumed to be made up by burning a fraction of the coal used in the process. Thus, a short ton of coal corresponds to 241 gallons of material

with density 1.0 g/cm^3 , or 5.74 barrels. An 80% efficient process would result in a yield not higher than $5.74 \text{ bbl} * 0.80 = 4.6 \text{ bbl}$.

Table 181. Comparative Efficiency and Yields for Synthetic Fuels.⁷⁸

	Gulf Direct Liquefaction	Sasol FT CTL	Shell FT GTL	Quantex CTL
Yield, Barrels Equivalent per short Ton	3	1.2	N/A	4.3
Thermal Conversion efficiency, percent	62	27	54	80

IV. SYSTEM DESIGN

4.1 Process Description

The FutureGen project was originally intended to form the core of the national capability of producing hydrogen. Currently the project has evolved to an oxyfuel plant rather than using gasification. Nevertheless future plants may one day be used for producing hydrogen.

A small amount of hydrogenation can be used in the current process to enhance coal solubility in aromatic oils.

A point design at 20,000 tons per year is nominated as a design point for a commercial demonstration unit capable of producing liquid products and carbon products using hydrogen-assisted solvent extraction. This design follows the suggestion in DE-FC26-03NT41873, Development of Continuous Solvent Extraction Processes for Coal Derived Carbon Products, that such a facility would be best located at a site already permitted to process coal tar pitch; e.g., at a pitch plant similar to sites at Follansbee WV or Clairton PA. Preliminary cost analysis suggests that an investment of some \$12 million dollars would be required. Since margins associated with commodity hydrocarbon products will likely be less than \$100 per ton, a cash-flow-positive operation would likely require a minimum of 20,000 tons per year of products.

According to the FutureGen Prospectus as of March 31, 2005, FutureGen or some similar gasification reactor would produce about 1 million tons of carbon dioxide to be sequestered. This corresponds to about 270,000 tons of carbon per year. Thus, 20,000 tons of carbon processed would be a reasonable fraction of the amount produced in a FutureGen plant.

FutureGen hydrogen is utilized to produce coal derived feedstocks for carbon products, chemicals and fuels. The basic process is illustrated in Figure 144. The process consists of the following steps:

a. A solvent feedstock is prepared by catalytically hydrotreating coal distillate at elevated temperature and pressure (approximately 400 °C and 1000 psig). Hydrogen would be optimally obtained from a coal gasification unit, such as which is expected to be available from the DOE FutureGen project. Alternatively, hydrogen could be obtained via tube trailer or pipeline. In either case, the result sought is the addition of about 0.5% hydrogen by weight. This process is accomplished in a high pressure reactor such as an autoclave reactor or trickle bed reactor.

b. Coal is crushed to -50 mesh and combined with the hydrotreated solvent feedstock in a second reactor at similar temperatures and pressures, but without the use of a catalyst. The ratio of coal to solvent is from 1:2 to 1:3. The result is a digested slurry that is about 90% liquid, and 10% solids (primarily mineral matter and fixed carbon).

c. The Slurry is separated into a 99.7% ash-free liquid stream, as well as a solid-containing medium. Depending on the desired characteristics of the solid-containing medium, the ash content can range from approximately 15% to 40% by weight, with the remainder being comprised of entrained solvent and liquefied coal.

d. The solid medium is to be qualified as a fuel for FutureGen. Alternatively, it can be blended with the inlet feedstock to a coal-fired power plant, or blended in asphalt mixtures.

e. The liquid phase can be considered to be a crude hydrocarbon source that can be refined by distillation and possibly other processes. Simple distillation can result in the production of two cuts. The overhead lights can be re-utilized as a coal solvent, or incorporated in liquid fuels products. The distillation bottoms can be blended as a binder pitch or impregnation pitch for the metals smelting industry. Alternatively, anisotropic coke can be produced by delayed coking, with the devolatilized liquids from that process being utilized as a blend for fuels such as gasoline, diesel, aviation fuel, home heating oil, etc. Combining coal derived liquids with alcohols such as ethanol is perceived to be a promising approach.

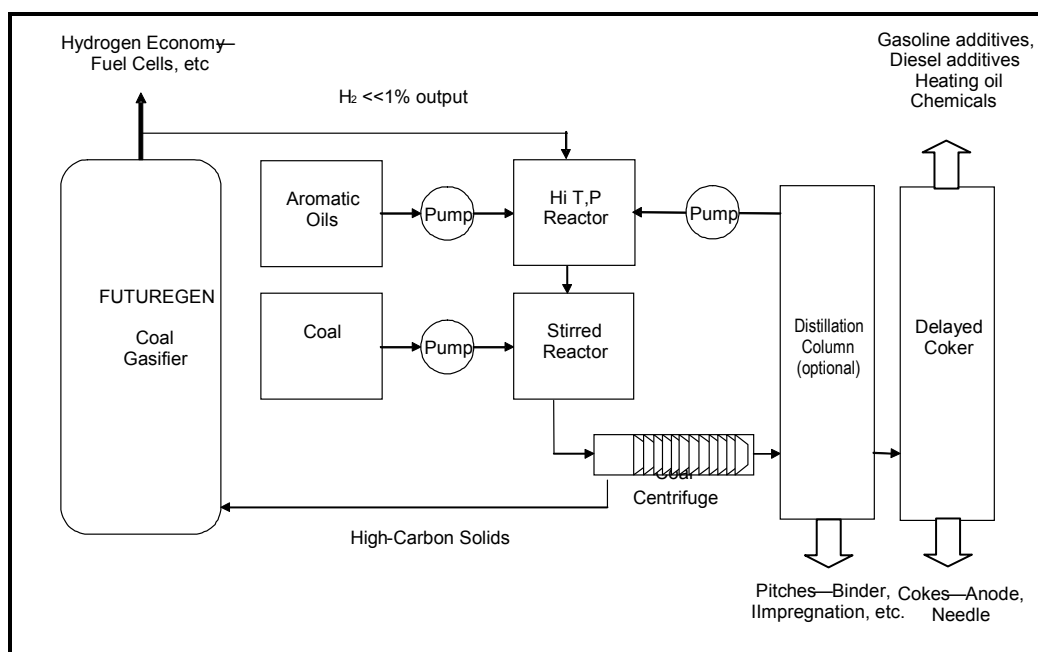


Figure 144. Process Diagram for Carbon Products Process for Synthetic Pitch and Coke Precursors.

CAPCOST, a computer model used to calculate chemical plant costs using standard data bases for equipment cost estimates, was used to establish preliminary economics for a plant dedicated to the production of carbon products.⁷⁹ It is presumed that the bottom line estimates vary considerably as a more refined design evolves.

These preliminary results suggest that coal-derived binder pitch can be profitable and competitive with petroleum derived products based on \$35 per barrel crude petroleum. The plant capacity is assumed to be 20,000 tons of product per year (or 104,000 barrels per year @ 1.1 specific gravity), based on 7000 hours of operation per year. The following assumptions were made:

a. The products are assumed to consist of the solid tails of the centrifugation process, as well as the bottoms from distilling the centrifuged liquids. The bottoms are assumed to be useful as blending agents for binder pitch or impregnation pitch with little or no additional processing.

The centrifuge tails are assumed to be of value for gasification (i.e., a fuel for FutureGen or other facility capable of accommodating a small amount of high ash material).

b. The plant would be located a site currently used for pitch processing; hence, a site that is already capable of distilling coal liquids. Hence the capital costs associated with distillation equipments and other refining equipment are not included.

c. Permitting costs are not included. Other material costs are listed in below.

d. FutureGen-produced hydrogen is assumed to be readily available at the site at a cost of \$1.50 per kg.

e. Reactor costs are pessimistically estimated based on autoclave reactors for both hydrogenation and coal digestion in order to be conservative, even though pipe reactors are now thought to be more effective and less costly.

f. An approximate mass balance is detailed in Table 183, along with economic values associated with feedstocks and products.

g. Other economic assumptions are listed in Table 184.

h. Uncertainties in market values, taxes, equipment costs, utility costs etc. are handled through a Monte Carlo analysis that assumes probabilistic values for each cost. These results are shown graphically from Figure 145 through Figure 151.

A mass balance was created based on the current protocol for producing binder pitch. Hydrogen is assumed to be available from FutureGen. The carbon products plant could be collocated with FutureGen, or at least close enough that pipeline costs to supply hydrogen are not excessive. If hydrogen were to be supplied via tube trailer, the cost to the plant could be easily 300% higher.

The coal is assumed to be an eastern bituminous coal such as the Kingwood type, containing about seven percent ash. A representative proximate analysis is shown in Table 182. The price of this coal is assumed to be \$55 per short ton.

The solvent is Koppers coal tar distillate (CTD), obtained from metallurgical coke production plants. Hydrogenation is assumed to require 0.5% hydrogen mass versus the mass of the solvent. The ratio of CTD to coal is 2:1 to 3:1.

Based on pilot scale tests, the dry-ash free coal has been measured to be as high as 90% soluble in hydrotreated coal tar distillate, although for the purposes of establishing a conservative baseline, that specification is dropped to 85%. If 7% ash is included in this basis, the resultant coal would be 79% converted to liquid and with 21% insolubles.

Centrifugation is required to reduce the ash content in the liquid phase to 0.5%, with a goal of 0.2%. Since the solid separations step is not 100% efficient, some of the liquid phase material would be entrained in the nominal solid phase tails. The fate of the liquefied coal stream is then 73% liquids and 27% “tails”. The liquid product is distilled to create a pitch. If the softening point is selected at about 110 °C, this pitch (with minor additional processing) can

be suitable for use as a binder pitch for use in metals smelting applications, or as an impregnation pitch.

A 20,000 ton per year plant can be profitable on the basis of relatively high margin specialty pitches, cokes and chemicals. For example, needle coke enjoys a world market price of some \$450-\$600 per ton depending on its grade. Conversely, fuel grade coke prices can be substantially less than \$100 per ton, and can even be negative if it is unacceptable for power plant use due to environmental constraints.

The overhead light distillation products can be recycled as a coal solvent, or refined into hydrocarbon products such as liquid fuels.

Alternatively, with additional coking (for example, in a delayed coker), the bottoms can be converted to a coke. In this case, the aromaticity of coal derivatives coupled with low metals content and near-zero quinoline insolubles can lead to an anisotropic needle grade coke. The additional liquids liberated from delayed coking have not been adequately characterized yet, but are expected to be suitable for liquid fuels.

Another product is the high-ash tails from the centrifuge. This material is expected to contain substantial ash and fixed carbon. One of the objectives of this effort is to determine whether the centrifuge tails can be converted to an acceptable fuel for FutureGen. Gasification processes such as FutureGen have the advantage of being able to accommodate high ash, high carbon materials in an environmentally sound process, since the ash is acquired in the form of slag, and CO₂ is captured and sequestered.

The process for producing a FutureGen-compatible fuel has not yet been identified. Options include blending the centrifuge tails directly with other FutureGen feedstocks; or carrying out additional processing prior to blending. The option of coking the centrifuge tails in order to produce liquid fuels is highly attractive owing to the prospect of creating high-value-added liquid products, but on the other hand the feedstock is substantially different from normal delayed coker feedstock. Hence it is not clear that the feedstock would be compatible with conventional delayed cokers.

Conventional delayed cokers produce coke by injecting hot fluid into a drum, and allowing the fluid to coke over a period of about a day (hence the term “delayed” coking). The drums are then open and the coke is literally cut out of the drum using a high pressure water jet. Thus, in the case of centrifuge tails that contain large amounts of ash as well as a carbon-rich hydrocarbon phase, it is feared that the resultant coke may be substantially denser than conventional delayed coker products and may be more difficult to remove from the drums. This possibility has not yet been evaluated experimentally. For that reason alternate coking methodologies may also need to be considered.

Table 182. Characteristics of Kingwood Lower Kittanning Coal.⁸⁰

Coal Bed	Kingwood
Seam	Lower Kittanning
County	Preston
State	WV
ASTM Rank	High Volatile Bituminous
% Volatile Matter (dry)	28.35
% Ash (dry)	7.36
% Fixed Carbon (dry)	64.29
% Sulfur (dry)	1.84
Mean-Max reflectance of vitrinite	1.08
Total Vitrinite	74.60
Total Liptinite	5.00
Total Inertinite	19.40

As described previously, the liquid phase can be completely recycled as solvent. The centrifuge tails are intended to be used as a fuel for FutureGen, possibly after additional processing to better utilize the light liquids available from such a feedstock (i.e., the Wolfe mild gasification process described above).

Table 183. Approximate Mass Balance for Carbon Products Plant with FutureGen.

Material Name	Classification	Cost (\$/kg)	Flowrate (kg/h)	Annual Cost
FutureGen Hydrogen	Raw Material	(\$1.25)	324	(\$2,838,240)
Coal (dry basis)	Raw Material	(\$0.06)	24345	(\$9,383,537)
Catalysts	Raw Material	(\$4.00)	25	(\$700,800)
CTD Solvent	Raw Material	(\$0.33)	4860	(\$11,239,430)
Synthetic Crude	Product	\$0.23	23711	\$36,993,590
FutureGen Coal/Ash Feed	Product	\$0.015	8764	\$921,272
Methane and other gases	Product	\$0.20	487	784,966
Total Revenue less Raw Materials				\$ 14,537,921

The overall mass balance as summarized in Table 183. Since there is more than one feedstock, and more than one product, it necessary to specify which products and which feedstocks are meant in speaking of the “percent yield.” From the standpoint of mass balance alone, there is in fact no waste material; hence the mass of the products equals the mass of the feedstocks.

In some cases it may be of interest to consider the net yield of liquid products versus the consumption of dry coal. In this case the net yield of liquids would be the mass of synthetic

crude minus the mass of the CTD consumed, or $23,711 \text{ kg} - 4617 \text{ kg} = 19094$. The mass of dry coal consumed is 24345 kg. In this case the “yield” would be 78%.

The process summarized in Table 183 consumes net solvent. However, it is suspected that low ash bituminous coals or even lignite coals may actually generate more liquid products than they consume, but this has not been proven at the pilot scale. This can be true if

- a. The H/C ratio is higher than bituminous coal,
- b. Conradson carbon (coking/charring) yield is low,
- c. Ash level is low to minimize losses,
- d. Losses to dealkylation (methane emission) must also be low.

Additional economic assumptions are listed in Table 184, based on a 20,000 tons per year plant. The estimates are based roughly on recent economic conditions in the coal producing regions of the eastern United States.

Table 184. Economic Assumptions.

Parameter	Value
Cost of Land	\$ 1,250,000
Taxation Rate	42%
Annual Interest Rate	10%
Salvage Value	\$ 1,412,400
Working Capital	\$ 2,630,000
FCI_L	\$ 6,420,000
Total Module Factor	1.18
Grass Roots Factor	0.50
Revenue From Sales	\$ 39,139,610
C_{RM} (Raw Materials Costs)	\$ 19,776,401
C_{UT} (Cost of Utilities)	\$ -
C_{WT} (Waste Treatment Costs)	\$ -
C_{OL} (Cost of Operating Labor)	\$ 150,000

Representative prices of basic utilities in the eastern United States industrial region are listed in Table 185. These values likewise are used in the CAPCOST model.

Table 185. Utility Price Assumptions.

Common Utilities	Cost (\$/GJ)
Electricity (110 V-440 V)	16.80
Cooling water (30 °C to 45 °C)	0.354
Refrigerated Water (15 °C to 25 °C)	4.43
Low Pressure Steam (5 barg, 160 °C)	6.08
Medium Pressure Steam (10 barg, 184 °C)	6.87
High Pressure Steam (41 barg, 254 °C)	9.83
Fuel Oil No. 2	6.00
Natural Gas	6.00
Coal (FOB mine mouth)	1.07
Thermal Systems	
Moderately High (up to 330 °C)	6.67
High (up to 400 °C)	7.00
Very High (up to 600 °C)	7.50
Refrigeration	
Moderately Low (5 °C)	4.43
Low (-20 °C)	7.89
Very Low (-50 °C)	13.11
Waste Disposal	Cost (\$/ Metric Tonne)
Non-hazardous	36
Hazardous	200

Table 186 lists the major equipment items associated with a 20,000 tpy plant to produce carbon products. The estimates are based upon standard equipment data bases. Because the design of such a system is currently not very detailed, the accuracy of the estimate can rightly be questioned.

In particular, two areas of concern are the reactors needed for hydrotreating and digestion. Recent advice from ChemTech, a subcontractor to Koppers (contract DE-FC26-03NT41873) is that pipe reactors would be much more economical and would likely provide higher performance than reactors of the autoclave type. Autoclave reactors would require custom manufacture and long lead times. Nevertheless, the price information for custom autoclave reactors is used to generate system cost estimates. Accordingly, it is believed that these estimates are highly conservative (pessimistic).

Table 186. Equipment Summary.

Centrifuges	Type	Diameter (meters)	# Spares			Purchased Equipment Cost	Bare Module Cost
Ct-101	Solid Bowl	1	1			\$ 187,000	\$ 293,000

Compressors	Compressor Type	Power (kilowatts)	# Spares	MOC		Purchased Equipment Cost	Bare Module Cost
C-101	Reciprocating	150	1	Carbon Steel		\$ 300,000	\$ 1,010,000

Conveyors	Type	Area (square meters)				Purchased Equipment Cost	Bare Module Cost
Cv-101	Belt	100				\$ 159,000	\$ 198,000

Exchangers	Exchanger Type	Shell Pressure (barg)	Pressure (barg)	MOC	Area (square meters)	Purchased Equipment Cost	Bare Module Cost
E-101	fixed, Sheet, or U-Tut	10	10	Stainless Steel / Stainless Steel	822	\$ 67,600	\$ 422,000

Fired Heaters	Type	Heat Duty (MJ/h)	Superheat (°C)	MOC	Pressure (barg)	Purchased Equipment Cost	Bare Module Cost
H-101	Process Heater	4070		Carbon Steel	62	\$ 476,000	\$ 1,110,000
H-102	Molten Salt Heater	1520				\$ 39,600	\$ 86,000
H-103	Molten Salt Heater	3600				\$ 58,900	\$ 128,000

Vessels	Orientation	Length/Height (meters)	Diameter (meters)	MOC	Demister MOC	Pressure (barg)	Purchased Equipment Cost	Bare Module Cost
V-101	Horizontal	7	1	Carbon Steel		20	\$ 7,680	\$ 40,500
V-102	Vertical	10	2	Stainless Steel		10	\$ 25,700	\$ 431,000
V-103	Vertical	10	2	Stainless Clad		10	\$ 25,700	\$ 267,000
V-104	Vertical	10	2	Carbon Steel		10	\$ 25,700	\$ 178,000

User Added Equipment	Description	BMF0	Actual BMF			Purchased Equipment Cost	Bare Module Cost
Z-101	Crusher	1	1.5			\$ 100,000	\$ 150,000
Z-102	Hydrotreatment Reactor	1	43628185907046			\$ 667,000	\$ 4,960,000
Z-103	Digestion Reactor	1	48571428571429			\$ 525,000	\$ 3,930,000

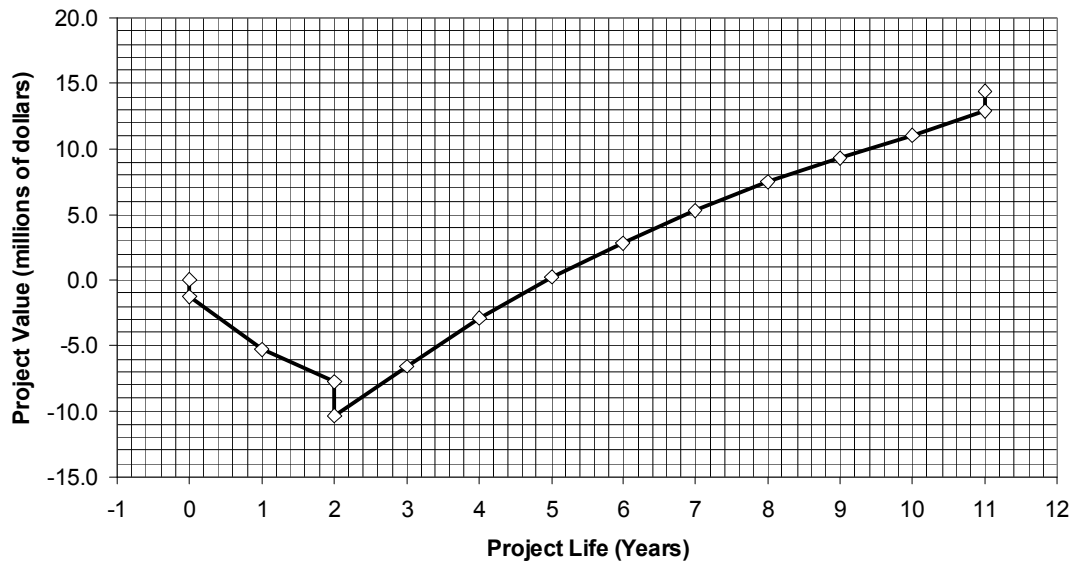


Figure 145. Estimated Cash Flow for a 20,000 TPY Carbon Products Plant with FutureGen.

There are a number of uncertainties in the design of any chemical plant. For example, the Fixed Capital Investment not including cost of land (FCIL) can not be predicted with certainty. Thus, lower and upper bounds are set for FCIL and other parameters, along with a probability distribution associated with each category, as listed in Table 187. CAPCOST then generates a large number of potential scenarios based on probabilities.

Table 187. Monte Carlo Analysis Parameters.

	Lower Limit	Maximum Limit	Base Value
FCIL	-20%	30%	\$ 8,600,000
Price of Product	-10%	10%	\$ 39,139,610
Working Capital	-50%	10%	\$ 2,860,000
Income Tax Rate*	-20%	20%	42%
Interest Rate*	-10%	20%	10%
Raw Material Price	-50%	100%	\$ 19,776,401
Salvage Value	-80%	20%	\$ 1,892,000

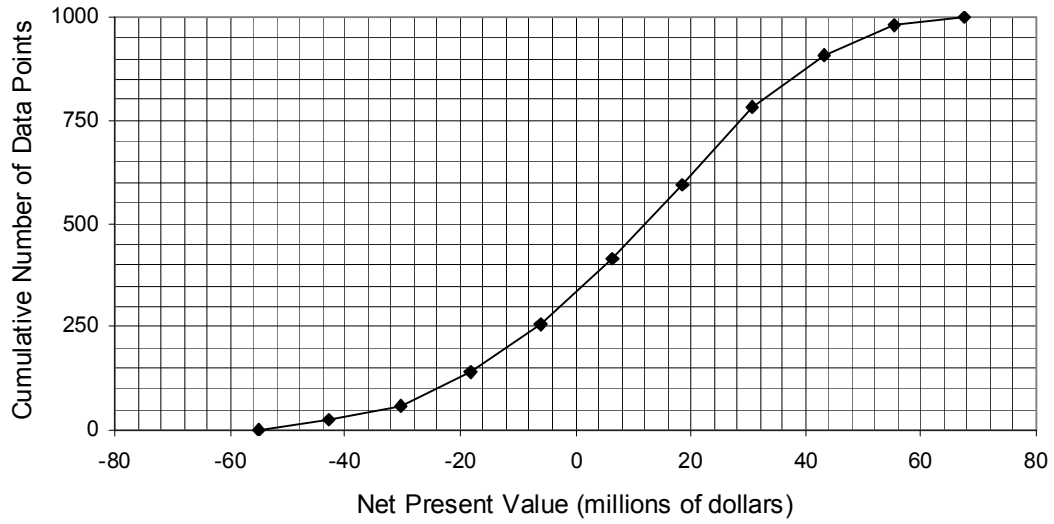


Figure 146. Estimated Net Present Value.

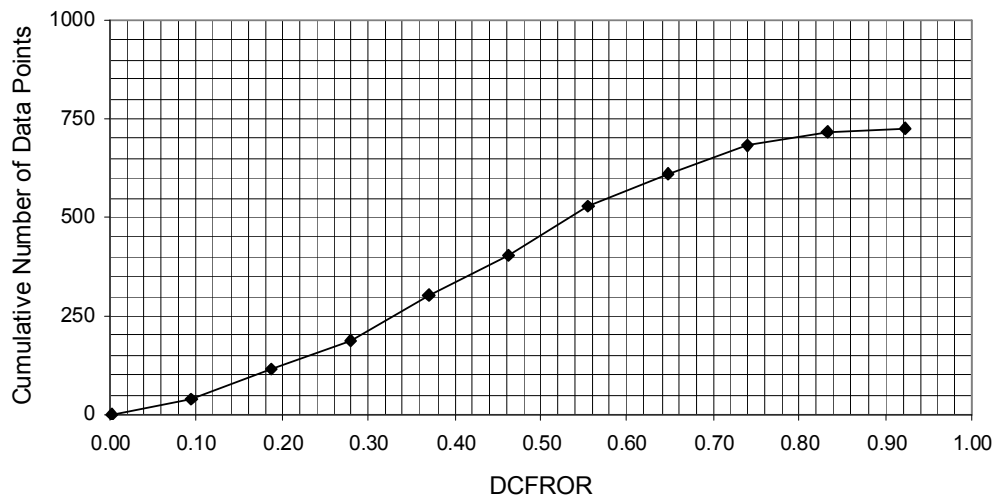


Figure 147. Estimated Discounted Cash Flow Rate of Return.

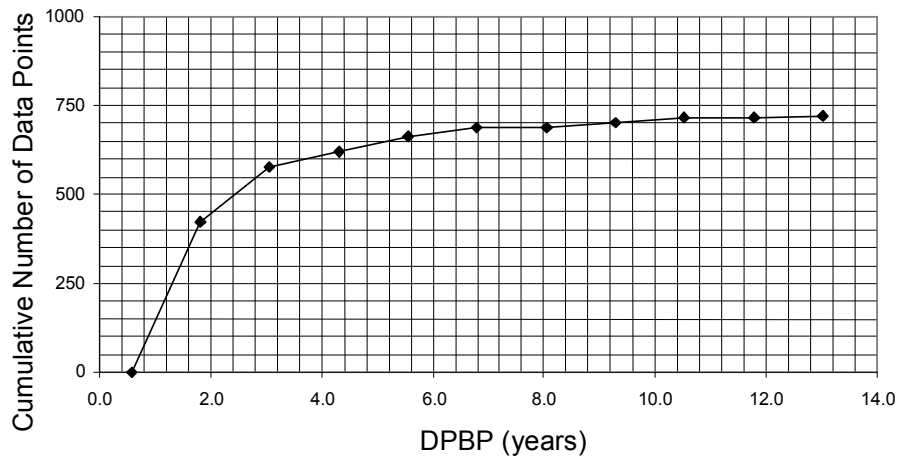


Figure 148. Estimated Discounted Payback Period.

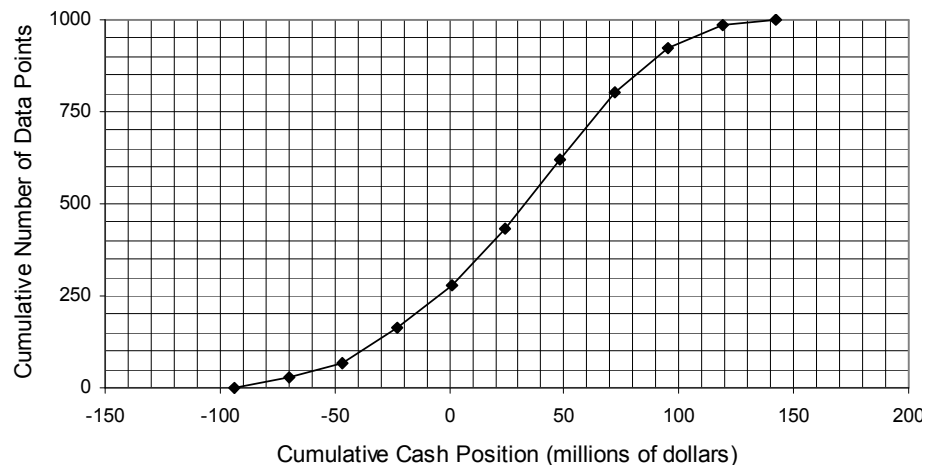


Figure 149. Cumulative Cash Position.

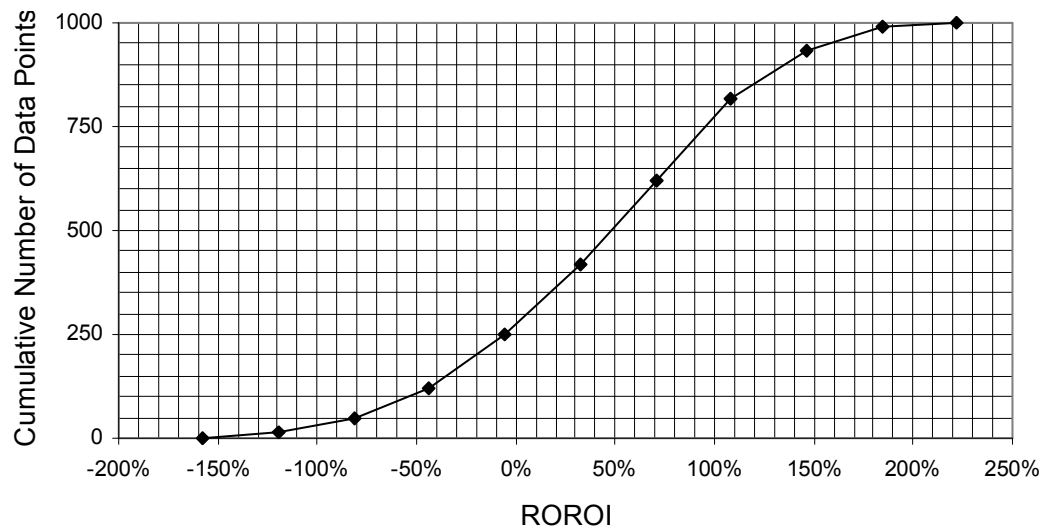


Figure 150. Estimated Rate of Return on Investment.

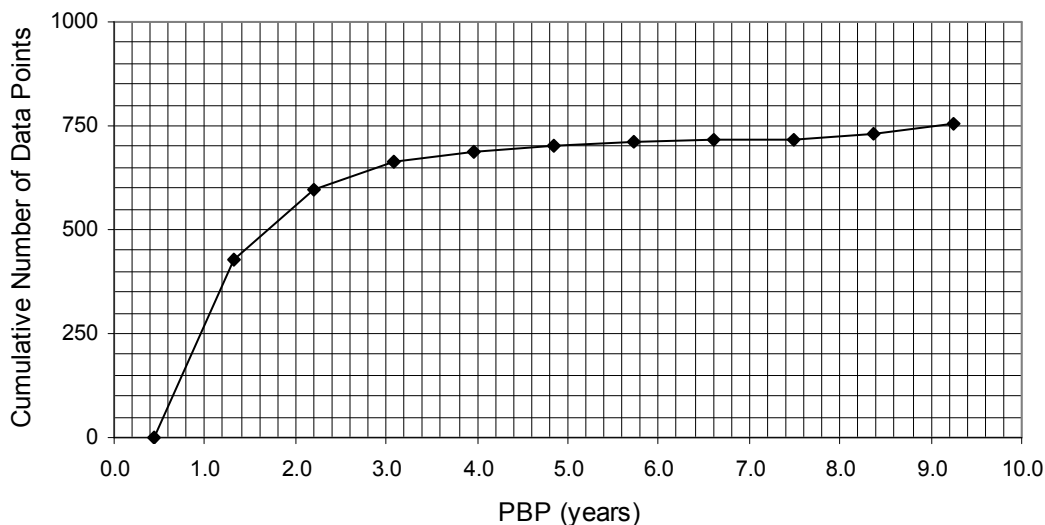


Figure 151. Estimated Payback Period.

4.2 Additional System Analysis

Although historically coal to liquid plants have been designed for maximum yield of transportation fuels, direct liquefaction can be considered as a means for producing a carbon-rich product stream with similar value. That is, the production of carbon rich pitches and cokes can be accomplished using coal-derived feedstocks with minimal hydrogen augmentation. This results in a lower H/C ratio than required for light crude. However, by utilizing carbon rich streams to create value added pitch or coke, the remainder can have a higher H/C ratio, while resulting in pitch and coke co-products to enhance revenue. In some cases, products such as needle grade coke and binder pitch can offer values comparable to fuels. Thus it is probably not necessary to upgrade all portions of the liquefied coal.

In the WVU solvent extraction process, the preferred approach is to generate a coal liquid from cracked coals. The coal liquid can then be used as a commodity solvent. Alternatively, a commodity solvent such as a coal tar distillate or decant oil, can be effective coal solvents if they are hydrogenated to enhance the solubility of coal. Crushed coal is then digested in the solvent at high pressure and high temperature resulting in conversion of up to 90% of the dry, ash-free coal to the liquid state. Solids are removed from the slurry via centrifugation, resulting in a refinable liquid.

Thus, two streams are created, a nominally solid phase composed of centrifuge tails, and a liquid phase. The centrifuged solids can be utilized as a gasification feedstock, or alternatively could be blended with other forms of coal or biomass. The solid product represents only several percent of the total output from the process. The liquid stream, i.e., the synthetic crude, is then distilled to produce at least two additional fractions. The overhead liquid fraction can be recycled as a coal solvent, or alternatively, upgraded to produce value-added fuels and chemicals. The distillation bottoms (that is, the heavy, carbon-rich fraction) can be utilized as a binder pitch. Alternatively, a delayed coker can be used to thermocrack the heavy molecules to produce lighter liquids in addition to an anode grade coke residue.⁸¹

Western sub-bituminous coals result in a lower yield of pitch and correspondingly higher yield of coal liquids. Moreover, the market price for sub-bituminous coals is lower than that for eastern bituminous coals, suggesting that western sub-bituminous coals can be excellent candidates for producing chemicals and fuels.

In addition to the favorable economics, the environmental aspects for coal to heavy crude need to be considered. The coal-to-heavy-crude conversion process reduces many potential pollutants such as mercury, sulfur and heavy metals, depending on their state in the liquid phase. Heavy products are transferred to the centrifuge tails and removed from the nominal liquid phase. The case for carbon dioxide is more complex. Generally, CO₂ is produced whenever fossil fuel is combusted to generate thermal energy to drive the process, although of course it is possible to consider thermal energy sources that do not produce CO₂, such as solar electrothermal, solar thermal storage, geothermal, nuclear, etc. Generally speaking, however, non-CO₂-generating processes are much more expensive than conventional gas reforming processes. Additional CO₂ is generally produced when hydrogen is generated. Because the coal-to-heavy-crude process requires much smaller amounts of hydrogen, the CO₂ footprint is correspondingly reduced. Thus it appears that both economic and environmental considerations favor the development of plants based on this concept.

To determine the materials costs associated with liquefaction, it is necessary to consider the hydrogen content of the feed material as well as the desired product. A representative coal sample was provided by the Kingwood Mine (Alpha Natural Resources) preparation plant. The elemental analysis in Table 188 lists the composition by mass. The atomic H/C ratio is described by

$$\left(\frac{H}{C}\right)_{at} = \frac{m_H A_C}{m_C A_H} \quad , \quad \text{(Equation 21)}$$

where m_H is the mass of hydrogen, m_C is the mass of Carbon, A_C is the atomic mass of carbon and A_H is the atomic mass of hydrogen. Thus from the data in Table 188, additional hydrogen is not needed to produce binder pitch, within the context of liquefaction reactions as depicted in Figure 152 below. The role of the hydrogen, then, is associated with enhancement of the chemical digestion process, *but is not necessary to produce a liquid product.*

Table 188. Elemental Analysis of Input Feedstocks and Products.

Name	%C	%H	%N	%S	%O	Molar H/C	Mass H/C	Enthalpy, MJ/kg
Lower Kittanning Bituminous Coal	77.93	5.333	1.738	1.830	12.16	0.821	0.0684	32.28
Canadian Sub-Bituminous Coal	47.97	5.697	1.277	0.2869	44.77	1.425	0.1187	17.54
Hydrogenated Oil	77.30	15.107	0.271	0	7.322	2.345	0.1954	39.6
Canadian Oil Sands Crude API -22	76.82	12.09	0.5258	3.664	6.901	1.889	0.1574	
Binder Pitch	93.2758	4.3239	1.2256	0.2793	0.8954	0.5563	0.0464	

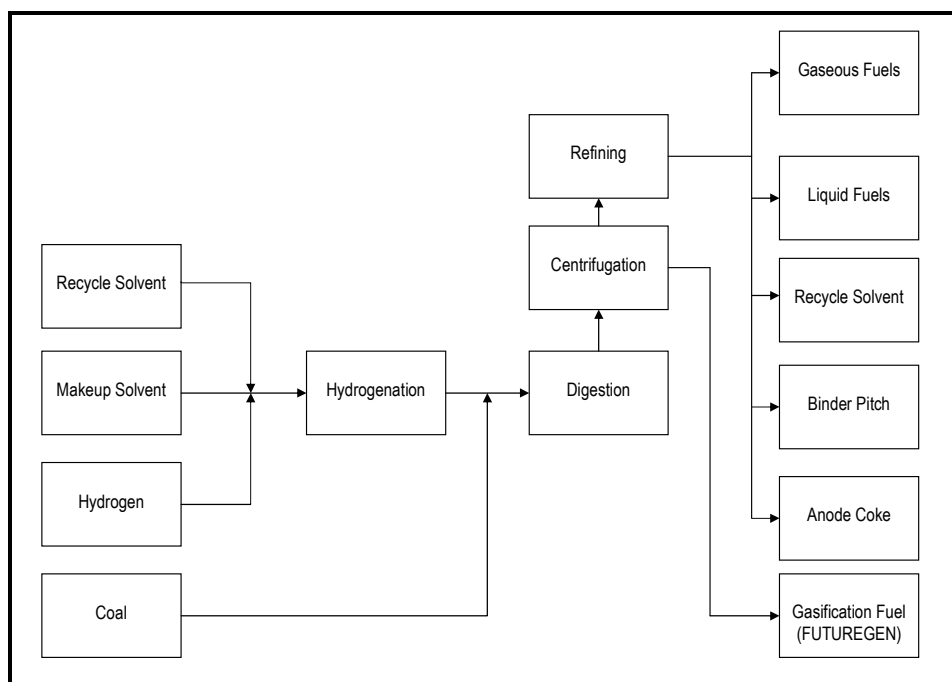


Figure 152. Simplified Mass Balance Options for Direct Liquefaction.

The H/C value is overstated in Table 188 since it includes the hydrogen present in moisture. If 27% of the sample is water, approximately 4% of the sample is hydrogen contained in water.

Table 189 shows a mass balance at different steps in the process for a representative protocol for liquefaction of sub-bituminous coal. The mass balance is normalized to one ton of moisture-free sub-bituminous coal (Stage 2, Dry Coal).

- a. Stage 1 corresponds to the starting raw materials. The coal is prepped and ground to about -20 mesh.
- b. Stage 2 involves boiling excess moisture at about 110 oC.
- c. Stage 3 results in formation of a slurry of the products.
- d. Stage 4 involves centrifugation to separate mineral matter and other solids from the liquid phase.
- e. Stage 5 involves distillation of the liquid to create a pitch with softening temperature of 110 °C, as well as lighter products that are separately recovered.
- f. Stage 6 corresponds to recovery of liquids from the centrifuge tails by heating to about 400 °C with recovery at approximately ambient temperature.
- g. Stage 7 conceptually integrates the liquids from centrifuge tails with those previously obtained at other phases in the process. In reality Stages 6 and 7 would be combined.

Table 189. Progressive Mass Balance for a Representative Sub-Bituminous Coal Conversion Process.

Mass Balance	Stage 1	Stage 2	Stage 3	Stage 4	Stage 5	Stage 6	Stage 7
Material List							
Coal, Sub-bituminous	1.370						
Dry Coal, Sub-bituminous		1.000					
Coal Liquids	2.750	2.750					
Hydrogenated Oil	0.250	0.250					
Slurry			4.000				
Centrate				3.299			
Binder Pitch					0.660	0.660	0.660
Tails				0.582	0.582		
Gasifier Fuel (coked Tails)						0.320	0.320
Gas				0.120	0.120	0.120	0.149
Coke Gas						0.029	
Overhead Distillates					2.639	2.639	2.871
Condensed Coking Liquids						0.233	
Water		0.370	0.370	0.370	0.370	0.370	0.370
Total Mass, kg	4.370	4.370	4.370	4.370	4.370	4.370	4.370
Processing Energy, kJ		836		3901	1475	887	0
Total Energy Consumed, kJ							7099
Estimated beginning Enthalpy, kJ							15293
Estimated Enthalpy, BTU							15547
Measured Enthalpy, BTU/lb							7545
Measured Enthalpy, KJ/kg							16531
Net Enthalpy kJ/k							9432
Efficiency = Net/Meas							0.571

The mass balance carried out above can be further normalized. Hydrogen balance is carried out on a dry ash-free basis, because the presence of moisture and clays can skew the results.

Enhanced output of liquid products can be achieved by upgrading the heavy hydrocarbons in much the same way that heavy petroleum crudes are upgraded. In this case, the workhorse of the industry is the delayed coker, which thermally cracks heavy hydrocarbons to produce a coke residue as well as lighter liquid products that are further refined in to fuels and chemical feedstocks. The complete cycle for delayed coking is generally about 16 hours with one drum filling on-line while its counterpart is off-line for stripping, cooling, and decoking. Delayed cokers are often built with very large capacity in order to take advantage of economy of scale.

Three plants were analyzed based on historical data, corresponding to three different concepts. These were rated for a plant capacity of 50000 BPD (Barrels per day) which was then scaled down to a pilot plant scale of 341 BPD.⁸²

All plants in the report were based upon Illinois 6 coal.

The first design, designated H-Coal, is based on an analysis by process developers in 1981. They used this data to calculate the values for the year 1999. Using the data obtained for the year 1999, values for current year 2008 were calculated.

The second plant designated ITSL (Integrated Two Stage Liquefaction) is based on a detailed preliminary design prepared for DOE by Bechtel in 1991-92 which was further modified to extrapolate the values for the year 1999. Performance assumed in this study was derived from test results from run 257 at the Wilsonville pilot plant.

The plant designated as CMSL (Catalytic Multi Stage Liquefaction) is based on a bench scale results at Hydrocarbon Technology Incorporated (HTI). Capital and operating costs are based on initial designs of HTI in 1997. The HTI design used natural gas as a feedstock but this was modified to coal only feedstock in order to be compatible with other plants. This was then used as a basis to calculate values for the year 2008.

10,000 to 30,000 tons per year of product is suggested as an appropriate range for a demonstration plant. This corresponds roughly to the falloff in North American production capacity since 1990.⁸³ In addition, this amount is comparable to 10-15 river barges per year, based on a barge capacity of 1800 tons. Anode grade coke is routinely calcined by the barge load, and supplied in similar quantities to the aluminum smelting industry. Hence 10,000 to 30,000 tons per year appears to be a desirable production capacity. To convert between tons per year and barrels per day, a density of 0.9218 g/cm³ (American Petroleum Institute gravity API-22) is assumed, resulting in a conversion factor of 0.01705 BPD/TPY. The midpoint of the range, or 20,000 TPY corresponds to 341 barrels per day.

To determine the costs of a demonstration plan, two methods were used. First, a bottoms-up design was created from the CAPCOST model.⁸⁴ Second, historical data was obtained on other coal liquefaction plants from the 1970s and extrapolated to a 2008 start of construction and a 20,000 TPY output..

CAPCOST modeling was based upon a hypothetical existing coal tar refining plant, meaning that environmental permitting, distillation, scrubbing and venting facilities were assumed to be already at the site. Under these conditions, a 2008 Capital Cost of some 18 million dollars is estimated, or \$53,000 per Barrel per Stream Day (BPSD) capacity.

Top-down costs based upon historical data were expected to yield higher estimates, since much greater processing was used in order to maximize fuels yield rather than carbon products yield. As mentioned in the summary report of the DOE Direct liquefaction process development campaign of the late twentieth century, the economic analysis of three full scale direct liquefaction plants was extrapolated from the 1970s to the year 1999 (H-Coal, ITSL (Integrated two stage liquefaction) and CMSL (Catalytic multi stage liquefaction)).^{85,86,87,88} These DOE estimates in turn were adjusted for 2008, and then further modified for a demonstration plant at the 20,000 ton per year level (341 barrels per day). Table 190 shows the assumptions that were used to convert 1999 estimates to 2008 dollars.

Table 190. Financial Assumptions for Extrapolation of 1999 Estimates to 2008.

Parameter	Value
Return on Equity (ROE)	15%
Equity	25%
Construction Period	4 years
Federal tax rate	34%
Loan Interest (16 Years)	8%
State/Local Property Tax	1%
Depreciation, DDB	16 years

The price of Northern Appalachian coal had soared to \$120 ton in the spot market as of May 2008 according to the Department of Energy Information Agency (EIA). Plant costs were calculated on the basis of 1999 plant value using the concept of future value and a rate of 4%. This leads to obtaining the escalation factor (which is the ratio of current plant cost to basis plant cost). Capital cost and Operations and maintenance costs (O&M) have been calculated by multiplying the escalation factors with their corresponding basis values. Coal cost (MM\$/day) has been calculated by multiplying coal feed (Ton/ day) and coal cost (\$/ton). This coal cost is then converted to MM\$/ year by multiplying the obtained value with 330 days (considering approximately 330 working days per year). Then total cost was calculated which is a summation of coal cost, O&M cost and the capital cost. (All the costs are million dollars per year). Yield was then converted into million barrels per year. Required selling price (RSP) was then calculated as the ratio of Total cost/Total yield. When these values of RSP are divided by their corresponding premium, the equivalent crude required price is obtained. Capital required per barrel per day is calculated by dividing the Plant cost(MM\$) with given yield (Barrels/Day).

All the capital investments calculated are based on the future value of money (USD\$). The standard rate of inflation has been taken as 4 % for all the calculations. All the costs would have to be scaled down or up depending on basis or the reference plant. A simple formula for scaling cost and capacity for two plants with capacity A and B respectively can be used to crudely evaluate economy of scale.⁸⁹

$$\left(\frac{\text{Capacity of } A}{\text{Capacity of } B} \right)^{0.6} = \frac{\text{Cost of } A}{\text{Cost of } B} \quad \text{Equation 22}$$

The future value of money is calculated by the formula:

$$FV = (1 + r)^n \quad , \quad \text{Equation 23}$$

where FV and PV are future value and present value of money respectively, r is the average inflation rate, which has been taken as 4 %, and n is the difference in years between present and future. Table 191 shows the estimated 1999 and 2008 capital costs for three projects, as well as the scaled estimate corresponding to a 20,000 TPY plant (341 BPD).

Table 191. Adjusted Capital Investment from CTL Plants.

	H- COAL		ITSL		CMSL	
	1999	2008	1999	2008	1999	2008
Yield,BBL/D	50000	50000	69000	69000	51500	51500
Coal Feed T/D	26370	26370	25415	25415	18090	18090
\$/Ton	\$20.5	\$84.3	\$20.5	84.3	\$20.5	\$84.3
Plant cost \$MM	\$4592	\$6284	\$4239	\$5801	\$2914	\$3988
Escalation factor		1.369		1.368569		1.368569
Capital interest	\$689	\$943	\$636	\$870	\$437	\$598
(\$ MM/ Yr)						
Coal cost,\$MM/Yr	178	734	172	707.0199	122	503.2457
O&M/Yr,\$MM/Yr	184	251	138	188.8625	87	119.0655
Total cost/Yr	1051	1928	946	1766.292	647	1220.376
MMbbls/Yr	16.5	16.5	22.77	22.77	17	17
RSP	63.69	116.86956	41.53	77.57103	38.06	71.78682
Premium	1	1	1.07	1.07	1.2	1.2
Eq Crude RSP	63.69	114.60174	38.81	72.49629	31.78	59.82235
Capital/BPSD		\$125,689		\$84,077		\$77,437.09
Cap/BPSD @ 20000 TPY (340 BPSD)		\$924,240		\$703,264		\$576,196

The bottom line estimates from H-Coal, for example (\$924,240 per BPSD) are vastly higher than the estimates generated from CAPCOST for mild direct liquefaction. This is not surprising, however, as the previous generation of plants aimed to maximize the yield of liquid transportation fuels, requiring the addition of some ~30 pounds of hydrogen versus 3 for the West Virginia process. In addition, the true scalability of the cost over two orders of magnitude of capacity is questionable.

Nevertheless, the numbers suggest that a significant investment is required in order to develop a limited production capability using conventional direct liquefaction technology. The contention of this project is that the reduction of hydrogen required for liquefaction results in significant savings in materials cost as well as scalability of the process.

4.3 Modular Plant Design

A transportable modular design philosophy has been emphasized in which the liquefaction plant is constructed in such a way that the modular sections of the plant can be transported by barge or by railcar to the site where liquefaction will take place (e.g., near a

pipeline or near the mine itself). The idea is to minimize the amount of labor time needed to erect the plant on-site. This is particularly attractive if the

This lesson was made evident during the boom period of 2005-2008, in which labor became very scarce in Alberta, for example, making new construction very difficult.

An example of a modular design is shown in Figure 153 through Figure 155 below. Figure 153 shows separate modules mounted on skids suitable for railcar transport. Figure 154 is a close-up view of the module in question, which houses a column for a wiped film evaporator used to distill reclaimed motor oil

Figure 155 shows the plant after the modules are assembled. Such plants are nicknamed “microplants” or “microrefineries” although in reality the plants are in fact macroscale plants.



Figure 153. Component modules for use in a microrefinery for reprocessing used motor oil.



Figure 154. Side view of a typical module.



Figure 155. A micro plant used for reprocessing spent motor oil.

4.4 Carbonite Plant in Virginia

Although the primary emphasis of this project was on solvent extraction, devolatilization has also been considered. Groundbreaking has already occurred based on the Carbonite concept.

At the beginning of this project, it was recognized that solvent extraction could be used to produce coal liquids as well as a carbon rich quasi-solid containing ash and fixed carbon. Hence, the initial interest was to use Dr. Wolfe's concept is to heat the centrifuge tails to about 600 °C in order to devolatilize the retentate as much as possible

In addition, however, devolatilization as means to co-produce liquid crude and upgraded coal (e.g., from steam coal to metallurgical grade) concept was studied by the DOE in the 1990's. The intention was to modify the properties of steam coal to create a substitute for coking coal (either metallurgical grade coke or its cousin, foundry grade coke).⁹⁰

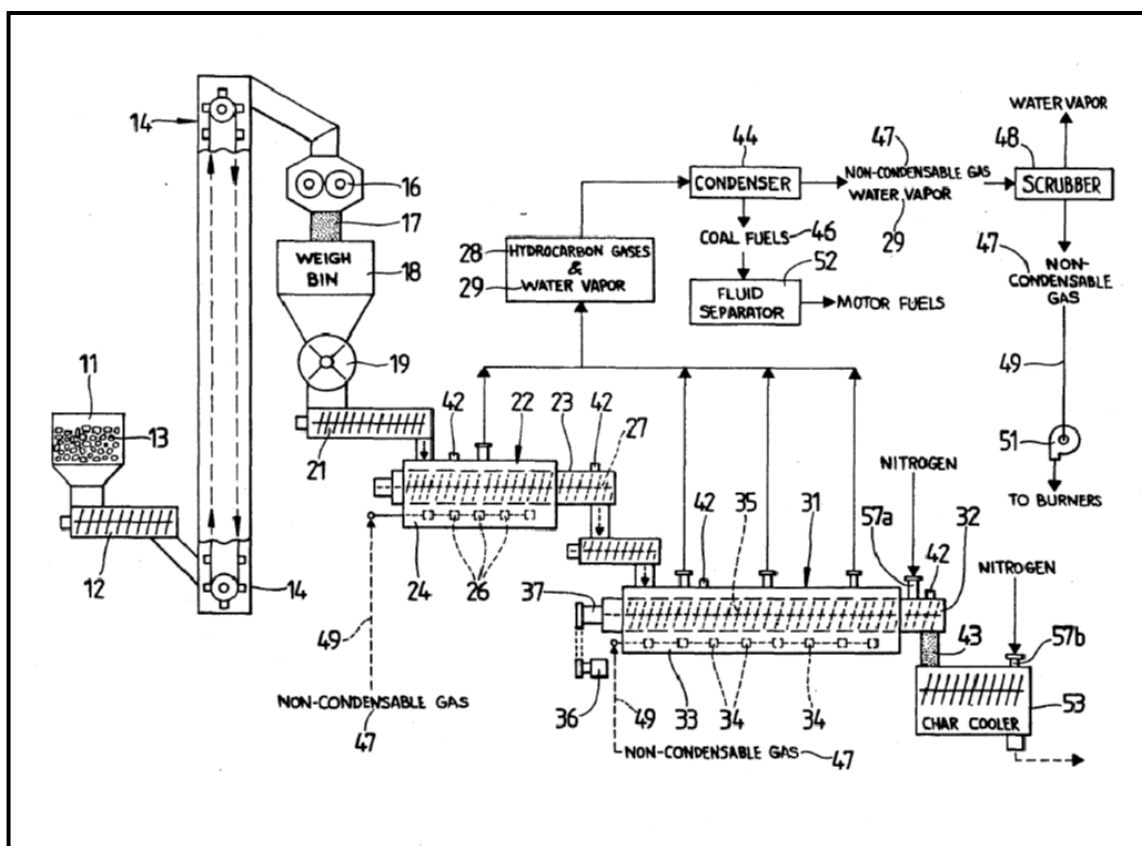


Figure 156. Wolfe process for devolatilizing coal to create crude oil and metcoke (www.USPTO.com).

Referring to the drawing from the patent application, coal is crushed (13), weighed (18) and conveyed to a pyrolyzer and screw conveyor (22). A twin screw extruder (31) is used to devolatilize the coal while creating a dense solid carbon which can be converted to a dense coke. The recovered volatiles are useful as a form of crude oil similar to coal tar obtained from metallurgical coke batteries. The twin screw machine serves to create a product with high

strength and modulus, making it suitable for use in blast furnaces. A briquetting machine is used to create briquettes, much like the charcoal briquettes used for home barbecues.

Hence the two main products are metallurgical grade or foundry grade coke plus oil. Approximately one barrel of oil is obtained from a ton of coal.

The economics have changed in recent years, as the price of coke has significantly outstripped inflation, as has crude oil. Demand for foundry coke is being driven by steel manufacturing, mainly overseas. Alibaba.com lists prices for foundry coke ranging from \$400 to \$600 per Metric Tonne. By comparison, the US International Trade Commission estimated an average price of \$176 per Metric Tonne in 1999. Using an inflation correction of 35.6% (according to www.usinflationcalculator.com, for the period 1999 to 2011), the equivalent price of foundry coke would be \$239 per Metric Tonne in 2011. Hence in real terms the price of foundry coke has approximately doubled since 1999.

Although forecasting the future of commodity prices is a treacherously difficult undertaking, at least some investors believe that the demand for foundry grade coke as well as metallurgical grade coke will continue for several years in the future.

Accordingly, a new company has been formed, Carbonite Incorporated. A plant to produce 50,000 short tons per year of solid and liquid products has been capitalized by private investors from West Virginia and Virginia, with some additional support from the Commonwealth of Virginia.^{91,92} The Carbonite plant is being built near Norton, Virginia. The plant will produce foundry grade coke as well as coal derived oil. It is projected to employ about thirty persons initially.

A second plant has been proposed for a location near Kingsport TN, although that has not been finalized.

The WVU process (now properly identified as the Quantex process) could, as one example, supply raw material to a Carbonite plant in order to produce cokes and crude oil.

The figures below (Figure 157 through Figure 167) highlight some of the activities.



Figure 157. Richard Wolfe (2nd from right) participated in experiments on-site at WVU, along with Liviu Magean, guest researcher Alain Lui, Elliot Kennel and Femi Olajide.

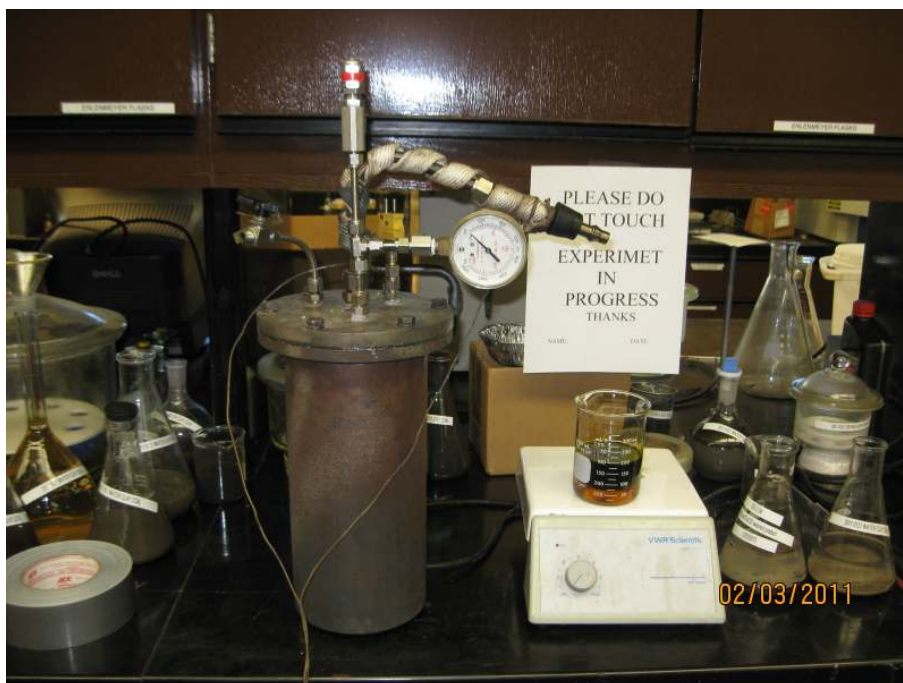


Figure 158. Bench scale coking reactor used to co-produce coked coal (Carbonite™) as well as coal liquids.



Figure 159. Olajide and Wolfe with heavy and light fractions of recovered coal oil from bench scale experiments.



Figure 160. Carbonite synthetic coke produced from Powder River Basin and other steam coals.



Figure 161. Coal conveyor at the Carbonite Plant near Norton VA.



Figure 162. A tunnel kiln is used to heat treat coke at high temperature, liberating additional volatiles. Similar kilns are in use in the ceramic industry.



Figure 163. Drying kilns at the Norton VA site.



Figure 164. Briquetting machine, used for producing coke briquettes.

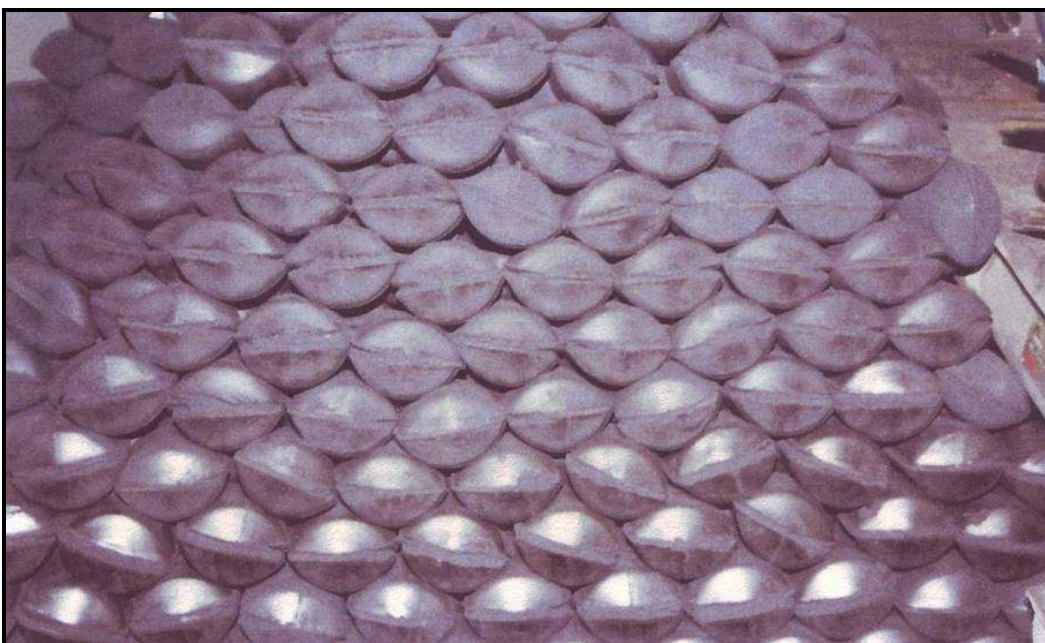


Figure 165. Synthetic foundry coke from the 1990's predecessor of Carbonite.



Figure 166. Foundries use coke to enhance the properties of metal products such as gray iron.



Figure 167. Carbonite compared with conventional coke. Carbonite coke was broken into pieces in order to more closely resemble the appearance of conventional slot oven metallurgical grade coke.

Appendix I. Gas and liquid analyses as measured by Koppers, Pittsburgh, Pa. and Environmental Laboratory Services, New Castle, Pa.

Reports are reproduced below. Originals are poor quality.

REPORT DATE: 03/02/07

Customer: Dr. Richard Wolfe
Generator: Dr. Richard Wolfe
Sample Name: RW-Poca Coal Liquid @ 560 °F
Sample Date: 02/20/07
Lab Sample #: HW62789

LABORATORY RESULTS

Parameter	Result	Method
*Benzene,	0.39 %	EPA 8260B
*Toluene,	2.23 %	EPA 8260B
*Ethyl Benzene,	0.19 %	EPA 8260B
*Xylenes, Total	2.32 %	EPA 8260B

Total Light Oil Compounds	5.13 %	
Flash Point	112 °F	EPA 1010A

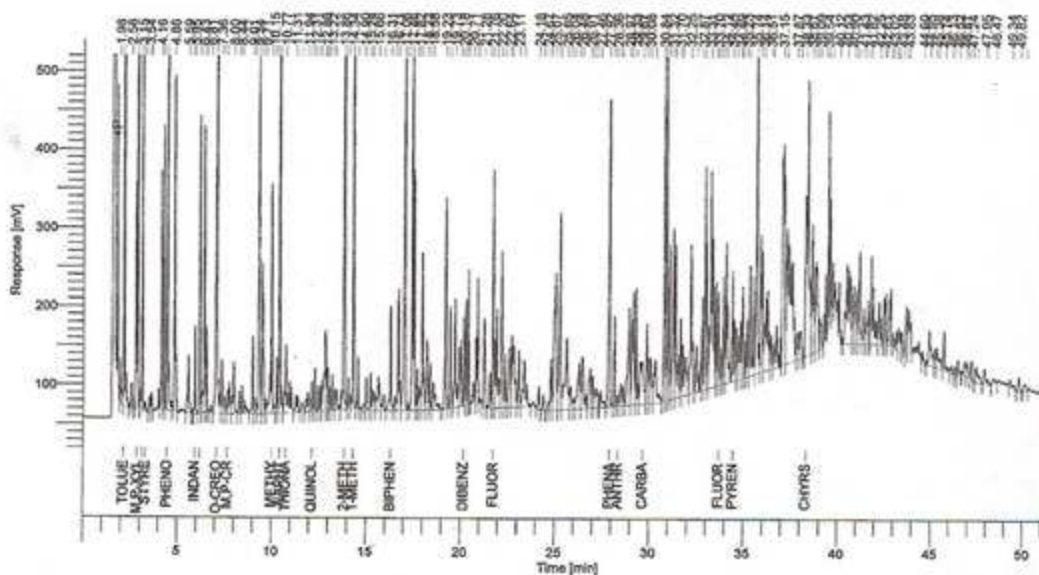
*The sample was centrifuged and the water layer removed prior to analysis of these compounds.

Mark Swansiger

Lab Director

Software Version	: 6.3.1.0504	Date	: 2/21/2007 3:13:30 PM
Reprocess Number	: 617d691: 1762		
Sample Name	: Coal liquid Dr. Wolfe	Data Acquisition Time	: 2/21/2007 2:21:53 PM
Instrument Name	: Clarus 500	Channel	: B
Rack/Vial	: 0/5	Operator	: TCWS
Sample Amount	: 1.000000	Dilution Factor	: 1.000000
Cycle	: 1		

Result File : C:\Data\datb002-20070221-151330.rst
Sequence File : C:\Sequences\february-21-2007-creo2.seq



DEFAULT REPORT

Peak #	Component Name	Time [min]	Area [uV*sec]	Area [%]
1		1.983	231464.06	0.20
2	Toluene	2.157	2800421.57	2.38
3		2.576	124343.21	0.11
4	m,p-Xylene	2.871	3568294.30	3.03
5	o-Xylene	3.145	1253378.86	1.07
6	styrene	3.315	45526.37	0.04
7		3.540	68877.04	0.06
8		3.630	94892.69	0.08
9		4.158	1074776.88	0.91

Peak #	Component Name	Time [min]	Area [uV*sec]	Area [%]
10		4.295	928173.66	0.79
11	Phenol	4.478	1821335.45	1.55
12		4.856	1510595.50	1.28
13		5.591	346516.87	0.29
14		5.823	27681.73	0.02
15	Indan	5.948	357353.75	0.30
16	Indene	6.197	1121297.80	0.95
17		6.429	1182465.51	1.01
18		6.558	320488.57	0.27
19		6.808	43517.51	0.04
20	o-creosol	7.094	2620353.76	2.23
21		7.358	314639.44	0.27
22		7.509	103289.61	0.09
23	m,p-creosol	7.670	276170.75	0.23
24		8.001	311226.78	0.26
25		8.305	131224.27	0.11
26		8.439	207195.64	0.18
27		9.007	328000.65	0.28
28		9.146	99597.35	0.08
29		9.337	2002572.99	1.70
30		9.524	906178.31	0.77
31		9.710	67866.06	0.06
32	Methyl-indene	10.019	1130067.34	0.96
33		10.150	61032.29	0.05
34		10.285	203790.55	0.17
35	Naphthalene	10.439	2482789.57	2.11
36	Thionaphthene	10.768	680916.78	0.58
37		11.306	161658.51	0.14
38		11.600	79273.08	0.07
39		11.940	204462.75	0.17
40	Quinoline	12.160	164880.74	0.14
41		12.307	183744.31	0.16
42		12.475	105719.05	0.09
43		12.615	92346.35	0.08
44		12.856	703747.51	0.60
45		12.948	311020.11	0.26
46		13.073	93843.48	0.08
47		13.222	169049.31	0.14
48		13.388	207430.94	0.18
49	2-Methylnaph	13.857	3872075.26	3.29
50		14.060	143019.48	0.12
51	1-Methylnaph	14.335	1531191.27	1.30
52		14.569	221801.48	0.19
53		14.904	52280.05	0.04
54		15.011	145731.89	0.12
55		15.241	160838.51	0.14
56		15.362	198360.20	0.17
57		15.660	345753.58	0.29
58		15.955	126142.38	0.11

1/2007 3:13:30 PM Result: C:\Data\datb002-20070221-151330.rst

ik	Component Name	Time [min]	Area [uV*sec]	Area [%]
9	Biphenyl	16.305	508005.22	0.43
0		16.537	101933.83	0.09
1		16.713	688171.49	0.58
2		17.065	2234355.41	1.90
3		17.221	31038.44	0.03
4		17.460	2588349.63	2.20
5		17.703	167687.35	0.14
6		17.824	205792.99	0.17
7		17.983	850328.14	0.72
8		18.227	435074.31	0.37
9	Dibenzofuran	18.394	227841.75	0.19
0		18.576	303446.45	0.26
1		19.234	1009970.84	0.86
2		19.462	473214.37	0.40
3		19.731	686987.08	0.58
4		20.028	510282.21	0.43
5		20.184	349777.31	0.30
6		20.309	447475.23	0.38
7		20.436	484766.70	0.41
8		20.715	125712.60	0.11
9	Fluorene	20.929	716486.06	0.61
0		21.278	566316.45	0.48
1		21.600	205121.01	0.17
2		21.756	1019217.78	0.87
3		21.948	958672.38	0.81
4		22.204	868919.90	0.74
5		22.397	271989.60	0.23
6		22.636	485858.48	0.41
7		22.749	836022.02	0.71
8		23.110	389812.59	0.33
9	Phenathrene	23.402	566279.97	0.48
0		24.177	133658.40	0.11
1		24.417	82310.23	0.07
2		24.672	59767.26	0.05
3		24.816	304745.73	0.26
4		25.065	1431049.03	1.22
5		25.299	1299718.09	1.10
6		25.651	908192.47	0.77
7		25.852	175061.98	0.15
8		26.043	90681.64	0.08
9	Anthracene	26.321	517518.64	0.44
0		26.480	586965.75	0.50
1		26.908	414592.89	0.35
2		27.034	216046.70	0.18
3		27.205	243769.32	0.21
4		27.456	169760.89	0.14
5		27.921	1940192.03	1.65
6		28.187	463345.67	0.39
7		28.361	56540.49	0.05

2/21/2007 3:13:30 PM Result: C:\Data\datb002-20070221-151330.rst

Peak #	Component Name	Time [min]	Area [uV*sec]	Area [%]
157		40.530	1419390.54	1.21
158		40.902	419688.36	0.36
159		41.044	420256.68	0.36
160		41.185	593634.73	0.50
161		41.428	250597.73	0.21
162		41.660	305322.01	0.26
163		41.819	893472.60	0.76
164		42.255	380275.35	0.32
165		42.525	277959.14	0.24
166		42.614	236358.17	0.20
167		42.870	405541.98	0.34
168		43.020	71304.18	0.06
169		43.198	73082.42	0.06
170		43.285	221179.20	0.19
171		43.477	137078.54	0.12
172		43.711	303967.03	0.26
173		43.835	452986.84	0.39
174		44.601	89315.14	0.08
175		44.952	407899.06	0.35
176		45.261	120185.85	0.10
177		45.384	240202.78	0.20
178		45.744	257088.27	0.22
179		46.132	62083.16	0.05
180		46.327	56431.21	0.05
181		46.517	98816.73	0.08
182		46.873	109050.04	0.09
183		47.024	136686.60	0.12
184		47.236	104144.15	0.09
185		47.473	215304.41	0.18
186		47.947	169208.88	0.14
187		48.472	64118.24	0.05
188		49.336	102284.75	0.09
189		49.820	114113.19	0.10
190		50.135	78918.56	0.07

1.18e+08 100.00

Warning -- Signal level out-of-range in peak

Missing Component Report

Component	Expected Retention (Calibration File)
-----------	---------------------------------------

Benzene	1.820
Benzo (b) furan	5.030

KOPPERS INC.
Tel: (724) 684-1000
Fax: (724) 684-1011

Coke Oven Gas Desulfurization - Daily Testing									
1. Desul Inlet:		Date		Time					
		02/23/07		11:11am					
H ₂	1.87	CO ₂	0.92	C ₂ H ₄	0.59	C ₂ H ₆	5.02	C ₂ H ₂	0.02
O ₂	10.94	N ₂	64.75	CH ₄	15.18	CO	0.71	BTU	259
Tutweiler Analysis		NA		grains/100 cu. ft.					
2. Desul Outlet:		Houston-Atlas				Tutweiler			
Time:	NA	NA				NA			
All H ₂ S analysis in grains per 100 cu. ft.									
Sample #1 @ 365°C.									

KOPPERS INC.
Tel: (724) 684-1000
Fax: (724) 684-1011

Coke Oven Gas Desulfurization - Daily Testing									
1. Desul Inlet:		Date		Time					
		02/23/07		12:20pm					
H2	8.93	CO2	0.37	C2H4	0.59	C2H6	5.02	C2H2	0.02
O2	9.22	N2	53.58	CH4	21.11	CO	1.16	BTU	344
Tutweiler Analysis		NA		grains/100 cu. ft.					
2. Desul Outlet:		Houston-Atlas				Tutweiler			
Time:	NA	NA				NA			
All H2S analysis in grains per 100 cu. ft.									
Sample #2 @ 450°C									

KOPPERS INC.
Tel: (724) 684-1000
Fax: (724) 684-1011

Coke Oven Gas Desulfurization - Daily Testing									
1. Desul Inlet:		Date		Time					
		02/28/07		9:47am					
H2	17.35	CO2	0.37	C2H4	0.37	C2H6	1.96	C2H2	0.02
O2	8.11	N2	46.47	CH4	23.53	CO	1.82	BTU	341
Tutweiler Analysis		NA		grains/100 cu. ft.					
2. Desul Outlet:		Houston-Atlas		Tutweiler					
Time:		NA		NA		NA			
All H2S analysis in grains per 100 cu. ft.									
Sample #3 @ 550°C.									

Table 3

Co-Products Collected from Wolfe's Mild Gasification Unit Operated by Coal Technology Corporation (CTC)

Note: Analysis conducted by Allied Signal, Inc in 1998

Heavy Coal Oil Liquid From Virginia Coal

Specific Gravity	60 F	1.108
Water	Vol. %	9.0 %
Quinoline Insolubles	Wt. %	4.4 %
Ash	Wt. %	0.089 %
Ammonium Chlorides	#/1000gal.	300

Pitch

Softening Point	C	54.40
Toluene Insolubles	Wt. %	16.40
Quinoline Insolubles	Wt. %	10.10
Coking Value	Wt. %	28.60
Ash	Wt. %	0.36
Sulfur	Wt. %	0.45
Distillation to 360 C	Wt. %	10.50

Flue Syn-Gas Analysis Collected from Wolfe's Mild Gasification Unit Operated by Coal Technology Corporation (CTC)

Note: Analysis conducted by Department of Energy at Morgantown Lab. in 1998

Flue Gas (Non-Condensable gas from Pyrolysis of Virginia Coal)

Gas	Volume %	Wt. #/cub ft.	Btu/cub ft.	Air Required
CH ₄	38.16	0.0171	366.3	3.66
C ₂ H ₆	1.46	0.0012	24.8	0.24
C _x H _{2x+2}	2.25	0.0038	38.3	0.09
H ₂	30.66	0.0017	89.5	0.89
O ₂	4.95	0.0044	--	--
N ₂	19.13	0.0150	--	--
CO	2.76	0.0022	22	0.07
CO ₂	0.65	0.0008	--	--
H ₂ S, COS, SO ₂	0.0037	0.2 X 10 ⁻⁶	1.1	0.01
Totals	100.0237	0.0462#/SCF	542 Btu/SCF (11,700 Btu/#)	4.96SCF/SCF

Data Assembled from CTC slides for Dr. Richard A. Wolfe

- last time very high CO₂

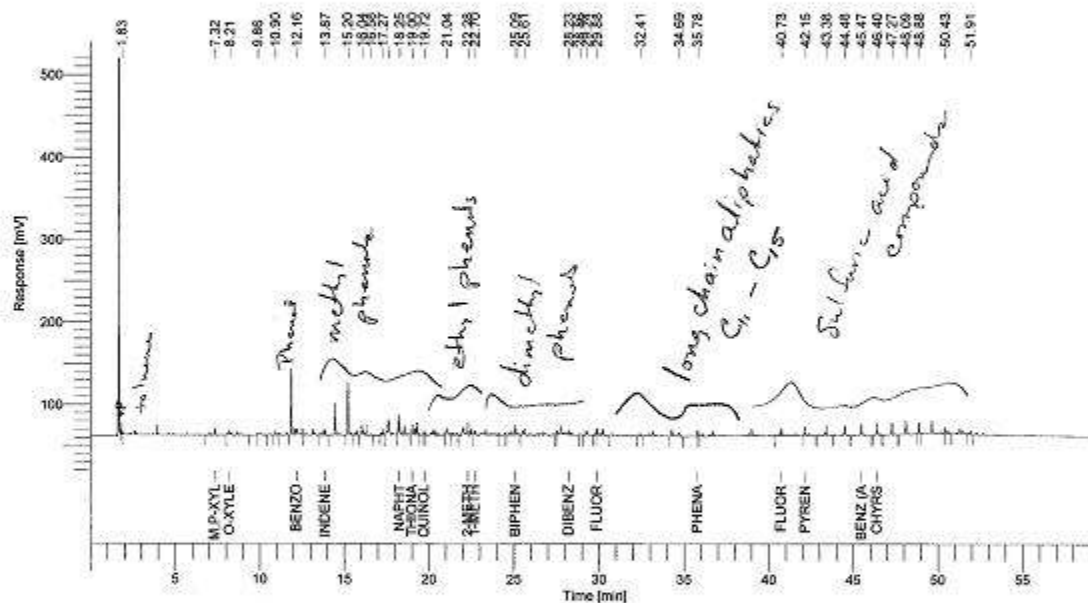
$$.38(0.0171) \left(\frac{11,700 \text{ Btu}}{\#} \right)$$

Software Version : 6.3.1.0504
 Reprocess Number : 617d691: 3682
 Sample Name : 08-2725
 Instrument Name : Clarus 500
 Rack/Vial : 0/13
 Sample Amount : 1.000000
 Cycle : 13

Date : 10/8/2008 6:51:39 AM
 Data Acquisition Time : 10/8/2008 5:51:43 AM
 Channel : B
 Operator : TCWS
 Dilution Factor : 1.000000

Result File : C:\Data\datb006-20081008-065138.rst

Sequence File : C:\Sequences\October 7-2008-pecreo-MSDSsolvent-WVU.seq



DEFAULT REPORT

Peak #	Component Name	Time [min]	Area [uV*sec]	Area [%]
1		1.825	15090.27	0.48
2	m,p-Xylene	7.324	53016.05	1.69
3	o-Xylene	8.206	75162.27	2.40
4		9.858	34293.11	1.09
5		10.905	23116.65	0.74
6	Benzofuran	12.165	295871.07	9.44
7	Indene	13.866	53128.24	1.69
8		15.199	276544.84	8.82
9		16.035	76993.96	2.46

More work

10/8/2008 4:12:28 AM Result: C:\Data\datb006-20081008-041227.rst

Warning -- Signal level out-of-range in peak

Missing Component Report

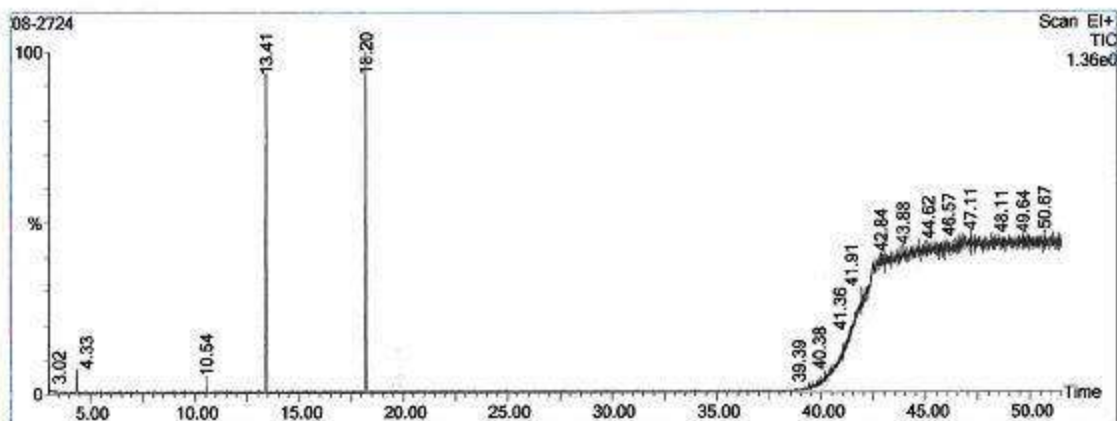
Component	Expected Retention (Calibration File)
Benzene	2.340
Toluene	3.930
o-Xylene	8.210
Indan	13.570
Indene	14.120
Naphthalene	18.610
Thionaphthene	18.750
Quinoline	20.240
2-Methylnaph	22.010
1-Methylnaph	22.510
Biphenyl	24.440
Acenaphthene	27.250
Dibenzofuran	28.090
Fluorene	29.750
Phenathrene	35.970
Anthracene	36.200
Carbazol	37.510
Fluoranthene	41.650
Pyrene	42.400
Benz (a) anthracene	46.210
Chrysene	46.350

Qualitative Report

File: C:\TURBOMASS\PAH.PRO\Data\08-2724.raw
 Acquired: 08-Oct-08 02:48:24 PM
 Description:
 GC/MS Method: GC: Creo.mth MS: Creo.EXP
 Sample ID:

Printed: 09-Oct-08 07:27 AM

Page 1 of 2
 Vial Number: 2



#	RT	Scan	Height	Area	Area %	Norm %	Name
1	4.328	198	91,593	3,181.3	0.563	5.23	
2	10.544	1125	67,859	2,361.2	0.418	3.88	
3	13.407	1552	1,273,365	59,363.7	10.498	97.60	
4	18.201	2267	1,354,616	60,822.2	10.756	100.00	
5	41.651	5764	41,845	2,143.9	0.379	3.52	
6	41.906	5802	100,024	2,023.2	0.358	3.33	
7	42.033	5821	54,834	2,451.7	0.434	4.03	
8	42.248	5853	42,234	1,719.2	0.304	2.83	
9	42.905	5951	60,657	1,988.9	0.352	3.27	
10	43.367	6020	53,961	1,776.4	0.314	2.92	
11	43.716	6072	41,004	1,983.2	0.351	3.26	
12	43.770	6080	73,406	1,929.1	0.341	3.17	
13	43.877	6096	77,478	3,269.7	0.578	5.38	
14	44.031	6119	64,427	2,058.8	0.364	3.38	
15	44.226	6148	46,691	1,796.6	0.318	2.95	
16	44.320	6162	49,866	1,756.9	0.311	2.89	
17	44.655	6212	61,921	2,034.9	0.360	3.35	
18	44.789	6232	68,509	2,158.5	0.382	3.55	
19	44.863	6243	60,394	1,913.0	0.338	3.15	
20	44.957	6257	54,240	1,746.6	0.309	2.87	
21	45.171	6289	60,534	2,138.9	0.378	3.51	
22	45.292	6307	81,895	1,852.3	0.328	3.05	

Inst() ACQUISITION PARAMETERS

Oven: Initial temp 80°C for 5 min, ramp 5°C/min to 165°C, hold 5 min, ramp 10°C/min to 310°C, hold 10 min, InjAauto=300°C,
 Volume=0 µL, Split=20:1, Carrier Gas=He, Solvent Delay=3.00 min, Transfer Temp=250°C, Source Temp=200°C, Scan: 50 to
 350Da, Column 30.0m x 250µm

10/8/2008 6:51:39 AM Result: C:\Data\datb006-20081008-065138.rst

Peak #	Component Name	Time [min]	Area [uV*sec]	Area [%]
10		16.578	15421.77	0.49
11		17.273	30239.06	0.96
12		17.621	159115.37	5.07
13	Naphthalene	18.254	193185.53	6.16
14	Thionaphthene	19.005	113341.37	3.61
15	Quinoline	19.718	11598.10	0.37
16		21.044	68125.57	2.17
17	2-Methylnaph	22.284	162524.17	5.18
18	1-Methylnaph	22.698	174553.14	5.57
19	Biphenyl	25.091	101833.43	3.25
20		25.605	158479.78	5.05
21	Dibenzofuran	28.230	171189.72	5.46
22		28.859	15791.89	0.50
23		29.241	41451.08	1.32
24	Fluorene	29.876	75293.25	2.40
25		32.412	18308.64	0.58
26		34.691	73008.15	2.33
27	Phenathrene	35.784	32659.78	1.04
28	Fluoranthene	40.732	80579.08	2.57
29	Pyrene	42.155	59474.75	1.90
30		43.383	65489.65	2.09
31		44.478	70612.63	2.25
32	Benz (a) anthracene	45.472	63012.65	2.01
33	Chrysene	46.397	55025.89	1.75
34		47.269	57716.56	1.84
35		48.093	59390.67	1.89
36		48.878	41366.71	1.32
37		50.427	37938.46	1.21
38		51.910	25645.60	0.82
			3135588.90	100.00

Warning -- Signal level out-of-range in peak

Missing Component Report

Component Expected Retention (Calibration File)

Benzene	2.340
Toluene	3.930
Phenol	11.850
Indan	13.570
Acenaphthene	27.250
Anthracene	36.200
Carbazol	37.510

10/8/2008 6:51:39 AM Result: C:\Data\datb006-20081008-065138.rst

Peak #	Component Name	Time [min]	Area [uV*sec]	Area [%]
10		16.578	15421.77	0.49
11		17.273	30239.06	0.96
12		17.621	159115.37	5.07
13	Naphthalene	18.254	193185.53	6.16
14	Thionaphthene	19.005	113341.37	3.61
15	Quinoline	19.718	11598.10	0.37
16		21.044	68125.57	2.17
17	2-Methylnaph	22.284	162524.17	5.18
18	1-Methylnaph	22.698	174553.14	5.57
19	Biphenyl	25.091	101833.43	3.25
20		25.605	158479.78	5.05
21	Dibenzofuran	28.230	171189.72	5.46
22		28.859	15791.89	0.50
23		29.241	41451.08	1.32
24	Fluorene	29.876	75293.25	2.40
25		32.412	18308.64	0.58
26		34.691	73008.15	2.33
27	Phenathrene	35.784	32659.78	1.04
28	Fluoranthene	40.732	80579.08	2.57
29	Pyrene	42.155	59474.75	1.90
30		43.383	65489.65	2.09
31		44.478	70612.63	2.25
32	Benz (a) anthracene	45.472	63012.65	2.01
33	Chrysene	46.397	55025.89	1.75
34		47.269	57716.56	1.84
35		48.093	59390.67	1.89
36		48.878	41366.71	1.32
37		50.427	37938.46	1.21
38		51.910	25645.60	0.82
			3135588.90	100.00

Warning -- Signal level out-of-range in peak

Missing Component Report

Component Expected Retention (Calibration File)

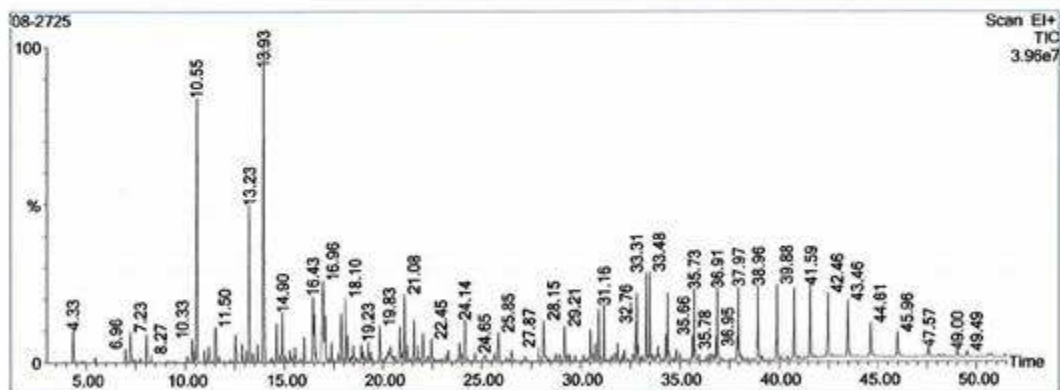
Benzene	2.340
Toluene	3.930
Phenol	11.850
Indan	13.570
Acenaphthene	27.250
Anthracene	36.200
Carbazol	37.510

Qualitative Report

File: C:\TURBOMASS\PAH.PRO\Data\08-2725.raw
 Acquired: 08-Oct-08 04:49:03 PM
 Description:
 GC/MS Method: GC: Creo.mth MS: Creo.EXP
 Sample ID:

Printed: 09-Oct-08 07:34 AM

Page 1 of 2
 Vial Number: 4



#	RT	Scan	Height	Area	Area %	Norm %	Name
1	4.328	198	4,105,657	184,636.7	0.740	7.77	
2	7.231	631	3,626,037	216,352.2	0.868	9.10	
3	8.022	749	3,517,355	167,634.0	0.672	7.05	
4	10.329	1093	2,766,095	129,440.5	0.519	5.44	
5	10.550	1126	32,948,130	1,618,660.4	6.491	68.07	
6	11.509	1269	4,301,846	334,565.8	1.342	14.07	
7	12.529	1421	3,450,386	200,562.3	0.804	8.43	
8	13.226	1525	19,651,444	920,693.4	3.692	38.72	
9	13.930	1630	39,569,912	2,377,782.2	9.535	100.00	
10	14.614	1732	4,798,806	222,405.4	0.892	9.35	
11	14.902	1775	6,170,466	266,229.4	1.068	11.20	
12	16.009	1940	3,125,378	140,093.6	0.562	5.89	
13	16.431	2003	8,265,476	394,757.6	1.583	16.60	
14	16.498	2013	6,005,142	279,016.3	1.119	11.73	
15	16.961	2082	9,687,884	937,771.2	3.761	39.44	
16	17.075	2099	5,485,274	262,662.2	1.133	11.89	
17	17.853	2215	6,034,056	328,602.2	1.318	13.82	
18	18.101	2252	7,777,412	342,680.9	1.374	14.41	
19	18.202	2267	3,247,738	169,754.2	0.761	7.98	
20	19.831	2510	4,250,688	220,656.9	0.885	9.28	
21	20.347	2587	1,779,973	135,163.7	0.542	5.68	
22	20.857	2663	4,130,844	200,505.5	0.804	8.43	

Inst() ACQUISITION PARAMETERS

Oven: Initial temp 80°C for 5 min, ramp 5°C/min to 165°C, hold 5 min, ramp 10°C/min to 310°C, hold 10 min, InjAauto=300°C, Volume=0 µL, Split=20:1, Carrier Gas=He, Solvent Delay=3.00 min, Transfer Temp=250°C, Source Temp=200°C, Scan: 50 to 350Da, Column 30.0m x 250µm

Qualitative Report

File: C:\TURBOMASS\PAH.PRO\Data\08-2725.raw
 Acquired: 08-Oct-08 04:49:03 PM
 Description:
 GC/MS Method: GC: Creo.mth MS: Creo.EXP
 Sample ID:

Printed: 09-Oct-08 07:34 AM

Page 2 of 2
 Vial Number: 4

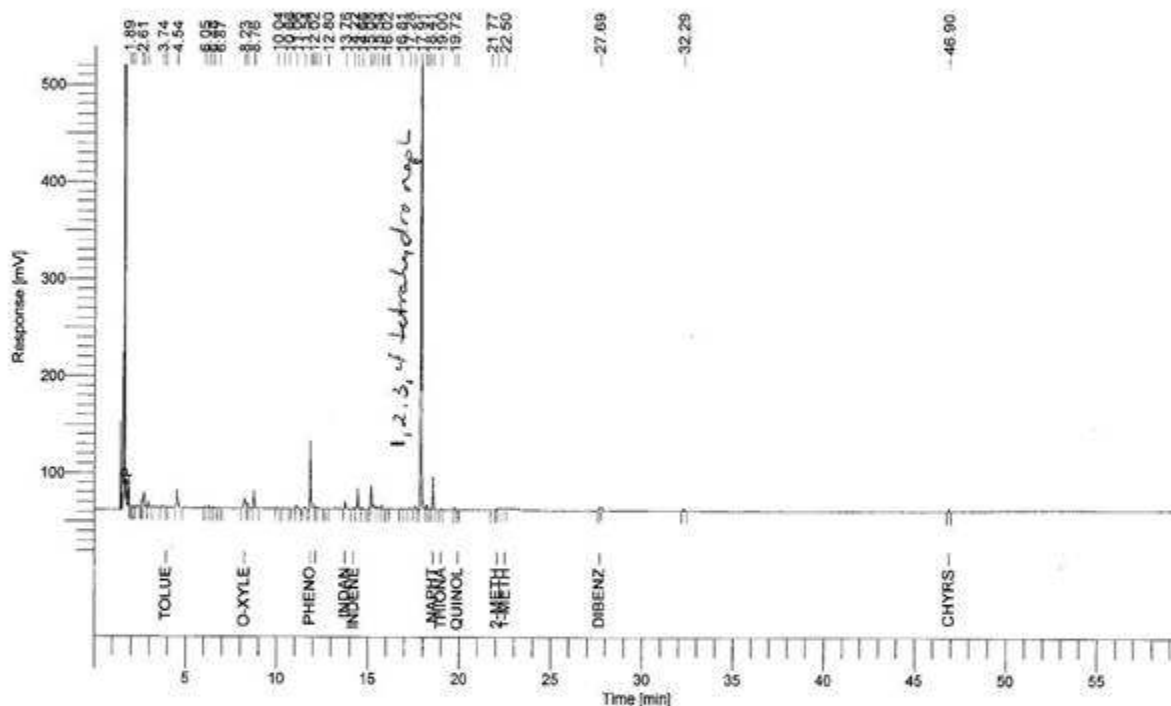
#	RT	Scan	Height	Area	Area %	Norm %	Name
23	21.085	2697	8,255,573	354,842.5	1.423	14.92	
24	21.554	2767	5,205,292	258,698.1	1.037	10.88	
25	22.030	2838	3,448,268	164,769.4	0.661	6.93	
26	22.446	2900	2,646,556	124,406.4	0.499	5.23	
27	24.136	3152	5,197,992	297,496.8	1.193	12.51	
28	25.853	3408	3,455,729	235,940.8	0.946	9.92	
29	28.146	3750	5,016,358	285,932.4	1.187	12.45	
30	29.206	3908	4,143,724	229,760.3	0.921	9.66	
31	30.507	4102	3,668,898	157,677.6	0.632	6.63	
32	30.909	4162	6,510,426	256,917.7	1.030	10.80	
33	31.164	4200	7,003,378	285,830.8	1.146	12.02	
34	32.760	4438	4,483,903	222,396.9	0.892	9.35	
35	32.854	4452	8,456,246	288,761.8	1.158	12.14	
36	33.310	4520	10,895,064	400,501.6	1.606	16.84	
37	33.484	4546	10,949,652	374,996.8	1.504	15.77	
38	34.316	4670	3,263,804	140,054.1	0.562	5.89	
39	34.410	4684	8,501,826	268,869.8	1.078	11.31	
40	35.731	4881	8,602,205	289,528.9	1.161	12.18	
41	36.905	5056	8,644,819	282,987.6	1.135	11.90	
42	37.972	5215	9,281,679	343,331.9	1.377	14.44	
43	38.958	5362	9,347,591	327,936.8	1.315	13.79	
44	39.883	5500	9,379,384	410,747.5	1.647	17.27	
45	40.755	5630	9,017,876	412,464.0	1.654	17.35	
46	41.594	5755	9,221,308	431,103.8	1.729	18.13	
47	42.459	5884	8,043,558	430,604.6	1.727	18.11	
48	43.459	6033	6,937,256	419,705.1	1.683	17.65	
49	44.612	6205	4,147,986	295,995.0	1.187	12.45	
50	45.960	6406	3,053,427	243,256.4	0.975	10.23	

Inst() ACQUISITION PARAMETERS

Oven: Initial temp 80°C for 5 min, ramp 5°C/min to 165°C, hold 5 min, ramp 10°C/min to 310°C, hold 10 min, InjAuto=300°C, Volume=0 µL, Split=20:1, Carrier Gas=He, Solvent Delay=3.00 min, Transfer Temp=250°C, Source Temp=200°C, Scan: 50 to 350Da, Column 30.0m x 250µm

Software Version	: 6.3.1.0504	Date	: 10/8/2008 11:17:44 AM
Reprocess Number	: 617d691: 3702		
Sample Name	: 08-2726	Data Acquisition Time	: 10/8/2008 10:18:08 AM
Instrument Name	: Clarus 500	Channel	: B
Rack/Vial	: 0/15	Operator	: TCWS
Sample Amount	: 1.000000	Dilution Factor	: 1.000000
Cycle	: 15		

Result File : C:\Data\datb006-20081008-111744.rst
Sequence File : C:\Sequences\October 7-2008-pecreo-MSDSsolvent-WVU.seq



DEFAULT REPORT

Peak #	Component Name	Time [min]	Area [uV*sec]	Area [%]
1		1.887	31281.83	0.70
2		2.003	1016.38	0.02
3		2.077	978.84	0.02
4		2.161	1722.86	0.04
5		2.605	14224.70	0.32
6		2.723	66805.27	1.50
7		2.940	13385.38	0.30
8		3.737	10526.50	0.24
9	Toluene	3.925	1667.59	0.04

10/8/2008 11:17:44 AM Result: C:\Data\datb006-20081008-111744.rst

Peak #	Component Name	Time [min]	Area [uV*sec]	Area [%]
10		4.537	83538.66	1.88
11		6.053	8568.29	0.19
12		6.282	6709.51	0.15
13		6.480	1601.20	0.04
14		6.553	5618.20	0.13
15		6.868	2271.03	0.05
16	o-Xylene	8.234	57463.96	1.29
17		8.385	16607.11	0.37
18		8.759	59742.84	1.34
19		10.043	4320.21	0.10
20		10.352	5971.54	0.13
21		10.656	4124.58	0.09
22		11.063	17814.30	0.40
23		11.541	6078.42	0.14
24	Phenol	11.853	188228.82	4.24
25		12.021	34607.13	0.78
26	Benzofuran	12.145	10946.52	0.25
27		12.314	6742.05	0.15
28		12.799	2311.51	0.05
29	Indan	13.757	29890.01	0.67
30	Indene	14.222	6084.61	0.14
31		14.450	58190.01	1.31
32		14.659	8706.46	0.20
33		15.076	5888.59	0.13
34		15.190	110036.36	2.48
35		15.336	26477.34	0.60
36		15.539	16568.33	0.37
37		15.764	13528.95	0.30
38		16.021	2180.67	0.05
39		16.136	1570.56	0.04
40		16.807	5476.99	0.12
41		17.277	6725.01	0.15
42		17.579	13926.63	0.31
43		17.915	3294577.27	74.17
44		18.178	12110.50	0.27
45		18.253	14507.88	0.33
46		18.408	2096.56	0.05
47	Naphthalene	18.560	97199.33	2.19
48	Thionaphthene	18.999	3979.84	0.09
49		19.721	9268.27	0.21
50	Quinoline	19.905	1646.40	0.04
51		21.766	4009.37	0.09
52	2-Methylnaph	22.057	2239.14	0.05
53	1-Methylnaph	22.495	2969.96	0.07
54	Dibenzofuran	27.687	6725.76	0.15
55		32.294	11053.88	0.25
56	Chrysene	46.897	9497.75	0.21
			4442007.65	100.00

10/8/2008 11:17:44 AM Result: C:\Data\datb006-20081008-111744.rst

Warning -- Signal level out-of-range in peak

Missing Component Report

Component	Expected Retention (Calibration File)
Benzene	2.340
m,p-Xylene	7.330
Biphenyl	24.440
Acenaphthene	27.250
Fluorene	29.750
Phenanthrene	35.970
Anthracene	36.200
Carbazol	37.510
Fluoranthene	41.650
Pyrene	42.400
Benz (a) anthracene	46.210

Qualitative Report

File: C:\TURBOMASS\PAH.PRO\Data\08-2726.raw

Acquired: 08-Oct-08 06:49:40 PM

Printed: 09-Oct-08 07:34 AM

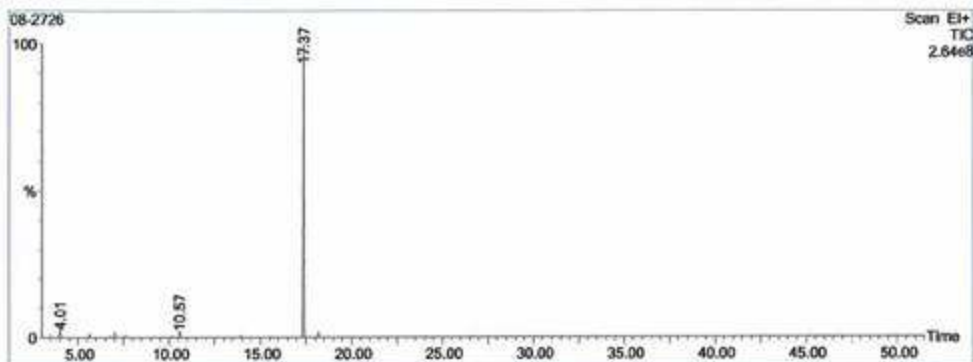
Description:

GC/MS Method: GC: Creo.mth MS: Creo.EXP

Page 1 of 2

Sample ID:

Vial Number: 6



#	RT	Scan	Height	Area	Area %	Norm %	Name
1	3.141	21	110,778	4,488.0	0.028	0.03	
2	3.469	70	2,833,176	214,805.0	1.350	1.62	
3	3.878	131	347,077	11,727.7	0.074	0.09	
4	4.012	151	7,234,720	514,853.9	3.235	3.88	
5	4.784	266	222,842	10,000.5	0.063	0.08	
6	5.822	391	3,390,718	130,027.7	0.817	0.98	
7	6.742	558	913,230	53,706.3	0.338	0.40	
8	7.003	597	4,223,902	228,340.7	1.435	1.72	
9	7.573	682	1,438,858	55,604.5	0.349	0.42	
10	8.076	757	56,079	2,519.5	0.016	0.02	
11	8.284	788	251,980	16,750.5	0.105	0.13	
12	9.149	917	502,551	19,171.1	0.120	0.14	
13	9.229	929	258,564	9,109.8	0.057	0.07	
14	9.652	992	203,201	7,312.8	0.046	0.06	
15	9.873	1025	90,309	3,431.1	0.022	0.03	
16	10.101	1059	577,654	33,179.6	0.209	0.25	
17	10.215	1076	989,141	65,228.3	0.410	0.49	
18	10.329	1093	51,737	2,578.0	0.016	0.02	
19	10.571	1129	5,828,504	375,003.9	2.357	2.83	
20	11.201	1223	214,093	7,608.0	0.048	0.06	
21	11.791	1311	354,795	12,571.2	0.079	0.09	
22	13.233	1526	451,036	17,327.0	0.109	0.13	

Inst() ACQUISITION PARAMETERS

Oven: Initial temp 80°C for 5 min, ramp 5°C/min to 165°C, hold 5 min, ramp 10°C/min to 310°C, hold 10 min, InjAauto=300°C, Volume=0 µL, Split=20:1, Carrier Gas=He, Solvent Delay=3.00 min, Transfer Temp=250°C, Source Temp=200°C, Scan: 50 to 350Da, Column 30.0m x 250µm

Qualitative Report

File: C:\TURBOMASS\PAH.PRO\Data\08-2726.raw
 Acquired: 08-Oct-08 06:49:40 PM
 Description:
 GC/MS Method: GC: Creo.mth MS: Creo.EXP
 Sample ID:

Printed: 09-Oct-08 07:34 AM

Page 2 of 2
 Vial Number: 6

#	RT	Scan	Height	Area	Area %	Norm %	Name
23	13.930	1630	1,405,239	72,497.8	0.456	0.55	
24	14.480	1712	143,619	4,543.2	0.029	0.03	
25	15.553	1872	267,052	9,139.2	0.057	0.07	
26	17.370	2143	263,972,800	13,273,797.0	83.416	100.00	
27	17.497	2162	715,975	25,641.5	0.161	0.19	
28	18.201	2267	4,529,298	209,442.8	1.316	1.58	
29	19.214	2418	76,326	2,832.1	0.018	0.02	
30	26.382	3484	57,517	2,648.8	0.017	0.02	
31	28.423	3493	71,774	2,592.2	0.016	0.02	
32	28.617	3522	320,169	90,210.2	0.567	0.68	
33	27.019	3582	48,841	3,658.7	0.023	0.03	
34	42.804	5936	48,281	2,361.7	0.015	0.02	
35	43.609	6056	71,599	2,568.6	0.016	0.02	
36	43.656	6063	63,966	3,119.2	0.020	0.02	
37	43.736	6075	69,876	2,652.8	0.017	0.02	
38	43.924	6103	64,044	3,972.3	0.025	0.03	
39	44.514	6191	61,372	2,429.1	0.015	0.02	
40	44.655	6212	86,003	3,162.7	0.020	0.02	
41	44.823	6237	67,706	2,555.3	0.016	0.02	
42	44.984	6261	57,007	2,673.4	0.017	0.02	
43	45.486	6333	60,789	2,197.0	0.014	0.02	
44	46.579	6499	49,806	3,915.4	0.025	0.03	
45	48.584	6796	162,713	2,415.0	0.015	0.02	
46	48.651	6808	53,828	2,520.3	0.016	0.02	
47	49.282	6902	58,610	2,247.3	0.014	0.02	
48	50.797	7128	73,764	4,887.7	0.031	0.04	
49	51.112	7175	75,760	4,315.6	0.027	0.03	
50	51.186	7186	62,196	2,436.4	0.015	0.02	

Inst() ACQUISITION PARAMETERS

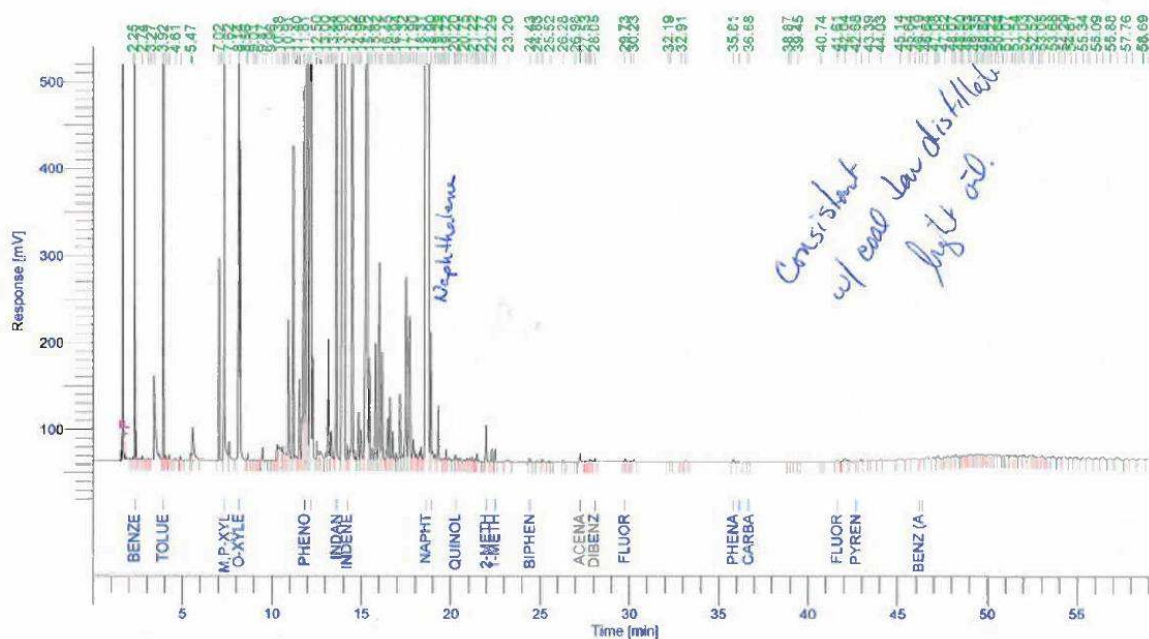
Over: Initial temp 80°C for 5 min, ramp 5°C/min to 165°C, hold 5 min, ramp 10°C/min to 310°C, hold 10 min, InjAuto=300°C, Volume=0 µL, Split=20:1, Carrier Gas=He, Solvent Delay=3.00 min, Transfer Temp=250°C, Source Temp=200°C, Scan: 50 to 350Da, Column 30.0m x 250µm

Software Version : 6.3.1.0504
 Reprocess Number : 617d691: 3705
 Sample Name : 08-2728
 Instrument Name : Clarus 500
 Rack/Vial : 0/18
 Sample Amount : 1.000000
 Cycle : 3

Date : 10/8/2008 4:28:24 PM
 Data Acquisition Time : 10/8/2008 3:28:46 PM
 Channel : B
 Operator : TCWS
 Dilution Factor : 1.000000

Result File : C:\Data\datb006-20081008-162824.rst

Sequence File : C:\Sequences\October 7-2008-pecreo-MSDSsolvent-WVU.seq



DEFAULT REPORT

Peak #	Component Name	Time [min]	Area [uV*sec]	Area [%]
1	Benzene	2.255	4940.91	0.01
2		2.328	2029478.49	2.94
3		2.739	8430.50	0.01
4		3.078	3396.30	0.00
5	Toluene	3.266	1374.34	0.00
6		3.441	472903.94	0.68
7		3.921	2529473.41	3.66
8		4.045	12281.07	0.02
9		4.232	12296.84	0.02

10/8/2008 4:28:24 PM Result: C:\Data\datb006-20081008-162824.rst

Peak #	Component Name	Time [min]	Area [uV*sec]	Area [%]
10		4.611	6130.72	0.01
11		4.889	11642.30	0.02
12		5.473	33188.19	0.05
13		5.546	204175.19	0.30
14		7.024	602290.20	0.87
15		7.173	6342.04	0.01
16	m,p-Xylene	7.341	3208475.93	4.64
17		7.619	96504.84	0.14
18	o-Xylene	8.144	2701043.19	3.91
19		8.556	5894.24	0.01
20		8.644	25574.65	0.04
21		9.006	5560.46	0.01
22		9.183	3256.49	0.00
23		9.472	42643.95	0.06
24		9.665	4331.19	0.01
25		9.961	3690.62	0.01
26		10.213	3553.17	0.01
27		10.296	59047.03	0.09
28		10.384	171625.72	0.25
29		10.595	79758.35	0.12
30		10.714	75126.17	0.11
31		10.912	654516.48	0.95
32		11.175	987555.17	1.43
33		11.271	30596.90	0.04
34		11.396	14945.58	0.02
35		11.539	437627.08	0.63
36	Phenol	11.815	1995660.92	2.89
37		12.006	5285544.14	7.64
38	Benzofuran	12.177	4346279.29	6.29
39		12.499	101107.39	0.15
40		12.680	106891.67	0.15
41		13.000	49744.64	0.07
42		13.142	456926.57	0.66
43		13.313	142742.44	0.21
44		13.436	10696.76	0.02
45	Indan	13.604	2946076.01	4.26
46		13.901	11290646.71	16.33
47	Indene	14.208	44896.44	0.06
48		14.267	29132.15	0.04
49		14.516	2156913.75	3.12
50		14.690	38223.91	0.06
51		14.849	194472.09	0.28
52		14.962	141263.81	0.20
53		15.325	5115276.49	7.40
54		15.421	333403.54	0.48
55		15.586	60584.37	0.09
56		15.818	522130.03	0.76
57		16.012	1027052.33	1.49
58		16.165	419167.42	0.61

10/8/2008 4:28:24 PM Result: C:\Data\datb006-20081008-162824.rst

Peak #	Component Name	Time [min]	Area [uV*sec]	Area [%]
59		16.454	163204.96	0.24
60		16.593	202923.48	0.29
61		16.745	103906.07	0.15
62		16.940	37896.50	0.05
63		17.177	221957.87	0.32
64		17.323	39076.05	0.06
65		17.508	911230.19	1.32
66		17.690	896403.48	1.30
67		17.895	132287.28	0.19
68		18.039	36507.52	0.05
69		18.231	50564.37	0.07
70		18.311	47276.87	0.07
71		18.419	20841.68	0.03
72	Naphthalene	18.601	12392030.11	17.92
73	Thionaphthene	18.900	411848.76	0.60
74		19.117	39321.92	0.06
75		19.292	184823.60	0.27
76		19.441	11435.97	0.02
77		19.544	11416.38	0.02
78		19.629	10287.21	0.01
79		19.722	40800.10	0.06
80		19.904	30029.29	0.04
81		20.195	12900.78	0.02
82	Quinoline	20.265	26769.68	0.04
83		20.399	10315.38	0.01
84		20.519	14593.26	0.02
85		20.746	6756.75	0.01
86		20.886	17783.59	0.03
87		21.079	19043.60	0.03
88		21.222	20207.32	0.03
89		21.414	10646.81	0.02
90		21.492	25114.17	0.04
91		21.574	6526.48	0.01
92		21.770	1258.23	0.00
93	2-Methylnaph	21.976	130640.09	0.19
94		22.286	39285.06	0.06
95	1-Methylnaph	22.463	40780.34	0.06
96		23.201	22456.69	0.03
97	Biphenyl	24.430	14162.87	0.02
98		24.829	9459.16	0.01
99		25.093	15314.90	0.02
100		25.522	6286.23	0.01
101		25.610	3199.11	0.00
102		26.280	9460.35	0.01
103		26.977	1873.84	0.00
104	Acenaphthene	27.223	35642.29	0.05
105		27.529	3822.38	0.01
106		27.731	9583.74	0.01
107		27.836	12830.05	0.02

10/8/2008 4:28:24 PM Result: C:\Data\datb006-20081008-162824.rst

Peak #	Component Name	Time [min]	Area [uV*sec]	Area [%]
108	Dibenzofuran	28.046	15293.05	0.02
109	Fluorene	29.731	12371.06	0.02
110		30.047	3191.76	0.00
111		30.234	11582.63	0.02
112		32.189	1982.19	0.00
113		32.305	4450.30	0.01
114		32.909	1744.19	0.00
115		33.160	10785.40	0.02
116	Phenathrene	35.808	15319.14	0.02
117	Anthracene	36.116	8018.83	0.01
118	Carbazol	36.676	3703.79	0.01
119		38.871	1629.47	0.00
120		39.010	4335.73	0.01
121		39.446	1686.25	0.00
122		40.739	2151.33	0.00
123	Fluoranthene	41.608	9280.17	0.01
124		42.040	41109.60	0.06
125	Pyrene	42.678	2533.14	0.00
126		42.858	6337.08	0.01
127		43.393	2530.97	0.00
128		44.030	8254.62	0.01
129		45.135	15145.87	0.02
130		45.641	11886.69	0.02
131		45.931	24135.06	0.03
132	Benz (a) anthracene	46.189	1117.48	0.00
133	Chrysene	46.395	9601.97	0.01
134		46.637	26972.87	0.04
135		47.076	15509.34	0.02
136		47.253	26546.99	0.04
137		47.618	2452.67	0.00
138		48.066	19055.50	0.03
139		48.234	25879.41	0.04
140		48.500	7847.55	0.01
141		48.635	12034.17	0.02
142		48.925	6273.47	0.01
143		49.072	19715.95	0.03
144		49.354	14755.02	0.02
145		49.447	23799.27	0.03
146		49.651	20670.99	0.03
147		49.802	13867.03	0.02
148		50.046	22726.95	0.03
149		50.216	22136.75	0.03
150		50.446	21223.37	0.03
151		50.636	21932.12	0.03
152		50.884	12864.81	0.02
153		51.073	27028.42	0.04
154		51.355	31402.13	0.05
155		51.541	21226.69	0.03
156		51.813	24029.37	0.03

10/8/2008 4:28:24 PM Result: C:\Data\datb006-20081008-162824.rst

Peak #	Component Name	Time [min]	Area [uV*sec]	Area [%]
157		52.029	27462.71	0.04
158		52.402	30662.02	0.04
159		52.523	25615.91	0.04
160		52.870	16624.72	0.02
161		53.050	28465.91	0.04
162		53.419	15854.05	0.02
163		53.676	30959.35	0.04
164		54.028	19169.38	0.03
165		54.286	40927.77	0.06
166		54.666	24295.71	0.04
167		54.922	39019.37	0.06
168		55.340	23046.81	0.03
169		55.662	30240.81	0.04
170		56.087	24316.50	0.04
171		56.436	38051.83	0.06
172		56.880	20403.95	0.03
173		57.252	41488.13	0.06
174		57.756	17407.81	0.03
175		58.109	25228.47	0.04
176		58.686	31650.44	0.05
177		58.992	33825.00	0.05
			69142130.40	100.00

Warning – Signal level out-of-range in peak

Missing Component Report

Component Expected Retention (Calibration File)

All components were found

08-2728

Injected On: 10-08-2008 15:28:46 by TCWS

Procedure File: SimDist_Calibration_Mix.pro

Page: 1

Data File: C:\Data\0808-2008\08-16204.CDF

Blank File: C:\Data\0808-2008\08-17141.CDF

Calib File:

Solvent Exclusions: None

BaseLine Zero: 63895.49219

Quench Region: No Quenching Correction

Uncon Total Sample Area: 1.097E10

Corr Total Sample Area: 1.0288E10

Start Of Material (mins): 2.648

End Of Material (mins): 21.472

Sample Weight (g): 1.0000

SOM Thrsh: (0.01000000%)

EOM Thrsh: (0.01000000%)

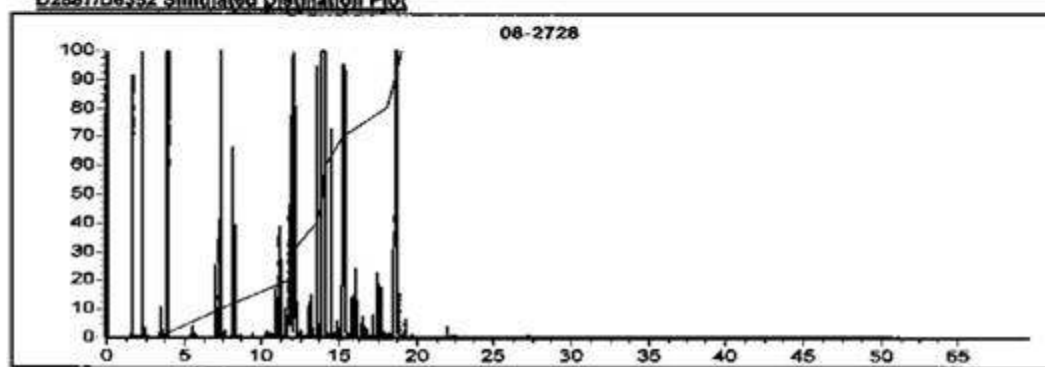
Solvent Weight (g): 0.0000

Material Search Restricted To: NO RESTRICTION

Material End Forced To: NO FORCE

Warnings: EOM Accuracy may be affected by BLEED at END OF RUN

D2887/D6352 Simulated Distillation Plot



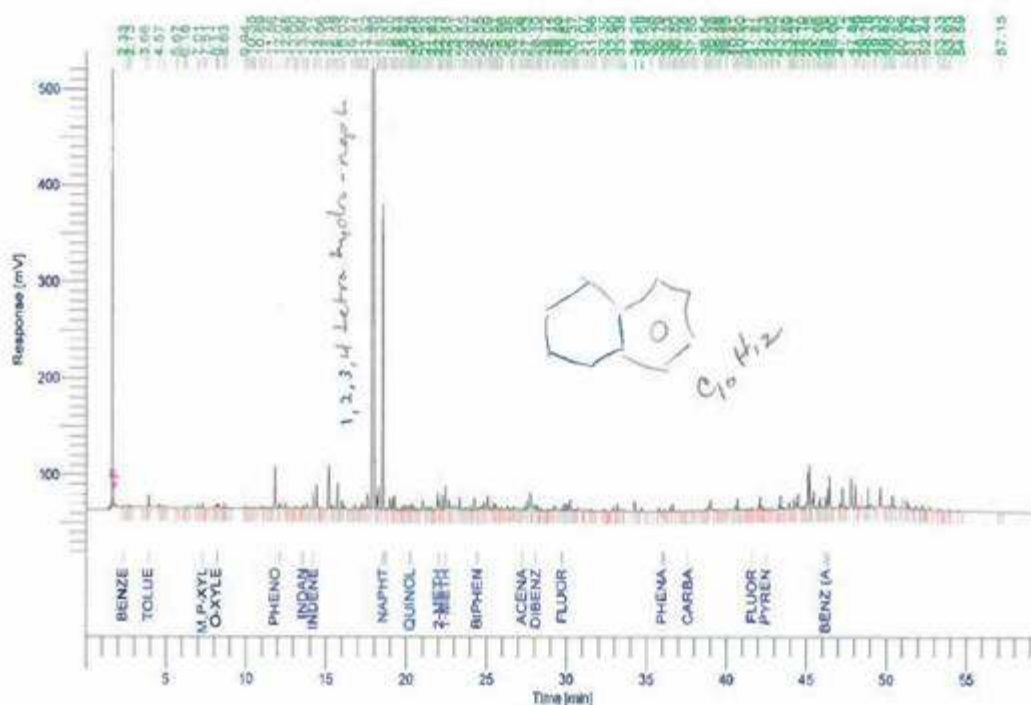
D2887/D6352 Boiling Point Mass Distribution

% OF BP(F)	% OF BP(F)	% OF BP(F)	% OF BP(F)	% OF BP(F)	% OF BP(F)	% OF BP(F)
IBP ... 232.41	20.00% ... 342.89	40.00% ... 363.59	60.00% ... 368.13	80.00% ... 414.55	FBP ... 424.00	
10.00% ... 283.83	30.00% ... 345.87	50.00% ... 367.78	70.00% ... 383.13	90.00% ... 420.74		

Software Version	: 6.3.1.0504	Date	: 10/8/2008 1:46:33 PM
Reprocess Number	: 617d691: 3703		
Sample Name	: 08-2729	Data Acquisition Time	: 10/8/2008 12:46:57 PM
Instrument Name	: Clarus 500	Channel	: B
Rack/Vial	: 0/16	Operator	: TCWS
Sample Amount	: 1.000000	Dilution Factor	: 1.000000
Cycle	: 1		

Result File : C:\Data\datb006-20081008-134633.rst

Sequence File : C:\Sequences\October 7-2008-pecreo-MSDSsolvent-WVU.seq



DEFAULT REPORT

Peak #	Component Name	Time [min]	Area [uV*sec]	Area [%]
1	Benzene	2.329	4155.22	0.03
2		2.606	4772.48	0.04
3		2.731	3821.94	0.03
4		3.664	3911.87	0.03
5	Toluene	3.920	26868.63	0.20
6		4.567	14065.82	0.10
7		4.877	6950.10	0.05
8		5.674	2755.15	0.02
9		6.183	1365.26	0.01

10/8/2008 1:46:33 PM Result: C:\Data\data\006-20081008-134633.rst

Peak #	Component Name	Time [min]	Area [uV*sec]	Area [%]
10		6.285	5507.33	0.04
11		7.007	8750.59	0.06
12	m,p-Xylene	7.311	17997.16	0.13
13		7.510	2917.47	0.02
14		8.110	8587.33	0.06
15	o-Xylene	8.192	13177.15	0.10
16		8.289	14728.16	0.11
17		8.829	15717.74	0.12
18		8.792	12044.70	0.09
19		9.937	7908.51	0.06
20		10.029	8107.54	0.06
21		10.202	4347.51	0.03
22		10.346	4911.25	0.04
23		10.485	2351.76	0.02
24		10.578	4749.87	0.04
25		10.893	14357.85	0.11
26		11.145	12367.25	0.09
27		11.561	5176.94	0.04
28	Phenol	11.846	120031.65	0.89
29		12.074	9547.46	0.07
30	Benzofuran	12.154	25959.66	0.19
31		12.481	16831.08	0.12
32		12.700	8107.50	0.05
33		12.896	2371.19	0.02
34		13.113	7325.47	0.05
35		13.255	9258.66	0.07
36	Indan	13.555	8814.62	0.07
37		13.766	17232.83	0.13
38		13.856	6692.16	0.05
39	Indene	14.215	48358.28	0.36
40		14.443	68786.66	0.51
41		14.658	4183.59	0.03
42		14.994	2247.51	0.02
43		15.187	191712.17	1.41
44		15.392	14374.49	0.11
45		15.593	11477.22	0.08
46		15.755	87268.79	0.64
47		16.027	27890.71	0.21
48		16.129	20863.95	0.15
49		16.571	4361.98	0.03
50		16.801	18472.20	0.14
51		17.008	2056.23	0.02
52		17.181	7960.09	0.06
53		17.297	19252.28	0.14
54		17.515	15295.67	0.11
55		17.593	80960.24	0.60
56		17.904	7653690.81	56.49
57		18.172	43179.29	0.32
58		18.250	68239.98	0.50

10/8/2008 1:46:33 PM Result: C:\Data\datb006-20081008-134633.rst

Peak #	Component Name	Time [min]	Area [uV*sec]	Area [%]
59		18.388	5265.22	0.04
60	Naphthalene	18.573	876519.86	6.47
61		18.682	5042.07	0.04
62	Thionaphthene	18.766	9913.32	0.07
63		18.999	47290.60	0.35
64		19.174	30629.04	0.23
65		19.277	44233.93	0.33
66		19.430	9607.60	0.07
67		19.624	7486.99	0.06
68		19.714	14229.45	0.11
69		19.820	1856.23	0.01
70		19.900	19116.12	0.14
71		20.088	21490.72	0.16
72		20.188	15025.15	0.11
73	Quinoline	20.260	18182.52	0.13
74		20.385	23504.39	0.17
75		20.523	12932.20	0.10
76		20.681	10287.25	0.08
77		20.800	4138.23	0.03
78		21.037	68905.55	0.51
79		21.240	14170.13	0.10
80		21.380	21571.56	0.16
81		21.555	9760.74	0.07
82		21.633	15764.55	0.12
83		21.965	68746.89	0.51
84	2-Methylnaph	22.034	30680.97	0.23
85		22.132	15808.20	0.12
86		22.277	49759.15	0.37
87	1-Methylnaph	22.452	94150.43	0.69
88		22.593	22594.21	0.17
89		22.692	42551.67	0.31
90		22.784	33718.61	0.25
91		23.006	64051.48	0.47
92		23.331	50735.47	0.37
93		23.553	15369.00	0.11
94		23.673	18021.25	0.13
95		23.847	24160.64	0.18
96		24.067	20226.12	0.15
97		24.270	44516.19	0.33
98	Biphenyl	24.445	11026.58	0.08
99		24.554	11456.94	0.08
100		24.670	28808.12	0.22
101		24.863	51024.87	0.38
102		25.085	54539.50	0.40
103		25.210	7723.00	0.06
104		25.287	3651.78	0.03
105		25.410	5782.02	0.04
106		25.509	23971.41	0.18
107		25.600	22179.24	0.16

10/8/2008 1:46:33 PM Result: C:\Data\datb006-20081008-134633.rst

Peak #	Component Name	Time [min]	Area [uV*sec]	Area [%]
108		25.735	5782.74	0.04
109		25.874	9500.81	0.07
110		25.961	6872.95	0.05
111		26.289	14148.04	0.10
112		26.449	4145.38	0.03
113		26.582	12391.48	0.09
114		26.749	10356.26	0.08
115		27.084	3540.94	0.03
116	Acenaphthene	27.221	13307.62	0.10
117		27.415	13982.11	0.10
118		27.526	36727.77	0.27
119		27.733	83827.56	0.62
120		27.856	39400.40	0.29
121	Dibenzofuran	28.102	33544.92	0.25
122		28.228	14831.33	0.11
123		28.361	6884.03	0.05
124		28.451	9206.23	0.07
125		28.723	2303.20	0.02
126		28.848	4062.79	0.03
127		29.110	4542.46	0.03
128		29.242	24612.70	0.18
129		29.495	7256.51	0.05
130	Fluorene	29.720	8983.54	0.07
131		29.874	24637.10	0.18
132		30.042	22266.78	0.16
133		30.230	46574.85	0.34
134		30.371	8461.90	0.06
135		30.482	7925.90	0.06
136		30.583	8002.24	0.06
137		30.740	25924.46	0.19
138		31.071	5523.78	0.04
139		31.309	16625.52	0.12
140		31.564	10586.49	0.08
141		31.759	3642.19	0.03
142		32.298	11938.60	0.09
143		32.412	8645.19	0.06
144		32.642	1953.56	0.01
145		32.903	16713.42	0.12
146		33.154	30946.66	0.23
147		33.377	12906.02	0.10
148		33.610	18055.73	0.13
149		34.256	50376.48	0.37
150		34.687	24374.51	0.18
151		35.281	4992.65	0.04
152		35.785	20800.97	0.15
153	Phenanthrene	35.962	7067.65	0.05
154	Anthracene	36.095	12019.68	0.09
155		36.332	5206.75	0.04
156		36.466	16265.53	0.13

10/8/2008 1:46:33 PM Result: C:\Data\datb006-20081008-134633.rst

Peak #	Component Name	Time [min]	Area [uV*sec]	Area [%]
157		36.673	29460.98	0.22
158		36.804	4295.42	0.03
159		36.940	9087.33	0.07
160		37.138	4078.02	0.03
161		37.275	2167.21	0.02
162		37.430	3831.95	0.03
163	Carbazol	37.578	9303.15	0.07
164		37.850	7263.49	0.05
165		37.997	2860.09	0.02
166		38.184	8077.04	0.06
167		38.639	4699.17	0.03
168		38.740	7601.50	0.06
169		38.862	15578.11	0.11
170		38.998	40330.04	0.30
171		39.159	6679.43	0.05
172		39.334	13312.00	0.10
173		39.559	3808.97	0.03
174		39.634	2520.85	0.02
175		39.949	3527.23	0.03
176		40.415	2568.18	0.02
177		40.627	16885.45	0.12
178		40.731	29415.07	0.22
179		40.896	3906.24	0.03
180		41.056	9351.56	0.07
181		41.213	4774.86	0.04
182		41.305	4570.45	0.03
183		41.392	3347.44	0.02
184		41.485	4172.44	0.03
185	Fluoranthene	41.588	8858.38	0.07
186		41.808	5044.63	0.04
187		42.073	13568.56	0.10
188		42.154	32624.48	0.24
189		42.335	8084.11	0.06
190	Pyrene	42.463	6298.35	0.05
191		42.684	8166.91	0.06
192		42.801	2170.17	0.02
193		42.888	8178.23	0.06
194		43.113	10803.89	0.08
195		43.317	14317.58	0.11
196		43.383	39417.60	0.29
197		43.616	7658.96	0.06
198		43.893	12113.55	0.09
199		43.970	22073.67	0.16
200		44.088	6393.49	0.05
201		44.179	7082.38	0.05
202		44.275	30229.83	0.22
203		44.480	59091.83	0.44
204		44.703	7762.37	0.06
205		44.798	3235.16	0.02

10/8/2008 1:46:33 PM Result: C:\Data\datb006-20081008-134633.rst

Peak #	Component Name	Time [min]	Area [uV*sec]	Area [%]
206		44.908	15421.78	0.11
207		45.150	109375.38	0.81
208		45.214	111898.32	0.83
209		45.473	80947.81	0.60
210		45.684	4028.30	0.03
211		45.799	17453.57	0.13
212		45.872	33829.79	0.25
213		46.051	9995.33	0.07
214	Benz (a) anthracene	46.191	6782.07	0.05
215		46.268	31249.10	0.23
216	Chrysene	46.399	61421.88	0.45
217		46.488	77672.11	0.57
218		46.605	4448.84	0.03
219		46.820	15187.47	0.11
220		47.118	13838.06	0.10
221		47.270	59413.66	0.44
222		47.406	3534.59	0.03
223		47.490	15573.33	0.11
224		47.837	83837.05	0.62
225		48.094	83822.04	0.47
226		48.293	4418.92	0.03
227		48.569	8708.65	0.06
228		48.777	7451.64	0.05
229		48.879	59671.24	0.44
230		49.070	20946.53	0.15
231		49.326	9080.65	0.07
232		49.639	67135.74	0.50
233		49.835	12511.87	0.09
234		49.956	3677.02	0.03
235		50.176	11673.60	0.09
236		50.254	9170.09	0.07
237		50.427	34151.48	0.25
238		50.564	5591.89	0.04
239		50.958	2281.20	0.02
240		51.072	2604.03	0.02
241		51.285	25952.90	0.19
242		51.421	18502.51	0.14
243		51.776	2995.82	0.02
244		51.912	14593.47	0.11
245		52.244	17541.64	0.13
246		52.442	1429.19	0.01
247		52.693	13593.67	0.10
248		53.334	10526.97	0.08
249		53.519	2276.67	0.02
250		53.676	2998.25	0.02
251		53.933	5514.67	0.04
252		54.589	8267.92	0.06
253		57.146	4637.53	0.03

10/8/2008 1:46:33 PM Result: C:\Data\datb006-20081008-134633.rst

Peak #	Component Name	Time [min]	Area [uV*sec]	Area [%]
			13549240.52	100.00

Warning -- Signal level out-of-range in peak

Missing Component Report

Component Expected Retention (Calibration File)

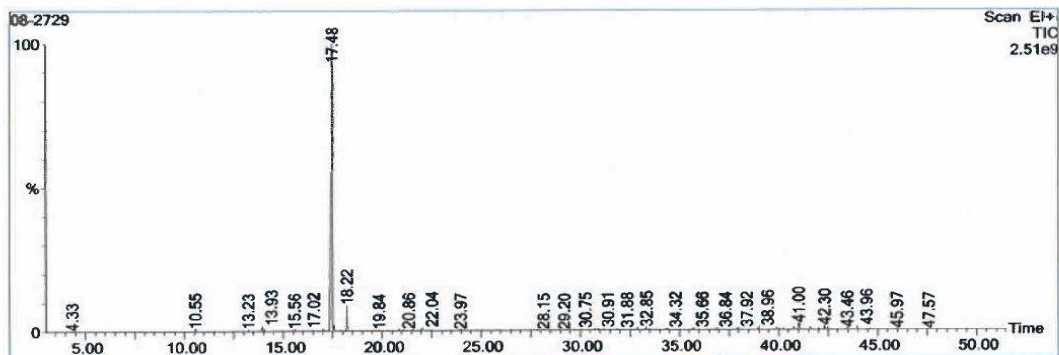
All components were found

Qualitative Report

File: C:\TURBOMASS\PAH.PRO\Data\08-2729.raw
 Acquired: 08-Oct-08 07:49:53 PM
 Description:
 GC/MS Method: GC: Creo.mth MS: Creo.EXP
 Sample ID:

Printed: 09-Oct-08 07:35 AM

Page 1 of 2
 Vial Number: 7



#	RT	Scan	Height	Area	Area %	Norm %	Name
1	10.550	1126	22,153,510	1,086,051.2	0.407	0.54	
2	13.226	1525	14,517,072	692,067.2	0.259	0.34	
3	13.930	1630	35,803,724	2,000,408.6	0.749	0.99	
4	14.037	1646	11,928,152	533,333.6	0.200	0.26	
5	15.559	1873	16,531,047	824,069.4	0.308	0.41	
6	16.445	2005	8,602,202	435,252.9	0.163	0.22	
7	17.021	2091	12,283,218	884,480.9	0.331	0.44	
8	17.484	2160	2,478,250,752	201,465,664.0	75.407	100.00	
9	17.558	2171	50,843,696	1,820,564.2	0.681	0.90	
10	17.860	2216	7,647,936	413,828.6	0.155	0.21	
11	18.108	2253	7,819,666	322,688.9	0.121	0.16	
12	18.222	2270	224,478,048	11,494,373.0	4.302	5.71	
13	19.838	2511	8,357,316	410,627.3	0.154	0.20	
14	20.864	2664	7,119,984	391,780.6	0.147	0.19	
15	21.086	2697	11,278,320	491,487.9	0.184	0.24	
16	21.555	2767	14,534,897	727,148.9	0.272	0.36	
17	22.038	2839	19,403,174	976,216.2	0.365	0.48	
18	22.447	2900	7,962,254	415,034.0	0.155	0.21	
19	23.970	3127	10,104,027	586,594.2	0.220	0.29	
20	24.138	3152	8,469,550	474,332.9	0.178	0.24	
21	28.148	3750	7,754,756	493,602.8	0.185	0.25	
22	29.201	3907	6,023,334	330,359.9	0.124	0.16	

Inst() ACQUISITION PARAMETERS

Oven: Initial temp 80°C for 5 min, ramp 5°C/min to 165°C, hold 5 min, ramp 10°C/min to 310°C, hold 10 min, InjAauto=300°C,
 Volume=0 µL, Split=20:1, Carrier Gas=He, Solvent Delay=3.00 min, Transfer Temp=250°C, Source Temp=200°C, Scan: 50 to
 350Da, Column 30.0m x 250µm

Qualitative Report

File: C:\TURBOMASS\PAH.PRO\Data\08-2729 raw
 Acquired: 08-Oct-08 07:49:53 PM
 Description:
 GC/MS Method: GC: Creo.mth MS: Creo.EXP
 Sample ID:

Printed: 09-Oct-08 07:35 AM

Page 2 of 2
 Vial Number: 7

#	RT	Scan	Height	Area	Area %	Norm %	Name
23	30.912	4162	11,014,080	427,245.8	0.160	0.21	
24	31.168	4200	8,813,239	363,428.2	0.136	0.18	
25	32.738	4434	6,962,810	345,992.8	0.130	0.17	
26	32.853	4451	14,199,972	487,053.4	0.182	0.24	
27	33.316	4520	25,694,190	962,434.8	0.368	0.49	
28	33.484	4545	12,239,816	464,771.0	0.174	0.23	
29	34.317	4669	7,492,210	346,493.5	0.130	0.17	
30	34.411	4683	15,088,754	477,597.7	0.179	0.24	
31	35.735	4880	16,121,780	485,942.5	0.182	0.24	
32	36.905	5054	16,511,487	519,568.4	0.194	0.26	
33	37.974	5213	19,717,420	733,013.8	0.274	0.36	
34	38.962	5360	20,049,374	714,930.4	0.268	0.35	
35	39.883	5497	19,681,312	710,370.1	0.266	0.35	
36	39.997	5514	11,505,565	371,849.2	0.139	0.18	
37	40.226	5548	14,301,690	557,449.4	0.209	0.28	
38	40.764	5628	24,249,462	1,139,154.6	0.426	0.57	
39	40.999	5663	58,002,068	1,798,050.6	0.673	0.89	
40	41.032	5668	54,811,368	2,287,265.5	0.856	1.14	
41	41.590	5751	23,544,002	980,735.2	0.367	0.49	
42	41.637	5758	18,023,510	680,392.8	0.255	0.34	
43	42.021	5815	12,639,776	453,290.3	0.170	0.22	
44	42.303	5857	37,027,064	1,344,462.0	0.503	0.67	
45	42.464	5881	21,577,070	1,037,747.8	0.388	0.52	
46	43.459	6029	19,467,454	1,203,484.8	0.484	0.64	
47	43.957	6103	25,177,514	1,229,246.9	0.460	0.61	
48	44.615	6201	13,240,169	947,481.4	0.355	0.47	
49	45.965	6402	10,228,119	880,450.0	0.330	0.44	
50	47.589	6641	4,525,362	446,674.0	0.167	0.22	

Inst() ACQUISITION PARAMETERS

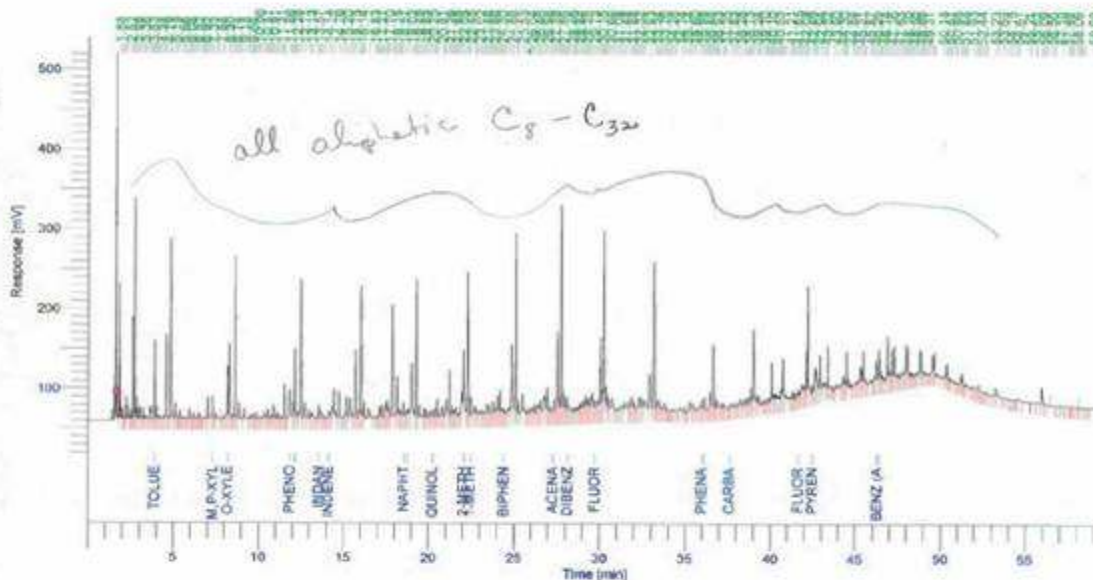
Oven: Initial temp 80°C for 5 min, ramp 5°C/min to 165°C, hold 5 min, ramp 10°C/min to 310°C, hold 10 min, InjAauto=300°C,
 Volume=0 µL, Split=20:1, Carrier Gas=He, Solvent Delay=3.00 min, Transfer Temp=250°C, Source Temp=200°C, Scan: 50 to
 350Da, Column 30.0m x 250µm

Software Version : 6.3.1.0504
Reprocess Number : 6f7d691: 3704
Sample Name : 08-2730
Instrument Name : Clarus 500
Rack/Vial : 0/17
Sample Amount : 1.000000
Cycle : 2

Date : 10/8/2008 3:07:26 PM
Data Acquisition Time : 10/8/2008 2:07:48 PM
Channel : B
Operator : TCWS
Dilution Factor : 1.000000

Result File : C:\Data\datb006-20081008-150725.rst

Sequence File : C:\Sequences\October 7-2008-pecreo-MSDSsolvent-WVU.seq



DEFAULT REPORT

Peak #	Component Name	Time [min]	Area [uV*sec]	Area [%]
1		1.884	271897.40	0.91
2		2.067	15851.18	0.05
3		2.157	4888.17	0.02
4		2.249	67937.21	0.23
5		2.519	13501.37	0.05
6		2.626	173770.55	0.58
7		2.732	377164.81	1.26
8		2.833	36346.49	0.12
9		2.953	29310.84	0.10

10/8/2008 3:07:26 PM Result: C:\Data\datb006-20081008-150725.rst

Peak #	Component Name	Time [min]	Area [uV*sec]	Area [%]
10		3.070	32249.42	0.11
11		3.259	21920.36	0.07
12		3.358	16980.57	0.06
13		3.579	6129.06	0.02
14		3.707	62156.14	0.21
15		3.830	4350.26	0.01
16	Toluene	3.922	187396.98	0.63
17		4.011	36066.81	0.12
18		4.104	11424.89	0.04
19		4.199	14161.88	0.05
20		4.375	3223.79	0.01
21		4.478	16189.85	0.05
22		4.603	267697.69	0.89
23		4.786	16855.06	0.06
24		4.881	562707.63	1.88
25		5.113	53609.98	0.18
26		5.191	17443.72	0.06
27		5.395	36291.93	0.12
28		5.531	13983.35	0.05
29		5.656	8228.38	0.03
30		5.792	5837.66	0.02
31		5.961	40645.94	0.14
32		6.078	1871.63	0.01
33		6.196	17909.41	0.06
34		6.394	6175.49	0.02
35		6.522	31707.29	0.11
36		6.705	1252.11	0.00
37		6.811	8581.68	0.03
38		6.918	5040.54	0.02
39		7.021	71746.56	0.24
40		7.225	20280.61	0.07
41	m,p-Xylene	7.328	118648.93	0.40
42		7.525	23745.33	0.08
43		7.678	7094.73	0.02
44		7.882	4318.88	0.01
45		7.975	16734.65	0.06
46	o-Xylene	8.204	204028.38	0.68
47		8.300	264837.63	0.88
48		8.494	21374.18	0.07
49		8.646	568957.12	1.90
50		8.739	8146.46	0.03
51		8.888	74007.33	0.25
52		8.977	9649.84	0.03
53		9.183	50849.62	0.17
54		9.384	9101.59	0.03
55		9.523	24883.40	0.08
56		9.664	19169.04	0.06
57		9.728	8908.24	0.03
58		9.850	25792.28	0.09

10/8/2008 3:07:26 PM Result: C:\Data\datb006-20081008-150725.rst

Peak #	Component Name	Time [min]	Area [uV*sec]	Area [%]
59		9.967	9445.06	0.03
60		10.057	13777.74	0.05
61		10.213	9862.45	0.03
62		10.418	45791.95	0.15
63		10.513	12306.18	0.04
64		10.592	36355.20	0.12
65		10.688	5256.82	0.02
66		10.802	24145.48	0.08
67		10.909	83659.23	0.28
68		11.050	14891.55	0.05
69		11.163	28183.73	0.09
70		11.315	10227.03	0.03
71		11.397	11320.25	0.04
72		11.481	10647.55	0.04
73		11.574	123166.03	0.41
74	Phenol	11.861	135505.63	0.45
75		11.959	34393.91	0.11
76		12.088	59435.93	0.20
77	Benzofuran	12.166	254104.66	0.85
78		12.281	32836.70	0.11
79		12.499	517907.49	1.73
80		12.710	90856.68	0.30
81		13.001	40609.67	0.14
82		13.127	26303.94	0.09
83		13.196	41085.30	0.14
84		13.401	4142.22	0.01
85	Indan	13.567	67347.85	0.22
86		13.698	49087.62	0.16
87		13.872	17190.89	0.06
88	Indene	14.140	41690.72	0.14
89		14.238	27540.99	0.09
90		14.459	207739.04	0.69
91		14.765	131998.04	0.44
92		15.024	12949.37	0.04
93		15.198	139799.71	0.47
94		15.405	123672.85	0.41
95		15.551	38847.99	0.13
96		15.750	272317.92	0.91
97		15.947	44585.81	0.15
98		16.045	453945.18	1.52
99		16.137	29272.53	0.10
100		16.222	72057.83	0.24
101		16.500	70513.82	0.24
102		16.827	15315.65	0.05
103		16.947	5251.19	0.02
104		17.013	5204.08	0.02
105		17.097	14191.37	0.05
106		17.173	51442.52	0.17
107		17.273	64387.11	0.21

10/8/2008 3:07:26 PM Result: C:\Data\datb006-20081008-150725.rst

Peak #	Component Name	Time [min]	Area [uV*sec]	Area [%]
108		17.454	50643.25	0.17
109		17.523	57530.52	0.19
110		17.585	106113.14	0.35
111		17.699	49458.77	0.17
112		17.893	471783.80	1.58
113		18.014	30560.18	0.10
114		18.152	182452.52	0.61
115		18.258	41180.88	0.14
116		18.337	23035.81	0.08
117		18.407	52575.22	0.18
118	Naphthalene	18.565	84932.62	0.28
119		18.682	29443.75	0.10
120	Thionaphthene	18.774	92706.13	0.31
121		19.023	338102.65	1.13
122		19.183	40676.34	0.14
123		19.292	462569.11	1.54
124		19.449	63989.27	0.21
125		19.607	18797.62	0.06
126		19.724	44241.30	0.15
127		19.830	6679.71	0.02
128		19.906	43188.42	0.14
129		20.101	31506.99	0.11
130	Quinoline	20.248	51206.94	0.17
131		20.394	49453.63	0.17
132		20.526	83986.17	0.28
133		20.807	81731.23	0.27
134		20.889	12376.20	0.04
135		21.039	174440.23	0.58
136		21.257	205243.68	0.69
137		21.387	56702.57	0.19
138		21.481	33841.05	0.11
139		21.566	26598.26	0.09
140		21.645	52735.69	0.18
141		21.771	13497.26	0.05
142		21.857	20551.55	0.07
143	2-Methylnaph	22.050	474859.56	1.59
144		22.296	500172.44	1.67
145	1-Methylnaph	22.453	115095.37	0.38
146		22.706	84547.86	0.28
147		22.826	55819.94	0.19
148		23.017	53163.24	0.18
149		23.172	26281.07	0.09
150		23.271	37260.89	0.12
151		23.435	69626.13	0.23
152		23.548	51713.25	0.17
153		23.663	29835.93	0.10
154		23.759	78092.55	0.26
155		23.864	35665.09	0.12
156		23.969	48502.36	0.16

10/8/2008 3:07:26 PM Result: C:\Data\datb006-20081008-150725.rst

Peak #	Component Name	Time [min]	Area [uV*sec]	Area [%]
157		24.091	137275.72	0.46
158		24.199	96348.45	0.32
159		24.301	49281.88	0.16
160	Biphenyl	24.405	33179.89	0.11
161		24.482	29427.33	0.10
162		24.675	79919.08	0.27
163		24.877	414670.55	1.38
164		25.106	641702.61	2.14
165		25.230	73872.11	0.25
166		25.528	193184.25	0.65
167		25.753	19887.19	0.07
168		25.876	32717.02	0.11
169		26.039	58275.10	0.19
170		26.195	58463.26	0.20
171		26.376	78126.65	0.26
172		26.456	47930.47	0.16
173		26.545	105625.68	0.35
174		26.772	207083.88	0.69
175		26.982	119540.34	0.40
176		27.132	47386.20	0.16
177	Acenaphthene	27.280	46031.16	0.15
178		27.391	81623.35	0.27
179		27.539	342633.91	1.14
180		27.628	78092.53	0.26
181		27.751	777749.13	2.60
182		27.863	119736.97	0.40
183		27.983	77907.93	0.26
184	Dibenzofuran	28.142	105441.92	0.35
185		28.228	68487.98	0.23
186		28.456	36918.92	0.12
187		28.545	22256.27	0.07
188		28.666	62513.42	0.21
189		28.845	58034.99	0.19
190		28.926	43268.52	0.14
191		29.032	86363.17	0.29
192		29.179	90517.36	0.30
193		29.250	64813.89	0.22
194		29.345	81074.27	0.27
195		29.429	46505.22	0.16
196		29.510	209697.93	0.70
197	Fluorene	29.727	79892.02	0.27
198		29.876	130905.76	0.44
199		30.058	329866.48	1.10
200		30.153	120473.39	0.40
201		30.257	727244.39	2.43
202		30.361	126758.12	0.42
203		30.458	102078.80	0.34
204		30.660	172564.71	0.58
205		30.878	39655.62	0.13

10/8/2008 3:07:26 PM Result: C:\Data\datb006-20081008-150725.rst

Peak #	Component Name	Time [min]	Area [uV*sec]	Area [%]
206		31.084	21388.76	0.07
207		31.283	74873.49	0.25
208		31.481	112338.08	0.38
209		31.737	54161.48	0.18
210		31.875	119952.42	0.40
211		32.018	56925.95	0.19
212		32.144	37222.21	0.12
213		32.315	113562.10	0.38
214		32.460	110942.35	0.37
215		32.615	164470.07	0.55
216		32.927	260254.34	0.87
217		33.189	831131.78	2.78
218		33.337	55620.59	0.19
219		33.464	77241.66	0.26
220		33.600	45527.77	0.15
221		33.757	28207.27	0.09
222		33.850	44035.46	0.15
223		33.977	10196.39	0.03
224		34.079	1407.42	0.00
225		34.276	11939.72	0.04
226		34.442	10910.61	0.04
227		34.743	32337.73	0.11
228		34.983	32043.91	0.11
229		35.142	4212.90	0.01
230		35.324	89747.48	0.30
231		35.478	57304.49	0.19
232		35.595	24511.64	0.08
233		35.841	65122.12	0.22
234	Phenathrene	35.994	63229.60	0.21
235	Anthracene	36.127	97002.63	0.32
236		36.283	8315.70	0.03
237		36.366	12341.59	0.04
238		36.475	103261.29	0.34
239		36.575	32205.17	0.11
240		36.687	287988.87	1.00
241		36.810	58037.49	0.19
242		36.930	67603.83	0.23
243		37.146	33321.49	0.11
244		37.258	33818.63	0.11
245		37.354	34041.36	0.11
246	Carbazol	37.623	35268.02	0.12
247		37.830	46869.81	0.16
248		37.985	39072.18	0.13
249		38.174	27055.69	0.09
250		38.282	67856.28	0.23
251		38.474	56388.42	0.19
252		38.640	41771.25	0.14
253		38.734	54685.98	0.18
254		38.875	100276.77	0.33

10/8/2008 3:07:26 PM Result: C:\Data\datb006-20081008-150725.rst

Peak #	Component Name	Time [min]	Area [uV*sec]	Area [%]
255		39.021	385736.33	1.29
256		39.244	58807.86	0.20
257		39.346	36069.19	0.12
258		39.523	19751.02	0.07
259		39.701	22120.81	0.07
260		39.769	12071.14	0.04
261		39.894	30261.14	0.10
262		39.988	17886.25	0.06
263		40.096	169285.87	0.57
264		40.219	47456.71	0.16
265		40.333	82093.04	0.27
266		40.534	30914.06	0.10
267		40.643	62265.20	0.21
268		40.742	217115.86	0.72
269		40.902	79970.45	0.27
270		41.211	21403.54	0.07
271		41.328	39036.03	0.13
272		41.413	23226.34	0.08
273		41.511	30199.16	0.10
274	Fluoranthene	41.651	49287.78	0.16
275		41.720	23996.96	0.08
276		41.841	111180.94	0.37
277		42.001	87329.23	0.29
278		42.081	46892.31	0.16
279		42.166	139716.29	0.47
280		42.235	374839.90	1.25
281	Pyrene	42.492	27373.24	0.09
282		42.647	118589.81	0.40
283		42.709	132949.20	0.44
284		42.937	151017.96	0.50
285		43.127	84068.88	0.28
286		43.322	23936.29	0.08
287		43.397	130351.75	0.44
288		43.672	13944.24	0.05
289		43.902	85094.20	0.28
290		44.194	36392.68	0.12
291		44.305	74948.38	0.25
292		44.358	60572.32	0.20
293		44.486	175810.60	0.59
294		44.839	17485.03	0.06
295		44.997	57093.75	0.19
296		45.144	60004.39	0.20
297		45.314	146075.08	0.49
298		45.483	142119.66	0.47
299		45.590	49447.34	0.17
300		45.872	70835.08	0.24
301		46.014	16834.61	0.06
302		46.082	54002.59	0.18
303	Benz (a) anthracene	46.286	188110.90	0.63

10/8/2008 3:07:26 PM Result: C:\Data\datb006-20081008-150725.rst

Peak #	Component Name	Time [min]	Area [uV*sec]	Area [%]
304	Chrysene	46.408	119773.36	0.40
305		46.527	53083.28	0.18
306		46.606	30471.92	0.10
307		46.745	42382.38	0.14
308		46.893	199266.93	0.67
309		47.058	34404.85	0.11
310		47.161	148783.01	0.50
311		47.276	173666.11	0.58
312		47.444	43244.52	0.14
313		47.629	31527.05	0.11
314		47.786	56802.64	0.19
315		47.853	46898.53	0.16
316		47.996	149222.47	0.50
317		48.101	123169.43	0.41
318		48.245	18937.67	0.06
319		48.349	41107.00	0.14
320		48.501	15811.33	0.05
321		48.584	34995.84	0.12
322		48.789	116024.70	0.39
323		48.887	90163.80	0.30
324		49.037	33319.56	0.11
325		49.136	19112.66	0.06
326		49.315	5882.94	0.02
327		49.552	81967.15	0.27
328		49.644	73619.33	0.25
329		50.176	10295.05	0.03
330		50.345	45900.36	0.15
331		50.436	51179.72	0.17
332		50.573	12445.70	0.04
333		50.644	22717.37	0.08
334		50.869	7486.51	0.02
335		50.982	6266.53	0.02
336		51.202	32173.21	0.11
337		51.291	52008.29	0.17
338		51.436	14705.26	0.05
339		51.544	22624.88	0.08
340		51.929	11071.81	0.04
341		52.152	23621.16	0.08
342		52.247	38039.21	0.13
343		52.441	6946.68	0.02
344		52.627	4247.51	0.01
345		52.706	24125.39	0.08
346		53.231	42942.13	0.14
347		53.336	35273.73	0.12
348		53.691	4983.21	0.02
349		53.931	10472.54	0.03
350		54.160	3137.38	0.01
351		54.358	1690.89	0.01
352		54.490	16099.11	0.05

10/8/2008 3:07:26 PM Result: C:\Data\datb006-20081008-150725.rst

Peak #	Component Name	Time [min]	Area [uV*sec]	Area [%]
353		54.611	24341.01	0.08
354		55.211	2451.00	0.01
355		55.321	9318.14	0.03
356		55.619	23403.27	0.08
357		55.960	96282.17	0.32
358		56.092	17163.90	0.06
359		56.255	7640.42	0.03
360		56.549	9322.81	0.03
361		56.745	3974.04	0.01
362		57.097	11527.99	0.04
363		57.493	12026.97	0.04
364		57.689	14647.80	0.05
365		57.806	13320.18	0.04
366		58.058	1546.00	0.01
367		58.164	3451.70	0.01
368		58.288	10148.68	0.03
369		58.433	4970.63	0.02
370		58.976	21634.49	0.07
			29947973.65	100.00

Missing Component Report

Component Expected Retention (Calibration File)

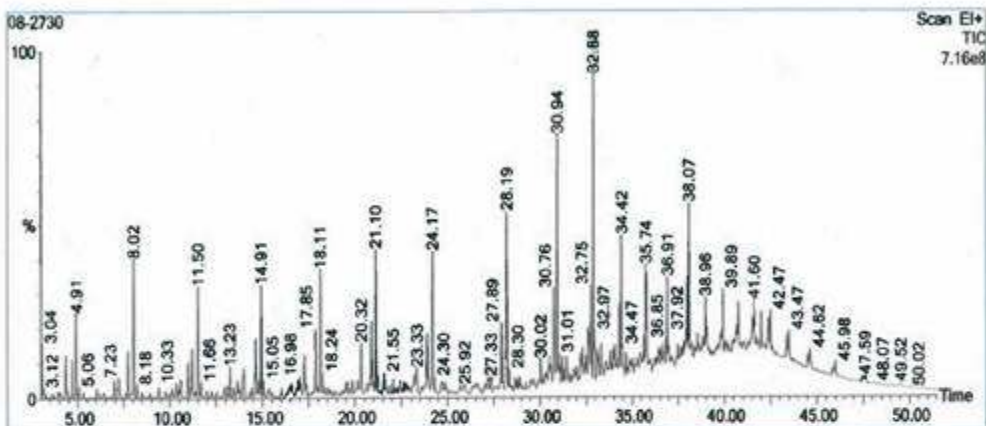
Benzene 2.340

Qualitative Report

File: C:\TURBOMASS\PAH.PRO\Data\08-2730.raw
 Acquired: 08-Oct-08 08:50:07 PM
 Description:
 GC/MS Method: GC: Creo.mth MS: Creo.EXP
 Sample ID:

Printed: 09-Oct-08 07:35 AM

Page 1 of 2
 Vial Number: 8



#	RT	Scan	Height	Area	Area %	Norm %	Name
1	4.911	285	176,934,464	9,054,689.0	1.019	34.74	
2	7.728	705	96,851,728	4,744,314.0	0.534	18.20	
3	8.023	749	287,936,128	14,791,547.0	1.664	56.74	
4	11.188	1221	99,703,864	4,725,972.5	0.532	18.13	
5	11.504	1268	227,955,392	11,808,121.0	1.328	45.29	
6	13.986	1638	60,180,024	5,521,223.0	0.621	21.18	
7	14.623	1733	118,945,928	7,351,838.5	0.827	28.20	
8	14.912	1776	228,886,144	10,498,303.0	1.181	40.27	
9	17.852	2214	130,153,416	6,793,724.5	0.764	26.06	
10	18.114	2253	254,927,872	12,004,810.0	1.351	46.06	
11	20.316	2581	106,288,704	6,847,193.5	0.770	26.27	
12	20.868	2663	146,059,840	7,425,672.0	0.835	28.49	
13	21.103	2698	293,707,808	13,387,160.0	1.506	51.36	
14	23.879	3111	121,692,064	9,144,034.0	1.029	35.08	
15	24.168	3154	286,813,888	17,407,190.0	1.958	66.78	
16	27.892	3708	139,627,264	11,284,403.0	1.269	43.29	
17	28.188	3752	362,599,232	22,830,824.0	2.568	87.59	
18	30.763	4135	184,007,408	9,203,232.0	1.035	35.31	
19	30.937	4161	496,967,776	21,377,098.0	2.405	82.01	
20	32.746	4430	173,127,024	8,989,666.5	0.786	26.81	
21	32.880	4450	660,780,928	26,066,756.0	2.932	100.00	
22	34.325	4685	136,277,840	7,232,519.5	0.814	27.75	

Inst() ACQUISITION PARAMETERS

Oven: Initial temp 80°C for 5 min, ramp 5°C/min to 165°C, hold 5 min, ramp 10°C/min to 310°C, hold 10 min, Inj/Auto=300°C,
 Volume=0 µL, Split=20:1, Carrier Gas=He, Solvent Delay=3.00 min, Transfer Temp=250°C, Source Temp=200°C, Scan: 50 to
 350Da, Column 30.0m x 250µm

Qualitative Report

File: C:\TURBOMASS\PAH.PRO\Data\08-2730.raw
 Acquired: 08-Oct-08 08:50:07 PM
 Description:
 GC/MS Method: GC: Creo.mth MS: Creo.EXP
 Sample ID:

Printed: 09-Oct-08 07:35 AM

Page 2 of 2
 Vial Number: 8

#	RT	Scan	Height	Area	Area %	Norm %	Name
23	34.419	4679	278,984,704	9,837,521.0	1.107	37.74	
24	35.744	4876	223,824,496	8,193,567.0	0.922	31.43	
25	35.791	4883	207,052,432	7,932,390.5	0.892	30.43	
26	36.665	5013	53,327,664	5,412,921.0	0.609	20.77	
27	36.913	5050	189,883,360	7,474,612.5	0.841	28.67	
28	37.976	5208	152,567,248	5,188,830.5	0.584	19.91	
29	38.070	5222	303,218,096	10,820,435.0	1.217	41.51	
30	39.011	5362	71,709,896	4,791,020.0	0.539	18.38	
31	39.765	5474	57,153,672	7,355,112.5	0.827	28.22	
32	39.886	5492	149,702,736	7,467,789.5	0.840	28.65	
33	40.209	5540	38,639,380	5,581,849.0	0.628	21.41	
34	40.647	5605	69,593,024	5,360,953.5	0.603	20.57	
35	40.761	5622	131,731,064	11,840,438.0	1.332	45.42	
36	41.037	5663	49,690,024	9,417,959.0	1.060	36.13	
37	41.280	5699	51,382,600	7,244,858.5	0.815	27.79	
38	41.509	5733	105,410,872	14,074,340.0	1.583	53.99	
39	41.597	5746	139,809,824	11,296,514.0	1.271	43.34	
40	41.745	5768	61,643,696	5,277,594.0	0.594	20.25	
41	41.866	5786	56,627,932	7,352,423.0	0.827	28.21	
42	42.001	5806	116,343,624	15,928,579.0	1.792	61.11	
43	42.379	5862	105,558,184	11,658,041.0	1.312	44.72	
44	42.473	5876	120,158,776	8,075,224.0	0.908	30.98	
45	42.574	5891	49,091,800	7,972,041.0	0.897	30.58	
46	42.823	5928	39,379,664	14,380,121.0	1.618	55.17	
47	43.369	6009	74,730,432	7,939,053.5	0.893	30.46	
48	43.470	6024	84,013,432	9,891,001.0	1.113	37.94	
49	44.164	6127	19,083,632	5,123,857.5	0.576	19.66	
50	44.623	6195	52,860,356	6,645,816.5	0.748	25.50	

Inst() ACQUISITION PARAMETERS

Oven: Initial temp 80°C for 5 min, ramp 5°C/min to 165°C, hold 5 min, ramp 10°C/min to 310°C, hold 10 min, Inj/Auto=300°C,
 Volume=0 µL, Split=20:1, Carrier Gas=He, Solvent Delay=3.00 min, Transfer Temp=250°C, Source Temp=200°C, Scan: 50 to
 350Da, Column 30.0m x 250µm

08-2730

Page: 1

Injected On: 10-08-2008 14:07:48 by TCWS

Procedure File: SimDist_Calibration_Mix.prc

Data File: C:\Data\data008-20081008-150725.CDF

Blank File: C:\Data\data001-20080325-081744.CDF

Cells File:

Solvent Exclusions: Mins

BaseLine Zero: 59744.09375

Quench Region: No Quenching Correction

Uncorr Total Sample Area: 1.2112E10

Corr Total Sample Area: 1.0972E10

Start Of Material (mins): 1.745

End Of Material (mins): 51.693

Sample Weight (g): 1.0000

SOM Thrsh: (0.01000000%)

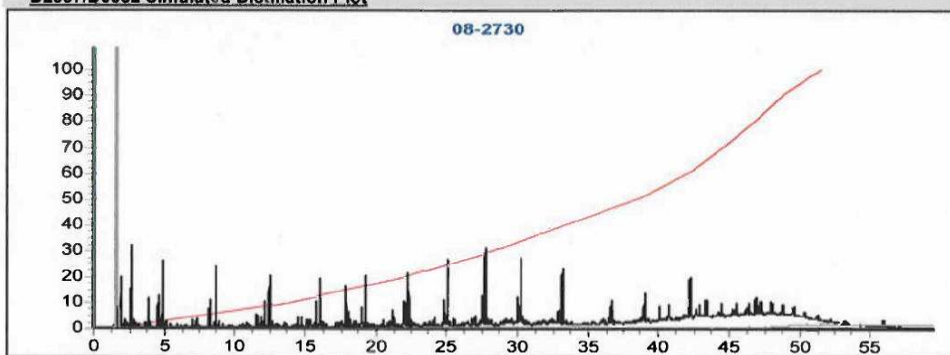
EOM Thrsh: (0.01000000%)

Solvent Weight (g): 0.0000

Material Search Restricted To: NO RESTRICTION

Material End Forced To: NO FORCE

Warnings: EOM Accuracy may be affected by BLEED at END OF RUN

D2887/D6352 Simulated Distillation Plot**D2887/D6352 Boiling Point Mass Distribution**

% Off BP(F)	% Off BP(F)	% Off BP(F)	% Off BP(F)	% Off BP(F)	% Off BP(F)	% Off BP(F)
IBP ... 182.31	20.00% ... 463.37	40.00% ... 579.52	60.00% ... 686.02	80.00% ... 776.08	FBP ... 872.04	
10.00% ... 364.69	30.00% ... 533.17	50.00% ... 633.84	70.00% ... 728.36	90.00% ... 819.23		

Arnel SimDist

10/10/2008 2:07:00 PM

APPENDIX II OTHER PROCESSES

A2.1 Exxon Donor Solvent Process

In this process, developed by the Exxon Corporation in the 1970s, the coal slurry along with a recycled solvent is treated with hydrogen in a tubular reactor at 425-470° C and 2000-2500 psi in the absence of any catalyst. Light hydrocarbons, a naphtha fraction and heavy distillates are formed in the reactor. The naphtha fraction and middle distillates are recovered while the solid residue from the bottom of the vacuum column can be converted into heavy oil using a process called flexicoking. The key feature of this process is to rehydrogenate the recycled solvent in order to regenerate its hydrogen donation capacity and thus improve its effectiveness. Rehydrogenation of the solvent is carried out in a separate fixed bed reactor using common hydrotreating catalysts such as Ni-Mo or Co-Mo on an alumina support at a temperature of about 370 °C and a pressure of 1500 psi of hydrogen. The process schematic of a typical Exxon Donor Solvent process is shown in Figure 168.

Although there are some similarities between the WVU/Quantex process and the EDS process PLEASE NOTE that Exxon's product yield does not even include pitch or coke as a product! That is a key item that clearly sets apart the current process from the previous one.

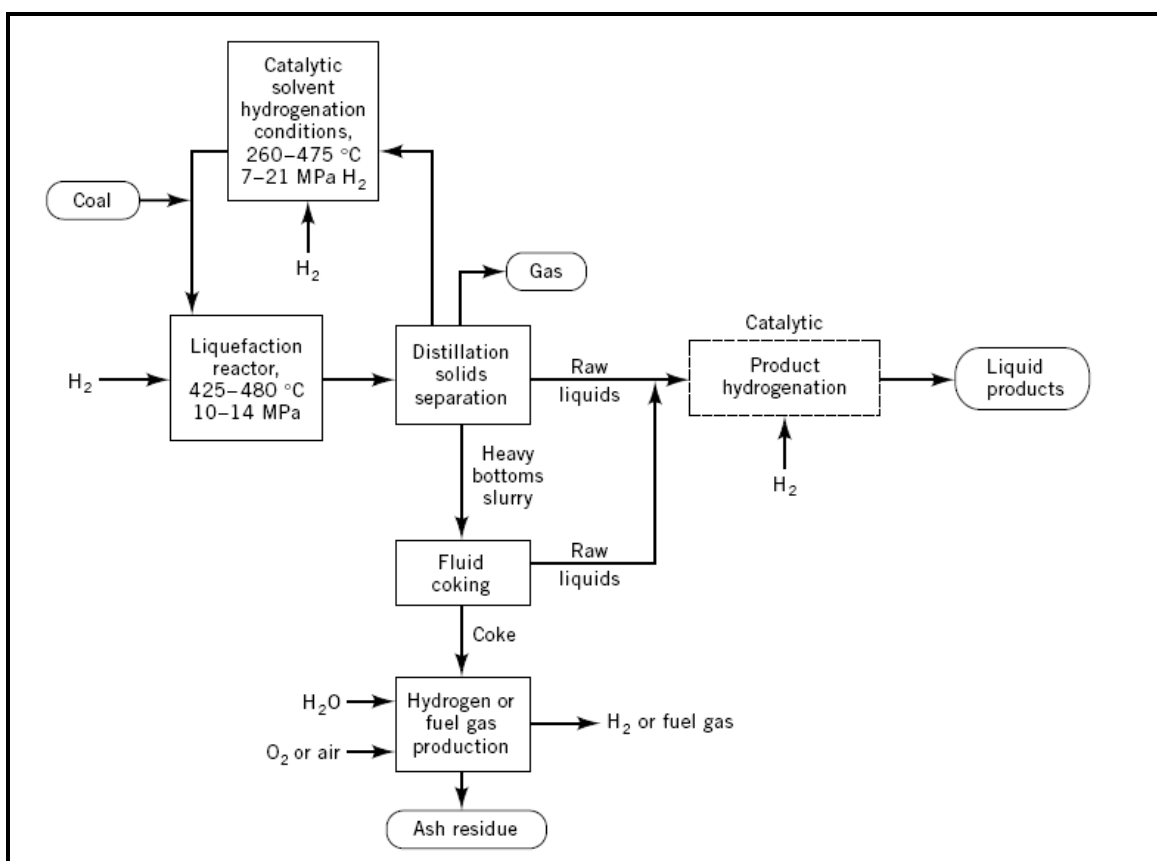


Figure 168. Process Schematic of a Typical Exxon Donor Solvent Process.⁹³

Exxon data from the 1970s shows that viable products can in fact be produced from Texas lignite, as shown in Table 192 and Figure 169 albeit with much higher hydrogen addition than contemplated in the current effort (4-6% versus ~0.5%).

Table 192. Exxon Conditions for Texas Lignite Conversion.

	Case i	Case ii	Case iii
Temperature, ° F	840	800	840
H ₂ Pressure, PSIG	1500	2000	2000
NRT, Minutes.	40	100	60
S/C/B, BY WT.	1.6/1/0	1.2/1/0.5	2.5/1/1
H ₂ Wt % on coal	4	6	6
RCLU NO.	1	2	2
Yield Periods	863-866	173-176	150-156
Mass Conversion (DAF basis), percent	53	64	72

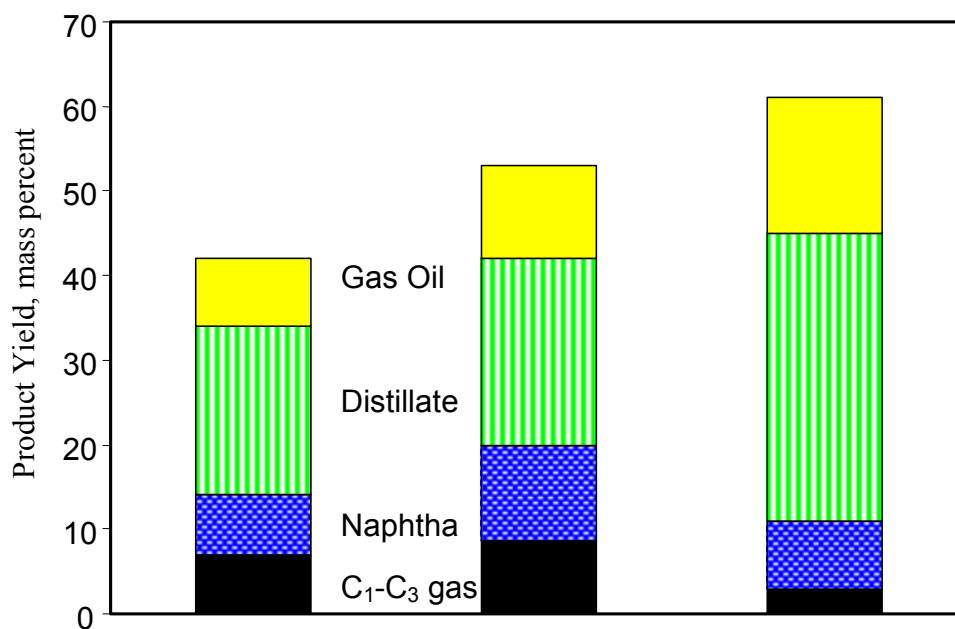


Figure 169. Graphical Representation of Product Yield from lignite, Dry-ash-free basis.

A2.2 H-COAL PROCESS

The H-Coal process was developed by Hydrocarbon Research Inc. (now a subsidiary of Headwaters Incorporated) as a variant of the commercialized H-Oil process for upgrading heavy oils. This process was mainly used to convert high sulfur coal into low sulfur boiler fuels and synthetic crude oil.⁹⁴

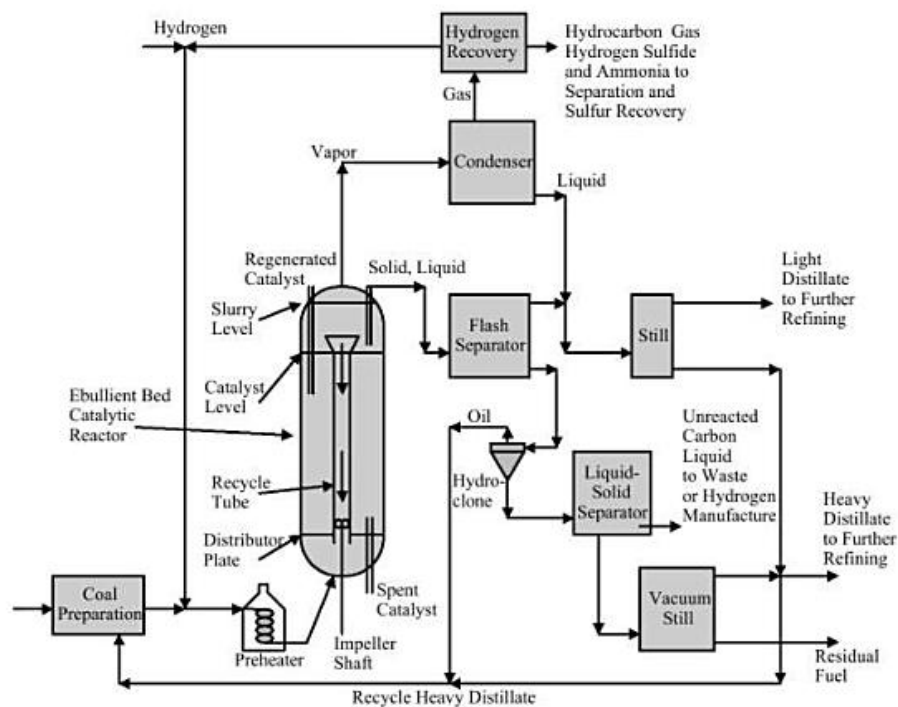


Figure 170. Process Schematic of a Typical H-Coal Process.⁹⁵

In this process, coal slurry along with a recycled solvent that consists of a solids-containing hydrocracker product with middle and heavy distillates, is treated with hydrogen in an ebullated bed hydrocracker at temperatures of 425-455° C and a pressure of 3000 psi in the presence of a hydrotreating catalyst such as Ni-Mo or Co-Mo on an alumina support. The reaction mixture is recycled upward through the reactor in order to maintain the catalyst in a fluidized state. The liquid-solid mixture from the reactor is separated using a flash separator to recover light and heavy hydrocarbons. Vapors in the overheads are condensed and fed into an atmospheric distillation unit to produce naphtha and middle distillate. The remaining solids and heavy oil are processed in hydrocyclones and a vacuum distillation unit. The conversion of coal to liquids and gaseous products for this process is about 95% with suitable coals. The liquid yield is about 50% on a dry basis. The process schematic of a typical H-Coal process is shown in Figure 170.

China is one of the largest producers of coal in the world and possesses huge reserves of all types of coal. The Shenhua Group Corporation, China's largest coal producer, has developed the Shenhua direct coal liquefaction process as an alternative source of liquid fuels to ensure energy security. West Virginia University (WVU) and China Shenhua Coal Liquefaction Co. Ltd. (CSCCLC), with support from U.S. Department of Energy are conducting joint research to understand the primary economic and environmental impacts of the facility. The technology of the plant is based on the process developed by Hydrocarbon Technologies Inc. The primary products of this process are diesel, LPG, naphtha and liquid ammonia. Also, a preliminary cost analysis conducted by Shenhua Group and WVU indicated that the liquid fuel production cost of the plant was approximately equal to crude oil price of US \$22/bbl.⁹⁶

The direct coal liquefaction process mainly consists of two backmixed reactor stages and a fixed bed in-line hydrotreater. The catalyst used in this process is a proprietary dispersed superfine iron catalyst. The process operates at a pressure of 17 MPa and reactor temperatures in the range of 400-460 °C. A slurry of pulverized coal along with recycled solvent (coal-derived heavy oil) is premixed and pumped through a preheater. Simultaneously, hydrogen is also pumped into the first stage reactor. The effluent from the first stage is separated in an interstage separator to remove gases and light ends. The slurry is then sent to the higher temperature second stage reactor. The effluent from the second stage is again separated in a hot separator and an atmospheric flash vessel consecutively. The vapor stream from the hot separator, combined with that from the interstage separator, flows to the fixed bed in-line hydrotreater for upgrading to very clean fuels. The overhead stream from the atmospheric flash vessel is condensed and pumped to the hydrotreater. The product from the hydrotreater is mainly naphtha and diesel fuel fraction. **Figure 171** illustrates the Shenhua direct coal liquefaction process.

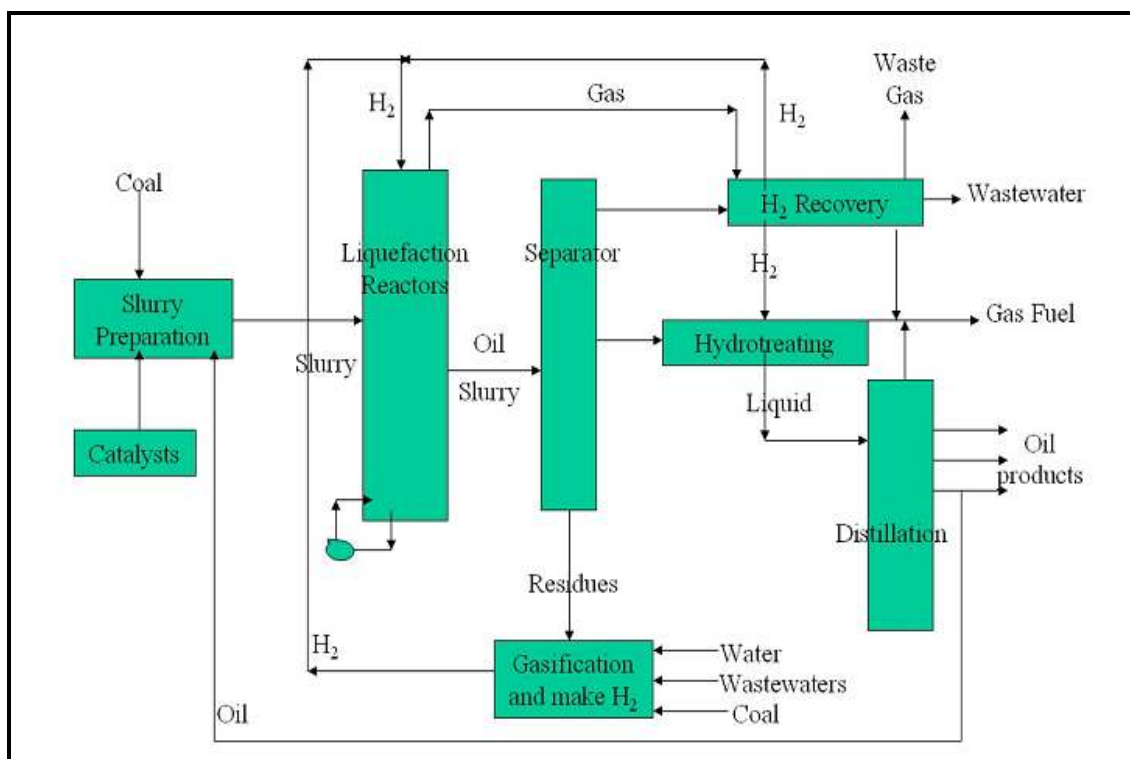


Figure 171. Process Schematic of Shenhua Direct Coal Liquefaction Process.

APPENDIX III. REFERENCES.

¹ The Carbon Products Industry Vision for the Future, Industries of the Future, Carbon Products Consortium, WVU-NRCCE, P.O. Box 6064, Morgantown, WV 26506.

² R. H. Wombles, "Experience with Petroleum Enhanced Coal Tar Pitch," 2000 Australasian Smelter Conference, Queenstown, Australia.

³ Franz Vogt, "A Review of Coke Quality Projections," Light Metals 2001, TMS, p. 587.

⁴ Zsolt Rummy, "The Future: It's Closer Than You Think" Convention of the Society for the Advancement of Material and Process Engineering — Anaheim, California. June 2, 1998. See also www.jeccomposites.com — "Toray to expand Carbon Fiber Production in France" Jan 20 2003. See also <http://netcomposites.com/news.asp?2507>, "Zoltek Announces \$20 Million Financing to Reduce Debt and Commence Capacity Expansion."

⁵ David Rigby Associates "The World Technical Textiles Industry and its Markets: Prospects to 2005." report prepared for Techtextil Messe Frankfurt GmbH. DRA can be reached at 44-161-236-0303, or by fax at 44-161-236-0310. Email: dra@dratex.co.uk. See also Dick J. Wilkins et al., JTEC Panel on Advanced Manufacturing Technology for Polymer Composite Structures in Japan, April 1994.

⁶ Freedonia Group; "World carbon black demand to reach 8.6 million metric tons in 2006" (News Release), Research Studies 3/27/2003. See also www.unitedcarbon.com.

⁷ Missile Defense Agency Newsletter, "C-Foam Hits the Beach," Article #4302, FALL 2003.

⁸ Cientifica, Nanotubes, March 2004.

⁹ Werner K. Fischer, Felix Keller and Ulrich Mannweiler, "The Changing World of Anode Raw Materials: Can Today's Carbon Technology Cope with it?" ARABAL Conference 1999, Kuwait.

¹⁰ Werner K. Fischer, Felix Keller and Ulrich Mannweiler, "The Changing World of Anode Raw Materials: Can Today's Carbon Technology Cope with it?" ARABAL Conference 1999, Kuwait.

¹¹ C. R. Manganaro, K. C. Krupinski & F. A. Smith, "A Study of the Mechanism of Needle Coke Formation," American Institute of Mining, Metallurgical, and Petroleum Engineers (AIME) Conference, March 1, 1971.

¹² HTI Direct Coal Liquefaction Technology,
<http://www.htigrp.com/data/upfiles/pdf/DCL%20Technology%2023Feb05.pdf>.

¹³ Jerald J. Fletcher, Qingyun Sun et al., "Coal to Clean Fuel – The Shenhua Investment in Direct Coal Liquefaction," 21st Annual International Pittsburgh Coal Conference, Osaka, JAPAN September 13-17, 2004.

¹⁴ Jerald J. Fletcher, Qingyun Sun et al., *ibid.*

¹⁵ Mieke Reece, Special Issue #9 Proposal for Oil Densities, International Energy Agency, Energy Statistics Working Group Meeting, 16-17 Nov 2004.

¹⁶ University of Kentucky, Phase II Quarterly Technical Progress Report, DE-AC22-91PC91040, April 2001.

¹⁷ The Carbon Products Industry Vision for the Future, Industries of the Future, Carbon Products Consortium, WVU-NRCCE, P.O. Box 6064, Morgantown, WV 26506.

¹⁸ R. H. Wombles, "Experience with Petroleum Enhanced Coal Tar Pitch," 2000 Australasian Smelter Conference, Queenstown, Australia.

¹⁹ Zsolt Romy, "The Future: It's Closer Than You Think" Convention of the Society for the Advancement of Material and Process Engineering — Anaheim, California. June 2, 1998. See also www.jecomposites.com – "Toray to expand Carbon Fiber Production in France" Jan 20 2003. See also <http://netcomposites.com/news.asp?2507>, "Zoltek Announces \$20 Million Financing to Reduce Debt and Commence Capacity Expansion."

²⁰ David Rigby Associates "The World Technical Textiles Industry and its Markets: Prospects to 2005." report prepared for Techtextil Messe Frankfurt GmbH. DRA can be reached at 44-161-236-0303, or by fax at 44-161-236-0310. Email: dra@dratex.co.uk. See also Dick J. Wilkins et al., JTEC Panel on Advanced Manufacturing Technology for Polymer Composite Structures in Japan, April 1994.

²¹ Freedonia Group; "World carbon black demand to reach 8.6 million metric tons in 2006" (News Release), Research Studies 3/27/2003. See also www.unitedcarbon.com.

²² Missile Defense Agency Newsletter, "C-Foam Hits the Beach," Article #4302, FALL 2003.

²³ Cientifica, Nanotubes, March 2004.

²⁴ N. Nakicenovic, "Freeing Energy from Carbon," *Daedalus*, Vol 125, #3 (1996), pp. 95-112.

²⁵ P. G. Stansberry et al., Modified Protocols for Synthetic Feedstocks for Anodes, 21st Annual Pittsburgh Coal Conference, Osaka JAPAN, Sept 13-17 2006.

²⁶ Ripudaman Malhotra, "Direct Coal Liquefaction: Lessons Learned," GCEP Advanced Coal Workshop, Brigham Young University, Provo, UT; Mar 16, 2005.

-
- ²⁷ John Morris Weiss, The Latent Heat of Vaporization of Coal Tar Oils, Journal of Industrial and Engineering Chemistry, Vol 14, 1, p. 72, 1922.
- ²⁸ Song C. and Schobert H., Fuel, 1996, 75(6), 724-736.
- ²⁹ Sapre A.V., Gates B.C., Hydrogenation of Aromatic Hydrocarbons Catalyzed by Sulfided CoO-MoO₃/Al₂O₃. Reactivities and Reaction Networks, Ind. Eng. Chem. Process Des. Dev. 1Q01, 20, 68-73.
- ³⁰ Frye, C. G.; Weitkamp, A. W. Equilibrium Hydrogenation of Multi-Ring Aromatics. J. Chem. Eng. Data 1969, 14, 372-376.
- ³¹ Al-Dahhan M.H., Dudukovic M.P., Catalyst wetting efficiency in trickle-bed reactors at high pressure, Chemical Engineering Science, Vol. 50, No. 15, pp. 2377-2389, 1995.
- ³² Jubert k., Stevens, G., Masudi, H., A Study of Coal formation Department of Mechanical Engineering, Prairie View A&M University, Prairie View, Texas
- ³³ Fenton D., "Direct Liquefaction of Coal with Coal-Derived Solvents to Produce Precursors from Coal", Thesis, Department of Chemical Engineering, West Virginia University, 2001.
- ³⁴ Song C. and Schobert H., Fuel, 1996, 75(6), 724-736.
- ³⁵ Gierman H. Appl. Catal. 1988, 43, 277.
- ³⁶ Girgis M.J., Gates B.C., Reactivities, Reaction Networks and Kinetics in High-pressure Catalytic Hydroprocessing, Ind. Eng. Chem. Res. 1991, 30, 2021-2058
- ³⁷ Van Krevelen D.W., Coal, Typology-Chemistry-Physics-Constitution. Elsevier Scientific Publishing Company, Amsterdam, 1981.
- ³⁸ E.L. Kugler, L. Feng, X. Li and D.B. Dadyburjor, "Effect of Ni on K-Doped Molybdenum-on-Carbon Catalysts: Temperature-Programmed Reduction and Reactivity to Higher-Alcohol Formation," Studies Surf. Sci. Catal., 130, 299-304 (2000).
- ³⁹ Schobert H., The Geochemistry of coal, Chem 1 supplement, Fuel Science Program, Pennsylvania state university.
- ⁴⁰ Coker A.K, Modeling of Chemical Kinetics and Reactor Design, Edition 2, July 2001, Elsevier Science and Technology Book.
- ⁴¹ Bej S.K., Performance Evaluation of Hydroprocessing Catalysts-A Review of Experimental Techniques, Department of Chemical Engineering, University of Michigan, Energy & Fuels 2002, 16, 774-784.
- ⁴² Zhan X., Guin J.A., High-pressure Hydrogenation of Naphthalene Using a Reduced Iron Catalyst, Energy & Fuels 1994, 8, 1384-1393

-
- ⁴³ Girgis M.J., Gates B.C., Reactivities, Reaction Networks and Kinetics in High-pressure Catalytic Hydroprocessing, *Ind. Eng. Chem. Res.* 1991,30, 2021-2058.
- ⁴⁴ Shaw J.M., A correlation for hydrogen solubility in alicyclic and aromatic solvents, *The Canadian Journal of Chemical Engineering*, 1987, 65, 293-298.
- ⁴⁵ Ali A.S., Thermodynamic aspects of aromatic hydrogenation, *Petroleum Science and Technology*, 2007, 25, 1293-1304.
- ⁴⁶ Rautanen P.A., Aittamaa J. R., Krause A. O. I., Liquid phase hydrogenation of tetralin on Ni/Al₂O₃, *Chemical Engineering Science*, 2001, 56, 1247-1254.
- ⁴⁷ Frye C. G.; Weitkamp A. W., Equilibrium Hydrogenation of Multi-Ring Aromatics. *Journal of Chemical and Engineering Data*, 1969, 14, 372-376.
- ⁴⁸ Sapre A.V., Gates B.C., Hydrogenation of Aromatic Hydrocarbons Catalyzed by Sulfided CoO-MoO₃/Al₂O₃, Reactivities and Reaction Networks, *Industrial and Engineering Chemistry Process Design and Development*. 1981, 20, 68-73.
- ⁴⁹ Zhan X., Guin J.A., High-pressure Hydrogenation of Naphthalene Using a Reduced Iron Catalyst, *Energy & Fuels* 1994, 8, 1384-1393.
- ⁵⁰ Satterfield, C. N, Trickle Bed Reactors, *AIChE Journal*, 1975, 21, 209-228.
- ⁵¹ Sapre and Gates, op cit.
- ⁵² Zhan and Guin, op. cit.
- ⁵³ Zhan and Guin, op. cit.
- ⁵⁴ Diaz-Real R.A., Mann R.S., Inderjeet S., Hydrotreatment of Athabasca Bitumen Derived Gas Oil over Ni-Mo, Ni-W, and Co-Mo Catalysts, *Industrial and Engineering Chemistry Research*, 1993, 32, 1354-1358.
- ⁵⁵ Goodman J.M., Kirby P.D., Haustedt L.O., Some calculations for organic chemists: Boiling point variation, Boltzmann factors and Eyring equation, *Tetrahedron Letters*, 2000, 41, 9879-9882.
- ⁵⁶ J. M. Shaw, op cit.
- ⁵⁷ Cai H.Y., Shaw J.M., Chung K.H., Hydrogen solubility measurements in heavy oil and bitumen cuts, *Fuel*, 2001, 80, 1055-1063.
- ⁵⁸ Mitra Motaghi et al., Anode-Grade Coke from Traditional Crudes, www.eptq.com.
- ⁵⁹ Mitra Motaghi et al., op. cit.
- ⁶⁰ Steel Times International, "Eurocoke 2011: Coke Consumption to rise to 750 MT by 2015," <http://www.steeltimesint.com/news/view/eurocoke-2011-coke-consumption-to-rise-to-750mt-by-2015/steel-news/> .
- ⁶¹ CRU Forecasts, The Annual Outlook for Metallurgical Coke, 2010 Edition, <http://cruonline.crugroup.com/SteelandFerroalloys/MarketForecasts/MetallurgicalCokeOutlook/tabid/161/Default.aspx> .

⁶² Steel Times International, “Eurocoke 2011: Coke Consumption to rise to 750 MT by 2015,” <http://www.steeltimesint.com/news/view/eurocoke-2011-coke-consumption-to-rise-to-750mt-by-2015/steel-news/> .

⁶³ InterTech Pira, The Future of Metallurgical Coke to 2015 - Global Market Forecasts, referenced in Nine Nice Minerals International Group Ltd., <http://www.e-reful.com/news/391.html>.

⁶⁴ Eric Johnson, Goodbye to carbon neutral: Getting biomass footprints right, Environmental Impact Assessment Review Volume 29, Issue 3, April 2009, Pages 165-168.

⁶⁵ M. E. Dias de Oliveira, B. E. Vaughan, E. J. Rykiel, Jr, BioScience, July 2005, Vol. 55, No. 7, Pages 593–602, Posted online on December 18, 2008.

⁶⁶ David Pimentel and T. W. Patzek, “Ethanol Production Using Corn, Switchgrass, and Wood; Biodiesel Production Using Soybean and Sunflower,” *Natural Resources Research*, Vol. 14, No. 1, March 2005.

⁶⁷ Richard Rhodes and Denis Beller , “The Need for Nuclear Power,” *Foreign Affairs*, Vol. 79, No. 1 (Jan. - Feb., 2000), pp. 30-44.

⁶⁸ Canadian Association of Petroleum Producers, “Environmental Challenges and Progress in Canada’s Oil Sands,” 10/23/2008.

⁶⁹ Merrill Lynch, “Biofuels Driving Global Oil Supply Growth,” Energy Commodities Weekly, 06 June 2008.

⁷⁰ John A. Organiscak and Steven J. Page, Investigation of Coal Properties and Airborne Respirable Dust Generation, NIOSH RI 9645, 2008.

⁷¹ M.C. Herweyer, A. Gupta, Unconventional Oil: Tar Sands and Shale Oil - EROI on the Web, Part 3 of 6, APPENDIX D TAR SANDS/OIL SANDS, April 15, 2008.

⁷² Eric H. Oelkers and David R. Cole, Carbon Dioxide Sequestration--A Solution to a Global Problem, ELEMENTS , VOL. 4, PP. 305–310.

⁷³ IEA Statistics, 2010 ed., CO2 Emissions from Fuel Combustion—Highlights. Page 74.

⁷⁴ Research Newsletter of Ecocosm Dynamics, Ltd., Volume 2 ~ Number 1 ~ February 1st, 2005. Weblink: <http://www.ecocosmdynamics.org/Pubs/EDLNewsletterVol2No1.html> .

⁷⁵ IEA Statistics, 2010 ed., CO2 Emissions from Fuel Combustion—Highlights. Page 13.

⁷⁶ CDIAC, <http://mdgs.un.org/unsd/mdg/SeriesDetail.aspx?srid=749&crid=> (the same information is compiled in Wikipedia.com).

⁷⁷ International Energy Annual, Energy Information Agency, 2006.

⁷⁸ Anthony Andrews, Jeffrey Logan, “Fischer-Tropsch Fuels from Coal, Natural Gas and Biomass: Background and Policy;” Congressional Research Services, Order Code RL 34133, March 27, 2008 .

⁷⁹ Richard Turton et al., *Analysis, Synthesis, and Design of Chemical Processes*, Prentice Hall ISBN 9780130647924, 2003.

⁸⁰ Final Report, NETL Contract Number: DE-FC26-02NT41596.

⁸¹ P. G. Stansberry, E. B. Kennel, and N. D. King, “Modified Protocols for Synthetic Feedstocks for Anodes,” *21st Annual Pittsburgh Coal Conference*, Osaka Japan, 2004.

⁸² Summary report of DOE direct liquefaction process development campaign of the late twentieth century: Topical report, July 2001.

⁸³ J. T. Baron, C. E. Kraynik and R. H. Wombles, “Strategies for a Declining North American Coal Tar Supply” in *Light Metals 1998 Métaux Légers*, edited by: M. Sahoo and C. Fradet, the Metallurgical Society.

⁸⁴ Richard Turton, Richard C. Bailie, Wallace B. Whiting, and Joseph A. Shaeiwitz, *Analysis, Synthesis, and Design of Chemical Processes, 2nd Edition* (Prentice Hall International Series in the Physical and Chemical Engineering Sciences), Prentice-Hall, Upper Saddle River NJ, 2002.

⁸⁵ CRESAP Test Facility, Final Report for the Period Sept 1 1977 to Sept 30, 1979 Vol I-III, DOE Contract AC01-76ET-10060.

⁸⁶ Robert E. Lumpkin, “Recent Progress in the Direct Liquefaction of Coal “ *Science* 239 (4842), 873 (19 February 1988).

⁸⁷ P. Wellman, Coal liquefaction - The H-Coal process, In: *Alternative energy sources; Proceedings of the Miami International Conference*, Miami Beach, Fla., December 5-7, 1977. Volume 7. (A79-34086 13-44) Washington, D.C., Hemisphere Publishing Corp., 1978, p. 3285-3305.

⁸⁸ Later, D.W., Two-stage coal liquefaction process materials from the Wilsonville Facility operated in the nonintegrated and integrated modes: chemical analyses and biological testing, OSTI ID: 6053786; DE85009992 Report Number(s) PNL-5215, DOE Contract Number AC06-76RL01830.

⁸⁹ James H. Gary, and Glenn E. Handwerk, *Petroleum Refining: Technology and Economics, 4th Edition*; CRC Press, February 15, 2001.

⁹⁰ Richard Wolfe et al., “Process for Converting Coal Into Liquid Fuel and Metallurgical Coke,” US Patent 5,296,005, March 22 1994.

⁹¹ Debra McCown, \$20 million carbonite plant being developed near Norton, Va. Published: March 22, 2011. Also see <http://www.istockanalyst.com/business/news/4999416/-20-million-carbonite-plant-being-developed-near-norton-va> .

⁹³ Dudukovic, M.P., Larachi, F., Mills, P.L., 2002. Multiphase catalytic reactors: a perspective on current knowledge and future trends. *Catalysis Reviews Science and Engineering* 44, 123.

⁹⁴ Technology Status Report 010, Coal Liquefaction, Cleaner Coal Technology Program, US Department of Trade and Industry, October 1999,

⁹⁵ S., Speight J. G., Loyalka K., *Handbook of Alternative Fuel Technologies*, 2007, CRC press.

⁹⁶ Zhang Y., Ren X., Sun Q., Fletcher J.J., Comparative analysis of costs of alternative coal liquefaction processes, *Energy & Fuels*, 2005, 19, 1160-1164.